

IL
NUOVO CIMENTO
ORGANO DELLA SOCIETÀ ITALIANA DI FISICA
SOTTO GLI AUSPICI DEL CONSIGLIO NAZIONALE DELLE RICERCHE

VOL. V, N. 6

Serie decima

10 Giugno 1957

**Ionization at the Origin
of High Energy Electron Positron Pairs.**

G. YEKUTIELI

Department of Physics, The Weizmann Institute of Science - Rehovoth, Israel

(ricevuto il 29 Dicembre 1956)

Summary. — The ionization at the origin of a high energy ($E > 50$ GeV) electron positron pair is calculated, and the results are compared with experiment.

The effect of decrease in the ionization of electron positron pairs of extremely high energy at the origin was suggested by D. T. KING ⁽¹⁾ and first measured by D. H. PERKINS ⁽²⁾.

The electron and the positron of an extremely energetic pair are produced into a very small angle and they travel together for a considerable length. According to BORSELLINO ⁽³⁾, the members of a 200 GeV electron positron pair will depart from each other by less than $5 \cdot 10^{-7}$ cm at a distance of 500 μ m from their origin. The impact parameter for distant collisions of relativistic singly charged particles in emulsions is extended up to about 10^{-6} cm. Thus a large number of electrons in the medium along the first few hundred microns of a 200 GeV electron pair will gain energy from the mutual electromagnetic field of the electron positron pair. In most of these cases the pair field will be weaker than twice the field of a single electron, and the electron positron pair will lose less energy by ionization than two independent electrons. This

⁽¹⁾ Private communication to PERKINS.

⁽²⁾ D. H. PERKINS: *Phil. Mag.*, **46**, 1146 (1955).

⁽³⁾ A. BORSELLINO: *Phys. Rev.*, **89**, 1023 (1953).

will make the total ionization of an electron positron pair near its origin less than twice the ionization of a single electron. As the electron positron pair travels further away from its origin less electrons will be within the mutual collision range of the two, and the ionization of the pair will increase. When the pair will be separated by more than twice the maximum impact parameter for distant collisions of a relativistic singly charged particle, the ionization of the pair will reach its saturation value of twice a single electron.

In what follows we shall calculate the energy loss of an electron positron pair by ionization. We shall assume that the electron and the positron are travelling parallel to each other with the same velocity v ($v \rightarrow c$) along a short distance x . They are separated from each other by b cm; b is assumed to be larger than twice the atomic radius ϱ_0 . The pair will lose energy to the electrons of the medium in two types of collisions (1) close collisions: collisions with electrons at distances less than ϱ_0 from one of the members of the pair, and (2) distant collisions: all other collisions. We shall see later that most of the contribution to the pair effect comes from distant collisions.

The contributions from distant collisions are calculated according to the Fermi model (4). The energy transmitted per unit time to the medium at distances larger than ϱ_0 from both the electron and the positron, is given by the Poynting vector $(c/4\pi)[E \times H]_n$ through the two cylindrical surfaces of radius ϱ_0 , having their axes on the paths of the electron and the positron. The electron-positron pair gives rise to a charge density

$$j_0 = e \delta(x - vt) [\delta(y) \delta(z) - \delta(y - b) \delta(z)]$$

and a current $\mathbf{j} = \mathbf{v} j_0$. The electron positron pair induces an electromagnetic field (A_0, A) in a medium of a dielectric constant $\epsilon(\omega)$. Solving the Maxwell equation for this pair, one finds that:

$$H_x = 0 \quad \text{and thus} \quad [E \times H]_n = E_x \frac{dA_x}{d\varrho},$$

where

$$(1) \quad \left\{ \begin{array}{l} A_x = \frac{e}{\pi c} \int_{-\infty}^{\infty} [K_0(k'\varrho) - K_0(k'\varrho')] \exp \left[i\omega' \left(\frac{x}{v} - t \right) \right] d\omega' , \\ E_x = -\frac{ie}{\pi v^2} \int_{-\infty}^{\infty} \left(\frac{1}{\epsilon} - \beta^2 \right) [K_0(k\varrho) - K_0(k\varrho')] \exp \left[i\omega \left(\frac{x}{v} - t \right) \right] \omega d\omega , \end{array} \right.$$

are the solutions for A_x and E_x (5) on a cylinder of radius ϱ with the positron

(4) E. FERMI: *Phys. Rev.*, **57**, 485 (1940).

(5) Compare M. SCHÖNBERG: *Nuovo Cimento*, **8**, 159 (1951).

as an axis (see Fig. 1), $\varrho'^2 = \varrho^2 + b^2 - 2b\varrho \cos \theta$, ϱ' is the distance to the electron, $k^2(\omega) = (\omega^2/v^2)(1 - \beta^2 \epsilon(\omega))$ and $k' = k(\omega')$.

The energy ΔW transmitted through a cylinder of radius ϱ_0 along Δx cm of the positron paths is:

$$(2) \quad \Delta W = \frac{e}{4\pi} \Delta x \int_{-\infty}^{\infty} \int_0^{2\pi} E_x \frac{dA_x}{d\varrho} dt \varrho d\theta .$$

An equal amount of energy is transmitted through a cylinder of radius ϱ_0 around the electron. Inserting in (2) the expressions of A_x and E_x from (1) and integrating on t and ω' the total energy loss by the pair in distant collisions per unit length is:

$$(3) \quad \left| \frac{dW}{dx} \right|_{>\varrho_0}^{\text{pair}} = \frac{ie^2 \varrho_0}{\pi^2 v^2} \int_{-\infty}^{\infty} \int_0^{2\pi} \left(\frac{1}{\varepsilon} - \beta^2 \right) [K_0(k'\varrho_0) - K_0(k'\varrho'_0)] \cdot \left[\frac{dK_0(k\varrho_0)}{d\varrho_0} - \frac{dK_0(k\varrho'_0)}{d\varrho_0} \right] \omega d\omega d\theta ,$$

where $k'(\omega) = k(-\omega)$.

The modified Bessel function $K_0(k\varrho')$ can be written as

$$(4) \quad K_0(k'\varrho') = I_0(k\varrho) K_0(kb) + 2 \sum_{m=1}^{\infty} I_m(k\varrho) K_m(kb) \cos m\theta .$$

Inserting this form of $K_0(k\varrho')$ under the integral, the integration on θ is carried out.

If ϱ_0 is of the order of magnitude of atomic dimensions, and b is not much larger, the corresponding arguments $k\varrho_0$ and kb of the modified Bessel functions have moduli smaller than one, and the Bessel functions may be replaced with their asymptotic expansions for $x \ll 1$ (compare with BUDINI (6)):

$$(5) \quad K_0(x) = \log \frac{2}{\gamma x}; \quad K_m(x) = \frac{(m-1)!}{2} \left(\frac{x}{2} \right)^{-m} \quad \text{and} \quad I_m(x) = \frac{1}{m!} \left(\frac{2}{x} \right)^m .$$

Neglecting all second order terms one finds:

$$(6) \quad \left| \frac{dW}{dx} \right|_{>\varrho_0}^{\text{pair}} = \frac{e^2}{\pi v^2} \left| \log \left(\frac{b}{\varrho_0} \right)^2 + \log \left[1 - \left(\frac{\varrho_0}{b} \right)^2 \right] \right| \int_{-\infty}^{\infty} \left(\frac{1}{\varepsilon} - \beta^2 \right) i\omega d\omega .$$

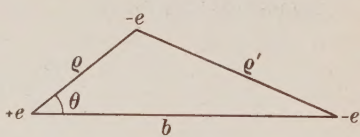


Fig. 1.

(6) P. BUDINI: *Nuovo Cimento*, **10**, 236 (1953).

Following BUDINI (6)

$$\int_{-\infty}^{\infty} \left(\frac{1}{\varepsilon} - \beta^2 \right) i\omega d\omega = \frac{4\pi^2 Ne^2}{m},$$

where M is the electron density in the medium, and m the electronic mass; finally

$$(7) \quad \left| \frac{dW}{dx} \right|_{>\varrho_0}^{\text{pair}} = \frac{4\pi N e^4}{mv^2} \left\{ \log \left(\frac{b}{\varrho_0} \right)^2 + \log \left| 1 - \left(\frac{\varrho_0}{b} \right)^2 \right| \right\}.$$

We shall use the Bohr classical model as a guide for calculating energy losses in close collisions. The momentum transferred to an electron in a plane normal to the motion of the pair is

$$(8) \quad P_{\perp} = \frac{2e^2}{v} \left(\frac{\rho}{\varrho^2} + \frac{\rho'}{\varrho'^2} \right).$$

where ϱ and ϱ' are the impact parameters of the two members of the pair $\varrho < \varrho_0 < \varrho'$ (see Fig. 1). The energy transferred by the pair per unit length is:

$$(9) \quad \left| \frac{dW}{dx} \right|_{<\varrho_0}^{\text{pair}} = \frac{4e^4 N}{mv^2} \int_{\varrho_{\min}}^{\varrho_0} \int_0^{2\pi} \left(\frac{\rho}{\varrho^2} + \frac{\rho'}{\varrho'^2} \right)^2 \varrho d\theta d\varrho.$$

Now $b^2 = \varrho^2 + \varrho'^2 - 2\rho(\rho')$ and

$$(10) \quad \begin{aligned} \left| \frac{dW}{dx} \right|_{<\varrho_0}^{\text{pair}} &= \frac{4e^4 N}{mv^2} \int_{\varrho_{\min}}^{\varrho_0} \int_0^{2\pi} \frac{b^2}{\varrho \varrho'^2} d\varrho d\theta = \\ &= \frac{4e^4 N \pi}{mv^2} \left\{ \log \left(\frac{\varrho_0}{\varrho_{\min}} \right)^2 - \log \left[1 - \left(\frac{\varrho_0}{b} \right)^2 \right] + \log \left[1 - \left(\frac{\varrho_{\min}}{b} \right)^2 \right] \right\}. \end{aligned}$$

The first term is twice the contribution of a single electron. We shall replace it by twice the expression $(2\pi Ne^4/Mv^2) \log(m\eta\varrho_0^2\gamma^2/2\hbar^2)$ given by BOHR (7) for the energy loss with energy transfer smaller than η at distance smaller than ϱ_0 . In spite of the fact that we cannot determine ϱ_{\min} we may infer that $\varrho_{\min} \ll \varrho_0 < b$, and thus the last term tends to zero and shall be neglected. Finally the contribution from close collision is:

$$(11) \quad \left| \frac{dW}{dx} \right|_{<\varrho_0}^{\text{pair}} = \frac{4\pi N e^4}{mv^2} \left\{ \log \frac{m\eta\varrho_0^2\gamma^2}{2b^2} - \log \left[1 - \left(\frac{\varrho_0}{b} \right)^2 \right] \right\}.$$

(7) N. BOHR: *Det. Kngl. Dans. Vid. Sels.*, **18**, 8 (1948).

The total energy loss of an electron positron pair in distant and close collision is obtained from (7) and (11):

$$(12) \quad \left| \frac{dW}{dx} \right|_{\text{pair}} = \frac{4\pi N e^4}{mv^2} \log \frac{m\eta b^2 \gamma^2}{2\hbar^2}.$$

To compare with experiment we define R :

$$(13) \quad R = \frac{\left| \frac{dW}{dx} \right|_{\text{pair}}}{2 \left| \frac{dW}{dx} \right|_{\text{single}}} = \frac{\log \frac{m\eta b^2 \gamma^2}{2\hbar^2}}{\log \left(\frac{mc^2 \eta}{\hbar^2 \alpha \sqrt{A}} \right) - 1}.$$

The ionization of a single electron was taken from BUDINI (6).

For emulsion the three parameters are: $\eta = 5 \text{ keV}$, $\alpha = 5.41 \cdot 10^{-33} \text{ s}^{-1}$ and $A \approx 1$. And we have for R :

$$(14) \quad R = \frac{40.7 + \log(b^2)}{13}.$$

The separation b between the two members of the pair at distance x from its origin is function of its opening angle ω and the multiple scatterings of the two electrons. According to BORSELLINO, the most probable angle for a pair of $E \text{ MeV}$ is $\omega_p = 2\varphi(a)/E$, where $\varphi(a)$ is function of the energy taken by the positron E_+ ($a = E_+/E$); $\varphi(a)$ is a slowly decreasing function of a , that changes from $\varphi(1/2) = 1$ to $\varphi(0.2) = 1.2$. We shall take $\varphi = 1$. Thus the separation of the pair, c at $x \text{ cm}$ from its origin due to an opening angle ω_p is $c = 2x/E$.

At the same time the pair is separated by multiple scatterings. The separation a , due to multiple scattering at distance x from the origin is governed by normal distribution law (8) $P(a)da = (1/\sigma^2) \exp[-a^2/2\sigma^2]da$, where $\sigma^2 = (96/E^2)x^3$; x is in cm and E the pair energy in MeV. The total separation at x , is $b = \sqrt{a^2 + c^2 - 2ac \cos \varphi}$, and the expected R is:

$$(15) \quad \langle R \rangle = \frac{40.7 + \langle \log(b^2) \rangle}{13},$$

$$(16) \quad \langle \log(b^2) \rangle = \int_0^\infty \int_0^{2\pi} \log(a^2 + c^2 - 2ac \cos \varphi) \frac{da}{2\pi} \exp \left[- \left(\frac{a^2}{2\sigma^2} \right) \right] \frac{da}{\sigma^2}.$$

(8) W. T. SCOTT: *Phys. Rev.*, **76**, 212 (1949) and S. ROSENDORFF: private communication.

Now

$$(17) \quad J = \int_0^{2\pi} \log(a^2 + c^2 - 2ac \cos \varphi) d\varphi = 2\pi \log(a^2) \quad \text{if } a \geq c;$$

$$\text{or } J = 2\pi \log(c^2) \quad \text{if } c \geq a.$$

Thus,

$$(18) \quad \langle \log(b^2) \rangle = \log(c^2) \int_0^c \exp\left[-\frac{a^2}{2\sigma^2}\right] \frac{a da}{\sigma^2} + \int_c^\infty \log(a^2) \exp\left[-\frac{a^2}{2\sigma^2}\right] \frac{a da}{\sigma^2},$$

or

$$(19) \quad \langle \log(b^2) \rangle = \log(c^2) - Ei\left(-\frac{c^2}{2\sigma^2}\right).$$

Using the expressions for $c = 2x/E$ and $\sigma^2 = (96/E^2)x^3$, and inserting (18) in (15) one gets

$$(20) \quad \langle R \rangle = \frac{40.7 + \log(4x^2/E^2) - Ei(-0.021/x)}{13}.$$

We have to bear in mind that the above derivation of the ionization loss by an electron positron pair is restricted only to pairs with a separation b not much larger than the atomic dimensions $\rho_0 \sim 10^{-8}$ cm. In the case of 180 GeV pair, this restricts us to the very first 100 μm from the origin. For $x = 100 \mu\text{m}$ the multiple scatterings contribution to $\langle R \rangle$ is only 0.3% and can be neglected. Further away from the pair's origin, i.e., for $x > 210 \mu\text{m}$ the multiple scattering becomes a dominant factor in the separation of the electron positron pair. The ionization of an electron positron pair in the region beyond 100 μm from its origin will be treated elsewhere.

PERKINS⁽²⁾ measured in emulsion the ionization at the origin of a group of electron-positron pairs with energy between 80 and 400 GeV, with an average of 180 GeV. In Table I the experimental results of PERKINS for the group is compared with our calculation (20), for $E = 180$ GeV.

TABLE I.

X μm	$R = \text{d}W/\text{d}x _{\text{pair}}/2 \text{d}W/\text{d}x _{\text{single}}$	
	Experiment	Theory
15	0.50 \pm .06	0.46
50	0.77 \pm .08	0.65
100	0.73 \pm .08	0.75
200	0.86 \pm .09	0.86

The agreement between experiment and theory displayed in Table I suggests that R as expressed in (20) is a good approximation even at 200 μm .

WOLTER and MIESOWICZ⁽⁹⁾ measured the ionization of an electron positron pair at the origin in photographic emulsion. They obtained an average R of $0.60 \pm .03$ for the first 260 μm from its origin. Comparing this measurement with R of (20) averaged on the first 260 μm from the pair's origin, we may estimate the opening angle ω_p and the energy E of this pair. In this way we find $\omega_p = 2 \cdot 10^{-6}$ radians and $E = 980 \text{ GeV}$, for the opening angle and the energy of the pair respectively; in good agreement with WOLTER and MIESOWICZ.

* * *

The author is very grateful to Dr. H. J. LIPKIN and Mr. S. ROSENDORFF for stimulating discussions in connection with this work.

(9) W. WOLTER and M. MIESOWICZ: *Nuovo Cimento*, **4**, 648 (1956). We learned from this publication that A. E. ČUDAKOV estimated theoretically the ionization at the origin, of an electron positron pair.

RIASSUNTO (*)

Si calcola la ionizzazione all'origine di una coppia elettrone-positrone di alta energia ($E > 50 \text{ GeV}$) e si confrontano i risultati con l'esperienza.

(*) Traduzione a cura della Redazione.

Examples of the Production of (K^0, K^0) and (K^+, K^0) Pairs of Heavy Mesons.

W. A. COOPER, H. FILTHUTH, J. A. NEWTH, G. PETRUCCI,
R. A. SALMERON and A. ZICHICHI

C.E.R.N. - Geneva

(ricevuto il 14 Gennaio 1957)

Summary. — Two simple nuclear interactions that produce pairs of K -mesons are described and discussed. They are interpreted as examples of the processes $n + p \rightarrow K^0 + \bar{K}^0 + n + p$ and $n + p \rightarrow K^+ + \bar{K}^0 + n + n$ where \bar{K}^0 is the anti-particle of the K^0 -meson.

1. — Introduction.

The production, in elementary reactions, of pairs of K -mesons without other strange particles has been predicted theoretically by GELL-MANN and PAIS⁽¹⁾. Two examples of (K^+, K^-) pairs, interpreted in this way, have been observed in emulsion experiments^(2,3). One event seen in a cloud chamber attached to the Berkeley accelerator has been interpreted as a (K^0, \bar{K}^0) pair in which only one of the K^0 -mesons was seen to decay⁽⁴⁾.

During a systematic study of the associated production of heavy mesons and hyperons in a cosmic-ray cloud chamber we have found two examples

⁽¹⁾ M. GELL-MANN and A. PAIS: *Proceedings of the Glasgow Conference on Meson and Nuclear Physics* (1954), p. 342.

⁽²⁾ M. W. FRIEDLANDER, D. KEEFE and M. G. K. MENON: *Nuovo Cimento*, **2**, 666 (1955).

⁽³⁾ M. CECCARELLI, M. GRILLI, M. MERLIN, G. SALANDIN and B. SECHI: *Nuovo Cimento*, **2**, 828 (1955).

⁽⁴⁾ W. B. FOWLER, G. MAENCHEN, W. M. POWELL, G. SAPHIR and R. W. WRIGHT: *Phys. Rev.*, **103**, 208 (1956).

of very simple nuclear interactions that give rise to pairs of K-mesons. In one case both the K-mesons are neutral, in the second case one is neutral and the other positively charged. The three neutral K-mesons are all seen to decay.

The importance of these observations is that they provide evidence to support the theoretical prediction that K^0 -mesons should exist in two states with opposite « strangeness »^(1,5).

2. – Selection of events.

In studying the production of heavy mesons and hyperons we have drawn heavily on the earlier work of JAMES and SALMERON⁽⁶⁾. They pointed out that nuclear interactions of low multiplicity occurring inside a cloud chamber were the most profitable to study. The probability of detecting V-particles produced in such interactions is relatively large and the chance of two V-particles being plurally produced, that is, produced in separate elementary reactions, is small. They also showed that nuclear scattering, at least of Λ^0 -particles, made the interpretation of production processes occurring in heavy nuclei extremely difficult. For this reason, and to reduce further the probability of plural production, they proposed the use of a light material inside the cloud chamber.

We have a collection of 60 000 cloud chamber photographs taken at the Jungfraujoch for all of which there was a solid plate placed across the centre of the chamber. For 5 000 photographs the plate was of lead, 30 mm thick, for 35 000 it was copper, 12 mm thick, and for the last 20 000 photographs a graphite plate 25 mm thick was used.

Nine nuclear interactions in these plates produced two strange particles. Table I lists these events giving the nature of the strange particles and the type of interaction.

The neutral V-events have been classified as compatible or incompatible with Λ^0 -decays. Events that cannot be Λ^0 -decays are assumed to be the decays of neutral K-mesons. All these K^0 -decays could be due to ℓ^0 -particles but the measurements do not exclude any of them being « anomalous » decays. In fact, among the thirteen neutral V-events of Table I there is no identified Λ^0 -decay. Eight of the V^0 -events are K^0 -decays and the other five could be either Λ^0 - or K^0 -decays.

Three of the nine nuclear interactions listed in Table I produce two K-mesons. Of these three, two have no fast charged secondary particles;

⁽⁵⁾ Discussion in Sect. 8, *Proceedings of the Sixth Rochester Conference* (1956).

⁽⁶⁾ G. D. JAMES and R. A. SALMERON: *Phil. Mag.*, **46**, 571 (1955).

therefore the probability that these interactions are elementary is very high. The description and discussion of these two events are given in the following sections.

TABLE I. - *Interactions in the cloud chamber producing associated strange particles.*

Picture No.	Identity of Strange Particles (*)	Details of Interaction			
		Material	Primary	Fast Secondaries	Slow Secondaries
VB 536	$K^0 + K^0$	Graphite	Neutral	0	1
SN 1534	$K^0 + K^+$	Copper	Neutral	0	0
TS 200	$K^0 + V^0$	Graphite	Charged	0	1
TF 1561	$K^0 + K^0$	Copper	Charged	1 (+ ?)	3 (+ ?)
TD 1183	$K^0 + V^0$	Copper	Charged	1 + e.p.	0
SO 1073	$K^+ + V^+$	Copper	Charged	1	1
TB 249	$K^0 + V^+$	Copper	Neutral	3	0
TH 1018	$V^0 + V^0$	Copper	Neutral	5 + e.p.	8
SL 496	$V^0 + V^+$	Copper	Neutral	5	4

(*) In this column K^0 stands for a V^0 -particle that cannot be a Λ^0 -particle and V^0 for a neutral V -particle that could be either a Λ^0 - or a K^0 -particle. The two K^+ -mesons are slow-moving particles whose decay is not observed; they are identified from momentum and ionization. The three V^+ -particles could be either K -mesons or hyperons.

In event TF 1561 the position of the interaction in the cloud chamber makes it unlikely that all the charged secondary particles are observed. The abbreviation "e.p." stands for "electron-positron pair".

3. - Description of the events.

3.1. *Event VB 536* (Plate 1). - This event shows two neutral V -particles and a single slow proton coming from an interaction in graphite. The interaction is produced by a neutral particle, presumably a neutron. The two V -events are not Λ^0 -decays. All the four decay products of these K^0 -particles have high momenta and we can only give lower limits to the Q -values of the decays. Assuming decay into two π -mesons, these lower limits are 77 MeV and 31 MeV.

On the assumption that the two particles are θ^0 -mesons, their momenta can be calculated quite accurately from the geometry of the decays. The values are 1400 MeV/c and 2550 MeV/c. The corresponding times of flight are $1.3 \cdot 10^{-10}$ s and $0.4 \cdot 10^{-10}$ s.

In the cloud chamber there are also the tracks of two fast particles that enter the chamber from above. These tracks are nearly vertical and if we assume that the neutron causing the interaction in the graphite plate was associated with them it is possible to make a dynamical analysis of the interaction.

W. A. COOPER, H. FILTHUTH, J. A. NEWTH, G. PETRUCCI,
R. A. SALMERON and A. ZICHICHI



Plate I. - Event VB 536. A , B and C , D are two K^- -decays and P is the track of a proton from the nuclear interaction producing the K^0 -mesons. The nuclear interaction occurs in a graphite plate and the primary particle is presumably a neutron. The two fast particles entering the chamber at the top suggest that the neutron was part of a nearly vertical shower. The measurements of the various tracks are given in Table II.

W. A. COOPER, H. FILTHUTH, J. A. NEWTH, G. PETRUCCI,
R. SALMERON and A. ZICHICHI



Plate 2. — Event SN 1534. A K^+ -meson and a K^0 -meson are produced in a nuclear interaction in copper. Track C is that of the K^+ -meson, A is a heavily-ionizing positive light meson and B is the negative secondary from the K^0 -decay. Track D is that of a K^+ -meson which stops in the copper plate and decays into a charged secondary particle (E). The similarity between tracks C and D makes possible the identification of particle C as a K^+ -meson. The measurements of the event are given in Table III.

3.2. *Event SN 1534* (Plate 2). — In this event a non-decaying K^+ -meson and a V^0 -particle are the only visible products of a nuclear interaction in copper. The primary of the interaction is again neutral but there are no fast charged particles to indicate its direction.

The identification of the K^+ -meson from this interaction is based on measurements of momentum and ionization and is extremely convincing since, on the same photograph, another K^+ -meson which stops in the copper plate producing a characteristic S -event has similar momentum and ionization.

The positive secondary particle from the V^0 -decay is a slow light meson and the decay cannot, therefore, be a Λ^0 -decay. The negative secondary particle has a high momentum and, again, only a lower limit to the Q -value of the decay can be calculated. Assuming decay into two π -mesons this lower limit is 146 MeV. If the V -particle is a Θ^0 -meson, the momentum of the Θ^0 -meson is 1090 MeV/c and its time of flight before decay is $1.6 \cdot 10^{-10}$ s.

The detailed measurements made on the two events and the method of identifying the various particles involved are given in the appendices.

4. — The production reactions.

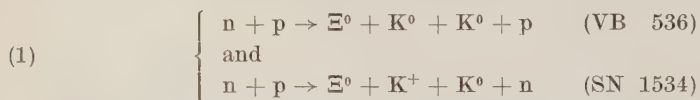
Accepting the phenomenological theory of strange particles (1) and its predictions about the allowed processes of associated production where the total «strangeness» (S) is conserved, there are three ways in which two K -mesons may arise from a nuclear interaction.

First is the possibility of plural processes. In our events one could assume that each K -meson ($S = +1$) was produced with a Σ - or Λ -hyperon ($S = -1$) in the well-established reactions leading to (Y , K) association. The strictness with which we have selected interactions of low multiplicity is strong evidence against this interpretation. If it were correct, four strange particles would have been produced in each interaction but no fast charged particle. Moreover, if a charged Σ -hyperon had been produced either it or its charged decay product would certainly have been seen. The hyperon most likely to escape detection is the neutral Λ^0 -particle and it is improbable that we should see no Λ^0 -decay if, in fact, a Λ^0 -particle was produced with each of the four K -mesons.

A second possible interpretation involves the production of a Ξ -particle ($S = -2$) and two K -mesons each with $S = +1$. An example of this process has been observed (2). The known Ξ^- -particle would almost certainly have been detected in either of our two events. But there are theoretical

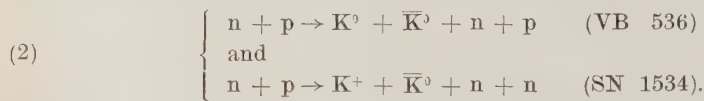
(1) J. D. SORRELS, R. B. LEIGHTON and C. D. ANDERSON: *Phys. Rev.*, **100**, 1457 (1955).

arguments for the existence of a Ξ^0 -particle whose immediate decay products (Λ^0, π^0) are also uncharged. The reactions



could thus account for our two events. These reactions are rather elaborate constructions to explain our events and since the events can be interpreted without introducing unobserved strange particles we prefer not to invoke the hypothetical Ξ^0 -particle.

The third, and most plausible, interpretation is that the events show the production of pairs of K-mesons with opposite strangeness ($S = +1$ and $S = -1$). If we follow the theory of GELL-MANN and PAIS ⁽¹⁾ these pairs would consist of a particle and an anti-particle and the production reaction would be



From the point of view of the dynamics of the reactions only there is little difference between (1) and (2) since both the Ξ^0 -particle and the neutron are heavy particles.

Assuming that reactions (2) are the correct interpretation of the two events, a lower limit may be set to the energy of the incident neutron in each case. For event VB 536 this limit is 5.7 GeV and for SN 1534 it is 3.8 GeV. If, further, we assume the direction of the incident neutron in event VB 536 to be that of the two fast particles in the top of the cloud chamber the dynamics of reaction (2) can be fully analyzed and the neutron energy is uniquely determined as 7.3 GeV. These values may be compared with the threshold energy of 2.5 GeV for reaction (2).

More detailed calculations of the dynamics of the reactions are not very reliable but one can say with confidence that the inelasticity of the neutron-proton collision is not more than about 50% in either of the events. In VB 536 this means that the secondary neutron travels forwards with considerable energy (~ 2 GeV) after the interaction. The same conclusion would hold for the Ξ -particle from reaction (1) and this is the reason for our confidence that a Ξ -particle would have been observed had it been produced. In event SN 1534 one of the two heavy particles that are not observed must be fast but the other can have a low energy.

5. — Discussion.

It would be of great value to know whether the K^0 -mesons produced in our two events could be identified as θ^0 -particles or not. Unfortunately the experimental measurements are not very helpful.

Concerning the dynamics of the decays, only lower limits can be set to the Q -values in all three cases. For the two V^0 -decays in event VB 536 the $Q(\pi\pi)$ -values are > 77 MeV and > 31 MeV. The $Q(\pi\pi)$ -value for the V^0 -event in SN 1534 is > 146 MeV. All one can say, therefore, is that the K^0 -decay in SN 1534 is not a τ^0 -decay.

The geometry of event VB 536 is of interest since the planes of the two V^0 -decays intersect in a line which, itself, intersects the proton track within the limits of experimental error. If either V^0 -decay were a three-body decay this would be an improbable situation. It therefore seems likely that both are decays into two bodies or, at least, that any third, neutral, particle is produced with a low momentum.

The lifetimes of the three K^0 -mesons are all of the order of 10^{-10} s. This provides no direct evidence for identifying them as θ^0 -mesons whose mean lifetime is 10^{-10} s since the cloud chamber would not have contained the decays if the lifetimes had been much longer than they were. Indirectly, one can argue that if one of the K^0 -mesons had a very long mean lifetime ($\sim 10^{-8}$ s) the probability of observing an event like VB 536 would be extremely small.

From the above points it is clear that all three K^0 -mesons could well be θ^0 -mesons but there is little direct evidence for this identification. In our calculations we have assumed that they are all θ^0 -mesons.

Finally, it is worth commenting on the general importance of the pair-production of K-meson. In an earlier paper⁽⁸⁾ we showed that the positive excess among charged K-mesons in the cosmic radiation was about 3.5:1. We pointed out that this implied that the frequency of reactions in which pairs of K-mesons were produced was comparable with that of processes leading to a hyperon and a K^+ -meson. For the neutral V-particles we find a similar situation. The observations in Table I include more K^0 -mesons than Λ^0 -hyperons. Among single V^0 -events we also find an excess of K^0 -decays. Considering only V-particles produced in carbon, the K^0 -particles exceed the Λ^0 -particles by a factor of two or three. This excess is not simple to interpret but processes of the type recorded in this paper could clearly explain it.

⁽⁸⁾ W. A. COOPER, H. FILTHUTH, J. A. NEWTH and R. A. SALMERON: *Nuovo Cimento*, **4**, 390 (1956).

6. — Conclusions.

The two events reported in this paper extend our knowledge of the production processes of heavy mesons. To the best of our knowledge, they are the first examples that have been observed of (K^0, K^0) and (K^+, K^0) pairs produced in simple interactions where the K -mesons have been identified directly.

The events are evidence that K^0 -mesons with both positive and negative strangeness exist. That this should be so was predicted by GELL-MANN and PAIS who suggested that the K^+ - and K^- -mesons were particle and anti-particle with $S = +1$ and $S = -1$ and that, likewise, the K^0 -mesons should exist in two states as particle and anti-particle with $S = +1$ and $S = -1$.

We interpret our observations, therefore, as being examples of (K^0, \bar{K}^0) and (K^+, \bar{K}^0) pairs produced in elementary neutron-proton interactions.

There seems to be good evidence that the production of K -meson pairs of this type is an important process at cosmic-ray energies.

* * *

We are grateful for the facilities provided for us at the Jungfraujoch Research Station where the photographs discussed in this paper were taken. In particular, we have received great help from the manager of the Station, Mr. HANS WIEDERKEHR.

Among our colleagues we should like to thank Mr. S. O. LARSON for the construction of apparatus and assistance in running it, Mlle. E. JOVET for making measurements of the photographs and Mr. A. H. CHAPMAN, Mr. G. D. JAMES and Mr. H. STEINER who all helped us with our work at the Jungfraujoch.

In writing this paper we have had the good fortune to be able to discuss it with Dr. B. d'ESPAGNAT and Dr. J. PRENTKI.

APPENDIX A

Event VB 536.

The measurements made on this event are given in Table II. None of the four tracks from the two neutral V-events shows a measurable curvature and the lower limits to the momenta of the four particles are given by the maximum detectable momentum. This is assumed to be proportional to the square of the track length for tracks less than 22 cm long and is equal to 4 GeV/c for tracks of this length or longer.

TABLE II. — Measurements made on event VB 536.

a) Tracks.

Track	Sign	Ionization (I_0)	Length (cm)	Momentum (MeV/c)	Calculated Momentum (MeV/c) (*)
<i>A</i>	±	< 2	8.0	> 530	540 ± 40
<i>B</i>	±	< 2	7.0	> 410	930 ± 50
<i>C</i>	±	< 2	12.5	> 1300	1450 ± 150
<i>D</i>	±	< 2	13.0	> 1400	1160 ± 150
<i>P</i>	+	3 to 6	11.5	330^{+144}_{-77}	—

b) Angles.

Tracks	Angle (°)	Tracks	Angle (°)
$A \cdot B$	33.0 ± 1	$C \cdot D$	18.5 ± 1
$V_{AB} \cdot A$	20.5 ± 2	$V_{CD} \cdot C$	7.0 ± 3
$V_{AB} \cdot B$	12.5 ± 2	$V_{CD} \cdot D$	11.5 ± 3
$V_{AB} \cdot V_{CD}$	5.0 ± 1	Plane (AB) · Plane (CD)	55 ± 2

The ionization densities given in column 3 are visual estimates. The momenta in column 5 are, for tracks *A*, *B*, *C* and *D*, the values of the maximum detectable momentum calculated for tracks of different length as explained in the text.

The angles have been calculated on the supposition that the V-particles come from an interaction in the graphite plate located by track *P* and the planes of the two V-decays.

(*) The momenta in column 6 have been calculated using the angles given in the table and assuming that the two V-decays are 0° -decays.

Neither V⁰-event can be a Λ^0 -decay since the value of $P \sin \varphi$ (where P is the momentum of the negative secondary and φ is the opening angle of the V⁰-decay) are both greater than 120 MeV/c (*). This criterion is completely satisfactory for V_{CD} but for V_{AB} the value of $P_B \sin \varphi$ is > 217 MeV/c if the value of P_B is taken equal to the maximum detectable momentum. If P_B were half the maximum detectable momentum the value of $P_B \sin \varphi$ would be less than 120 MeV/c allowing interpretation of V_{AB} as a Λ^0 -decay.

If we accept the interaction in the carbon plate as the origin of the V-particles there is complete certainty that V_{AB} is not a Λ^0 -decay. From the angle measurements given in Table II the momenta of particles *A* and *B* can be calculated assuming V_{AB} to be a Λ^0 -decay. One finds that either *A* or *B* should be the track of a proton with momentum 260 MeV/c or less. A proton of this momentum has an ionization of $10I_0$ and would easily be recognised.

Using the measurements in Table II lower limits to the $Q(\pi\pi)$ -values for the two V⁰-events can be calculated. The values are 106 MeV for V_{AB} and 236 MeV for V_{CD} if the momenta of the four particles *A*, *B*, *C* and *D* are all taken to be equal to the appropriate maximum detectable momentum. If we

(*) J. P. ASTBURY: *Nuovo Cimento*, **12**, 387 (1954).

make the pessimistic assumption that all the momenta are, in fact, only half the maximum detectable momentum the lower limits to the Q -values become 31 MeV and 77 MeV respectively. It is thus possible that the two V-particles are θ^0 -particles with $Q(\pi\pi) = 215$ MeV but they could also be «anomalous» decays. If we assume that they are θ^0 -particles their momenta and also the momenta of the secondary particles can be calculated from the angles in Table II. The momenta of the V-particles are found to be 1400 MeV/c and 2550 MeV/c; the corresponding momenta of the secondaries are given in column 6 of Table II.

APPENDIX B

Event SN 1534.

The measurements made on this event are given in Table III. The V 0 -decay cannot be a Λ^0 -decay since the positive secondary particle has a mass less than 500 m.. Assuming the negative particle to have a momentum equal to the maximum detectable momentum the $Q(\pi\pi)$ -value for the decay is 276 MeV. If the momentum is half the maximum detectable momentum, the $Q(\pi\pi)$ -value is reduced to 146 MeV. Again, the V-event could well be a θ^0 -decay and, in this case, it could not be a τ^0 -decay ($Q(\pi\pi) \leq 80$ MeV). If the decay is assumed to be a θ^0 -decay the negative particle's momentum is found from P_+ and φ to be 1050 MeV/c and the momentum of the θ^0 -particle is 1090 MeV/c.

TABLE III. — Measurements made on event SN 1534.

Track	Sign	Ionization (I_0)	Length (cm)	Momentum (MeV/c)	Mass (m _e)
<i>A</i>	+	3 to 6	13.0	64 ± 5	220 to 430
<i>B</i>	±	< 2	13.0	> 1400	—
<i>C</i>	+	3 to 6	23.0	220 ± 15	770 to 1400
<i>D</i>	+	4 to 8	10.0	155^{+34}_{-26}	560 to 1400
<i>E</i>	+	< 2	19.0	188 ± 12	< 520

$$\text{Angle } \widehat{AB} = 26^\circ \pm 1^\circ$$

$$\text{Angle } \widehat{V_{AB}C} = 69.5^\circ \pm 2^\circ$$

The measurements of this event have been made as described in the text. The masses of the various particles have been found by combining the estimated ionization densities with the measured momenta. The angle $\widehat{V_{AB}C}$ is found on the assumption that the line of flight of the V 0 -particle intersects track C in the copper plate.

The track *C* cuts the plane of the V 0 -decay in a point which lies inside the copper plate. This point lies very close to the continuation of track *B* — as would be expected if the V-event were a θ^0 -decay and the θ^0 -particle were produced with particle *C* in the copper plate.

From the measurements made on track C it is apparently due to a heavy meson. An isolated track of this sort could not be reliably identified because of the uncertainties attached to visual estimates of ionization. Fortunately, event SN 1534 shows a second heavy meson (track D) which stops and decays in the copper plate giving a single charged secondary (E). The resemblance between tracks C and D is so close that C can be confidently identified as a K^+ -meson.

Analysis of the S-event shows that the particle E was emitted from the decay point of D with a momentum of (204^{+18}_{-15}) MeV/c if E is assumed to be a μ -meson or with (207^{+19}_{-15}) MeV/c if it is assumed to be a π -meson. The decay is probably an example of $K_{\pi 2}$ -decay ($p^* = 205$ MeV/c) but could also be $K_{\mu 2}$ -decay ($p^* = 236$ MeV/c).

RIASSUNTO (*)

Si descrivono e discutono due semplici interazioni nucleari producenti coppie di mesoni K . Si interpretano come esempi dei processi $n+p \rightarrow K^0 + \bar{K}^0 + n + p$ e $n+p \rightarrow K^+ + \bar{K}^0 + n + n$, dove \bar{K}^0 è l'antiparticella del mesone K^0 .

(*) Traduzione a cura della Redazione.

Meson Production by a Meson Nucleon Collision in the Heisenberg Representation.

G. R. SCREATON (*)

Emmanuel College - Cambridge

(ricevuto il 17 Gennaio 1957)

Summary. — A relation between the interaction operator, the Heisenberg operator and the interaction Hamiltonian is established. The matrix element for the production of mesons by a meson nucleon collision is obtained with all its renormalization terms. A causality condition is shown to be involved in this matrix element.

1. — Introduction.

The causality condition has recently been used with considerable success in obtaining dispersion relations for pion nucleon scattering. The method for obtaining these relations is essentially to use the Low equation (¹) for the scattering amplitude in terms of Heisenberg operators and to relate this to an amplitude which is causal. Then from the properties of the causal amplitude, usually as a function of the meson energy in the Breit frame, dispersion relations are obtained (²).

For inelastic scattering it is much more difficult to see what the causal amplitude should be. Part of the difficulty lies in the absence to date of a notation and technique which can readily handle the inelastic case. In this paper we give a notation which enables us to express the inelastic scattering

(*) Grant provided by the Department of Scientific and Industrial Research.

(¹) F. E. Low: *Phys. Rev.*, **97**, 1392 (1955).

(²) M. L. GOLDBERGER: *Phys. Rev.*, **99**, 979 (1955); M. L. GOLDBERGER, H. MIYAZAWA and R. OEHME: *Phys. Rev.*, **99**, 986 (1955); A. SALAM: *Nuovo Cimento*, **3**, 424 (1956); A. SALAM and W. GILBERT: *Nuovo Cimento*, **3**, 607 (1956); R. OEHME: *Phys. Rev.*, **100**, 1503 (1955).

amplitude, with all its renormalization terms, in a concise way and at the same time allows us to give a generalized causal amplitude in a simple form. Finally we give a relativistic form of the condition for the scattering and causal amplitudes to be equal. The causal amplitude obtained here reduces, in a neater form, to that obtained by Polkinghorne⁽⁵⁾ for one incoming and n outgoing mesons, when put in the Breit frame.

2. – Interaction representation.

We define interaction representation operators in terms of Heisenberg operators by a unitary transformation in the usual way. If $A(x)$ is a Heisenberg operator then the interaction operator $A_\tau(x)$ which is equal to $A(x)$ at time τ , is given by

$$(1) \quad A_\tau(x) = S_\tau(t) A(x) S_\tau^\dagger(t) \quad x = (t, \mathbf{x})$$

with $S_\tau(t)$ satisfying

$$(2) \quad i \frac{\partial S_\tau(t)}{\partial t} = S_\tau(t) H(t),$$

$$(3) \quad S_\tau(\tau) = 1.$$

$H(t)$ is the interaction Hamiltonian. It follows from (2) and the boundary condition (3) that

$$(4) \quad S_\tau(t) = S_\tau(\tau) S_\tau(t),$$

$$(5) \quad (*) \quad S_\tau(t) S_\tau^\dagger(t) = S_\tau^\dagger(t) S_\tau(t) = 1.$$

As $S_\tau(t)$ is unitary we can rewrite (2) as

$$(6) \quad i \frac{\partial S_\tau(t)}{\partial t} = H_\tau(t) S_\tau(t)$$

and so

$$(7) \quad S_\tau(t) = 1 - i \int_{\tau}^t H_\tau(t') S_\tau(t') dt'.$$

We are now in a position to show that if Q is any operator

$$(8) \quad S_\tau^\dagger(t) Q S_\tau(t) = Q + i \int_{\tau}^t dt' S_\tau^\dagger(t')[H_\tau(t'), Q] S_\tau(t')$$

(*) The unitarity of $S_\tau(t)$ is true for finite t and τ but we know that in the meson nucleon case $S_\tau(t)$ becomes indeterminate when $t = \pm \infty$ or $\tau = \pm \infty$. To get over this difficulty we will introduce the adiabatic hypothesis.

this we do by substituting for $S_\tau(t)$ and $S_\tau^\dagger(t)$ their integral equation forms ((7) and its Hermitian conjugate). Then

$$(9) \quad S_\tau^\dagger(t) Q S_\tau(t) = Q + i \int_{\tau}^t \{ S_\tau^\dagger(t') H_\tau(t') Q - Q H_\tau(t') S_\tau(t') \} dt' + \\ + \int_{\tau}^t \int dt' dt'' S_\tau^\dagger(t') H_\tau(t') Q H_\tau(t'') S_\tau(t'');$$

if $t \geq \tau$ the last integral is split into integrals over the two regions $\tau < t' < t'' < t$ and $\tau \leq t'' < t' \leq t$. If $\tau \geq t$ we make the split $\tau \geq t' \geq t'' \geq t$ and $\tau \geq t'' \geq t' \geq t$. Integrating w.r.t. t' or t'' for the two regions respectively and using equation (7) and its Hermitian conjugate we obtain (8). If Q is an interaction operator introduced at time τ , the integrand in (8) is independent of τ because

$$(10) \quad S_\tau^\dagger(t')[H_\tau(t'), Q_\tau(x)] S_\tau(t') = H(t') S_\tau^\dagger(t') S_\tau(t) Q(x) S_\tau^\dagger(t) S_\tau(t') - \\ - S_\tau^\dagger(t') S_\tau(t) Q(x) S_\tau^\dagger(t) S_\tau(t') H(t') = [H(t'), Q_\tau(x)]$$

and so we can rewrite (8) as

$$(11) \quad [S_\tau(T), Q_\tau(x)] = -i S_\tau(T) \int_{\tau}^T dt' [H(t') Q_\tau(x)].$$

This equation will be used in a discussion of the meson nucleon problem. There the interaction Hamiltonian in the Heisenberg representation is

$$H(t) = \int \mathcal{H}(x) d^3x,$$

with

$$(12) \quad \mathcal{H}(x) = G \bar{\psi}(x) \tau_i \gamma_5 \psi(x) \varphi_i(x) - \frac{1}{2} \delta \mu^2 \varphi_i^2(x) - \delta M \bar{\psi}(x) \psi(x) - \frac{1}{4} \lambda [\varphi_j^2(x)]^2,$$

this leads to the equations of motion

$$(13) \quad (i \gamma^\mu \partial_\mu - M) \psi(x) = -\delta M \psi(x) + G \tau_i \gamma_5 \psi(x) \varphi_i(x) \equiv -J(x),$$

$$(14) \quad (\square + \mu^2) \varphi_i(x) = -G \bar{\psi}(x) \gamma_5 \tau_i \psi(x) + \delta \mu^2 \varphi_i(x) + \lambda [\varphi_j^2(x)] \varphi_i(x) \equiv -j_i(x).$$

From the commutation relations for the interaction field variables we obtain

$$(15) \quad [\psi_\tau(x), \mathcal{H}_\tau(y)] = i S(x-y) J_\tau(y),$$

$$(16) \quad [\varphi_{i\tau}(x), \mathcal{H}_\tau(y)] = i \Delta(x-y) j_{i\tau}(y).$$

Thus from (11) we have for $\varphi_i(x)$

$$(17) \quad [S_\tau(T), \varphi_{i\tau}(x)] = -S_\tau(T) \int_T^T \Delta(x-x') j_i(x') d^4x' .$$

We notice that when $T=t$ this gives the relation for the interaction operator in terms of Heisenberg operators

$$(18) \quad \varphi_i(x) = \varphi_{i\tau}(x) + \int_T^t \Delta(x-x') j_i(x') d^4x' .$$

Two similar equations hold for $\psi(x)$.

3. – Matrix element.

The matrix element for the scattering of mesons by a nucleon into a nucleon and mesons will be considered. We wish the word scattering to be understood as including inelastic processes in which mesons can be created or annihilated. The scattering matrix element for incoming mesons $q_{n+1}\alpha_{n+1}, q_{n+2}\alpha_{n+2}, \dots, q_m\alpha_m$ (*) and a nucleon Q going into an outgoing nucleon P and mesons $q_1\alpha_1, q_2\alpha_2, \dots, q_n\alpha_n$ is

$$(19) \quad {}_{\text{out}}\langle P; q_1\alpha_1, q_2\alpha_2, \dots, q_n\alpha_n | Q; q_{n+1}\alpha_{n+1}, q_{n+2}, \alpha_{n+2}, \dots, q_m\alpha_m \rangle_{\text{in}} .$$

We will drop the reference to the isotopic spin states of the mesons whenever we can without causing ambiguity. (19) is related to

$$(20) \quad \langle P | \varphi_{\text{out}}^{(+)}(x_n) \varphi_{\text{out}}^{(+)}(x_{n-1}) \dots \varphi_{\text{out}}^{(+)}(x_1) \varphi_{\text{in}}^{(-)}(x_m) \dots \varphi_{\text{in}}^{(-)}(x_{n+2}) \varphi_{\text{in}}^{(-)}(x_{n+1}) | Q \rangle ,$$

the superscript (\pm) refer to the $\pm ve$ frequency parts of the « in » and « out » meson field operators. Following YANG and FELDMAN⁽³⁾ we relate the « in » and « out » fields to one another by the « S » matrix

$$(21) \quad \varphi_{\text{out}}(x) = S^{-1} \varphi_{\text{in}}(x) S .$$

Introducing the adiabatic hypothesis we have $S = S_{-\infty}(\infty)$; having used this

(*) $q\alpha$ denotes a meson with four momentum q and isotopic component α .

⁽³⁾ C. N. YANG and D. FELDMAN: *Phys. Rev.*, **79**, 972 (1950).

we cannot consider initial or final states in which bound states are present (4). Only those matrix elements are considered in which the mesons in the final state have different values for their charge and momentum states from those in the initial state. This does not cause any loss in generality, as we are only interested in this case or the limit of it, as it approaches the excluded case. The restriction is equivalent to taking the commutator of $\varphi_{\tau}^{(+)}(x)$ and $\varphi_{\tau}^{(-)}(y)$ to be zero. Using (21) we can write (20) as

$$(22) \quad PS^{\dagger}\varphi_{in}^{(+)}(x_n)\varphi_{in}^{(+)}(x_{n-1})\dots\varphi_{in}^{(+)}(x_1)S\varphi_{in}^{(-)}(x_m)\dots\varphi_{in}^{(-)}(x_{n+2})\varphi_{in}^{(-)}(x_{n+1})|Q\rangle = \\ = (-)^n\langle P|S^{\dagger}\left[\left[\dots\left[\left[S,\varphi_{in}^{(-)}(x_m)\right],\varphi_{in}^{(-)}(x_{m-1})\right],\dots\right],\varphi_{in}^{(+)}(x_2)\right],\varphi_{in}^{(+)}(x_1)\rangle|Q\rangle,$$

because all the unwanted terms on the right hand side vanish as $\varphi_{in}^{(+)}(x)|Q\rangle$ and $\langle P|\varphi_{in}^{(-)}(x)$ give zero.

We find it convenient to introduce the symbol $(y)^n$ defined by

$$(23) \quad (-i)^n\Delta(y_1-y)\Delta(y_2-y)\dots\Delta(y_n-y)(y)^n = \\ = \left[\left[\dots\left[\left[\mathcal{H}(y),\varphi_y(y_1)\right],\varphi_y(y_2)\right],\dots\right],\varphi_y(y_n)\right],$$

the subscript y means the operators are the interaction operators introduced at time y_0 . It will be noticed that $(y)^n$ is a Heisenberg operator at the space time point y and that

$$(24) \quad [(y)^n,\varphi_y(y_{n+1})] = (-i)\Delta(y_{n+1}-y)(y)^{n+1}.$$

$(y)^n$ is zero for $n > 4$, the non zero values are

$$(25) \quad \begin{cases} (y)_{\alpha_1}^1 & \equiv j_{\alpha_1}(y) \equiv G\psi(y)\gamma_5\tau_{\alpha_1}\psi(y) - \delta\mu^2\varphi_{\alpha_1}(y) - \lambda[\varphi_j^2(y)]\varphi_{\alpha_1}(y) \\ (y)_{\alpha_1\alpha_2}^2 & \equiv -\delta\mu^2\delta_{\alpha_1\alpha_2} - \lambda\varphi_j^2(y)\delta_{\alpha_1\alpha_2} - 2\lambda\varphi_{\alpha_2}(y)\varphi_{\alpha_1}(y) \\ (y)_{\alpha_1\alpha_2\alpha_3}^3 & \equiv -2\lambda\{\delta_{\alpha_1\alpha_2}\varphi_{\alpha_3}(y) + \delta_{\alpha_3\alpha_2}\varphi_{\alpha_1}(y) + \delta_{\alpha_3\alpha_1}\varphi_{\alpha_2}(y)\} \\ (y)_{\alpha_1\alpha_2\alpha_3\alpha_4}^4 & \equiv -2\lambda\{\delta_{\alpha_1\alpha_2}\delta_{\alpha_3\alpha_4} + \delta_{\alpha_2\alpha_3}\delta_{\alpha_1\alpha_4} + \delta_{\alpha_3\alpha_1}\delta_{\alpha_2\alpha_4}\}. \end{cases}$$

It can now be proved by induction (see the Appendix) that

$$(26) \quad \left[\left[\dots\left[\left[S,\varphi_{in}(y_1)\right],\varphi_{in}(y_2)\right],\dots\right],\varphi_{in}(y_n)\right] = \\ = (-)^n S \int \int \dots \int dy'_1 dy'_2 \dots dy'_n \Delta(y_1 - y'_1) \Delta(y_2 - y'_2) \dots \Delta(y_n - y'_n) C \mathcal{D}\{(y'_1)^1 (y'_2)^1 \dots (y'_n)^1\},$$

(4) S. S. SCHWEBER, H. A. BETHE and F. DE HOFFMAN: *Mesons and Fields*, Vol. 1. Sect. 16b.

the integrals are to be taken over all space time, \mathcal{D} is Dyson's chronological operator and C stands for the sum over all contractions. When we contract $(y'_r)^1, (y'_{r+1})^1, \dots, (y'_{r+s})^1$ we insert $(i)^s \delta(y'_r - y'_{r+1}) \delta(y'_{r+1} - y'_{r+2}) \dots \delta(y'_{r+s-1} - y'_{r+s})$ in the integrand and replace $(y'_r)^1 (y'_{r+1})^1 \dots (y'_{r+s})^1$ by $(y'_r)^{s+1}$.

Thus

$$(27) \quad \langle P | \varphi_{\text{out}}^{(+)}(x_n) \dots \varphi_{\text{out}}^{(+)}(x_1) \varphi_{\text{in}}^{(-)}(x_m) \dots \varphi_{\text{in}}^{(-)}(x_{n+1}) | Q \rangle = \\ = (-)^{m+n} \langle P | \int \int \dots \int dx'_1 dx'_2 \dots dx'_m \Delta^{(+)}(x_1 - x'_1) \dots \Delta^{(+)}(x_n - x'_n) \cdot \\ \cdot \Delta^{(-)}(x_{n+1} - x'_{n+1}) \dots \Delta^{(-)}(x_m - x'_m) C \mathcal{D}\{(x'_1)^1 (x'_2)^1 \dots (x'_m)^1\} | Q \rangle$$

and as $a_\tau(q)$, the interaction annihilation operator for mesons of type q , is given by

$$a_\tau(q) = \sqrt{\frac{(2q_0)}{(2\pi)^3}} \int \varphi_\tau^{(+)}(x) \exp[iqx] d^3x,$$

we have for the matrix element (19), after doing the space integrations,

$$(28) \quad (-i)^m \{ (2\pi)^{3m} (2q_{10})(2q_{20}) \dots (2q_{m0}) \}^{-\frac{1}{2}} \int \int \dots \int dx_1 dx_2 \dots dx_m \exp[iq_1 x_1] \dots \\ \dots \exp[iq_n x_n] \exp[-iq_{n+1} x_{n+1}] \dots \exp[-iq_m x_m] \langle P | C \mathcal{D}\{(x_1)^1 (x_2)^1 \dots (x_m)^1\} | Q \rangle .$$

As an example we give

$$(29) \quad {}_{\text{out}} \langle P; q_1, q_2 | Q; p \rangle_{\text{in}} = (-i)^3 \{ (2\pi)^9 (2q_{10})(2q_{20})(2p_0) \}^{-\frac{1}{2}}$$

$$(29.1) \quad \langle P | \left\{ \int \int \int dx_1 dx_2 dx_3 \exp[iq_1 x_1] \exp[iq_2 x_2] \exp[-ipy] \mathcal{D}\{(x_1)^1 (x_2)^1 (y)^1\} \right.$$

$$(29.2) \quad \left. + i \int \int dx_1 dy \exp[i(q_1 + q_2)x_1] \exp[-ipy] \mathcal{D}\{(x_1)^2 (y)^1\} \right.$$

$$(29.3) \quad \left. + i \int \int dx_1 dy \exp[iq_1 x_1] \exp[-i(p - q_2)y] \mathcal{D}\{(x_1)^1 (y)^2\} \right.$$

$$(29.4) \quad \left. + i \int \int dx_2 dy \exp[iq_2 x_2] \exp[-i(p - q_1)y] \mathcal{D}\{(x_2)^1 (y)^2\} \right.$$

$$(29.5) \quad \left. - \int dy \exp[-i(p - q_1 - q_2)y] (y)^3 \right\} | Q \rangle .$$

The terms arise as follows: (29.1) no contractions; (29.2) $(x_1)^1$ and $(x_2)^1$ contracted; (29.3) $(x_2)^1$ and $(y)^1$ contracted; (29.4) $(x_1)^1$ and $(y)^1$ contracted; (29.5) $(x_1)^1$, $(x_2)^1$ and $(y)^1$ contracted.

4. – Causality.

The matrix element is now further specialised to the physically most interesting case; one incoming meson p and n outgoing mesons q_1, q_2, \dots, q_n . The corresponding matrix element in terms of Heisenberg operators is

$$(30) \quad \{(2p_0)(2q_{10})(2q_{20}) \dots (2q_{n0})(2\pi)^{3(n+1)}\}^{-\frac{1}{2}}(-i)^{n+1} \int \int \dots \int dx_1 dx_2 \dots dx_n dy \cdot \\ \cdot \exp[iq_1x_1] \exp[iq_2x_2] \dots \exp[iq_nx_n] \exp[-ipy] \langle P | C \mathcal{D}\{(x_1)^1(x_2)^1 \dots (x_n)^1(y)^1\} | Q \rangle.$$

In the Heisenberg representation

$$(31) \quad A(x) = \exp[iMx]A(0)\exp[-iMx],$$

M is the energy momentum four vector operator. Using this and at the same time making the transformation $x \rightarrow x - y$ in (30) we extract the δ -function corresponding to overall energy momentum conservation, i.e. we have

$$(32) \quad (2\pi)^4 \delta^4(P + q_1 + q_2 + \dots + q_n - Q - p) \cdot \\ \cdot \{(2p_0)(2q_{10})(2q_{20}) \dots (2q_{n0})(2\pi)^{3(n+1)}\}(-i)^{n+1} \int \int \dots \int dx_1 dx_2 \dots dx_n \cdot \\ \cdot \exp[iq_1x_1] \exp[iq_2x_2] \dots \exp[iq_nx_n] \langle P | C \mathcal{D}\{(x_1)^1(x_2)^1 \dots (x_n)^1(0)^1\} | Q \rangle.$$

For the moment we omit all the contraction terms and use Ω to denote all the factors occurring in front of the integral. We pick out from (32) the term with $\theta(x_1 > x_2 > \dots > x_r > 0 > x_{r+1} > x_{r+2} > \dots > x_n)$ viz.

$$(33) \quad \Omega \int \int \dots \int dx_1 dx_2 \dots dx_n \exp[iq_1x_1] \exp[iq_2x_2] \dots \exp[iq_nx_n] \theta(x_1 > x_2 > \dots > x_r > 0 > x_{r+1} > \dots > x_n) \langle P | (x_1)^1(x_2)^1 \dots (x_r)^1(0)^1(x_{r+1})^1(x_{r+2})^1 \dots (x_n)^1 | Q \rangle,$$

where $\theta(x > y > z \dots > a > b)$ means $\theta(x - y)\theta(y - z) \dots \theta(a - b)$. We now show that $\theta(x_1 > x_2 > \dots > x_r > 0 > x_{r+1} > \dots > x_n)$ can be replaced by $(-)^{n-r}\theta(x_1 > x_2 > \dots > x_r > 0)\theta(x_n > x_{n-1} > \dots > x_{r+1} > 0)$. Because

$$(34) \quad \theta(x) = \frac{1}{2\pi i} \int_{-\infty}^{\infty} \frac{\exp[ikx_0]}{k - i\varepsilon} dk, \quad \theta(-x) = -\frac{1}{2\pi i} \int_{-\infty}^{\infty} \frac{\exp[ikx_0]}{k + i\varepsilon} dk \quad \varepsilon > 0$$

and so replacing ε by $-\varepsilon$ is equivalent to changing $\theta(x)$ to $-\theta(-x)$. Introducing a set of intermediate states $|\gamma^1\rangle, |\gamma^2\rangle, \dots, |\gamma^n\rangle$, which are eigen states

of energy and momentum for the complete Hamiltonian, we have for (33)

$$(35) \quad \sum_{\gamma} \mathcal{Q} \iint \dots \int dx_1 dx_2 \dots dx_n \exp[iq_1 x_1] \exp[iq_2 x_2] \dots \exp[iq_n x_n] \cdot \\ \cdot \langle P | \exp[iMx_1](0)^1 \exp[-iMx_1] | \gamma^1 \rangle \langle \gamma^1 | \dots | \gamma^n \rangle \langle \gamma^n | \exp[iMx_n](0)^1 \cdot \\ \cdot \exp[-iMx_n] | Q \rangle \left(\frac{1}{2\pi i} \right)^n \frac{\exp[ik_1(x_1 - x_2)_0]}{k_1 - i\varepsilon_1} \dots \frac{\exp[ik_n(x_{n-1} - x_n)_0]}{k_n - i\varepsilon_n} dk_1 dk_2 \dots dk_n.$$

Doing the space time integrations for x_1, x_2, \dots, x_n we obtain a product of δ -functions which are equivalent to requiring that

$$(36) \quad k_i = (\gamma^i + \alpha^i - Q)_0, \quad \Upsilon^i = \mathbf{Q} - \boldsymbol{\alpha}^i$$

where

$$\alpha^i = q_n + q_{n-1} + \dots + q_i \quad i > r$$

and

$$(37) \quad k_i = (\gamma^i + \beta^i - P)_0, \quad \Upsilon^i = \mathbf{P} - \boldsymbol{\beta}^i$$

where

$$\beta^i = -(q_1 + q_2 + \dots + q_i) \quad i \leq r.$$

Using overall energy momentum conservation we can rewrite (37) in the form of (36) with

$$\alpha^i = q_n + q_{n-1} + \dots + q_r - p + q_{r-1} + \dots + q_{i-1} \quad i \leq r.$$

The states $|\gamma\rangle$ which are going to contribute will contain at least a nucleon and so taking into account the momentum equations for the intermediate states, we have

$$(38) \quad (\gamma_0 + \alpha_0)^2 - Q_0^2 = \gamma_0^2 + 2\gamma_0\alpha_0 + \alpha_0^2 - (M^2 + \Upsilon^2) - 2\Upsilon \cdot \alpha - \alpha^2 \geq 2\gamma \cdot \alpha + \alpha^2.$$

For $i > r$, γ and α are timelike vectors with positive 0-th component and so $2\gamma \cdot \alpha + \alpha^2 > 0$. Thus $k_i > 0$ for $i > r$, and because k_i is the real part of the denominator in the integrand (35), we can change ε_i to $-\varepsilon_i$ without altering the value of the integral. This shows that $\theta(x_1 > x_2 > \dots > x_r > 0 > x_{r+1} > x_{r+2} > \dots > x_n)$ can be replaced by $(-)^{n-r} \theta(x_1 > x_2 > \dots > x_r > 0) \theta(x_n > x_{n-1} > \dots > x_{r+1} > 0)$.

Now we can replace the \mathcal{Q} product in the integral (32) by what we call a θ product i.e. instead of $\mathcal{Q}\{(x_1)^1(x_2)^1 \dots (x_n)^1(0)^1\}$ we can write $\theta[(x_1)^1(x_2)^1 \dots (x_n)^1:(0)^1]$. The θ product is a sum of multiple commutators in which the x 's

are put in a time ordered sense but with 0 always occurring earliest. Explicitly

$$(39) \quad \theta[(x_1)^1(x_2)^1 \dots (x_n)^1:(0)^1] = \\ = \sum \theta(x_1 > x_2 > \dots > x_n > 0) [(x_1)^1, [(x_2)^1, [\dots, [(x_{n-1})^1, [(x_n)^1, (0)^1]] \dots]]],$$

where the sum is over all permutations of x_1, x_2, \dots, x_n . To see this we notice that the coefficient of $(x_1)^1(x_2)^1 \dots (x_r)^1(0)^1(x_n)^1(x_{n-1})^1 \dots (x_{r+1})^1$ in

$$\theta(x_{i_1}) > x_{i_2} > \dots > x_{i_n} > 0) [(x_{i_1})^1, [(x_{i_2})^1, [\dots, [(x_{i_{n-1}})^1, [(x_{i_n})^1, (0)^1]] \dots]]],$$

where i_1, i_2, \dots, i_n is a permutation of $1, 2, \dots, n$, is

$$(40) \quad (-)^{n-r} \theta(x_{i_1} > x_{i_2} > \dots > x_{i_n} > 0) \theta(x_1 > x_2 > \dots > x_r) \theta(x_{r+1} > x_{r+2} > \dots > x_n),$$

for either the second two θ functions are, (a) consistent with the first and are consequently equivalent to unity, or (b) not consistent with the first and so equivalent to zero. In case (a) the term we are considering can occur with coefficient $(-)^{n-r} \theta(x_{i_1} > x_{i_2} > \dots > x_{i_n} > 0)$ but in case (b) the term cannot occur. Hence the coefficient of this term in $\theta[(x_1)^1(x_2)^1 \dots (x_n)^1:(0)^1]$ is

$$(41) \quad (-)^{n-r} \theta(x_i > x_2 > \dots > x_r) \theta(x_{r+1} > x_{r+2} > \dots > x_n) \cdot \\ \cdot \sum_i \theta(x_{i_1} > x_{i_2} > \dots > x_{i_n} > 0),$$

where the sum is over all i corresponding to permutations of $1, 2, \dots, n$. But

$$(42) \quad \sum_i \theta(x_{i_1} > x_{i_2} > \dots > x_{i_n} > 0) = \theta(x_1 > 0) \theta(x_2 > 0) \dots \theta(x_n > 0)$$

and so the coefficient in the θ product is

$$(43) \quad (-)^{n-r} \theta(x_1 > x_2 > \dots > x_r > 0) \theta(x_{r+1} > x_{r+2} > \dots > x_n > 0)$$

but we have already shown that the coefficient $\theta(x_1 > x_2 > \dots > x_r > 0 > > x_n > \dots > x_{r+1})$ of this term arising from the \mathcal{D} product in (32), can be replaced by (43). Hence we can replace the \mathcal{D} product by the θ product in (32).

We have not used the fact that the $(x)^1$'s are identical operators and so the above argument will go through unchanged for the contraction terms. However care must be taken to be sure that when a contraction is made with $(0)^1$ the associated contraction term is written to the right of the colon. The

matrix element in our new notation can be written

$$(44) \quad \Omega \int \int \dots \int dx_1 dx_2 \dots dx_n \exp [iq_1 x_1] \exp [iq_2 x_2] \dots \exp [iq_n x_n] \cdot \\ \cdot \langle P | C\theta[(x_1)^1 (x_2)^1 \dots (x_n)^1 : (0)^1] | Q \rangle .$$

We now establish a property of the θ product, the proof of which depends on a simple property of the commutator, namely

$$(45) \quad [(z_n), [(z_{n-1}), [\dots, [(z_2), (z_1)]] \dots]] + [(z_{n-1}), [(z_{n-2}), [\dots, [(z_1), (z_n)]] \dots]] + \\ + \dots + [(z_1), [(z_n), [\dots, [(z_3), (z_2)]] \dots]] = 0 .$$

When z_n is separated spacially from z_1, z_2, \dots, z_{n-1}

$$(46) \quad [(z_n), [(z_{n-1}), [\dots, [(z_2), (z_1)]] \dots]] = 0 ,$$

for we can use (45) to give a proof by induction as the result is certainly true for the case $n = 2$ by the causality condition. We use this to show that we do not get a contribution to the θ product in (44) unless all the points of x_1, x_2, \dots, x_n which are left after the contractions are made, lie in the future light cone of 0. We select for consideration a particular term of the θ product with time ordering given by $\theta(x_1 > x_2 > \dots > x_N > 0)$ where x_1, x_2, \dots, x_N are the space time points occuring in this term. Suppose that $x_i^2 > 0$ for $i = r+1, r+2, \dots, N$ but that $x_r^2 < 0$, then $(x_r - x_i)^2 < 0$ for

$$(47) \quad (x_r - x_i)_0^2 - (x_r - x_i)^2 < (|x_r| - |x_i|)^2 - (x_r - x_i)^2 \leq 0$$

and so using (46) the term will be zero. Therefore we obtain the interesting result that after the δ -functions due to the contractions have been eliminated in (44) the integrations for the remaining x 's need only be carried out over the future light cone of 0. This gives us a generalised causality condition in our definition of matrix elements.

5. – Discussion.

The expression (44) provides us with a relativistic covariant causal amplitude, which we have shown to be equal to the scattering amplitude for all physically possible initial and final states involved in the production of mesons by a meson nucleon collision. We can use it to obtain dispersion relations for

this process. In fact if with POLKINGHORNE⁽⁵⁾ we write

$$(48) \quad \begin{cases} p_0 = -\omega v_{n+1} & v_{n+1} < 0 \\ q_{i0} = \omega v_i & v_i > 0, \quad i = 1, 2, \dots, n \\ \mathbf{P} + \mathbf{Q} = 0 & P_0 = Q_0 = \sqrt{M^2 + P^2} \\ v_1 + v_2 + \dots + v_n + v_{n+1} = 0, \end{cases}$$

where v 's are fixed but ω is allowed to vary, we find a dispersion relation of the form

$$(49) \quad M(\omega) = \frac{i}{\pi} P \int_{-\infty}^{\infty} \frac{M(\omega') d\omega'}{\omega - \omega'}$$

where

$$(50) \quad M(\omega) = \iint \dots \int \exp [iq_1 x_1] \exp [iq_2 x_2] \dots \exp [iq_n x_n] dx_1 dx_2 \dots dx_n \cdot \\ \cdot (-i)^{n+1} \langle P | C\theta[(x_1)^1 (x_2)^1 \dots (x_n)^1 : (0)^1] | Q \rangle + i \langle P | (0)^{n+1} | Q \rangle .$$

The first term is related to the scattering amplitude while the second is a constant due to renormalization.

The situation in which there are more than one incoming and more than one outgoing mesons is more complicated. We saw it was impossible to change $\theta(x)$ to $-\theta(-x)$ when there existed a real intermediate state $|\gamma\rangle$ with

$$\gamma = Q - \alpha .$$

We have only had to consider the case where α was the sum of a series of meson four momenta and was consequently time like with positive 0-th component. The proof that a real intermediate state did not exist was then easy. However in the more general case we are interested not only in sums of meson four momenta but also in their differences, if we wish to obtain dispersion relations by the method due to Polkinghorne. Unfortunately it does not follow in the general case that if α_0 is greater than zero a real intermediate state does not exist, as POLKINGHORNE would seem to assert in his paper.

A causal amplitude similar to (44) will exist for the case of n incoming mesons going into one outgoing meson.

* * *

The author wishes to thank Dr. J. HAMILTON and Dr. A. SALAM for the continued interest they have shown in this work.

⁽⁵⁾ J. C. POLKINGHORNE: *Nuovo Cimento*, **4**, 216 (1956).

APPENDIX

Here we prove equation (26) by induction. From (11) and (24) we have

$$(A.1) \quad [(y)^e, \varphi_{in}(x)] = [S_y^\dagger(-\infty)[S_y(-\infty), \varphi_y(x)], (y)^e] + [(y)^e, \varphi_y(x)] = \\ = \left[\int_{-\infty}^{y_0} dx' \Delta(x - x')(x')^1, (y)^e \right] + (-i) \Delta(x - y)(y)^{e+1},$$

where the integration is over all space but only over the time range $-\infty$ to y_0 . We have then to consider the expression

$$(A.2) \quad \left[(-)^n S \iint \dots \int dy'_1 dy'_2 \dots dy'_n \Delta(y_1 - y'_1) \cdot \right. \\ \left. \cdot \Delta(y_2 - y'_2) \dots \Delta(y_n - y'_n) C \mathcal{D}\{(y'_1)^1 (y'_2)^1 \dots (y'_n)^1\}, \varphi_{in}(y_{n+1}) \right],$$

to simplify the argument we take only one time ordering in the integrand, together with all the contraction terms that are consistent with it. For convenience take the term corresponding to the time ordering $\theta(y'_1 > y'_2 > \dots > y'_n)$, for consistent contractions only consecutive (y') 's in this ordering can be contracted. Thus the term in the integrand that we are considering is

$$\Delta(y_1 - y'_1) \Delta(y_2 - y'_2) \dots \Delta(y_n - y'_n) \theta(y'_1 > y'_2 > \dots > y'_n) \sum_e (y'_1)^{e_1} (y'_2)^{e_2} \dots (y'_n)^{e_n} \delta^e,$$

where

$$\delta^e = \prod_i \delta^{e_i}$$

$$\delta^{e_i} = (i)^{e_{i-1}} \delta^4(y'_i - y'_{i+1}) \delta^4(y'_i - y'_{i+2}) \dots \delta^4(y'_i - y'_{i+e_i-1})$$

and the contractions have been labelled by the (y') with the lowest suffix. The sum is over all e corresponding to the various contractions, this implies

$$e_1 + e_2 + \dots + e_n = n$$

$$e_i < n + 1 - i$$

and that if $e_i > 1$ the next e_{i-1} , e 's must be zero. Whenever an e_i is zero $(y'_i)^{e_i}$ together with the δ^{e_i} associated with it has to be omitted. Using equa-

tions (11) and (A.1), (A.2) for this time ordering becomes

$$\begin{aligned}
 & (-)^{n+1} S \int_{-\infty}^{\infty} dy'_1 \int_{-\infty}^{y'_1} dy'_2 \int_{-\infty}^{y'_2} dy'_3 \dots \int_{-\infty}^{y'_{n-1}} dy'_n \Delta(y_1 - y'_1) \Delta(y_2 - y'_2) \dots \Delta(y_n - y'_n) \cdot \\
 & \cdot \sum_e \delta^e \left[\int_{-\infty}^{\infty} dy'_{n+1} \Delta(y_{n+1} - y'_{n+1}) (y'_{n+1})^1 (y'_1)^{e_1} (y'_2)^{e_2} \dots (y'_n)^{e_n} + \right. \\
 & + \left\{ - \int_{-\infty}^{y'_1} dy'_{n+1} \Delta(y_{n+1} - y'_{n+1}) [(y'_{n+1})^1, (y'_1)^{e_1}] + i \Delta(y_{n+1} - y'_1) (y'_1)^{e_1+1} \right\} (y'_2)^{e_2} \dots (y'_n)^{e_n} - \\
 & + (y'_1)^{e_1} \left\{ - \int_{-\infty}^{y'_2} dy'_{n+1} \Delta(y_{n+1} - y'_{n+1}) [(y'_{n+1})^1, (y'_2)^{e_2}] + i \Delta(y_{n+1} - y'_2) (y'_2)^{e_2+1} \right\} \\
 & \cdot (y'_3)^{e_3} \dots (y'_n)^{e_n} + \dots + (y'_1)^{e_1} (y'_2)^{e_2} \dots (y'_{n-1})^{e_{n-1}} \cdot \\
 & \cdot \left. \left\{ - \int_{-\infty}^{y'_n} dy'_{n+1} \Delta(y_{n+1} - y'_{n+1}) [(y'_{n+1})^1, (y'_n)^{e_n}] + i \Delta(y_{n+1} - y'_n) (y'_n)^{e_n+1} \right\} \right],
 \end{aligned}$$

the first term in each of the {} gives rise to the term in which (y'_{n+1}) is not contracted and the second those terms in which it is contracted with the various (y') 's. When we add the terms together we get the appropriate term in the expansion of

$$\begin{aligned}
 & (-)^{n+1} S \iint \dots \int dy'_1 dy'_2 \dots dy'_{n+1} \Delta(y_1 - y'_1) \Delta(y_2 - y'_2) \dots \\
 & \dots \Delta(y_{n+1} - y'_{n+1}) C \mathcal{D} \{ (y'_1)^1 (y'_2)^1 \dots (y'_{n+1})^1 \}.
 \end{aligned}$$

Now (17) shows that the equation (26) holds when $n = 1$ and so by induction the equation holds for all n .

RIASSUNTO (*)

Si mette in evidenza una relazione tra l'operatore d'interazione, l'operatore di Heisenberg e l'hamiltoniana d'interazione. Si ottiene l'elemento di matrice per la produzione di mesoni da parte di una collisione mesone-nucleone con tutti i suoi termini di rinormalizzazione. Questo elemento di matrice sembra implicare una condizione di causalità.

(*) Traduzione a cura della Redazione.

Review of the Experimental Evidence for the Law of Variation of the Electron Mass with Velocity.

P. S. FARAGÓ and L. JÁNOSSY

Central Research Institute for Physics - Budapest

(ricevuto il 18 Gennaio 1957)

Summary. — The paper reviews the actual experiments in which the dependence of electron mass on velocity is investigated. It is found that the most precise verification of the relativistic formula follows from the fine structure doublet separation of hydrogen-like spectra. Regarding the direct experiments on the behaviour of free electrons, the results do not contradict the relativistic formula, although the experimental error of the available measurements is rather high; i.e. it is in most cases comparable with the difference between theoretical formulae derived from different assumptions. Recent measurements on the velocity dependence of the mass of protons are also reviewed.

1. — Introduction.

One of the most important consequences of the special theory of relativity is the relation expressing the dependence of mass on velocity:

$$(1) \quad m = \frac{m_0}{\sqrt{1 - (v/c)^2}}.$$

For velocities v not too near the velocity c of light, (1) can be expanded in a power series:

$$(2) \quad m = m_0 \left(1 + \gamma_1 \left(\frac{v}{c} \right)^2 + \gamma_2 \left(\frac{v}{c} \right)^4 + \dots \right),$$

with $\gamma_1 = \frac{1}{2}$, $\gamma_2 = \frac{3}{8}$, etc.

As is well known this formula for the electron was derived already by Lorentz on the assumption that the mass of the electron is of electromagnetic origin, and that when moving with high velocity it suffers a contraction in the direction of the velocity. By assuming the electron to be a perfectly rigid sphere, another law is obtained, namely that due to ABRAHAM:

$$(3) \quad m = m_0 \frac{3}{4(v/c)^2} \left[\frac{1 + (v/c)^2}{2(v/c)} \log \frac{1 + (v/c)}{1 - (v/c)} - 1 \right],$$

which again is given approximately by the power series (2) with

$$\gamma_1 = \frac{2}{5}, \quad \gamma_2 = \frac{9}{35}, \quad \text{etc. .}$$

Other formulae could be obtained by postulating for the electron types of structures different from those postulated by Abraham or Lorentz.

It is generally asserted that the validity of equ. (1) is completely confirmed by a number of experiments (see e.g. MØLLER⁽¹⁾, footnote § 32, p. 89). Furthermore, it is often claimed that the successful operation of high-energy particle accelerators gives an indirect confirmation of the validity of (1).

Analysing the available experimental material, the authors of this article have come to the conclusion that the experiments carried out so far support the validity of (1) far less than is usually supposed to be the case. As a matter of fact it is only a study of the fine structure of hydrogen-like spectra which confirms equ. (1) with high precision. Regarding the direct experiments on the behaviour of free electrons, although there is no experimental evidence which would contradict equation (1), the experimental results we were able to analyse seem in most cases to be compatible not only with (1) but also with (3). In fact we were at a loss to find results in this field which would prove the validity of (1) with a margin of error much smaller than, say the difference between expressions (1) and (3). We are, however, indebted to Prof. W. PAULI for drawing our attention to a little-known paper by ROGERS, McREYNOLD and ROGERS which seems to be the only one giving results with an accuracy sufficient to distinguish clearly between formulae (1) and (3). Even so we have to conclude that it would be highly desirable to carry out further direct experiments proving the validity of (1) quantitatively and with still greater precision than obtained up to now. Should new experiments on the subject be forthcoming, the publication of a detailed treatment of the experimental results would be welcomed, similar to e.g. the classical papers of KAUFMANN. This seems the more indicated as equ. (1) is one of the most fundamental

⁽¹⁾ C. MØLLER: *The Theory of Relativity* (Oxford, 1952).

relations of modern physics and—after all—should an experiment lead even to the slightest discrepancy between the theoretical formula and the actual behaviour of a particle, such a discrepancy would present a serious problem for the theory.

Analysing the results of direct experiments the following facts can be regarded as established beyond doubt:

- 1) mass does change with velocity;
- 2) the velocity of light is an upper limit;
- 3) quantitative results do not contradict equ. (1).

In fact the first two of the above statements must be expected from any kind of theoretical assumption, and they follow from equ. (1) just as from equ. (3). So as to obtain a quantitative proof of the validity of equ. (1) it is necessary to carry out precise measurements on particles with velocities v well in between zero and c . To show the deviation of Abraham's formula (3) from Lorentz' formula (1) we have plotted both in Fig. 1. In the $(m_0/m)^2$ is plotted against $(v/c)^2$.

In Sect. 2 we shall give an account of the results of fine-structure measurements in relation to the problem of mass variation of electrons. In Sect. 3 we shall briefly review those experiments whose results were already critically discussed in the literature, as well as those which cannot be analysed because of the lack of detailed experimental data. In Sect. 4 the results of the experiments of GUYE, RATNOWSKY and LAVANCHY (2)—usually considered to be the most exact experiments existing—will be analysed. The result of the latter analysis will be found to show that the experimental errors are comparable with the difference existing between the theoretical formulae derived from different assumptions. Finally, in Sect. 5 and 6 further indirect experimental evidence will be considered.

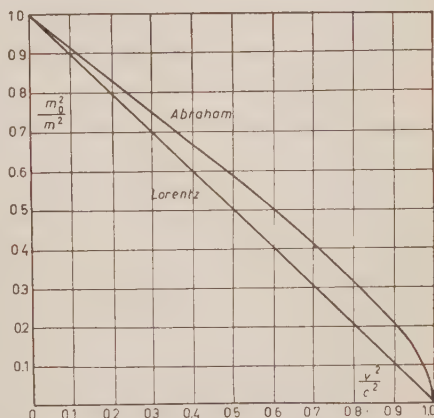


Fig. 1. Deviation between Abraham's and Lorentz' laws over the full range of variation of v/c .

(2) C. E. GUYE, S. RATNOWSKY and C. LAVANCHY: *Mém. Soc. Phys. Genève*, **39**, fasc. 6, 273 (1921).

2. — Fine structure separation and the change of mass with velocity.

The technical difficulty of measuring the exact form of the law governing the change of mass of the electron with velocity led the SOMMERFELD school to look for indirect methods of approach. For this purpose use was made of the close relation existing between the fine-structure splitting of spectral lines and the variation of mass of the electron in the course of its motion in an atomic orbit; in particular, for the hydrogen atom and also for hydrogen-like atoms quantitative predictions could be made as to the expected magnitude of the fine-structure splitting for any given law of mass variation.

As is well known, the original non-relativistic theory of Bohr does not give the fine-structure splitting of atomic spectral lines. It was shown by SOMMERFELD that the fine-structure separation can be accounted for if the momentum and the energy of the electron are considered in their relativistic form; thus splitting is connected with the relativistic change of mass with velocity. If, however, the variation of the mass of the electron is considered according to some other theory, e.g. according to the theory of Abraham instead of the theory of relativity, a different splitting up has to be expected. Thus the experimental determination of the fine structure provides evidence as to the form of the law of variation of the electron mass with velocity. If the two theories lead to different values for the fine-structure splitting, the choice between the two competing theories could be made experimentally.

A detailed study of the problem was carried out by GLITSCHER in 1917 (3). He used the power series expansion of the expression for the kinetic energy and the momentum as first approximation, considering only terms up to the order of $(v/c)^4$. In this case the corresponding expressions obtained from the theory of relativity and the Abraham theory, respectively differ only in the coefficients of the terms retained. The calculations were carried out along the lines of the old Bohr theory and an expression for the fine-structure splitting in terms of the coefficients of expansion (2) was obtained. If the mass of the nucleus is assumed to be infinite, the expected fine structure separation is thus found

$$(4) \quad \Delta\nu = 2\gamma_1 \left(\frac{Z}{2}\right)^2 R_\infty \alpha^2,$$

where γ is the coefficient of (v^2/c^2) in (2), i.e. $\gamma_1 = \frac{1}{2}$ for the relativistic case and $\gamma_1 = \frac{2}{3}$ for the Abraham case, R_∞ is the Rydberg constant without correction for the motion of the nucleus and $\alpha = e^2/\hbar c$ Sommerfeld's fine-structure constant.

(3) K. GLITSCHER: *Ann. d. Phys.*, **52**, 608 (1917).

To decide between the two theories Glitscher proceeded as follows. Using the fine-structure splitting $\Delta\nu$ of He^+ as measured by PASCHEN and the values of the constants e , c , \hbar and R_∞ , he compared the value of α in terms of e , c and \hbar with those obtained from (4) putting once $\gamma_1 = \frac{1}{2}$ and then $\gamma_1 = \frac{2}{3}$.

Agreement could only be obtained for $\gamma_1 = \frac{1}{2}$.

Our knowledge as to the precise values of the universal constants has greatly increased since the publication of the above investigations, it seems thus reasonable to repeat the above analysis using more recent values for the constants involved.

In doing so we must of course be careful not to be involved in a vicious circle, i.e. we must use values of e and \hbar obtained by experiments other than the fine-structure measurements.

Great efforts have been made to determine the «best» adjusted values of the fundamental constants, that is to form a consistent set of the values themselves and their standard errors, least violating experimental results from any known source of information. The latest achievements in this field are due to DUMOND and COHEN (4). Selecting—to some extent arbitrarily—a set of «primary» unknowns, their best adjusted values were determined with the aid of the method of least squares, other atomic constants being evaluated by combining the primary ones with certain auxiliary constants.

The success of such a procedure greatly depends first on the choice of quantities to be taken as auxiliary constants, i.e. constants known with sufficient accuracy relative to the rest and treated as known quantities and secondly on the choice of as many independent equations as there are *reliable* determinations of the unknowns. Evidently both conditions are satisfied the better, the more exact the experimental data made use of. It should be emphasized, however, that in the majority of experiments one does not measure *one* of the primary unknowns but rather some function of several of them. The primary unknowns and the experimental data actually chosen by DUMOND and COHEN made necessary the use of some relativistic relations in setting up the system of equations to be solved for the «best» compromise values of the unknowns. In fact they use both the relativistic expression for the fine-structure splitting of hydrogen-like spectra and the relation $\alpha = e^2/c\hbar$ in setting up their equations. Thus, as already mentioned, it would be a logical fallacy to use their results for the proof of the validity of the relativistic change of mass with velocity.

For the above reasons we used data which were obtained more directly from experiments. Such values of c , e , \hbar/e , R_p and $\Delta\nu_p$ are given in Table I. The authors referred to in the last column of the Table derived the values

(4) J. W. M. DUMOND and E. R. COHEN: *Rev. Mod. Phys.*, **25**, 691 (1953).

given by careful analysis of experiments of one type for each constant. (It should be mentioned that the values given in Table I are compatible with those derived by DuMond and Cohen within the error limits stated.)

TABLE I.

Symbol	Value	Experimental source	Ref.
c	$(299\,792.6 \pm 0.7) \cdot 10^5 \text{ cm s}^{-1}$	Free space microwave interferometry	(a)
e	$(4.8029 \pm 0.0004) \cdot 10^{-10} \text{ e.s.u.}$	Ruled grating	(b)
\hbar/e	$(1.37938 \pm 0.00008) \cdot 10^{-17} \text{ cgs}$	Excitation energy limit in continuous X-ray spectrum	(c)
R_D	$109\,707.419 \pm 0.012 \text{ cm}^{-1}$	Spectroscopy	(d)
$\Delta\nu_D$	$0.365969 \pm 0.000008 \text{ cm}^{-1}$	Atomic beam magnetic resonance	(e)
(a) K. D. FROOME: <i>Proc. Roy. Soc., A</i> 213 , 123 (1952).			
(b) F. G. DUNNINGTON: <i>Rev. Mod. Phys.</i> , 11 , 68 (1939).			
(c) J. A. BEARDEN and G. SCHWARZ: <i>Phys. Rev.</i> , 79 , 674 (1950).			
(d) E. R. COHEN: <i>Phys. Rev.</i> , 88 , 353 (1952).			
(e) E. S. DAYHOFF: <i>Preprinted Report No. VI on Fine Structure of the Hydrogen Atom</i> (Columbia University, 1952), referred to by DUMOND and COHEN (*).			

With the aid of the data given in Table I, we calculated the value of γ_1 from the measured fine-structure splitting of the spectrum of deuterium ($Z = 1$):

$$\gamma_1 = \frac{8 \cdot \Delta\nu_D \cdot c^2 (\hbar/e)^2}{R_D \cdot e^2} = 0.5012, \quad \Delta\gamma/\gamma = 0.0002.$$

The discrepancy between the theoretical value and the observation amounts to 2.4%, and is equal twelve times the standard error. The deviation is in itself not very small since the elementary constants are claimed to be known with accuracies of the order of 10^{-5} .

One might try to attribute the discrepancy to the fact that the expression (2) is only approximate in so far as it is derived by neglecting higher powers in e^2/hc . The exact energy for the state of quantum numbers n and j is given by

$$E/m_0c^2 = \left\{ 1 + \left[n - (j + \frac{1}{2}) + \sqrt{(j + \frac{1}{2})^2 - \alpha^2 Z^2} \right]^2 \right\}^{-\frac{1}{2}} - 1.$$

Developing in powers of $\alpha Z/n$, we get

$$E/m_0c^2 = -\frac{1}{2} \left(\frac{\alpha Z}{n} \right) \left\{ 1 + \left(\frac{n}{j + \frac{1}{2}} - \frac{3}{4} \right) \frac{\alpha Z}{n} \right\}^2 + \left[\frac{1}{4} \left(\frac{n}{j + \frac{1}{2}} \right)^3 + \frac{3}{4} \left(\frac{n}{j + \frac{1}{2}} \right)^2 - \frac{3}{2} \frac{n}{j + \frac{1}{2}} + \frac{5}{8} \right] \left(\frac{\alpha Z}{n} \right)^4 + \dots \right\}.$$

So as to get the energies of the fine-structure components from which we may determine γ , we have to insert

$$Z = 1, \quad n = 2, \quad j = \frac{3}{2} \text{ resp. } j = \frac{1}{2}.$$

We thus get for the energy difference between the fine-structure components in suitable units

$$\frac{\Delta E/m_0 c^2}{(\alpha/2)^4} = \frac{1}{2} \left[1 + \frac{5}{2} \left(\frac{\alpha}{2} \right)^2 \right] = 0.50003,$$

instead of the value $\frac{1}{2}$ of the approximate procedure. We see that the discrepancy between the exact formula and the observed fine-structure splitting is practically the same as the discrepancy between the approximate formula and the measurement, and therefore it is not caused by the approximate nature of equ. (4).

In conclusion it would seem desirable to investigate the above discrepancy more closely. At any rate, the best confirmation of the relativistic formula for the change of the mass of the electron with velocity was obtained by the above method of Glitscher.

As, however, there seems to exist a numerical discrepancy between theory and measurements, furthermore as the theoretical formula is based on several assumptions, one of which is the mass law (another assumption is that the magnetic moment of the electron is exactly a Bohr magneton), it seemed highly desirable to check the mass law with high accuracy by more direct methods.

3. - Direct experiments on the velocity dependence of mass.

3.1. Experiments with β -particles. - As is well known the first experimental investigation concerning the dependence of mass on velocity was carried out by KAUFMANN⁽⁵⁾ with the aid of the parabola method. His results yielded no decision between the competing theories of Abraham and Lorentz. Soon after the publication of Kaufmann's paper PLANCK discussed the results in detail⁽⁶⁾, i.e. he re-evaluated them in a manner slightly different from that of Kaufmann. Planck's examination of Kaufmann's results showed that they justify the theory of Abraham more than that of Lorentz—if the phrase « more » or « less » has any meaning in this connection. PLANCK himself says: « The fact that the deviations from one theory are less than those from the other does not favour the first one ». It is worth mentioning that the problem

⁽⁵⁾ W. KAUFMANN: *Ann. d. Phys.*, (4), **19**, 487 (1906).

⁽⁶⁾ M. PLANCK: *Phys. Zeits.*, **7**, 753 (1906).

is nowhere exposed so clearly as is done by PLANCK in the discussions following his article. Among others he emphasizes that the final word in the debate between competing theories must be that of the experimental facts.

For a long time the greatest precision was claimed for the measurements of BUCHERER (⁷), although they were criticized by BESTELMEYER (⁸). The experiments were repeated and continued by NEUMANN (⁹). The principles of the method can be summarized as follows (see Fig. 2). In the centre between the circular plates of a condenser there is a source of β -particles. The system is placed in a magnetic field which is perpendicular to the electric field between the condenser plates. Thus only such electrons can leave the condenser whose velocity has a certain value defined by the electric and magnetic field intensities: those electrons for which the effect of the two kinds of field is just compensated. Outside the condenser the motion of the electrons is influenced only by the magnetic field and thus their deflection is inversely proportional to their momentum. Consequently the electric and magnetic field intensities

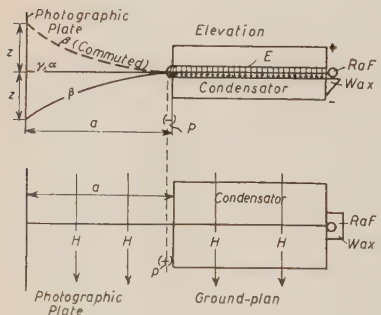


Fig. 2. — Scheme of the experimental arrangement used by Bucherer reproduced from (⁷).

define the velocity of the escaping electrons and their momentum as well, and with the aid of a β -source of continuous energy spectrum, the mass of the particles as a function of their velocity can be determined directly.

It was ZAHN and SPEES (¹⁰) who in 1938 called attention to the fact that the most important feature of the experimental device of BUCHERER and NEUMANN, its resolving power, has never been properly studied, excepting some notes on the effect of the scattering of β -particles along the condenser plates and on the asymmetries of the experimental arrangement. With the aid of elementary electron-optical considerations ZAHN and SPEES obtained the following results.

The velocity filter under consideration, even for the case of negligible scattering of electrons along the condenser plates, must have completely broken down for values of $v/c > 0.7$. For the lower velocities observed the resolution width was approximately as great as that equivalent to the whole relativistic mass effect. Besides it was found that, with a certain choice of geometrical

(⁷) A. H. BUCHERER: *Ann. d. Phys.*, (4), **28**, 585 (1909); **30**, 974 (1909).

(⁸) A. BESTELMEYER: *Ann. d. Phys.*, (4), **30**, 166 (1909); **32**, 231 (1910).

(⁹) G. NEUMANN: *Ann. d. Phys.*, (4), **45**, 529 (1914).

(¹⁰) C. T. ZAHN and A. H. SPEES: *Phys. Rev.*, **53**, 357 (1938); **53**, 511 (1938).

constants, a very poor resolving power may be concealed by spurious focusing effects—and it was just this choice that NEUMANN, by trial and error, found necessary to make in order to obtain sharp lines. Thus quoting the conclusion of ZAHN and SPEES verbally, «it seems fair to say that the Bucherer-Neumann experiment actually proved very little, if anything more than the Kaufmann experiments. The uncertainties of interpretation are so great as to give one very little feeling of certainty as regards a 10% effect».

Electron-optical considerations led ZAHN and SPEES to a modification of the experimental arrangement of BUCHERER and NEUMANN, which, based on the same principle, greatly improved its resolving power, even if secondary effects (as scattering of electrons on the condenser plates) are considered. The source of electrons was placed within the magnetic field but outside the condenser, and the electrons after passing the crossed magnetic and electric fields were detected by a G.M.-counter tube (see Fig. 3). The authors claim to have found the variation of mass with velocity in accord wity the Lorentz expression within 1.5% which is well within the limits of experimental error. It is unfortunate that their papers do not contain the numerical data obtained directly from the measurements, and thus one cannot follow the calculations.

The same reasons which led ZAHN and SPEES to the investigations outlined above, caused also another experiment to be undertaken. ROGERS, McREYNOLDS and ROGERS⁽¹¹⁾ made use of the high-precision absolute value of $H\varrho = mv/e$ of the most intense lines of the RaB β -particle spectrum (determined by one of the authors mentioned) and measured $XR = mv^2/e$ for the same electrons in a radial electrostatic field X . From these one gets $r = (XR)/(H\varrho)$ and $m/e = (H\varrho)^2/(XR)$. Because of the focusing action of the radial electric field the chief source of uncertainty discussed by ZAHN and SPEES can be avoided in the new experiments. The maximum errors in the $H\varrho$ values are no more than 0.03%. The accuracy of XR depends on the precision with which the geometrical constants of the experimental set-up, the voltage on the deflecting electrodes, and—last but not least—the corrections due to the stray fields can be determined. The authors quoted—without giving a detailed discussion—estimate the maximum relative error of v to be less than 0.9% and that of m/e to be well within 1%. The values calculated from equ. (1) agree with the experimental results within these error limits, and the possibility of the validity of equ. (3) is clearly excluded.

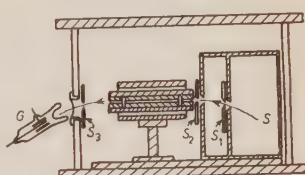


Fig. 3. Scheme of the experimental arrangement used by Zahn and Spees, reproduced from⁽¹⁰⁾.

⁽¹¹⁾ M. M. ROGERS, A. W. McREYNOLDS and F. T. ROGERS: *Phys. Rev.*, **57**, 379 (1940).

In the period between the experiments of BUCHERER and NEUMANN and those of ZAHN and SPEES, TRICKER⁽¹²⁾ carried out measurements with a modified β -spectrograph (see Fig. 4). The method makes use of the focusing effect of a longitudinal magnetic field, the focal length depending on the velocity of the electrons.

The β -source applied had discrete momentum spectrum accurately known from other measurements. Although the author himself considers his results to be of a preliminary nature and does not claim them to be final or exhaustive, we do not know whether he ever continued his experiments. As a matter of fact, repetition would have been very interesting as in the velocity range of the measurements expressions (1) and (3) differ only by about 5% and the error of the results is estimated by the author as about 2%. This error, however, is not a consequence of the limitations of the method, but results rather from the lack of sufficient experimental data: the results published were derived from measurements on some nine photographs, the lines on which are sharp and easily seen and which were taken under standard conditions. Five of these, however, were probably not quite so accurate as the others.

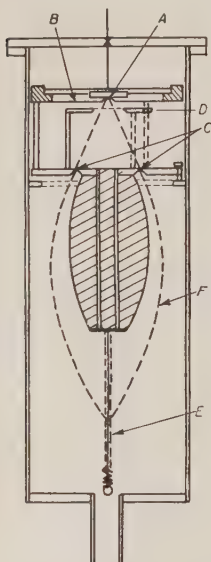


Fig. 4. — Scheme of the experimental arrangement used by Tricker, reproduced from⁽¹²⁾.

3.2. Experiments with cathode rays. — The first experiments on the variation of mass of artificially accelerated electrons were carried out in 1908 by HUPKA⁽¹³⁾. At that time high-voltage and high-vacuum techniques were in their infancy and electron optics was nowhere at all. The experiments were carried out up to about 90 kV accelerating voltage. In spite of the primitive experimental set-up, HUPKA applied a very ingenious null method, thus increasing the accuracy of the results. The electron beam was deflected by the magnetic field of a pair of coils. The deflecting field was varied in such a manner that for each value of the accelerating voltage the deflection was kept constant. Since the deflecting coils did not contain iron, the deflecting field intensity was proportional to the coil current. By measuring the accelerating voltage and the coil current, the relation between mass and velocity could be determined with the aid of the expression for the momentum and the kinetic

⁽¹²⁾ R. A. TRICKER: *Proc. Roy. Soc., A* **109**, 384 (1925).

⁽¹³⁾ E. HUPKA: *Ann. d. Phys.* (4), **31**, 169 (1910).

energy. One can also calculate the rest mass from the values obtained for the various velocities. Doing this, HUPKA found that by using the relativistic formulae throughout, a constant value is obtained within the limits of a very small error, while Abraham's theory leads to a «rest» mass, which is decreasing systematically, if values corresponding to increasing energies are used. Thus the relativistic theory is confirmed, the plots published by HUPKA seem to be most convincing.

Not much later, however, HEIL analyzed the above experiment critically (14), and pointed out serious difficulties as regards the reliability of the results obtained.

It is obvious that the accuracy of the results chiefly depends on the precision with which the coil current and the accelerating potential is measured. There is no difficulty with the first one. As to the second, it is shown that the two kinds of mass variation can be distinguished only if the error in the measurement of the accelerating potential is below 1%. It is about this error which occurs in the measurements of HUPKA. Thus the assumption underlying the treatment of the experimental data is of greatest importance. While with the aid of certain assumptions as to the error distribution HUPKA obtained results confirming the Lorentz expression, HEIL has shown that the same experimental data can be evaluated in favour of the Abraham theory as well. Thus it is safe to state that the investigations of HUPKA do not add anything to the experimental facts in favour of or against the relativistic expression under consideration.

Several series of experiments carried out with artificially accelerated electrons, which are claimed to have confirmed the Lorentz expression with a very high degree of accuracy were performed by GUYE, RATNOWSKY and LAVANCHY in 1907-1915 (2). Their result is quoted by a number of modern textbooks as the most precise experimental evidence of the validity of the relativistic variation of mass.

The principle of the experiment is the following: Electrons accelerated in a cathode ray tube to a high velocity (up to $v/c \sim 0.5$) are deflected once by an electric field and once by a magnetic field. The two kinds of deflections are measured separately, thus two values are obtained, one being inversely proportional to the kinetic energy, the other to the momentum of the electrons. The electrical deflection is

$$(5) \quad X = A \frac{V}{mv^2},$$

(14) W. HEIL: *Ann. d. Phys.* (4), **31**, 519 (1910); **33**, 403 (1910); E. HUPKA: *Ann. d. Phys.* (4), **34**, 400 (1910).

and the magnetic deflection:

$$(6) \quad Y = B \frac{I}{mv},$$

where m is the mass and v the velocity of the electron, V is the voltage applied to the deflecting plates. I is the magnetizing current through the air-cored deflecting coil; A and B are constants depending on the geometry of the experimental arrangement. From the above expression we have

$$(7) \quad v = \frac{A}{B} \frac{Y}{X} \frac{V}{I},$$

$$(8) \quad m = \frac{B^2}{A} \frac{X}{Y^2} \frac{I^2}{V}.$$

Thus from the experimental values X , Y , I , V quantities proportional to velocity and mass respectively are obtained.

Two measurements at different accelerating potentials result in two sets of values X_1 , Y_1 , V_1 , I_1 ; X_2 , Y_2 , V_2 , I_2 . From these the ratios of the velocities v_1/v_2 and the corresponding masses m_1/m_2 can be determined independently of the «form-factors» A and B . At low velocities the accelerating potential can be measured with great accuracy. Thus the absolute value of the kinetic energy is obtained. If the other quantities are measured at the same accelerating voltage, the absolute value of the velocity may be determined as well, i.e. the constant A can be determined. Using the value of the rest mass m_0 from other experiments, values of m/m_0 for various velocities are obtained. If the experimental data are evaluated according to the relativistic relations, the results for the variation of mass with velocity agree with the Lorentz expression within 0.02%; if the experimental data are treated according to the theory of Abraham a systematic deviation occurs and an average deviation of 1.12% is found.

The results of the relativity theory seem thus to be confirmed in a most convincing way. However, the method followed in the treatment of the experimental data can be seriously criticized.

The method followed by all authors mentioned above can be summarized as follows. The experimental data are evaluated twice; namely on the assumption that either the one or the other theory is valid. The correct theory is then deemed to be that one for which the values derived from the experimental data are in accordance with those expected theoretically, or in other words for which the calculated values of m/m_0 plotted against v/c fall on the theoretical curve. Owing to the experimental errors, however, the experimental points do not fit exactly in either of the cases: The experimental values lie closer to the one than to the other theoretical curve.

The method followed is reminiscent of that which PLANCK criticized in

connection with Kaufmann's experiments. Regarding the paper of GUYE et al. further difficulties can be found. The deviation of the experimental results from the theory is characterized by these authors by evaluating the arithmetic mean value of the difference between some averaged experimental values and the theoretically expected values. In our opinion this procedure does not reflect clearly upon the validity of the assumed theories.

Fortunately the paper referred to contains all the experimental data explicitly and thus we were in a position to re-evaluate the material in a more satisfactory way. We presently give our analysis of the original data.

4. – Analysis of the results of Guye et al.

4.1. – The experiments of GUYE et al. were carried out in a rather small range of velocities ($v/c < 0.5$). We assume the dependence of mass upon velocity in this region to be given by a polynomial in powers of $q = (v/c)^2$; we determine the coefficients of this polynomial (and their respective experimental errors) from data given by GUYE et al. and compare the values of the coefficients obtained from the analytical approximation of the theoretical formulae by polynomials; the analytical approximation must of course be carried out for that interval of velocities in which the measured values were obtained. For convenience of the numerical work we make use of the approximation through orthogonal polynomials as described e.g. by RUNGE and KÖNIG (15). As the method employed for the analysis of the experimental data seems to be of paramount importance for the reliability of the result of the analysis and as in our opinion too little stress has been laid on this side of the problem, we reproduce our analysis in some detail.

From equ. (7) and (8) it is seen that the experimental data yield a quantity proportional to the mass of the electron

$$(9) \quad \eta = \frac{X}{Y^2} I^2 = k_1 m,$$

and another quantity proportional to the square of v/c

$$(10) \quad \zeta = \left(\frac{Y}{X} \frac{V}{I} \right)^2 = k_2 \left(\frac{v}{c} \right)^2,$$

k_1 and k_2 being constants.

Having obtained from the experiment n sets of quantities ζ_i , η_i , one

(15) C. RUNGE and H. KÖNIG: *Vorlesungen über numerisches Rechnen* (Berlin, 1924).

can define the following quantities:

$$(11) \quad X_i = \zeta_i - \frac{\sum_j \zeta_j}{n},$$

$$(12) \quad Y_i = \eta_i - \frac{\sum_j \eta_j}{n},$$

with the property

$$(13) \quad \sum_{i=1}^n X_i = \sum_{i=1}^n Y_i = 0.$$

Plotting the points Y_i against X_i one has to find that function

$$Y = f(X)$$

which best fits the points (X_i, Y_i) , i.e. for which

$$(14) \quad \sigma^2 = \sum_i (f(X_i) - Y_i)^2 = \text{minimum}.$$

If the expression $Y = f(X)$ is found, (9), (10), (11) and (12) yield

$$(15) \quad \frac{Y}{\sum \eta_i/n} = \frac{m}{m^0} - 1 = \frac{1}{\sum \eta_i/n} \cdot f[k_2(q - q^0)],$$

where

$$q^0 = \frac{1}{k_2} \sum_i \frac{\zeta_i}{n}, \quad m^0 = \frac{1}{k_1} \sum_i \frac{\eta_i}{n},$$

are the mean values of the quantities $q = (v/c)^2$ within the range of the experiment and that of the mass resp. It is this expression, whose explicit form will be compared with the theory. For this purpose the determination of the constant k_2 is of course also necessary, this will be done later.

Let the function $Y = f(X)$ have the form

$$(16) \quad Y = a_1 X + a_2 P_2(X),$$

where $P_2(X)$ is a polynomial of second order, orthogonal to X and normalized:

$$(17) \quad P_2(X) = A_0 + A_1 X + A_2 X^2$$

satisfying the following conditions:

$$(18) \quad \begin{cases} \sum_i P_2(X_i) = 0, \\ \sum_i X_i P_2(X_i) = 0, \\ \sum_i P_2^2(X_i) = 1. \end{cases}$$

The condition expressed by equ. (14) yields two equations for a_1 and a_2 respectively:

$$\frac{\partial(\sigma^2)}{\partial a_1} = 2 \sum [a_1 X_i + a_2 P_2(X_i) - Y_i] X_i = 0,$$

$$\frac{\partial(\sigma^2)}{\partial a_2} = 2 \sum [a_1 X_i + a_2 P_2(X_i) - Y_i] P_2(X_i) = 0.$$

Taking the relations (18) into consideration, the above equations are found to be independent, and give

$$(19) \quad a_1 = \frac{\sum X_i Y_i}{\sum X_i^2} \quad \text{and} \quad a_2 = \sum Y_i P_2(X_i).$$

Using the explicit form of P_2 and remembering the relations (13) and (18), one can write also

$$(20) \quad a_2 = \sum Y_i P_2(X_i) = A_1 \sum X_i Y_i + A_2 \sum X_i^2 Y_i.$$

The constants in $P_2(X)$ are determined by solving the simultaneous equations (18), remembering equ. (13):

$$(21) \quad \begin{cases} A_0 = \frac{1}{n} \left[\frac{\sum X_i^4}{\sum X_i^2} - \frac{(\sum X_i^3)^2}{(\sum X_i^2)^3} - \frac{1}{n} \right]^{-\frac{1}{2}}, \\ A_1 = A_0 \frac{n \sum X_i^3}{(\sum X_i^2)^2}, \\ A_2 = -A_0 \frac{n}{\sum X_i^2}. \end{cases}$$

With the aid of the relations derived above and the numerical results of the experiments published by GUYE *et al.*, the explicit expression for the function $Y = f(X)$ can be given. The authors mentioned carried out two

series of measurements, the tables giving the results contain 85 sets of data for the first, and 67 sets of data for the second series. The original diagram showing the relation of m/m_0 to v/c as found by the authors is reproduced in Fig. 5. In the course of the numerical calculations we found that two data

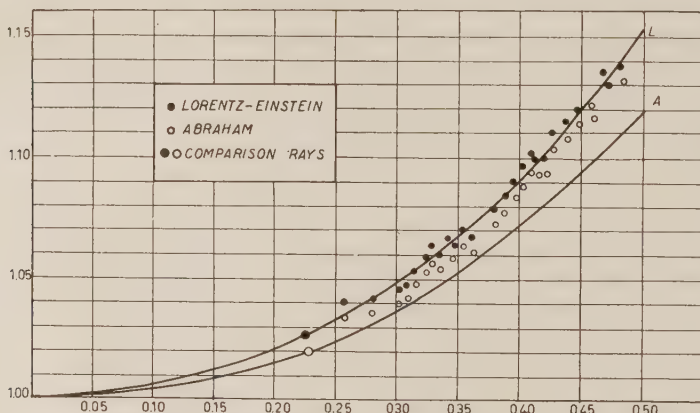
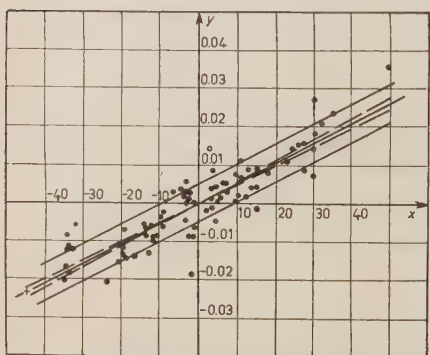


Fig. 5. - Change of mass with velocity according to Lorentz-Einstein (L) and Abraham (A) reproduced from Guye, Ratnowsky and Lavanchy (2). Circles and dots represent measured values.

of Series 1 and one of Series 2 are likely to be misprints. If we were to include these results in the calculation we would obtain a decrease of mass with velocity.

Leaving out these data we obtained the results given in Table II. They are shown also graphically in Fig. 6. The dots represent the points (X_i, Y_i) as calculated with (11) and (12) from the



ries 1. The two lines parallel to the fully drawn thick line are obtained by a shift of the latter by $\pm \delta Y$, the broken lines by changing the direction of the thick line by $\pm \delta a_1$.

Fig. 6. - Normalized values of mass versus normalized values of velocity. The fully drawn thick line through the origin represents the linear relation best fitting the experimental values of Series 1.

experimental data. The thick solid lines represent

$$Y = a_1 X \quad \text{with} \quad a_1 = 5.2 \cdot 10^4 \quad \text{and} \quad a_1 = 6.2 \cdot 10^4 \quad \text{resp.,}$$

i. e. the straight lines best fitting the experimental points. The other straight lines in the Figure characterize the dispersion of the experimental errors and its consequences, as will be explained presently.

TABLE II.

	Series 1, $n = 83$	Series 2, $n = 66$
$\sum X_i^2$	$3.0343 \cdot 10^4$	$4.3415 \cdot 10^4$
$\sum X_i^3$	$-1.8295 \cdot 10^4$	$-1.2330 \cdot 10^3$
$\sum X_i^4$	$3.0444 \cdot 10^7$	$1.4817 \cdot 10^4$
$(\sum \eta_i)/n$	0.731	0.7836
$\sum X_i Y_i$	15.82	27.049
$\sum X_i^2 Y_i$	54.407	799.56
$\sum Y_i^2$	$1.0404 \cdot 10^{-2}$	$1.8537 \cdot 10^{-2}$
A_0	0.0831	0.0718663
A_1	$-1.37 \cdot 10^{-4}$	$-3.1028 \cdot 10^{-3}$
A_2	$-2.272 \cdot 10^{-4}$	$-1.09252 \cdot 10^{-4}$
$\sum X_i P_2(X_i)$	-0.01453	0.0034261
a_1	$5.2137 \cdot 10^{-4}$	$6.23034 \cdot 10^{-4}$
a_2	-0.01453	0.0034261

Using the numerical results given in Table II, the function $Y = f(X)$ can be written as follows:

$$(22) \quad Y(X) = 5.21 \cdot 10^{-4}X + 3.30 \cdot 10^{-6}(X^2 + 0.6X - 365.8) \quad \text{for Series 1,}$$

$$(23) \quad Y(X) = 6.23 \cdot 10^{-4}X - 3.74 \cdot 10^{-7}(X^2 + 28.4X - 657.8) \quad \text{for Series 2.}$$

Evidently these are the most probable functional relations compatible with the two series of experimental results. However, the dispersion of the experimental results does not allow the determination of an exact relation of the quantities considered. The most important feature of the method followed here is the fact that the errors and the uncertainties characterizing the experiment can be estimated quantitatively.

The mean square deviation of Y is

$$(24) \quad (\delta Y)^2 = \frac{\sigma^2}{n} = \frac{1}{n} \left(\sum Y_i^2 - a_1^2 \sum X_i^2 - a_2^2 \right),$$

from (14), (16), (17) and the orthogonality relations. Using the data of Table II, we get:

$$\text{for Series 1: } (\delta Y)^2 = 2.34 \cdot 10^{-5},$$

$$\text{for Series 2: } (\delta Y)^2 = 2.53 \cdot 10^{-5}.$$

It is interesting to see how the mean square deviation $(\delta Y)^2$ decreases with increasing order of the approximating polynomial. Let the mean square deviation for a linear approximation be $(\delta_1 Y)^2$ and that for a second order approximation $(\delta_2 Y)^2$. For these quantities (24) gives the relation

$$(25) \quad (\delta_2 Y)^2 = (\delta_1 Y)^2 \left[1 - \frac{a_2}{n(\delta_1 Y)^2} \right],$$

from which

$$(\delta_2 Y)^2 = 0.903(\delta_1 Y)^2 \quad \text{for Series 1,}$$

and

$$(\delta_2 Y)^2 = 0.997(\delta_1 Y)^2 \quad \text{for Series 2.}$$

It is seen that the approximation is not improved essentially when proceeding from the linear to the quadratic approximation. The physical meaning of this result is that the spread of the experimental data within the relatively small interval is rather high, and there is not much sense in fitting a parabola to the experimental points instead of a straight line. It should be noted that this is evidently a property of the actual experimental data, and not of the theoretical formula to be verified.

As a matter of fact, it is not $(\delta Y)^2$ we are interested in, but rather the uncertainty of the parameters a_1 and a_2 , where a_1 —contenting ourselves with the linear approximation—gives the direction of our straight line. Supposing that the X_i values are exact and only the Y_i values possibly erroneous, all having the same standard error δY , one obtains

$$(\delta a_1)^2 = \sum \left(\frac{\partial a_1}{\partial Y_i} \right)^2 (\delta Y_i)^2; \quad \delta Y_i = \delta Y_1,$$

which together with (19) gives

$$(\delta a_1)^2 = \frac{(\delta Y)^2}{\sum X_i^2} \quad \text{and} \quad (\delta a_2)^2 = (\delta Y)^2.$$

Substituting the necessary numerical data from Table II, we get for Series 1

$$\frac{\delta a_1}{a_1} = 0.053 \quad \text{and} \quad \frac{\delta a_2}{a_2} = 0.33,$$

and for Series 2

$$\frac{\delta a_1}{a_1} = 0.039 \quad \text{and} \quad \frac{\delta a_2}{a_2} = 1.47.$$

We note the very high relative error $\delta a_2/a_2$ in both series showing that the experimental data give no real information beyond the first approximation. The uncertainty of our linear approximation is characterized by $\delta a_1/a_1$. This quantity enables us to judge the reliability of the whole experiment, i.e. how far its results are decisive for our problem.

Returning to Fig. 6 the two lines parallel to the thick line are obtained by a shift of the latter by $\pm \delta Y$, the broken lines are obtained by changing the direction of the thick line by $\pm \delta a_1$.

4.2. — As shown by equ. (15) our empirical formula for the change of mass with velocity within the velocity range covered by the experiments can be written as

$$(26) \quad \frac{m}{m^0} - 1 = \frac{1}{\sum \eta_i/n} \{ a_1 [k_2(q - q^0)] + a_2 P_2[k(q - q^0)] \},$$

where q^0 is the mean value of the quantities $q - (c/e)^2$ within the range of the experiments and m^0 the corresponding mass. In order to compare (26) with the theory, the constant k_2 must be eliminated and corresponding approximations for the theoretical formulae derived.

For a direct determination of the constant k_2 , i.e. without using the method of evaluation of GUYE *et al.*, the experimental data given by them are insufficient. However, at the beginning of the velocity range studied, the velocity is so low that the values obtained for it from the accelerating potential and the deviation of the cathode ray agree within 1 %, no matter whether constant mass or any of the formulae for the velocity dependence of mass are assumed. Thus it seems justified to take k_2 as the ratio of the smallest value of ζ_i and the smallest velocity occurring among the data given by the paper under consideration. In this way

$$k_2 \sim 730$$

is obtained. Using this value for k_2 (26) with (22) and (23) yields

$$(27) \quad \frac{m}{m^0} - 1 = 0.52(q - q^0) + 2.48[(q - q^0)^2 + 8.35 \cdot 10^{-4}(q - q^0) - 6.87 \cdot 10^{-4}],$$

$$(28) \quad \frac{m}{m^0} - 1 = 0.58(q - q^0) - 0.255[(q - q^0)^2 + 3.9 \cdot 10^{-2}(q - q^0) + 1.29 \cdot 10^{-3}],$$

as the empirical formula for the variation of mass with velocity within the experimental range. Regarding the value of the coefficient of the linear term the relative error $\delta a_1/a_1$ determined earlier must be taken into consideration. As is usual in the statistical treatment of observational data, *the possible error is taken to be 3 times the root mean square deviation.* Thus the coefficient of the first term is found to be

$$0.52 \pm 0.09 \quad \text{and} \quad 0.58 \pm 0.08$$

for the respective series.

In order to compare equ. (27) or (28) with the theory, a corresponding approximation of the theoretical expressions is necessary. Although an analogous approximation would be the expansion of the theoretical formulae within the range of the experiments into a series of spherical harmonics, it will suffice to determine the parabola passing through the points corresponding to q_1 , q_2 and $q^0 = (q_1 + q_2)/2$, i.e. the lowest, highest and the mean value of $(v/c)^2$ occurring in one series of experiments. In this manner an expression of the following form is obtained:

$$(29) \quad \frac{m}{m^0} - 1 = B_1(q - q^0) + B_2(q - q^0)^2,$$

where

$$B_1 = \frac{m_2 - m_1}{m^0(q_2 - q_1)},$$

and

$$B_2 = \frac{m_1 + m_2}{m^0(q_2 - q_1)},$$

with $m_i = (m)_{q=q_i}$.

In consequence of the simplified method of approximation in (29) only a second order term occurs instead of a second order polynomial. This term, however, does not play an important role at all, partly because the interval of the approximation is very small and partly because of the uncertainty of the corresponding terms in the empirical formulae.

Table III gives the coefficients of the linear terms of the approximate formulae derived above. In the second and third column no errors are given because they are negligible as compared to those given in the first column.

The results shown in Table III justify the statement that the experimental results published by GUYE *et al.* are compatible with the theory of relativity; the spread in the measured data, however, produces an error which is com-

parable with the difference existing between the relativistic and Abraham's expressions.

TABLE III.

	Empirical	Lorentz	Abraham
Series 1	0.52 ± 0.09	0.55	0.44
Series 2	0.58 ± 0.08	0.59	0.47

It must further be added that in our analysis we have taken into consideration only the errors caused by the straggle of the measured points around a parabola; we were unable to consider errors which are involved in the determination of k_2 . The value of k_2 is, however, most critical because any change of it would influence the value of B_1 . Thus the limits of error given by us represent lower limits. It is curious that the two series of measurements which were actually evaluated give better agreement between the individually obtained B_1 values than might be expected from their comparatively large standard errors.

5. - Collision of electrons in a cloud chamber.

The collision of fast electrons with atomic electrons can be observed in a cloud chamber. These collisions can be regarded in first approximation as elastic collisions between two free particles. By measuring the momentum of the colliding particle before and after the collision, and also the momentum of the recoiling particle, conclusions concerning the law of collision can be drawn. CHAMPION (16) carried out such measurements in an attempt to verify the relativistic laws of collision; as the theory of relativistic collisions is closely related to the relativistic law of change of mass with velocity, the measurements of CHAMPION can be regarded as an experimental investigation into the relativistic mass law.

Denote the momentum of the incident particle P_1 , that of the incident particle after collision P_2 and the momentum of the recoil particle P_3 . In case of the non-relativistic collision the vectors P_2 and P_3 are expected to be perpendicular upon each other; the observation of CHAMPION showed clearly that the actual angle between the track of the particle and the track of the recoiling particle deviates strongly from 90° , thus the observations prove in a qualitative manner that the mass of the electron changes with velocity indeed.

Regarding the quantitative analysis, CHAMPION estimates the error of his

(16) F. C. CHAMPION: *Proc. Roy. Soc., A* **136**, 630 (1932).

measurements to be about 2% and he claims them to be in agreement with the theory of relativity inside this margin of error. It seems, however, that CHAMPION has greatly overestimated the accuracy of his measurements. CHAMPION's work appeared before the investigations of E. J. WILLIAMS⁽¹⁷⁾ upon spurious curvature of cloud-chamber tracks caused by scattering; thus the latter source of error was not taken into account in CHAMPION's work.

CHAMPION measured the momentum P_1 of the primary particle by means of its curvature in a magnetic field inside the chamber. The momenta P_2 and P_3 are not measured but instead the angles

$$\vartheta = \measuredangle(P_1, P_2), \quad \varphi = \measuredangle(P_1, P_3)$$

between primary direction and scattered direction and also between primary direction and recoil particle.

Supposing the law of conservation of momentum to hold, we have from simple geometry

$$(30) \quad P_2 = P_1 \frac{\sin \varphi}{\sin(\varphi + \vartheta)}, \quad P_3 = P_1 \frac{\sin \vartheta}{\sin(\varphi - \vartheta)};$$

the latter assumption holds for both the classical and the relativistic theory; therefore by postulating (30) we do not assume anything which would prejudice the answer as to the exact form of the law of mass change. A check of the relativistic theory is obtained if we evaluate from the measured values P_1 , φ , ϑ the momenta P_2 and P_3 according to (30) and investigate to what accuracy the momenta thus obtained obey the relativistic law of the conservation of energy. Thus we must investigate to what accuracy the relativistic energy equation

$$1 + \sqrt{1 + P_1^2} = \sqrt{1 + P_2^2} + \sqrt{1 + P_3^2},$$

where we have chosen as the unit of momentum mc (m mass of electron), is fulfilled. Substituting (30) into the above equation, we may write

$$(31) \quad \varepsilon = 1 + \sqrt{1 + P_1^2} - \sqrt{1 + P_1^2 \frac{\sin^2 \varphi}{\sin^2(\varphi + \vartheta)}} - \sqrt{1 + P_1^2 \frac{\sin^2 \vartheta}{\sin^2(\varphi - \vartheta)}},$$

where the theory demands $\varepsilon = 0$ within the accuracy of measurement.

Denoting by δP_1 , $\delta \vartheta$, $\delta \varphi$ the standard errors of P_1 , ϑ and φ , the standard

⁽¹⁷⁾ E. J. WILLIAMS: *Phys. Rev.*, **58**, 292 (1940).

error of ε is determined from (31) by

$$\delta\varepsilon = \left\{ \left(\frac{\delta\varepsilon}{\delta P_1} \right)^2 \delta P_1^2 + \left(\frac{\delta\varepsilon}{\delta\vartheta} \right)^2 \delta\vartheta^2 + \left(\frac{\delta\varepsilon}{\delta\varphi} \right)^2 \delta\varphi^2 \right\}^{1/2}.$$

As a typical example we consider numerical data which have the same order of magnitude as those considered by CHAMPION:

$$P_1 = \sqrt{8}, \quad \vartheta = 45^\circ, \quad \varphi = 25^\circ$$

(the above data correspond to a velocity of the primary of $v/c \sim 0.94$ and a mass increase by a factor of 3). We find thus

$$\delta\varepsilon = (0.01 \delta P_1^2 + 1.3 \delta\varphi^2 + 0.87 \delta\vartheta^2)^{1/2}.$$

While it is difficult to estimate the errors $\delta\varphi$ and $\delta\vartheta$ of the angles from the published data, a minimum estimate of the error δP_1 of the momentum measurement can be obtained directly from Williams' theory of scattering. Applying this theory we obtain for a track of about 10 cm length in a magnetic field of $H = 280$ Gauss

$$\delta P_1/P_1 \sim 0.15.$$

Thus

$$\delta\varepsilon \gtrsim 4\%.$$

The above estimation gives a lower limit of the uncertainty involved in the method discussed, the actual uncertainty must be larger as the errors of measurement of angles are not considered in the above estimate. ε is measured in units of the rest energy of the electron. Thus allowing for errors of the order of 3 times the standard error, deviations from the energy law amounting to 12% of the rest energy of the electron are compatible with any of the collision measurements. Thus we conclude that on account of the considerable uncertainties involved in the interpretation of the results, these measurements do not add much to our knowledge of the relation between energy and momentum and thus the law of the change of mass with velocity.

6. – Remark on some further experimental evidence.

6.1. – In this category we discuss first the arguments which can be derived from the operation of high-energy particle accelerators.

As is well known, mass and velocity of a particle moving in a cyclic re-

sonance accelerator are given by

$$m = \frac{e}{c} H \frac{1}{\omega} \quad \text{and} \quad v = \omega \varrho ,$$

where H is the magnetic field, ϱ the radius of the orbit and ω the angular velocity, the other symbols having their usual meaning. Resonance occurs if the angular velocity of the particle and the angular frequency of the accelerating field are equal. In the synchro-cyclotron we have $H = \text{const}$, the energy of the particle is increased—through increasing its mass—by decreasing ω ; of course ϱ increases at the same time. In the synchrotron obtains $\varrho = \text{const}$, and the energy of the particle is increased—through increasing the mass—by the simultaneous variation of H and ω .

Since the quantities ω , ϱ and H can be measured with an extremely high accuracy, it seems reasonable to suppose that the relation between mass and velocity can be studied very precisely in an accelerator. As a matter of fact, however, the situation is not quite so simple.

If ω means the angular frequency of the accelerating field, the relations given above are the expressions for resonance. The accelerated beam, however, contains also particles which, oscillating around the resonance particle, do not satisfy exactly the condition of resonance. The angular frequency of the individual particles in a beam is varying in an interval $\omega \pm \Delta\omega$ and the radius of their orbits is varying in a corresponding interval $\varrho + \Delta\varrho$. Furthermore the magnetic field is more or less inhomogeneous, inhomogeneity is deliberately introduced so as to improve the focusing of the beam and its stability.

One of us (P.S.F.) was informed that when the 1 GeV proton synchrotron was put into operation in Birmingham, there were carried out measurements which are supposed to confirm the relativistic mass-velocity relation to a high degree of accuracy. The method used for these measurements was also communicated in a private discussion, but no detailed results have been given, and thus no analysis could be carried out from the present point of view.

As far as the authors know, the only report of experiments devised for the study of the mass variation of protons with velocity is that of GROVE and FOX⁽¹⁸⁾. They determined the angular velocity of the protons in a 140 in. synchrocyclotron, and by measuring the magnetic field intensity along the orbit they calculated the e/m ratio. The same quantity was determined from the relativistic formula with the aid of the known orbit radius and angular velocity. The authors claim an accuracy of 0.1%, but on account of the extremely short communication, the validity of this claim cannot be assessed.

FARAGÓ, TYAPKIN and ZRELYOV have recently determined the mass of

⁽¹⁸⁾ D. J. GROVE and I. C. FOX: *Phys. Rev.*, **90**, 378 (1953).

660 MeV protons by measuring simultaneously their momentum p and velocity v in the external beam of the 6 m synchrocyclotron of the International Institute for Nuclear Research, Dubna, USSR. The momentum was measured with the aid of a current carrying wire and an accuracy of 0.2% was obtained. To determine the velocity of the protons the absorption of protons in copper was measured. The Bragg curve thus obtained was compared with similar curves obtained in earlier experiments with protons of approximately the same energy whose velocity was directly measured with the aid of their Čerenkov radiation. Thus, although not quite directly, the velocity of the protons was determined by means of Čerenkov radiation. The accuracy of the value thus obtained is well within 0.1%. The mass $m_1 - p/v$ is obtained therefore with an accuracy of 0.2% and its value can be compared with m_2 the mass given by the Lorentz formula. The discrepancy is found to be $(m_2 - m_1)/m_1 = -0.004(1 \pm 0.8)$. Although this discrepancy is somewhat greater than the experimental error, it is not significant, as three times the standard error is still compatible with the experimental results. A more detailed report on these experiments will be published soon in the *Acta Physica Hungarica*.

6'2. – It was shown by JÁNOSSY (19) that there is a close connection between the transversal Doppler effect and equ. (1) applied to electrons. The measurements of OTTING (20) are compatible with the theory and thus with the validity of (1), but the experimental error of the measurements is too large to permit stricter conclusions as to the validity of the formula (1) than those which can be drawn from direct measurements.

6'3. – Finally we mention that the negative outcome of the Michelson-Morley experiments allows certain conclusions as to the law of the mass variation of the electron. It was shown (21) that the relativistic length contraction can be derived as a change of equilibrium distance between the atoms of a lattice when the relativistic properties of the electromagnetic field and the relativistic properties of the electrons are taken into consideration. If we were to suppose a deviation from equ. (1) this would cause a perturbation and would affect the equilibrium distance in a lattice under translation, and this should be detectable experimentally. Preliminary calculations show, however, that the equilibrium distances depend to a much greater extent on the purely electromagnetic forces than the kinetic energy of the electron and therefore a large deviation from equ. (1) would lead to a relatively small correction in the contraction formula.

(19) L. JÁNOSSY: *Acta Phys. Hung.*, **5**, 215 (1955).

(20) G. OTTING: *Phys. Zeits.*, **40**, 681 (1939).

(21) L. JÁNOSSY: *Uspechi* **62** (1957).

7. — Conclusions.

Analyzing the available experimental material, we have come to the conclusion that it is the fine-structure splitting in the spectra of atoms of the hydrogen type which give the only high-precision confirmation of the relativistic law of the variation of electron mass with velocity. This evidence, however, is a rather indirect one, and it does not cover a range of velocities which is wide enough.

Regarding the fairly large number of direct experiments on the behaviour of free electrons we could hardly find such results which would prove the validity of the relativistic relation with a margin of error much less than, say, the difference between the results of the relativity theory and the theory of Abraham.

Quantitative experimental results concerning particles other than electrons or protons are not available.

RIASSUNTO (*)

Il lavoro passa in rassegna gli attuali esperimenti coi quali si investiga la dipendenza dalla massa elettronica dalla velocità. Si trova che la verifica più esatta della formula relativistica segue dalla separazione dei doppietti degli spettri idrogenoidi. Gli esperimenti diretti sul comportamento degli elettroni liberi danno risultati che non contraddicono la formula relativistica, per quanto l'errore sperimentale delle misure disponibili sia abbastanza elevato, nella maggior parte dei casi dell'ordine della differenza fra le formule teoriche derivanti da differenti ipotesi. Si passano in rassegna anche misure recenti sulla dipendenza della massa protonica dalla velocità.

(*) Traduzione a cura della Redazione.

A New Method for Solving Multiple Scattering Problems in Inhomogeneous Media.

P. GOSAR

Institut za Elektrosvrize - Ljubljana, Yugoslavia

(ricevuto il 28 Gennaio 1957)

Summary. — The theory of the multiple small angle scattering of waves, published by the author in a recent paper, is extended to be applicable in the case of the inhomogeneous medium composed of the equal and centrally symmetrical scatterers embedded in an homogeneous medium. Further, a new method is developed for the numerical calculation of the angular distribution of the scattered waves. As an example the multiple scattering by dielectric spheres is discussed. In this case the angular distribution of the scattered waves is similar to the angular distribution of the electrons passing through thin metal foils. It proves that the mutual interaction of the spheres has an influence on the angular distribution, if the average distance between neighboring spheres is of order of their diameter.

1. — Introduction.

In the previous paper ⁽¹⁾ we developed a theory of the multiple small angle scattering of scalar waves by a special type of the inhomogeneous medium. This theory is applicable to an inhomogeneous medium having the following properties:

- 1) The inhomogeneous medium is non-absorbing and the differences of the dielectric constants between different parts of the medium are very small.
- 2) The medium can be divided in domains of fluctuations of the dielectric constant, called scatterers. The dimensions of domains are great in

⁽¹⁾ P. GOSAR: *Nuovo Cimento*, **4**, 688 (1956). References to formulae of this paper will be preceded by the symbol G.

comparison with the wave length. The space between individual scatterers is filled with homogeneous matter, the dielectric constant of which is equal to the average value $\langle \epsilon \rangle$, taken over the whole inhomogeneous medium.

3) The distribution of the dielectric constant in scatterers is such, that equal positive and negative phase shifts $\varphi(\mathbf{r}, \mathbf{s})$ and equal positive and negative total phase shifts $\varphi(\mathbf{p})$ of the rays emerging from the scatterers occur with equal frequency.

In this paper we shall extend the theory for another case of the inhomogeneous medium, which does not fulfill the third postulate and a part of the second. We shall investigate the multiple scattering of waves by an inhomogeneous medium composed of the equal and spherically symmetrical domains of the fluctuations of the dielectric constant embedded in an homogeneous medium. Let these domains or scatterers be distributed in some random way through the volume of the medium. The dimensions of the scatterers are great in comparison with the wave length and the above first postulate is fulfilled.

The theory developed in the previous paper needs some modifications to be used in this case. We further shall show here a new method for solving multiple scattering problems.

In the last section we shall give an example for the application of the theory. We shall examine the multiple scattering by the dielectric spheres embedded in a homogeneous medium.

2. - Statement of the problem and its solution.

A plane wave, which propagates in a homogeneous infinite medium in the direction of the z axis of the space co-ordinate system, falls upon a plan-parallel sheet of the inhomogeneous medium. The boundary planes of this medium are parallel to the co-ordinate plane (x, y) . The thickness of the sheet is d , the area S_0 and the volume V .

The inhomogeneous medium is composed of N equal and spherically symmetric scatterers embedded in the homogeneous medium of dielectric constant ϵ . Additionally we choose the dielectric constant of the medium surrounding the sheet also equal to ϵ . The radial distribution of the dielectric constant in a single scatterer is given by the function

$$(1) \quad \epsilon(\mathbf{r}') - \epsilon = q(r') ,$$

where $\epsilon(\mathbf{r}')$ is the dielectric constant at the point \mathbf{r}' in the co-ordinate system with the origin in the center of the chosen scatterer, and r' is the radial

distance. We assume, that the function $q(r')$ is regular and finite in an interval from 0 to r_0 and zero for $r' > r_0$. r_0 is the radius of the scatterer.

In our calculations we do not need to know the exact distribution of the scatterers through the volume of the inhomogeneous medium. It is enough to know the average distribution of the scatterers around some chosen one. We obtain this average distribution, if we plot in the same co-ordinate system the distribution of the centers of the scatterers around each scatterer being in the origin of the co-ordinate system. We assume, that the average density $D(\mathbf{r}')$ of the centers of scatterers in the relative position \mathbf{r}' to the center of the chosen scatterer is only a function of the radial distance r' and is given by

$$(2) \quad D - D(\mathbf{r}') = w(r') ,$$

where D is the average density of the scatterers in the inhomogeneous medium, i.e. $D = N/V$. If the distance r' is greater than the average distance between the centers of scatterers, the probability function $w(r')$ approaches zero. It follows from the definition of the function $w(r')$ that

$$(3) \quad \int w(r') d\mathbf{r}' = 1 ,$$

where $d\mathbf{r}'$ is the volume element and the integral extends over all space. The value of the function $w(r')$ at $r' = 0$ is N/V .

We are interested in the angular distribution of the scattered waves emerging from the sheet of the inhomogeneous medium. Following the way of the calculation outlined in the previous paper we must first choose the reference dielectric constant ϵ_0 so that the average value of the quantity $\Delta\epsilon(\mathbf{r})g(\mathbf{r}, \mathbf{s})$ taken over the whole inhomogeneous medium is equal to zero. $\Delta\epsilon(\mathbf{r})$ is $\epsilon(\mathbf{r}) - \epsilon_0$ and $g(\mathbf{r}, \mathbf{s})$ is the macrostructural correction factor defined by the equation (G 11). The reference dielectric constant ϵ_0 is complex

$$(4) \quad \epsilon_0 = \epsilon' + i\kappa .$$

As the differences of the dielectric constants between different parts of the medium are small and as the scatterers are large, we approximate $g(\mathbf{r}, \mathbf{s})$ with the expression (G 13). The phase shift $\varphi(\mathbf{r}, \mathbf{s})$ of the wave passing through the point \mathbf{r} , due to the fluctuations of the dielectric constant, is here given by

$$(5) \quad \varphi(\mathbf{r}, \mathbf{s}) = \frac{2\pi}{\lambda} \int_s [n(s) - n'] ds ,$$

where n' is $\sqrt{\epsilon'}$. This integral extends over the variable s , which measures the distance along the line passing through the point \mathbf{r} in the direction \mathbf{s} of

the propagation of the chosen macrostructural wave, from an initial point, which we shall determine in the following, to the point \mathbf{r} . In the integrand $n(s)$ is the refractive index of a given point s of the line. The initial point or the lower limit of the integral (5) is determined in the following way. We divide the whole inhomogeneous medium in cells in such a way, that in each cell there is one and only one scatterer. This division in cells should be performed by the construction of the symmetry planes between pairs of the neighboring scatterers. Thus we obtain the division of the medium in polyhedra. Now we determine the lower limit of the integral with the first intersection of the line, going through the point \mathbf{r} in the direction \mathbf{s} , and the surface of the polyhedron containing the point \mathbf{r} . In this way we can determine the factor $g(\mathbf{r}, \mathbf{s})$ for every point of the medium. This method of determination is rather arbitrary, but is reasonable.

Using the above approximation for $g(\mathbf{r}, \mathbf{s})$ the reference dielectric constant ε_0 is determined from the equations

$$(6) \quad \begin{cases} \langle [\varepsilon(\mathbf{r}) - \varepsilon'] \cos [\varphi(\mathbf{r}, \mathbf{s})] \rangle + \kappa \langle \sin [\varphi(\mathbf{r}, \mathbf{s})] \rangle = 0, \\ \langle [\varepsilon(\mathbf{r}) - \varepsilon'] \sin [\varphi(\mathbf{r}, \mathbf{s})] \rangle - \kappa \langle \cos [\varphi(\mathbf{r}, \mathbf{s})] \rangle = 0. \end{cases}$$

It is easy to see, that for cases in which this theory is applicable the real part of the reference dielectric constant ε_0 is very near to the average value $\langle \varepsilon \rangle$. The theory can only be used in the cases, where the product of the extinction coefficient for macrostructural waves μ , which is equal to $2\pi\kappa/n'\lambda$, and the average distance c between the centers of the neighboring scatterers is rather below 1. We derive from $\mu c < 1$ the following restriction for the value of κ

$$(7) \quad \kappa < \frac{n' \lambda}{2\pi c}.$$

On the other hand we obtain from the second equation of (6), taking into account that $\varepsilon(\mathbf{r}) - \varepsilon'$ is nearly equal to $2n'[n(\mathbf{r}) - n']$ and considering the expression (5) for $g(\mathbf{r}, \mathbf{s})$,

$$(8) \quad \kappa = \frac{n' \lambda}{\pi} \frac{\sum_{m=1}^N \int_{S_m} \{1 - \cos [\varphi(\mathbf{p})]\} dS}{V \langle \cos [\varphi(\mathbf{r}, \mathbf{s})] \rangle}.$$

Here we evaluate the average value $\langle [\varepsilon(\mathbf{r}) - \varepsilon'] \sin [\varphi(\mathbf{r}, \mathbf{s})] \rangle$ in such a way, that in each cell of the medium we perform the integration over one space co-ordinate of the direction \mathbf{s} . The m -th integral in (8) is evaluated over the plane S_m , which passes through the center of the m -th scatterer and is per-

perpendicular to the direction \mathbf{s} . The function $q(\rho)$ in the integrand represents the total phase shift of the ray emerging from the m -th cell and passing through point ρ of the plane S_m . The function $q(\rho)$ is equal to zero for the rays, which do not traverse the m -th cell. We can write the expression (8) also in the form

$$(9) \quad \kappa = \frac{n' \lambda}{\pi c'} \frac{\langle \{1 - \cos[\varphi(\rho)]\} \rangle_s}{\langle \cos[\varphi(\mathbf{r}, \mathbf{s})] \rangle},$$

where c' is a distance nearly equal to the average dimension of the cells and the average in the numerator, denoted with the subscript s , is evaluated over the planes S_m .

Comparing the expressions (7) and (9) we see, that the phase shift $q(\rho)$ must be smaller than 1 over a great part of the area of the cross-sections S_m of the cells, if we wish the restriction (7) to be fulfilled. This is the case in a very dense packing of scatterers only, if the differences of the dielectric constants are so small, that the phase shifts of rays passing through a single scatterer are in the average smaller than 1. We shall investigate here in more detail another case, where the system of scatterers is not too dense. Here the phase shifts of the rays passing through the scatterers can be also greater than 1, but the phase shifts of the rays, which do not pass through the scatterers must be much smaller than 1. The phase shifts of the rays, which do not pass through the scatterers, are only due to the mutual influence of the scatterers. Here we assume a relatively small mutual interaction.

The next step in the theory is the evaluation of the autocorrelation function $\gamma(\mathbf{r}'', \mathbf{s})$ for $\Delta\epsilon(\mathbf{r})g(\mathbf{r}, \mathbf{s})$ defined by the formula (G 24). The vector \mathbf{r}'' is the autocorrelation distance vector. The integrals in (G 24) are performed over the whole volume of the inhomogeneous medium. We now divide these integrals in the sum of the integrals over the volumes of the individual cells of the medium. Thus

$$(10) \quad \gamma(\mathbf{r}'', \mathbf{s}) = \frac{\sum_{m=1}^N \int \Delta\epsilon(\mathbf{r}') g(\mathbf{r}', \mathbf{s}) \Delta\epsilon^*(\mathbf{r}' + \mathbf{r}'') g^*(\mathbf{r}' + \mathbf{r}'', \mathbf{s}) d\mathbf{r}'}{\sum_{m=1}^N \int \Delta\epsilon(\mathbf{r}') \Delta\epsilon^*(\mathbf{r}') d\mathbf{r}'},$$

where V_m is the volume of the m -th cell.

The evaluation of $\gamma(\mathbf{r}'', \mathbf{s})$ can be here very simplified due to the smallness of the difference $\epsilon(\mathbf{r}) - \epsilon'$ for the points outside the scatterers. This difference is for $r' > r_0$ in the average much smaller than for the points in the scatterers. It follows from this reasoning, that those volume elements of the cells, which do not belong to the scatterers, contribute only little to $\gamma(\mathbf{r}'', \mathbf{s})$. Hence we make a very small error in the evaluation of $\gamma(\mathbf{r}'', \mathbf{s})$, if we take all

the cells mutually equal with the average dimensions. In this approximation let the cells be spheres of radius R_0 , where R_0 is determined from the equation $4\pi R_0^3/3 = V/N$. Further the factor $\varkappa g(\mathbf{r}, \mathbf{s})$, which appears in $\gamma(\mathbf{r}'', \mathbf{s})$, is generally so small in comparison with the other terms, that it can be dropped or, if we wish, changed to $\varkappa \langle g(\mathbf{r}, \mathbf{s}) \rangle$.

The part of the autocorrelation function, which is due to the correlations of $\Delta\varepsilon(\mathbf{r}')g(\mathbf{r}', \mathbf{s})$ between points in the same cell, is thus

$$(11) \quad \gamma_1(\mathbf{r}'', \mathbf{s}) = \frac{\int_{V_0} [\varepsilon(\mathbf{r}') - \varepsilon'] g(\mathbf{r}', \mathbf{s}) [\varepsilon(\mathbf{r}' + \mathbf{r}'') - \varepsilon'] g^*(\mathbf{r}' + \mathbf{r}'', \mathbf{s}) d\mathbf{r}'}{\int_{V_0} [\varepsilon(\mathbf{r}') - \varepsilon']^2 d\mathbf{r}'}.$$

The dielectric constant $\varepsilon(\mathbf{r}')$ is here equal to $\varepsilon + q(r')$ and the integration extends over the volume V_0 of the sphere of radius R_0 . The numerator of (11) represents the convolution of two functions $[\varepsilon(\mathbf{r}') - \varepsilon']g(\mathbf{r}', \mathbf{s})$ and $[\varepsilon(\mathbf{r}') - \varepsilon']g^*(\mathbf{r}', \mathbf{s})$ and can be written, with the use of the Fourier transforms, in the form

$$(12) \quad \int G(\boldsymbol{\eta}, \mathbf{s}) G^*(\boldsymbol{\eta}, \mathbf{s}) \exp [ir''\boldsymbol{\eta}] d\boldsymbol{\eta},$$

where the integration extends over all space and the function $G(\boldsymbol{\eta}, \mathbf{s})$ is the Fourier transform of the function $[\varepsilon(\mathbf{r}') - \varepsilon']g(\mathbf{r}', \mathbf{s})$, i.e.

$$(13) \quad G(\boldsymbol{\eta}, \mathbf{s}) = \frac{1}{(\sqrt{2\pi})^3} \int_{V_0} [\varepsilon(\mathbf{r}') - \varepsilon'] g(\mathbf{r}', \mathbf{s}) \exp [-i\boldsymbol{\eta}\mathbf{r}'] d\mathbf{r}'.$$

The integration field is here the volume of the sphere of radius R_0 . Thus we obtain

$$(14) \quad \gamma_1(\mathbf{r}'', \mathbf{s}) = \frac{\int G(\boldsymbol{\eta}, \mathbf{s}) G^*(\boldsymbol{\eta}, \mathbf{s}) \exp [ir''\boldsymbol{\eta}] d\boldsymbol{\eta}}{\int G(\boldsymbol{\eta}, \mathbf{s}) G^*(\boldsymbol{\eta}, \mathbf{s}) d\boldsymbol{\eta}}.$$

We must now evaluate that part of the autocorrelation function, which is due to the correlations between the points in different cells. In calculating the integrals in the numerator of (10) we consider only those volume elements of the cells, for which the points in the relative position \mathbf{r}'' lie in some of the neighboring cells. Further we substitute the sum of the integrals over individual cells with the product of the number of cells and the average integral over the volume of one cell. By this procedure the average value

$\Delta\varepsilon^*(\mathbf{r})g^*(\mathbf{r}, \mathbf{s})|_{\mathbf{r}' + \mathbf{r}''}$ appears in the integrand of the average integral instead of $\Delta\varepsilon^*(\mathbf{r}' + \mathbf{r}'')g^*(\mathbf{r}' + \mathbf{r}'', \mathbf{s})$. The subscript $\mathbf{r}' + \mathbf{r}''$ denotes that the average

is here taken over all points, which are in the position $\mathbf{r}' + \mathbf{r}''$ in reference to the center of each scatterer, and not over the whole medium. We write

$$(15) \quad \langle \Delta \varepsilon^*(\mathbf{r}) g^*(\mathbf{r}, \mathbf{s}) \rangle_{\mathbf{r}' + \mathbf{r}''} = \langle [\varepsilon(\mathbf{r}) - \varepsilon'] g^*(\mathbf{r}, \mathbf{s}) \rangle_{\mathbf{r}' + \mathbf{r}''} + i\varepsilon \langle g^*(\mathbf{r}, \mathbf{s}) \rangle_{\mathbf{r}' + \mathbf{r}''}.$$

In this expression we replace the last term, which is very small, by $i\varepsilon \langle g^*(\mathbf{r}, \mathbf{s}) \rangle$, where the average is taken over the whole medium. The term $i\varepsilon \langle g^*(\mathbf{r}, \mathbf{s}) \rangle$ is on the other hand equal to $-\langle [\varepsilon(\mathbf{r}) - \varepsilon'] g^*(\mathbf{r}, \mathbf{s}) \rangle$. Thus we have

$$(16) \quad \langle \Delta \varepsilon^*(\mathbf{r}) g^*(\mathbf{r}, \mathbf{s}) \rangle_{\mathbf{r}' + \mathbf{r}''} \approx \langle [\varepsilon(\mathbf{r}) - \varepsilon'] g^*(\mathbf{r}, \mathbf{s}) \rangle_{\mathbf{r}' + \mathbf{r}''} - \langle [\varepsilon(\mathbf{r}) - \varepsilon'] g^*(\mathbf{r}, \mathbf{s}) \rangle.$$

Using the probability function $w(r')$ for the distribution of the scatterers around a chosen one and taking into account the relation (16) we obtain

$$(17) \quad \langle \Delta \varepsilon^*(\mathbf{r}) g^*(\mathbf{r}, \mathbf{s}) \rangle_{\mathbf{r}' + \mathbf{r}''} \approx - \int [\varepsilon(\mathbf{r}'_2) - \varepsilon'] g^*(\mathbf{r}'_2, \mathbf{s}) w(\mathbf{r}'_1) d\mathbf{r}'_1.$$

Here, $\mathbf{r}'_2 = \mathbf{r}' + \mathbf{r}'' - \mathbf{r}'_1$ and the integration extends over all space; further $\varepsilon(\mathbf{r}'_2) = \varepsilon + q(\mathbf{r}'_2)$ for $\mathbf{r}'_2 < R_0$ and $\varepsilon(\mathbf{r}'_2) = \varepsilon'$ for $\mathbf{r}'_2 > R_0$. The integral (17) represents the convolution of the function $[\varepsilon(\mathbf{r}') - \varepsilon'] g^*(\mathbf{r}', \mathbf{s})$ and $w(r')$ and can be written in the form

$$(18) \quad - \int G^*(\xi, \mathbf{s}) W(\xi) \exp[-i(\mathbf{r}' + \mathbf{r}'')\xi] d\xi,$$

where the integration extends over all space and $W(\xi)$ is the Fourier transform of $w(r')$, i.e.

$$(19) \quad W(\xi) = \frac{1}{(\sqrt{2\pi})^3} \int w(r') \exp[i\xi r'] dr',$$

the whole space being the integration field, and $G^*(\xi, \mathbf{s})$ is the transform (13).

The part of the autocorrelation function $\gamma(\mathbf{r}'', \mathbf{s})$, which is due to the correlations between different cells, is thus

$$(20) \quad \gamma_n(\mathbf{r}'', \mathbf{s}) = - \frac{\int \left\{ \int G^*(\xi, \mathbf{s}) W(\xi) \exp[-i(\mathbf{r}' + \mathbf{r}'')\xi] d\xi \right\} [\varepsilon(\mathbf{r}') - \varepsilon'] g(\mathbf{r}', \mathbf{s}) d\mathbf{r}'}{\int [\varepsilon(\mathbf{r}') - \varepsilon']^2 d\mathbf{r}'}$$

For the evaluation of the convolution in the numerator of (20) we need the Fourier transform of the function (18)

$$(21) \quad - \frac{1}{(\sqrt{2\pi})^3} \int \left\{ \int G^*(\xi, \mathbf{s}) W(\xi) \exp[-ir'\xi] d\xi \right\} \exp[i\eta r'] dr' = \\ = - (\sqrt{2\pi})^3 G^*(\eta, \mathbf{s}) W(\eta).$$

The integration extends here over all space. Hence,

$$(22) \quad \gamma_{II}(\mathbf{r}'', \mathbf{s}) = -\frac{\sqrt{(2\pi)^3} \int G(\boldsymbol{\eta}, \mathbf{s}) G^*(\boldsymbol{\eta}, \mathbf{s}) W(\boldsymbol{\eta}) \exp [i\mathbf{r}''\boldsymbol{\eta}] d\boldsymbol{\eta}}{\int G(\boldsymbol{\eta}, \mathbf{s}) G^*(\boldsymbol{\eta}, \mathbf{s}) d\boldsymbol{\eta}}.$$

The approximation, which we made in (17) and (20) taking all the cells as mutually equal, is here quite justified. Namely those volume elements of the scatterers, for which the points in the realtive position \mathbf{r}'' also lie in some of the neighboring scatterers, contribute far most to the value of $\gamma_{II}(\mathbf{r}'', \mathbf{s})$.

Summing (14) and (22) we obtain the final expression for the autocorrelation function

$$(23) \quad \gamma(\mathbf{r}'', \mathbf{s}) = \frac{\int G(\boldsymbol{\eta}, \mathbf{s}) G^*(\boldsymbol{\eta}, \mathbf{s}) [1 - (\sqrt{2\pi})^3 W(\boldsymbol{\eta})] \exp [i\mathbf{r}''\boldsymbol{\eta}] d\boldsymbol{\eta}}{\int G(\boldsymbol{\eta}, \mathbf{s}) G^*(\boldsymbol{\eta}, \mathbf{s}) d\boldsymbol{\eta}}.$$

We have now the needed data for the calculation of the angular distribution of the flux of waves emerging from the planparallel sheet of the inhomogeneous medium. The angular distribution is given by the formula (G 43)

$$(24) \quad I(\theta, d) = \frac{I_0}{2\pi} \int_0^\infty \exp [d(H(\alpha) - H(0))] J_0(\theta\alpha) \alpha d\alpha,$$

where I_0 is the flux of the incident waves and θ the angle of scattering. Further $H(\alpha)$ is the Bessel-Fourier transform of the function $h(\theta)$ defined by (G 38)

$$(25) \quad h(\theta) = \frac{\pi^2 \langle \Delta \varepsilon(\mathbf{r}) \Delta \varepsilon^*(\mathbf{r}) \rangle}{\lambda^4} E(\theta).$$

The function $E(\theta)$ is the transform (G 25) of the autocorrelation function $\gamma(\mathbf{r}'', \mathbf{s})$, θ being the angle between the directions \mathbf{s} and \mathbf{s}_1 and $k' = 2\pi n'/\lambda$. We consider here only small angle scatterings so that the vector $\mathbf{s} - \mathbf{s}_1$ is nearly perpendicular to the direction \mathbf{s}_1 and $|\mathbf{s} - \mathbf{s}_1|$ nearly equal to ϑ . We have

$$(26) \quad h(\theta) = h(\mathbf{s}, \mathbf{s}_1) = \\ = \frac{N}{V} \frac{\pi^2}{\lambda^4} (2\pi)^3 \left\{ G(k'(\mathbf{s} - \mathbf{s}_1), \mathbf{s}_1) G^*(k'(\mathbf{s} - \mathbf{s}_1), \mathbf{s}_1) [1 - (\sqrt{2\pi})^3 W(k'(\mathbf{s} - \mathbf{s}_1))] \right\}.$$

Due to the fact, that $\varepsilon(\mathbf{r}') - \varepsilon'$ is the spherically symmetrical function, the evaluation of $G(k'(\mathbf{s} - \mathbf{s}_1), \mathbf{s}_1)$ can be very simplified. The function $[\varepsilon(\mathbf{r}') - \varepsilon'] g(\mathbf{r}', \mathbf{s}_1)$ axially symmetric with regard to the line passing through the origin of the co-ordinate system in the direction \mathbf{s}_1 . We may perform the integration in (13) first over the surface of a cylinder, whose axis is the line of the direction \mathbf{s}_1 and whose radius is ϱ . Thus we obtain, taking

into account the relation between $\varepsilon(\mathbf{r}') - \varepsilon'$ and $g(\mathbf{r}', \mathbf{s})$ as is given by (G 13) and (5),

$$(27) \quad G(k'(\mathbf{s} - \mathbf{s}_1), \mathbf{s}_1) = \frac{n'\lambda}{i\pi} \frac{1}{\sqrt{2\pi}} \int_0^{R_0} \left\{ \exp [i\varphi(\varrho)] - 1 \right\} J_0(k'\varrho) \varrho d\varrho,$$

where $\varphi(\varrho)$ is the total phase shift of the ray passing through the cell at the distance ϱ from the center.

Substituting the expression (27) in (26) we obtain the following formula for $h(\vartheta)$

$$(28) \quad h(\vartheta) = \frac{N}{V} \left(\frac{n'}{\lambda} \right)^2 \left\{ 2\pi \int_0^{R_0} \left\{ \exp [i\varphi(\varrho)] - 1 \right\} J_0(k'\varrho) \varrho d\varrho \cdot \right. \\ \left. \cdot 2\pi \int_0^{R_0} \left\{ \exp [-i\varphi(\varrho)] - 1 \right\} J_0(k'\varrho) \varrho d\varrho \cdot [1 - (\sqrt{2\pi})^3 W(k'\vartheta)] \right\}.$$

The transform $W(k'(\mathbf{s} - \mathbf{s}'))$ is only a function of the absolute value $|k'(\mathbf{s} - \mathbf{s}_1)|$ and so we may write $W(k'\vartheta)$ instead of $W(k'(\mathbf{s} - \mathbf{s}_1))$.

Putting (28) in the formula for the Bessel-Fourier transform (G 39) and introducing a new variable $u = \alpha/k'$ we obtain

$$(29) \quad H(u) = \frac{N}{V} 2\pi \int_0^{R_0} \int_0^{R_0} \int_0^{\infty} \left\{ \exp [i\varphi(\xi)] - 1 \right\} \left\{ \exp [-i\varphi(\eta)] - 1 \right\} \cdot \\ \cdot [1 - (\sqrt{2\pi})^3 W(\zeta)] J_0(\xi\zeta) J_0(\eta\zeta) J_0(u\zeta) \xi\eta\zeta d\xi d\eta d\zeta.$$

It is convenient for the later calculation of $H(u)$ to divide the integral (29) in two parts

$$(30) \quad H(u) = \frac{N}{V} [H_1(u) - H_2(u)],$$

where

$$(31) \quad H_1(u) = 2\pi \int_0^{R_0} \int_0^{R_0} \int_0^{\infty} \left\{ \exp [i\varphi(\xi)] - 1 \right\} \cdot \\ \cdot \left\{ \exp [-i\varphi(\eta)] - 1 \right\} J_0(\xi\zeta) J_0(\eta\zeta) J_0(u\zeta) \xi\eta\zeta d\xi d\eta d\zeta,$$

and

$$(32) \quad H_2(u) = 2\pi \int_0^{R_0} \int_0^{R_0} \int_0^{\infty} \left\{ \exp [i\varphi(\xi)] - 1 \right\} \cdot \\ \cdot \left\{ \exp [-i\varphi(\eta)] - 1 \right\} (\sqrt{2\pi})^3 W(\zeta) J_0(\xi\zeta) J_0(\eta\zeta) J_0(u\zeta) \xi\eta\zeta d\xi d\eta d\zeta.$$

The term $H_2(u)$ is due only to the influence of the neighboring scatterers on the scattering of a single isolated scatterer. The important part of this influence is included also in the first term $H_1(u)$, namely indirectly in the value of ε' and R_0 .

Before we proceed to the discussion of the methods for the evaluation of the integrals $H_1(u)$ and $H_2(u)$, we wish to derive another expression for $H(\alpha)$, which is of some interest.

In the formula (G 39) we substitute $h(\vartheta)$ by the expression (G 38) with $E(\vartheta)$ given by (G 26). Changing the order of the integration we have

$$(33) \quad H(\alpha) = \frac{\pi^2 \langle \Delta\varepsilon(\mathbf{r}) \Delta\varepsilon^*(\mathbf{r}) \rangle}{\lambda^4} 4\pi^2 \int_0^\infty dr \int_0^\pi d\beta \gamma(r, \cos \beta) r^2 \sin \beta \cdot \\ \cdot \int_0^\infty J_0(k'r \sin \beta \vartheta) J_0(\alpha \vartheta) \vartheta d\vartheta.$$

The value of the last integral is $\delta(k'r \sin \beta - \alpha)/\alpha$, where $\delta(k'r \sin \beta - \alpha)$ denotes the Dirac δ function. Integrating over β we obtain

$$(34) \quad H(u) = \frac{\pi^2}{\lambda^2} \frac{\langle \Delta\varepsilon(\mathbf{r}) \Delta\varepsilon^*(\mathbf{r}) \rangle}{\varepsilon'} \int_{-\infty}^{+\infty} \gamma \left(\sqrt{u^2 + s^2}, \frac{s}{\sqrt{u^2 + s^2}} \right) ds.$$

This integral represents the integration of the autocorrelation function $\gamma(\mathbf{r}'', \mathbf{s})$ along the line with direction \mathbf{s} and distance $u = \alpha/k'$ from the origin of the co-ordinate system. The formula (34) gives a simple connection between the autocorrelation function $\gamma(\mathbf{r}'', \mathbf{s})$ and $H(\alpha)$.

3. – Evaluation of $H_1(u)$.

In the formula (31) we first perform the integration over ζ . The value of the integral containing three Bessel functions of zero order under the integral sign is

$$(35) \quad \int_0^\infty J_0(\xi\zeta) J_0(\eta\zeta) J_0(u\zeta) \zeta d\zeta = \frac{1}{2\pi A},$$

(WATSON (2), p. 411), where A is the area of a triangle having the sides ξ , η , u , if the construction of such a triangle is possible. In the contrary case the

(2) G. N. WATSON: *A Treatise on the Theory of Bessel Functions* (London, 1952).

value of the integral is zero. Hence, we have

$$(36) \quad H_1(u) = \iint \{ \exp [i\varphi(\xi)] - 1 \} \cdot \{ \exp [-i\varphi(\eta)] - 1 \} \frac{\xi\eta}{4} d\xi d\eta.$$

The field of integration in the (ξ, η) plane is shown in Fig. 1.

Using new variables $x = (\xi + \eta)/\sqrt{2}$, $y = (\xi - \eta)/\sqrt{2}$ and writing

$$(37) \quad f(x, y) = \left\{ \exp \left[i\varphi \left(\frac{x+y}{\sqrt{2}} \right) \right] - 1 \right\} \left\{ \exp \left[-i\varphi \left(\frac{x-y}{\sqrt{2}} \right) \right] - 1 \right\},$$

we obtain from (36) that

$$(38) \quad H_1(u) = \iint \frac{f(x, y)(x^2 - y^2)}{\sqrt{x^2 - \omega^2} \sqrt{\omega^2 - y^2}} dx dy,$$

where $\omega = u/\sqrt{2}$.

The evaluation of the integral (38) is usually difficult. Fortunately it suffices, if the thickness d of the inhomogeneous medium is great enough, to know the function $H(u)$ only in the immediate neighborhood of the point $u = 0$. In this case the field of integration is a very narrow strip along the axis x of the co-ordinate system. We divide the field of integration in three parts I, II and III. The division is made with the lines $x = \varepsilon''$ and $x = \sqrt{2}R_0 - \varepsilon''$; ε'' being some small constant, but greater than ω .

To perform the integration in the first integration field we substitute in (38) $f(x, y)$ by its expansion in Taylor series of ascending powers of x and y , if this expansion is possible. We choose the constant ε'' small enough to ensure the convergence of the series. Integrating over x from ω to ε'' and over y from $-\omega$ to $+\omega$ term by term we obtain

$$(39) \quad \pi \left\{ -\frac{\omega^2}{4} f(0, 0) - \frac{\omega^4}{16} \left[\frac{3}{4} \frac{\partial^2 f(0, 0)}{\partial x^2} + \frac{\partial^2 f(0, 0)}{\partial y^2} \right] + \frac{\omega^4}{16} \left(\log \frac{2}{\omega} \right) \left[\frac{\partial^2 f(0, 0)}{\partial x^2} - \frac{\partial^2 f(0, 0)}{\partial y^2} \right] + \dots \right\} + O(\varepsilon'').$$

Here $O(\varepsilon'')$ represents the series of powers of ε'' and terms with $\log \varepsilon''$. As the value of $H_1(u)$ does not depend on the choice of ε'' , all the terms in the series $O(\varepsilon'')$ must be concealed after the summation of the integrals over the fields I and II. Therefore we do not give the explicit expression for $O(\varepsilon'')$.

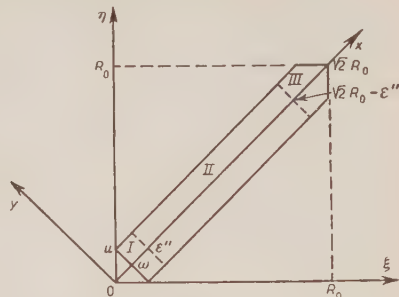


Fig. 1.

The integration in the second field can easily be performed, if it is possible to expand the function $f(x, y)$ into a series of ascending powers of y for all values of x in the interval $(\epsilon'', \sqrt{2}R_0 - \epsilon'')$. Integrating over y from $-\omega$ to $+\omega$ term by term we have

$$(40) \quad \pi \int_{\epsilon''}^{\sqrt{2}R_0 - \epsilon''} \frac{dx}{\sqrt{x^2 - \omega^2}} \left\{ x^2 \left[f(x, 0) + \frac{1}{2} \frac{\omega^2}{2!} \frac{\partial^2 f(x, 0)}{\partial y^2} + \frac{1 \cdot 3}{2 \cdot 4} \frac{\omega^4}{4!} \frac{\partial^4 f(x, 0)}{\partial y^4} + \dots \right] - \right. \\ \left. - \omega^2 \left[\frac{1}{2} f(x, 0) + \frac{1 \cdot 3}{2 \cdot 4} \frac{\omega^2}{2!} \frac{\partial^2 f(x, 0)}{\partial y^2} + \dots \right] \right\}.$$

Now we expand $1/\sqrt{x^2 - \omega^2}$ into a series of ascending powers of ω/x and than we integrate over x term by term. We need here usually only few of the first terms.

The third integration field is small. To perform the integral (38) over this field we may therefore substitute the function $f(x, y)$ in the integrand by some approximate expression for $f(x, y)$, if we so facilitate the integration. Further we expand the function $1/\sqrt{x^2 - \omega^2}$ in the integrand, as in the former case, into a series of ascending powers of ω/x .

4. – Evaluation of $H_2(u)$.

Due to the spherical symmetry of the average distribution of the scatterers around a chosen one we substitute in the formula (32) for $H_2(u)W(\zeta)$ by

$$(41) \quad W(\zeta) = \frac{1}{(\sqrt{2}\pi)^3} \int_0^\infty 4\pi r'^2 w(r') \frac{\sin \zeta r'}{\zeta r'} dr' = \frac{1}{(\sqrt{2}\pi)^3} \sqrt{\frac{\pi}{2}} \int_0^\infty 4\pi r'^2 w(r') \frac{J_{\frac{1}{2}}(\zeta r')}{(\zeta r')^{\frac{1}{2}}} dr'.$$

Further, using the Gegenbauer integral expression for the product of two Bessel functions of the same order (WATSON, l. c., p. 367), we write in (32)

$$(42) \quad J_0(\xi\zeta)J_0(\eta\zeta) = \frac{1}{\pi} \int_0^\pi J_0(v\zeta) \alpha' d\alpha',$$

where $v = \sqrt{\xi^2 + \eta^2 - 2\xi\eta \cos \alpha'}$. Thus we obtain.

$$(43) \quad H_2(u) = 2\pi \int_0^{R_0} d\xi \int_0^{R_0} d\eta \int_0^\pi \xi \eta \{ \exp[i\varphi(\xi)] - 1 \} \{ \exp[-i\varphi(\eta)] - 1 \} \cdot \\ \cdot \frac{1}{\pi} \int_0^\pi d\alpha' \int_0^\infty dr' 4\pi r'^2 w(r') \sqrt{\frac{\pi}{2}} \int_0^\infty \frac{J_{\frac{1}{2}}(r'\zeta)}{(r'\zeta)^{\frac{1}{2}}} J_0(r\zeta) J_0(u\zeta) d\zeta.$$

The last integral in (43) can be evaluated (WATSON, i.e., p. 411) and we get

$$(44) \quad H_2(u) = 2\pi \int_0^{R_0} \int_0^{R_0} d\xi d\eta \xi \eta \{ \exp[i\varphi(\xi)] - 1 \} \{ \exp[-i\varphi(\eta)] - 1 \} \cdot \\ \cdot \frac{1}{\pi} \int_0^{\pi} d\alpha' \int_0^{\infty} dr' 4\pi r' w(r') \frac{1}{\pi} \int_0^A \frac{d\beta'}{\sqrt{r'^2 - v^2 - u^2 + 2vu \cos \beta'}} ,$$

where the value of A is

$$(45) \quad A = \begin{cases} 0 & ; \quad r' < |v - u|, \\ \arccos\left(\frac{v^2 + u^2 - r'^2}{2vu}\right) & ; \quad |v - u| < r' < |v + u|, \\ \pi & ; \quad r' > |v + u|. \end{cases}$$

The further evaluation of $H_2(u)$ depends on the analytical form of the function $w(r')$. The example for this is given in the following section.

5. – The multiple scattering by spheres.

In this section we shall give an example for the application of the theory. Let the scatterers be dielectric spheres of dielectric constant ϵ_1 and of radius r_0 . Further we assume, that the average distribution of the scatterers around a chosen one is given by the Gauss probability function, i.e.

$$(46) \quad w(r') = \frac{N}{V} \exp[-r'^2/l^2] ,$$

where $l = (1/\sqrt{\pi})\sqrt[3]{V/N}$, to fulfill the condition (3).

In this case the total phase shift of the ray passing through the spherically symmetrical cell at the distance ϱ from the center is

$$(47) \quad \varphi(\varrho) = \varphi_1(\varrho) - \varphi_2(\varrho) ,$$

where

$$(48) \quad \varphi_1(\varrho) = \begin{cases} b_1 \sqrt{1 - \varrho^2/r_0^2} ; & \varrho < r_0 \\ 0 & ; \quad \varrho > r_0 , \end{cases}$$

with $b_1 = 4\pi(n_1 - n)r_0/\lambda$, n_1 being $\sqrt{\varepsilon_1}$ and n is $\sqrt{\varepsilon}$, and

$$(49) \quad \varphi_2(\varrho) = b_2 \sqrt{1 - \varrho^2/R_0^2},$$

with $b_2 = 4\pi(n' - n)R_0/\lambda$. Here b_2 is much smaller than b_1 . To satisfy the restriction (7) b_2 must be also much smaller than 1.

We shall evaluate here only a few terms of the expansion of $H(u)$ into a series of terms containing ascending powers of u . We shall calculate only the terms with less than the fourth power of u . Further we shall neglect the terms containing $\varphi_2(\varrho)$ or b_2 in the square, as b_2 is small.

Using the expression (47) for $\varphi(\varrho)$ we obtain

$$(50) \quad \begin{aligned} & \{\exp[i\varphi(\xi)] - 1\}\{\exp[-i\varphi(\eta)] - 1\} \approx \\ & \approx \{\exp[i\varphi_1(\xi)] - 1\}\{\exp[-i\varphi_1(\eta)] - 1\} + \\ & + i\varphi_2(\eta)\{\exp[i\varphi_1(\xi)] - 1\} - i\varphi_2(\xi)\{\exp[-i\varphi_1(\eta)] - 1\} - \\ & - i[\varphi_2(\xi) - \varphi_2(\eta)]\{\exp[i\varphi_1(\xi)] - 1\}\{\exp[-i\varphi_1(\eta)] - 1\}. \end{aligned}$$

Inserting this function in the formula (36) we can see that the last term of (50) contributes very little to $H_1(u)$ in comparison with the first three terms. The difference $\varphi_2(\xi) - \varphi_2(\eta)$ is namely small and besides the imaginary part of the integral

$$(51) \quad \iint \{\exp[i\varphi_1(\xi)] - 1\}\{\exp[-i\varphi_1(\eta)] - 1\} \frac{\xi\eta}{A} d\xi d\eta,$$

is zero. So we neglect this term. Thus we obtain the following approximate expression for $H_1(u)$

$$(52) \quad \begin{aligned} H_1(u) = & \iint \{\exp[i\varphi_1(\xi)] - 1\}\{\exp[-i\varphi_1(\eta)] - 1\} \frac{\xi\eta}{A} d\xi d\eta - \\ & - 2 \iint \varphi_2(\eta) \sin \varphi_1(\xi) \frac{\xi\eta}{A} d\xi d\eta. \end{aligned}$$

In the second integral of (52) we approximate $\varphi_2(\eta)$ with $b_2(1 - \eta^2/2R_0^2)$, as η is much smaller than R_0 throughout the whole integration field.

The evaluation of the integrals (52) follows chiefly the way outlined in section 3. The integration field is in this case smaller due to the approximation made for $\varphi(\varrho)$. Here we make the division between the second and the third field of integration by the line $x = \sqrt{2}r_0 - \varepsilon''$. Note, that the field III for the second integral of (52) is different from the field III for the first integral.

To perform the integration in the field III we put

$$(53) \quad \left\{ \exp \left[i\varphi_1 \left(\frac{x+y}{\sqrt{2}} \right) \right] - 1 \right\} \left\{ \exp \left[-i\varphi_1 \left(\frac{x-y}{\sqrt{2}} \right) \right] - 1 \right\} \approx \\ \approx \frac{\sqrt{2}b_1^2}{r_0} \sqrt{(\sqrt{2}r_0 - x)^2 - y^2},$$

and

$$(54) \quad \varphi_2 \left(\frac{x-y}{\sqrt{2}} \right) \sin \left[\varphi_1 \left(\frac{x+y}{\sqrt{2}} \right) \right] \approx \frac{\sqrt{2}b_1 b_2}{\sqrt{r_0}} \left(1 - \frac{r_0^2}{2R_0^2} \right) \sqrt{(\sqrt{2}r_0 - x) + y},$$

as in this field the difference $z = \sqrt{2}r_0 - x$ is small. Further we retain in the integrand of the integral (38) only the terms, which contribute mostly to the result. Therefore we approximate this integral in the field III by

$$(55) \quad \sqrt{2}r_2 \iint \frac{f(x, y)}{\sqrt{\omega^2 - y^2}} dx dy.$$

Introducing a new variable $z = \sqrt{2}r_0 - x$ and first integrating over z and than over y , we obtain for the value of the first integral of (52) over the field III

$$(56) \quad \pi b_1^2 \frac{\omega^2}{2} \left[\left(\log \frac{\omega}{2} - \frac{1}{2} \right) + \frac{4}{\pi} \int_0^1 \frac{x^2 \log x}{\sqrt{1-x^2}} dx \right] + O(\varepsilon''),$$

where $O(\varepsilon'')$ represents, as in (39), the series of powers of ε'' and terms with $\log \varepsilon''$, and must be dropped in the final result. The value of the integral in (56) is $(\pi/4)(\frac{1}{2} - \log 2)$ (GRÖBNER (3), p. 79). Hence, (56) reads

$$(57) \quad \pi b_1^2 \frac{\omega^2}{2} \log \frac{\omega}{4} + O(\varepsilon'').$$

The second integral of (52) over the field III contains only the terms $O(\varepsilon'')$.

Summing the integrals over the three fields and introducing a new variable $x = bu/r_0$ we finally obtain the following result for $H_1(u)$

$$(58) \quad H_1(u) = 2\pi r_0^2 \left(1 - \frac{2 \sin b_1}{b_1} - \frac{2 \cos b_1}{b_1^2} + \frac{2}{b_1^3} \right) - \\ - 4\pi r_0^2 \frac{b_2}{b_1} \left| \frac{\sin b_1}{b_1} - \cos b_1 + \left(\frac{r_0}{R_0} \right)^2 \frac{1}{b_1} \left(\sin b_1 + \frac{3 \cos b_1}{b_1} - \frac{3 \sin b_1}{b_1^2} \right) \right| + \\ + \pi r_0^2 \frac{x^2}{4} \left[\log \frac{x}{4b_1} + 8 \left(\frac{r_0}{R_0} \right)^2 \frac{b_2}{b_1^3} \left(\frac{\sin b_1}{b_1} - \cos b_1 \right) \right].$$

(3) W. GRÖBNER and N. HOFREITER: *Integraltafeln* (Wien, 1950).

There remains the calculation of $H_2(u)$. We substitute in the formula (44) $w(r')$ by (46) and than we integrate over r' from $r' = \sqrt{v^2 + u^2 - 2ru \cos \beta'}$ to $r' = \infty$. We obtain

$$(59) \quad H_2(u) = \frac{N}{V} 4\pi^2 \sqrt{\pi} l \exp[-u^2/l^2] \int_0^{R_0} \int_0^{R_0} d\xi d\eta \xi \eta \{ \exp[i\varphi(\xi) - 1] \cdot \\ \cdot \{ \exp[-i\varphi(\eta)] - 1 \} \frac{1}{\pi} \int_0^\pi d\alpha' \exp[-v^2/l^2] \frac{1}{\pi} \int_0^\pi \exp[2vu \cos \beta'/l^2] d\beta' .$$

Now we integrate over β' . Thus

$$(60) \quad H_2(u) = \frac{N}{V} 4\pi^2 \sqrt{\pi} l \exp[-u^2/l^2] \int_0^{R_0} \int_0^{R_0} d\xi d\eta \xi \eta \{ \exp[i\varphi(\xi) - 1] \cdot \\ \cdot \{ \exp[-i\varphi(\eta)] - 1 \} \frac{1}{\pi} \int_0^\pi \exp[-v^2/l^2] I_0(2vu/l^2) d\alpha' .$$

We must know the function $H_2(u)$ only for the small values of u . Therefore we expand the modified Bessel function $I_0(2ru/l^2)$ into a series and than we integrate over α' term by term. Retaining only the first two terms of the series we obtain

$$(61) \quad H_2(u) = \frac{N}{V} 4\pi^2 \sqrt{\pi} l \exp[-u^2/l^2] \int_0^{R_0} \int_0^{R_0} \{ \exp[i\varphi(\xi)] - 1 \} \cdot \\ \cdot \{ \exp[-i\varphi(\eta)] - 1 \} \{ [1 + u^2(\xi^2 + \eta^2)/l^4] I_0(2\xi\eta/l^2) + \\ + 2u^2(\xi\eta/l^4) I_1(2\xi\eta/l^2) \} \exp[-(\xi^2 + \eta^2)/l^2] \xi\eta d\xi d\eta .$$

We make a small error in the value of $H_2(u)$, if we substitute $\varphi(\varrho)$ in (61) by $\varphi_1(\varrho)$; the integration field being now a square of the sides r_0 . Further we expand $H_2(u)$ into a series of decreasing powers of l . If the system of scatterers is not too dense, ξ and η of the new integration field are small in comparison with l . Therefore we are satisfied with the first terms of the series. Hence the following approximation for $H_2(u)$

$$(62) \quad H_2(u) = \frac{N}{V} 4\pi^2 \sqrt{\pi} l \int_0^{r_0} \int_0^{r_0} \{ \exp[i\varphi_1(\xi)] - 1 \} \{ \exp[-i\varphi_1(\eta)] - 1 \} \cdot \\ \cdot \left(1 - \frac{\xi^2 + \eta^2}{l^2} - \frac{u^2}{l^2} \right) \xi\eta d\xi d\eta = \\ = H_2(0) - \pi r_0^2 u^2 \left(\frac{r_0}{l} \right)^4 \frac{1}{b_1^2} \left[\left(1 - \frac{2 \sin b_1}{b_1} - \frac{2 \cos b_1}{b_1^2} + \frac{2}{b_1^2} \right)^2 + \frac{4}{b_1^2} \left(\frac{\sin b_1}{b_1} - \cos b_1 \right)^2 \right] .$$

In the evaluation of the last term of (62) we took into account the relation between l and V/N , i.e. $l = (1/\sqrt{\pi})\sqrt{V/N}$. We do not give here the explicit expression for $H_2(0)$, as this term is not of interest and also does not appear in the formula for the angular distribution of the scattered waves.

Substituting (58) and (62) in (30) to obtain $H(u)$ and than inserting $H(u)$ in (24) we get the final formula for the angular distribution of the flux of waves, multiply scattered by spheres

$$(63) \quad I(\theta, d) = \frac{I_0}{2\pi} \left(\frac{k'r_0}{b_1} \right)^2 \int_0^t \exp \left[\frac{N}{V} \pi r_0^2 d \frac{x^2}{4} \left\{ \log \frac{x}{4b_1} + \right. \right. \\ + 8 \left(\frac{r_0}{R_0} \right)^2 \frac{b_2}{b_1^3} \left(\frac{\sin b_1}{b_1} - \cos b_1 \right) + 4 \left(\frac{r_0}{R_0} \right)^4 \frac{1}{b_1^2} \left(\left(1 - \frac{2 \sin b_1}{b_1} - \frac{2 \cos b_1}{b_1^2} + \frac{2}{b_1^2} \right)^2 + \right. \\ \left. \left. + \frac{4}{b_1^2} \left(\frac{\sin b_1}{b_1} - \cos b_1 \right)^2 \right) \right] J_0 \left(\frac{k'r_0 \theta}{b_1} x \right) x dx .$$

We replaced here the integration over x from 0 to ∞ by the integration in the finite limits from 0 to t , where t is a constant great enough for the value of the integral to depend very little on the choice of it. But the constant t must not be too great, as otherwise the exponential function of the integrand begins to increase at greater values of the argument because of the logarithmic term in the exponent. This increase of the value of the integrand is not real, it is only caused by the use of the approximate expression for $H(u)$ instead of the exact. The integral (63) is of the Molière's type ⁽⁴⁾. MOLIÈRE gives more strict arguments for this method. He also evaluated the integral of type (63) in the form of quickly convergent series.

The formula (63) gives some interesting features of the multiple scattering by spheres. The angular distribution of the waves, multiply scattered by spheres, is similar to the angular distribution of the electrons passing through thin metal foils.

The factor $(N/V)\pi r_0^2 d$ in the exponent of the integrand of (63) can be interpreted as the average number of the scatterings of a ray passing through the inhomogeneous medium, if we assume the scattering cross-section of the spheres to be equal to their geometrical cross-section. The real scattering cross-section σ differs a lot from the geometrical cross-section and is given, in the case of a rare system, by the first term in the formula (58)

$$(64) \quad \sigma = 2\pi r_0^2 \left(1 - \frac{2 \sin b_1}{b_1} - \frac{2 \cos b_1}{b_1^2} + \frac{2}{b_1^2} \right) .$$

⁽⁴⁾ G. MOLIÈRE: *Zeits. f. Naturforsch.*, **3a**, 78 (1948).

The cross-section σ , as function of b_1 , oscillates and at greater values of b_1 approaches the double value of the geometrical cross-section (Fig. 2). This

is in accord with Mie's theory. It is of interest, that the oscillatory nature of σ does not appear in the formula for $I(\theta, d)$. The term in the exponent of (63), which corresponds to the scattering by isolated scatterers, i.e. $(N/V)\pi r_0^2 d(x^2/4) \log(x/4b_1)$, has no oscillatory tendency. This can be explained by the fact, that the scatterings at greater angles chiefly determine the shape of the angular distribution function. But the oscillatory nature of σ is due

to the modifications of the scattering distribution function of a isolated sphere at very small angles.

The other terms in the exponent of (63) besides $(N/V)\pi r_0^2 d(x^2/4) \log(x/4b_1)$ are result of the mutual influence of the neighboring scatterers. These terms are only important in dense systems, for instance if $R_0 \approx 2r_0$. We have not given attention in this paper to the exact determination of b_2 by the solution of the equations (6), as it appears only in the correction terms. We make a very small error, if we put $\epsilon' = \langle \epsilon \rangle$. With this approximation we have $(n' - n)/(n_1 - n) = (r_0/R_0)^3$ and $b_2/b_1 = (r_0/R_0)^2$. As an example we consider the multiple scattering of light ($\lambda = 5 \cdot 10^{-5}$ cm) by dielectric spheres ($r_0 = 5 \cdot 10^{-3}$ cm, $n_1 - n = 10^{-3}$) embedded in the sheet of an optically homogeneous medium ($d = 10$ cm, $n = 1.5$, $N/V = 25 \cdot 10^4$ cm $^{-3}$). Substituting these values in (63) we see, that in a great part of the integration interval the value of the exponent function in the integrand is over ten per cent greater due to the correction terms. The influence of the correction terms on the angular distribution is greater for smaller b_1 .

Our determination of the first and second correction term in the exponent of (63) is too approximate for very dense systems with $R_0 < 2r_0$. In such a case we cannot approximate the cells with spheres. The first correction term is due to the curvature of the surface of the cell, as can be seen from the evaluation of the second integral of (52). The shape of the cell has great influence on the value of this correction term. Also our way of evaluation of $H_1(u)$ is too approximate for small values of R_0 . The same holds about the evaluation of $H_2(u)$. Here however much work remains to be done.

For some experimental evidence of the validity of the formula (63) and for the comparison of our result with the other theories of the multiple scattering by spheres see GOSAR (5).

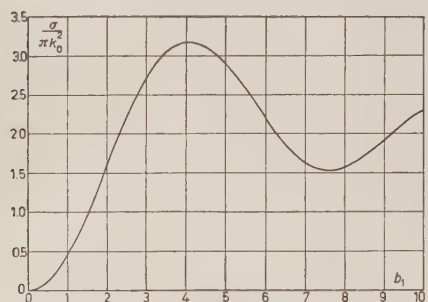


Fig. 2.

(5) P. GOSAR: *Razprave SAZU* (Ljubljana, in press).

RIASSUNTO

La teoria dello scattering multiplo pubblicata dall'autore in un articolo recente è estesa al caso di un mezzo non omogeneo composto di centri di scattering eguali e di simmetria centrale racchiusi in un mezzo omogeneo. Si presenta un nuovo metodo per il calcolo numerico della distribuzione angolare delle onde disperse. Come esempio si discute lo scattering multiplo da parte di sfere dielettriche. In questo caso la distribuzione angolare delle onde disperse è simile alla distribuzione angolare degli elettroni attraverso lamine metalliche. Si mostra che la interazione mutua delle sfere ha una influenza sulla distribuzione angolare, se la distanza media fra le sfere vicine è dell'ordine del loro diametro.

Radiation from ^{192}Pt and Proposed Decay Scheme (*).

M. S. HUQ

Physics Department, Dacca University - East Pakistan

(ricevuto il 7 Febbraio 1957)

Summary. — By bombarding a gold target at proton energy of 61 MeV the isotopes ^{192}Pt and ^{191}Pt were indirectly produced. Photographs were taken with the help of a 180° focussing β -ray spectrograph. Of the 207 lines examined, 170 were identified. Those assigned to ^{192}Pt and ^{191}Pt are given in separate tables. Assignments were aided by intensity measurements under the high resolution of a 180° β -ray spectrometer with crystal detector. A tentative decay scheme for ^{192}Pt was also made.

1. — Introduction.

This investigation is concerned with the radiations from the isotopes ^{192}Pt and ^{191}Pt which have been indirectly produced by $^{197}\text{Au}(\text{p} \cdot 6\text{n})^{192}\text{Hg}$ and $\text{Au}(\text{p} \cdot 7\text{n})^{191}\text{Hg}$ reactions in the McGill 100 MeV cyclotron. The activated mercury decays to gold by electron capture and gold in its turn decays to Pt by the same process.

A large number of techniques are now available for the study of radioactive decay schemes. The most powerful methods today, involve mainly the use of spectrographs. First a γ -ray spectrum may be taken of a radioactive source to give a quick indication of most of the activities. Once these activities are established in a rough way, the β -ray spectrometers can be used for accurate determination of half-lives, relative intensities and conversion coefficients of internal conversion lines. Finally the high resolution 180° spectrograph is used to establish fine structures and to find exact energy levels.

(*) This work was done in the Radiation Laboratory, McGill University, Montréal, Canada.

Additional information concerning the fine structures is supplied by a 180° spectrometer.

We used in our investigations a 180° β -ray spectrograph for fine structure studies and a 180° β -ray spectrometer for determining the intensities of the conversion lines and the half-lives of faint lines close to the strong ones. These instruments have relative advantages over each other in their respective fields. Thus in the present investigation the information gained from the plates of the spectrographs is supplemented by the runs in the spectrometer.

2. - Experimental.

Chemically pure gold (197) sheets of 0.001 in. thickness were used as target material. These sheets were bombarded in the 100 MeV McGill Proton Cyclotron at different energies. In order to find out a suitable exciting voltage necessary for the highest activity of the particular isotope ^{192}Hg , the target was bombarded at 50, 55, 60, 65, 70 MeV proton energy. A typical excitation curve of Fig. 1 shows that at a bombarding energy of 61 MeV mass 192 gives the highest activity. Thus 61 MeV was the exciting voltage for this investigation. Bombardment for one hour gave strong activity and therefore was used in all subsequent work. Within fifteen minutes after bombardment the active mercury was evaporated and deposited on an aluminium block along a central line of 0.002 in. width.

This central line of active Hg served as a line source. After deposition, a period of two hours was allowed in every case for the decay of active mercury. Then the sources were heated for 15 min. Hg by K capture and β^+ emission decays to gold, gold decays to Pt and active Pt decays to Ir. The source on an Al-block is about four times more active than that on a wire.

Sources prepared in this way were placed inside the 180° β -ray spectrograph⁽¹⁾. Throughout the investigation the slit width remained fixed at 0.100 in.. Eastman X-ray no screen emulsion on glass plates was used in this investigation.

A line corresponding to any moderate energy can be made to fall anywhere on the photographic plate by an appropriate choice of the magnetic field strength.

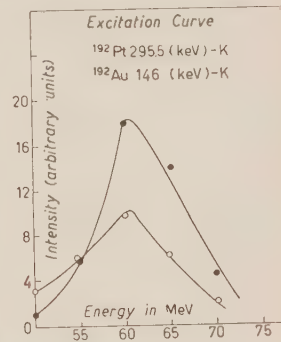


Fig. 1.

⁽¹⁾ F. A. JOHNSON: *Ph. D. Thesis* (McGill University, 1952).

An active source gave 165 lines on a plate at a field strength of about 90 G/cm. About 100 more lines were observed when the field was changed to about 150 G/cm. Photographs are shown in Fig. 2. For each source, exposure times were varied from half an hour to three days. From the resulting plates the decay of different lines was studied. Energy values corresponding to these lines on the plate were calculated from the formula

$$E = 510.98(\sqrt{1 + 0.3443 H^2 \rho^2 \cdot 10^{-6}} - 1).$$

Au 61 MeV-2Hrs. (1)
($H \sim 90$ g/cm)

γ 61 MeV-2Hrs. (2)
($H \sim 155$ g/cm)

Fig. 2.

We got the different values of H^2 from the calibration curve. ρ^2 is related to X^2 by the formula $\rho^2 = (X^2 + 15.0435)/4$. The values of X come from the distances of different lines on the plate. Sources for 180° β -ray spectrometer (²) were prepared in the same way. In this apparatus the photographic plate is replaced by an anthracene crystal detector and an electronic recording apparatus. Source and detector slits were set at 0.14 in. and 0.02 in. respectively and thus we got 0.3% resolution and transmission was satisfactory. A range of 21 cm was scanned in about five hours time. Two count-rate meters with two recorders were connected in parallel. Times were denoted on the chart at the beginning and at end of each scan. The same process was repeated three or four times. Thus a number of charts were obtained. Decay rates and intensities of different lines were computed from the charts.

3. - Results.

Altogether there were 207 lines on the plates for a source excited at a proton energy of 61 MeV. The observed half-lives and the correspondence of different lines with conversion K , L , M , N electrons of different isotopes helped us in making the assignments of different lines. About 170 of them were assigned.

(²) M. A. BADIOUR: *M. Sc. Thesis* (McGill University, 1954).

Most (³⁻⁶) of them corroborate the results previously obtained. Electrons thus observed correspond to conversion lines of ^{195}Au , ^{193}Au , ^{192}Au , ^{191}Au , ^{193}Pt , ^{192}Pt , ^{191}Pt and ^{191}Ir . This is due to the fact that gold decayed to platinum and platinum in its turn decayed to iridium.

In the present work our idea was to observe the radiations from ^{192}Pt and if possible, from ^{191}Pt . We tried to observe as many γ -rays as possible for ^{192}Pt especially in the low energy region. EWAN and THOMPSON (⁴) reported the presence of 16 γ -rays in ^{192}Pt . In the lower energy region we observed a few more, viz. 45, 97, 105,

167 and 308 keV γ -rays of which 45, 97, 308 keV γ -rays fit nicely into the latest decay scheme proposed for ^{192}Pt by TAYLOR and PRINGLE (⁷) from the study of irradiated Ir with the help of a scintillation spectrometer. Further study may help in finding some other levels for fitting 105 and 167 keV new γ -rays. Observed γ -rays with their possible polarity are given in Table I and the proposed decay scheme is shown in Fig. 3.

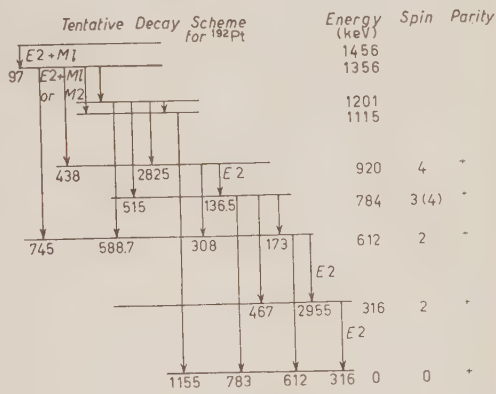


Fig. 3.

TABLE I. — Conversion line designation for ^{192}Pt .

Electron Energy (keV)	γ -Rays (keV)	Designation	Intensity (Arbitrary Units)	Polarity
31.11	44.97	L_I	8	
31.91	45.17	L_{II}	2.0	
33.50	45.05	L_{III}	7.0	
42.17	45.20	M_{II}	1	
18.56	96.91	K	3.5	
82.92	96.79	L_I	1	
85.39	96.94	L_{III}	1	
95.95	96.66	N_I	1.5	$E_2 + M_1$

(³) L. P. GILLON, K. GOPALA KRISHNAN and A. DE-SHALIT: *Phys. Rev.*, **93**, 124 (1954).

(⁴) G. T. EWAN and A. L. THOMPSON: *Trans. Roy. Soc. Canada*, **47**, 126 (1953).

(⁵) J. M. CORK, J. M. LEBLANC, A. E. STODDARD, W. J. CHILDS, C. E. BRANYAN

and D. H. MARTIN: *Phys. Rev.*, **82**, 930 (1952).

(⁶) K. I. ROULSTON and R. W. PRINGLE: *Phys. Rev.*, **87**, 930 (1952).

(⁷) H. W. TAYLOR and R. W. PRINGLE: *Phys. Rev.*, **99**, 1345 (1955).

TABLE I: *continued.*

Electron Energy (keV)	γ -Rays (keV)	Designation	Intensity (Arbitrary Units)	Polarity
26.31	104.66	K	6	
90.89	104.75	L_I	2	M_2
91.45	104.71	L_{II}	0.5	
58.10	136.45	K	6	
123.61	137.47	L_I	8	E_2
124.15	137.41	L_{II}	2.5	
142.91	156.77	L_I	16	E_1 or M_1
143.38	156.64	L_{II}	2	
89.46	167.81	K	3	
153.52	167.40	L_I	1.5	M_3
156.26	167.31	L_{III}	1.0	
126.38	204.73	K	3	$E_2 + M_1$
190.93	204.79	L_I	1	or M_2
203.13	282.48	K	4	
269.60	282.66	L_{II}	9	E_3
217.20	295.55	K	16	
281.34	295.20	L_I	4	
281.96	295.22	L_{II}	5	
283.62	295.17	L_{III}	3.0	E_2
292.12	295.40	M	3	
229.65	308.00	K	9	
294.40	308.26	L_I	4	E_2
237.78	316.13	K	35	
301.93	315.80	L_I	6	
302.40	315.66	L_{II}	7	
304.25	315.80	L_{III}	5	
312.80	315.81	M_{II}	4	
314.95	315.66	N_I	2	
386.89	400.75	L_I	V.W.	
387.76	401.02	L_{II}	V.W.	
401.24	415.40	L_I	4	
359.00	437.35	K	1.5	
388.12	466.47	K	1.5	

γ -rays observed in ^{191}Pt are shown in Table II. Some of them were previously reported by MOON and THOMPSON (⁸).

(⁸) J. H. MOON and A. L. THOMPSON: *Phys. Rev.*, **83**, 892 (1951).

TABLE II. — Conversion line designation for ^{191}Pt .

Electron Energy (keV)	γ -rays (keV)	Designation	Intensity (Arbitrary Units)
34.33	48.20	L_I	2
34.91	48.17	L_{II}	3
36.68	48.23	L_{III}	2
44.91	48.20	M_I	1
39.24	53.10	L_I	15
39.85	53.11	L_{II}	2
50.27	64.10	L_I	15
50.94	64.20	L_{II}	18
77.80	91.06	L_{II}	8
79.50	91.05	L_{III}	9
44.10	122.45	K	1
110.98	122.55	L_{III}	3
33.17	111.52	K	2
97.65	111.52	L_I	2
37.30	115.65	K	3
101.60	115.46	L_I	1.5
51.60	129.95	K	6
115.75	129.62	L_I	4.5
117.31	130.57	L_{II}	0.7
55.15	133.50	K	12
119.00	132.86	L_I	2.5
119.53	132.79	L_{II}	1.5
80.40	158.75	K	4
147.44	161.30	L_I	4
148.38	161.64	L_{II}	V.W.
149.92	161.47	L_{III}	V.W.
136.53	214.88	K	V.W.
201.76	215.02	L_{II}	V.W.
211.73	215.02	M_I	V.W.
214.62	215.33	N_I	V.W.
170.11	248.46	K	2.5
235.51	248.77	L_{II}	1
326.90	405.25	K	V.W.

* * *

The Author wishes to express his gratitude to Prof. J. S. FOSTER, F.R.S., Director of Radiation Laboratory, McGill University, for giving all sorts of facilities for carrying out this research work in his laboratory and he is also thankful to the Government of Canada for financial help during his stay in Canada.

RIASSUNTO (*)

Bombardando un bersaglio d'oro con protoni di 61 MeV di energia furono prodotti indirettamente gli isotopi ^{192}Pt e ^{191}Pt . Furono prese fotografie con l'ausilio di uno spettrografo focalizzatore di 180° a raggi β . Delle 207 righe esaminate se ne identificarono 170. In tabelle separate si riportano quelle assegnate al ^{192}Pt e al ^{191}Pt . Le assegnazioni furono facilitate da misure d'intensità eseguite per mezzo di uno spettrometro di 180° a raggi β con rivelatore a cristallo. Si è anche ipotizzato uno schema di decadimento per il ^{192}Pt .

(*) Traduzione a cura della Redazione.

Measurement of the Alpha Particle Flux at 41° N Geomagnetic Latitude Using Nuclear Emulsions.

B. J. O'BRIEN and J. H. NOON

*The F.B.S. Falkiner Nuclear Research and Adolph Basser Computing Laboratories,
School of Physics (*), The University of Sydney - Sydney, N. S. W., Australia*

(ricevuto il 7 Febbraio 1957)

Summary. — Values obtained for the α -particle flux by counter measurements at 41° N over the U.S.A. are significantly higher than those obtained using nuclear emulsions at 41° N over Sardinia. We have measured the α -particle flux at 41° N over the U.S.A. using nuclear emulsions and the results in agreement with counter measurements are higher than those over Sardinia. These measurements are of interest in view of the proposed modifications to geomagnetic co-ordinates.

Recent measurements have indicated that calculations using geomagnetic co-ordinates based on the centred dipole approximation yield erroneous values for cosmic ray fluxes at certain parts of the earth's surface ^(1,2). Two modifications to the above co-ordinate system have been proposed, which would lead to different calculated cut-off energies and hence different fluxes for places formerly considered to be at the same geomagnetic latitude, but different longitudes. One of these is a theoretical one which involves an eccentric dipole field for the earth rather than a centred dipole ⁽³⁾, while the other is purely empirical.

The value of the α -particle flux at 55° geomagnetic latitude over England (longitude 0°) differs significantly ⁽¹⁾ from that at the same latitude over the U.S.A. (longitude 90° W). The discrepancy may be explained ⁽²⁾ by either of the proposed modifications to the geomagnetic co-ordinates. However the

(*) Also supported by the Nuclear Research Foundation within the University of Sydney.

⁽¹⁾ C. J. WADDINGTON: *Nuovo Cimento*, **3**, 930 (1956).

⁽²⁾ J. A. SIMPSON, K. B. FENTON, J. KATZMANN and D. C. ROSE: *Phys. Rev.*, **102**, 1648 (1956).

⁽³⁾ F. S. JORY: *Phys. Rev.*, **102**, 1167 (1956).

discrepancy by a factor of two between values for the α -particle flux obtained at 41° geomagnetic latitude over Sardinia (longitude 10° E) and over the U.S.A. (90° to 105° W) is too large to be explained by the eccentric dipole field (2).

Since the experiment in Sardinia (4) was carried out with nuclear emulsions whereas values reported (5-9) over U.S.A. were obtained from counter measurements, we believed that it was worth while to measure the flux of primary α -particles in a nuclear emulsion stack flown at 41° N geomagnetic latitude over Texas U.S.A. (longitude 105° W) in February, 1956, so that direct comparison of results obtained by nuclear emulsion techniques, could be made. The stack consisted of 15 600 μm G-5 Ilford stripped emulsions 9 in. \times 10 in., all in contact, flown with vertical orientation of the 9 in. side for around 6 hours at over 110 000 feet (8.6 g/cm^2 residual atmosphere + 2 g/cm^2 packing). Further details can be obtained from a previous report on this stack (10).

The plateau grain density g_{pl} of the plates was found to be (8 ± 0.5) grains/100 μm from measurements on an unbiassed sample of electrons from π - μ -e decays. Scanning was then carried out for tracks with grain density between 3 and 5 times the plateau value. Tracks were traced for 4 cm and counted for 100 grains in the central 400 μm of the emulsion sheets at the beginning and end of this range. Twelve such tracks whose grain density changed by less than 10% over a range of 4 cm or more of emulsion, gave a mean grain density of 34 ± 1 per 100 μm for fast α -particles.

Horizontal line scanning was then carried out with $450\times$ magnification for all tracks entering the scanning sheet from the outside, which had grain density ≥ 25 per 100 μm , projected length ≥ 5 mm in the scanning plate, and projected zenith angle $\leq 45^\circ$. The grain-density acceptance limit is more than two standard deviations below the mean value for alphas. Only those tracks which had a projected length of 7.5 mm or more, and a projected zenith angle of less than 30° , were accepted for tracing and analysis. In the original scan of 45.4 cm 117 such tracks were found, and in a rescan of 22.7 cm, 2 more tracks were found. Scanning efficiency is therefore estimated as 96%. Tracks accepted for analysis were traced until they led to a star or had travelled at least 4 cm (16 g/cm^{-2}). 400 grains were counted in the central 400 μm of the emulsion sheet at each end of the tracks.

(4) A. DE MARCO, A. MILONE and M. REINHARZ: *Nuovo Cimento*, **3**, 1150 (1956).

(5) G. J. PERLOW, L. R. DAVIS, C. W. KISSINGER and J. D. SHIPMAN: *Phys. Rev.*, **88**, 321 (1952).

(6) N. HORWITZ: *Phys. Rev.*, **98**, 165 (1955).

(7) L. BOHL: *Ph. D. Thesis*, University of Minnesota [quoted by WADDINGTON (1)].

(8) W. R. WEBBER and F. B. McDONALD: *Phys. Rev.*, **100**, 1460 (1955).

(9) J. LINSLEY: *Phys. Rev.*, **101**, 826 (1956).

(10) J. H. NOON, A. J. HERZ and B. J. O'BRIEN: *Nuovo Cimento*, in press.

At geomagnetic latitude 41° N, the cut-off kinetic energy of α -particles with zenith angles of less than 30° is more than 1.3 GeV/nucleon, hence all primary alphas at flight altitude are relativistic.

It is essential to separate with certainty α -particles from the background of slow singly-charged particles, protons, deuterons, and tritons, which originate from nuclear interactions either above or within the stack. These spurious tracks traced into the stack from the survey plate should show an increase or decrease in grain density, whereas fast α -particles should show no such variation.

The residual ranges (R) in emulsion of protons, deuterons and tritons having a grain density of 4 times minimum, calculated from the tables of BARKAS *et al.* (1), are 2.7, 5.4 and 8.1 cm respectively. In Table I are given the

TABLE I.

Particle		($R + 3.5$) cm	R cm	($R - 3.5$) cm
Proton	$g/100 \mu\text{m}$	24	34	—
	% change	29%	0%	—
Deuteron	$g/100 \mu\text{m}$	28	34	55
	% change	19%	0%	63%
Triton	$g/100 \mu\text{m}$	29	34	45
	% change	14%	0%	31%

grain counts for these particles at ($R + 3.5$), R , and ($R - 3.5$) cm. Since all grain counts are done to 5% statistical accuracy and only tracks which changed in grain density by less than 12% over 3.5 cm of emulsion were accepted as α -par-

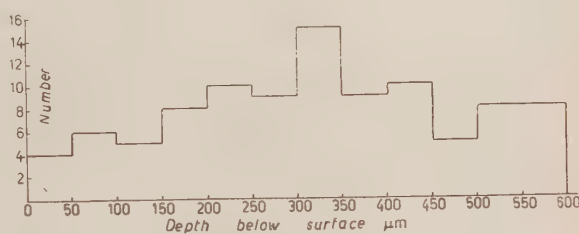


Fig. 1. — Depth distribution of all tracks found which satisfied the acceptance criteria for analysis.

(1) W. H. BARKAS and D. M. YOUNG: *Heavy Particle Functions*, University of California Radiation Laboratory Report UCRL-2579 Rev. (Berkeley, Calif. Univ. of Calif., 1954).

ticles, only a slow triton may possibly be identified as an α -particle. The percentage change in grain density over a range of at least 3.5 cm of emulsion for all tracks accepted as α -particles is shown in Fig. 2. The distribution has a mean of $(-2 \pm 1)\%$, rather than the expected zero value, and has a standard deviation of 5%. As seen from Table I, a triton will show a variation of at least 14% over the same range, and the slight skewness of the α -particle distribution in Fig. 2 should not result in erroneous rejection of true α -particles or in erroneous acceptance of background tracks to any significant extent.

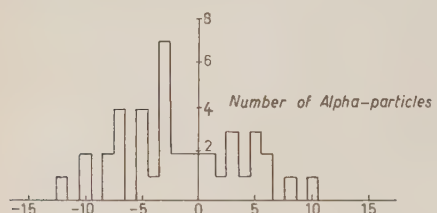


Fig. 2. - Percentage change in grain density of all α -particles after 3.5 cm of emulsion.

between 70 and 300 MeV) from stars indicated a proton-to-deuteron ratio between 0.3 and 0.1, and a triton-to-deuteron ratio of 0.25. Accordingly an upper limit to the background due to slow tritons is 8% of the background due to slow protons. In our experiment 3 of the 72 background tracks were classified by their change in grain density as due to tritons, and accordingly it is certain that the correction to the α -particle flux for incorrectly-identified background tracks is less than 5%. Grain density distributions of all tracks which satisfied the acceptance criteria are shown in Fig. 3, together with the grain-density distribution of the α -particles. The spread in the α -particle distribution is 7%, i.e. slightly larger than that expected from statistical fluctuations alone, but it is not enough to affect the separation from background.

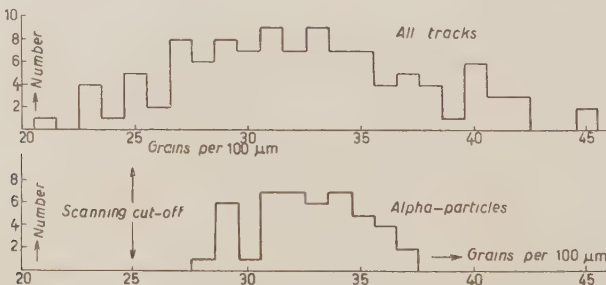


Fig. 3. - Grain density distributions of α -particles and all tracks analysed in the survey plate.

(12) C. DAHANAYAKE, P. F. FRANCOIS, Y. FUJIMOTO, P. IKEDALE, C. J. WAD-DINGTON and M. YASIN: *Nuovo Cimento*, **1**, 888 (1955).

10 tracks were also found which had grain density between 28 and 38 grains/100 μm and led to a star on tracing without showing any appreciable change in grain density. In 9 of these the star contained one or more shower particles in a narrow forward cone at less than 5° to the direction of the track traced. These were accepted as α -particle-induced stars. The other track, 16 mm long, led to a star with no emergent shower particles, and this was also taken to be an incident α .

The above results are in reasonable agreement with WADDINGTON (13), who found that, for a median α -particle energy of 1.3 GeV/nucleon, 5 of the 68 stars caused by α -particles contained no shower particles. The interaction mean free path obtained $(218.9/10) = 21.9 \text{ cm}$, is in agreement with previous measurements (13,14).

Of the total length scanned, viz. 45.4 cm, two lines of 11.4 cm each were separated by 2 cm, and the remainder of the lines were 7.5 cm apart; 45 α -particles were found in the first scan. After correction for tracks which crossed more than one swath and for scanning efficiency (given above) the flux of the α -particles at flight altitude is 92 particles $\text{m}^{-2} \text{s}^{-1} \text{sr}^{-1}$.

Calculation of the primary flux at the top of the atmosphere was made, using an attenuation mean free path in air of 45 g/cm², and correcting for α -particles which entered the stack during ascent and descent of the balloon (about 10%), and for fast alphas produced above the stack in interactions of heavier particles (about 5%). In the latter estimate, fragmentation probabilities were taken from NOON and KAPLON (15) and flux values from NOON *et al.* (16). The resulting primary α -particle flux at the top of the atmosphere at 41° N geomagnetic latitude is (102 ± 15) particles $\text{m}^{-2} \text{s}^{-1} \text{sr}^{-1}$. The error quoted is the statistical standard deviation only.

This value is in good agreement with previous measurements made with counter apparatus at 41° N over the U.S.A., given in Table II. However,

TABLE II. — Counter Measurements at 41° N geomagnetic latitude of the Flux of α -Particles
(particles $\text{m}^{-2} \text{s}^{-1} \text{sr}^{-1}$).

110 \pm 20	G. J. PERLOW <i>et al.</i> (5)
99 \pm 16	N. HORWITZ (6)
88 \pm 10	L. BOHL (7)
82 \pm 9	W. R. WEBBER (8)
88 \pm 8	J. LINSLEY (9)
87 \pm 9	F. B. McDONALD (16)

(13) C. J. WADDINGTON: *Phil. Mag.*, **1**, 105 (1956).

(14) M. V. K. APPER RAO, R. R. DANIEL and K. A. NEELAKANTAN: *Proc. Ind. Acad.*, **43**, 181 (1956).

(15) J. H. NOON and M. F. KAPLON: *Phys. Rev.*, **97**, 769 (1955).

(16) F. B. McDONALD: *Phys. Rev.*, **104**, 1723 (1956).

it is in marked disagreement with the only other measurement at this latitude reported by nuclear emulsion workers (⁴), who obtained a value of (39 ± 8.6) particles $\text{m}^{-2} \text{s}^{-1} \text{sr}^{-1}$ from a stack flown in Sardinia.

A similar discrepancy by a factor of two exists between the measurements in emulsion of the flux of nuclei heavier than boron. FAY (¹⁷) obtained a figure of (4.0 ± 0.8) from a stack also flown in Sardinia, whereas the Sydney group has found a flux of (8.1 ± 1.5) in the stack flown over Texas (¹⁰). The latter figure is in agreement with previous measurements (^{18,19}) in the U.S.A.

The measurements on the flux of heavy nuclei and of α -particles over Sardinia were carried out by two different laboratories on stacks flown on two different flights. The measurements over U.S.A. were made by many workers, using a variety of techniques. Accordingly the discrepancy by a factor of two between these fluxes at different longitudes appears to be a real effect and it seems necessary to invoke a shift in geomagnetic co-ordinates to explain it (*).

* * *

The authors acknowledge with pleasure the help given by Dr. A. J. HERZ in discussions on this paper. The team of scanners who have taken part in this work consisted of Mrs. B. CHARTRES, Mrs. I. DOCHERTY, Mrs. I. THOW, Mrs. K. WOODGER and Miss M. WOODWARD. The figures were prepared by Miss S. A. O'REILLY. Our thanks are due to the U.S. Office of Naval Research, who arranged the balloon exposure, and to Professor H. MESSEL and the Nuclear Research Foundation within the University of Sydney for the excellent facilities put at our disposal. One of us (B.J. O'B.) is indebted to the Research Committee of the University of Sydney for a Research Studentship.

(¹⁷) H. FAY: *Zeits. f. Naturfor.*, **10a**, 572 (1955).

(¹⁸) M. F. KAPLON, B. PETERS, H. L. REYNOLDS and D. M. RITSON: *Phys. Rev.*, **85**, 295 (1952).

(¹⁹) M. F. KAPLON, J. H. NOON and G. W. RACETTE: *Phys. Rev.*, **95**, 1408 (1954).

(*) Recently ALY and WADDINGTON have obtained a value of (72 ± 9) for the α -particle flux from an emulsion stack flown in Sardinia. Although much higher than that found by DE MARCO *et al.* it is still significantly lower than our value over the U.S.A. Private communication C. J. WADDINGTON (1957).

RIASSUNTO (*)

I valori ottenuti eseguendo misure con contatori per il flusso delle particelle α a 41°N sugli Stati Uniti sono significativamente maggiori di quelli ottenuti per mezzo di emulsioni nucleari a 41°N sulla Sardegna. Abbiamo misurato il flusso di particelle α a 41°N sugli Stati Uniti per mezzo di emulsioni nucleari e i risultati, che si accordano con quelli delle misure per mezzo di contatori, sono superiori a quelli ottenuti in Sardegna. Tali misure sono d'interesse per le proposte modificazioni alle coordinate geomagnetiche.

On the Impossibility of the Hamiltonian Formulation of Theory with the Form-Factor.

V. S. BARAŠENKOV

Joint Institute for Nuclear Research - Dubna, USSR

(ricevuto l'11 Febbraio 1957)

Summary. — It is shown that the Hamiltonian structure is not proper to the theory with non-local interaction; the latter may be formulated, however, both in Lagrangian $\mathbf{x}_k; \dot{\mathbf{x}}_k; A_\mu; \dot{A}_\mu$ and Hamiltonian variables $\mathbf{x}_k; \mathbf{p}_k; A_\mu; \pi_\mu$. With the help of an example of one-dimensional oscillator Pauli's method is considered (⁷). The initial integro-differential equation of motion and the canonical system of equations of motion obtained by the Pauli method are not equivalent. The many-time equations of motion obtained by Hayashi's method (¹⁴) turn out to be incompatible in any K -approximation of the perturbation theory.

1. — Introduction.

A considerable number of recent papers have been devoted to the theory of field with «spread» or, as is usual now, non-local interaction. Such theories may be regarded as attempts at a phenomenological description of the internal structure of elementary particles. But even independently of physical ideas concerning the understanding of elementary particle size, the examination of theories with non-local interaction is very important as an inquiry into the possibilities of the mathematical apparatus of linear field theory.

Theoretical investigation of possible deviations in small space-time regions from the principles and concepts which have proved true for the phenomena in macroscopic space-time regions acquires nowadays quite a particular significance in view of the great difficulties the field theory has been facing of late (¹).

(¹) L. D. LANDAU and I. Ja. POMERANČUK: *Dokl. Akad. Nauk SSSR*, **102**, 489 (1955); I. Ja. POMERANČUK: *Dokl. Akad. Nauk SSSR*, **103**, 1005 (1955).

« Searching » studies of this kind make it possible to detect the points in which actual theory is the least « stable » and which may serve as a beginning for further generalizations of the theory.

A characteristic feature of the theory with non-local interaction is that it allows for velocities of signals greater than that of light in small spacetime regions. In this case equations of motion contain dynamic variables concerning different instants of time; as a consequence, it is insufficient to know the behaviour of the dynamic variables only in the near neighbourhood $[t; t + \delta t]$ in order to determine the solution at the point $t + \delta t$, and the Hamiltonian formulation of theory becomes impossible.

For theories with the Schrödinger wave equation this has been clearly demonstrated by M. A. MARKOV in papers ⁽²⁾.

After the appearance of the papers by D. I. BLOHINCEV ⁽³⁾ and R. E. PEIERLS ⁽⁴⁾ the theory with non-local interaction has been formulated in the relativistic invariant Heisenberg representation ⁽⁵⁾ (*).

In this case, however, the theory cannot be formulated either in the Hamiltonian form. This may be simply exemplified by a system of classical oscillators with non-local interaction.

2. – Oscillatory model with non-local interaction.

2.1. – The function of action S for a system of N interacting oscillators will be written as follows:

$$(1) \quad S = \frac{1}{2} \sum_{i=1}^N m_i \int_{-\infty}^{+\infty} \dot{q}_i^2(t) dt - \frac{1}{2} \sum_{i=1}^N \omega_i^2 \int_{-\infty}^{+\infty} q_i^2(t) dt - \\ - \frac{1}{2} \sum_{i,j=1}^N \gamma_{ij} \int_{-\infty}^{+\infty} q_i(t) F_{ij}(t_1 - t_2) q_j(t_2) dt_1 dt_2,$$

where q_i and \dot{q}_i are the coordinate and the velocity of the oscillator; F_{ij} is the

⁽²⁾ M. A. MARKOV: *Žu. Éksper. Teor. Fiz.*, **10**, 1311 (1940); **16**, 790 (1946); **21**, 11 (1951); *Usp. Fiz. Nauk*, **29**, 269 (1946); **51**, 317 (1953).

⁽³⁾ D. I. BLOHINCEV: *Moscow Univ. Herald Physics*, **77**, 3 (1946); *Žu. Éksper. Teor. Fiz.*, **16**, 480 (1946); **17**, 267 (1947); **18**, 556 (1948).

⁽⁴⁾ R. E. PEIERLS: 8^{me} *Conseil de Physique, Inst. Solvay* (1948), p. 291; R. E. PEIERLS and H. MC MANUS: *Proc. Roy. Soc.*, **195**, 323 (1948).

⁽⁵⁾ P. KRISTENSEN and G. MØLLER: *Det Kon. Vid. Selsk. Medd.*, **27**, n. 7 (1952); C. BLOCH: *Det Kon. Vid. Selsk. Medd.*, **27**, no. 8 (1952).

(*) As is known, in the theory with non-local interaction the interaction representation and the Heisenberg representation are not equivalent.

form-factor satisfying the conditions

$$(2) \quad \gamma_{ii} F_{ii} = \gamma_{ji} F_{ji} ;$$

when $|t| \gg \lambda$

$$(3) \quad F_{ij}(t) \rightarrow 0 ;$$

when $\lambda \rightarrow 0$

$$(4) \quad F_{ij}(t) \rightarrow \delta(t) .$$

From the variation principle

$$(5) \quad \delta S = 0 ,$$

by varying the dynamic variables $q_i(t)$ and $\dot{q}_i(t)$ we get the equation of motion:

$$(6) \quad \ddot{q}_i(t) + \omega_i^2 q_i(t) + \sum_{j=1}^N \gamma_{ij} \int_{-\infty}^{+\infty} F_{ij}(t-t_1) q_j(t_1) dt_1 = 0 . \quad i = 1, 2, \dots, N .$$

2.2. – The solution of the system of integro-differential equations (6) may be obtained with the help of the Laplacian or Fourier transformation. For the form-factors F_{ij} satisfying the condition

$$(7) \quad \int_{-\infty}^{+\infty} \exp[\alpha|t|] |F_{ij}(t)| dt \leq R < \infty , \quad \alpha > 0 ,$$

this solution is the following:

$$(8) \quad q_i(t) = \sum_{k=1}^N \sum_{j=1}^{M_k} f_{ik}(w_k^2) t^{j-1} (c_{kj}^+ \exp[w_k t] + c_{kj}^- \exp[-w_k t]) ; \quad i = 1, 2, \dots, N .$$

Here c_{kj}^\pm are arbitrary constants; the kind of the functions $f_{ik}(w_k^2)$ and the root values w_k are found from the linear homogeneous system of algebraic equations:

$$(9) \quad (w_k^2 - \omega_i^2) f_{ik}(w_k^2) - \sum_{j=1}^N \gamma_{ij} F_{ij}(w_k^2) f_{jk}(w_k^2) = 0 \quad i = 1, 2, \dots, N ,$$

where

$$(10) \quad F_{ij}(w_k^2) = \sqrt{2\pi} \int_{-\infty}^{+\infty} F_{ij}(t) \exp[-iwt] dt ;$$

M_k is the root multiplicity.

It is clear from a direct substitution that the functions (8) satisfy the system of equations (6). It may also be shown that (8) is the unique solution of the system of equations (6) in the class of continuous functions satisfying the condition:

$$(11) \quad \int_{-\infty}^{\infty} |q_i(t)| \exp[-\beta|t|] dt \leq R < \infty,$$

where

$$0 < \beta < \alpha. \quad (\text{cf. (7)}).$$

The condition (11) shows limitations for the admissible root values w_k in (8).

The $2NM$ values of the constants c_{kj}^{\mp} are determined from the initial conditions

$$(12) \quad q_i(t) \Big|_{t=t_0} = q_{i0}; \quad \frac{dq_i(t)}{dt} \Big|_{t=t_0} = \dot{q}_{i0}; \quad \text{etc.}$$

$2NM$ initial conditions at the instant of time $t = t_0$ and the condition (11) concerning the whole infinity interval $[-\infty; +\infty]$ fully determine the solution of the system of equations (6).

In the general case of the form-factors F_{ij} , limited only by the requirements (2)-(4), the multiplicity of the root w_k is

$$M_k > 1,$$

i.e. to determine the kind of solution a number of initial conditions greater than that in the system of oscillators with local interaction is needed. The required number of initial conditions also depends upon the value of the coefficients γ_{ii} which determine the degree of interaction of the oscillators.

A part of the roots w_k will have, in this case, a real part which is not zero

$$\operatorname{Re}(w_k) \neq 0$$

and determine the divergent solutions which have no physical meaning:

$$q_{ik}(t) \sim \exp[\operatorname{Re}(w_k)t].$$

There exists, however, a large class of values of form-factors F_{ij} and bond coefficients γ_{ii} for which all roots w_k are purely imaginary, the number of these roots being the same as for the oscillators with local interaction.

The case is analogous, in particular, when the coefficients γ_{ii} in the class of form-factors satisfying the condition (3) are small enough. To show

this it suffices to re-write the system of equations (6), with the help of the Green functions $G_i(t_0; t; t_1)$, as a system of integral equations:

$$(13) \quad q_i(t) = q_{0i}(t) + \sum_{j=1}^N \gamma_{ij} \int_{-\infty}^{+\infty} G_{ij}(t_0; t; t_1) F_{ij}(t_1 - t_2) q_j(t_2) dt_1 dt_2, \quad i = 1, 2, \dots, N,$$

where

$$G_i(t_0; t; t_1)|_{t=t_0} = 0; \quad \dot{G}_i(t_0; t; t_1)|_{t=t_0} = 0$$

and to substitute the finite limits $A > \lambda$ for the infinite integration limits, which is always possible owing to (3).

According to the well-known theory the system of integral equations (16) with the coefficients γ_{ij} sufficiently small and $q_{0i}(t)$ limited has a unique solution which may be obtained by the method of successive approximations (6). The requirement of limited $q_{0i}(t)$ in (13) concerns the infinity interval $t \in [t_0; \infty]$ in contrast with the theory with local interaction where the functions $q_{0i}(t)$ must satisfy the requirement of limitation only in the interval $[t_0; t]$.

The demand of limited $q_{0i}(t)$ at the infinite interval $t \in [t_0; \infty]$ is analogous to the requirement (11) for the solution of equations of motion by the method of the Fourier or Laplacian transformations and is essential to the demonstration of the theorem that the system of equations (6) and (13) has a univocal solution. In the theory with local interaction all dynamic variables in the system of equations of motion belong to the infinitesimal neighbourhood of the instant of time t , and to determine the kind of solution at the point $t + \delta t$ we have to know the behaviour of the variables only in this infinitesimal neighbourhood $[t; t + \delta t]$.

2.3. — The system of equations (6) may be re-written as follows:

$$(14) \quad \frac{d}{dt} \left(\frac{\partial L}{\partial \dot{q}_i} \right) - \frac{\partial L}{\partial q_i} = 0; \quad i = 1, 2, \dots, N,$$

if we determine

$$(15) \quad L \equiv L(q_i; \dot{q}_i) = \frac{1}{2} \sum_{i=1}^N m_i \dot{q}_i^2(t) - \frac{1}{2} \sum_{i=1}^N \omega_i^2 q_i^2(t) - \\ - \frac{1}{2} \sum_{i,j=1}^N (2 - \delta_{ij}) \gamma_{ij} \int F_{ij}(t - t_1) q_j(t_1) dt_1.$$

(1) I. G. PETROVSKIJ: *Lectures on Integral Equations* (Moscow, 1948).

By determining then the function

$$(16) \quad H = -L + \sum_{i=1}^N p_i q_i - \lambda H(p_i; q_i) = \\ = \frac{1}{2} \sum_{i=1}^N \frac{p_i^2(t)}{m_i} + \frac{1}{2} \sum_{i=1}^N \omega_i^2 q_i^2(t) + \frac{1}{2} \sum_{i; j=1}^N (2 - \delta_{ij}) \gamma_{ij} \int F_{ij}(t - t_1) q_j(t_1) dt_1,$$

the system of equations (14) may be re-written as follows:

$$(17) \quad \dot{p}_i = -\frac{\partial H}{\partial q_i}; \quad \dot{q}_i = \frac{\partial H}{\partial p_i}; \quad i = 1, 2, \dots, N.$$

However, the system of equations (17) is not a Hamiltonian one as its dynamic variables concern different instants of time, while the Hamiltonian system of equations supposed the dynamic variables bound only in the infinitesimal interval of time dt . Besides, with $\lambda \rightarrow 0$ the functions L and H with $N > 1$ do not become the Lagrangian and Hamiltonian functions of the theory with local interaction (*).

2'4. — PAULI (7) has suggested to construct the theory with non-local interaction in the Hamiltonian form using the known fact of analytical dynamics that the Hamiltonian system of equations of motion is connected with a certain bilinear differential form obtained from the equation of motion (6) (8).

For instance, for an oscillator with non-local interaction it is easy to derive from the equations of motion (6) the bilinear differential form

$$(18) \quad I(t; D; \delta) = (Dq(t); \delta \dot{q}(t)) + \frac{\omega^2}{2} \int_{-\infty}^{+\infty} \epsilon(t - t_2) F(t_2 - t_1) (Dq(t_2); \delta \dot{q}(t_1)) dt_1 dt_2,$$

which satisfies the condition

$$(19) \quad \frac{d}{dt} I(t; D; \delta) = 0.$$

(*) However, the writing of the equations of motion in terms of the auxiliary functions L and H proves to be of much use when studying the many-time generalizations of the theory with non-local interaction (9,10).

(7) W. PAULI: *Nuovo Cimento*, **10**, 648 (1953).

(8) M. D. WHITTAKER: *Analytic Dynamics* (Moscow, 1937).

(9) V. S. BARAŠENKOV: *Zh. Éksper. Teor. Fiz.* (in the press).

(10) V. S. BARAŠENKOV: *Thesis* (1955).

Here

$$(Dq(t); \delta\dot{q}(t)) = [Dq(t) \delta\dot{q}(t) - \delta q(t) D\dot{q}(t)];$$

$$\varepsilon(t) = \begin{cases} +1, & \text{when } t > 0 \\ -1, & \text{when } t < 0 \end{cases}$$

$I(t; D; \delta)$ contains dynamic variables concerning different instants of time, which hinders the direct application of analytical dynamics theorems. To overcome this difficulty PAULI has proposed, proceeding from the equation of motion (6) ($N = 1$), to express $q(t_1)$ and $q(t_2)$ through independent dynamic variables q and \dot{q} taken at the instant of time t :

$$(8') \quad q(t_j) = q(t) \cos w(t_j - t) + \dot{q}(t) \frac{1}{w} \sin w(t_j - t).$$

The differential form (18) expressed through the dynamic variations $Dq(t)$; $\delta q(t)$; $dq(t)$ satisfies than the conditions

$$dI(t; D; \delta) + \delta I(t; d; D) + DI(t; \delta; d) = 0$$

and may be considered as the bilinear covariant of a Pfaff form which may be reduced by an appropriate transformation of the dynamic variables to the canonical form (11). It is clear from the above considerations that the canonical system of Pauli equations is constructed with the help of the found solution (8) of the integro-differential equations (6), which leads to the fact that this system of equations is actually superfluous and cannot give anything new with comparison to the equations (6).

Besides, for the solution of the initial equations of motion (6), requirements of the kind of solution concerning the whole infinite time interval are obligatorily employed.

The necessity of such additional requirements makes a substantial difference between the equations of motion (6) and the canonical system of Pauli equations (6). From this point of view Pauli's method is equivalent to the substitution of the integro-differential equations of motion for differential equations for which the Cauchy problem may be formulated (i.e. no additional conditions in the infinity interval are needed) and the solutions of which coincide with those of the initial integro-differential equations derived from the variation principle.

(11) N. K. RAŠEVSKIJ: *Geometric Theory of Equations with Quotient Derivatives* (Moscow, 1948).

2·5. – An attempt may be made at obtaining the Hamiltonian formulation of the theory by re-writing the system of equations of motion (6) as a system of differential equations with higher derivatives (12,13)

$$(20) \quad \ddot{q}_i + \omega_i^2 q_i + \sum_{j=1}^N \gamma_{ij} F_{ij} \left(\frac{d}{dt} \right) q_j = 0; \quad i = 1, 2, \dots, N.$$

Paper (12) contains a method of constructing the Hamiltonian formalism for the general case when

$$(21) \quad F_{ij} \left(\frac{d}{dt} \right) = \exp f \left(\frac{d}{dt} \right) \prod_{j=1}^k \left(\frac{d}{dt} - \Omega_j \right).$$

But again the system of integro-differential equations (6) is equivalent to that of differential equations (20) only with definite requirements superposed on the kind of the functions q_i in the whole infinity interval $t \in [-\infty; +\infty]$.

3. – Theory of field with non-local interaction.

3·1. – The results obtained in the preceding section are true for the Blohineev-Peierls theory of extended particles (3,4) and the theory of field with non-local interaction as well (5).

3·2. – For the Hamiltonian formulation of the system of equations of motion with non-local interaction HAYASHI (14) has suggested to use the method (15) which was successfully applied before to the theory with local interaction. Let us consider this method in the application to the non-local interaction of a scalar neutral field $A(x)$ and a scalar charged field $\psi(x)$.

Let us write the system of equations of motions as follows:

$$(22) \quad \frac{\delta A_0[x; \sigma]}{\delta \sigma(x')} = -g \int A_\mu(x - x') \psi^*(x_1) \psi(x_3) F(x_1 x' x_3) d^4(x_1 x_3) - \\ - \frac{\delta}{\delta \sigma(x')} \sum_{k=1}^{\infty} g^k a[x; \sigma];$$

$$(23) \quad \frac{\delta \psi_0[x; \sigma]}{\delta \sigma(x')} = -g \int A_\mu(x - x') A(x_2) \psi(x_3) F(x' x_2 x_3) d^4(x_2 x_3) - \\ - \frac{\delta}{\delta \sigma(x')} \sum_{k=1}^{\infty} g^k \varphi[x; \sigma],$$

(12) A. PAIS and G. UHLENBECK: *Phys. Rev.*, **79**, 145 (1950).

(13) Y. KATAYAMA: *Progr. Theor. Phys.*, **10**, 31 (1953); I. RZEWSKI: *Acta Phys. Polonica*, **12**, 100 (1953).

(14) C. HAYASHI: *Progr. Theor. Phys.*, **10**, 533 (1953); **11**, 226 (1954).

(15) H. UMEZAWA and Y. TAKAHASHI: *Progr. Theor. Phys.*, **9**, 14, 501 (1953).

where

$$(24) \quad A(x) = \sum_{k=0}^{\infty} g^k A_k[x; \sigma]; \quad \psi(x) = \sum_{k=0}^{\infty} g^k \psi_k[x; \sigma].$$

If the equations (22), (23) are re-written as follows

$$(25) \quad \frac{\delta A_0[x; \sigma]}{\delta \sigma(x')} = i[H(x'/\sigma); A_0[x; \sigma]];$$

$$(26) \quad \frac{\delta \psi_0[x; \sigma]}{\delta \sigma(x')} = i(H(x'/\sigma); \psi_0[x; \sigma]),$$

then, comparing the right sides of the equations (22) and (25) and (26) and properly choosing expressions for the additional fields $a_k[x; \sigma]$ and $\varphi_k[x; \sigma]$ it is possible to find a formal expression for the functional $H[x; \sigma]$ in form of a power series of g :

$$(27) \quad H[x; \sigma] = \sum_{k=1}^{\infty} g^k H_k[x; \sigma].$$

The equations (25), (26) are integrable only if

$$(28) \quad \left[\frac{\delta}{\delta \sigma(x'')}; \frac{\delta}{\delta \sigma(x')} \right] A_0[x; \sigma] = 0; \quad \left[\frac{\delta}{\delta \sigma(x'')}; \frac{\delta}{\delta \sigma(x')} \right] \psi_0[x; \sigma] = 0,$$

or, taking into account the expansion (27):

$$\begin{aligned} \left[\frac{\delta}{\delta \sigma(x'')}; \frac{\delta}{\delta \sigma(x')} \right] A_0[x; \sigma] &= i \sum_{k=1}^{\infty} g^k \left\{ \left[H_k(x'/\sigma); \frac{\delta A_0[x; \sigma]}{\delta \sigma(x'')} \right] - \right. \\ &\quad \left. - \left[H_k(x''/\sigma); \frac{\delta A_0[x; \sigma]}{\delta \sigma(x')} \right] + \left[\frac{\partial H_k(x'/\sigma)}{\partial \sigma(x'')}; A_0[x; \sigma] \right] - \left[\frac{\partial H_k(x''/\sigma)}{\partial \sigma(x')}; A_0[x; \sigma] \right] \right\} \text{ etc.}, \end{aligned}$$

where the symbol $\partial/\partial \sigma(x)$ means differentiation with respect to the hyper-surface σ which is explicitly included into the expression for the Hamiltonian $H_k[x; \sigma]$. Using the expression for $H_k[x; \sigma]$ obtained in (14) we get:

$$\begin{aligned} \sum_{k=1}^{\infty} g^k \left\{ \left[H_k(x'/\sigma); \frac{\delta A_0[x; \sigma]}{\delta \sigma(x'')} \right] - \left[H_k(x''/\sigma); \frac{\delta A_0[x; \sigma]}{\delta \sigma(x')} \right] \right\} &= \\ = i([H_1(x'/\sigma); H_1(x''/\sigma)]; A_0[x; \sigma]) + O(g^3) &= i \int F(x_1 x_2 x_3) F(x'_1 x'_2 x'_3) \cdot \\ \cdot \sum_{i,j=1}^3 a_i a_j [\delta(x' - x_i) \delta(x'' - x'_j) - \delta(x' - x'_j) \delta(x'' - x_i)] A_m(x'_3 - x_1) \psi_0^*[x'_j; \sigma] \psi_0[x_3; \sigma] \cdot \\ \cdot \{ A_\mu(x_2 - x) A_0[x'_2; \sigma] + A_\mu(x'_2 - x) A_0[x_2; \sigma] \} d^4(x_1 \dots x'_3) + O(g^3), \end{aligned}$$

where $a_1 + a_2 + a_3 = 1$; $a_1 = a_3$.

$$(29) \quad \left\{ \begin{array}{l} \left[\frac{\partial H_k[x'; \sigma]}{\partial \sigma(x'')} ; A_0[x; \sigma] \right] = -\frac{i}{2} \int F(x_1 x_2 x_3) F(x'_1 x'_2 x'_3) \sum_{i,j=1}^3 a_i a_j \delta(x' - x_i) \delta(x'' - x'_j) \cdot \\ \quad \cdot \{ A_\mu(x_2 - x) A_0[x'_2; \sigma] + A_\mu(x'_2 - x) A_0[x_2; \sigma] \} \{ A_m(x_1 - x'_1) \psi_0[x'_1; \sigma] \\ \quad \cdot [x'_3; \sigma] \psi_0[x_3; \sigma] + A_m(x_3 - x'_3) \psi_0^*[x_1; \sigma] \psi_0^*[x'_1; \sigma] \} \dot{d}^3(x_1 \dots x'_3) . \\ \\ \left[\frac{\delta}{\delta \sigma(x'')} ; \frac{\delta}{\delta \sigma(x')} \right] A_0[x; g] = -g^2 \int d^4(x_1 \dots x'_3) F(x_1 x_2 x_3) F(x'_1 x'_2 x'_3) \cdot \\ \quad \cdot \sum_{i,j=1}^3 a_i a_j [\delta(x' - x_i) \delta(x'' - x'_j) - \delta(x' - x'_j) \delta(x'' - x_i)] \cdot \\ \quad \cdot \{ A_\mu(x_2 - x) A_0[x'; \sigma] + A_\mu(x'_2 - x) A_0[x_2; \sigma] \} \cdot \\ \quad \cdot \{ A_m(x'_3 - x_1) \psi_0^*[x'_1; \sigma] \psi_0[x_3; \sigma] - \frac{1}{2} A_m(x_1 - x'_1) \psi_0[x'_1; \sigma] \psi_0[x_3; \sigma] - \\ \quad - \frac{1}{2} A_m(x_3 - x'_3) \psi_0^*[x_1; \sigma] \psi_0^*[x'_1; \sigma] \} + O(g^3) . \end{array} \right.$$

An analogous expression may be derived for $\psi_0[x; \sigma]$ too. In the theory with non-local interaction these expressions do not vanish and, consequently, the conditions (28) are not satisfied.

So the Hayashi procedure in any K -approximation ($K \neq \infty$) is internally contradictory and the equations of motion are not Hamiltonian.

However, from the equations (22) and (23) follows that the conditions of integrability of (28) will be satisfied in the limit $K \rightarrow \infty$ if for any $K > 1$

$$(30) (*) \quad \left[\frac{\delta}{\delta \sigma(x'')} ; \frac{\delta}{\delta \sigma(x')} \right] a_k[x; \sigma] = 0; \quad \left[\frac{\delta}{\delta \sigma(x'')} ; \frac{\delta}{\delta \sigma(x')} \right] \varphi.[x; \sigma] = 0 ,$$

and the expansions (24) and (27) converge. In this case the many-time equations of motion for the fields $A_0[x; \sigma]$ and $\psi_0[x; \sigma]$ as well as the corresponding Tomonaga-Schwinger equation in the interaction representation would have solutions with velocities of signals greater than that of light. These equations would have unique solutions in finite time-like regions and when passing to the limit $\lambda \rightarrow 0$.

Investigation of convergence of the series (24), (27) presents considerable difficulties just because of the complicated procedure for the determination of the expressions $H_k[x; \sigma]$; $a_k[x; \sigma]$ and $\varphi_k[x; \sigma]$.

(*) As the fields $a_k[x; \sigma]$ and $\varphi_k[x; \sigma]$ in (14) may be also expanded into a series with respect to the degrees of the constant g , it is comprehensible that from the satisfaction of the condition (30) for a certain value of $k = k^* > 1$ does not follow that (28) is satisfied in g^{k^*} -approximation.

But an extremely rapid increase of the number of terms in the expressions for $H_k[x; \sigma]$, $a_k[x; \sigma]$; $\varphi_k[x; \sigma]$ leaves no ground for expecting that the series (24), (27) will be convergent.

In this point there is a substantial difference from the theory with local interaction where, in spite of divergence of the expansions in powers of the interaction constant g , it is possible to use after renormalization a certain number of initial terms in these expansions, which give in many cases, as the comparison with experiment shows, a good enough asymptotical representation of the quantities discussed.

In the theory with non-local interaction one cannot limit oneself to a finite number of terms as in this case the conditions (28) are not satisfied.

To construct the canonical system of equations (25), (26) a preliminary solution of the equations (22), (23) is needed and that is why all the above remarks concerning the canonical system of equations obtained by Pauli's method hold for this system as well.

So both in the Heisenbergian representation and in the interaction representation we fail to construct theories with non-local interaction which would have the Hamiltonian structure.

None the less, the impossibility of applying the Hamiltonian method to the theory with non-local interaction does not exclude the formulation of such a theory within the limits of the phenomenological scattering matrix (^{9,16}).

* * *

The author takes pleasure in thanking Prof. D. I. BLOHINCEV for fruitful discussions and valuable advice and also Prof. M. A. MARKOV for interesting discussions concerning general questions of form-factor theories.

(¹⁶) B. V. MEDVEDEV: *Dokl. Akad. Nauk SSSR*, **103**, 37 (1955).

RIASSUNTO (*)

Si dimostra che la struttura hamiltoniana non è propria della teoria della interazione non locale; quest'ultima può, tuttavia, essere formulata sia in variabili lagrangiane \mathbf{x}_k ; $\dot{\mathbf{x}}_k$; A_μ ; \dot{A}_μ che in variabili hamiltoniane \mathbf{x}_k ; \mathbf{p}_k ; A_μ ; π_μ . Considerando a titolo d'esempio il caso dell'oscillatore unidimensionale, si esamina il metodo di Pauli (⁷). L'equazione integro-differenziale iniziale del moto e il sistema canonico delle equazioni del moto ottenute col metodo di Pauli non sono equivalenti. Le equazioni pluritemporali del moto ottenute col sistema di Hayashi risultano incompatibili in qualsiasi approssimazione K della teoria delle perturbazioni.

(*) Traduzione a cura della Redazione.

Zur Energieverteilung der inelastischen Streuung von K^+ -Mesonen an Kernen.

P. MITTELSTAEDT

Max-Planck-Institut für Physik - Göttingen, Deutschland

(ricevuto l'11 Febbraio 1957)

Summary. — The energy distribution in the inelastic scattering of K^+ -mesons by complex nuclei is calculated using the Goldberger method. The results are found to be in fair agreement with the 80 MeV experimental data of the Göttingen group.

1. – Einleitung und Problemstellung.

In der Arbeit von BISWAS u. a. ⁽¹⁾ wird berichtet über Streuexperimente mit künstlich erzeugten K^+ -Mesonen einer Energie von etwa 80 MeV an mittelschweren Kernen ($A = 100$) in Photoplatten. Aus 154 Einzelereignissen konnte die Energie und Winkelverteilung der sekundären K^+ -Mesonen bestimmt werden.

Derartige Experimente sind deshalb von Interesse, weil aus der Energie und Winkelverteilung der sekundären K^+ -Mesonen eventuell Rückschlüsse gezogen werden können auf die Wechselwirkung zwischen K^+ -Mesonen und Nukleonen. Anderseits kann man bei genauer Kenntnis der Querschnitte σ_{K^+} und σ_{K^+N} zwischen den Einzelteilchen aus den Streuexperimenten an komplexen Kernen Aussagen über die Eigenschaften der Kernmaterie gewinnen.

In der vorliegenden Arbeit soll versucht werden, die Energieverteilung der sekundären K^+ -Mesonen nach der Goldberger-Methode zu berechnen. Es werden dabei die individuellen Querschnitte σ_{K^+p} und σ_{K^+N} als bekannt angenommen und daraus die Energieverteilung der Streuung an einem komplexen

⁽¹⁾ N. N. BISWAS, L. CECCARELLI-FABBRICHESI, M. CECCARELLI, K. GOTTSSTEIN, N. C. VARSHNEYA and P. WALOSCHEK: *Nuovo Cimento*, 5, 123 (1957).

Kern berechnet. Diese Methode wurde früher bereits mit Erfolg auf die Streuung von Protonen (²) bzw. Neutronen (³) an schweren Kernen angewandt. Der Unterschied der vorliegenden Rechnungen von diesen Arbeiten besteht einmal in der Verschiedenheit der Massen von K^+ -Meson und Nukleon, zum anderen in der Tatsache, daß das K^+ -Meson nicht dem Pauliprinzip unterworfen ist. Beide Effekte zusammen bewirken wesentliche Veränderungen in den Rechnungen und in den Ergebnissen.

Nach dieser Methode wird die Streuung des Primärteilchens am Kern durch einen «klassischen» Stoßvorgang zwischen dem K^+ -Meson und einem Nukleon im Kern beschrieben. Es wird angenommen, daß das Primärteilchen innerhalb des Kernes nur einen solchen Stoß durchführt, d.h. die mittlere freie Weglänge wird als groß gegenüber dem Kernradius angenommen. Die Wirkung der übrigen Nukleonen auf das Primärteilchen wird dabei durch ein gemeinsames Potential dargestellt, in dem sich das K^+ -Meson im Inneren des Kernes bewegt. Die Energie- und Winkelverteilung der K^+ -Mesonen nach der Streuung an einem Kern gewinnt man dann durch Mittelbildung über alle möglichen Stöße zwischen K^+ -Meson und einem Nukleon des Kerns. Dabei spielt die Kenntnis der Impulsverteilung der Nukleonen im Kerninneren eine wesentliche Rolle.

Dieses Modell ist eine umso bessere Näherung, je höher die Energie des Primärteilchens ist. Auf Grund der Erfolge dieser Methode bei Nukleonen mit wesentlich kleineren Energien als 80 MeV kann man jedoch hoffen, daß es sich im vorliegenden Fall um eine gute Näherung handelt. Die Geschwindigkeit der K^+ -Mesonen ist anderseits noch nicht so groß, daß relativistische Effekte eine wesentliche Rolle spielen. Wir werden daher im Folgenden stets in der unrelativistischen Näherung rechnen.

Die geschilderte Methode erlaubt es, aus der Gesamtheit der an einem Kern gestreuten K^+ -Mesonen die Energie- und Winkelverteilung der sog. inelastischen Prozesse zu berechnen, also der Prozesse, bei denen wirklich ein Einzelstoß zwischen K^+ -Meson und Nukleon stattfindet, d.h. daß der Kern sich nach dem Stoß in einem angeregten Zustand befindet, wenn er vor dem Stoß im Grundzustand war. Dadurch entsteht bei dem Vergleich mit dem Experiment eine gewisse Unsicherheit insbesondere bei kleinen Energieabgaben, die zum großen Teil durch die elastischen Prozesse hervorgerufen werden, da die Trennung der elastischen von den inelastischen Ereignissen mit großen Schwierigkeiten verbunden ist. (Vgl. dazu die Diskussion dieser Frage bei BISWAS u. a. (¹)).

Eine weitere Unsicherheit entsteht dadurch, daß die individuellen Querschnitte σ_{K^+N} und σ_{K^+p} in ihrer Energie- und Winkelabhängigkeit nur sehr

(²) W. HEISENBERG: *Ber. Sächs. Akad.*, **89**, 369 (1937).

(³) M. L. GOLDBERGER: *Phys. Rev.*, **74**, 1269 (1948); S. HAYAKAWA, M. KAWAI und K. KIKUCHI: *Progr. Theor. Phys.*, **13**, 415 (1955).

schlecht bekannt sind, da nur eine sehr kleine Zahl von Einzelstößen experimentell gefunden werden konnte.

Aus diesem Grunde soll in der vorliegenden Arbeit auch die Winkelverteilung der sekundären K^+ -Mesonen, die stark von der Winkelverteilung von σ_{K^+N} und σ_{K^+p} abhängt, nicht berechnet werden. Dazu kommt, daß zu einer Berechnung der Winkelverteilung außerdem eine ziemlich genaue Kenntnis der Potentialverteilung im Atomkern erforderlich wäre, um die Brechung und Reflektion im Oberflächengebiet des Kernes berücksichtigen zu können. Diese beiden genannten Fehlerquellen bringen eine so große Unsicherheit in die Rechnungen, daß es vorläufig noch nicht zweckmäßig ist, die Winkelverteilung genauer zu berechnen.

2. – Ansatz und Rechenmethode.

Um den Einzelstoß zwischen einem K^+ -Meson und einem Nukleon zu behandeln, führen wir folgende Größen ein: m_1 sei die Masse des K^+ -Mesons, m_2 die des Nukleons. (Von dem Massenunterschied zwischen Proton und Neutron soll hier abgesehen werden). \mathbf{P}_1 und \mathbf{P}_2 bzw. E_1 und E_2 seien die Impulse bzw. Energien der Teilchen vor dem Stoß, \mathbf{P}'_1 , \mathbf{P}'_2 bzw. E'_1 , E'_2 die entsprechenden Größen nach dem Stoß. Dann lautet der Energiesatz

$$\frac{P_1^2}{2m_1} + \frac{P_2^2}{2m_2} = \frac{P'_1^2}{2m_1} + \frac{P'_2^2}{2m_2},$$

und der Impulssatz

$$\mathbf{P}_1 + \mathbf{P}_2 = \mathbf{P}'_1 + \mathbf{P}'_2.$$

Führen wir noch die Relativimpulse vor und nach dem Stoß ein,

$$\mathbf{P} = \frac{\mathbf{P}_1 m_2 - \mathbf{P}_2 m_1}{m_1 + m_2}, \quad \mathbf{P}' = \frac{\mathbf{P}'_1 m_2 - \mathbf{P}'_2 m_1}{m_1 + m_2},$$

so gilt

$$P = P'.$$

Die eingeführten Energien E_1 , E_2 , E'_1 , E'_2 beziehen sich auf die Energie, die die Teilchen im Inneren des Kernes haben. Da, wie sich später zeigen wird, für die K^+ -Teilchen zwischen dem Innenraum und dem Außenraum des Kernes ein Potentialunterschied von $V = 20$ MeV existiert, ist die Energie E_1^A bzw. E'_1 der K^+ -Mesonen außerhalb des Kernes mit den Werten im Inneren durch

$$E_1^A = E_1 + V, \quad E'_1 = E'_1 + V$$

verbunden.

Außer durch die Erhaltungssätze sind die Stöße mit den Nukleonen noch eingeschränkt durch die Forderung, daß die Nukleonen vor dem Stoß alle Energien unterhalb der Maximalenergie E_p haben, und daß nach dem Stoß die Energie der Nukleonen größer als E_p ist. Also

$$E_2 \leq E_p \leq E'_2$$

woraus unmittelbar folgt, daß die K^+ -Mesonen nur Energie an den Kern verlieren, aber keine gewinnen können.

Der Streuquerschnitt zwischen dem K^+ -Meson und dem einzelnen Nukleon ist eine Funktion von \mathbf{P} und \mathbf{P}' . Da wegen der Stoßgesetze $P = P'$ ist, genügt es, $\sigma(\mathbf{P}, \mathbf{P}')$ in Abhängigkeit von P und ϑ' zu behandeln, wenn ϑ' der Winkel zwischen \mathbf{P} und \mathbf{P}' ist. Bezeichnen wir mit $d\Omega'$ das Winkelement in Richtung \mathbf{P}' , so ist der differentielle Querschnitt $\sigma(\mathbf{P}, \mathbf{P}') d\Omega'$.

$\sigma(\mathbf{P}, \mathbf{P}') d\Omega'$ ist der Querschnitt dafür, daß der Vektor \mathbf{P}' im Winkelement $d\Omega'$ liegt, wenn \mathbf{P} der Relativimpuls vor dem Stoß war. Den über alle möglichen Stöße, also über die möglichen Werte von P_2 gemittelten Querschnitt erhält man durch Mittelbildung über das Produkt von $\sigma(\mathbf{P}, \mathbf{P}') d\Omega'$ mit der Relativgeschwindigkeit v_r , dividiert durch die Geschwindigkeit v_i des Primärteilchens ⁽³⁾

$$(1) \quad \bar{\sigma} = \frac{3(m_1 + m_2)}{P_1 P_F^3 4\pi m_2} \int d\mathbf{P}_2 \int d\Omega' \mathbf{P} \sigma(\mathbf{P}, \mathbf{P}').$$

Die Streuexperimente zwischen K^+ -Mesonen und Nukleonen zeigen keine eindeutige Winkelabhängigkeit von $\sigma(\mathbf{P}, \mathbf{P}')$, ebenso ist wegen des sehr geringen experimentellen Materials nichts über die Energieabhängigkeit von $\sigma(\mathbf{P}, \mathbf{P}')$ bekannt. Es soll daher im Folgenden als einfacher Ansatz

$$\sigma(\mathbf{P}, \mathbf{P}') = \frac{\sigma_t(P)}{4\pi} = \frac{\sigma_t}{4\pi},$$

versucht werden, wobei $\sigma_t(P)$ der totale Querschnitt eines Nukleon- K^+ -Mesonstößes mit dem Relativimpuls P ist und auch unabhängig von P sein soll. Der Zusammenhang von σ_t mit dem Querschnitt σ_{K^+N} und σ_{K^+p} für den K^+ -Meson-Proton bzw. K^+ -Meson-Neutron-Stoß ist für den jeweils untersuchten Kern durch

$$\sigma_t = \frac{Z\sigma_{K^+p} + (A - Z)\sigma_{K^+N}}{A},$$

gegeben.

Mit diesen Annahmen erhält man

$$\bar{\sigma} = \frac{3\sigma_t(m_1 + m_2)}{P_1 P_F^3 m_2 (4\pi)^2} \int d\mathbf{P}_2 \int d\Omega' \mathbf{P}.$$

Den Querschnitt des gesamten Atomkernes erhält man daraus durch Multiplikation mit dem Atomgewicht A

$$\sigma_A = A \bar{\sigma} .$$

Die Größe σ_A ist anderseits in Photoplatten experimentell bestimmt worden, sodaß sich daraus die Konstante σ_t festlegen läßt.

Da im Folgenden vorwiegend die Energieverteilung der sekundären K^+ -Mesonen interessiert, fragen wir zunächst nach dem Querschnitt, der alle Ereignisse mit einer Sekundärenergie E'_1 erfaßt, die oberhalb einer Grenzenergie E liegen. Damit erhält man die integrale Energieverteilung $\bar{\sigma}(E)$ aus der die differentielle Verteilung $d\sigma/dE$ gewonnen werden kann.

Das Integral ist also unter den Nebenbedingungen

$$(2) \quad E'_1 \geq E, \quad E_2 \leq E_F, \quad E'_2 > E_F$$

auszuführen. Wir untersuchen dazu zunächst das Winkelement $d\Omega'$. Mit $d\Omega' = d\varphi dz$, wobei

$$z = \cos \varphi (\mathbf{P}_1 + \mathbf{P}_2, \mathbf{P}')$$

ist, lautet das Integral

$$\bar{\sigma} = \frac{3\sigma_t(m_1 + m_2)}{P_1 P_F^2 m_2 (4\pi)^2} \int d\mathbf{P}_2 \int d\varphi dz d\mathbf{P} .$$

Führt man $x = -\cos \varphi (\mathbf{P}_1, \mathbf{P}_2)$ ein, so kann z geschrieben werden als Funktion $z = z(E_1, P_2, x)$, wenn P_1 als bekannt angenommen wird. Da bei der Integration über $d\Omega'$ die Größen vor dem Stoß festgehalten werden, ist

$$dz = \frac{\partial z}{\partial E'_1} dE'_1 = \frac{(m_1 + m_2)}{|\mathbf{P}_1 + \mathbf{P}_2| P} dE'_1 .$$

Ist weiter $d\mathbf{P}_2 = d\varphi_2 dx P_2^2 dP_2$ und führt man die Integrationen über $d\varphi$ und $d\varphi_2$ aus, so ist

$$(3) \quad \bar{\sigma} = \frac{3\sigma_t(m_1 + m_2)^2}{P_1 P_F^3 4m_2} \int P_2^2 dP_2 \int dE'_1 \int \frac{dx}{|\mathbf{P}_1 + \mathbf{P}_2|} .$$

Die Grenzen von P_2 sind wegen (2)

1. $E + E_F - E_1 \leq E_2 \leq E_F \quad \text{wenn} \quad E + E_F - E_1 \geq 0 ,$
2. $0 \leq E_2 \leq E_F \quad \text{wenn} \quad E + E_F - E_1 \leq 0 .$

Die Grenzen der E_1 -Integration lauten

$$E \leq E'_1 \leq E_1 + E_2 - E_F ,$$

sind also von P_2 abhängig. Die Grenzen der x -Integration werden im allgemeinen außer von P_2 noch von E_1 abhängen. Der Integrand $1/|P_1 + P_2|$ muß daher zuerst nach x , dann nach E_1 und schließlich nach P_2 integriert werden.

3. – Durchführung der Rechnung.

Die Grenzen für die x -Integration gewinnt man durch die Forderung, daß für x und $x' = -\cos \varphi(P'_1, P'_2)$ gilt

$$|x| \leq 1, \quad |x'| \leq 1.$$

Bestimmt man x in Abhängigkeit von E_1 und x' , so erhält man

$$x = \frac{1}{2P_1P_2} \left\{ \left(\frac{m_2}{m_1} - 1 \right) (2m_1E'_1 - P_1^2) + 4\sqrt{m_1m_2E'_1(E_1 + E_2 - E'_1)}x' \right\}.$$

Für jeden E_1 -Wert wird der größte bzw. kleinste Wert von x bei $x' = +1$ bzw. $x' = -1$ erreicht. Betrachtet man x als Kurvenparameter, so ist der durch die Kurven $x = x(E'_1, +1)$ und $x = x(E'_1, -1)$ begrenzte Bereich der $x - E'_1$ -Ebene der durch die Forderung $|x'| \leq 1$ zugelassene Bereich (Abb. 1 und 2). Anderseits muß auch $|x| \leq 1$ sein, weshalb die zulässige Wertemenge in dem Rechteck $0 \leq E'_1 \leq E_1, -1 \leq x \leq +1$ enthalten sein muß. Durch diese beiden Forderungen ist der zulässige x -Bereich gegeben. Entsprechend den Abb. 1 und 2 gibt es zwei Möglichkeiten, je nachdem ob der Punkt $x(0, x') = -\mu P_1/2P_2$ größer oder kleiner als -1 ist ($\mu = (m_2/m_1) - 1$). Ist $E_M = \mu^2 P_1 / 8m_2$, so kommt es also darauf an, ob $E_2 \leq E_M$ oder $E_2 \geq E_M$. Die Schnittpunkte

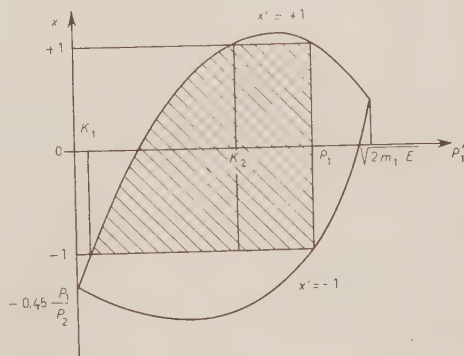


Abb. 1. – Wertebereiche für x bei $P_2 < 0.45P_1$.

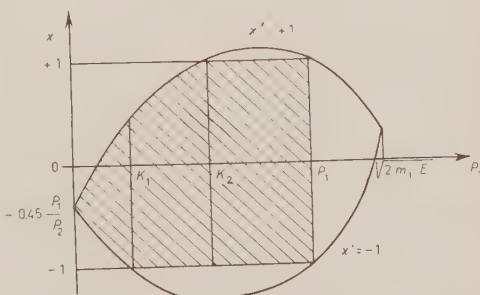


Abb. 2. – Wertebereiche für x bei $P_2 > 0.45P_1$.

E_{k_1} und E_{k_2} der x -Kurven mit den Geraden $x = \pm 1$ sind

$$E_{k_1}(E_2) = \frac{1}{2m_1} \left(\frac{\mu P_1 - 2P_2}{\mu + 2} \right)^2, \quad E_{k_2} = \frac{1}{2m_1} \left(\frac{\mu P_1 + 2P_2}{\mu + 2} \right)^2.$$

Für die Integration über x gewinnt man damit folgende Grenzen:

TABELLE I.

	Grenzen	Integral
$E_2 < E_M$		
1.	$0 < E'_1 < E_{k_1}$	$J_{11} = 0$
2.	$E_{k_1} < E'_1 < E_{k_2}$	J_{12}
3.	$E_{k_2} < E'_1 < E_1 + E_2 - E_F$	J_{13}
$-1 < x < x(E'_1, +1)$	$-1 < x < x(E'_1, +1)$	
$E_2 \geq E_M$		
1.	$0 < E'_1 < E_{k_1}$	J_{21}
2.	$E_{k_1} < E'_1 < E_{k_2}$	J_{22}
3.	$E_{k_2} < E'_1 < E_1 + E_2 - E_F$	J_{23}
$-1 < x < x(E'_1, +1)$	$-1 < x < x(E'_1, +1)$	

Diese komplizierten Grenzen für x sind ein wesentlicher Unterschied gegenüber den Rechnungen, bei denen die Streuung eines Nukleons am Kern untersucht wird. Wegen der gleichen Massen fallen dort die Punkte E_{k_1} und E_{k_2} zusammen, und es ist

$$E_{k_1} = E_{k_2} = E_2.$$

Da im Falle von Nukleonen auch für das einfallende Teilchen das Pauli-prinzip gelten muß, ist also

$$E_2 < E_F < E'_1.$$

Somit ist innerhalb des zulässigen E_1 -Gebietes $E_2 < E'_1 < E_1 + E_2 - E_F$ die x -Grenze stets $-1 < x < +1$.

Die Tatsache, daß der zulässige x -Bereich bei dem K^+ -Mesonen Problem zu kleineren Sekundärenergie hin immer kleiner wird, macht sich später sehr deutlich in der differentiellen Energieverteilung bemerkbar. Die Häufigkeit der erlaubten Stöße nimmt mit abnehmender Sekundärenergie stark ab und verschwindet stetig in $E'_1 = 0$.

Die Integration über x ist elementar auszuführen und ergibt

$$\int_{x_A}^{x_B} \frac{dx}{|\mathbf{P}_1 + \mathbf{P}_2|} = \frac{1}{P_1 P_2} (\sqrt{P_1^2 + P_2^2 - 2P_1 P_2 x_A} - \sqrt{P_1^2 + P_2^2 - 2P_1 P_2 x_B}).$$

Man erhält somit 6 Integrale $J_{kl}(E'_1, P_2)$, deren Indizes entsprechend der in Tab. I angegebenen Bezeichnung gewählt sind. Der Index k bezieht sich dabei auf das jeweilige E_2 -Gebiet, der Index j auf das E'_1 -Gebiet. Die explizite Form dieser Integrale ist in Anhang 1 angegeben. Dabei ist zu bemerken, daß $J_{12} = J_{22}$ und $J_{13} = J_{23}$ gilt.

Bei der Integration über E'_1 , die zwischen den Grenzen $E \leq E'_1 \leq E_1 + E_2 - E_F$ zu erfolgen hat, sind wiederum 3 Fälle zu unterscheiden.

1. $0 \leq E \leq E_{k_1},$
2. $E_{k_1} \leq E \leq E_{k_2},$
3. $E_{k_2} \leq E \leq E_1 + E_2 - E_F.$

Entsprechend erhält man 6 Integrale ($k=1, 2$), wobei sich der Index k wiederum auf das E_2 -Gebiet bezieht.

$$\begin{aligned} J_k^1(P_2) &= \int_E^{E_{k_1}} J_{k_1} dE'_1 + \int_{E_{k_1}}^{E_{k_2}} J_{k_2} dE'_1 + \int_{E_{k_2}}^{E_1 + E_2 - E_F} J_{k_3} dE'_1, \\ J_k^2(P_2) &= \int_E^{E_{k_2}} J_{k_2} dE'_1 + \int_{E_{k_2}}^{E_1 + E_2 - E_F} J_{k_3} dE'_1, \\ J_k^3(P_2) &= \int_E^{E_1 + E_2 - E_F} J_{k_3} dE'_1, \end{aligned}$$

wobei jetzt $J_1^2(P_2) = J_2^2(P_2)$ und $J_1^3(P_2) = J_2^3(P_2)$ gilt. Die genaue Form der Integrale ist in Anhang 2 angegeben.

Um das gesuchte Integral

$$f(E) = \int P_2^2 dP_2 \int dE'_1 \int \frac{dx}{|\mathbf{P}_1 + \mathbf{P}_2|},$$

zu erhalten, muß noch über P_2 integriert werden. Entsprechend Gl. (2) sind dabei zwei Fälle zu unterscheiden:

1. $E \leq E_1 - E_F, \quad 0 \leq E_2 \leq E_F,$
2. $E \geq E_1 - E_F, \quad E + E_F - E_1 \leq E_2 \leq E_F.$

Da die Integrale $J_k^l(P_2)$ (der Index l bezieht sich auf das E -Gebiet) über P_2 integriert werden sollen, ist hierbei zu beachten, daß in den verschiedenen E -Bereichen jeweils verschiedene J_k^l als Integrand gewählt werden müssen.

Es sind hierbei 6 Fälle zu unterscheiden:

	$(k = 1) \quad E_2 \leq E_M$	$(k = 2) \quad E_2 > E_M$
1.	$0 \leq E \leq E_{k_1}$	$0 \leq E \leq E_{k_1}$
2.	$E_{k_1} \leq E \leq E_{k_2}$	$E_{k_1} \leq E \leq E_{k_2}$
3.	$E_{k_2} \leq E \leq E_1 + E_2 - E_F$	$E_{k_2} \leq E \leq E_1 + E_2 - E_F$

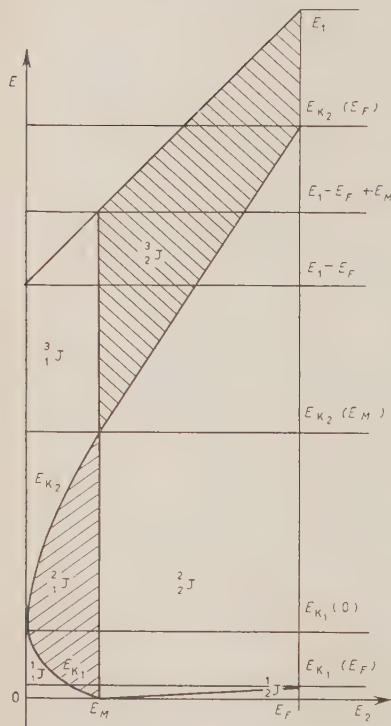


Abb. 3. – Integrationsgebiete in der (E, E_2) -Ebene.

In Abb. 3 sind in der $E-E_2$ -Ebene die verschiedenen Integrationsgebiete für E_2 jeweils bei entsprechendem E angegeben. In den 6 verschiedenen Gebieten (zur Unterscheidung sind 3 Gebiete schraffiert) ist jeweils der dort gültige Integrand $J_k^l(E, E_2)$ angegeben. Man hat entsprechend der Abb. 3 zunächst 7 Wertebereiche für E zu unterscheiden, bei denen die Integranden bzw. die Grenzen der einzelnen Integranden jeweils verschieden sind. Wegen $J_1^2 = J_2^2$ und $J_1^3 = J_2^3$ sind jedoch nur 5 Bereiche voneinander zu unterscheiden. Entsprechend gibt es 5 Integrale (der Index S bezieht sich auf ein E -Bereich) von dem Typ

$$^S J = \int_A^B J_k^l P_2^2 dP_2 + \int_{A'}^{B'} J_{k'}^l P_2^2 dP_2 + \int_{A''}^{B''} J_{k''}^l P_2^2 dP_2$$

Betrachtet man die Grenzkurven $E_{k_1}(E_2)$ und $E_{k_2}(E_2)$ als Grenzen für P_2 , so muß man die entsprechenden Gleichungen nach P_2 auflösen. Man erhält $P = \sqrt{2m_1 E}$)

E_{k_1}	linker Zweig	$P_2 = (\mu/2) P_1 - ((\mu+2)/2) P \equiv G_1$
E_{k_1}	rechter Zweig	$P_2 = (\mu/2) P_1 + ((\mu+2)/2) P \equiv G_2$
E_{k_2}		$P_2 = -(\mu/2) P_1 + ((\mu+2)/2) P \equiv G_3$

Als weitere Grenze kommt $E = E_1 + E_2 - E_F$ in Betracht, also

$$P_2 = \sqrt{2m_2(E - E_1 + E_F)} \equiv G_4 .$$

In Tab. II sind für die 5 Bereiche von E die jeweils entsprechenden Integrale angegeben. Der in jedem Integral auftretende Faktor $P_2^2 dP_2$ wurde wegen der Übersichtlichkeit in der Tabelle weggelassen.

TABELLE II.

$$\begin{aligned} {}^1J &= \int_0^{G_1} J_1^1 + \int_{G_1}^{G_2} J_1^2 + \int_{G_2}^{P_F} J_2^1 \quad 0 < E < E_{k_1}(E_F) \\ {}^2J &= \int_0^{G_1} J_1^1 + \int_{G_1}^{P_F} J_1^2 \quad E_{k_1}(E_F) < E < E_{k_1}(0) \\ {}^3J &= \int_0^{G_3} J_1^3 + \int_{G_3}^{P_F} J_1^2 \quad E_{k_1}(0) < E < E_1 - E_F \\ {}^4J &= \int_{G_4}^{G_3} J_1^3 + \int_{G_3}^{P_F} J_1^2 \quad E_1 - E_F < E < E_{k_2}(E_F) \\ {}^5J &= \int_{G_4}^{P_F} J_1^3 \quad E_{k_2}(E_F) < E < E_1 \end{aligned}$$

Die Integrationen über P_2 sind sämtlich elementar auszuführen. Die expliziten Formeln für die sJ werden jedoch so unübersichtlich, daß sie hier nicht angegeben werden sollen. Der im nächsten Abschnitt durchgeföhrte Vergleich an den berechneten mit den experimentellen Energieverteilungen soll dort nur an Hand der graphischen Darstellung durchgeföhrt werden.

4. – Vergleich mit dem Experiment.

Der gesuchte integrale Querschnitt $\bar{\sigma}(E)$ kann jetzt für die oben angegebenen verschiedenen Bereiche der Variablen E bestimmt werden. Es ist

$$\bar{\sigma}(E) = \frac{3\sigma_t(m_1 + m_2)^2}{P_1 P_F^2 4m_2} f(E).$$

Dabei ist die Masse m_1 des K^+ -Mesons nach den neuesten experimentellen Ergebnissen $966 m_e$ (m_e ist die Elektronenmasse), während für die Masse m_2 eines Nukleons der Wert $1837 m_e$ gewählt wurde. In der berechneten integralen Energieverteilung $\bar{\sigma}(E)$ ist jedoch zunächst noch ein unbestimmter Parameter vorhanden, das Potential V , das im Kerninneren auf die K^+ -Mesonen wirkt.

Die Bedeutung dieses Potentials V besteht zunächst darin, daß die Primär-energie $E_1 = E_1^A - V$ ist, wenn E_1^A die Energie außerhalb des Kernes bedeutet. Je nachdem, ob V positiv oder negativ ist, ist E_1 kleiner oder größer als E_1^A . Für E_1^A haben die Experimente den Wert von 80 MeV ergeben (1).

Eine Aussage über das gesuchte V läßt sich unmittelbar aus der experimentellen Kurve für die differentielle Energieverteilung gewinnen: Sekundär-energien unter 12 MeV kommen in der experimentellen Statistik überhaupt nicht vor, die meisten liegen sogar über 20 MeV.

Daraus kann man schließen, daß ein Potential im Kern existiert mit einer Höhe von etwa 20 MeV (Abb. 4). Die Verwendung eines Potentials von 20 MeV liefert bei der Berechnung der differentiellen Energieverteilung auch sonst die beste Anpassung an die Form der experimentellen Kurve.

Abb. 4. – Das Potential im Inneren und Äußeren des Kernes [Kastenpotential] für die K^+ -Mesonen.

Auch die von BISWAS u. a. (1) durchgeführte Monte-Carlo-Rechnungen zur Winkelverteilung ergaben eine optimale Anpassung an die Experimente bei einem Potential von 200 MeV. Für die folgenden Rechnungen soll daher der Wert von $V = 20$ MeV zugrunde gelegt werden.

Bevor wir jedoch die integrale und differentielle Energieverteilung genauer diskutieren, soll zuerst der Gesamtquerschnitt $\bar{\sigma}(0)$ untersucht werden. Der Wert $\bar{\sigma}(0)$ umfaßt alle vorkommenden Ereignisse und ist daher mit den Experimenten besonders gut zu vergleichen. Bezeichnen wir mit σ_A den totalen Querschnitt eines Kernes aus A Nukleonen, so ist:

$$\sigma_A = A\bar{\sigma}(0).$$

Der Wert σ_A ist experimentell aus der mittleren freien Weglänge der K^+ -Mesonen in der Photoemulsion bekannt. Wählt man für m_1 und m_2 die angeführten Werte und setzt $V = 20$ MeV, so ist

$$\sigma_t = 1,48 \cdot \frac{\sigma_A}{A}.$$

Mit $A = 100$, was angenähert als Mittelwert der in der Photoemulsion vorkommenden Kerne angesehen werden kann, und dem experimentellen Wert

$$\sigma_A = 0.44 \text{ barn}$$

erhält man

$$\sigma_t = 6.5 \text{ mb}.$$

Anderseits ist

$$\sigma_t = \frac{Z\sigma_{K^{+}p} + (A - Z)\sigma_{K^{+}N}}{A}.$$

Setzen wir näherungsweise $N = Z$, so lässt sich aus dem aus Einzelereignissen bekannten Querschnitt

$$\sigma_{K^+ p} = (15 \pm 5) \text{ mb}$$

der entsprechende Querschnitt für den Stoß von K^+ -Mesonen und Neutronen bestimmen. Infolge der Fehlergrenzen von $\sigma_{K^+ p}$ erhält man:

$$\sigma_{K^+ N} < 3.0 \text{ mb}$$

oder

$$\frac{\sigma_{K^+ p}}{\sigma_{K^+ N}} \geq 3.3 .$$

Ein Vergleich von $\sigma_{K^+ N}$ mit dem Experiment ist bisher leider nicht möglich, da ein entsprechendes Ereignis noch nicht gefunden werden konnte.

Mit dem eben berechneten Wert für σ_t kann jetzt nach den Formeln des letzten Kapitels der integrale Querschnitt $\sigma(E)$ berechnet werden. In Abb. 5 ist dieser integrale Querschnitt als Kurve dargestellt. Die Ordinate gibt hierbei den relativen Querschnitt $Q(E) = \bar{\sigma}(E)/\bar{\sigma}(0)$ an, während auf der Abszisse der relative Energieverlust $\epsilon^A = ((E_1 - E)/E_1^A) = \Delta E/E_1^A$ aufgetragen ist. Dabei ist $0 < \epsilon^A < 0.75$ und $0 < Q < 1$. Aus dieser Funktion lässt sich die differentielle Energieverteilung $dQ/d\epsilon^A$ berechnen. Die entsprechende Kurve ist in Abb. 6 graphisch dargestellt. Der berechnete Verlauf von $dQ/d\epsilon^A$ ist physikalisch leicht zu verstehen. Der Anstieg der Kurve zwischen $0 < \epsilon^A < 0.3$ wird durch das Pauliprinzip hervorgerufen. Je höher die Energieabgabe des Primärteilchens ist, um so mehr Möglichkeiten für einen Stoß sind vorhanden, bei dem die gestossenen Nukleonen nach dem Stoß eine Energie von $E'_2 > E_p$ haben. Der Anstieg von $dQ/d\epsilon^A$ erfolgt solange, bis ΔE genügend groß ist, damit alle Nukleonen gestoßen werden können, auch die, die im Mittelpunkt der Fermikugel liegen. Das ist der Fall, wenn $\Delta E = E_p$ also $\epsilon^A = 0.3$ ($E_p = 24 \text{ MeV}$). Genau an dieser Stelle erreicht die Kurve auch ihr Maximum.

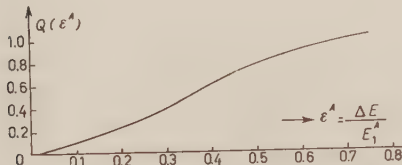


Abb. 5. - Integrale Energieverteilung.

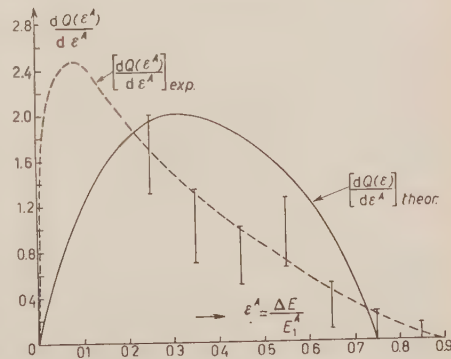


Abb. 6. - Differentielle Energieverteilung.

Der Abfall nach dem Maximum wird durch einen anderen Effekt verursacht: Findet ein Stoß mit einer Energieabgabe ΔE statt, so steht für den Primärwinkel dieses Stoßes $x = \cos \vartheta$ ein Bereich Δx zur Verfügung, der umso kleiner ist, je größer ΔE wird. (Vgl. dazu auch Abb. 1 und 2.) Dieser Effekt wird wirksam wenn $\varepsilon^4 \geq 0.089$ ist. Eine deutliche Abnahme von $dQ/d\varepsilon^4$ macht sich allerdings nur in dem Gebiet $0.3 \leq \varepsilon^4 \leq 0.75$ bemerkbar, wo das Pauliprinzip keinen weiteren Anstieg der Querschnitte mehr bewirkt. Bei $\varepsilon^4 = 0.75$, also wenn $\Delta E = E_1$, ist nur noch ein Winkel für den Stoß erlaubt $x = (\mu/2)P_1/P_2$, sodaß hier also der differentielle Querschnitt auf 0 abgefallen ist.

Die experimentellen Daten sind in Abb. 6 durch senkrechte Striche einge tragen. Versucht man, die experimentellen Werte durch eine möglichst glatte Kurve zu verbinden, so entsteht die mit $[dQ(\varepsilon^4)/d\varepsilon^4]_{\text{exp}}$ bezeichnete gestrichelte Kurve (Abb. 6). Die Extrapolation der Kurve nach links über den kleinsten experimentellen Wert bei $\varepsilon^4 = 0.25$ hinaus ist dabei keineswegs willkürlich, sondern durch zwei wesentliche Bedingungen eingeschränkt. Einerseits bewirkt das Pauliprinzip zwischen den Nukleonen, daß bei $\varepsilon^4 = 0$ auf den Wert Null abfallen muß. Anderseits ist die gesamte von der Kurve umrandete Fläche immer gleich 1, wodurch der starke Anstieg der Werte zwischen $\varepsilon^4 = 0$ und 0.2 bewirkt wird.

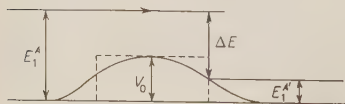
Der Vergleich zwischen der theoretischen und der experimentellen Kurve zeigt zunächst noch keine sehr befriedigende Übereinstimmung. Die Abweichungen der beiden Kurven voneinander lassen sich jedoch qualitativ gut verstehen, wenn man einige vereinfachende Annahmen, die in der Theorie gemacht wurden, berücksichtigt.

Das Vorhandensein von Ereignissen mit einer Sekundärenergie $E'_1 \leq 20$ MeV also $\varepsilon^4 > 0.75$ ist vermutlich darauf zurückzuführen, daß das Potential nicht die in Abb. 4 angegebene Gestalt hat. Zahlreiche frühere Untersuchungen

über die Struktur der Atomkerne haben gezeigt, daß eine stetig nach außen abnehmende DichteVerteilung der Nukleonen existieren muß. Es ist daher zu vermuten, daß auch das Potential V nicht wie in Abb. 4 am Kernrand unstetig Null wird, sondern wie in Abb. 7 allmählich abfällt. Die Berücksichtigung dieser Tatsache hätte zur Folge, daß besonders bei höheren Werten von ε^4 die dif-

Abb. 7. – Allmählich abfallendes Potential eines Kernes für die K^+ -Mesonen.

ferentielle Verteilung etwas flacher zu Null werden würde. Dadurch würden auch größere Energieabgaben, also kleinere Sekundärenergien möglich. Man wird daher annehmen können, daß die unterhalb 20 MeV liegenden Sekundärenergien, also die oberhalb von $\varepsilon^4 = 0.75$ liegenden Werte von $dQ/d\varepsilon^4$ durch eine solche diffuse Oberfläche erklärt werden können.



Die im Gebiet zwischen $0 < \varepsilon^4 \leq 0.25$ liegenden experimentellen Daten sind gegenüber den theoretischen Werten viel zu groß. Eine Korrektur der theoretischen Kurve in dieser Hinsicht ließe sich jedoch erreichen, wenn man beachtet, daß die in der Theorie angenommene Energieverteilung der Nukleonen im Kern, die einem vollständig entarteten Fermigas entspricht (Abb. 8), nicht ganz mit der Wirklichkeit übereinstimmt. Die Berücksichtigung der Wechselwirkung zwischen den Nukleonen ergibt eine Energieverteilung, die angenähert, der eines schwach aufgeheizten Fermigases entspricht (4,5). Für diese Tatsache sprechen auch einige neuere Streuexperimente mit Protonen und π -Mesonen (6), sowie mit Neutronen durchgeführte « pick-up-Prozesse ». Eine Korrektur in derselben Richtung ergibt sich auch, wenn man an Stelle eines unendlich großen Kernes (ebene Wellen) zu einem Kern mit endlichem Radius übergeht.

Die Verwendung einer solchen aufgelockerten Energieverteilung in den hier durchgeführten Rechnungen hat zur Folge, daß der durch das Pauliprinzip bewirkte Anstieg von $dQ/d\varepsilon^4$ im Gebiet $0 < \varepsilon^4 < 0.3$ schneller erfolgt als in der in Abb. 6 angegebenen theoretischen Kurve. Dadurch wird das Maximum der Kurve etwas nach links verschoben. Der Verlauf der differentiellen Energieverteilung wird dann in diesem Gebiet vermutlich einen ähnlichen Verlauf haben, wie die gestrichelte (experimentelle) Kurve. Eine Vergrößerung der Werte in dem Gebiet zwischen 0 und 0.2 hat andererseits wegen der Normierung der Fläche, die von der Kurve umrandet wird, zur Folge, daß die Werte zwischen 0.2 und 0.7 gegenüber der bisherigen Rechnung verkleinert werden, was ebenfalls der experimentellen Kurve besser entsprechen würde.

Diese Ergebnisse zeigen, daß durch einige geringfügige Korrekturen der hier gemachten theoretischen Ansätze (diffuse Oberfläche der Potentialverteilung und Energieverteilung eines schwach aufgeheizten Fermigases) vermutlich eine weitgehende Übereinstimmung zwischen Theorie und Experiment erreicht werden kann. Die beiden erwähnten Korrekturen sind insofern unproblematisch, als sich derartige Annahmen auch in zahlreichen anderen Arbeiten über den Aufbau der Atomkerne als richtig und notwendig erwiesen haben (*).

(4) S. WATANABE: *Zeits. Phys.*, **113**, 482 (1939).

(5) K. A. BRUECKNER, R. SERBER und K. M. WATSON: *Phys. Rev.*, **84**, 258 (1951).

K. A. BRUECKNER, N. C. FRANCIS und R. J. EDEN: *Phys. Rev.*, **98**, 1445 (1955).

(6) J. B. CLADIS, W. N. HESS und B. J. MOYER: *Phys. Rev.*, **87**, 425 (1952); P. A. WOLF: *Phys. Rev.*, **87**, 435 (1952); J. HADLEY und H. F. YORK: *Phys. Rev.*, **80**, 345 (1950).

(*) Anmerkung bei der Korrektur. - Nimmt man näherungsweise an, daß in dem « aufgeheizten » Fermigas mit der « Temperatur » kT bereits alle Nukleonen gestoßen

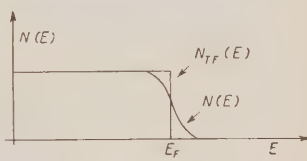


Abb. 8. - Energieverteilung der Nukleonen in schweren Kernen. $N_{TF}(E)$: Thomas-Fermi-Verteilung; $N(E)$: wirkliche Verteilung.

* * *

Herrn Prof. W. HEISENBERG, sowie den Herren Dr. CECCARELLI, Dr. DEUTSCHMANN, Dr. LÜDERS und Dr. WALOSCHEK möchte ich für zahlreiche wertvolle Diskussionen vielmals danken.

Ferner danke ich der Göttinger Plattengruppe über die freundliche Überlassung ihrer experimentellen Resultate vor deren Veröffentlichung.

ANHANG I

Das Integral

$$\int_{x_A}^{x_B} \frac{dx}{|\mathbf{P}_1 + \mathbf{P}_2|}$$

zerfällt für die verschiedenen in Tab. I und Abb. 1 und 2 angegebenen Bereiche der Variablen E'_1 und E_2 in 6 Integrale

$$J_{11} = 0,$$

$$J_{12} = \frac{1}{P_1 P_2} (P_1 + P_2 + P'_1 - P'_2),$$

$$J_{13} = \frac{2}{P_1},$$

$$J_{21} = \frac{2P'_1}{P_1 P_2},$$

$$J_{22} = \frac{1}{P_1 P_2} (P_1 + P_2 + P'_1 - P'_2),$$

$$J_{23} = \frac{2}{P_1}.$$

werden können, wenn die Energieabgabe des Primärteilchens $\Delta E = E_F - 2kT$ beträgt (kT wird hier als klein gegen E_F vorausgesetzt), so würde das Maximum der Energieverteilungskurve bei

$$\varepsilon_{\text{Max}} = \frac{E_F - 2kT}{E_1^A},$$

liegen. Die eingezeichnete experimentelle Kurve entspricht dann einem Fermigas mit einer Temperatur von $kT = 8$ MeV, in guter Übereinstimmung mit (4), (5) und (6).

Dabei ist zu bemerken, daß bei den Integralen J_{12} und J_{22} an sich

$$J_{12} = J_{22} = \frac{1}{P_1 P_2} (P_1 + P_2 - |P'_1 - P'_2|),$$

stehen müßte. In den Bereichen

$$\begin{aligned} E_{k_1} &< E'_1 < E_{k_2}, \\ 0 &< E_2 < E_F, \end{aligned}$$

ist jedoch stets

$$-|P'_1 - P'_2| \leq P'_1 - P'_2,$$

weshalb die Betragsstriche in den obigen Formeln weggelassen wurden.

Die Funktionen J_{k_i} hängen ihrerseits noch von P'_1 und P'_2 ab. (P_1 gilt hier als konstant, während P'_2 durch den Energiesatz eliminiert werden kann.).

ANHANG II

Von den 6 Integralen, $J_k^l(P_2)$, die durch die Integration über E'_1 entstehen, sind einige einander gleich. Es ist:

$$J_1^2(P_2) = J_2^2(P_2), \quad J_1^3(P_2) = J_2^3(P_2).$$

Es sollen daher nur 4 von diesen Integralen explizit angegeben werden.

$$\begin{aligned} J_1^1 &= \frac{1}{P_1 P_2} \left\{ (P_1 + P_2)(E_{k_2} - E_{k_1}) + \frac{2}{3} \sqrt{2m_1(E_{k_2}^{\frac{1}{2}} - E_{k_1}^{\frac{1}{2}})} - \right. \\ &\quad \left. - \frac{2}{3} \sqrt{2m_2} [(E_1 + E_2 - E_{k_2})^{\frac{1}{2}} - (E_1 + E_2 - E_{k_1})^{\frac{1}{2}}] \right\} + \frac{2}{P_1} (E_1 + E_2 - E_F - E_{k_2}), \end{aligned}$$

$$\begin{aligned} J_1^2 &= \frac{1}{P_1 P_2} \left\{ (P_1 + P_2)(E_{k_2} - E) + \frac{2}{3} \sqrt{2m_1(E_{k_2}^{\frac{3}{2}} - E^{\frac{3}{2}})} + \right. \\ &\quad \left. + \frac{3}{2} \sqrt{2m_2} [(E_1 + E_2 - E_{k_2})^{\frac{3}{2}} - (E_1 + E_2 - E)^{\frac{3}{2}}] \right\} + \frac{2}{P_1} (E_1 + E_2 - E_F - E_{k_2}), \end{aligned}$$

$$J_1^3 = \frac{2}{P_1} (E_1 + E_2 - E_F - E),$$

$$\begin{aligned}
 J_{\frac{1}{2}}^1 = & \frac{1}{P_1 P_2} \left\{ (P_1 + P_2)(E_{k_2} - E_{k_1}) + \frac{2}{3} \sqrt{2m_1} (E_{k_2}^{\frac{3}{2}} - E_{k_1}^{\frac{3}{2}}) + \right. \\
 & + \frac{2\sqrt{2m_2}}{3} [(E_1 + E_2 - E_{k_2})^{\frac{3}{2}} - (E_1 + E_2 - E_{k_1})^{\frac{3}{2}}] \Big\} + \\
 & + \frac{2}{P_1} (E_1 + E_2 - E_F - E_{k_2}) + \frac{4\sqrt{2m_1}}{3P_1 P_2} (E_{k_1}^{\frac{3}{2}} - E^{\frac{3}{2}}).
 \end{aligned}$$

RIASSUNTO (*)

Servendosi del metodo di Goldberger si calcola la distribuzione di energia nello scattering anelastico dei mesoni K^+ da parte di nuclei complessi. I risultati si trovano in buon accordo con i dati sperimentali per 80 MeV ottenuti dal gruppo di Göttingen.

(*) Traduzione a cura della Redazione.

Inelastic Scattering of Electrons by Nuclei.

L. J. TASSIE

*Research School of Physical Sciences
The Australian National University - Canberra, A.C.T.*

(ricevuto il 18 Febbraio 1957)

Summary. — It is shown that the variation with energy of the differential cross section for the scattering of high energy electrons by nuclei depends on whether the nuclear transition occurs with $\Delta M=0$ or with $\Delta M=\pm 1$, where M is the component of the nuclear spin in the direction of the vector change of momentum of the scattered electron. The electron excitation of $\Delta M=0$ transitions is then considered using the independent particle model of the nucleus and comparison is made with the experimental results of FREIKAU for ^{12}C .

1. — Introduction.

The study of the elastic scattering of high energy electrons by nuclei has yielded considerable information about nuclear ground states. The inelastic scattering should also provide information about the excited states. However, the theoretical treatment of the inelastic scattering presents more difficulties than that of the elastic scattering. By using the first Born approximation, which should be valid for light nuclei, SCHIFF (¹) has given a treatment of the inelastic scattering which relates the scattering cross-section to nuclear charge, current and magnetization densities which are treated as classical quantities. Some general results which are independent of the structure of the nucleus can be obtained from this theory, but to obtain detailed expressions for the scattering cross-sections some nuclear model must be assumed. The

(¹) L. I. SCHIFF: *Phys. Rev.*, **96**, 765 (1954).

independent particle model of the nucleus is used to calculate the electron scattering accompanying the electric excitation of the nucleus, and the theoretical cross-sections are compared with the experimental results of FREGEAU⁽²⁾ on the scattering of electrons by ^{12}C .

2. - $\Delta M = 0$ and $\Delta M = \pm 1$ excitation.

SCHIFF⁽¹⁾ finds that there are three possible kinds of electron excitation of nuclei, *a*) electric multipole with $\Delta M = 0$; *b-1*) electric multipole with $\Delta M = \pm 1$; *b-2*) magnetic multipole with $\Delta M = \pm 1$. M is the component of the nuclear spin along the direction of the vector change in momentum of the scattered electron. The experiments are performed at high energies and large angles, so that we can neglect the rest mass energy and the energy loss of the electron in comparison with the incident energy. Using the matrix elements given by SCHIFF⁽¹⁾, the differential scattering cross-sections then become,

$$(1) \quad a) \quad (\mathrm{d}\sigma/\mathrm{d}\omega)^{(E)}_0 = (e/\hbar c)^2 \cot^2 \frac{1}{2}\theta q^{-2} |\sum_v \{\pi(2v+1)\}^{\frac{1}{2}} i^v \int j_v(qr) Y_{v0} \varrho \mathrm{d}V|^2 ,$$

$$(2) \quad b-1) \quad (\mathrm{d}\sigma/\mathrm{d}\omega^{(E)}_{\pm 1}) = (e/\hbar c)^2 (1 + \sin^2 \frac{1}{2}\theta) \cosec^2 \frac{1}{2}\theta \cdot \\ \cdot |\sum_v \{\pi(2v+1)/v(v+1)\}^{\frac{1}{2}} i^v \int j_v(qr) Y_{v\pm 1}^* \mathbf{r} \cdot \mathrm{curl} [\mathbf{M} + (eq^2)^{-1} \mathrm{curl} \mathbf{j}] \mathrm{d}V|^2 ,$$

$$(3) \quad b-2) \quad (\mathrm{d}\sigma/\mathrm{d}\omega)^{(M)}_{\pm 1} = (e/\hbar c)^2 (1 + \sin^2 \frac{1}{2}\theta) \cosec^2 \frac{1}{2}\theta \cdot \\ \cdot (qe)^{-2} |\sum_v \{\pi(2v+1)/v(v+1)\}^{\frac{1}{2}} i^v \int j_v(qr) Y_{v\pm 1}^* \mathbf{r} \cdot \mathrm{curl} [\mathbf{j} + e \mathrm{curl} \mathbf{M}] \mathrm{d}V|^2 ,$$

where $j_v(z) \equiv (\pi/2z)^{\frac{1}{2}} J_{v+\frac{1}{2}}(z)$ is the spherical Bessel function,

$$q = 2k \sin \frac{1}{2}\theta = (2E/\hbar c) \sin \frac{1}{2}\theta ,$$

hk is the momentum of the incident electron, and ϱ , \mathbf{j} and \mathbf{M} are the transition nuclear charge, current and magnetization densities respectively.

From equation (1) it is seen that for electric transitions with $\Delta M = 0$

$$(4) \quad \mathrm{tg}^2 \frac{1}{2}\theta (\mathrm{d}\sigma/\mathrm{d}\omega)^{\Delta M=0} ,$$

is a function of $E \sin \frac{1}{2}\theta$, and from equations (2) and (3) that for electric and

⁽²⁾ J. H. FREGEAU: *Phys. Rev.*, **104**, 225 (1956).

magnetic transitions with $\Delta M = \pm 1$

$$(5) \quad \sin^2 \frac{1}{2}\theta (1 + \sin^2 \frac{1}{2}\theta)^{-1} (\frac{d\sigma}{d\omega})^{\Delta M= \pm 1},$$

is a function of $E \sin \frac{1}{2}\theta$ (*). By comparing experimental angular distributions at two or more different energies, it should be possible to test this result of the theory, and to determine whether a particular transition involves $\Delta M = 0$ or $\Delta M = \pm 1$ excitation. Where both types of excitation occur, it may be possible to separate the contributions from these two types of excitation.

The experimental results of FREGEAU and HOFSTADTER (3) for the electron excitation of the 4.43 MeV level of ^{12}C are plotted in Fig. 1 in the forms (4) and

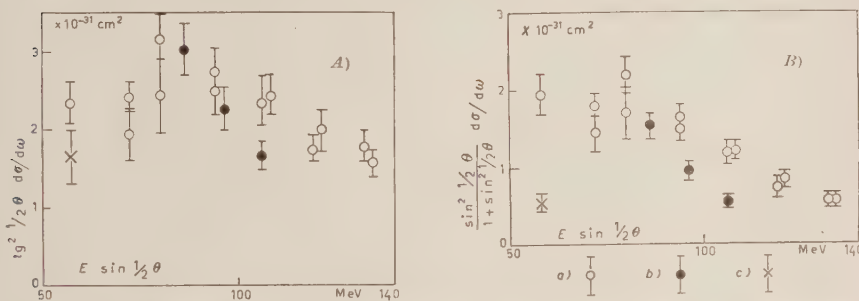


Fig. 1. - The experimental results of FREGEAU and HOFSTADTER (3) on the inelastic scattering of electrons of energies a) 187 MeV; b) 150 MeV and c) 80 MeV, with excitation of the 4.43 MeV level of ^{12}C . If the excitation involves only $\Delta M = 0$, the points plotted in A should lie on a single curve, and if only $\Delta M = \pm 1$ excitation occurs, the points plotted in B should lie on a single curve.

(5) against $E \sin \frac{1}{2}\theta$. These results would seem to indicate that $\Delta M = 0$ excitation predominates for this transition. Measurement of the scattering at 80 MeV through larger angles may give a more definite result. The experimental results of FREGEAU and HOFSTADTER (3) for the excitation of the 7.68 MeV and 9.61 MeV levels of ^{12}C were also examined but the difference in the incident energies, 37 MeV, is not sufficient to distinguish between $\Delta M = 0$ and $\Delta M = \pm 1$ excitation. More extensive measurements of the excitation of the 7.68 MeV level could test the theory for $\Delta M = 0$ excitation, as both the ground state and the 7.68 MeV level have zero spin. Measurements at several energies associated with the magnetic dipole transition $J = 1 \rightarrow J' = 0$ (no change

(*) FREGEAU (2) has used a formula different to our (5), but no derivation is given.

(3) J. H. FREGEAU and R. HOFSTADTER: *Phys. Rev.*, **99**, 1503 (1955).

in parity), such as the excitation of the 3.57 MeV level of ^6Li , would be needed to test the theory for $\Delta M = \pm 1$ excitation, since for any transition where electric excitation can occur we can expect at least some contribution from $\Delta M = 0$ excitation.

SCHIFF (1) has made rough estimates of the relative importance of $\Delta M = 0$ and $\Delta M = \pm 1$ excitation and finds that $\Delta M = 0$ excitation is expected to predominate for collective transitions, but that the $\Delta M = 0$ and $\Delta M = \pm 1$ excitations may be of equal importance for single particle transitions. Neglecting spin-orbit coupling it has been shown (4) that the $\Delta M = 0$ excitation is more important than $\Delta M = \pm 1$ excitation for some single particle transitions, but the $\Delta M = \pm 1$ excitation may be sensitive to the spin-orbit coupling. As there is the possibility of separating the two types of excitation we shall confine our treatment to $\Delta M = 0$ excitation since this is the simpler and there is some experimental evidence of its importance.

3. - Independent particle model.

Equation (1) can be written as

$$(6) \quad d\sigma/d\omega = (d\sigma/d\omega)_p \left| \sum_{\nu} i^{\nu} F_{\nu} \right|^2,$$

where $(d\sigma/d\omega)_p$ is the point charge elastic scattering cross-section and

$$(7) \quad F_{\nu} = (Ze)^{-1} \{4\pi(2\nu + 1)\}^{1/2} \int j_{\nu}(qr) Y_{\nu 0} \varrho dV.$$

Assuming that the nuclear charge density arises only from the nuclear protons we can write

$$(8) \quad F_{\nu} = (Ze)^{-1} \sum_{k=1}^A \langle i | X_k | f \rangle,$$

where

$$(9) \quad X_k = \{4\pi(2\nu + 1)\}^{1/2} \varepsilon_k j_{\nu}(qr_k) Y_{\nu 0}(\theta_k, \varphi_k).$$

r_k, θ_k, φ_k are the coordinates of the k -th nucleon and ε_k is its charge. In isotopic spin notation

$$\varepsilon_k = \frac{e}{2} (1 - \tau_{3k}).$$

(1) L. J. TASSIE: *Proc. Phys. Soc. London, A* **69**, 205 (1956).

We now use the independent particle model to calculate F_r using the method of fractional parentage (5). Since X_k operates on only one nucleon, only transitions involving a single nucleon can occur. The angular part of the operator X_k is similar to that of the operators involved in the matrix elements of electric multipole radiative transitions, and can be obtained using the methods of LANE and RADICATI (6). If n particles are required to define the transition, $(n_0 l_0)^n \rightarrow (n_0 l_0)^{n-1} (n_1 l_1)^1$, where $n_0 l_0$ and $n_1 l_1$ are not necessarily different, then

$$(10) \quad F_r = (Ze)^{-1} n \langle i | X_n | f \rangle = \\ = Z^{-1} n (-1)^{J' - J + l_0 - l_1} P C_{000}^{v l_0 l_1} C_{0MM}^{v J' J} (2\nu + 1) \langle n_0 l_0 | j_v(qr) | n_1 l_1 \rangle .$$

J and J' are the initial and final spins of the nucleus.

$$(11) \quad \langle n_0 l_0 | j_v(qr) | n_1 l_1 \rangle = \int_0^\infty R_{n_0 l_0}(r) R_{n_1 l_1}(r) j_v(qr) r^2 dr ,$$

is the single particle radial matrix element. P is the parentage overlap which is given (6) in $L-S$ coupling by

$$(12) \quad P_{L-S} = \delta_{SS'} \sum_P U(vl_1 LL_P, l_0 L') U(vL'JS, L J') \langle \alpha_P | \{\alpha\} \alpha \rangle \langle \alpha_P | \{\alpha'\} \alpha' \rangle (\frac{1}{2} \delta_{TT} - J_P) ,$$

and in $j-j$ coupling by

$$(13) \quad P_{j-j} = (-1)^{l_0 + l_1 + j_1 - j_0} \sum_P U(vj_1 JJ_P, j_0 J') \cdot \\ \cdot U(vl_1 j_0 s, l_0 j_1) \langle \alpha_P | \{\alpha\} \alpha \rangle \langle \alpha_P | \{\alpha'\} \alpha' \rangle (\frac{1}{2} \delta_{TT'} - \mathcal{C}_P) ,$$

where

$$\mathcal{C}_P = (-1)^{2T_P - T' - 2} \frac{\sqrt{3}}{2} U(1 \frac{1}{2} TT_P, \frac{1}{2} T') C_{0MTM_T}^{1 T' T} .$$

The notation is the same as that of LANE and RADICATI (6). The fractional parentage coefficients, $\langle \alpha_P | \{\alpha\} \alpha \rangle$ are tabulated for the $1p$ shell by JAHN and VAN WIERINGEN (7) for $L-S$ coupling and by EDMONDS and FLOWERS (8) for $j-j$ coupling.

(5) A. M. LANE and D. H. WILKINSON: *Phys. Rev.*, **97**, 1199 (1955).

(6) A. M. LANE and L. A. RADICATI: *Proc. Phys. Soc. London*, A **67**, 167 (1954).

(7) H. A. JAHN and H. VAN WIERINGEN: *Proc. Roy. Soc. London*, A **209**, 502 (1951).

(8) A. R. EDMONDS and B. H. FLOWERS: *Proc. Roy. Soc. London*, A **214**, 515 (1952).

The following selection rules are obtained:

$$|J - J'| \leq v \leq J + J' : |l_1 - l_0| \leq v \leq l_1 + l_0 :$$

change in parity is $(-1)^v$: $v = 0$ (electric monopole) is forbidden for $n_0 l_0 = n_1 l_1$. For $j-j$ coupling, $|j_1 - j_0| \leq v \leq j_1 + j_0$; and for $L-S$ coupling,

$$|L' - L| \leq v \leq L' + L, \quad S = S' .$$

Averaging over M , equation (6) can be written as

$$(14) \quad d\sigma/d\omega = (d\sigma/d\omega)_P \sum_v |F'_v|^2 ,$$

where

$$(15) \quad F'_v = Z^{-1} n (-1)^{l_0 - l_1} P C_{00}^{vl_0 l_1} \cdot (2v + 1)^{\frac{1}{2}} \langle n_0 l_0 | j_v(qr) | n_1 l_1 \rangle .$$

4. - The radial matrix elements.

The general single particle radial matrix element can be obtained by using the harmonic oscillator wave functions

$$(16) \quad R_{nl}(r) = \left(\frac{2\Gamma(n+l+\frac{3}{2})}{n} \right)^{\frac{1}{2}} \frac{a^{-\frac{3}{2}}}{\Gamma(l+\frac{3}{2})} \cdot (r/a)^l \exp[-\frac{1}{2}(r/a)^2] F(-n|l+\frac{3}{2}|r^2/a^2) ,$$

where the energy is

$$E_{nl} = (\hbar^2/Ma^2)(2n+l+\frac{3}{2}) .$$

The result is

$$(17) \quad \begin{aligned} \langle n_0 l_0 | j_v(qr) | n_1 l_1 \rangle &= (-1)^{n_1 2 - \frac{1}{2}(v+n_0+n_1)} \frac{(2n_0+2l_0+1)!! n_0!}{(2n_1+2l_1+1)!! n_1!} \cdot \\ &\cdot K^v \exp[-K^2/4] \sum_{i=0}^{\infty} \frac{(-1)^i K^{2i}}{2i! (2v+2i+1)!!} \cdot \\ &\cdot \sum_{m_0=0}^{n_0} \frac{(-1)^{m_0} (2s+2n_1+2m_0+1)!! (n_1+m_0+s-v)!}{m_0! (n_0-m_0)! (2l_0+2m_0+1)!! (n_1+m_0+s-v-i)!} \cdot \\ &\cdot {}_3F_2 \left(\begin{matrix} -n_1, & -l_1-n_1-\frac{1}{2}, & -n_1-m_0-(s-v)+i \\ -n_1-m_0+(s-v), & -s-n_1-m_0-\frac{1}{2} \end{matrix} \right) , \end{aligned}$$

where $s = (v + l_0 + l_1)/2$, and $K = qa$. As only finite series are involved,

(17) can be readily evaluated provided n_0 , n_1 , l_0 , l_1 and r are small as is the case for light nuclei. Some results are given in Table I.

Where only one value of r is important, the relative angular distribution of the inelastically scattered electrons depends only on r and the radial wave functions, and is independent of the angular matrix elements and thus of whether there is L - S , j - j or intermediate coupling. Also, for $qR \ll 1$,

$$(18) \quad \frac{d\sigma/d\omega}{(d\sigma/d\omega)_P} \propto' q^{2r},$$

TABLE I. — Single particle radial matrix elements for harmonic oscillator wave functions.
 $\langle n_0 l_0 | j_\nu(qr) | n_1 l_1 \rangle = a K^\nu (1 + b_1 K^2 + \dots) \exp[-K^2/4]$.

ν	$n_0 l_0$	$n_1 l_1$	a	b_1	b_2
0	1s	1s	1	—	—
0	1p	1p	1	-1/6	—
0	2s	2s	1	-1/3	1/24
0	1d	1d	1	-1/3	1/60
1	1s	1p	1/6 $^{\frac{1}{2}}$	—	—
1	1p	2s	-1/3	-1/4	—
1	1p	1d	(5/2) $^{\frac{1}{2}}$ /3	-1/10	—
2	1p	1p	-1/6	—	—
2	1d	1d	7/30	-1/14	—
2	1d	2s	-(2/5) $^{\frac{1}{2}}$ /3	-1/8	—
2	1s	1d	(1/15) $^{\frac{1}{2}}$ /2	—	—
2	1p	2p	-(1/10) $^{\frac{1}{2}}$ /3	-1/4	—
2	1p	1f	(7/5) $^{\frac{1}{2}}$ /6	-1/14	—

EO transitions $\nu = 0$.

$$\langle n_0 l_0 | j_0(qr) | n_1 l_1 \rangle = a K^0 (1 + b_1 K^2 + \dots) \exp[-K^2/4].$$

$n_0 l_0$	$n_1 l_1$	a	b_1
1s	2s	(1/6) $^{\frac{1}{2}}$ /2	—
1p	2p	(5/2) $^{\frac{1}{2}}$ /6	-1/10

except for electric monopole transitions, $\nu = 0$, for which

$$\frac{d\sigma/d\omega}{(d\sigma/d\omega)_P} \propto' q^4.$$

It may be possible by these means to determine the values of ν from experiment and thus obtain information about the spins and parities of nuclear

energy levels. However, it would be rather difficult to distinguish between $\nu = 0$ and $\nu = 2$.

5. – Application to ^{12}C .

FREGEAU and HOFSTADTER (3) and FREGEAU (2) have measured the elastic and inelastic scattering of high energy electrons by ^{12}C . Several calculations have been made of the elastic (⁹⁻¹²) scattering and the inelastic scattering (⁹⁻¹¹) using the independent particle model and of the inelastic scattering using a modified liquid drop model (13), but no completely satisfactory theory has been given for the inelastic scattering. Since it appears that $\Delta M = 0$ excitation predominates for the 4.43 MeV level and as only $\Delta M = 0$ excitation can occur for the 7.68 MeV level, the results of Sect. 3 can be applied to these two levels.

5.1. 4.43 MeV excitation. – The ground state of ^{12}C has $J = 0^+$, $T = 0$ and the 4.43 MeV state has $J = 2^+$, $T = 0$ (14). Only $E2$ ($\nu = 2$) excitation can occur. Assuming both states belong to the $(1s)^2(1p)^8$ configuration, the result for $L-S$ coupling is obtained from equations (14), (12) and Table I, using the fractional parentage tables of JAHN and VAN WIERINGEN (7).

$$(19) \quad \frac{(\text{d}\sigma/\text{d}\omega)_{L-S}}{(\text{d}\sigma/\text{d}\omega)_P} = \frac{7}{1620} K^1 \exp[-K^2/2].$$

As ^{12}C has a completed $1p$ -shell, the result for $j-j$ coupling is readily obtained.

$$(20) \quad \frac{(\text{d}\sigma/\text{d}\omega)_{j-j}}{(\text{d}\sigma/\text{d}\omega)_P} = \frac{1}{650} K^4 \exp[-K^2/2].$$

These results have been previously obtained by MORPURGO (9).

From the elastic scattering experiments, FREGEAU (2) obtains the root mean square radius of the ^{12}C nucleus as $\langle r^2 \rangle^{\frac{1}{2}} = 2.40 \cdot 10^{-13}$ cm using harmonic oscillator wave functions. This corresponds to $a = 1.63 \cdot 10^{-13}$ cm. The

(⁹) G. MORPURGO: *Nuovo Cimento*, **3**, 430 (1956).

(¹⁰) D. G. RAVENHALL: unpublished. This work is referred to in reference (2) where some of the results are given.

(¹¹) R. A. FERRELL and W. M. VISSCHER: *Phys. Rev.*, **104**, 475 (1956).

(¹²) L. J. TASSIE: *Austr. Journ. Phys.*, **9**, 400 (1956).

(¹³) L. J. TASSIE: *Austr. Journ. Phys.*, **9**, 407 (1956).

(¹⁴) F. AJZENBERG and T. LAURITSEN: *Rev. Mod. Phys.*, **27**, 77 (1955).

ratio to point charge scattering calculated from equation (19) using this value of a is compared in Fig. 2 with the experimental results of Fregeau (2) for the inelastic scattering with 4.43 MeV energy loss. The result of equation (19) multiplied by 1.4 is also shown in Fig. 2. It is seen that the observed intensity is approximately 40% larger than that calculated using L - S coupling. j - j coupling, equation (20), gives an even lower cross section than L - S coupling. The theoretical relative angular distribution, which is independent of the nuclear coupling scheme, falls off too slowly with increasing scattering angle (increasing q).

It can be shown that intermediate coupling cannot give a larger cross-section than L - S coupling for this transition. The values of P_{L-S} for transitions between various L - S states with $J = 0$ and $J = 2$ are given in Table II. The two states with $J = 0$ in Table II are the only L - S states likely to be present to any appreciable extent in the ground state. P_{L-S} vanishes for transitions from either of these two states to any other $J = 2$ states not shown in TABLE II. The maximum value of $|P|$ for a transitions between the [431]0110 state and an arbitrary mixture of the [431]01L2 states is 0.137.

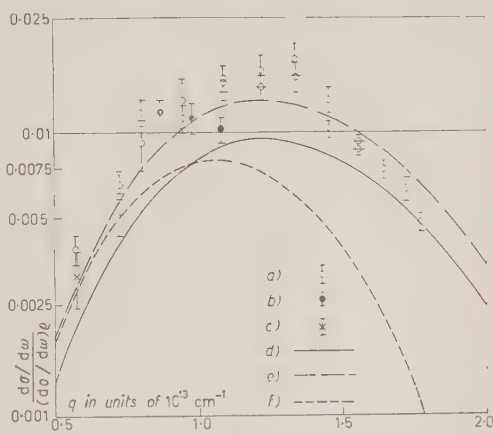


Fig. 2. — The ratio to point charge scattering of the inelastic scattering of electrons with excitation of the 4.43 MeV level of ^{12}C . The experimental points are those of FREGEAU (2) for electrons with incident energies of a) 187 MeV; b) 150 MeV and c) 80 MeV. d) calculated from eq. (19) for an $E2\ 1p \rightarrow 1p$ transition with LS coupling. e) curve (d) multiplied by 1.4. f) calculated from eq. (21) for an $E2\ 1p \rightarrow 1f$ transition assuming maximum parentage overlap of the initial and final states.

TABLE II. — $\nu = 2$.

Initial state				Final state				P	
T	S	L	J	T	S	L	J		
[44]	0	0	0	[44]	0	0	2	— 0.209	
[431]	0	1	1	0	[431]	0	1	1	+ 0.088
					[431]	0	1	2	+ 0.079
					[431]	0	1	3	— 0.066

Thus it can be concluded that equation (19) gives the maximum scattering cross-section for this transition according to the independent particle model, assuming that the 4.43 MeV state belongs to the same configuration as the ground state.

The possible $E2$ transitions between the ground state and the $J' = 2$ levels of the first few excited configurations, $(1s)^3(1p)^8(1d)$, $(1s)^4(1p)^7(1f)$ and $(1s)^4(1p)^7(2p)$ have also been examined. The inelastic electron scattering is given by

$$(21) \quad \frac{d\sigma/d\omega}{(d\sigma/d\omega)_p} = AK^4(1 + b_1K^2)^2 \exp[-K^2/2],$$

here the b_1 are given in Table I. For maximum parentage overlap, i.e. where the excited state has the same parent state as the ground state, we obtain

$$A_{1\text{-}1d} = \frac{1}{432}; \quad A_{1p\text{-}1f} = \frac{7}{1080}; \quad A_{1p\text{-}2p} = \frac{1}{810}.$$

The scattering cross-sections for the $1s \rightarrow 1d$ and $1p \rightarrow 2p$ transitions are always smaller than that for the $1p \rightarrow 1p$ transition, equation (19). The ratio to point charge scattering for the $1p \rightarrow 1f$ transition is shown in Fig. 2. Although this curve is consistent with the experimental results for small q , it decreases too quickly as q increases to account for the experimental scattering.

5.2. 7.68 MeV transition. — The 7.68 MeV level has $J = 0^+$ (¹⁴), and for this case we have $E0$ excitation ($\nu = 0$). In the limit of small q , the matrix element for $E0$ electron excitation is related to the electric monopole matrix element

$$\mathcal{M}_{E0} = \langle i | \sum_{k=1}^A \varepsilon_k r_k^2 | f \rangle,$$

occurring in the theory (¹⁵) of $E0$ decay by internal conversion or pair emission and several calculations of \mathcal{M}_{E0} have been made for this transition. If the 7.68 MeV level belongs to the $(1s)^4(1p)^8$ configuration, both the electron excitation matrix element and \mathcal{M}_{E0} vanish (using unperturbed wave functions). SCHIFF (¹⁶) and SHERMAN and RAVENHALL (¹⁷) have calculated \mathcal{M}_{E0} for such a transition using perturbation theory but the calculated matrix element is too small to account for the observed electron excitation of this level. However,

(¹⁵) R. G. SACHS: *Nuclear Theory* (Addison-Wesley, 1953).

(¹⁶) L. I. SCHIFF: *Phys. Rev.*, **98**, 1281 (1955).

(¹⁷) B. F. SHERMAN and D. G. RAVENHALL: *Phys. Rev.*, **103**, 949 (1956).

the excited 0^+ level can be also interpreted as belonging to an excited configuration. Possible configurations, which are all degenerate for the harmonic oscillator, are

$$(22) \quad \left\{ \begin{array}{l} (1s)^3(1p)^8(2s) \\ (1s)^4(1p)^7(2p) \\ (1s)^4(1p)^6(2s)^2 \\ (1s)^4(1p)^6(1d)^2 \\ (1s)^4(1p)^7(1f)^1 \\ (1s)^2(1p)^{10}. \end{array} \right.$$

REDMOND (18) has calculated \mathcal{M}_{E0} for ^{16}O and ^{12}C by considering the excited 0^+ state as due to excitation of a nucleon into the $2s$ state and ELLIOTT (19) has made a similar calculation by treating the excited 0^+ level of ^{16}O as a mixture of excited configurations. Only the first two configurations in (22) can contribute to the $E0$ matrix elements. We shall consider the electron excitation of the 7.68 MeV level, assuming that this level belongs to only one or the other of these two configurations. Mixing with the other four configurations or the $(1s)^4(1p)^8$ configuration will not alter the relative angular distribution of the scattering, but will only diminish the absolute cross-section. We can expect our results to give an upper limit to the scattering cross-section for the independent particle model. Again assuming maximum parentage overlap and also that $T' = 0$, we obtain

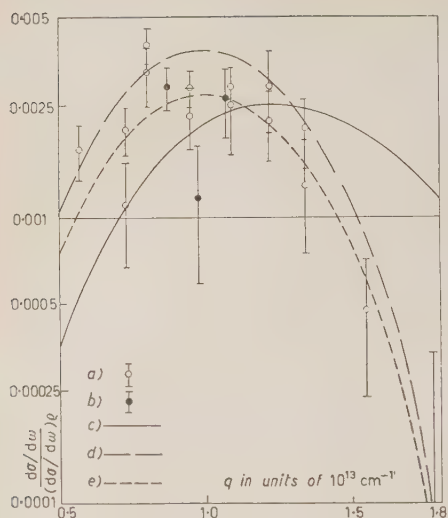
$$(23) \quad \frac{(d\sigma/d\omega)_{1s \rightarrow 2s}}{(d\sigma/d\omega)_p} = \frac{1}{864} K^4 \exp[-K^2/2],$$

$$(24) \quad \frac{(d\sigma/d\omega)_{1p \rightarrow 2p}}{(d\sigma/d\omega)_p} = \frac{5}{1296} K (1 - K^2/10) \exp[-K^2/2].$$

Fig. 3 shows the curves calculated from equations (23) and (24) in comparison with the experimental results of Fregeau (2). Also shown in Fig. 3 is the curve calculated from equation (24) reduced by a factor of 0.7. Thus, the experimental results are consistent with the 7.68 MeV excited state consisting of 70% of the $(1s)^4(1p)^7(2p)$ configuration and 30% of other configurations which do not contribute towards the electron excitation matrix element. The relative angular distribution indicates that the $(1s)^4(1p)^7(2p)$ configuration

(18) P. J. REDMOND: *Phys. Rev.*, **101**, 751 (1956).

(19) J. P. ELLIOTT: *Phys. Rev.*, **101**, 1212 (1956).



predominates over the $(1s)^3(1p)^8(2s)$ configuration, but the experimental results are not sufficiently accurate to determine the relative proportions of these two configurations with any accuracy.

Fig. 3. — The ratio to point charge scattering of the inelastic scattering of electrons with excitation of the 7.68 MeV level of ^{12}C . The experimental points are those of FREGEAU (²) for electrons with incident energies of *a*) 187 MeV and *b*) 150 MeV; *c*) calculated from eq. (23) for an $E0\ 1s \rightarrow 2s$ transition; *d*) calculated from eq. (24) for an $E0\ 1p \rightarrow 2p$ transition; *e*) curve *(d)* multiplied by 0.7.

6. — Discussion.

It can be concluded that the independent particle model can explain the observed (²) electron excitation of the 7.68 MeV level of ^{12}C , but cannot explain the observed (²) electron excitation of the 4.43 MeV level. Calculations (¹³) have been made of the electron excitation of the 4.43 MeV level using the liquid drop model and a modified form of the liquid drop model which takes into account the non-uniform nuclear charge distribution. The calculated scattering for these models is larger than the experimental scattering and falls off too rapidly with increasing angle. It would seem that a full explanation of the experimental scattering would require a description of the nucleus including both independent particle and collective effects.

In Sect. 3, the centre of the potential well has been treated as a fixed point and thus the effect of the difference between the centre of the well and the centre of mass of the nucleus has been neglected. This effect has been investigated for small q by BARKER (²⁰) and except for very light nuclei the effect is small except for electric dipole transitions with $T' = T$. The results given here cannot therefore be applied to electric dipole transitions with $T' = T$.

* * *

The author wishes to thank Dr. F. C. BARKER for many valuable discussions.

(²) F. C. BARKER: private communication.

RIASSUNTO (*)

Si dimostra che la variazione con l'energia della sezione d'urto differenziale per lo scattering di elettroni di alta energia su nuclei dipende dall'avvenire la transizione nucleare con $\Delta M=0$ o $\Delta M=\pm 1$, dove M è la componente dello spin nucleare nella direzione della variazione nucleare del momento dell'elettrone che ha subito lo scattering. Si considera poi l'eccitazione dell'elettrone nelle transizioni con $\Delta M=0$ servendosi del modello del nucleo a particelle indipendenti e si fa il confronto coi risultati sperimentali di Fregeau per il ^{12}C .

(*) Traduzione a cura della Redazione.

Derivation of the Functional Integral Formalism for Fermi Systems from the Canonical Formalism.

W. K. BURTON and A. H. DE BORDE

Department of Natural Philosophy - University of Glasgow, Scotland

(ricevuto il 19 Febbraio 1957)

Summary. — Using the canonical formulation of the quantum theory of fields, the functional integral formalism is derived for systems obeying anticommutation rules. A prescription for the evaluations of the appropriate functional integrals, using normal techniques is thereby obtained.

In a previous paper ⁽¹⁾, we showed how an explicit evaluation of the Feynman path integral could be made to give the propagators for Fermi fields. Special attention was paid to the one body propagator and apart from a sign, the prescription given led to the usual results. If, however, the same prescription is used for the evaluation of many body propagators, it leads to functions with the incorrect symmetry properties. To investigate this situation we show how the functional integral formalism for a Fermi field may be derived directly from the canonical formalism. We follow closely a method due to SYMANZIK ⁽²⁾ but differ from him in indicating a specific process whereby the integration over « anticommuting » functions is reduced to a series of normal integrations over numerical variables.

1. — We define the propagator by

$$(1) \quad \langle \psi(x_1) \dots \psi(x_n) \rangle = \frac{(\text{vac} | T\tilde{\psi}(x_1) \dots \tilde{\psi}(x_n) | \text{vac})}{(\text{vac} | \text{vac})},$$

⁽¹⁾ W. K. BURTON and A. H. DE BORDE: *Nuovo Cimento*, **4**, 254 (1956).

⁽²⁾ K. SYMANZIK: *Zeits. f. Naturfors.*, **9a**, 809 (1954).

where T indicates the time ordered product of the hermitian field operators $\psi(x)$ in the sense of WICK, and take the equation of motion of the system to be

$$L\psi(x) = 0 ; \quad L = -L^* = -L^{tr} = L^\dagger ,$$

where L is a suitable linear differential operator. Then it can be shown from the canonical formalism ⁽³⁾ that

$$(2) \quad 2L\langle\psi(x)\psi(x_1)\dots\psi(x_n)\rangle = \\ = i \sum_{j=1}^n (-1)^{j+1}\langle\psi(x_1)\dots\psi(x_{j-1})\psi(x_{j+1})\dots\psi(x_n)\rangle\delta(x-x_j)$$

and

$$(3) \quad \langle\psi(x)\psi(x_1)\dots\psi(x_n)\rangle = 0 \quad \text{if } n \text{ is even.}$$

The propagator (1) is completely antisymmetric in the variables x_1, \dots, x_n :

Our aim is to present $\langle\psi(x_1)\dots\psi(x_n)\rangle$ in terms of L as a functional integral. To this end we introduce the functional

$$(4) \quad F\{\eta\} = \sum_{n=0}^{\infty} \frac{i^n}{n!} \int \eta(x_1)\dots\eta(x_n) \langle\psi(x_1)\dots\psi(x_n)\rangle dx_1\dots dx_n = \\ = \sum_{n=0}^{\infty} \frac{(-1)^n}{(2n)!} \int \eta(x_1)\dots\eta(x_{2n}) \langle\psi(x_1)\dots\psi(x_{2n})\rangle dx_1\dots dx_{2n} ,$$

where we have appealed to (3) in writing down the second version of $F\{n\}$. Since the propagators are antisymmetric in all variables, $F\{\eta\} = 1$ if the $\eta_i(x)$ are numerical. We therefore take

$$(5) \quad \eta(x) = \sum_r \eta_r \sigma_r \varphi_r(x) ,$$

where the η_r are real, and the $\varphi_r(x)$ form a complete orthonormal set of real functions

$$(6) \quad \varphi_r \varphi_s \equiv \int \varphi_r(x) \varphi_s(x) dx = \delta_{rs} ; \quad \sum_r \varphi_r(x) \varphi_r(x') = \delta(x-x') .$$

The σ_r form an anticommuting system:

$$(7) \quad \{\sigma_r, \sigma_s\} = 2\delta_{rs} .$$

⁽³⁾ P. T. MATTHEWS and A. SALAM: *Proc. Roy. Soc., A* **221**, 128 (1954).

We can now write (4) as

$$(8) \quad F\{\eta\} = \sum \frac{i^n}{n!} \eta_{r_1} \sigma_{r_1} \dots \eta_{r_n} \sigma_{r_n} F_{r_1 \dots r_n},$$

where

$$(9) \quad F_{r_1 \dots r_n} = \int \varphi_{r_1}(x_1) \dots \varphi_{r_n}(x_n) \langle \psi(x_1) \dots \psi(x_n) \rangle dx_1 \dots dx_n$$

is completely antisymmetric in its suffixes. Accordingly, the only non-vanishing contributions to $F\{\eta\}$ in the sum (8) are those where no two of the r 's are equal. In these contributions the σ 's anticommute with one another, by (7).

2. — The next step is to find a functional differential equation satisfied by $F\{\eta\}$; this equation is then solved by using functional integration. We introduce the (left) functional derivative $\delta F/\delta\eta(x)$ as follows:

$$(10) \quad \delta F = \int \delta\eta(x) \frac{\delta F}{\delta\eta(x)} dx = \sum_r \int \delta\eta_r \sigma_r \varphi_r(x) \frac{\delta F}{\delta\eta(x)} dx = \sum_r \delta\eta_r \frac{\partial F}{\partial\eta_r}.$$

Then

$$(11) \quad \frac{\partial F}{\partial\eta_r} = \sigma_r \int \varphi_r(x) \frac{\delta F}{\delta\eta(x)} dx,$$

which, using (6) and (7), gives

$$(12) \quad \sum_r \sigma_r \varphi_r(x') \frac{\partial F}{\partial\eta_r} = \frac{\delta F}{\delta\eta(x')}.$$

A short calculation now shows that

$$(13) \quad -i \frac{\delta F\{\eta\}}{\delta\eta(x)} = \sum \frac{i^n}{n!} \int \varphi\eta(x_1) \dots \eta(x_n) \langle \psi(x) \psi(x_1) \dots \psi(x_n) \rangle dx_1 \dots dx_n.$$

If we write

$$(14) \quad S = \psi L \psi \equiv \int \psi(x) L \psi(x) dx,$$

we find, by expressing $\psi(x)$ as $\sum a_r \sigma_r \varphi_r(x)$ that

$$(15) \quad \frac{\delta S}{\delta\psi(x)} = 2L\psi(x).$$

Hence, using (2)

$$(16) \quad \frac{\delta S}{\delta \psi} \Big|_{\psi = -i(\delta/\delta \eta)} \cdot F\{\eta\} = - \sum \frac{i^n}{(n+1)!} \cdot \\ \cdot \int \{ \eta(x) \eta(x_1) \dots \eta(x_n) - \eta(x_1) \eta(x) \eta(x_2) \dots \eta(x_n) + \dots \} \langle \psi(x_1) \dots \psi(x_n) \rangle dx_1 \dots dx_n = \\ = - \sum \frac{i^n}{n!} \int A\{\eta(x), \eta(x_1) \dots \eta(x_n)\} \langle \psi(x_1) \dots \psi(x_n) \rangle dx_1 \dots dx_n,$$

where

$$(17) \quad A\{\eta(x), \eta(x_1) \dots \eta(x_n)\} = \\ = \frac{1}{n+1} [\eta(x) \eta(x_1) \dots \eta(x_n) - \eta(x_1) \eta(x) \eta(x_2) \dots \eta(x_n) + \dots],$$

is the « antisymmetric part » of $\eta(x) \eta(x_1) \dots \eta(x_n)$.

3. — It is not immediately apparent how to solve (16) so we study the related equation

$$(18) \quad \frac{\delta S}{\delta \psi} \Big|_{\psi = -i(\delta/\delta \eta)} \cdot F_1\{\eta\} = -\eta(x) F_1\{\eta\}.$$

If the function η obeyed anticommutation rules $\{\eta(x), \eta(x')\} = 0$ equations (16) and (18) would be identical. Since this relation is not obeyed, F_1 and F will not be the same, but we shall see that, in a sense to be explained later, $F\{\eta\}$ is the antisymmetric part of $F_1\{\eta\}$ and the functional derivatives of $F\{\eta\}$ are calculable from F_1 .

Introduce the Fourier transform $G_1\{\lambda\}$ of $F_1\{\eta\}$ by

$$(19) \quad F_1\{\eta\} = \int \exp[i\lambda\eta] G_1\{\lambda\} d(\lambda); \quad \lambda\eta = \int \lambda(x) \eta(x) dx = \sum_r \lambda_r \eta_r,$$

where

$$(20) \quad \lambda(x) = \sum_r \lambda_r \sigma_r \varphi_r(x).$$

Regarding $G_1\{\lambda\}$ as a function of the λ_r , the integration is over all the λ_r :

$$(21) \quad d(\lambda) = \prod_r \frac{d\lambda_r}{\sqrt{2\pi}}.$$

We have the inverse formula

$$(22) \quad G_1\{\lambda\} = \int \exp[-i\lambda\eta] F_1\{\eta\} d(\eta),$$

interpretable in a similar sense. It may be necessary to modify the volume elements in these two integrals in order to secure convergence: $d(\lambda) \rightarrow d(K\lambda)$, $d(\eta) \rightarrow d(K^{-1}\eta)$ as suggested by SYMANZIK. If so we continue to use the notation $d(\lambda)$ instead of $d(K\lambda)$. From (19) we obtain

$$-i \frac{\delta F_1}{\delta \eta(x)} = \int \lambda(x) \exp[i\lambda\eta] G_1\{\lambda\} d(\lambda),$$

so that

$$(23) \quad \left. \frac{\delta S}{\delta \Psi} \right|_{\psi = -i(\delta/\delta\eta)} \cdot F_1\{\eta\} = \int \frac{\delta S\{\lambda\}}{\delta \lambda} \exp[i\lambda\eta] G_1\{\lambda\} d(\lambda).$$

Integration by parts shows that

$$\int_{\eta_s} \exp[i\lambda\eta] G_1\{\lambda\} d(\lambda) = \int \exp[i\lambda\eta] i \frac{\partial}{\partial \lambda_s} G_1\{\lambda\} d(\lambda).$$

Hence

$$(24) \quad \eta(x) F_1\{\eta\} = \int \exp[i\lambda\eta] i \frac{\delta}{\delta \lambda(x)} G_1\{\eta\} d(\lambda)$$

Combining (18), (23) and (24) we have

$$(25) \quad \left(\frac{\delta S\{\lambda\}}{\delta \lambda(x)} + i \frac{\delta}{\delta \lambda(x)} \right) G_1\{\lambda\} = 0.$$

Put

$$(26) \quad G_1\{\lambda\} = \exp[iT\{\lambda\}].$$

Then

$$\left(\frac{\delta S}{\delta \lambda} - \frac{\delta T}{\delta \lambda} \right) \exp[iT\{\lambda\}] = 0.$$

Hence, if $G_1\{\lambda\} \neq 0$ we have $T = S + D$ where

$$\frac{\delta D\{\lambda\}}{\delta \lambda(x)} = 0.$$

This gives

$$(27) \quad F_1\{\eta\} = \int \exp [i(\psi L\psi + \psi\eta)] \cdot d(\psi),$$

if we absorb the contribution from D into the volume element $d(\psi)$.

4. - We now evaluate the functional integral using $\psi(x) = \sum_r a_r \sigma_r \varphi_r(x)$ and integrating over the a_r , first making a suitable choice of the orthonormal set $\{\varphi_r\}$. We introduce the normalized eigenfunctions of L :

$$(28) \quad L\psi_r = \lambda_r \psi_r.$$

Since L is Hermitian, the λ_r are real and we have, since L is imaginary

$$(29) \quad L\psi_r^* = -\lambda_r \psi_r^*.$$

We can label the ψ_r so that

$$(30) \quad L\psi_r = \lambda_r \psi_r; \quad \lambda_r > 0 \quad \text{and} \quad \lambda_{-r} = -\lambda_r \quad \text{for } r > 0.$$

We then have

$$(31) \quad \psi_r^* = -\psi_{-r}.$$

If L contains the appropriate imaginary part to secure the correct boundary conditions on the $\langle \psi(x_1) \dots \psi(x_n) \rangle$, the value $r = 0$ does not come into consideration. We can construct a real complete orthonormal set from the ψ_r as follows:

$$\psi_{1r} = (\psi_r + \psi_{-r})/\sqrt{2}, \quad \psi_{2r} = (\psi_r - \psi_{-r})/i\sqrt{2}; \quad r > 0.$$

We have

$$(32) \quad \begin{cases} \psi_{1r}\psi_{1s} = \delta_{rs} \\ \psi_{2r}\psi_{2s} = \delta_{rs} \\ \psi_{1r}\psi_{2s} = 0, \end{cases}$$

since $\psi_r^* \psi_s = \int \psi_r^*(x) \psi_s(x) dx = \delta_{rs}$. We shall use the $\psi_{1r}(x)$ and $\psi_{2r}(x)$ as the set $\varphi_r(x)$ mentioned above. The functions $\eta(x)$ and $\psi(x)$ are expanded as

$$(33) \quad \begin{cases} \eta(x) = \sum_{r>0} [\eta_{1r}\sigma_{1r}\psi_{1r}(x) + \eta_{2r}\sigma_{2r}\psi_{2r}(x)], \\ \psi(x) = \sum_{r>0} [a_{1r}\sigma_{1r}\psi_{1r}(x) + a_{2r}\sigma_{2r}\psi_{2r}(x)], \end{cases}$$

where the square of each σ is 1 and two different σ 's anticommute. To evaluate $\psi L \psi$ we need

$$(34) \quad \left\{ \begin{array}{l} \psi_{1r} L \psi_{1s} = \psi_{1r} L(\psi_s + \psi_{-s})/\sqrt{2} = \psi_{1r}(\lambda_s \psi_s - \lambda_{-s} \psi_{-s})/\sqrt{2} = i\lambda_s \psi_{1r} \psi_{2s} = 0 \\ \psi_{2r} L \psi_{2s} = 0 \\ \psi_{1r} L \psi_{2s} = -i\lambda_r \delta_{rs} \\ \psi_{2r} L \psi_{1s} = i\lambda_r \delta_{rs} . \end{array} \right.$$

Hence

$$(35) \quad \psi L \psi = - \sum_{r>0} 2\lambda_r a_{1r} a_{2r} \sigma_{3r} ,$$

where

$$(36) \quad \sigma_{3r} = \frac{1}{2} i[\sigma_{1r}, \sigma_{2r}] \quad (\text{not summed}).$$

Now

$$(37) \quad \eta \psi = \sum_{r>0} (\eta_{1r} a_{1r} + \eta_{2r} a_{2r}) = \psi \eta$$

and hence

$$(38) \quad \exp [i(\eta_{1r} a_{1r} + \eta_{2r} a_{2r} - 2\lambda_r a_{1r} a_{2r} \sigma_{3r})] = \\ = \exp [i(\eta_{1r} a_{1r} + \eta_{2r} a_{2r})] (\cos 2\lambda_r a_{1r} a_{2r} - i\sigma_{3r} \sin 2\lambda_r a_{1r} a_{2r}) = \\ = \frac{1}{2}(1 - \sigma_{3r}) \exp [i(\eta_{1r} a_{1r} + \eta_{2r} a_{2r} + 2\lambda_r a_{1r} a_{2r})] + \\ + \frac{1}{2}(1 + \sigma_{3r}) \exp [i(\eta_{1r} a_{1r} + \eta_{2r} a_{2r} - 2\lambda_r a_{1r} a_{2r})] .$$

We have

$$(39) \quad \left\{ \begin{array}{l} 2\lambda_r a_{1r} a_{2r} + \eta_{1r} a_{1r} + \eta_{2r} a_{2r} = 2\lambda_r \left(a_{1r} + \frac{\eta_{2r}}{2\lambda_r} \right) \left(a_{2r} + \frac{\eta_{1r}}{2\lambda_r} \right) - (\eta_{2r} \eta_{1r} / 2\lambda_r) , \\ -2\lambda_r a_{1r} a_{2r} + \eta_{1r} a_{1r} + \eta_{2r} a_{2r} = -2\lambda_r \left(a_{1r} - \frac{\eta_{2r}}{2\lambda_r} \right) \left(a_{2r} - \frac{\eta_{1r}}{2\lambda_r} \right) + (\eta_{2r} \eta_{1r} / 2\lambda_r) , \end{array} \right.$$

so that the contribution to $F_1\{\eta\}$ from the integration over a_{1r} and a_{2r} is given by

$$\int \exp [i(2\lambda_r a_{1r} a_{2r})] da_{1r} da_{2r} / 2\pi = \int \delta(2\lambda_r a_{1r}) da_{1r} = \\ = (2\lambda_r)^{-1} = \int \exp [-i(2\lambda_r a_{1r} a_{2r})] da_{1r} da_{2r} .$$

Hence

$$(40) \quad \left\{ \begin{aligned} F_1\{\eta\} &= (\det L)^{-\frac{1}{2}} D_1 \prod_{r>0} \left[\frac{1}{2} (1 - \sigma_{3r}) \exp[-i\eta_{1r}\eta_{2r}/2\lambda_r] + \right. \\ &\quad \left. + \frac{1}{2}(1 + \sigma_{3r}) \exp[i\eta_{1r}\eta_{2r}/2\lambda_r] \right] \\ &= (\det L)^{-\frac{1}{2}} D_1 \prod_{r>0} [\cos(\eta_{1r}\eta_{2r}/2\lambda_r) + i\sigma_{3r} \sin(\eta_{1r}\eta_{2r}/2\lambda_r)] \\ &= (\det L)^{-\frac{1}{2}} D_1 \exp[i/2 \sum_{r>0} \eta_{1r} \lambda^{-1} \eta_{2r} \sigma_{3r}] = \\ &= (\det L)^{-\frac{1}{2}} D_1 \exp[-(i/4)\eta L^{-1}\eta]. \end{aligned} \right.$$

In the latter formula, which has a direct interpretation only so long as we limit ourselves to a finite subset (of order $2N$) of the orthonormal set $\{q_r\}$, $\det L$ is the determinant formed by the matrix elements of L with respect to this subset. Further, the factor D_1 consists of the *arbitrary* factor D introduced into the volume element (see remark after (27)) and a weighting factor K (see remark after (22)) which must be included in the volume element to make the functional integral (22) or (27) converge in the limit $N \rightarrow \infty$. For example, factors such as the $\frac{1}{2}$ in the equation before (40) are absorbed in this way. Since D_1 contains an arbitrary factor we choose it so that the combined product $D_1(\det L)^{-\frac{1}{2}}$ converges when $N \rightarrow \infty$.

If we introduce

$$(41) \quad G_0(xx') = \langle \psi(x) \psi(x') \rangle; \quad LG_0(xx') = \frac{1}{2}i \delta(x - x'),$$

we can write this last result as

$$(42) \quad F_1\{\eta\} = (\det G_0)^{\frac{1}{2}} D_0 \exp[-\frac{1}{2}\eta G_0\eta].$$

For the purpose of later developments it may be desirable to consider a range of problems which differ from one another by having L dependent on an external field φ : $L = L_\varphi$. Let us identify the problem considered so far with the case $\varphi = 0$. In this case, if we want $F_1\{0\} = 1$ we must choose

$$(43) \quad D_0 = (\det G_0)^{-\frac{1}{2}}.$$

If we now consider a general φ , the quantity G_0 will be a functional of φ , and we may write it G_φ . Then, *providing the functional integral (27) converges with the same volume element for all φ considered, including $\varphi = 0$* we have

$$(44) \quad F_1^{(\varphi)}\{\eta\} = (\det G_0^{-1}G_\varphi)^{\frac{1}{2}} \exp[-\frac{1}{2}\eta G_\varphi\eta] = (\det L_0^{-1}L_\varphi)^{-\frac{1}{2}} \exp[-\frac{1}{2}\eta G_\varphi\eta].$$

5. — We now try to establish a connection between $F_1^{(0)}\{\eta\}$ and $F\{\eta\}$. To do this we expand the exponential as follows

$$(45) \quad \left\{ \begin{array}{l} F_1^{(0)}\{\eta\} = \sum \frac{(-1)^n}{n! 2^n} \int \eta(x_1) G_0(x_1 x'_1) \eta(x'_1) \dots \eta(x_n) G_0(x_n x'_n) \eta(x'_n) dx_1 dx'_1 \dots dx_n dx'_n \\ = \sum \frac{(-1)^n}{n! 2^n} \int \eta(x_1) \dots \eta(x_{2n}) G_0(x_1 x_2) \dots G_0(x_{2n-1} x_{2n}) dx_1 \dots dx_{2n}. \end{array} \right.$$

Now consider the functional

$$(46) \quad F_2\{\eta\} = \mathcal{A}F_1^{(0)}\{\eta\}$$

derived from $F_1^{(0)}\{\eta\}$ by replacing the kernels $G_0(x_1 x_2) \dots G_0(x_{2n-1} x_{2n})$ by their antisymmetric parts

$$(47) \quad \frac{1}{(2n)!} \sum \varepsilon(i_1 \dots i_{2n}) G_0(x_{i_1} x_{i_2}) \dots G_0(x_{i_{2n-1}} x_{i_{2n}}),$$

where $\varepsilon(1, 2, 3, \dots, 2n) = 1$ and is completely antisymmetric in $(1, \dots, 2n)$. In the indicated summation, each term appears in $n! 2^n$ equal copies arising from it by those permutations which do not sever any two arguments bracketed together by $G_0(\)$ in that term. Defining

$$(48) \quad G(x_1 \dots x_{2n}) \equiv \frac{1}{n! 2^n} \sum \varepsilon(i_1 \dots i_{2n}) G_0(x_{i_1} x_{i_2}) \dots G_0(x_{i_{2n-1}} x_{i_{2n}}),$$

which is a Pfaffian (*) in $G_0(xx')$ we can write

$$(49) \quad F_2\{\eta\} = \sum \frac{(-1)^n}{(2n)!} \int \eta(x_1) \dots \eta(x_{2n}) G(x_1 \dots x_{2n}) dx_1 \dots dx_{2n}.$$

We have from the definition of G , noting that there is only one term in $G_0(x_1 x_2)$, only one term containing $G_0(x_1 x_3)$ and so on:

$$(50) \quad \left\{ \begin{array}{l} G(x_1 \dots x_n) = G(x_1 x_2) G(x_3 x_4 \dots x_n) - G(x_1 x_3) G(x_3 x_4 x_5 \dots x_n) + \dots \\ = \sum_{j=2}^n G(x_1 x_j) (-1)^j G(x_2 \dots x_{j-1} x_{j+1} \dots x_n); \quad G(xx') \equiv G_0(xx') \end{array} \right.$$

which may be written

$$(51) \quad G(xx_1 \dots x_n) = \sum_{i=1}^n (-1)^{i+1} G(xx_i) G(x_1 \dots x_{i-1} x_{i+1} \dots x_n).$$

(*) Using this function we can write $(\det G)^{\frac{1}{2}} = PfG$ etc., in (44).

Hence

$$(52) \quad 2LG(xx_1 \dots x_n) = i \sum_{j=1}^n (-1)^{j+1} \delta(x - x_j) G(x_1 \dots x_{j-1} x_{j+1} \dots x_n).$$

We conclude that $F_2\{\eta\}$ satisfies the same functional differential equations as $F\{\eta\}$, by comparing (52) with (1) and (52) with (2). We also see from this comparison that

$$(53) \quad \langle \psi(x_1) \dots \psi(x_n) \rangle = G(x_1 \dots x_n)$$

and in fact $F\{\eta\} = F_1\{\eta\}$.

6. – Since

$$(54) \quad (-i)^n \frac{\delta^n F\{\eta\}}{\delta \eta(x_n) \dots \delta \eta(x_1)} \Big|_{\eta=0} = \langle \psi(x_1) \dots \psi(x_n) \rangle,$$

and

$$(55) \quad (-i)^n \frac{\delta^n F_1^{(0)}\{\eta\}}{\delta \eta(x_n) \dots \delta \eta(x_1)} = \int \psi(x_n) \dots \psi(x_1) \exp [i(\psi L \psi + \eta \psi)] \cdot d(\psi),$$

we see that

$$(56) \quad \langle \psi(r_1) \dots \psi(r_n) \rangle = \text{Antisymmetric part of } \int \psi(r_n) \dots \psi(r_1) \exp [i\psi L \psi] d(\psi),$$

the symmetric part arising from the presence of equal suffixes on the σ_r 's appearing in the expansion of the factor $\psi(r_n) \dots \psi(r_1)$. It is these symmetrical parts which are eliminated in formal prescriptions such as SYMANZIK's (2). The foregoing analysis can be regarded as a justification for such prescriptions.

RIASSUNTO (*)

Basandosi sulla formulazione canonica della teoria quantistica dei campi, si deriva per sistemi obbedienti a regole di anticommutazione il formalismo dei funzionali integrali. Si ottiene così una regola per il calcolo degli adatti funzionali integrali facendo ricorso solo a tecniche normali.

(*) Traduzione a cura della Redazione.

A Generalization of Reissner-Nordström Solution. II.

R. L. BRAHMACHARY

Institut für Theoretische Physik - Universität Hamburg ()*

(ricevuto il 21 Febbraio 1957)

Summary. — This is a continuation of the work on a generalization of Reissner-Nordström solution, namely the interior solution of a charged (material) sphere. Following TOLMAN (²) we may easily obtain two special solutions of the field-equations, when the energy-tensor consists of two parts, namely the electromagnetic and the material parts. The second solution, obtained by assuming $e^{\nu}(\nu'/2r) = \text{const}$ is discussed here. We further obtain another solution based on the very restrictive assumption $\varrho = -p$. We also show the validity of Birkhoff's theorem for the case of a charged sphere.

1. — In order to obtain the second solution mentioned in the first part of our note (¹) we start from the simplified form of field-equations as obtained by TOLMAN (²) namely the set of equations

$$(1) \quad 8\pi(T_1^1 - T_2^2)\frac{2}{r} = \frac{d}{dr}\left(\frac{\exp[-\lambda] - 1}{r^2}\right) + \frac{d}{dr}\left(\exp[-\lambda]\frac{\nu'}{2r}\right) + \\ + \exp[-(\lambda + \nu)]\frac{d}{dr}\left(e^\nu\frac{\nu'}{2r}\right), \quad (T_1^1 = T_2^2),$$

$$(2) \quad 8\pi p = \exp[-\lambda]\left(\frac{\nu'}{r} + \frac{1}{r^2}\right) - \frac{1}{r^2} + A,$$

$$(3) \quad 8\pi\varrho = \exp[-\lambda]\left(\frac{\lambda'}{r} - \frac{1}{r^2}\right) + \frac{1}{r^2} - A.$$

(*) Present address: Research and Training School, Indian Statistical Institute, Calcutta.

(¹) R. L. BRAHMACHARY: *Nuovo Cimento*, **4**, 1216 (1956).

(²) R. C. TOLMAN: *Phys. Rev.*, **55**, 364 (1939).

In case of our charged sphere, we now obtain the following three equations

$$(4) \quad 8\pi(t_1^1 - t_2^2) \frac{2}{r} = \frac{d}{dr} \left(\frac{\exp[-\lambda] - 1}{r^2} \right) + \frac{d}{dr} \left(\exp[-r] \frac{\nu'}{2r} \right) + \\ + \exp[-(\lambda + \nu)] \frac{d}{dr} \left(e^\nu \frac{\nu'}{2r} \right), \quad 8\pi t_1^1 = 4\pi\epsilon r^2,$$

$$(5) \quad 8\pi p - 8\pi t_1^1 = \exp[-\lambda] \left(\frac{\nu'}{r} + \frac{1}{r^2} \right) - \frac{1}{r^2} + A,$$

$$(6) \quad 8\pi\varrho + 8\pi t_4^4 = \exp[-\lambda] \left(\frac{\lambda'}{r} - \frac{1}{r^2} \right) + \frac{1}{r^2} - A.$$

Let us assume

$$e^\nu \frac{\nu'}{2r} = B^2 = \text{const},$$

$$\nu' = \frac{2B^2r}{B^2r^2 + D}.$$

Equation (4) now reduces to

$$\frac{\exp[-\lambda] - 1}{r^2} + \exp[-\lambda] \frac{\nu'}{2r} = 8\pi\epsilon r^2 + C,$$

where C is a constant of integration, whence we obtain

$$e^\lambda = \frac{1 + (2r^2B^2/D)}{(1 + (r^2B^2/D))(1 + Cr^2 + 8\pi\epsilon r^4)}.$$

Putting these values of λ , ν in equations (5), (6) we obtain the values of p and ϱ . Thus our complete solution is

$$e^\nu = B^2r^2 + D,$$

$$e^\lambda = \frac{1 + (2B^2r^2/D)}{(1 + (r^2B^2/D))(1 + Cr^2 + 8\pi\epsilon r^4)}.$$

The expressions for p and ϱ are naturally very complicated but at $r = 0$, they reduce to

$$8\pi p = \frac{4B^2}{D} + \frac{B^2C}{D} + C + A,$$

$$8\pi\varrho = -3C + \frac{6B^2}{D} - \frac{B^2C}{D} - A.$$

2. - A further solution can be obtained under very restrictive physical conditions. The equations (4) and (5) can be combined to yield

$$(7) \quad \frac{dp}{dr} = \frac{-(\varrho + p)\nu'}{2} + 3\varepsilon r,$$

we have now to solve equations (5), (6), (7). Integrating equation (6), we obtain

$$\exp[-\lambda] = 1 - \frac{r^2}{R^2} - \frac{4\pi\varepsilon r^4}{5} - 8\pi \int \varrho r^2 dr.$$

If we now assume the very restricting condition $\varrho + p = 0$ which may be physically realized only in case of a «neutron-fluid» sphere, equation (7) reduces to

$$p = \frac{3}{2}\varepsilon r^2 + c$$

and hence we obtain

$$\varrho = -\frac{3}{2}\varepsilon r^2 - c.$$

Thus

$$\exp[-\lambda] = 1 - \frac{r^2}{R^2} - \frac{4}{5}\pi\varepsilon r^4 + \frac{12}{5}\varepsilon r^5 + \frac{8}{3}Cr^3 - 8\pi D.$$

As any value of ν' , will satisfy (7) we can substitute $p, e^{-\lambda}$ in equation (5) and obtain the value of

$$\nu' = \frac{-\alpha r^5 - \beta r^4 - \gamma r^3 - \delta r^2 - (2 + 8\pi D)}{\alpha r^6 - (\beta r^6/4) - \gamma r^4 - (1/R^2)r^3 + r(1 - 8\pi D)}.$$

For very small values of r , say the case of a nucleus, we may neglect the higher powers of p and simplify ν' .

External solution: outside the charged sphere we have again the Reissner-Nordström solution if $p = 0, \varrho = 0$. The well known method of boundary conditions and equations of fit can be employed to find the value of constants, such as c in the first part of our note, B , etc.

It may be mentioned that Birkhoff's theorem is valid in case of a charged sphere. Outside the sphere,

$$\mathcal{C}_1^1 = (T_1^1 + t_1^1) = t_1^1, \quad \mathcal{C}_2^2 = t_2^2, \quad \text{etc.}$$

Thus,

$$T_1^1, T_2^2, T_3^3 = 0$$

$$t_1^1, t_2^2, t_3^3 \neq 0$$

and further,

$$T_4^1, t_4^1, T_1^4, t_1^4 = 0.$$

We have however the general equations

$$8\pi C_4^1 = - \exp[-\lambda] \frac{\dot{\lambda}}{r},$$

$$8\pi C_1^4 = - \exp[-\nu] \frac{\dot{\lambda}}{r}.$$

As $C_4^1 = (T_4^1 + t_4^1)$ and $C_1^4 = (T_1^4, t_1^4) = 0$.

We have

$$\dot{\lambda} = 0.$$

This condition leads to the validity of Birkhoff's theorem.

RIASSUNTO (*)

L'articolo è la continuazione del lavoro sulla generalizzazione della soluzione di Reissner-Nordström, cioè la soluzione interna di una sfera (materiale) carica. Secondo Tolman, quando il tensore dell'energia consiste di due parti, l'elettromagnetica e la materiale, possiamo facilmente ottenere due soluzioni particolari delle equazioni del campo. Qui discutiamo la seconda soluzione ottenuta assumendo $e^r(\nu'/2r) = \text{cost}$. Ottieniamo inoltre un'altra soluzione basata sull'ipotesi molto restrittiva $\varrho = -p$. Dimostriamo anche la validità del teorema di Birkhoff per il caso di una sfera carica.

(*) Traduzione a cura della Redazione.

On the Neutron Deficient Isotopes of Thallium, ^{200}Tl and ^{202}Tl .

R. K. GUPTA and S. JHA

Tata Institute of Fundamental Research, - Bombay

(ricevuto il 22 Febbraio 1957)

Summary. — The scintillation spectrometer studies of ^{200}Ti have shown that this isotope emits, in addition to the γ -rays reported by GERHOLM, γ -rays of energy round 1580 keV, 1680 keV, 1800 keV, 1950 keV and 2100 keV. In the study of ^{202}Ti , the ratio of the probabilities of L electron captures and K electron captures has been measured by the summing technique. The ratio P_L/P_K , leading to the 440 keV state, is $0.555_{-0.033}^{+0.036}$, from which the total decay energy has been calculated to be 600_{-7}^{+5} keV.

In this note we report the results of some of our work on ^{200}Tl and ^{202}Tl . A mercury oxide target was bombarded with deuterons in the cyclotron at the Birmingham University and immediately flown to Bombay. Thallium was separated chemically from mercury and deposited on mica. The γ -radiation from the Tl isotopes was studied in a single crystal scintillation spectrometer with a duMont photomultiplier, 6292 and a NaI(Tl) Crystal $1\frac{3}{4}$ in. in diameter and 2 in. high. The spectrum is reproduced in Fig. 1.

One can see from the spectrum that the source consisted of the 27-hr ^{200}Tl , 3-days ^{201}Tl and 12.5-days ^{202}Tl .

1. — Thallium 200.

A decay scheme for ^{200}Tl has been published by GERHOLM (¹). The energies of the γ -rays from this isotope are 116 keV, 252 keV, 289 keV, 309 keV, 368 keV, 594 keV, 627 keV, 712 keV, 758 keV, 828 keV, 1206 keV, 1227 keV,

(¹) T. R. GERHOLM: *Ark. f. Fys.*, **44** (2), 55 (1956).

1362 keV and 1516 keV, and the excited states of ^{200}Hg have been placed at 368 keV, 947 keV, 1575 keV, 1595 keV, 1660 keV, 1730 keV, 1776 keV, 1885 keV and 2137 keV. The highest energy γ -ray observed is of energy 1516 keV and another of about 1800 keV is suspected.

One observes in Fig. 1 that there are perhaps two γ -rays emitted in the region 1500–1700 keV. The energies of the γ -rays have been estimated to be 1580 keV and 1680 keV. In addition to these, γ -rays of energy 1800 keV, 1950 keV and 2100 keV are emitted. When examined in the well of a NaI(Tl) crystal 4 in. in diameter and 4 in. high, the final sum peak of feeble intensity appeared near 2400 keV. It seems that the decay energy of ^{200}Tl is about 2.4 MeV.

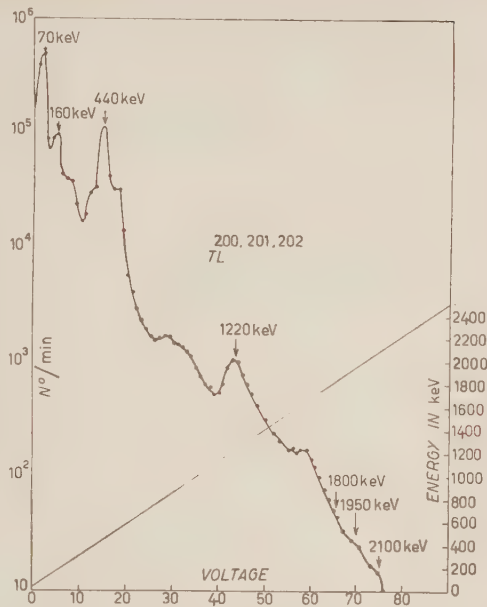


Fig. 1. – The γ -ray spectrum of ^{200}Tl , ^{201}Tl and ^{202}Tl in a single crystal spectrometer.

2. – Thallium 202.

Thallium 202 is known to decay with a half-life of 12.5-days by electron captures to the ground state of ^{202}Hg in 63% of the cases and to the first excited state at 440 keV in 37% of the cases (2,3). The decay energy of ^{202}Tl has been determined by KRAMER *et al.* (3) within rather wide limits. The summing technique has been used here to measure the decay energy (4,5).

The radiations from ^{202}Tl were studied in a single crystal spectrometer after ^{201}Tl and ^{200}Tl had decayed away. The spectrum is reproduced in Fig. 2. One notices the K X-ray peak at 68 keV along with the escape peak, the γ -ray

(2) I. BERGSTROM, R. D. HILL and G. DE PASQUATE: *Phys. Rev.*, **92**, 918 (1953).

(3) P. KRAMER, H. C. HAMERS and G. MEIJIR: *Physica*, **22**, 205 (1956).

(4) R. K. GUPTA and S. JHA: *Nuovo Cimento*, **4**, 88 (1956).

(5) A. BISI, E. GERMANOLI and L. ZAPPA: *Nuclear Physics*, **1**, 205 (1956).

peak at 440 keV and a peak at 510 keV due to the simultaneous detection of the K X-ray and the γ -ray.

The ratio of the number of coincidences between the γ -ray and the K X-ray, $I_{\gamma x}$ to the number of γ -rays, I_γ ,

$$I_{\gamma x}/I_\gamma = (N_K/N)\omega_K S \varepsilon_x \exp[-\mu_x t] = (1/(1 + P_L/P_K))\omega_K S \varepsilon_x \exp[-\mu_x t],$$

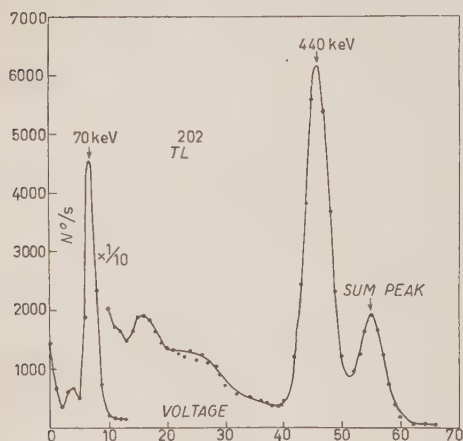


Fig. 2. — The γ -ray spectrum of ^{202}Tl with the source kept close to the NaI(Tl) crystal.

The spectra were taken with the source at various distances from the crystal, and $I_{\gamma x}/I_\gamma$ was plotted against the solid angle (Fig. 3).

The value of $I_{\gamma x}/I_\gamma$ for $S = 0.5$ was read from Fig. 3 to be 0.29 ± 0.01 . When corrected for the random summing, the value comes out to be 0.284 ± 0.01 , which gives $P_L/P_K = 0.555^{+0.036}_{-0.033}$ and the decay energy to the 440 keV state is calculated to be $161.5^{+5.4}_{-7.3}$.

The total decay energy of ^{202}Tl is 600^{+5}_{-7} keV which gives the $\log ft$ for the transition to the ground state as 7, and that for transition to the 440 keV state as 6.3. The ground state and the first excited state of the even-even isotope ^{202}Hg are 0^+ and 2^+

where N_K is the number of the K electron captures leading to the excited state, N is the total number of captures leading to the 440 keV state, ω_K the K -fluorescence yield, S the solid angle subtended by the source at the crystal, ε_x the efficiency of the detection of the K X-ray and $\exp[-\mu_x t]$ the absorption of the K X-rays in the cover of the crystal, P_K the probability of K electron capture and P_L the probability of L electron capture. The decay energy for the calculated value of P_L/P_K can be read from the curves of BRYSK and ROSE (6).

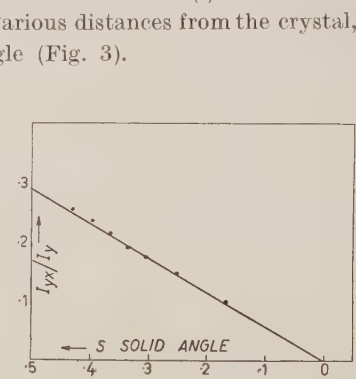


Fig. 3. — $I_{\gamma x}/I_\gamma$ is plotted against the solid angle subtended by the source at the crystal.

() H. BRYSK and M. E. ROSE: ORNL 1830.

respectively. From the log ft values, one can perhaps conclude that the electron capture decay of the odd-odd isotope ^{202}Tl both to the ground state and to the first excited state of ^{203}Hg are of the first forbidden character. The assignment of only 1^- would be consistent. This is rather surprising, as one would expect ^{202}Tl to be 2^- like ^{204}Tl .

* * *

Our thanks are due to Mr. K. S. BHATKI who separated Tl from the mercury target for us. We are grateful to Mr. B. SARAF for all the help we have received from him.

RIASSUNTO (*)

Gli studi sul ^{200}Tl fatti con l'ausilio dello spettrometro a scintillazione hanno dimostrato che questo isotopo emette, oltre ai raggi γ riferiti da GERHOLM, i γ di energie prossime a 1580 keV, 1680 keV, 1800 keV, 1950 keV e 2100 keV. Nello studio del ^{202}Tl , è stato misurato per mezzo della tecnica additiva il rapporto fra la probabilità di cattura degli elettroni L e quella degli elettroni K . Il rapporto P_L/P_K , che conduce allo stato di 440 keV è $0.555^{+0.036}_{-0.03}$ da cui si calcola l'energia di decadimento totale in 600^{+5}_{-7} keV.

(*) Traduzione a cura della Redazione.

A Method for Calculating the Anomalous Magnetic Moment of the Electron.

S. KAHANA and J. C. POLKINGHORNE

Tait Institute of Mathematical Physics, University of Edinburgh, Scotland

(ricevuto il 26 Febbraio 1957)

Summary. — A method of calculating the anomalous magnetic moment of the electron is outlined, making use of zero-photon-energy uncrossed Compton scattering diagrams. It is illustrated by a calculation of the Schwinger term.

1. — Introduction.

Recently FRANKEN and LIEBES⁽¹⁾ have measured the magnetic moment of the electron and find that their result disagrees with the theoretical estimate of KARPLUS and KROLL⁽²⁾. The value FRANKEN and LIEBES obtain for the electron magnetic moment is given, in units of the Bohr magneton, by

$$\mu_e = 1.001165 \pm .000011$$

$$1 + \frac{\alpha}{2\pi} + (0.7 + 2.0) \frac{\alpha^2}{\pi^2},$$

where α is the fine structure constant. KARPLUS and KROLL arrived at the value

$$\mu_e = 1.0011454$$

$$1 + \frac{\alpha}{2\pi} - 2.973 \frac{\alpha^2}{\pi^2}.$$

⁽¹⁾ P. FRANKEN and S. LIEBES, Jr.: *Phys. Rev.*, **104**, 1197 (1956).

⁽²⁾ R. KARPLUS and N. M. KROLL: *Phys. Rev.*, **77**, 537 (1950).

It therefore seems desirable to seek to confirm the intricate calculation of KARPLUS and KROLL by an independent method. The present authors propose to outline a method which could yield such a check, and illustrate this method by calculating the magnetic moment to first order in the fine structure constant.

2. — Method of calculation.

It is well known⁽³⁾ that the magnetic moment of the electron can be deduced by inspection of the vertex function $\Gamma_\mu(p, p')$ for small values of the momentum difference $(p' - p)$. In fact the magnetic moment term is obtained as the term of type

$$\mu_e \bar{u}(p) \sigma_{\mu\nu} (p' - p)^\nu u(p') ,$$

when $\Gamma_\mu(p, p')$ is evaluated between free spinors $u(p)$ and $u(p')$. The method proposed then consists in isolating the required terms by performing a Taylor expansion of $\Gamma_\mu(p, p')$ and using Ward's identity to simplify the calculation of these terms.

Since we are interested only in the anomalous magnetic moment (a.m.m.) of the electron, we may confine ourselves to the quantity $A_\mu(p, p')$ where

$$\Gamma_\mu(p, p) = \gamma_\mu + A_\mu(p, p') .$$

We recall that for $A_\mu(p, p')$ Ward's identity takes on the form

$$(1) \quad A_\mu(p, p) = -i \frac{\partial \Sigma^*}{\partial p^\mu}(p) ,$$

where $\Sigma^*(p)$ is the proper self energy part for the electron. The Taylor expansion of $A_\mu(p, p')$ is then seen to be

$$(2) \quad A_\mu(p, p') = -i \frac{\partial \Sigma^*}{\partial p^\mu}(p) + (p' - p)^\nu \left[\frac{\partial}{\partial p'^\nu} A_\mu(p, p') \right]_{p' = p} + \dots .$$

A slight extension of the technique involved in deducing Ward's identity allows us to interpret the coefficient of $(p' - p)^\nu$ in (2) as a sum of uncrossed Feynman diagrams contributing to the Compton scattering of zero energy photons. The operation of differentiating $A_\mu(p, p')$ with respect to p'^ν and

⁽³⁾ See for example: J. M. JAUCH and F. ROHRLICH: *The Theory of Photons and Electrons*, (Cambridge Mass. 1955). Our notation is that of JAUCH and ROHRLICH.

then setting $p' = p$ corresponds to inserting zero energy photons, in a definitely ordered fashion, into the open line of all diagrams $A_\mu(p, p)$.

We may then write

$$(3) \quad A_\mu(p, p') = -i \frac{\partial}{\partial p^\mu} \Sigma^*(p) + (p' - p)^\nu M_{\mu\nu}(p).$$

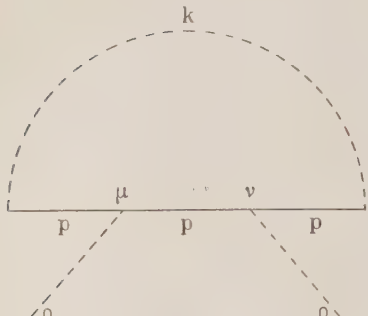


Fig. 1.

$M_{\mu\nu}(p)$ is defined as the contribution of uncrossed diagrams to zero-energy photon Compton scattering. It is given in lowest order by Fig. 1.

3. — First order calculation.

In the remaining part of this paper we will compute the a.m.m. to first order in the fine structure constant. We note that both terms in (3) will contribute to

the a.m.m. However we make use of the well known result for $\Sigma_{(2)}^*(p)$ (4) to deduce the contribution of the first term.

In fact

$$(4) \quad \Sigma^{(2)}(p) = (i\gamma p + m) \cdot$$

$$\left\{ \frac{x}{2\pi} \int_0^1 dx \frac{x(1-x)}{x^2} \int_0^1 dz \frac{m(1+x) + (i\gamma p - m)[1 - x - 2z(x - 1/x)]}{m^2 x^2 + (p^2 + m^2)x(1-x)z} \right\} \cdot (i\gamma p + m).$$

From the fashion in which we have written $\Sigma^{(2)}(p)$ it is clear that on differentiation the term we are interested in reduces to

$$(5) \quad \frac{\alpha}{2\pi m} \int_0^1 dx \frac{x(1-x^2)}{x^2} \cdot \bar{u}(p) \gamma_\mu (i\gamma p + m) u(p') = \\ = \frac{\alpha}{2\pi m} \int_0^1 dx \frac{x(1-x^2)}{x^2} \bar{u}(p) (p' - p)^\nu \sigma_{\mu\nu} u(p').$$

All the other non-zero terms in $-i\bar{u}(p)(\partial/\partial p^\mu)\Sigma^{(2)}(p)u(p')$ are proportional to higher powers of the momentum p^ν and hence do not contribute to the a.m.m.

(4) The symbol (2) appearing in $\Sigma_{(2)}^*(p)$ indicates second order in perturbation theory. The value for $\Sigma_{(2)}^*(p)$ we quote, is that given in JAUCH and ROHRLICH, loc. cit.

In addition we have from Fig. 1 (5)

$$(6) \quad M_{\mu\nu}^{(2)}(p) = -i \cdot \frac{ie^2}{(2\pi)^4} \cdot \int \frac{d^4k}{k^2} \gamma_\varepsilon \frac{1}{i\gamma(p-k) + m} \gamma_\mu \frac{1}{i\gamma(p-k) + m} \gamma_\nu \frac{1}{i\gamma(p-k) + m} \gamma^\nu.$$

The remaining part of the calculation is greatly simplified if we note that γ_μ, γ_ν appearing in (6) can be considered to anti-commute with all terms $\gamma(p-k)$ present in (6). The terms ignored in this fashion, if retained, would introduce higher powers of p^μ, p^ν or else terms proportional to $g_{\mu\nu}$. None of these would therefore contribute to the a.m.m.

If we also shift the origin of integration in (6), we find $M_{\mu\nu}^{(2)}$ reduces to

$$(7) \quad M_{\mu\nu}^{(2)} = i \cdot \frac{ie^2}{(2\pi)^4} \int \frac{d^4k}{(p-k)^2} \frac{1}{(k^2 + m^2)^2} (2i\gamma k) \gamma_\mu \gamma_\nu.$$

Thus the contribution of $M_{\mu\nu}^{(2)}$ to the a.m.m. is (6)

$$(8) \quad -\frac{\alpha}{2\pi m} \int_0^1 dx \frac{x(1-x)}{x^2} \bar{u}(p)(p'-p)^\nu \sigma_{\mu\nu} u(p').$$

Combining (5) and (8) the infrared divergences cancel and we obtain finally for the a.m.m.

$$\mu \bar{u}(p)(p'-p)^\nu \sigma_{\mu\nu} u(p') = \frac{e}{2m} \frac{\alpha}{2\pi} \bar{u}(p)(p'-p)^\nu \sigma_{\mu\nu} u(p').$$

That is the a.m.m. up to first order in the fine structure constant is $\mu_a/\mu_0 - z/2\pi$. This is the well known Schwinger term.

4. — Discussion.

Although the method employed above yields the lowest order a.m.m. with very little effort, it is questionable whether in the next order of perturbation theory it is any improvement on a direct renormalization calculation of $A_\mu(p, p')$. Firstly, the number of graphs to be evaluated for $M_{\mu\nu}^{(n)}(p)$ is greater

(5) Care needs to be taken to obtain the correct number of factors i in $M_{\mu\nu}$.

(6) The 4-momentum integration in equation (7) is performed using the symmetrical integration technique of R. P. FEYNMAN (*Phys. Rev.*, **76**, 769 (1949)).

than the corresponding number for $A_\mu^{(0)}(p, p')$. Secondly, the renormalization of $\Sigma^*(p)$ is considerably more difficult in fourth order than in second order perturbation theory. However, some simplifications may be introduced by referring to a result due to PETERMANN (?). He is able to demonstrate that if one can represent $M_{\mu\nu}(p)$ in the fashion

$$M_{\mu\nu}(p) = g_{\mu\nu}\beta + \delta\gamma_\mu\gamma_\nu + \dots$$

then the a.m.m. is given simply by the coefficient β . This result is understood if one notes that

$$M_{\mu\nu} + M_{\nu\mu} = \frac{\partial}{\partial p^\nu} \left(\frac{\partial}{\partial p^\mu} \Sigma^*(p) \right).$$

Thus one could avoid the renormalization of $\Sigma^*(p)$ in fourth order, and in fact the entire calculation is then free of ultraviolet divergences. From Petermann's point of view the simplest fashion in which to proceed would be to compute δ from $M_{\mu\nu}^{(1)}$ by methods similar to those we have used in extracting the a.m.m. contribution of $M_{\mu\nu}^{(2)}$; and also to evaluate the trace of $M_{\mu\nu}^{(1)}$, thus obtaining $\beta + \delta$.

* * *

One of us (S.K.) wishes to thank the National Research Council, Ottawa, Canada, for the award of a Special Scholarship.

(?) A. PETERMANN: *Nucl. Phys.*, **1**, 355 (1956). After this work was completed our attention was drawn to this paper. The author obtains similar results by arguments of invariance.

RIASSUNTO (*)

Metodo per calcolare il momento magnetico anomalo dell'elettrone per mezzo di diagrammi di scattering Compton non incrociati per fotoni di energia zero. Il metodo è illustrato dal calcolo del termine di Schwinger.

(*) Traduzione a cura della Redazione.

Low Energy K-Nucleon Interaction.

D. AMATI

*Istituto di Fisica Teorica dell'Università - Napoli
Istituto Nazionale di Fisica Nucleare - Sezione di Roma*

B. VITALE

*Istituto di Fisica dell'Università - Catania
Centro Siciliano di Fisica Nucleare - Catania*

(ricevuto il 4 Marzo 1957)

Summary. — The low energy K-nucleon interaction has been studied using the Salam interaction Hamiltonian for the Nucleon-Heavy Meson-Hyperon system. The K-N scattering amplitude has been calculated disregarding K virtual state contributions, recoil and virtual barion-antibarion pair effects. Results are rather independent of the cut-off energy η . The experimental data on $K^+ - N$ scattering cross sections are obtained with a renormalized coupling constant $G^2/4\pi = 0.3$. With this choice for the coupling constants, the phase shifts are small and negative for the $T = 0$ isobaric spin eigenstate and rather larger and positive for the $T = 1$ eigenstate.

Several laboratories have already obtained experimental results on K-N interaction, relative to the cross-section for K-N scattering and to the relative weights of the two possible isobaric spin amplitudes ($T = 0$ and $T = 1$). Experiments have been carried on at low energy using K-meson beams up to energies of about 200 MeV. The first results indicate (1-6):

(¹) J. E. LANNUTTI, W. W. CHUPP, G. GOLDHABER, S. GOLDHABER, E. HELMY, E. ILOFF, A. PEVSNER and D. H. RITSON: *Phys. Rev.*, **101**, 1617 (1956).

(²) N. N. BISWAS, L. CECCARELLI-FABBICHESI, M. CECCARELLI, K. GOTTSSTEIN, N. C. VARSHNEYA and P. WALOSCHEK: *Nuovo Cimento*, **3**, 825 (1956).

(³) N. N. BISWAS, L. CECCARELLI-FABBICHESI, M. CECCARELLI, M. CRESTI, K. GOTTSSTEIN, N. C. VARSHNEYA and P. WALOSCHEK: *Nuovo Cimento*, **3**, 1481 (1956).

(⁴) N. N. BISWAS, L. CECCARELLI-FABBICHESI, M. CECCARELLI, K. GOTTSSTEIN, N. C. VARSHNEYA and P. WALOSCHEK: *Nuovo Cimento*, **5**, 123 (1957).

(⁵) G. COCCONI, G. PUPPI, G. QUARENINI and A. STANGHELLINI: *Nuovo Cimento*, **5**, 172 (1957).

(⁶) M. BALDO-CEOLIN, M. CRESTI, N. DALLAPORTA, M. GRILLI, L. GUERRIERO, M. MERLIN, G. SALANDIN and G. ZAGO: *Nuovo Cimento*, **5**, 402 (1957).

a) the cross-section for K^+ -p elastic scattering is of about 15 mb at energies below 200 MeV. The Bologna group (5) gives $\sigma(K^+ \text{-} p) = (14 \pm 3) \text{ mb}$ ($E_K^{\text{kin}} = 40 \div 150 \text{ MeV}$); the Padua group (6) gives $\sigma(K^+ \text{-} p) = (14 \pm 6) \text{ mb}$ ($E_K^{\text{kin}} = 50 \div 150 \text{ MeV}$); the Göttingen group (4) gives $\sigma(K^+ \text{-} p) = (14 \pm 3) \text{ mb}$.

b) the center of mass angular distribution for K^+ -p elastic scattering does not differ significantly from an isotropic differential cross-section (4);

c) at low energy the $T = 1$ state contributes much more than the $T = 0$ state to K^+ interactions in nuclei (5,6);

d) the total K^+ -nucleus potential seems to be repulsive; this last conclusion is still of a rather tentative nature.

We have investigated if this enhancement of the $T = 1$ scattering amplitude for scattering at low energy in s waves can be attributed to the very structure of the usually assumed K-N interaction Hamiltonian; in other words, if a theory developed in a consistent way from this Hamiltonian, disregarding recoil, virtual barion-antibarion pairs, \bar{K} effects and pion interactions, will correctly describe the K-N scattering at low energies and give a good agreement with the observed behaviour (7).

1. - K-N scattering states.

Nucleons and K-mesons are assumed to be iso-spinors; Σ -particles are taken as components of an iso-vector; Λ^0 -particles as an iso-scalar. We have therefore:

$$(1) \quad N = \begin{vmatrix} p \\ n \end{vmatrix}; \quad K = \begin{vmatrix} K^+ \\ K^0 \end{vmatrix}; \quad \Sigma = \begin{vmatrix} \Sigma_1 \\ \Sigma_2 \\ \Sigma_3 \end{vmatrix},$$

where: $\Sigma^\pm = 2^{-\frac{1}{2}}(\Sigma_1 \mp i\Sigma_2)$.

The total Hamiltonian for the N-K- Σ - Λ^0 system will be (8):

$$(2) \quad H = H_N^0 + H_K^0 + H_{\Lambda^0}^0 + H_\Sigma^0 + g_\Lambda [\Psi_N \varphi_\Lambda A_k + A_k^+ \bar{\varphi}_\Lambda \Psi_N] + \\ + g_\Sigma [\bar{\Psi}_N \boldsymbol{\tau} \cdot \boldsymbol{\varphi}_\Sigma A_k + A_k^+ \boldsymbol{\varphi}_\Sigma \cdot \boldsymbol{\tau} \Psi_N] + \delta m_N \int \bar{\Psi}_N \Psi_N d\tau + \\ + \delta m_\Lambda \int \bar{\varphi}_\Lambda \varphi_\Lambda d\tau + \delta m_\Sigma \int \bar{\varphi}_\Sigma \cdot \boldsymbol{\varphi}_\Sigma d\tau,$$

(7) Interesting considerations on K-N scattering were made by A. PAIS and R. SERBER: *Phys. Rev.*, **99**, 1551 (1955).

While this work was in progress, we received a preprint of a paper by C. CEOLIN and L. TAFFARA: *Nuovo Cimento*, **5**, 435 (1957), where lowest order perturbation calculations are done on K-N scattering.

(8) B. D'ESPAGNAT and J. PRENTKI: *Nucl. Phys.*, **1**, 33 (1956); A. SALAM: *Nucl. Phys.*, **2**, 173 (1956-57).

where

$$A_k(r) = \sum_k \frac{r(k)}{(2\omega_k)^{\frac{1}{2}}} \cdot (a_k \exp[ikr] + b_k^+ \exp[-ikr]),$$

(a_k and b_k are the annihilation operators for K and \bar{K} , respectively; a_k^+ and b_k^+ the corresponding creation operators; $\omega_k = (k^2 + m_k^2)^{\frac{1}{2}}$; $r(k)$ is the usual form factor in momentum space necessary in a theory that neglects recoil effects. This also eliminates «ghost» inconsistencies; see, for instance W. PAULI *Suppl. Nuovo Cimento* 4, 703 (1956)). g_Λ and g_Σ are the rationalized but not renormalized coupling constants; the masses involved into (2) are always the «observed» masses.

The assigned spins of K-mesons and hyperons are 0 and $\frac{1}{2}$, respectively; besides the parity of the K-meson is assumed to be equal to the relative parity of hyperon and nucleon. We shall not take into account in the following recoil effects of barions and virtual barion-antibarion pair formation; therefore (2) will describe only K-N interaction in a s state.

Let $|N\rangle$ and $|N\rangle$ be the «undressed» and the «dressed» [by the interaction part of (2)] nucleon states respectively. We shall now disregard contributions to K-N interaction coming from virtual \bar{K} creation and annihilation. Because of conservation of strangeness, the processes that are not taken into account in scattering states are those that involve at least three heavy mesons at the same time. We can then express $|N\rangle$ as a linear combination of bare nucleon, bare meson plus Λ^0 and bare meson plus Σ states:

$$(3) \quad |N\rangle = A(|N\rangle + \sum_k g(k) a_k^+ |\Lambda^0\rangle + \sum_{k,l} f_l(k) a_k^+ |\Sigma_l\rangle),$$

where l is the isobaric index of the Σ .

The assumption that m_N is the «observed» nucleon mass gives:

$$(4) \quad H|N\rangle = m_N|N\rangle.$$

Substitution of (3) into (4) easily gives:

$$(5) \quad g(k) = -\frac{g_\Lambda v(k)}{\sqrt{2\omega_k} (\omega_k + m_\Lambda - m_N)},$$

$$(6) \quad f_l(k) = -\frac{g_\Sigma v(k) \tau^l}{\sqrt{2\omega_k} (\omega_k + m_\Sigma - m_N)},$$

$$(7) \quad \delta m_N = g_\Lambda \sum_k \frac{g(k)v(k)}{\sqrt{2\omega_k}} + g_\Sigma \sum_{k,l} \frac{\tau^l f_l(k)v(k)}{\sqrt{2\omega_k}}.$$

The normalization of $|N\rangle$ gives:

$$(8) \quad A^2 = [1 + \sum_k g^2(k) + \sum_{k,l} f_l^2(k)]^{-1}.$$

A^2 and δm_N are related to the coupling constant renormalization and to the nucleon mass renormalization, respectively.

In the assumptions made, the Hamiltonian (2) presents many analogies with the Hamiltonian studied by LEE⁽⁹⁾, and the scattering states ($K-N$) can be solved and the relative phase shifts found as function of the energy, without using perturbation methods. We shall express the physical state $|N + K\rangle$, in analogy with (3), by the expansion:

$$(9) \quad |N + K\rangle = [\sum_k \chi(k) a_k^+ |N\rangle + \sum_{k,l} \Psi(k, k') a_k^+ a_{k'}^+ |\Lambda^0\rangle + \\ + \sum_{k,k',l} \varphi_l(k, k') a_k^+ a_{k'}^+ |\Sigma_l\rangle],$$

and the relation:

$$(10) \quad H|N + K\rangle = (m_N + \omega_p)|N + K\rangle,$$

where ω_p is the total energy of the K , gives (putting $(g_\Lambda^2 A^2) = G_\Lambda^2$; $(g_\Sigma^2 A^2) = G_\Sigma^2$) the following integral equation for the scattering amplitude:

$$(11) \quad \chi(k)(\omega_k - \omega_p)h(k) = G_\Lambda^2 \int K_\Lambda(k, k') \chi(k') d^3 k' + \\ + G_\Sigma^2 \sum_l \tau^l \cdot \tau^l \int K_\Sigma(k, k') \chi(k') d^3 k',$$

where

$$(12) \quad K_V(k, k') = \frac{1}{16\pi^3} \frac{v(k)v(k')}{\sqrt{\omega_k \omega_{k'} (\omega_k + \omega_{k'} - \omega_p - m_N + m_Y)}},$$

and

$$(13) \quad h(k) = 1 - \frac{G_\Lambda^2}{16\pi^3} \int \frac{v^2(k')(\omega_k - \omega_p)d^3 k'}{\omega_k(\omega_{k'} + m_\Lambda - m_N)^2(\omega_k + \omega_{k'} - \omega_p + m_\Lambda - m_N)} - \\ - \frac{3G_\Sigma^2}{16\pi^3} \int \frac{v^2(k')(\omega_k - \omega_p)d^3 k'}{\omega_k(\omega_{k'} + m_\Sigma - m_N)^2(\omega_k + \omega_{k'} - \omega_p + m_\Sigma - m_N)}.$$

Projecting now $\chi(k)$ into the two isobaric spin eigenstates χ_0 and χ_1 , cor-

(9) T. D. LEE: *Phys. Rev.*, **95**, 1329 (1954).

responding to the eigenvalues $T = 0$ and $T = 1$, and using the projection operators:

$$(14) \quad P_0 = \frac{1 - \mathbf{\tau} \cdot \mathbf{\tau}}{4}; \quad P_1 = \frac{3 + \mathbf{\tau} \cdot \mathbf{\tau}}{4},$$

we obtain:

$$(15) \quad \chi_0(k)(\omega_k - \omega_p)h(k) = \frac{G_\Lambda^2}{16\pi^3} \int K_\Lambda \chi_0(k') d^3k' - \frac{3G_\Sigma^2}{16\pi^3} \int K_\Sigma \chi_0(k') d^3k',$$

$$(16) \quad \chi_1(k)(\omega_k - \omega_p)h(k) = \frac{G_\Lambda^2}{16\pi^3} \int K_\Lambda \chi_1(k') d^3k' + \frac{G_\Sigma^2}{16\pi^3} \int K_\Sigma \chi_1(k') d^3k'.$$

2. - Solution of the integral equation for the scattering amplitudes.

Equations (15) and (16) can be put into the form:

$$(17) \quad \chi_\alpha(k) = \delta(k - p) + C_\alpha \int \frac{K_\alpha(k, k') \chi_\alpha(k') d^3k'}{(\omega_k - \omega_p)h(k)}.$$

The Fredholm method gives the solution in the form:

$$(18) \quad \chi_\alpha(k) = \delta(k - p) + \frac{A_\alpha(p; k, p)}{D_\alpha(p)},$$

where $A_\alpha(p; k, p)$ and $D_\alpha(p)$ are given, in first approximation, by:

$$(19) \quad A_\alpha(p; k, p) = p^2 C_\alpha \frac{K_\alpha(k, p)}{(\omega_k - \omega_p)h(k)},$$

$$(20) \quad D_\alpha(p) = 1 - C_\alpha \int \frac{K_\alpha(k, k) d^3k}{(\omega_k - \omega_p)h(k)}.$$

In order to understand how good is the first approximation of the Fredholm method as applied to our problem, we have tried to solve our integral equation in another approximate way by slightly modifying its kernel in order to have it separable into the variables k and k' . When this is done the equation can be easily solved by the Schmidt method; the results that follow are not modified in a significant way when this second method is applied.

3. - Results.

The expression (13) for $h(k)$, when a square cut-off with $\omega_{\max} = \eta$ is introduced, can be easily integrated using some trivial approximations and disregarding the nucleon-hyperon mass differences; we get then:

$$(21) \quad h(k) = \left[1 - \frac{\hbar}{\sqrt{3\pi}} \left(\frac{G_\Lambda^2 + 3G_\Sigma^2}{4\pi} \right) \left(\frac{(2\omega_k - 2\omega_p + m_k)(\eta - m_k)}{(2m_z + \omega_k - \omega_p)(2\eta + \omega_k - \omega_p)} - \frac{\eta - m_k}{\eta} \right) \right],$$

$D_0(k)$ and $D_1(k)$ have been integrated numerically, using (21). From the values of A_α and D_α we can get the value of the phase shift at the energy ω_p , using the expression (10):

$$(22) \quad \operatorname{tg} \eta_\alpha(p) = \frac{\pi}{D_\alpha(p)} \lim_{k \rightarrow p} [(k - p) A_\alpha(p; k, p)],$$

and the corresponding scattering cross-section:

$$(23) \quad \sigma_\alpha(\omega_p) = \frac{4\pi}{p^2} \sin^2 \eta_\alpha(p),$$

Numerical results will depend on the values taken for the two coupling constants G_Λ^2 and G_Σ^2 and for the cut-off energy η . Numerical values for the phase-shifts are however rather insensitive to variations of η from 2000 to about 3000 MeV. We shall give in the following the numerical results obtained with $\eta = 2000$ MeV and $\eta = 3000$ MeV.

We shall now make the following assumptions on the numerical values of the coupling constants:

a) $G_\Lambda^2 = G_\Sigma^2 = G^2$.

The Fredholm method, with $G^2/4\pi = 0.3$, gives a small negative phase shift for the $T = 0$ state and a positive phase shift for the $T = 1$ state. We get:

	η_0	σ_0	η_1	σ_1
$\eta = 2 \text{ GeV}$				
$E_K^{\text{kin}} = 100 \text{ MeV}$	— 8°	$\sim 1 \text{ mb}$	+ 27°	9 mb
$E_K^{\text{kin}} = 200 \text{ MeV}$	— 11°	$\sim 1 \text{ mb}$	+ 32°	6 mb
$\eta = 3 \text{ GeV}$				
$E_K^{\text{kin}} = 100 \text{ MeV}$	— 8°	$\sim 1 \text{ mb}$	+ 32°	13 mb
$E_K^{\text{kin}} = 200 \text{ MeV}$	— 10°	$\sim 1 \text{ mb}$	+ 38°	9 mb

(10) W. KOHN: *Phys. Rev.*, **84**, 495 (1951).

The qualitative aspect of these results is not modified in a significant way by small variations for the numerical value of $G^2/4\pi$; the $T=0$ phase shifts are always small and negative, the $T=1$ phase shifts are always rather larger and positive. The value $G^2/4\pi = 0.3$ was chosen in order to give a good agreement with experiment for the $T=1$ cross-section ($K^+ N$ scattering) when $\eta = 3$ GeV.

b) $G_\Lambda^2 \neq G_\Sigma^2$.

There is no value for $G_\Lambda^2/4\pi$ that can give the correct $T=1$ cross-section at 100 MeV and at the same time a negligible $T=0$ interaction if we put $G_\Sigma^2 = 0$; the same holds if we put $G_\Lambda^2 = 0$. Therefore, in order to account for the experimental data, we have to consider both the $N-K-\Lambda^0$ and the $N-K-\Sigma$ coupling.

4. - Conclusions.

We conclude from the previous analysis that the observed experimental behaviour in $K-N$ scattering is related probably to the structure of the interaction Hamiltonian, at least so far as the two coupling constants involved are of the same order of magnitude.

These results have to be taken with some care as the neglect of recoil effects is less justifiable here than in the pion-nucleon case; and besides the presence of \bar{K} and π in the intermediate states could modify them in a way that we cannot at present foresee. We feel however confident that the enhanced character of the $T=1$ scattering amplitude at low energy is not a result of our approximations but is bound to the nature of the interaction Hamiltonian.

* * *

We wish to thank here Prof. M. CINI for useful discussions; and the Bologna and Padua groups who sent us prepublication copies of their papers.

One of us (D.A.) is grateful to the Consiglio Nazionale delle Ricerche for financial support.

RIASSUNTO

È stata studiata l'interazione K -Nucleone a bassa energia, usando l'hamiltoniana di Salam e risolvendo per l'ampiezza di diffusione $K-N$ trascurando i contributi dei K virtuali e del rinculo. I risultati sono poco sensibili al valore del taglio in energia per i K . Un buon accordo con i dati sperimentali è ottenuto ponendo le costanti di accoppiamento entrambe uguali a $G^2/4\pi = 0.3$. Con questa scelta per le costanti di accoppiamento gli sfasamenti risultano piccoli e negativi per l'autostato di spin isobare con $T = 0$, e piuttosto più grandi e positivi per l'autostato di spin isobarico $T = 1$.

**Expérience sur les gerbes pénétrantes produites par les mesons μ
dans une grande chambre de Wilson sous terre.**

D. KESSLER and R. MAZE

Ecole Normale Supérieure - Paris

(ricevuto il 4 Marzo 1957)

Summary. — A large cloud chamber containing 12 Pb plates (1 cm thick) and internal Geiger counters has been operated for 5000 h at 65 m w.e. underground. 28 penetrating showers produced inside the chamber by high energy μ -mesons have been observed. These showers have been analysed with the following results: 1) As far as the relative number of secondary π^\pm , π^0 and protons is concerned, the penetrating showers observed underground do not differ significantly from those obtained at sea-level and mountain altitudes. The observed mean free path for star production and nuclear scattering by the ionizing secondaries (the outgoing μ -meson being excluded) is 233 ± 52 g/cm $^{-2}$ Pb. This corresponds to a geometrical mfp, taking into account the finite plate thickness. 2) The angle of deviation of the μ -meson in the interaction is shown to be very small, less than 2° in most cases. This is about one order of magnitude less than the estimated ratio q/E of energy transfer to primary energy, in agreement with the interpretation of the events in terms of inelastic photo-nuclear interactions. 3) The mean number of ionizing penetrating secondaries (without the outgoing μ -meson) is 3.7. The mean energy of the observed events has been estimated from the electron cascades produced by disintegration of π^- -mesons: 16 GeV. 4) The observed cross-section of $(0.43 \pm 0.08) \cdot 10^{-31}$ cm 2 /nucleon for production of penetrating showers of more than 12 GeV by μ -mesons at 65 m w.e. underground is in good agreement with the predictions of a refined Williams-Weizsäcker theory and an assumed photo-nuclear cross-section of 10^{-23} cm 2 /nucleon at those high energies. 5) There is some evidence that the secondaries are not emitted isotropically in the center-of-momentum system of the virtual photon and the target nucleon. An anisotropic distribution of the type $(1 + \cos \Phi) d\Omega$ in the CM system would agree with the observed angular distribution in the laboratory. In the same experiment, we have observed 12 cases of parallel non-interacting penetrating particles, presumably μ -mesons from extensive air showers. 2 pictures show as much as 9 and 11 parallel μ -mesons in the illuminated region of the cloud-chamber, which leads to a density of about 55 particles per m 2 at 65 m w.e. and is estimated to arise from air-showers of about $3 \cdot 10^{18}$ eV. This energy estimate would agree with the observed frequency.

1. - Introduction.

Depuis 1950, plusieurs chercheurs ont mis en évidence l'existence d'interactions nucléaires de mésons μ à l'aide de diverses techniques. Nous avons résumé les résultats de ces expériences dans le Tableau I.

En vue d'interpréter leur propres résultats, GEORGE *et al.*⁽¹⁾ ont utilisé la théorie de Williams-Weizsäcker⁽²⁾: cette dernière revient à décomposer le champ électromagnétique du méson μ relativiste en un spectre de photons virtuels, ce qui permet d'exprimer la section efficace σ_{μ} en termes de σ_{ph} , section efficace d'interaction nucléaire des photons de grande énergie, au moyen d'une formule du type $\sigma_{\mu}(E) = \int N(E, q) \sigma_{ph}(q) dq/q$. Au moyen d'une théorie un peu plus précise qui consiste à comparer les graphiques de Feynman relatifs à l'interaction du μ et du photon, ce qui permet de tenir compte également du spin du μ et de l'angle de déviation fini, on a obtenu⁽³⁾:

$$N(E, q) = (2\alpha/\pi)[\ln(E/m) - \frac{1}{2}] .$$

Les résultats expérimentaux semblent être en bon accord avec cette interprétation si l'on adopte pour la section efficace du photon $\sigma_{ph}(q)$ à grande énergie une valeur de $(1 \div 3) \cdot 10^{-28} \text{ cm}^2/\text{nucleon}$ ⁽⁴⁾. Cependant, les incertitudes expérimentales sont grandes: en ce qui concerne les expériences avec émulsions, si la fréquence des étoiles en profondeur est en équilibre avec le flux des mésons μ , il faut souligner qu'une grande partie de ces étoiles ne sont pas produites directement par les mésons μ , mais par des mésons π , neutrons et protons, eux-mêmes secondaires d'une interaction du méson μ . Comme nous l'avons remarqué en fin du travail cité⁽⁵⁾, même les étoiles de type 1_p de George doivent contenir une proportion appréciable d'événements secondaires.

Cette remarque vaut également pour les expériences de comptage de neutrons, où de plus on peut avoir affaire à des neutrons d'origine photo-nucléaire produits surtout dans les gerbes électro-photoniques consécutives à la Bremsstrahlung du méson μ et aux neutrons émis dans la capture de mésons μ arrivés au repos.

⁽¹⁾ E. P. GEORGE et J. EVANS: *Proc. Phys. Soc. (Londres)*, A **63**, 1248 (1950); A **64**, 193 (1951); A **68**, 829 (1955).

⁽²⁾ E. J. WILLIAMS: *Proc. Roy. Soc. (Londres)*, A **139**, 163 (1933); C. F. v. WEIZSÄCKER: *Zeits. f. Phys.*, **88**, 612 (1934).

⁽³⁾ D. KESSLER et P. KESSLER: *Compt. Rend. Acad. Sc. (Paris)*, **242**, 3045 (1956); *Nuovo Cimento*, **4**, 601 (1956).

⁽⁴⁾ P. H. BARRETT, L. M. BOLLINGER, G. COCCONI, Y. EISENBERG et K. GREISEN: *Rev. Mod. Phys.*, **24**, 133 (1952).

TABLEAU I.

Méthode expérimentale	Auteurs	Prof. m H ₂ O	Section efficace $10^{-31} \text{ cm}^2/\text{nucleon}$	Remarques
Emulsions	GEORGE <i>et al.</i> (1)	8	4.5 \pm 1.1	Calculé d'après le nombre d'étoiles 1 _p + gerbes, la moyenne est 4.6 \pm 0.5.
		25	4.7 \pm 0.8	
		45	4.4 \pm 1.2	
		57	4.8 \pm 0.9	
		8	1.9 \pm 0.7	Calculé d'après les étoiles comportant des gerbes de secondaires relativistes. La moyenne est 1.7 \pm 0.3.
		25	0.82 \pm 0.4	
		45	2.6 \pm 0.8	
		57	1.35 \pm 0.4	
	AVAN (5)	300	12–18 ($\pm 40\%$)	Pour des mésons d'énergie ~ 100 GeV.
	COCCONI <i>et al.</i> (6)	0–60	10 \pm 5	—
			20 \div 150	—
Comptage de neutrons	Rome (8)	50	2.4 \pm 0.4	Gerbes pénétrantes comportant au moins 2 particules traversant 15 cm Pb.
		200	7.5 \pm 1.0	
	Paris (9)	10	1.16 \pm 0.54	
		65	1.22 \pm 0.45	
	Osaka (10)	32	0.28 \pm 0.07	
		200	0.29 \pm 0.11	
	Cornell (1)	1 600	40 \pm 20	—
Chambre	Milan (11)	55	1.2	—
	Osaka (12)	50	0.5 \pm 0.3	—
	Paris	65	0.43 \pm 0.08	Travail présent: énergie minima estimée à 12 GeV.

(5) L. AVAN: *Thèses* (Caen, France, 1955).(6) G. COCCONI et V. COCCONI-TONGIORGI: *Phys. Rev.*, **82**, 335 (1951); **84**, 29 (1951).(7) M. ANNIS, H. C. WILKINS et J. D. MILLER: *Phys. Rev.*, **94**, 1038 (1954).(8) E. AMALDI, C. CASTAGNOLI, A. GIGLI et S. SCIUTI: *Nuovo Cimento*, **9**, 453 (1952); **9**, 969 (1952); *Proc. Phys. Soc. (Londres)*, **65**, 556 (1952); C. CASTAGNOLI, A. GIGLI et S. SCIUTI: *Nuovo Cimento*, **10**, 893 (1953); E. AMALDI: *Conférence de Bagnères de Bigorre* (1953); P. E. ARGAN, A. GIGLI et S. SCIUTI: *Nuovo Cimento*, **11**, 1277 (1954).(9) D. KESSLER et R. MAZE: *Physica*, **22**, 69 (1956).

(10) S. HIGASHI, M. ODA, T. OSHIO, H. SHIBATA, K. WATANABE et Y. WATASE: communication privée (1956).

(11) A. LOVATI, A. MURA, C. SUCCI et G. TAGLIAFERRI: *Conférence de Bagnères de Bigorre* (1953); *Nuovo Cimento*, **10**, 105, 1201 (1953).(12) S. HIGASHI, T. OSHIO, H. SHIBATA, K. WATANABE et Y. WATASE: *Nuovo Cimento*, **5**, 592 (1957).

Quant aux expériences au moyen d'hodoscopes de compteurs, on est généralement à la fois par les interactions électromagnétiques multiples (knock-ons, Bremsstrahlung, production directe de paires d'électrons) au niveau des bances de compteurs (^{13,11}) et par les gerbes électromagnétiques énergétiques qui touchent plusieurs bances de compteurs simultanément si ces bances ne sont pas séparées par au moins 15 cm Pb (¹⁵). De plus, il est souvent difficile d'éliminer les gerbes pénétrantes produites dans les plafonds ou les murs du laboratoire souterrain. D'autre part, la comparaison des résultats fournis par des groupes différents dépend de leur définition.

Par exemple, les résultats donnés dans le Tableau I pour le groupe de Paris (⁹) ont été corrigés pour tenir compte des probabilités de déclenchement de l'hodoscope. La section efficace citée se réfère donc à toutes les gerbes pénétrantes d'au moins 2 particules traversant 18.5 cm Pb. On aurait pu également donner une section efficace pour les événements réellement détectés, que l'on aurait alors dû définir par leur énergie minima ou leur énergie moyenne. On aurait alors obtenu (0.34 ± 0.13) et $(0.36 \pm 0.11) \cdot 10^{-30} \text{ cm}^2/\text{nucléon}$ pour les gerbes dont l'énergie moyenne est de l'ordre de 10 GeV, mais plus élevée à 65 m H₂O qu'à 10 m H₂O sous terre. Ceci illustre les difficultés que l'on rencontre dans l'interprétation des expériences avec hodoscopes.

Malgré ces incertitudes expérimentales, les résultats cités ci-dessus sont en bon accord avec l'interprétation de GEORGE. Inversement, si l'on s'en tient à cette interprétation, l'étude des gerbes pénétrantes produites par les mésons fournit un moyen excellent, et peut-être le seul moyen pour l'étude des interactions photo-nucléaires de haute énergie.

Jusqu'ici très peu d'expériences ont été tentées au moyen d'une chambre de Wilson, la plupart en vue d'élucider le problème des particules pénétrantes associées (PPA) qui semblent finalement avoir été une illusion (^{16,17}). Dans ces expériences, le nombre de gerbes pénétrantes obtenues était de quelques unités tout au plus. Les expériences les plus importantes dont nous avons connaissance sont les suivantes: le groupe de Milan (¹¹) a publié des clichés Wilson obtenus sous terre à ~55 m H₂O et montrant des interactions nucléaires de mésons μ , comportant la production de secondaires pénétrants. La chambre contenait 8-9 écrans de 1.6 cm Pb et 5 gerbes furent observées, toutes produites par une particule pénétrante isolée à l'intérieur de la chambre. Cinq événements produits dans un absorbant immédiatement au-dessus de la chambre

(¹³) D. KESSLER et R. MAZE: *Physica*, **21**, 425 (1955); *Nuovo Cimento*, **1**, 966 (1955).

(¹¹) G. CAGLIOTI et S. SCIUTI: *Nuovo Cimento*, **1**, 851 (1955).

(¹⁵) D. KESSLER et R. MAZE: *Physica*, **18**, 528 (1952).

(¹⁷) V. APPAPILLAI, A. W. MAILVAGANAM et A. W. WOLFENDALE: *Phil. Mag.*, **45**, 1059 (1954).

(¹⁷) H. J. J. BRADDICK et B. LEONTIC: *Phil. Mag.*, **45**, 1287 (1954).

ont été obtenus dans la même expérience. Les interactions étaient semblables aux interactions nucléaires observées en altitude. Les secondaires interagissent fortement et sont donc des mésons π . De plus, la production de mésons π neutres a été observée. La section efficace pour la création de gerbes de 3 particules et plus est compatible avec la section efficace indiquée par GEORGE et EVANS, soit environ $1.2 \cdot 10^{-30} \text{ cm}^2/\text{nucleon}$, ce qui équivaut à un parcours de 1200 m Pb.

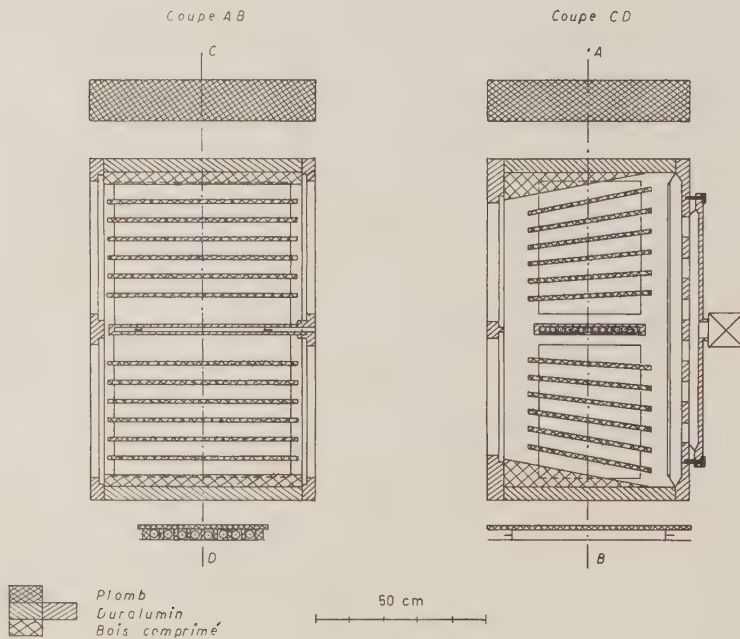


Fig. 1. — Dispositif expérimental.

Le groupe d'Osaka (12) a récemment obtenu au moyen d'une chambre à écrans travaillant à $50 \text{ mH}_2\text{O}$, 13 gerbes pénétrantes, dont 5 produites à l'intérieur de la chambre. Trois de ces dernières sont produites par une particule pénétrante isolée, donc probablement un méson μ . La section efficace est estimée à $(0.5 \pm 0.3) \cdot 10^{-30} \text{ cm}^2/\text{nucleon}$.

L'expérience que nous allons décrire a été réalisée en 1955-1956 en vue d'obtenir des résultats supplémentaires et plus quantitatifs sur les gerbes pénétrantes produites par les mésons μ .

2. — Dispositif expérimental.

Le dispositif expérimental représenté dans la Fig. 1 a été installé dans le laboratoire souterrain de l'Ecole Normale Supérieure sous 65 m H₂O équiv. de sol. La chambre de Wilson de forme parallélépipédique a été fabriquée à partir de planches de duralumin de 4 et 5 cm d'épaisseur. Les dimensions externes de la chambre sont: hauteur 100 cm, largeur 65 cm, profondeur 58 cm. Le volume éclairé utile est de 82 cm de hauteur en moyenne, 50 cm de largeur et 30 cm de profondeur. Les glaces latérales, servant à l'éclairage, et les glaces antérieures, servant à la photographie, sont en verre « sécurit » de 14 mm d'épaisseur.

La chambre contient 12 écrans de plomb de 10 mm d'épaisseur qui convergent vers les objectifs photographiques. De plus, la chambre contient une boîte étanche de duralumin comportant des logements pour 15 compteurs Geiger. Les parois de cette boîte ont 5 mm d'épaisseur; des cloisons de 5 mm également séparent les logements des compteurs et évitent l'écrasement de la boîte par la surpression qui règne dans la chambre. Ces logements des compteurs communiquent avec l'extérieur sur le côté gauche de la chambre, dispositif pratique pour réaliser les connexions électriques ainsi que pour remplacer les compteurs sans démontage de la chambre. Le plafond et le plancher de la chambre portent des coins en bois comprimé, comme indiqué sur la figure, en vue de régulariser la détente du gaz.

Le piston est une membrane de caoutchouc naturel chargé de graphite de 2 mm d'épaisseur, collée sur la face postérieure sur une planche de dural « fortal traité » de 1 mm qui lui confère sa rigidité, et portant sur la face antérieure un velours noir qui constitue le fond photographique. La charge de graphite du caoutchouc a le double avantage de rendre le caoutchouc noir (ce qui diminue la lumière diffusée par les bords du piston) et conducteur (ce qui évite l'accumulation de charges statiques, celles-ci étant évacuées par une mise à la masse).

La chambre est remplie d'argon commercial à une pression de 280 g au-dessus de la pression atmosphérique à l'état détendu et d'un mélange eau-alcool éthylique en parties égales.

L'arrière-chambre s'ouvre vers l'extérieur par deux rangées de huit ouvertures de 216 cm² de surface totale permettant une évacuation très rapide. Ces ouvertures sont obturées en état de marche par la membrane d'un relai pneumatique gonflé lui-même à 1.5 kg au-dessus de la pression atmosphérique et commandé par une soupape électromagnétique conventionnelle.

(13) G. PFOTZER: *Mitt. Max Planck-Instit. (Weissenau)*, n. 2 (1954).

La détente de la chambre est du type « régulation de volume ». La position antérieure du piston est déterminée au moyen d'un dispositif semblable à celui décrit par PFOTZER (18), à cette différence près que l'axe du régulateur n'est pas fixé au piston, mais maintenu en contact avec celui-ci au moyen d'un ressort. Cette modification évite les effets de torsion et de grippage sur le passage de l'axe et facilite le montage en rendant le régulateur indépendant. Finalement, l'avantage décisif de ce dispositif est le suivant: le nettoyage de la chambre pendant le cycle de remise en état est grandement amélioré en surcomprimant la chambre pendant les détentes lentes, et ceci n'est possible que si l'on rend le régulateur en question indépendant du piston. Le taux de détente de la chambre est de 7.5% en marche normale (compte tenu du volume des plaques de plomb et de la boîte de compteurs) et d'environ 8.5% en détente lente. La surecompression en détente lente est réalisée par un jeu de vannes électromagnétiques et une alimentation particulière en air comprimé à une pression stabilisée et réglable. Le cycle de remise en état de la chambre après détente rapide dure 3 minutes et comporte 3 détentes lentes et un temps de repos de 45 secondes, largement suffisant vu la faible fréquence des événements.

En dehors d'un léger chauffage de la glace avant pour éviter la formation de buée, aucun dispositif de régulation thermique n'a été employé, la température étant stable à 0.5 °C près dans le laboratoire souterrain utilisé.

Un champ de balayage des ions de 40 V est appliqué entre les écrans de plomb, ce champ est coupé électroniquement au moment de la détente.

L'éclairage de la chambre est effectué par 3 tubes flash de 90 cm de longueur utile de part et d'autre de la chambre et des miroirs cylindriques en aluminium poli. Les tubes flash sont alimentés par une batterie de condensateurs fournissant 4300 J à chaque éclair.

La photographie est prise par 3 appareils situés à une distance de 168 cm de la glace antérieure. Un appareil est situé dans l'axe de la chambre, les deux autres sont inclinés de 9.5° sur cet axe. Les objectifs sont des objectifs An-génieux U2 de 75 mm de focale et diaphragmés à f: 6.5. On a utilisé du film Kodak Plus-X de 35 mm. Trois fils métalliques verticaux tendus sur la face interne de la glace servent de référence.

La chambre est surmontée d'une couche de plomb de 12 cm d'épaisseur. Les compteurs utilisés pour la commande sont du type Maze (en verre à cathode externe). Sur les 15 logements à compteurs, les 4 extrêmes étaient inoccupés, les autres contenaient 11 compteurs internes de 13 mm de diamètre et de 36 cm de longueurs utile, formant 2 groupes de compteurs alternés de 6 et 5 compteurs connectés en parallèle. Sous la chambre se trouvent 8 compteurs de 30 mm de diamètre et de 45 cm de longueur utile, placés perpendiculairement aux précédents et formant deux groupes de 4 compteurs alternés. Ils sont surmontés d'une couche de 8 mm de plomb et séparés par des cloisons de 12 mm d'épaisseur, pour diminuer la contribution d'effets locaux de basse énergie.

Le déclenchement est commandé par la coïncidence des 4 groupes de compteurs, ce qui exige au moins 2 particules au niveau de la boîte à compteurs au centre de la chambre et au moins 2 particules sous la chambre. Le télescope de compteurs a un demi-angle d'ouverture de 29° aussi bien de face que de profil.

L'appareil était en fonctionnement pendant environ 10 mois sous terre et a opéré d'une façon satisfaisante, ne nécessitant pratiquement aucune surveillance. On rajustait le taux de détente une fois par semaine tout au plus.

3. — Résultats expérimentaux.

La durée totale de l'expérience a été de 5 055 heures, soit 4 915 heures effectives, déduction faite du temps mort des cycles. 2 793 clichés ont été pris. Par suite de la disposition d'un train de compteurs internes il a été possible dans la grande majorité des cas de déterminer la façon dont la chambre a été déclenchée. Ces événements ont été classés parmi les types suivants dans le Tableau II.

TABLEAU II.

Mésons isolés	(a) (67+93)	160
	(b) électrons touchant seulement les compteurs supérieurs AB (404+228)	632
	(c) électrons touchant seulement les compteurs inférieurs CD (30+23)	53
Mésons + composante électronique	(d) mésons produisant 2 électrons ou gerbes indépendantes qui touchent respectivement les trains AB et CD (132+61)	193
	(e) mésons produisant une gerbe électronique énergique qui touche simultanément les deux trains de compteurs (203+170)	373
Composante électronique sans particules pénétrantes visibles (side-showers)	(f) de faible énergie (moins de 10 électrons)	385
	(g) moyens (10 à 50 électrons)	290
	(h) énergiques (plus de 50 électrons)	229
Divers (pour la plupart des mésons μ accompagnés de composante électronique qui n'ont pu être classés)	(i)	89
Clichés blanches	(j)	252
Evénements nucléaires	(k) d'origine externe (dont 16 dans l'aluminium et dans le Pb du plafond)	86
Particules pénétrantes associées	(l) produits dans les écrans de Pb à l'intérieur de la chambre (19+9)	28
	(n) concourantes	11
	(p) parallèles	12
	Total	2 793

La catégorie la plus nombreuse est fournie par les mésons μ visibles dans la chambre et qui actionnent les trains AB et CD par des secondaires de nature

électronique. Dans de nombreux cas, les trains *AB* et *CD* sont visiblement touchés par des secondaires indépendants (*d*), mais il n'est pas douteux que les cas où un seul train est touché de façon apparente par des électrons, (*b*) et (*c*), sont de nature identique, et même les cas où le méson seul est vu dans la chambre (*a*) sans secondaires visibles. La proportion des événements où le secondaire qui touche les compteurs *AB* intérieurs à la chambre, n'est pas visible est de 20% et cette proportion est de 75% pour les compteurs inférieurs (rappelons que les compteurs inférieurs sont séparés de la chambre par 3.5 cm de bois comprimé, 4 cm de dural et 0.8 cm Pb. De plus, les secondaires issus du dernier écran de Pb dans le bas de la chambre ne sont pas toujours bien visibles dans le dernier compartiment éclairé). Les deux nombres entre parenthèse se réfèrent le premier aux cas où le méson est entièrement contenu dans le volume éclairé et le deuxième aux mésons obliques qui sont vus seulement en partie.

Le groupe (*e*) désigne les mésons qui produisent une gerbe électrophotonique assez énergique pour traverser toute la moitié inférieure de la chambre et touchent ainsi les deux trains *AB* et *CD* simultanément (Fig. 2). Ces gerbes sont beaucoup plus nombreuses que les interactions nucléaires, mais moins pénétrantes. Ceci résulte du Tableau III où les 203 gerbes électroniques et les 19 interactions nucléaires dont le primaire est tout entier dans le volume éclairé, sont classés suivant leur origine. On y a inclus également 16 interactions nucléaires produites dans le plafond ou la couverture de Pb. On voit que pour un parcours minimum de 10 cm Pb, les interactions électromagnétiques dominent encore sur les interactions nucléaires, mais pour les interactions dont l'origine est dans le plafond de la chambre (parcours minimum 13 cm Pb), le rapport est inversé. Ceci justifie *a posteriori* la conclusion d'un précédent travail (⁹) et la précaution que nous avons prise d'exiger une traversée d'an-

TABLEAU III. — *Origine des interactions.*

Origine	Gerbes molles	Gerbes pénétrantes
Couverture Pb	5	11
Plafond Al		5
Ecran n. 1	5	1
2	15	1
3	24	4
4	37	3
5	64	3
6	52	6
7	1	1
8 et suiv.	0	0
Total	203	35

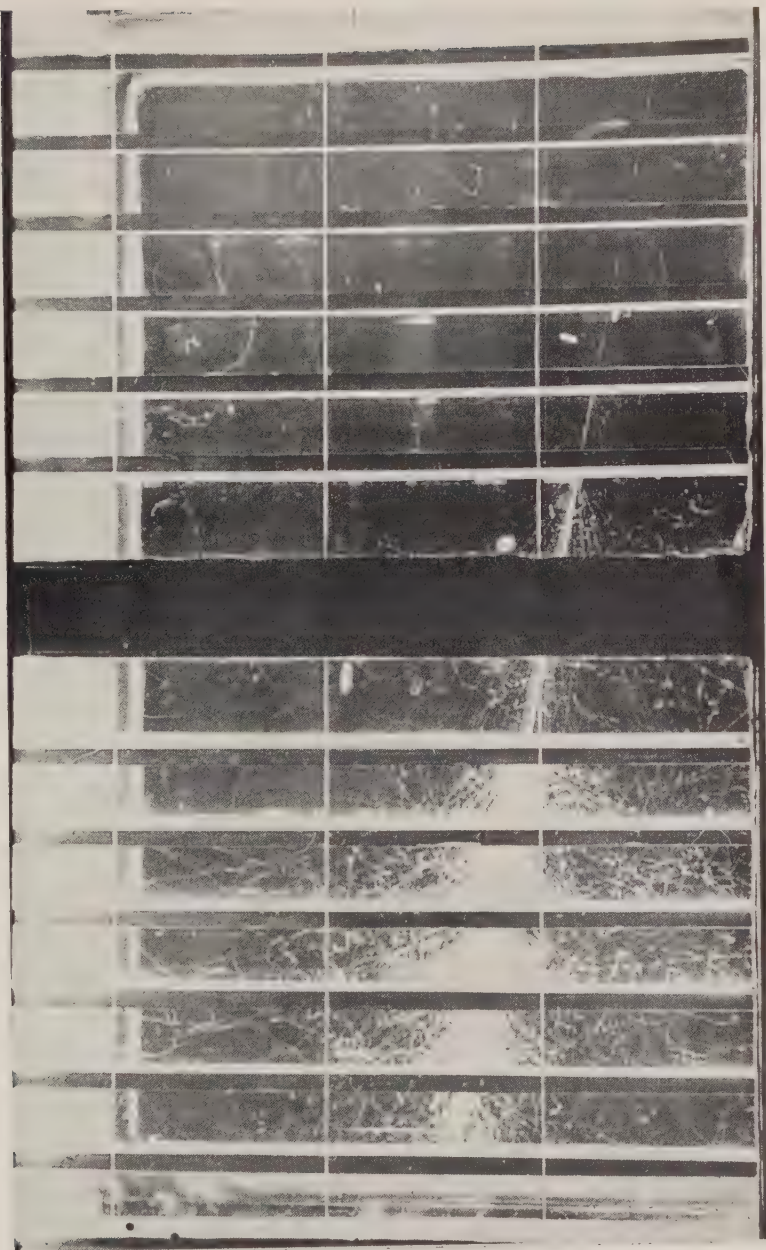


Fig. 2. — Exemple de gerbe électronique produite par un méson μ dans le 5^e écran et traversant tout le bas de la chambre (événement du type « e »).



moins 18.5 cm Pb pour éliminer la composante molle. Remarquons en passant que les cas où le train AB est touché par des particules diffusées en arrière à partir du 7^e écran, sont très rares. Ils sont inexistant pour les écrans suivants.

Les groupes (*j*), (*g*) et (*h*) du Tableau II sont des gerbes électrophotoniques produites au voisinage de la chambre ou dans le sol, ainsi sans doute que la plupart des clichés « blanches » (*j*): nous avons classé comme « blanches » tous les clichés ne comportant que des électrons de faible énergie (rayons δ) sans multiplication en cascade. Le groupe « divers » (*i*) comporte tous les clichés qui n'ont pu être classés avec certitude: la plupart de ces clichés montrent une particule pénétrante (méson μ) de type « rayonnant » produisant 3 secondaires électroniques ou plus dans les écrans ou bien accompagnés tout le long de leur trajectoire par des électrons isolés ou des paires, sans multiplication importante en cascade.

Les clichés (*k*) comportent des gerbes mixtes (particules pénétrantes, composante électronique, interactions nucléaires secondaires) dont l'origine se trouve à l'extérieur de la chambre. Parmi ces événements, il y en a 16 dont l'origine se projette soit dans le plafond de la chambre (Al), soit dans la couverture de Pb. Les clichés (*u*) qui représentent des particules pénétrantes de même âge et approximativement concourantes, mais sans interaction nucléaire visible, sont probablement de même origine.

Il n'en est pas de même des 12 clichés (*p*), qui figurent des particules pénétrantes approximativement parallèles et sans interaction nucléaire. Ces clichés représentent sans doute des mésons μ provenant des grandes gerbes de l'air. Nous en dirons un mot à la fin de cet article.

Notre étude actuelle a pour objet de présenter une analyse des 28 clichés (*m*), c'est-à-dire des gerbes pénétrantes produites à l'intérieur de la chambre par un primaire isolé. Nous supposerons par la suite que nous avons affaire dans tous ces cas à une interaction directe des mésons μ . En effet, les secondaires d'interactions produites au-dessus de l'appareil et suffisamment énergiques pour produire à leur tour une gerbe pénétrante, ont peu de chance de paraître isolés. Effectivement, nous avons observé 7 gerbes pénétrantes secondaires parmi les événements (*k*) produits à l'extérieur de la chambre: dans tous ces cas la particule produisant l'interaction dans la chambre est accompagnée d'au moins deux autres PP provenant manifestement de la même origine. Dans 5 cas elle est accompagnée en outre par une abondante composante électronique. Ces gerbes pénétrantes secondaires sont en général peu énergétiques: 3 comportent 2 PP, 2 comportent 3 PP et une seule 6 PP. Les primaires sont ionisants dans 6 cas et neutre dans 1 cas.

Nous estimons donc que le critère d'isolement du primaire est suffisant pour garantir que la très grande majorité des 28 événements ainsi sélectionnés, sinon la totalité, soit produite directement par des mésons μ .

4. - Primaires des interactions.

L'observation directe des primaires permet de préciser les remarques précédentes.

1) Les primaires des 28 événements sélectionnés sont tous ionisants, alors que le système de déclenchement n'oppose aucun biais contre d'éventuels primaires neutres.

2) L'ensemble des primaires traverse 74 écrans avant de produire les gerbes pénétrantes qui déclenchent l'appareil, ce qui correspond, compte tenu de l'angle d'incidence, à $812 \text{ g} \cdot \text{cm}^{-2}$ Pb. Sur ce parcours on ne constate aucune interaction nucléaire, ni aucun scattering des primaires (le scattering mesurable est inférieur à 1° dans la grande majorité des traversées (80%) et à 3° dans tous les cas).

3) Une preuve supplémentaire de l'identité des primaires est fournie par l'étude de la distribution angulaire des secondaires dans le paragraphe suivant: il sera en effet possible de mettre en évidence le méson μ sortant dans la plupart des événements.

Quoique les arguments précédents pris individuellement ne constituent pas une preuve absolue du fait que les 28 primaires sont effectivement des mésons μ , nous considérons que l'ensemble fournit une base solide pour les traiter comme tels.

5. - Secondaires relativistes.

Nous définissons comme «secondaires relativistes» ou «particules pénétrantes» (PP) les particules qui ionisent moins que $2 I_{\min}$ et pénètrent au moins 2 écrans Pb sans multiplication. On peut tenter d'identifier ces PP en examinant celles qui s'arrêtent à l'intérieur de la chambre.

Les protons qui s'arrêtent dans la chambre doivent être ionisants (plus de $2 I_{\min}$) dans les 4 derniers intervalles, tandis que les mésons π^\pm ne peuvent être ionisants que dans les 2 derniers intervalles tout au plus. On a ainsi observé 6 cas d'arrêt dans la chambre, dont 5 π^\pm et 1 p. Cependant, parmi les PP identifiées comme π^\pm , 3 s'arrêtent sans avoir traversé plus de 3 écrans et n'auraient pas été identifiées comme PP si elles avaient été des protons.

D'autre part, on a observé 13 étoiles secondaires à plus de 2 branches produites par des PP et 3 étoiles similaires produites apparemment par des secondaires neutres. Si l'on suppose que le parcours d'interaction et le spectre d'énergie des protons, neutrons et mésons π^\pm sont semblables et que les p

et n sont produits en nombre sensiblement égal, on trouve que nos résultats sont compatibles avec une proportion de $2\pi^\pm : 1 p : 1 n$, sensiblement la même que celle que l'on trouve au sol^(19,20) dans les gerbes pénétrantes produites par la composante nucléaire du rayonnement cosmique. Ce résultat sera confirmé plus loin avec une meilleure statistique par l'observation des π^0 .

Ce que nous venons de dire ci-dessus ne s'applique qu'aux secondaires qui s'arrêtent dans la chambre ou qui ont une forte interaction nucléaire. Le méson μ sortant se trouve cependant également parmi les PP secondaires. Nous avons mesuré l'angle entre les secondaires et le méson μ primaire. Cette mesure a été faite au moyen d'une méthode semblable à celle de Duller et Walker⁽²⁰⁾, mais plus précise du fait que nous disposions de 3 photographies stéréoscopiques pour chaque événement. Dans 95% des cas, l'angle zénithal des traces est déterminé à mieux que $\frac{1}{2}$ degré et l'angle entre deux traces comporte une erreur maxima de 1°. Dans le Tableau IV nous avons présenté le résultat de ces mesures pour tous les clichés qui ne comportent pas une importante composante molle susceptible de cacher une partie des particules pénétrantes.

TABLEAU IV.

N° de cliché	Nombre total de PP	Angle θ pour particules sans arrêt, ni scattering ($< 2^\circ$), ni interaction	Angle θ pour particules éliminées en raison d'un scattering de $2^\circ \div 5^\circ$
1	5	0.5°; 8°; 18°	12°
2	8	4°; 15°; 17°	13°; 26°
3	4	1°; 14°	7°; 15°
4	2	$< 1^\circ$; 2°	
7	8	0.5°; 1.5°; 6°; 12.5°	27°
9	3	2°; 28°	
10	4	1°	
13	4	1.5°	
14	4	1.5°	
15	5	$< 4^\circ$; 6°; 10°	
16	5	$< 1^\circ$; 1.5°; 3.5°; 13°	12°
18	3	$< 2^\circ$	7°
19	3	2°; 12°	
21	5	2°	7°; 22.5°
22	4	1°	
23	4	$< 2^\circ$; 8°	
26	3	1°	
27	7	1°; 5°; 9°; 15°	17°
28	7	0.5°; 4°; 6.5°; 7.5°; 47°	

(19) F. E. FROELICH, E. M. HARTH et K. SITTE: *Phys. Rev.*, **87**, 504 (1952).

(20) N. M. DULLER et W. D. WALKER: *Phys. Rev.*, **93**, 215 (1954).

La colonne 3 de ce tableau donne les angles θ entre les PP secondaires et le primaire pour tous les PP qui obéissent aux conditions suivantes: 1) Ils ne s'arrêtent pas dans la chambre et quittent le champ éclairé avec une ionisation inférieure à $2 I_{\min}$. 2) Ils ne produisent pas d'interaction nucléaire visible. 3) Ils ne présentent pas de scattering supérieur à 2° . Cette dernière condition peut sembler sévère, c'est pourquoi nous ajoutons dans la colonne 4 les angles d'émission θ pour les particules qui ont été éliminées en raison d'un scattering compris entre 2° et 5° . L'adjonction de ces particules ne changera pas notre argumentation. Les particules portées dans la colonne 3 sont donc celles qui sont susceptibles d'être le méson μ sortant et leur distribution angulaire apparaît dans la Fig. 3. Nous pouvons en tirer les arguments suivants:

1) Parmi les 19 gerbes pénétrantes du Tableau VI, 7 comportent *une seule* particule émise qui puisse être identifiée avec le méson μ sortant. Dans ces 7 cas, l'angle d'émission θ est toujours inférieur ou égal à 2° .

2) Dans 16 cas sur 19, il figure parmi les particules de la colonne 2 au moins un secondaire émis à moins de 2° , et dans tous les cas un secondaire émis à moins de 5° . La particule « ? » du cliché n. 27 est cachée par une gerbe électronique, l'angle θ est probablement inférieur à 4° .

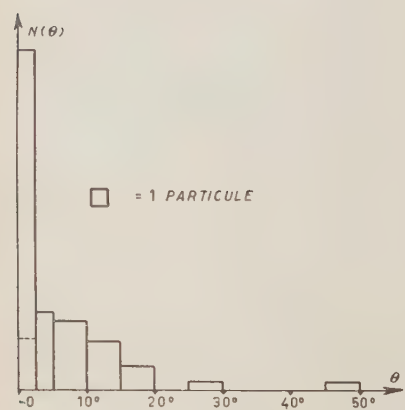


Fig. 3. — Distribution angulaire des secondaires pénétrants susceptibles d'être identifiés avec le méson μ sortant.

est émis à un angle inférieur ou égal à 2° et dans tous les cas à un angle inférieur à 5° .

Inversement, la présence dans toutes les gerbes pénétrantes d'une particule émise à petite angle, qui n'est pas arrêtée et ne subit aucune interaction in scattering fournit l'argument supplémentaire que nous avons laissé prévoir quant à l'identification des primaires comme mésons μ .

3) Trois clichés comportent 2 particules dans l'intervalle $0 \pm 2.5^\circ$, ils sont indiqués en pointillé sur la Fig. 3. Cette dernière montre clairement que la distribution angulaire résulte de la superposition d'une distribution étalée et d'une distribution très pointue au voisinage de $\theta = 0^\circ$. Cet argument est valable également si l'on ajoute à la distribution les particules de la colonne 4.

On peut donc conclure: dans au moins 85% des cas, le méson μ sortant

Nous reviendrons plus loin à la question de la faible déviation angulaire des mésons μ sortants.

Pour obtenir le libre parcours d'interaction des secondaires des gerbes pénétrantes, nous éliminons d'abord les mésons μ identifiés comme tels ou vraisemblables. Pour les autres particules, nous avons observé un parcours total de $4660 \text{ g} \cdot \text{cm}^{-2}$ Pb. Sur ce parcours on a compté 13 étoiles (dont une gerbe pénétrante secondaire à 2 PP) et 7 scatterings nucléaires de plus de 15° . Le libre parcours qui en résulte est $233 \pm 52 \text{ g} \cdot \text{cm}^{-2}$ Pb. Ce libre parcours apparent est le même que celui que l'on trouve au sol (FROEHLICH *et al.* (¹⁹) trouvent $(250 \pm 30) \text{ g} \cdot \text{cm}^{-2}$) et correspond à un libre parcours géométrique, compte tenu de l'épaisseur des écrans utilisés (²¹). Remarquons que si l'on avait compris également les secondaires considérés comme μ dans ce calcul, on aurait obtenu un libre parcours de 10% plus élevé et l'accord avec les observations au sol aurait été moins bon.

6. – Composante molle.

Parmi les 28 événements produits à l'intérieur de la chambre, on a observé 19 gerbes mixtes comportant des cascades électroniques traversant au moins un écran de plomb. La proportion de ces gerbes mixtes ($68 \pm 16\%$) est du même ordre que celle que l'on trouve au niveau du sol et en montagne. Par exemple, FROEHLICH *et al.* (¹⁹) en ont trouvé 59% . Les gerbes électroniques que nous observons présentent les mêmes caractères que dans les gerbes mixtes bien connues: elles convergent vers l'origine de l'interaction et se matérialisent dans le même écran ou l'écran de plomb suivant. Nous considérons qu'elles sont toutes produites par des mésons π^0 .

Pour déterminer le nombre de π^0 produits, nous comptons le nombre n de gerbes électroniques identifiées dans chaque événement et nous faisons $N(\pi^0) = n/2$ pour n pair et $N(\pi^0) = (n-1)/2$ pour n impair. On obtient ainsi au total 26 π^0 . Dans les mêmes clichés on a identifié 113 PP, dont il convient de déduire les 28 mésons μ sortants; on obtient alors 87 PPN (particules pénétrantes nucléaires, c'est-à-dire mésons π chargés et protons).

Il faut remarquer ici qu'un certain nombre de PP, estimé à 16, échappent à l'observation, soit qu'elles quittent la chambre avant d'avoir traversé 2 écrans de Pb, soit qu'elles soient cachées par la composante molle. Il est cependant probable que le nombre de π^0 a été sous-estimé dans la même proportion et pour les mêmes raisons. Nous nous en tiendrons donc aux nombres cités ci-dessus.

Le rapport $N(\pi^0)/N(\pi^0 + \text{PPN}) = 26/113 = 0.23$, est en bon accord avec le rapport trouvé en montagne par DULLER et WALKER (²⁰), soit 0.25.

(²¹) A. LOVATI, A. MURA, C. SUCCI et G. TAGLIAFERRI: *Nuovo Cimento*, **8**, 271 (1956).

En supposant $N(\pi^0)/N(\pi^\pm) = \frac{1}{2}$, le résultat ci-dessus est de nouveau compatible avec l'estimation précédente $N(\pi^\pm):N(p) = 2:1$.

L'énergie des gerbes électroniques peut être estimée en comptant le nombre d'électrons m au maximum de la gerbe et en prenant $E \sim 100 m$ (MeV) (22). En faisant la somme de toutes les gerbes et en divisant par le nombre de π^0 , on obtient l'énergie moyenne par π^0 , soit 2.3 GeV.

Nous supposerons que l'énergie moyenne des π^0 , π^\pm , neutrons et protons énergiques est la même et que les rapports de fréquence estimés plus haut sont applicables, à savoir $N(\pi^0):N(\pi^\pm):N(p):N(n) = 1:2:1:1$. Compte tenu du nombre estimé de particules non observées (environ 15% du total), on obtient une multiplicité moyenne (mésons π et nucléons rapides, à l'exclusion du méson μ sortant) de 5.9 par gerbe. Nous ajouterons également 2 GeV par événement pour tenir compte de l'énergie dissipée sous forme de particules de faible énergie. On obtient ainsi une estimation de l'énergie moyenne des événements, soit environ 16 GeV.

7. - Section efficace.

Conformément à nos remarques dans l'introduction, il importe de définir avec précision à quoi s'appliquera la section efficace que nous allons calculer. L'expérience opère une sélection entre toutes les interactions en imposant un parcours minimum aux gerbes pénétrantes ainsi qu'une certaine densité de particules. La probabilité de détection augmentera avec l'énergie des interactions, mais d'autre part le spectre d'énergie des gerbes pénétrantes sera évidemment décroissant, de sorte que le spectre des gerbes pénétrantes détectées devra présenter un maximum.

Nous avons donc le choix entre deux procédés: 1) on peut tenter de corriger le nombre d'interactions obtenues pour tenir compte de la sélection introduite par l'expérience et ramener les résultats à l'exigence minima du système, en donnant une section efficace relative à toutes les gerbes pénétrantes d'au moins 2 particules traversant plus de 6 cm Pb; c'est le procédé que nous avons employé faute de mieux dans notre précédente expérience avec compteurs (9), favorisée à ce point de vue car le producteur était compacte et peu épais par rapport à l'extension verticale du télescope de compteurs. Présentement, au contraire, le producteur étant fractionné en 6 écrans et reparti sur une distance comparable à la distance entre les trains de compteurs, il s'introduirait une correction géométrique supplémentaire difficile à évaluer.

(22) I. E. TAMM et S. BELENKY: *Journ. Phys. U.R.S.S.*, **1**, 177 (1939) cité par B. ROSSI: *High Energy Particles* (New York, 1952), chapitre 5.22.

2) Nous pouvons donner la section efficace pour les événements effectivement détectés et caractériser ces derniers par leur énergie moyenne, environ 16 GeV dans le cas présent. En vue de la comparaison avec la théorie, il serait cependant plus commode de parler d'une énergie minima au lieu d'une énergie moyenne. Or, le système de détection ne produit évidemment pas de coupure nette selon l'énergie ou la multiplicité des événements. Nous pouvons cependant introduire une « énergie de coupure » telle que le nombre d'événements détectés en-dessous de cette énergie soit égal au nombre d'événements non détectés au-dessus. Dans la Fig. 4, nous avons porté les multiplicités des gerbes pénétrantes (π^0 et PPN), le trait pointillé indique la « coupure » estimée des multiplicités. Celle-ci correspond à une énergie d'environ 12 GeV, déterminée selon les mêmes méthodes que l'énergie moyenne plus haut. L'énergie moyenne par particule ne semble pas varier beaucoup avec la multiplicité, ce qui a été vérifié pour les π^0 . On a donc:

Nombre d'événements: 27 événements d'énergie supérieure à 12 GeV produits dans les écrans 1 à 6 (au-dessus des compteurs AB).

Flux de mésons μ : On a mesuré le flux de mésons qui traversent les compteurs AB et CD , et on a corrigé ce résultat du nombre de mésons qui passent par les cloisons de plomb ou d'aluminium entre les compteurs. Le flux total de mésons qui passent dans l'angle solide du télescope (compteurs et séparations) est $2.53 \cdot 10^6$ pour toute la durée de l'expérience. On n'a pas tenu compte des mésons qui passent en dehors du télescope et produisent une gerbe pénétrante touchant les compteurs, ni des mésons qui passent à l'intérieur du télescope et produisent une gerbe pénétrante qui manque les compteurs. On estime en effet que ces événements doivent se compenser dans une large mesure.

Epaisseur efficace du producteur: Les 6 écrans de plomb ne couvrent pas complètement l'angle solide déterminé par le télescope de compteurs. L'épais-

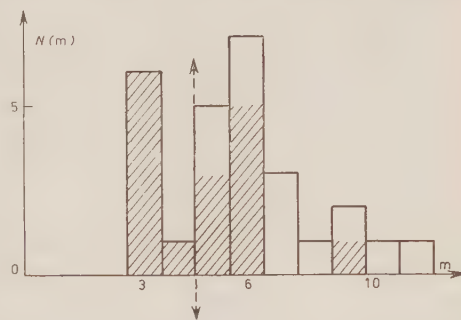


Fig. 4. – Distribution des multiplicités des secondaires (π^0 et PPN) dans les 27 événements produits dans la moitié supérieure de la chambre. Les parties hachurées correspondent à des événements dont la multiplicité est déterminée avec certitude, les parties blanches proviennent d'estimations qui sont en général bonnes à ± 1 particule près. Les flèches verticales marquent l'estimation de la « coupure » des multiplicités définie dans le texte.

seur moyenne du producteur a été déterminée en multipliant l'épaisseur de chaque écran par la fraction de l'angle solide du télescope qu'il couvre, et en divisant par le cosinus de l'angle d'incidence moyen des mésons μ (15°). On obtient ainsi $41 \text{ g} \cdot \text{cm}^{-2}$ Pb.

Il en résulte la section efficace suivante pour la production de gerbes pénétrantes d'énergie supérieure à 12 GeV par les mésons μ à 65 m H₂O sous terre: $(0.43 \pm 0.08) \cdot 10^{-30} \text{ cm}^2/\text{nucloen}$. Cette section efficace correspond à un libre parcours de 3 400 mètres de Pb.

8. - Comparaison avec la théorie.

Soit $N(E, x) dE$ le spectre différentiel des mésons μ à la profondeur $x = 65 \text{ m H}_2\text{O}$ et $\sigma(E, q) dq$ la section efficace différentielle pour la production d'un effet nucléaire comportant un transfert d'énergie compris entre q et $q+dq$ par un méson μ d'énergie E . La section efficace totale $\sigma(q_{\min}, x)$ relative à un transfert d'énergie minimum déterminé par l'expérience à la profondeur x est donné par la formule

$$(1) \quad \sigma(q_{\min}, x) = \int_{E_{\min}}^{\infty} N(E, x) dE \int_{q_{\min}}^{E} \sigma(E, q) dq / \int_{E_{\min}}^{\infty} N(E, x) dE,$$

E_{\min} est l'énergie minima des mésons qui traversent le télescope au moyen duquel on mesure le flux de mésons qui entre dans la détermination expérimentale de la section efficace, soit environ 0.5 GeV dans notre cas. Dans la première intégrale E_{\min} peut être remplacé par q_{\min} étant donné que $\sigma(E, q)$ est égale à zéro pour $E < q$, mais dans la troisième intégrale, qui est l'intégrale de normalisation du flux de mésons, on doit intégrer à partir de E_{\min} :

Comme spectre des mésons nous employerons le spectre utilisé précédemment (13) à savoir:

$$(2) \quad \left\{ \begin{array}{ll} N(E, x) dE = K(E + ax)(E_c + E + ax)^{-3.6} dE & \text{pour } E + ax \leq 60 \text{ GeV} \\ \text{et} & \\ N(E, x) dE = KE_s(E + ax)^{-3.6} dE & \text{pour } E + ax > 60 \text{ GeV} \end{array} \right.$$

K est une constante de normalisation, E_c l'énergie perdue par un méson dans la traversée de l'atmosphère soit 2 GeV, $E_s = 60 \text{ GeV}$ et $a = 2 \text{ MeV} \cdot \text{g}^{-1} \cdot \text{cm}^2$, la perte d'énergie des mésons μ dans la terre.

Pour $\sigma(E, q) dq$ on ne peut employer ni la formule originale de Williams-Weizsäcker, ni une formule assez semblable calculée par nous (3) car ces expressions ne sont valables que pour $q \ll E$, alors que l'intégration doit s'étendre

sur tout le domaine de q jusqu'à E . On emploiera la formule suivante que nous avons calculée pour la production de pions par des électrons (23):

$$(3) \quad \sigma(E, q) dq = (2\alpha/\pi) \sigma_{ph}(q) \frac{dq}{q} \left\{ \frac{2E^2 - 2Eq + q^2}{2E^2} \cdot \ln \left[(E - q)/m \right] - \frac{E - q}{2E} \right\}.$$

Contrairement aux formules antérieures, cette expression tient compte à la fois: 1) de l'effet de spin du méson; 2) de l'angle de déviation du méson; 3) et surtout elle est valable dans tout le domaine de q .

En effectuant les intégrations (1) avec $q_{min} = 12$ GeV et $\sigma_{ph}(q) = 10^{-28}$ cm²/nucléon, on obtient $\sigma(12 \text{ GeV}, 65 \text{ m H}_2\text{O}) = 0.48 \cdot 10^{-30}$ cm²/nucléon à comparer avec la valeur expérimentale ($0.43 \pm 0.08 \cdot 10^{-30}$ cm²/nucléon).

La section efficace trouvée est donc compatible avec l'interprétation des effets observés en termes d'interaction photonucléaire, en prenant une section efficace photonucléaire voisine de 10^{-28} cm²/nucléon dans le domaine de 12 GeV et au-dessus. Il est peu vraisemblable que $\sigma_{ph}(q)$ puisse être aussi élevé que l'ont proposé BARRET *et al.* (3) soit $2 \text{ à } 3 \cdot 10^{-28}$ cm²/nucléon. Nous pensons que la section efficace élevée trouvée par ces auteurs est due à une sous-estimation des interactions électromagnétiques multiples au niveau des bâches des compteurs (voir les conclusions des références (13,14)).

Nous avons représenté dans la Fig. 5 la section efficace pour la production d'effets photonucléaires d'énergie supérieure à 12 GeV en fonction de l'énergie du méson μ primaire. La Fig. 6 représente la fonction $N(E) \int_{q_{min}}^E \sigma(E, q) dq$ pour

$q_{min} = 12$ GeV: cette fonction constitue la contribution différentielle des mésons d'énergie E à la section efficace totale. Il en résulte que l'énergie la plus probable des mésons qui produisent les interactions est 33 GeV et l'énergie moyenne 47 GeV.

On constate que le rapport du transfert d'énergie à l'énergie du primaire est de l'ordre $q/E = 1/3$, alors

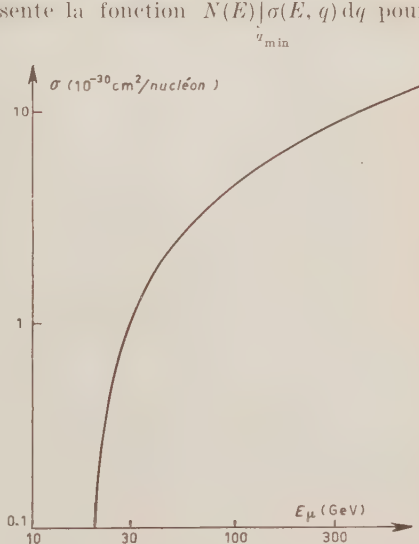


Fig. 5. — Section efficace pour la production d'interactions à transfert d'énergie supérieur à 12 GeV en fonction de l'énergie du méson μ primaire (calculée par intégration de la formule (3))

(23) P. KESSLER et D. KESSLER: *Comp. Rend. Acad. Sc. (Paris)* **244**, 1893 (1957).

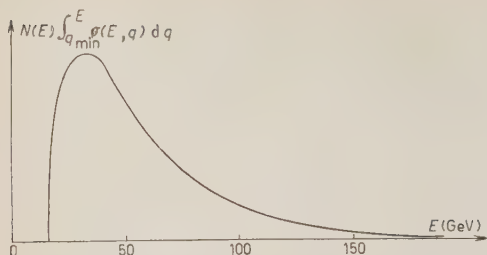


Fig. 6. — Représentation de l'intégrand de la formule (1) (à 65 m H₂O de profondeur et pour $q_{\min} = 12 \text{ GeV}$): spectre des mésons μ qui contribuent aux événements observés.

gerbes pénétrantes dans une chambre à écrans a été utilisée par DULLER et WALKER (²⁰), que nous suivrons ici de près. L'angle d'émission θ d'une particule dans le système du laboratoire (système L) est relié à l'angle φ dans le système du centre des moments (système CM) par la formule suivante:

$$(4) \quad \operatorname{tg} \theta = \sin \varphi / \gamma_c (\cos \varphi + \beta_c / \beta_s),$$

où β_c est la vitesse du système CM, β_s est la vitesse du secondaire dans le système CM et $\gamma_c = 1/(1 - \beta_c^2)^{\frac{1}{2}}$. En faisant l'approximation $\beta_c / \beta_s = 1$, on a:

$$(5) \quad \operatorname{tg} \theta = \operatorname{tg}(\varphi/2) / \gamma_c.$$

Si les secondaires sont émis isotropiquement dans le système CM, la fraction F de particules émises à l'intérieur de l'angle q dans le système CM est $F = \sin^2(\varphi/2)$, de sorte que l'on a finalement dans le système L:

$$(6) \quad \operatorname{tg}^2 \theta = \gamma_c^{-2} \frac{F(\theta)}{1 - F(\theta)}.$$

En portant sur un graphique $\log \operatorname{tg} \theta$ en fonction de $\log [F/(1 - F)]$, on doit obtenir une droite de pente 2 qui permet de déterminer γ_c et par conséquent l'énergie du primaire. Cette méthode connue sous le nom de « *F plot* » a été utilisée avec succès par DULLER et WALKER (²⁰) et d'autres. Pour obtenir une statistique valable, on est obligé de grouper ensemble un grand nombre de gerbes pénétrantes. Notons tout de suite que l'application de cette méthode aux étoiles de Bristol dont les énergies sont connues par des mesures directes, fournit plutôt une sous-estimation de l'énergie et la courbe dévie d'une ligne droite aux grands angles θ (²⁰). D'après les auteurs cités (²⁰), ceci provient très probablement de la contribution d'interactions secondaires à l'intérieur du noyau frappé et peut-être en plus du fait que $\beta_c / \beta_s < 1$.

Pour notre analyse nous avons groupé ensemble tous les clichés remplissant les conditions suivantes:

que la déviation du méson μ est de l'ordre de 1/30 radian. Ceci confirme notre prédition théorique (³) et l'interprétation que nous en avons donnée en termes d'interaction photonucléaire *inelastique*.

9. — Distribution angulaire des particules de gerbe.

Une méthode différente pour déterminer l'énergie des



Fig. 7. - Exemple de gerbe pénétrante produite par un méson μ dans le 2^e écran de plomb (cliché n. 7). On distingue 8 PP secondaires, dont un proton qui s'arrête dans le dernier écran dans le bas de la chambre, et 2 gerbes électroniques de faible énergie (4 et 8 particules respectivement).

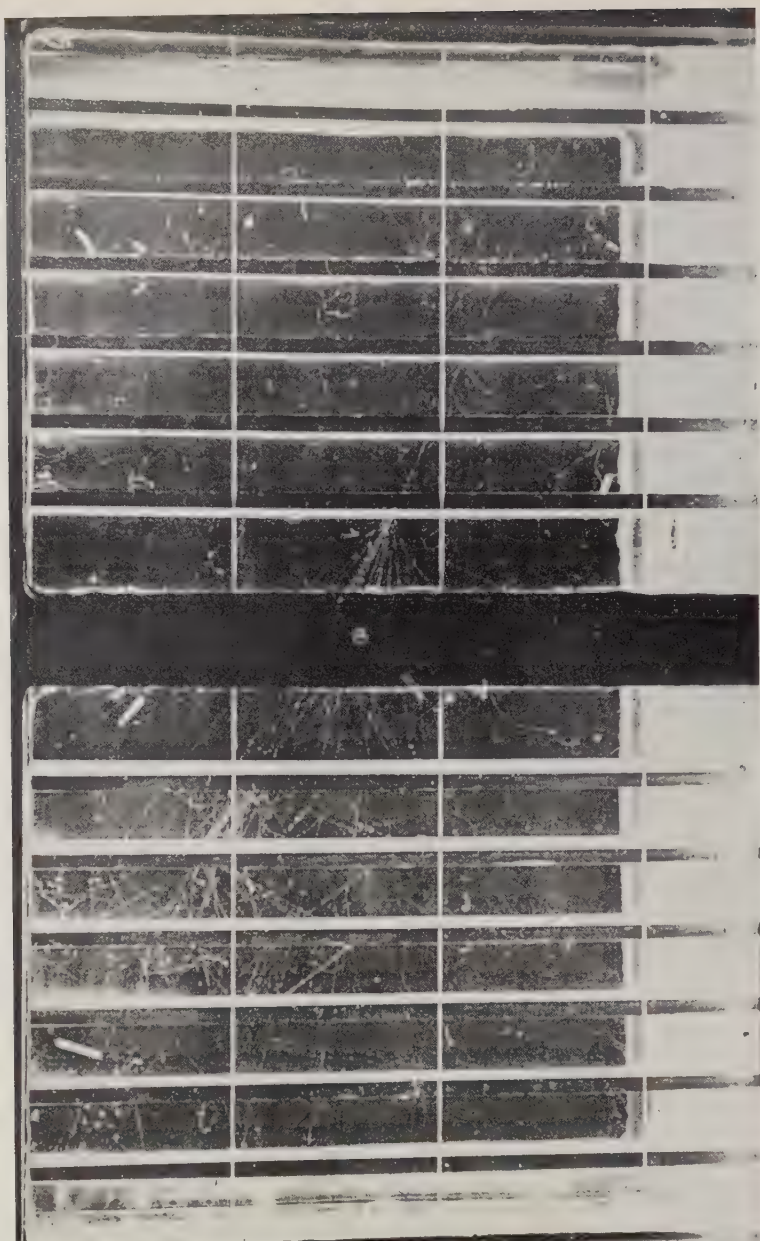


Fig. 8. — Exemple de gerbe pénétrante produite par un méson μ dans le 6^e écran (cliché n. 6). On distingue 4 PP secondaires et 4 gerbes électroniques. D'autres PP sont probablement cachées par la composante électronique ou partent vers le fond de la chambre.

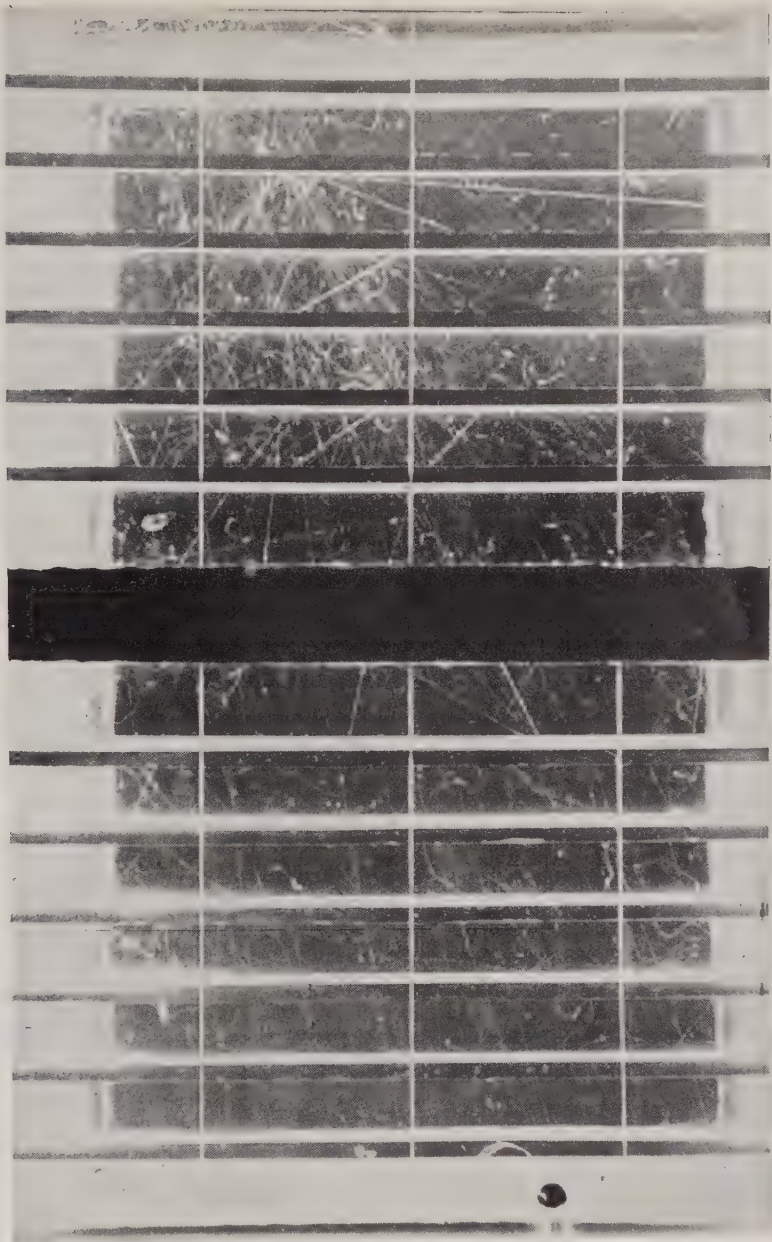


Fig. 9. - Gerbe pénétrante très énergique produite dans la couverture de plomb au-dessus de la chambre. On distingue environ 25 PP, de nombreuses interactions secondaires et une composante molle d'environ 40 électrons.

1) Ils sont bien placés dans la chambre et ne comportent pas une composante électronique importante, de sorte que les secondaires pénétrants peuvent être identifiés comme tels avec certitude.

2) Ils comportent au maximum 1 PP non mesurable.

3) Ils comportent au moins 4 PP (3 PPN + le méson μ sortant).

Les angles d'émission ont été mesurés par rapport au primaire; ils sont à peu de chose près égaux aux angles d'émission par rapport au photon virtuel. Les mesures ont été faites au moyen d'une méthode semblable à celle de Duller et Walker (20), à ceci près que nous disposions de 3 photographies stéréoscopiques pour chaque événement. Ceci nous a permis d'obtenir une précision bien supérieure dans les mesures d'angle (généralement inférieure à 1°). Dans le Tableau V nous présentons l'ensemble des clichés utilisés.

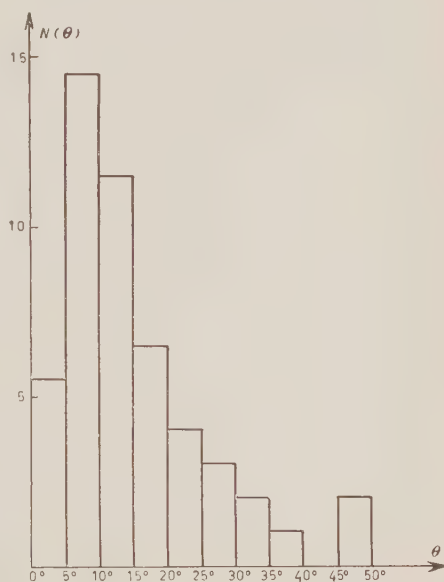


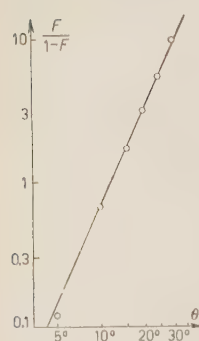
Fig. 10. — Distribution angulaire des PPN dans les 11 événements sélectionnés.

TABLEAU V.

Numéro du cliché	Nombre de π	Nombre de PP	Angles d'émission des PP		
			Méson μ sortant	PPN	
1	1	5	0.5°	8°; 12°; 14°; 18°	
2	0	8	4°	6°; 13°; 13°; 15°; 17°; 23°; 26°	
7	1	8	0.5°	1.5°; 6°; 12.5°; 16°; 18°; 27°; 27°	
13	1	4	1.5°	10°; 15°; ?	
15	1	5	< 4°	6°; ?; 10°; 22°	
16	1	5	< 1°	1.5°; 3.5°; 12°; 13°	
21	1	5	2°	7°; 8°; 11.5°; 22.5°	
22	1	4	1°	12°; 32°; 48°	
23	0	4	2°	3°; 7°; 8°; 17°	
27	0	7	?	5°; 7°; 9°; 15°; 33°; 39°	
28	0	7	0.5°	4°; 6.5°; 7.5°; 7.5°; 22°; 47°	

On voit que sur 52 PPN, seulement 2 traces n'ont pu être mesurées. Les 11 événements considérés comportent en moyenne $0.6\pi^0$ et 4.7 PPN. On voit que nos critères nous ont amené à sélectionner des interactions particulièrement pauvres en π^0 . L'énergie moyenne de ces événements est estimée à 17 GeV, soit un peu supérieure à l'énergie de l'ensemble des gerbes.

La distribution angulaire des 50 PPN mesurées est portée en Fig. 10 et



le «F-plot» en Fig. 11. Ce dernier constitue une ligne droite de pente très voisine de 2 et le γ_c déterminé d'après le point $F/(1-F) = 1$ est $\gamma_c = 4.65$. Ce γ_c est relatif au système CM du photon virtuel et du nucléon de la cible. Il est lié à l'énergie du photon virtuel par la formule $E_{ph} = Mc^2(2\gamma_c^2 - 1)$, où Mc^2 est l'énergie de masse du nucléon. On obtient $E_{ph} = 40$ GeV.

10. — Discussion.

Fig. 11.

L'énergie de 40 GeV obtenue à partir de cette analyse de la distribution angulaire semble être beaucoup trop élevée. Rappelons que l'estimation précédente basée

sur l'évaluation de l'énergie des π^0 est confirmée par le bon accord entre la section efficace expérimentale avec la théorie. Vu la sélection sévère des clichés, il ne semble pas que la distribution angulaire ait pu être faussée du fait que des PP émises à grand angle ont été omises dans la statistique. Si tel avait été le cas, on aurait d'ailleurs obtenu une courbe incurvée vers le haut au lieu d'une ligne droite.

Au contraire, il y a lieu de penser que l'énergie obtenue d'après la distribution angulaire a plutôt été sous-estimée, car deux effets tendent à élargir la distribution angulaire des secondaires de l'interaction, à savoir: 1) les interactions secondaires à l'intérieur du noyau frappé et 2) le fait que les angles ont été mesurés par rapport au méson μ incident et non par rapport à la direction du photon virtuel.

Il semble donc que l'on soit obligé de réviser l'hypothèse de l'émission isotropique dans le système CM. Les distributions symétriques dans le système CM par rapport au plan perpendiculaire aux moments produiraient toutes des courbes passant par le même point $F/(1-F) = 1$ sur le graphique et donneraient donc le même γ_c , ce qui n'arrangerait pas le désaccord.

On est donc obligé de s'orienter vers une distribution asymétrique dans le système CM avec une prépondérance de particules émises en avant, c'est-à-dire dans la direction du photon virtuel. Différentes distributions ont été essayées, dont la meilleure semble être une distribution de la forme $(1 + \cos q) d\Omega$ dans le système CM. Une telle distribution conduirait à la formule suivante, ana-

logue de (6):

$$(7) \quad \operatorname{tg}^2 \theta = \gamma_e^{-2} \frac{1 - \sqrt{1 - F}}{\sqrt{1 - F}}.$$

On a donc porté $\log[(1 - \sqrt{1 - F})/\sqrt{1 - F}]$ en fonction de $\log \operatorname{tg} \theta$ dans la Fig. 12. Les points expérimentaux s'alignent sur une droite de pente 1.7 et le γ_e est 2.8, ce qui correspond à une énergie de photon de 14 GeV, en accord raisonnable avec les autres estimations de l'énergie des événements. Le fait que la pente est inférieure à 2 et l'énergie un peu inférieure à l'énergie estimée par ailleurs pourrait être interprété par un élargissement de la distribution angulaire par suite des deux effets cités plus haut.

L'asymétrie qui est suggérée par cette expérience peut fournir des indications intéressantes en ce qui concerne les théories de production multiple. Nous ne tiendrons pas d'interpréter ce résultat avant qu'il ne soit confirmé par d'autres expériences.

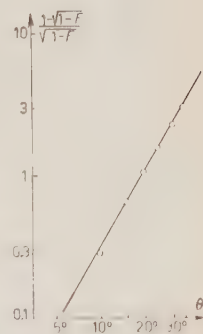


Fig. 12.

11. — Mésons μ « parallèles ».

Nous avons observé 12 cas de particules pénétrantes « parallèles » et contemporaines. En réalité, le parallélisme n'est pas parfait, mais nous n'avons pas jugé utile d'imposer un critère très strict, car ces clichés sont assez caractéristiques et ne peuvent guère être confondus avec d'autres événements:

1) Il ne s'agit pas de coïncidences fortuites de mésons μ , car leur nombre calculé est négligeable et en fait on n'en a pas observé.

2) Il ne s'agit pas non plus de particules pénétrantes concourantes produites dans le sol à une assez grande distance de la chambre. Les angles observées dans le cas de particules concourantes sont assez grands et il n'y a pas de continuité entre les deux distributions.

Ces événements doivent sans aucun doute être interprétés comme mésons μ associés aux grandes gerbes de l'air. A cet égard, il est significatif de constater que le rapport de fréquence des mésons parallèles et des gerbes pénétrantes locales apparemment produites dans le sol ou dans l'appareil même, est 12:115, c'est-à-dire très proche du rapport 1/10 déterminé par GEORGES *et al.* (21) au moyen d'une mesure de décoherence avec des télescopes de comp-

teurs à 60 m H₂O sous terre. La distribution des multiplicités observées est portée dans le Tableau VI.

TABLEAU VI.

Multiplicités de mésons	2	3	4	5	6	7	8	9	10	11	>11
Nombre de cas observés	7	1	1	1	0	0	0	1	0	1	0

Les cas de faible densité se prêtent difficilement à l'analyse car le biais de la commande de l'appareil intervient ici. Les deux cas de forte multiplicité (9 et 11, voir Fig. 13) sont intéressants: l'angle formé par les trajectoires avec leur direction moyenne est inférieur à $\pm 2.5^\circ$ pour toutes les trajectoires sauf une, qui a un angle de 3.5° . Ces angles sont faciles à interpréter en termes de scattering Coulombien dans le sol.

Les angles zénitaux sont de 37° et 19° respectivement. On a observé 45 traversées d'écran dans le cliché à 9 trajectoires (environ $590 \text{ g} \cdot \text{cm}^{-2}$ Pb) et 66 traversées ($730 \text{ g} \cdot \text{cm}^{-2}$ Pb) dans le cliché à 11 trajectoires, soit au total environ 11 parcours nucléaires sans interaction, ni scattering appréciable.

La densité de mésons observés dans ces 2 cas est environ 55 m^{-2} à 65 m H₂O de profondeur. Si on prend le modèle de George (24) selon lequel la moitié des mésons μ d'une gerbe de l'air arrivant à cette profondeur sont contenus dans un cercle de 60 m de rayon, on obtient au total environ 10^6 mésons à 65 m H₂O. L'absorption des mésons des grandes gerbes ne semble pas être différente de celle des mésons ordinaires entre le sol et 65 m H₂O (25) et on aura ainsi au sol 10^7 mésons μ . Le nombre total de particules des gerbes correspondantes sera de l'ordre de 10^9 , ce qui correspond à une énergie de primaire d'environ $3 \cdot 10^{18}$ eV! D'autre part, si l'on calcule, en extrapolant le spectre d'énergie connu, le nombre de primaires produisant des gerbes dont les axes tombent à l'intérieur d'un cercle de 60 m de rayon, on trouve 2 événements pour 5 000 heures d'observation, ce qui semble confirmer notre interprétation.

Nous désirons remercier ici Monsieur A. CACHON pour des discussions intéressantes sur le problème des mésons parallèles et leur rapport avec les grandes gerbes de l'air.

Cette expérience a été effectuée grâce à des subventions du Centre National de la Recherche Scientifique et du Haut Commissariat pour l'Energie Atomique (France) auxquels nous exprimons ici toute notre reconnaissance.

(24) E. P. GEORGE, J. W. MACANUFF et J. W. STURGESS: *Proc. Phys. Soc. (Londres)*, A 66, 345 (1953).

(25) K. GREISEN: *Progress in Cosmic Ray Physics*, III (Amsterdam, 1956), chap. 6.10.

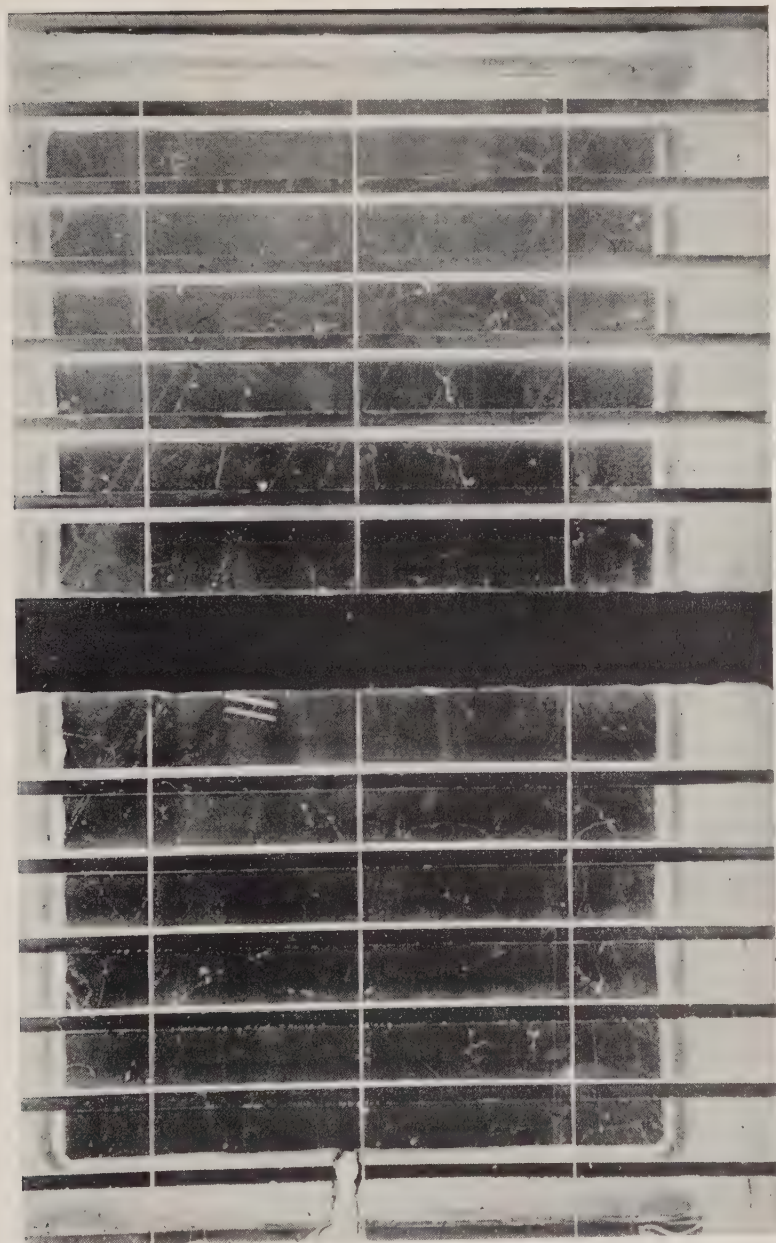


Fig. 13. - Exemple de mésons parallèles. On distingue 9 mésons μ qui traversent la chambre d'avant en arrière.

RIASSUNTO (*)

Una grande camera a nebbia contenente 12 piastre di Pb (spesse 1 cm) e contatori Geiger interni è stata fatta funzionare per 5000 h sotto terra a 65 m a.e. Si sono osservati 28 sciami penetranti prodotti dentro la camera da mesoni μ di alta energia. Tali sciami sono stati analizzati coi seguenti risultati: 1) Per quanto riguarda il numero relativo dei π^+ , dei π^0 secondari e dei protoni, gli sciami penetranti osservati sotto terra non differiscono in modo significativo da quelli ottenuti al livello del mare e in osservatori di montagna. Il cammino libero medio osservato per la produzione di stelle e lo scattering nucleare da parte dei secondari ionizzanti (escluso il mesone μ uscente) è (233 ± 52) g/cm $^{-2}$ Pb, corrispondente a un cammino libero medio geometrico, tenuto conto dello spessore finito delle piastre. 2) L'angolo di deviazione del mesone μ nell'interazione risulta assai piccolo, nella maggioranza dei casi inferiore a 2° , cioè circa un ordine di grandezza minore del rapporto q/E stimato per il trasferimento di energia a energia primaria, d'accordo con l'interpretazione degli eventi in termini di interazioni fotonucleari anelastiche. 3) Il numero medio di secondari penetranti ionizzanti (escluso il mesone μ uscente) è di 3.7. L'energia media degli eventi osservati è stata stimata in base alle cascate elettroniche prodotte dalla disintegrazione di mesoni π , in 16 GeV. 4) La sezione d'urto di $(0.43 \pm 0.08) \cdot 10^{-3}$ cm 2 /nucleone osservata per la produzione di sciami penetranti di più di 12 GeV da parte di mesoni μ a 65 m a.e. sotto terra è in buon accordo con le predizioni di una teoria di Williams-Weizsäcker perfezionata ed una sezione d'urto fotonucleare presunta in 10^{-28} cm 2 /nucleone a queste alte energie. 5) Si hanno alcune prove che i secondari non sono emessi isotropicamente nel sistema del centro d'impulso del fotone virtuale e del nucleone bersaglio. Una distribuzione anisotropa del tipo $(1 + \cos \Phi) d\Omega$ nel sistema del centro di massa sarebbe in accordo con la distribuzione angolare osservata in laboratorio. Nella stessa esperienza abbiamo osservato 12 casi di particelle penetranti non interagenti parallele, presumibilmente mesoni μ provenienti da sciami estesi dell'aria. Due fotografie mostrano 9 e 11 mesoni μ paralleli nella regione illuminata della camera a nebbia, il che porta a stimare una densità di circa 55 particelle per m 2 a 65 m a.e. derivanti da sciami dell'aria di circa $3 \cdot 10^{18}$ eV. Questa energia sarebbe d'accordo con la frequenza osservata.

(*) Traduzione a cura della Redazione.

RIASSUNTO (*)

Una grande camera a nebbia contenente 12 piastre di Pb (spesse 1 cm) e contatori Geiger interni è stata fatta funzionare per 5000 h sotto terra a 65 m a.e. Si sono osservati 28 sciami penetranti prodotti dentro la camera da mesoni μ di alta energia. Tali sciami sono stati analizzati coi seguenti risultati: 1) Per quanto riguarda il numero relativo dei π^\pm , dei π^0 secondari e dei protoni, gli sciami penetranti osservati sotto terra non differiscono in modo significativo da quelli ottenuti al livello del mare e in osservatori di montagna. Il cammino libero medio osservato per la produzione di stelle e lo scattering nucleare da parte dei secondari ionizzanti (escluso il mesone μ uscente) è (233 ± 52) g/cm $^{-2}$ Pb, corrispondente a un cammino libero medio geometrico, tenuto conto dello spessore finito delle piastre. 2) L'angolo di deviazione del mesone μ nell'interazione risulta assai piccolo, nella maggioranza dei casi inferiore a 2° , cioè circa un ordine di grandezza minore del rapporto q/E stimato per il trasferimento di energia a energia primaria, d'accordo con l'interpretazione degli eventi in termini di interazioni fotonucleari anelastiche. 3) Il numero medio di secondari penetranti ionizzanti (escluso il mesone μ uscente) è di 3.7. L'energia media degli eventi osservati è stata stimata in base alle cascate elettroniche prodotte dalla disintegrazione di mesoni π , in 16 GeV. 4) La sezione d'urto di $(0.43 \pm 0.08) \cdot 10^{-3}$ cm 2 /nucleone osservata per la produzione di sciami penetranti di più di 12 GeV da parte di mesoni μ a 65 m a.e. sotto terra è in buon accordo con le predizioni di una teoria di Williams-Weizsäcker perfezionata ed una sezione d'urto fotonucleare presunta in 10^{-28} cm 2 /nucleone a queste alte energie. 5) Si hanno alcune prove che i secondari non sono emessi isotropicamente nel sistema del centro d'impulso del fotone virtuale e del nucleone bersaglio. Una distribuzione anisotropa del tipo $(1 + \cos \Phi) d\Omega$ nel sistema del centro di massa sarebbe in accordo con la distribuzione angolare osservata in laboratorio. Nella stessa esperienza abbiamo osservato 12 casi di particelle penetranti non interagenti parallele, presumibilmente mesoni μ provenienti da sciami estesi dell'aria. Due fotografie mostrano 9 e 11 mesoni μ paralleli nella regione illuminata della camera a nebbia, il che porta a stimare una densità di circa 55 particelle per m 2 a 65 m a.e. derivanti da sciami dell'aria di circa $3 \cdot 10^{18}$ eV. Questa energia sarebbe d'accordo con la frequenza osservata.

(*) Traduzione a cura della Redazione.

Velocity-Dependent Nuclear Interaction.

W. E. FRAHN and R. H. LEMMER

*Nuclear Physics Division of the National Physical Research Laboratory
C.S.I.R. - Pretoria, South Africa*

(ricevuto il 5 Marzo 1957)

Summary. — The single particle wave equation describing the motion of nucleons in nuclei, as derived from the nuclear many-body problem, is of a non-local form in coordinate space. It is shown, that in the effective mass approximation, this equation reduces to a velocity-dependent Schrödinger equation, which contains a spatially variable effective nucleon mass in a properly symmetrized kinetic energy operator. The eigenvalue problem is treated for the special case of the infinite harmonic oscillator potential as the local part of the interaction.

1. — Introduction.

Recent developments in the many-body problem of nuclear structure (¹) led to a deeper understanding of the fact, that the nucleon-nucleus interaction can be successfully described by an overall potential in spite of the strong, short-range internuclear forces, thus giving a firmer basis to the single particle models.

The overall potential resulting from this treatment appears, however, not as a local potential $V(r)$, as assumed in earlier Hartree-Fock calculations, but as an essentially non-local interaction. Therefore, the wave equation for the relative motion of a nucleon in the nucleus has the general form in co-ordinate

(¹) A very comprehensive study of this problem, based on the work of K. A. BRUECKNER, K. M. WATSON, C. A. LEVINSON, H. M. MAHMOUD, R. J. EDEN and N. C. FRANCIS, has been given by H. A. BETHE: *Phys. Rev.*, **103**, 1353 (1956); it also contains the references to the earlier literature.

space:

$$(1) \quad -\frac{\hbar^2}{2M_0} \Delta \psi(\mathbf{r}) + E\psi(\mathbf{r}) = \int K(\mathbf{r}, \mathbf{r}') \psi(\mathbf{r}') d\mathbf{r}' .$$

Some implications of this type of interaction have been studied previously (2), viz., the modified propagation properties of nucleons in nuclear matter, reflected in a reduced effective nucleon mass, and the energy dependence of the real parts of the optical model parameters. For mathematical convenience and in order to point out the essential features only, a very simple form of the interaction kernel was used, viz.,

$$(2) \quad K(\mathbf{r}, \mathbf{r}') = -V_0 \delta_a(\mathbf{r} - \mathbf{r}'),$$

δ_a being an approximation function to the δ -function. The kernel thus describes a «small» non-local deviation from a constant local potential characterizing infinitely extended nuclear matter.

In the present paper we will consider the more general kernel

$$(3) \quad K(\mathbf{r}, \mathbf{r}') = V \left(\frac{\mathbf{r} + \mathbf{r}'}{2} \right) \delta_a(\mathbf{r} - \mathbf{r}'),$$

$\delta_a(\mathbf{r} - \mathbf{r}') = \pi^{-1/2} a^{-3} \exp[-((\mathbf{r} - \mathbf{r}')/a)^2]$ again being the Gaussian approximation of $\delta(\mathbf{r} - \mathbf{r}')$ with parameter a . Thus, for $a \rightarrow 0$, the non-local interaction reduces to the local potential $V(r)$.

A development of the interaction term in powers of a up to a certain order, leads to a velocity dependent potential of that order. It will be shown in the following Sect. 2, that in the first non-vanishing approximation, eq. (1) reduces to an equivalent Schrödinger equation with the local potential $V(r)$, but with a spatially variable effective nucleon mass, appearing in a properly symmetrized kinetic energy operator. In the subsequent sections we specify $V(r)$ to be the harmonic oscillator potential. In Sect. 3 we consider the one-dimensional case in order to explain the relation of the wave equation to the differential equation of the spheroidal functions. In Sect. 4 the 3-dimensional isotropic oscillator is treated and the energy level structure calculated in first approximation.

2. – The effective mass approximation.

The radial part of eq. (1) is obtained by writing

$$(4) \quad \psi(\mathbf{r}) = \frac{u_l(r)}{r} Y_{lm}(\theta, \varphi),$$

(2) W. E. FRAHN: *Nuovo Cimento*, **4**, 313 (1956).

where the Y_{lm} are the normalized spherical harmonics and

$$(5) \quad K(\mathbf{r}, \mathbf{r}') = \sum_{l=0}^{\infty} \frac{2l+1}{4\pi} \frac{k_l(r, r')}{rr'} P_l(\cos \theta) = \\ = \sum_{l=0}^{\infty} \sum_{m=-l}^{+l} \frac{k_l(r, r')}{rr'} Y_{lm}(\theta, \varphi) Y_{lm}^*(\theta', \varphi'),$$

θ, φ and θ', φ' being the polar angles of \mathbf{r} and \mathbf{r}' , respectively. The resulting radial equation is

$$(6) \quad \frac{\hbar^2}{2M_0} \left(\frac{d^2 u_l}{dr^2} - \frac{l(l+1)}{r^2} u_l \right) + Eu_l = \int_0^{\infty} k_l(r, r') u_l(r') dr',$$

where

$$(7) \quad k_l(r, r') = 2\pi rr' \int_{-1}^{+1} K(\mathbf{r}, \mathbf{r}') P_l(\zeta) d\zeta.$$

With the kernel (3) and using the Gaussian approximation for δ_a , we obtain

$$(8) \quad k_l(r, r') = \frac{2rr'}{\sqrt{\pi} \cdot a^3} \int_{-1}^1 V \left(\left| \frac{\mathbf{r} + \mathbf{r}'}{2} \right| \right) \exp \left[- \left(\frac{\mathbf{r} - \mathbf{r}'}{a} \right)^2 \right] P_l(\zeta) d\zeta.$$

In order to study the effect of a small non-local deviation from a local potential, we develop the right hand side of eq. (6) in powers of the parameter a . Retaining contributions up to the order a^2 only, we find

$$(9) \quad \int_0^{\infty} k_l(r, r') u_l(r') dr' = V(r) u_l(r) + \\ + \frac{a^2}{4} \left[V(r) \frac{d^2 u_l}{dr^2} + V'(r) \frac{du_l}{dr} + \left(\frac{1}{4} V''(r) - \frac{1}{2r} V'(r) - \frac{l(l+1)}{r^2} V(r) \right) u_l(r) \right].$$

In deriving this equation, we use the integral relations

$$(10) \quad \int_{-1}^{+1} \zeta^n P_l(\zeta) \exp \left[\frac{2rr'\zeta}{a^2} \right] d\zeta = 2(-1)^l i^{l+n} j_l^{(n)} \left(\frac{2irr'}{a^2} \right),$$

and the asymptotic expressions for the derivatives, $j_l^{(n)}$, of the spherical Bessel-functions up to order a^{-4} .

The Schrödinger equation (6) with its right hand side given by (9) can be rewritten in the form

$$(11) \quad -\frac{\hbar^2}{8M_0} \left\{ A_r \left[\left(1 - \frac{a^2 M_0}{2\hbar^2} V(r) \right) \frac{u_l}{r} \right] + 2 \left[\frac{d}{dr} \left(1 - \frac{a^2 M_0}{2\hbar^2} V(r) \right) \frac{d}{dr} + \right. \right. \\ \left. \left. + \left(1 - \frac{a^2 M_0}{2\hbar^2} V(r) \right) A_r \right] \left(\frac{u_l}{r} \right) + \left(1 - \frac{a^2 M_0}{2\hbar^2} V(r) \right) A_r \left(\frac{u_l}{r} \right) \right\} + \\ + \frac{\hbar^2}{2M_0} \frac{l(l+1)}{r^2} \left(1 - \frac{a^2 M_0}{2\hbar^2} V(r) \right) \frac{u_l}{r} + V(r) \frac{u_l}{r} = E \frac{u_l}{r},$$

where $A_r = (1/r^2)(d/dr)(r^2(d/dr))$. This is seen to be the radial part of the following wave equation:

$$(12) \quad \frac{1}{8} \left[\mathbf{P}^2 \frac{1}{M(r)} + \mathbf{P} \frac{2}{M(r)} \mathbf{P} + \frac{1}{M(r)} \mathbf{P}^2 \right] \psi(\mathbf{r}) + V(r)\psi(\mathbf{r}) = E\psi(\mathbf{r}),$$

with the local potential $V(r)$, but with a spatially variable effective nucleon mass

$$(13) \quad M(r) = \frac{M_0}{1 - (a^2 M_0 / 2\hbar^2) V(r)},$$

appearing in a properly symmetrized kinetic energy operator. In regions where $V(r)$ is negative, the effective nucleon mass is always smaller than the mass of the free nucleon, the reduction depending on the local strength of the overall potential. In field-free regions or in the limit $a = 0$, we have $M = M_0$. For a potential well with depth $V(0) = -V_0$ at the centre of the nucleus, we have

$$(13a) \quad M(0) = \frac{M_0}{1 + (a^2 M_0 / 2\hbar^2) V_0} = M^*,$$

in agreement with the expression derived previously (2) for the case of infinitely extended nuclear matter, characterized by a constant potential $-V_0$, in the effective mass approximation in momentum space. Both empirical and theoretical evidence leads consistently to the value $M^* \approx \frac{1}{2} M_0$.

The single particle wave equation (12) represents the correct effective mass approximation of eq. (1) with the kernel (3) in co-ordinate space. It may be noted, that the result in this approximation is independent of the special choice of the approximation for the δ -function.

An equation of a similar type has been derived by DUERR (3) in his rela-

(3) H. P. DUERR: *Phys. Rev.*, **103**, 469 (1956).

tivistically covariant formulation of the model of JOHNSON and TELLER (4). In this treatment, the equation results as the non-relativistic limit obtained from the Dirac-Hamiltonian assumed by DUERR, after a Foldy-Wouthuysen transformation. In addition, however, a large spin-orbit coupling term appears, which does not result from the present formalism because of its essentially non-relativistic nature.

3. – One-dimensional oscillator.

We now specify the potential $V(r)$ to be that of the infinite isotropic harmonic oscillator. In this case, eq. (12) reduces to a form which has a close connection with the differential equation of the spheroidal functions. In order to clarify this relation, we first consider the one-dimensional case. Eq. (12) then takes the form

$$(14) \quad -\frac{\hbar^2}{8} \left[\frac{d^2}{dx^2} \frac{1}{M(x)} + \frac{d}{dx} \frac{2}{M(x)} \frac{d}{dx} + \frac{1}{M(x)} \frac{d^2}{dx^2} \right] \psi(x) + V(|x|)\psi(x) = E\psi(x),$$

which is the effective mass approximation of the one-dimensional analogue of (1).

With the oscillator potential

$$(15) \quad V(x) = -V_0 + \frac{1}{2} M_0 \omega^2 x^2,$$

we have

$$(16) \quad \frac{1}{M(x)} = \frac{1}{M^*} \left(1 - \frac{2M^*}{\hbar^2} \kappa^2 \cdot x^2 \right),$$

where

$$(17) \quad \kappa^2 = \frac{1}{8} M_0 \omega^2 a^2,$$

and from (14) we obtain with the substitution $\varrho = ((2M^*)^{1/2}\kappa/\hbar) \cdot x$:

$$(18) \quad \frac{d}{d\varrho} \left[(1 - \varrho^2) \frac{d\psi}{d\varrho} \right] + [\lambda' + \gamma^2(1 - \varrho^2)]\psi = 0,$$

where

$$(19) \quad \lambda' = \frac{1}{\kappa^2} \left[E + V_0 - \frac{1}{2} \kappa^2 - \frac{1}{4\kappa^2} (\hbar\omega^*)^2 \right]; \quad \gamma = \frac{\hbar\omega^*}{2\kappa^2}; \quad \omega^* = \left(\frac{M_0}{M^*} \right)^{1/2} \omega.$$

(4) M. H. JOHNSON and E. TELLER: *Phys. Rev.*, **98**, 783 (1955).

Equation (18) is the differential equation of the spheroidal functions⁽⁵⁾ $\psi = ps_n^0(\varrho; \gamma^2)$.

In the approximation of small a , i.e. $\gamma^2 \gg 1$, the spectrum of the γ -asymptotic equation of (18) up to the order γ^{-1} is given by⁽⁵⁾

$$(20) \quad \lambda_n^{(0)}(\gamma^2) = -\gamma^2 + \gamma(2n' + 1) - \frac{1}{2}[n'(n' + 1) + \frac{3}{2}] - \\ - \frac{1}{16\gamma} (2n' + 1)[n'(n' + 1) + 3]; \quad (n' = 0, 1, 2, \dots),$$

and the eigenfunctions are in first approximation

$$(21) \quad ps_n^0(\varrho; \gamma^2) = \left(\frac{4\gamma}{\pi}\right)^{\frac{1}{2}} \frac{1}{[n!(2n+1)]^{\frac{1}{2}}} D_n[(2\gamma)^{\frac{1}{2}}\varrho] + O(\gamma^{-\frac{3}{2}}),$$

where D_n denotes the parabolic cylinder functions

$$(22) \quad D_n(z) = (-1)^n \exp\left[\frac{z^2}{4}\right] \frac{d^n}{dz^n} \exp\left[-\frac{z^2}{2}\right].$$

Inserting the abbreviations (19), we get from (20):

$$(23) \quad E_{n'} + V_0 = (n' + \frac{1}{2})\hbar\omega^* - \frac{\varkappa^2}{2}[n'(n' + 1) + \frac{1}{2}] - \\ - \frac{\varkappa^*}{4} \frac{1}{\hbar\omega^*} (n' + \frac{1}{2})[n'(n' + 1) + 3].$$

The same result is obtained by writing eq. (14) in the form

$$(24) \quad \frac{\hbar^2}{2M^*} \psi''(x) + (E + V_0 - \frac{1}{2}M^*\omega^{*2})\psi(x) = \varkappa^2[x^2\psi''(x) + 2x\psi'(x) + \frac{1}{2}\psi(x)],$$

and by treating the right hand side of this equation as a perturbation of the static oscillator problem, defined by the left hand side, up to the order \varkappa^4 .

4. – Three-dimensional isotropic oscillator.

The radial part of the wave equation (12) was given by (6) and (9). With the isotropic oscillator potential

$$(25) \quad V(r) = -V_0 + \frac{1}{2}M_0\omega^2r^2,$$

⁽⁵⁾ J. MEIXNER and F. W. SCHÄFKE: *Mathieu'sche Funktionen und Sphäroidfunktionen* (Berlin, 1954).

we obtain

$$(26) \quad \frac{\hbar^2}{2M^*} \left(u_i''(r) - \frac{l(l+1)}{r^2} u_i(r) \right) + (E + V_0 - \frac{1}{2} M^* \omega^* r^2) u_i(r) = \\ = \varkappa^2 [r^2 u_i''(r) + 2r u_i'(r) - (l(l+1) + \frac{1}{2}) u_i(r)] .$$

This can be written in the form

$$(27) \quad \frac{d}{d\varrho} \left[(1 - \varrho^2) \frac{du_i}{d\varrho} \right] + \left[\lambda + \gamma^2 (1 - \varrho^2) - \frac{l(l+1)}{\varrho^2} \right] u_i = 0 ,$$

where

$$(28) \quad \lambda = \frac{1}{\varkappa^2} \left[E + V_0 + (l(l+1) + \frac{1}{2}) \varkappa^2 - \frac{1}{4\varkappa^2} (\hbar \omega^*)^2 \right] .$$

For $l = 0$, eq. (27) is again the differential equation of the spheroidal functions, but for $l \neq 0$ an additional centrifugal term appears (*).

Analogous to the one-dimensional case, the eigenvalue-spectrum in the approximation of small a , i.e. in the asymptotic form for $\gamma \rightarrow \infty$, can be obtained by a perturbation calculation starting from the local isotropic oscillator problem defined by the left hand side of eq. (26). The normalized unperturbed radial solutions are

$$(29) \quad u_{nl}(r) = \frac{\beta^{\frac{1}{2}} (2n!)^{\frac{1}{2}}}{[\Gamma(n+l+\frac{3}{2})]^{\frac{1}{2}}} (\beta r^2)^{(l+1)/2} \exp[-\frac{1}{2}\beta r^2] L_n^{l+\frac{1}{2}}(\beta r^2) ,$$

with $\beta = M^* \omega^* / \hbar$, and

$$(30) \quad L_n^\mu(z) = \frac{\Gamma(\mu+n+1)}{\Gamma(n+1)} \frac{e^z}{z^\mu} \frac{d^n}{dz^n} (z^{n+\mu} e^{-z}) ,$$

are the Laguerre polynomials (6).

Using the recurrence formulae and the normalization integrals of the La-

(*) *Note added in proof:* Meanwhile, J. MEIXNER has treated the generalized equation (27) of the spheroidal functions, i.e. including the centrifugal term, for $\gamma^2 \gg 1$ with a method similar to that used previously (J. MEIXNER: *Z. angew. Math. Mech.*, 28, 304 (1948)) for the ordinary equation (18). His results agree exactly with ours, obtained by perturbation calculation, up to the order γ^{-2} . One of us (W.E.F.) is much indebted to Professor MEIXNER for a private communication of his results.

(6) P. M. MORSE and H. FESHBACH: *Methods of Theoretical Physics*, vol. I (New York, 1953).

guerre polynomials (6), we find up to the order κ^2 :

$$(31) \quad E_{nl} + V_0 = (N + \frac{3}{2})\hbar\omega^* - \frac{\kappa^2}{2}[N(N + 3) + l(l + 1) + \frac{9}{2}],$$

where $N = 2n + l = 0, 1, 2, \dots$.

For s -states, the differential equation (26) reduces to that of the spheroidal functions and the spectrum (31) for $l = 0$ becomes similar to that of the one-dimensional case (23). In this case we have $N = 2n$, and the connection between the two level schemes follows from the fact, that, because of the boundary condition $u(0) = 0$, only the odd values of n' in the one-dimensional case have an analogue to the n -values of the three-dimensional case. With the substitutions $n' \rightarrow 2n + 1$ and $\lambda' \rightarrow \lambda$ the scheme (23) up to the order κ^2 becomes identical with (31) for $l = 0$.

The comparison of (31) with the spectrum of the static oscillator,

$$(32) \quad E_{nl}^{(0)} + V_0 = (N + \frac{3}{2})\hbar\omega,$$

shows the following effects of the velocity dependence:

1) The spacing $\hbar\omega$ of the static oscillator levels is increased by the factor $\omega^*/\omega = (M_0/M^*)^{1/2} \approx \sqrt{2}$. In order to bind the same number of particles as in the static case, the potential well depth V_0 has to be increased by about a factor 2.

2) Apart from the increased level spacing, the velocity dependence causes a general depression of the oscillator levels, as indicated by the term $-(\kappa^2/2)[N(N + 3) + \frac{9}{2}]$.

3) The (n, l) -degeneracy of the static isotropic oscillator is removed in the velocity-dependent case, as a consequence of the term $-(\kappa^2/2)l(l+1)$. This is formally equivalent to an additional term $-(\kappa^2/2)l^2$ in the interaction Hamiltonian. Such a term causes a depression of the higher angular momentum states and induces a level sequence which goes into the direction of that obtained from a square well potential.

The velocity-dependent oscillator potential can thus be regarded as an interpolation between the static isotropic oscillator and the spherical well potentials, such an interpolation usually being assumed as a starting point for the construction of the level scheme of the Mayer-Jensen shell model (7). Indeed, the spectrum (31) gives the correct level sequence assumed in this

(7) M. GOEPPERT-MAYER and J. H. D. JENSEN: *Elementary Theory of Nuclear Shell Structure* (New York, 1955).

interpolation, the energy difference between two adjacent l -levels in a given oscillator shell being $\Delta E_{l,l+2} = (2l + 3)\pi^2$. However, in order to compare the level structure arising from the velocity-dependent oscillator spectrum with that required by empirical nuclear properties, a phenomenological spin-orbit coupling term has to be added. A detailed discussion of this comparison will be given in a subsequent paper.

ROSS, LAWSON and MARK⁽⁸⁾ have recently calculated the nucleon energy levels derived from a velocity-dependent wave equation very similar to eq. (12). The local potential $V(r)$ used by these authors is the diffuse well potential proposed by Woods and SAXON⁽⁹⁾. It has been shown, that with a certain choice of the interaction parameters for a velocity-dependent potential of this type, a satisfactory nucleon shell structure and level sequence can be obtained.

* * *

The authors are indebted to Dr. S. J. du Toit, head of the Nuclear Physics Division, for his interest and to the South African Council for Scientific and Industrial Research for permission of publication.

⁽⁸⁾ A. A. ROSS, R. D. LAWSON and H. MARK: *Phys. Rev.*, **104**, 401 (1956).

⁽⁹⁾ R. D. WOODS and D. S. SAXON: *Phys. Rev.*, **95**, 577 (1954).

RIASSUNTO (*)

L'equazione d'onda di una singola particella che descrive il moto di nucleoni nei nuclei, come si deriva dal problema nucleare di più corpi, è di forma non locale nello spazio delle coordinate. Si dimostra che nell'approssimazione della massa effettiva quest'equazione si riduce a un'equazione di Schrödinger dipendente dalla velocità che contiene una massa nucleonica spazialmente variabile in un operatore di energia cinetica opportunamente simmetrizzato. Il problema degli autovalori è trattato per il caso speciale del potenziale di oscillatore armonico infinito come parte locale della interazione.

(*) Traduzione a cura della Redazione.

A Model for the Weak Interactions.

S. GOTŌ

Institute of Physics, Tokyo Gakugei University - Tokyo

(ricevuto il 17 Marzo 1957).

Summary. — By assigning iso-spin to be zero and strangeness u to be $2, -2$ and 0 for the leptons μ^+ , e^- and ν respectively, the universality of the weak interactions including the lepton processes is shown to be consistently derived if the strong primary interactions are assumed to be of the Yukawa type and the weak primary interactions of the Fermi one.

1. — Introduction.

As is well known, the charge independence hypothesis proposed by NISHIJIMA⁽¹⁾ and GELL-MANN⁽²⁾ has succeeded in explaining the curious natures of the strange particles as far as the strong interactions are concerned. But such a theory, as it stands, seems to be unsatisfactory in explaining the lepton processes^(3,4).

In the customary scheme the leptons are not assigned any iso-spin and strangeness. This view point is usually accepted on the ground that the lepton interactions, except for the electromagnetic ones, are about 10^{-14} weaker than the strong ones, and are charge dependent. According to the current scheme,

⁽¹⁾ T. NAKAMO and K. NISHIJIMA: *Prog. Theor. Phys.*, **10**, 531 (1953); K. NISHIJIMA: *Prog. Theor. Phys.*, **12**, 107 (1955); **13**, 285 (1955).

⁽²⁾ M. GELL-MANN: *Phys. Rev.*, **92**, 833 (1953).

⁽³⁾ S. GOTŌ: *Prog. Theor. Phys.*, **17**, 107 (1957). We call this paper as (I).

⁽⁴⁾ M. GELL-MANN: *Proceedings of the 6th Rochester Conference*, VIII (1956).

we are obliged to allow such unwanted processes:

$$(1.1) \quad K^0 \rightarrow \mu^+ + \mu^-$$

$$(1.2) \quad \rightarrow e^+ + e^-$$

$$(1.3) \quad \begin{aligned} K^+ &\rightarrow \pi^+ + \mu^+ + \mu^- \\ &\rightarrow \pi^+ + e^+ + e^- \\ &\rightarrow \pi^+ + v + \bar{v} \end{aligned}$$

etc.

On the contrary we are allowed to take a different attitude and assign an appropriate iso-spin and strangeness for leptons, since the charged leptons as well as the baryons and bosons interact universally with the electromagnetic field which characterizes the third axis in the iso-space ⁽³⁾.

In this paper we take this second attitude and assume, for each lepton having strangeness quantum number s , the following relation between the third component of iso-spin I_3 and charge Q :

$$(1.6) \quad Q = I_3 + \frac{1}{2}u, \quad u = n + s,$$

where n means the number of leptons. This relation is an extension of that introduced by NISHIJIMA and GELL-MANN for each « strongly » (baryon and boson) with strangeness S :

$$(1.7) \quad Q = I_3 + \frac{1}{2}U, \quad U = N + S.$$

N in (1.7) is the number of baryons. The two equations (1.6) and (1.7) can be summarized as follows, giving

$$(1.8) \quad Q = I_3 + \frac{1}{2}V, \quad V = U + u,$$

which hold for all particles.

We assume in this paper, as shown in Table I, the iso-spin of any one of the leptons to be zero. μ^+ and e^- are considered to be normal ⁽⁵⁾, so μ^- and e^+ are antiparticles. The iso-spin assignment for baryons and bosons has been assumed to be the same as that of the paper (I).

(5) E. J. KONOPINSKI and H. M. MAHMOUD: *Phys. Rev.*, **92**, 1045 (1953).

TABLE I. — Iso-spin assignment for leptons (*).

Particle	I	I_3	$Q = I_3 + \frac{1}{2}u$	$u = n + s$	s	Transformation properties
μ^+	0	0	1	$I_3 + 1$	2	1
e^-	0	0	-1	$I_3 - 1$	-2	-3
ν	0	0	0	I_3	0	-1

(*) After the present paper was written, the author knew by private communication that the same iso-spin as taken in this paper for leptons was considered also by SENBA and OUCHI.

All the processes realized in nature are classified into the following three categories according to the interaction strength:

(i) *strong interactions* ($G^2 \sim 1$)

$$\Delta N = 0, \quad \Delta I = 0, \quad \Delta U = 0, \quad (\Delta Q = 0), \quad n = 0$$

($n = 0$ means that no leptons belong to this group).

(ii) *electromagnetic interactions* ($e^2 = 1/137$)

$$\Delta N = 0, \quad \Delta I_3 = 0, \quad \Delta U = 0, \quad (\Delta Q = 0), \quad (\text{for baryons}),$$

$$\Delta n = 0, \quad \Delta I = 0, \quad \Delta u = 0, \quad (\Delta Q = 0), \quad (\text{for leptons}).$$

(iii) *weak interactions* (*) ($f^2 \sim 10^{-14}$)

(a) *strongly-strongly*

$$\Delta N = 0, \quad \Delta Q = 0, \quad |\Delta I| = \frac{1}{2} \text{ or } \frac{3}{2}, \quad |\Delta U| = 1, \quad n = 0.$$

(b) *strongly-lepton*

$$\Delta N = \Delta n = 0, \quad \Delta Q = 0, \quad |\Delta I| = \frac{1}{2} \quad \text{or} \quad |\Delta I| = |\Delta I_3| = 1, \quad |\Delta u| = 2.$$

(c) *lepton-lepton*

$$\Delta n = 0, \quad \Delta I = 0, \quad \Delta u = 0, \quad (\Delta Q = 0), \quad N = 0.$$

($N = 0$ means that any one of baryons is not concerned to this process.)

(*) S. GOTŌ: *Prog. Theor. Phys.*, **17**, No. 3 (1957).

It is the main purpose of this paper that, among the various interactions realized in nature, the strong interactions are derived from appropriate combinations of the primary strong interactions of the Yukawa type, and the weak ones are obtained by the combination of one of the weak primary interactions of the Fermi type and some of the strong primary interactions of the Yukawa type (?).

2. - A model for the weak interactions.

We set the following assumptions on the interactions of the elementary particles.

ASSUMPTION I. The strong primary interactions are of the Yukawa type, and the weak primary interactions are of the Fermi type.

Justification of this assumption will be discussed in the next sections. Now, according to the above assumption, a copious production of hyperons occurs through a combination of several strong interactions of the Yukawa type, while the weak lepton processes are derived from the combination of some of the strong interactions of the Yukawa type and one of the weak interactions of the Fermi type, except the μ -e decay where the decay interaction is of Fermi type between leptons.

The primary interactions between the elementary particles are summarized as follows:

strong interactions ($G^2 \sim 1$)

$$\text{Yukawa type: } \Delta U = 0, \quad \Delta I = 0, \quad (\tilde{B}_K B'_K) K$$

$$(\tilde{B}_\pi B'_\pi) \pi$$

weak interactions ($f^2 \sim 10^{-14}$)

$$\text{Fermi type: } \left\{ \begin{array}{ll} |\Delta V| = 1, & |(\Delta I)| = \frac{1}{2} \text{ or } \frac{3}{2}, \\ |\Delta V| = 1, & |\Delta I| = \frac{1}{2}, \\ |\Delta V| = 2, & |\Delta I| = |\Delta I_3| = 1, \\ \Delta u = 0, & \Delta I = 0, \end{array} \right. \quad \begin{array}{l} (\tilde{B}_K B'_K \tilde{B}_\pi B'_\pi) \\ (\tilde{B}_K B'_K \tilde{l} l') \\ (\tilde{B}_\pi B'_\pi \tilde{l} l') \\ (\tilde{l} l' \tilde{l}' l') \end{array}$$

In the above table, $(\tilde{B}_K B'_K)$ and $(\tilde{B}_\pi B'_\pi)$ mean respectively the baryon pairs interacting strongly with the K and π -mesons, and the wave symbol \sim designates anti-particle. l , l' , l'' mean leptons. Besides the assumption I we set the following assumption in order to derive results consistent with the experiments.

(?) M. GELL-MANN: *Proceedings of the 6-th Rochester Conference*, VIII (1956), p. 25.

ASSUMPTION II. In the primary weak interactions, the coupling strengths are of the same order, but the type of coupling may be different from process to process (8).

For the convenience of later calculations we list here the more concrete expression of the above table.

strong interactions ($\Delta I = 0$, $\Delta U = 0$)

$$(\tilde{\Sigma}\Xi)K, \quad (\tilde{N}\Sigma)K, \quad (\tilde{N}\Lambda^0)K, \quad (\tilde{\Lambda}^0\Xi)K; \\ (\tilde{\Xi}\Xi)\pi, \quad (\tilde{\Sigma}\Sigma)\pi, \quad (\tilde{N}N)\pi, \quad (\tilde{\Lambda}\Lambda^0)\pi.$$

weak interactions

(i) baryon-baryon type ($|\Delta U| = 1$, $|\Delta I| = \frac{1}{2}$ or $\frac{3}{2}$)

$$\{(\tilde{\Sigma}\Xi), (\tilde{\Lambda}^0\Xi), (\tilde{N}\Sigma), (\tilde{N}\Lambda^0)\} \times \{(\tilde{\Xi}\Xi), (\tilde{\Sigma}\Sigma), (\tilde{N}N), (\tilde{\Lambda}\Lambda^0)\}.$$

(ii) lepton-lepton type ($\Delta u = 0$, $\Delta I = 0$)

$$(\tilde{\mu}v)(\tilde{e}v).$$

(iii) baryon-lepton type

(a) $|\Delta V| = 2$, $|\Delta I| = |\Delta I_3| = 1$.

$$\{(\tilde{\Xi}\Xi), (\tilde{\Sigma}\Sigma), (\tilde{N}N), (\tilde{\Lambda}\Lambda^0)\} \times \{(\tilde{\mu}v), (\tilde{e}v)\};$$

(b) $|\Delta V| = 1$, $|\Delta I| = \frac{1}{2}$

$$\{(\tilde{\Sigma}\Xi), (\tilde{\Lambda}^0\Xi), (\tilde{N}\Sigma), (\tilde{N}\Lambda^0)\} \times \{(\tilde{\mu}v), (\tilde{e}v)\}.$$

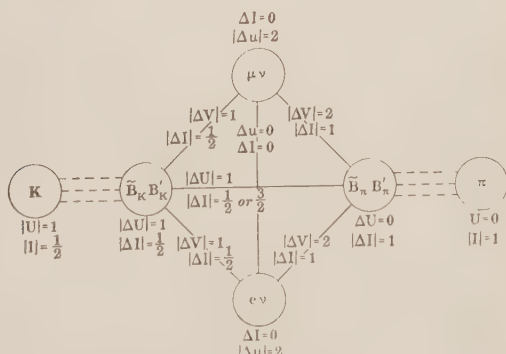


Fig. 1. — Model for the weak interactions. Full lines mean the weak Fermi interactions ($f^2 \sim 10^{-4}$), and bundles of three dotted line denote the strong Yukawa interactions ($G^2 \sim 1$).

(8) S. ŌNEDA and A. WAKASA: *Nucl. Phys.*, **1**, 445 (1956).

In order to derive the weak interactions of baryon-lepton type as secondary processes, we use the model which was proposed by GELL-MANN (⁷) and DALLAPORTA to unify the weak interactions. But our model differs from theirs, because we assign iso-spin and strangeness for leptons, while in their case leptons are not assigned any iso-spin and strangeness.

3. - Assumption of primarity of the strong Yukawa interactions.

By using a beam of 1.3 GeV π^- -mesons, it has been observed that the K^0 particles produced in the reactions

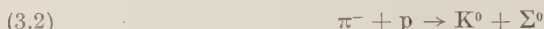
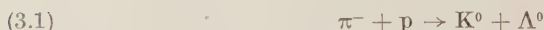
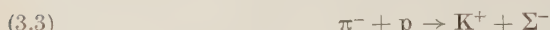


exhibit a pronounced forward asymmetry in the centre of mass system, while the angular distribution of K^+ -particles, produced by



is comparatively isotropic and favours the backward direction.

In this section we calculate the cross-sections for the reactions (3.1) ~ (3.3) by the lowest order perturbation for the cases where (3.1) ~ (3.3) are considered to occur through one step direct reactions and through two step reactions with interactions of the Yukawa type. It is shown that two step reactions are more apt than the one step reaction to interpret the experimental result mentioned above.

3.1. Case of the one step reaction (⁸). — We assume that the spins of the hyperons are all one half, and that of the K -meson zero. The interaction Hamiltonian including the reactions (3.1) ~ (3.3) through one step reactions is assumed to be

$$(3.4) \quad H = G_0 \bar{\Psi} \Gamma \psi \Phi^* \varphi + \text{h.c.},$$

where Ψ , ψ , Φ , and φ are respectively the wave functions of hyperon, proton, K -meson and π -meson, and Γ takes the value 1 or γ_5 . Throughout this paper

(⁸) W. B. FOWLER, R. D. SHUTT, A. M. THORNDIKE and W. L. WHITTEMORE: *Phys. Rev.*, **93**, 861 (1954); **98**, 121 (1955); R. BUDDE, M. CHRETIEN, J. LEITNER, N. P. SAMIOS, M. SCHWARTZ and J. STEINBERGER: *Phys. Rev.*, **103**, 1827 (1956).

we take the γ -matrices as follows:

$$(3.5) \quad \begin{cases} \gamma_\mu \gamma_\nu + \gamma_\nu \gamma_\mu = 2\delta_{\mu\nu} & (\mu, \nu = 1, 2, 3, 4) \\ \delta_{44} = -\delta_{11} = -\delta_{22} = -\delta_{33} = 1 \\ \gamma_5 = \gamma_1 \gamma_2 \gamma_3 \gamma_4 . \end{cases}$$

According to the interaction Hamiltonian (3.1), the production cross-section ($\hbar = e = 1$) for the reaction (3.1) is given in the centre of mass system as follows:

$$(3.6) \quad \frac{d\sigma}{d\Omega} = \frac{G_0^2}{2E^2} \frac{k'}{k} (E_p E_\Lambda + \varepsilon M_p M_\Lambda) \left(1 - \frac{kk'}{E_p E_\Lambda + \varepsilon M_p M_\Lambda} \cos \theta \right),$$

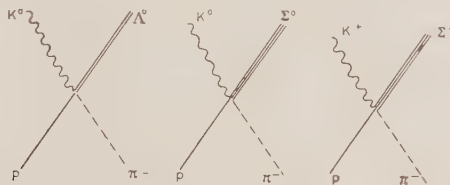


Fig. 2. · Feynman graphs for the reactions (3.1)~(3.3) regarded to be one step reactions

where θ is the angle between the directions of the incident π^- and the emitted K^0 . M_p and M_Λ mean respectively the rest masses of proton and Λ^0 . k and k' are the values of the momenta of the incident and final particles. E_p , E_π , E_Λ , E_K mean respectively the energy of proton, π^- , Λ^0 and K , and E the total energy of the incident (or emitted) particles. ε is equal to 1 (-1) according to $\Gamma = 1$ ($\Gamma = \gamma_5$).

The cross-sections for (3.2) and (3.3) are obtained simply by replacing M_{Σ^0} , E_{Σ^0} and M_{Σ^-} , E_{Σ^-} into (3.1) instead of M_Λ , E_Λ . Therefore the interaction Hamiltonian (3.4) gives no dissimilar asymmetries in the angular distributions of K^0 and K^+ particles in pion nucleon collisions. The tendency to similar angular distributions of K^0 and K^+ particles will not be altered by taking other types of coupling if (3.1)~(3.3) are considered to occur through the one step reaction.

3.2. Case of the two step reaction (10). — We take the interaction Hamiltonian as follows:

$$(3.6) \quad H = GH(NN\pi) + G_1H(\Lambda NK) + G_2H(\Sigma NK) + G_3H(\Sigma\Lambda\pi) + G_4H(\Sigma\Sigma\pi)$$

$$(3.7) \quad H(NN\pi) = \sqrt{2}(\bar{\psi}_p \gamma_5 \psi_n \varphi_+ + \bar{\psi}_n \gamma_5 \psi_p \varphi_-) + (\bar{\psi}_p \gamma_5 \psi_p - \bar{\psi}_n \gamma_5 \psi_n) \varphi_0$$

(11) H. IWAO: *Soryushiron Kenkyu*, **10**, 192 (1955) (mimeographed circular in Japanese).

$$(3.8) \quad H(\Lambda NK) = \bar{\Psi}_\Lambda \gamma_5 \psi_\nu \Phi_+^* + \bar{\Psi}_\Lambda \gamma_5 \psi_n \Phi_0^* + \text{h.c.}$$

$$(3.9) \quad H(\Sigma NK) = \sqrt{2} (\bar{\psi}_\nu \gamma_5 \Psi_{\Sigma^+} \Phi_0 + \bar{\psi}_n \gamma_5 \Psi_{\Sigma^-} \Phi_+) + \\ + (\bar{\psi}_\nu \gamma_5 \Psi_{\Sigma^0} \Phi_+ - \bar{\psi}_n \gamma_5 \Psi_{\Sigma^0} \Phi_0) + \text{h.c.}$$

$$(3.10) \quad H(\Sigma \Lambda \pi) = \bar{\Psi}_{\Sigma^+} \gamma_5 \Psi_{\Lambda^0} \varphi_+ + \bar{\Psi}_{\Sigma^0} \gamma_5 \Psi_{\Lambda^0} \varphi_0 + \bar{\Psi}_{\Sigma^-} \gamma_5 \Psi_{\Sigma^0} \varphi_- + \text{h.c.}$$

$$(3.11) \quad H(\Sigma \Sigma \pi) = \sqrt{2} \{ (\bar{\Psi}_{\Sigma^0} \gamma_5 \Psi_{\Sigma^+} - \bar{\Psi}_{\Sigma^+} \gamma_5 \Psi_{\Sigma^0}) \varphi_+ + (\bar{\Psi}_{\Sigma^-} \gamma_5 \Psi_{\Sigma^0} - \bar{\Psi}_{\Sigma^0} \gamma_5 \Psi_{\Sigma^-}) \varphi_- + \\ + (\bar{\Psi}_{\Sigma^+} \gamma_5 \Psi_{\Sigma^+} - \bar{\Psi}_{\Sigma^-} \gamma_5 \Psi_{\Sigma^-}) \varphi_0 \} + \text{h.c.}$$

Here the intrinsic parity for each particle is assigned according to Table II.

TABLE II. — Parity assignment.

Particle	N	Λ	Σ	π	K
parity	+	-	-	-	+
	+	+	+	--	-

If we use the parity assignment in Table II, the strong interactions of Yukawa type are given by the γ_5 -type (11):

$$G \bar{\Psi}_\alpha \gamma_5 \Psi_\beta \varphi .$$

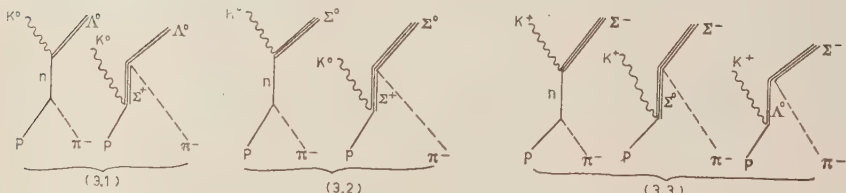


Fig. 3. — Feynman graphs for the reactions (3.1) ~ (3.3) regarded to be two step reactions.

The differential cross sections for the reactions (3.1) ~ (3.3) in the center of

(11) R. UTIYAMA and W. TOBOCMAN: *Phys. Rev.*, **98**, 780 (1955).

mass system are given by the following expressions:

$$(3.1a) \quad \frac{d\sigma(3.1)}{d\Omega} = \frac{1}{E^2} \frac{k'}{k} \left[\frac{G^2 G_1^2}{(E^2 - M_p^2)^2} (C + D \cos \theta) - \right.$$

$$\left. \frac{2GG_1 G_2 G_3}{(E^2 - M_p^2)(2E_p E_K + M_\Sigma^2 - M_p^2 - m_K^2)} \frac{C'_{12} + D'_1 \cos \theta}{1 + \varepsilon'_\Sigma \cos \theta} + \right.$$

$$\left. + \frac{G_z^2 G_3^2}{(2E_p E_K + M_\Sigma^2 - M_p^2 - m_K^2)^2} \frac{C''_2 + D''_2 \cos \theta}{(1 + \varepsilon''_\Sigma \cos \theta)^2} \right],$$

$$(3.2a) \quad \frac{d\sigma(3.2)}{d\Omega} = \frac{2}{E^2} \frac{k''}{k} \left[\frac{G^2 G_2^2}{(E^2 - M_p^2)^2} (C''_1 + D''_1 \cos \theta) - \right.$$

$$\left. - \frac{2GG_2^2 G_4}{(E^2 - M_p^2)(2E_p E'_K + M_\Sigma^2 - M_p^2 - m_K^2)} \frac{C''_{12} + D''_1 \cos \theta}{1 + \varepsilon''_\Sigma \cos \theta} + \right.$$

$$\left. + \frac{G_z^2 G_4^2}{(2E_p E'_K + M_\Sigma^2 - M_p^2 - m_K^2)^2} \frac{C''_2 + D''_2 \cos \theta}{(1 + \varepsilon''_\Sigma \cos \theta)^2} \right],$$

$$(3.3a) \quad \frac{d\sigma(3.3)}{d\Omega} = \frac{1}{E^2} \frac{k''}{k} \left[\frac{2G^2 G_2^2}{(E^2 - M_p^2)^2} (C''_1 + D''_1 \cos \theta) + \right.$$

$$+ \frac{2G_2^2 G_4^2}{(2E_p E'_K + M_\Sigma^2 - M_p^2 - m_K^2)} \frac{C''_2 + D''_2 \cos \theta}{(1 + \varepsilon''_\Sigma \cos \theta)^2} +$$

$$+ \frac{G_1^2 G_3^2}{2(2E_p E'_K + M_\Lambda^2 - M_p^2 - m_K^2)^2} \frac{C''_3 + D''_3 \cos \theta}{(1 + \varepsilon''_\Lambda \cos \theta)^2} -$$

$$- \frac{2\sqrt{2}GG_2^2 G_4}{(E^2 - M_p^2)(2E_p E'_K + M_\Sigma^2 - M_p^2 - m_K^2)} \frac{C''_{12} + D''_1 \cos \theta}{1 + \varepsilon''_\Sigma \cos \theta} -$$

$$- \frac{2GG_1 G_2 G_3}{(E^2 - M_p^2)(2E_p E'_K + M_\Lambda^2 - M_p^2 - m_K^2)} \frac{C''_{13} + D''_1 \cos \theta}{1 + \varepsilon''_\Lambda \cos \theta} +$$

$$+ \frac{\sqrt{2}G_1 G_2 G_3 G_1}{(2E_p E'_K + M_\Lambda^2 - M_p^2 - m_K^2)(2E_p E'_K + M_\Sigma^2 - M_p^2 - m_K^2)} \frac{C''_{23} + D''_{23} \cos \theta}{(1 + \varepsilon''_\Lambda \cos \theta)(1 + \varepsilon''_\Sigma \cos \theta)} \right],$$

with the abbreviation of

$$\begin{cases} C'_1 = (E^2 + M_p^2)(E_p E_\Lambda + M_p M_\Lambda) - 2EM_p(M_p E_\Lambda + M_\Lambda E_p) \\ D'_1 = kk'(E^2 - M_p^2) \end{cases}$$

$$\begin{cases} C'_2 = 2\{(E_\Lambda E_K + k'^2) + M_\Lambda(M_\Sigma - M_p)\}E_p E_K + \{(M_\Sigma - M_p)^2 - m_K^2\}E_p E_\Lambda + \\ + 2M_p(M_\Sigma - M_p)(E_\Lambda E_K + k'^2) + M_\Lambda M_p\{(M_\Sigma - M_p)^2 + m_K^2\} \end{cases}$$

$$\begin{cases} D'_2 = \{2(E_\Lambda E_K + k'^2) + 2M_\Lambda(M_\Sigma - M_p) - (M_\Sigma - M_p)^2 + m_K^2\}kk' \end{cases}$$

$$\begin{aligned} C'_{12} = & (EE_p - M_p)(E_\Lambda E_\kappa + k'^2) + M_\Lambda(M_\Sigma - M_p)(EE_p - M_p^2) + \\ & + M_p M_\Lambda E_\kappa E_\pi + M_p(M_\Sigma - M_p)E_\Lambda E_\pi \end{aligned}$$

$$\left\{ \begin{array}{l} \varepsilon'_\Sigma = \frac{2kk'}{2E_p E_\kappa + M_\Sigma^2 - M_p^2 - m_\kappa^2}, \quad E_\Lambda = \frac{1}{2E}(E^2 + M_\Lambda^2 - m_\kappa^2), \\ E_\theta = \frac{1}{2E}(E^2 - M_\Lambda^2 + m_\kappa^2), \quad k'^2 = \frac{1}{4E^2}[(E^2 - M_\Lambda^2 - m_\kappa^2)^2 - 4M_\Lambda^2 m_\kappa^2] \end{array} \right.$$

$$\left\{ \begin{array}{l} C''_1 = (E^2 + M_p^2)(E_p E_\Sigma + M_p M_\Sigma) - 2EM_p(M_p E_\Sigma + M_\Sigma E_p) \\ D''_1 = kk''(E^2 - M_p^2) \end{array} \right.$$

$$\left\{ \begin{array}{l} C''_2 = 2\{(E_\Sigma E'_\kappa + k'^2) + M_\Sigma(M_\Sigma - M_p)\}E_p E'_\kappa + \{(M_\Sigma - M_p)^2 - m_\kappa^2\}E_p E_\Sigma + \\ \quad + \{(M_\Sigma - M_p)^2 + m_\kappa^2\}M_p M_\Sigma + 2M_p(M_\Sigma - M_p)(E_\Sigma E'_\kappa + k'^2) \\ D''_2 = \{2(E_\Sigma E'_\kappa + k'^2) + 2M_\Sigma(M_\Sigma - M_p) - (M_\Sigma - M_p)^2 + m_\kappa^2\}kk'' \end{array} \right.$$

$$\begin{aligned} C''_{12} = & (EE_p - M_p^2)(E_\Sigma E'_\kappa + k'^2) + M_\Sigma(M_\Sigma - M_p)(EE_p - M_p^2) + \\ & + M_p M_\Sigma E'_\kappa E_\pi + M_p(M_\Sigma - M_p)E_\Sigma E_\pi \end{aligned}$$

$$\left\{ \begin{array}{l} \varepsilon''_\Sigma = \frac{2kk''}{2E_p E'_\kappa + M_\Sigma^2 - M_p^2 - m_\kappa^2}, \quad E_\Sigma = \frac{1}{2E}(E^2 + M_\Sigma^2 - m_\kappa^2), \\ E'_\theta = \frac{1}{2E}(E^2 - M_\Sigma^2 + m_\kappa^2), \quad k''^2 = \frac{1}{4E^2}[(E^2 - M_\Sigma^2 - m_\kappa^2)^2 - 4M_\Sigma^2 m_\kappa^2] \end{array} \right.$$

$$\left\{ \begin{array}{l} C''_3 = 2\{(E_\Sigma E'_\kappa + k'^2) + M_\Sigma(M_\Lambda - M_p)\}E_p E'_\kappa + \{(M_\Lambda - M_p)^2 - m_\kappa^2\}E_p E_\Sigma + \\ \quad + 2M_p(M_\Lambda - M_p)(E_\Sigma E'_\kappa + k'^2) + M_\Sigma M_p \{(M_\Lambda - M_p)^2 + m_\kappa^2\} \\ D''_3 = \{2(E_\Sigma E'_\kappa + k'^2) + 2M_\Sigma(M_\Lambda - M_p) - (M_\Lambda - M_p)^2 + m_\kappa^2\}kk'' \end{array} \right.$$

$$\begin{aligned} C''_{13} = & (EE_p - M_p^2)(E_\Sigma E'_\kappa + k'^2) + M_\Sigma(M_\Lambda - M_p)(EE_p - M_p^2) + \\ & + M_p M_\Sigma E'_\kappa E_\pi + M_p(M_\Lambda - M_p)E_\Sigma E_\pi \end{aligned}$$

$$\left\{ \begin{array}{l} C''_{23} = \{2E_p E'_\kappa + M_p(M_\Sigma + M_\Lambda - 2M_p)\}(E_\Sigma E'_\kappa + k'^2) + \\ \quad + \{(M_\Sigma - M_p)(M_\Lambda - M_p) - m_\kappa^2\}E_p E_\Sigma + m_\kappa^2 M_p M_\Sigma + \\ \quad + (M_\Sigma + M_\Lambda - 2M_p)M_\Sigma E_p E'_\kappa + M_p M_\Sigma(M_\Sigma - M_p)(M_\Lambda - M_p) \\ D''_{23} = \{2(E_\Sigma E'_\kappa + k'^2) + m_\kappa^2 + M_p(M_\Lambda - M_p) + M_\Sigma(M_\Sigma - M_p)\}kk'' \end{array} \right.$$

$$\varepsilon''_\Lambda = \frac{2kk''}{2E_p E'_\kappa + M_\Lambda^2 - M_p^2 - m_\kappa^2}.$$

Now, taking $G^2 = 10$, $G_1^2 = 1$, $G_2^2 = 0.8$, $G_3^2 = 1$, $G_4^2 = 0.05$, we write the graphs of (3.1) ~ (3.3) which are given in Fig. 4. As is seen from Fig. 4, the result of our calculation is qualitatively consistent with experiments. When the lowest order perturbation is used, the case of the two step reaction is better than the case of the one step reaction as far as the angular distribution of the K-particles is concerned.

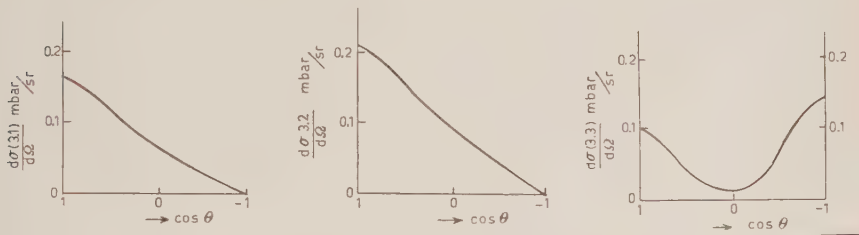


Fig. 4. – Angular distributions of the K-particles (C.M.S.).

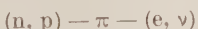
4. – Primarity of the weak Fermi interactions.

As is well known there is the μ -e decay as the first example of maintaining the primarity of Fermi interaction which is weak, i.e. the μ -e decay



should be considered to be primary as far as a new field is not introduced, since it is a decay process between leptons which have no strong interactions.

The β -decay should be considered to be primary since the β -decay which is considered to occur through intermediate states such as



is inconsistent with the experiment of the π -e decay. If we assume that the free neutron decay is primary and without pseudoscalar and pseudovector interactions, the π -decays $\pi^- \rightarrow e^- + \bar{\nu}$ and $\pi^+ \rightarrow e^+ + \nu$ are forbidden by relativistic considerations. According to the β -decay experiments a linear combination of S and T seems to be favourable to the interactions. If we assume the above interactions for the β -decay, the branching ratio of the decay mode $\pi \rightarrow e + \nu$ relative to the normal pion decay mode $\pi \rightarrow \mu + \nu$ can be made small enough to be consistent with the experimental value such as ⁽¹²⁾

$$\varrho = \frac{w(\pi \rightarrow e + \nu)}{w(\pi \rightarrow \mu + \nu)} \leq 5 \cdot 10^{-4}.$$

⁽¹²⁾ Cf. for example, R. P. FEYNMAN: *Meson Theories* (1951), p. 72.

Summarizing the above facts the primarity of the weak Fermi interactions among four Fermions seems to be the natural assumption.

5. — Secondary decay processes.

It is shown here that by using the model proposed in Sect. 2, any weak decay interactions can be derived as a secondary process from combination of a weak Fermi interaction and several strong Yukawa interactions. In this case it is remarkable that only special combinations are allowable by the selection rules derived from the assignment of iso-spin and strangeness for leptons. We will show these facts in the following by using the Feynman graphs shown in Fig. 5.

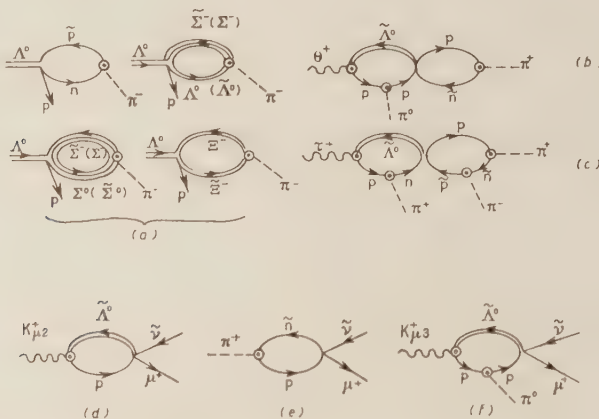


Fig. 5. — Feynman graphs for the various decay processes considered to be secondary.

In the following we denote the Fermi coupling constant by f , the Yukawa coupling constant by G , and write the coupling constants contained in the matrix element in the lowest order perturbation in parenthesis.

(1) *Strongly-strongly.* — The following three types of decays are included in this category.

(1) **Hyperon decay (fG).** — We consider here the Λ^0 -decay only. The Σ and Ξ decay can be similarly treated. In this case the four types of baryon loops shown in Fig. 5-a are allowable.

(2) **$K_{2\pi}$ -decay (fG^2).** — If we don't care about the position of π -meson vertex, there are different graphs like Fig. 5-b.

(3) $K_{3\pi}$ -decay (fG^4). — This case is obtained from the $K_{2\pi}$ -decay by adding one meson external line to an appropriate baryon internal line, as is shown in Fig. 5-e.

(II) *Strongly-leptons*. — To this category the following three types of decay are included.

(1) $K_{\mu 2}$ -decay (fG) ($K_{\nu 2}$ -decay). — Four types of graphs, one of which is shown in Fig. 5-d, are allowed.

(2) π - μ decay (fG) (π -e decay). — Four types of graphs, one of which is shown in Fig. 5-e, are allowed.

(3) $K_{\mu \pi}$ -decay (fG^2) ($K_{\nu \pi}$ -decay). — This type of graph is obtained from the $K_{\mu 2}$ -decay by adding one external π -meson line to the baryon loop. One graph as an example is shown in Fig. 5-f.

6. — Some results expected from the present model.

In this section we describe a few results which can be derived at once from our model.

(1) *All the processes including neutrino and antineutrino pairs are forbidden.* — This statement follows as an immediate consequence of the present model shown in Fig. 1. The restriction mentioned above is very useful to forbid the following unwanted processes

$$(6.1) \quad \left\{ \begin{array}{l} K^- \rightarrow \pi^- + \nu + \bar{\nu} \\ \quad \rightarrow \mu^- + \bar{\nu} + \nu + \bar{\nu} \\ \quad \rightarrow \pi^- + \pi^0 + \nu + \bar{\nu} \\ \quad \rightarrow e^+ + \nu + \bar{\nu} + \bar{\nu} \\ \pi^+ \rightarrow \mu^+ + \bar{\nu} + \nu + \bar{\nu} \\ \quad \rightarrow e^- + \nu + \bar{\nu} + \bar{\nu} \\ \quad \text{etc.} \end{array} \right.$$

It is remarkable here that the process $K^+ \rightarrow \pi^+ + \nu + \bar{\nu}$ being allowed in the formalism given in the paper (I) is now forbidden in conformity with the experiments.

(2) *Decay of π -mesons.* — It is known experimentally that, relative to the normal pion decay mode $\pi^- \rightarrow \mu^- + \nu$, the branching ratios ϱ and ϱ_γ for the

alternate decay modes $\pi \rightarrow e + \nu$ and $\pi \rightarrow e + \nu + \gamma$ are very small (13), i.e.

$$(6.2) \quad \left\{ \begin{array}{l} \varrho = \frac{w(\pi \rightarrow e + \nu)}{w(\pi \rightarrow \mu + \nu)} \lesssim 5 \cdot 10^{-5}, \\ \varrho_\gamma = \frac{w(\pi \rightarrow e + \nu + \gamma)}{w(\pi \rightarrow \mu + \nu)} \lesssim 5 \cdot 10^{-5}. \end{array} \right.$$

Since we consider in the present model that the pion decays $\pi \rightarrow \mu + \nu$ and $\pi \rightarrow e + \nu$ occur as the secondary processes through virtual baryon pairs, these reactions are forbidden for any one of the scalar (S), vector (V), and tensor (T) couplings of four Fermion interactions. If the mixed S and T coupling predominant in nuclear β -decay is generally applicable to the four Fermion interactions including electron-neutrino pairs and the axial vector (A) coupling is assumed in the four Fermion interactions to include muon-neutrino pairs, a pion decay into an electron and a neutrino is forbidden, whereas a pion decay into a muon and a neutrino is allowed in conformity with the first relation in (6.2). Though the pion decay $\pi \rightarrow e + \nu$ is forbidden for the mixed scalar and tensor coupling, the radiative decay $\pi \rightarrow e + \nu + \gamma$ occurs by the tensor coupling (14), and the ratio ϱ_γ of the rates of the two decay modes $\pi \rightarrow e + \nu + \gamma$ and $\pi \rightarrow \mu + \nu$ is obtained such as

$$(6.3) \quad \varrho_\gamma = 0.067 \left(\frac{1}{137} \right) \left(\frac{f'_T}{f_A} \right)^2 \left(\frac{m_\pi}{m} \right)^2,$$

by using the result given by TREIMAN and WYLD (eq. (25) in their paper (15)). If we take $f'_T = f_A$, m = nucleon mass, the ratio becomes

$$(6.4) \quad \varrho_\gamma \sim 10^{-6},$$

a result which is consistent with the experimental upper limit.

A similar discussion as above can also be applied to the K-meson decays $K \rightarrow e + \nu$, $K \rightarrow \mu + \nu$ and $K \rightarrow e + \nu + \gamma$. In this discussion we effectively use the intrinsic parity assignment for the stronglys given in Table II.

(3) *The decays of $K_{\mu 3}$ and $K_{e 3}$.* — The energy spectra of the secondary μ^- and e^- emitted in the decays of $K_{\mu 3}$ and $K_{e 3}$ seem to be different from each other as far as the results of the present experiments are concerned, though a definite conclusion may not be drawn for lack of experimental data.

(13) R. SHERR and R. H. MILLER: *Phys. Rev.*, **93**, 1076 (1954).

(14) K. IWATA, S. OGAWA, H. OKONOGI, B. SAKITA and S. ONEDA: *Prog. Theor. Phys.*, **13**, 19 (1955).

(15) S. B. TREIMAN and H. W. WYLD: *Phys. Rev.*, **101**, 1552 (1956).

According to the calculation of YONEZAWA *et al.* (16), a combination of S and T coupling which is similar to the case of nuclear β -decay is sufficient to explain the energy spectrum of the secondary electrons in the K_{e3} -decay. In the case of the $K_{\mu 3}$ -decay agreement of the theoretical and experimental energy spectrum of the secondary μ^+ seems to be good provided A or V interaction is assumed. The above circumstances will be easily understood by using the present model since in our model appropriate linear combination of the four different types of baryon loops are allowable for the K_{e3} and $K_{\mu 3}$ decays and there are sufficient degrees of freedom to explain the experiments.

Finally we add a remark on the selection rule $|\Delta I| = \frac{1}{2}$ or $\frac{3}{2}$ in the $K_{\mu 3}$ and K_{e3} decays. The branching ratios are given as follows:

	$ \Delta I = \frac{1}{2}$	$ \Delta I = \frac{3}{2}$	
(6.5)	$K^+ \rightarrow \mu^+ + \pi^0 + \bar{\nu}$	1	2
	$K^- \rightarrow \mu^- + \pi^0 + \nu$	1	2
	$K^0 \rightarrow \mu^+ + \pi^- + \bar{\nu}$	2	1
	$\tilde{K}^0 \rightarrow \mu^- + \pi^+ + \nu$	2	1

	$ \Delta I = \frac{1}{2}$	$ \Delta I = \frac{3}{2}$	
(6.6)	$K^+ \rightarrow e^+ + \pi^0 + \nu$	1	2
	$K^- \rightarrow e^- + \pi^0 + \bar{\nu}$	1	2
	$K^0 \rightarrow e^+ + \pi^- + \nu$	2	1
	$\tilde{K}^- \rightarrow e^- + \pi^+ + \bar{\nu}$	2	1

The selection rule $|\Delta I| = \frac{3}{2}$ seems to be more favourable than $|\Delta I| = \frac{1}{2}$, though the number of experimental data (17) is very small and it is too early to draw any conclusion.

7. - Conclusion.

In this paper we have proposed to use the modified model of Gell-Mann and Dallaporta for the weak interactions by assigning zero iso-spin and appropriate strangeness for leptons, and have constructed the compatible theory in a general consideration.

(16) M. YONEZAWA, S. FURUICHI and S. OGAWA: private communication.

(17) J. BALLAM, M. CRISARU and S. B. TREIMAN: *Phys. Rev.*, **101**, 1439 (1956); M. M. BLOCK, E. M. HARTH, M. E. BLEVINS and G. C. SLAUGHTER: *Nuovo Cimento*, **4**, 46 (1956).

As was stated in Sect. 1 and 2, the present theory shows that the transformation properties of leptons in the iso-space are meaningful even in the lepton processes practically observed, while according to the formalism stated in the paper (I) the transformation properties of leptons in the iso-space lose their meaning in the lepton processes observed though definite transformation properties have been assigned to each lepton when the self energy effects are all neglected. It is noteworthy to remark that the process $K^+ \rightarrow \pi^+ + \nu + \bar{\nu}$ being allowed by the selection rule given in the paper (I) is forbidden according to the present theory in accordance with the experiments.

The accumulation of experimental data will enable us in future to compare with experiments the various calculations resulting from the present model.

RIASSUNTO (*)

Assegnando isospin zero e stranezza 2, — 2 e 0 ai leptoni μ^+ , e^- e ν rispettivamente, si dimostra che si può coerentemente derivare l'universalità delle interazioni deboli, compresi i processi leptonici se le interazioni primarie forti si assumono essere di tipo Yukawa e le interazioni primarie deboli di tipo Fermi.

(*) Traduzione a cura della Redazione.

Polarization in Neutron Proton Scattering at 95 MeV.

G. H. STAFFORD, C. WHITEHEAD and P. HILLMAN

The Atomic Energy Research Establishment - Harwell, Berkshire, England

(ricevuto il 17 Marzo 1957)

Summary. — The free neutron-proton polarization has been measured at centre-of-mass angles from 20° to 160° . The asymmetries were obtained using fixed detectors and by rotating the plane of polarization of the neutron beam with respect to the scattering plane by means of a long solenoid. The polarization cross-section was found to be strongly non-antisymmetrical about 90° centre-of-mass and evidence for *D*-wave interaction was obtained.

1. — Introduction.

In a recent paper in this journal HILLMAN and STAFFORD⁽¹⁾ reported measurement of the polarization in free neutron proton scattering at energies in the region of 100 MeV with the 110 in. Harwell cyclotron. The asymmetries were obtained in the conventional manner by measuring counting rates to the left and to the right of the direction of the incident partially polarized neutron beam. Recoil protons were detected at centre of mass angles between 60° and 160° . The polarization of the incident neutron beam was low (less than 10%), the measured asymmetries small and the possibility of false asymmetries correspondingly important. As a result of a new method of measuring asymmetries in neutron polarization experiments (HILLMAN, STAFFORD and WHITEHEAD⁽²⁾) effects due to false asymmetries have been made entirely negligible and this has enabled us to repeat the previous measurements with improved precision and to extend the measurements to smaller scattering angles. In the present experiment neutrons were detected in the centre-of-mass angular region from 20° to 76° and protons from 78° to 160° .

(¹) P. HILLMAN and G. H. STAFFORD: *Nuovo Cimento*, **3**, 633 (1956).

(²) P. HILLMAN, G. H. STAFFORD and C. WHITEHEAD: *Nuovo Cimento*, **4**, 67 (1956).

2. - Method.

If an incident beam of neutrons has a polarization P_1 then the asymmetry obtained after a second scattering is given by

$$e = \frac{I(\theta, 0) - I(\theta, \pi)}{I(\theta, 0) + I(\theta, \pi)} = P_1 P_2,$$

where P_2 is the polarization in the second scattering and $I(\theta, \varphi)$ is the intensity of the scattered particle at scattering angle θ and azimuthal angle φ with respect to the plane perpendicular to the direction of polarization. In conventional measurements of asymmetries $I(\theta, 0)$ and $I(\theta, \pi)$ are the scattered intensities to the left and to the right of the direction of the incident beam. In this experiment, instead of rotating the counters about the plane of polarization from an angle $(\theta, 0)$ to (θ, π) , the counters were kept fixed and the plane of polarization was rotated first through 90° in one direction and then through 90° in the opposite direction by passing the partially polarized neutron beam through a longitudinal magnetic field. This method has been described in detail by HILLMAN, STAFFORD and WHITEHEAD (2). Briefly, the principle is that if a spinning magnetic moment is acted on by a uniform magnetic field it will precess in a direction normal to the plane containing the spin and the magnetic field vectors, the frequency of precession being given by

$$\nu_p = \hbar^{-1} g \mu_n H,$$

where: \hbar = Planck's constant,
 g = gyromagnetic ratio,
 μ_n = nuclear magneton,
 H = magnetic field.

In this experiment a solenoid was used to produce the magnetic field. It can be shown that if the neutron velocity is v and the length of the solenoid is l_0 then the integrated field strength required to precess the neutrons through 90° is given by

$$l_0 H_0 = \frac{v \hbar}{4 g \mu_n (1 - \beta^2)^{\frac{1}{2}}},$$

where: $H_0 = 4\pi n I / 10$,
 n = number of turns per centimetre,
 I = current through the solenoid in amperes.

For 95 MeV neutrons a value of $l_0 H_0 = 1.18 \cdot 10^6$ G cm was required and

this was obtained using a solenoid of 903 turns approximately 11 feet long and a current of 1030 A.

3. - Apparatus.

3.1. *The experiment in which neutrons were detected.* - In the measurement of the polarization in the neutron forward scattering hemisphere a large liquid scintillation counter and a liquid hydrogen target were used. The procedure adopted in the use of this counter as a threshold neutron detector has been described fully by THRESHER, VOSS and WILSON⁽³⁾ who used it to measure the neutron-proton differential cross-section. Their method of varying the counter bias as $\cos^2 \theta$ (where θ is the scattering angle in the laboratory system) to keep the effective energy constant was adopted. A correction for the non-linear response of the scintillator as a function of energy was also made. This procedure proved successful in THRESHER, VOSS and WILSON's experiment and should be satisfactory in the present experiment as the polarization is not expected to vary rapidly with energy.

The liquid hydrogen target was 18 cm long by 10 cm wide by 4 cm high. The counting volume was defined by the dimensions of the neutron beam which were 7 cm wide by 2.5 cm high. The counter was placed 2 metres from the target. Its dimensions were 45 cm long by 15 cm wide by 7.5 cm high. The upper diagram in Fig. 1 shows in vertical section the geometry used in this experiment. The boron trifluoride slow neutron detector which was used as a beam monitor was located between the two shielding walls. During the runs no changes were made in the cyclotron operating conditions.

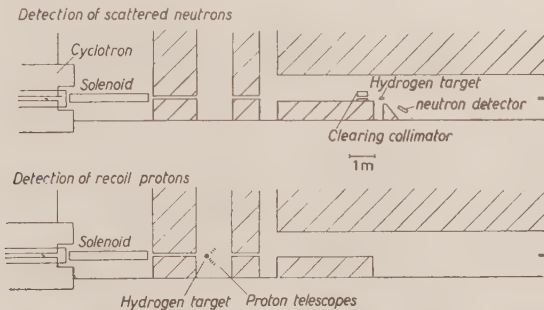


Fig. 1. - The upper diagram shows the vertical section of the geometry employed in the experiment in which scattered neutrons were detected and the lower diagram shows the geometry for the recoil proton experiment.

⁽³⁾ J. J. THRESHER, R. G. P. VOSS and R. WILSON: *Proc. Roy. Soc., A* **229**, 492 (1955).

3·2. The experiment in which the recoil protons were detected. – Two identical four-unit scintillation telescopes were used. They were arranged in triple coincidence plus anticoincidence with aluminium absorbers placed between units 2 and 3 to maintain the same effective energy at all angles and between unit 3 and anticoincidence unit 4 to place a limit on the maximum energy of protons recorded as coincidences. As the neutron energy spectrum was known, the corresponding recoil proton energy spectrum at each angle was calculable and it was possible to adjust the absorber between units 3 and 4 to stop all genuine recoil protons before unit 4. The anticoincidence counter then helped to reduce background effects. Pulses from the individual photomultipliers were fed into a coincidence unit with a resolving time of 10^{-8} s. The coincidence output was counted at two discriminator levels as a check on the stability of the apparatus. The proton telescopes were placed above and below the beam at scattering angles similar to within $\pm 0.5^\circ$. By suitably combining the results from the two telescopes any error introduced by the boron trifluoride monitor into the measurement was made very small.

A different liquid hydrogen target was used for this part of the experiment. The target hydrogen was contained in a 2.5 cm diameter cylinder made from 0.0025 cm nickel foil 10 cm in width. The reservoir held 4.5 litres of hydrogen which was sufficient for a 9 hour measurement, although the liquid nitrogen jacket required replenishing every 3 hours. Measurements were made at angles between 80° and 160° (centre of mass). The size of the neutron beam at the target was 2.5 cm high by 3.75 cm wide.

4. – The neutron spectrum and the effective neutron energy.

The maximum neutron energy in the incident beam was 120 MeV. The neutrons used in the experiment had energies from approximately 75 MeV to the maximum and the shape of the spectrum was approximately triangular. For convenience the measurements are said to have been made at an effective energy of 95 ± 2 MeV where the effective energy was calculated using the measured attenuation of the neutron beam in polythene and the total cross-sections for hydrogen and carbon given by TAYLOR, PICKAVANCE, CASSELS and RANDLE (⁴). The attenuation measurement was made with the neutron counter in the direct beam. In the experiment in which neutrons were detected the effective energy was kept constant by suitably adjusting the bias level with angle as mentioned in Sect. 3·1 above. In the experiment in which recoil protons were detected the effective energy was maintained constant

(⁴) A. E. TAYLOR, T. G. PICKAVANCE, J. M. CASSELS and T. C. RANDLE: *Phil. Mag.*, **42**, 328 (1951).

by changing the absorber thickness with angle. The correct absorber thickness was calculated from the known shape of the neutron spectrum (measured with a similar telescope in a previous experiment (¹)). Allowance was made for the shape and thickness of the hydrogen target and as the same target was used for all angles the low energy cut-off decreased slightly with decreasing centre of mass scattering angle.

The attenuation experiment defined an effective energy \bar{E} given by

$$\int \varepsilon(E) N(E) \exp[-x\sigma(E)] dE = \exp[-x\overline{\sigma(\bar{E})}] \int \varepsilon(E) N(E) dE,$$

where $\varepsilon(E)$ is the detection efficiency of the counter for a neutron of energy E , $\sigma(E)$ is the total neutron cross-section for polythene and \bar{E} is the effective energy deduced from the measured total cross-section $\sigma(E)$. The effective energy used in the present experiment should be calculated from

$$\int \varepsilon(E) N(E) \left(P \frac{d\sigma}{d\Omega} \right)_E dE = P \left(\frac{d\sigma}{d\Omega} \right)_E \int \varepsilon(E) N(E) dE,$$

where P is the measured polarization for the band of neutron energies used and $(d\sigma/d\Omega)_E$ is the mean neutron proton differential cross-section. The variation of the polarization P with energy is not known and so it is impossible to estimate reliably how much this will affect the value of the effective energy given. This should be borne in mind in fitting theoretical curves to the experimental results.

5. — Background effects.

Background measurements were made at each angle before and after the liquid hydrogen runs. In the neutron experiment, background counting rates were comparable in magnitude to the true counting rate but in the proton experiment the background was less than 10% of the true rate at all angles. It is possible to tolerate large backgrounds with some confidence (as was the case in the neutron experiment) because it should be independent of the sign or magnitude of the solenoid current; the asymmetry observed in the background measurements was, in fact, not significantly different from zero.

6. — The magnitude of the polarization of the neutron beam.

The best value of P_1 , the polarization of the incident beam, was obtained by combining the results of VOSS and WILSON (⁵) at 97 MeV and 104 MeV and our results (²) at 95 MeV and 99 MeV.

(⁵) R. G. P. VOSS and R. WILSON: *Phil. Mag.*, **1**, 175 (1956).

The polarization P_1 was measured by scattering the neutron beam off uranium at an angle of $(1/3)^\circ$. The polarization produced at this angle by the interaction between the magnetic moment of the neutron and the coulomb field of the uranium nucleus is large and calculable. It was assumed that from 95 MeV to 104 MeV the polarization of the incident beam changed linearly with energy. A least squares fit to the experimental points gave a value 0.088 ± 0.007 for the polarization at 95 MeV. This revises the value given in a previous report (2).

7. - Errors and corrections.

The measured asymmetries were small (never greater than 5%) and drifts in the electronics during the day were about 1% but by cycling the measurements the effect of this slow drift was very much reduced. Asymmetries were measured in the following cycle of solenoid current settings: anti-clockwise rotation, clockwise rotation, clockwise rotation, anti-clockwise rotation; each set being completed in about 35 minutes. At all angles the ratios «clockwise rotation»:«anti-clockwise rotation» were analysed statistically for both hydrogen runs and background runs, and all were found to have the expected statistical standard deviations with a satisfactory « χ^2 -square» probability.

The angular resolution of the neutron detector was $\pm 4^\circ$ base width at small angles increasing to $\pm 7^\circ$ at the large angles but calculation showed that the error introduced by this coarse resolution in no case exceeded 3%. The acceptance angle of the proton telescope was $\pm 3^\circ$. A correction has been applied to the measurements made with the neutron counter at centre of mass angles of 22.5° , 29.8° and 41.0° as the background runs were made with the hydrogen target filled with air.

8. - Results.

The results are presented in Table I. In column 2 of the table the measured asymmetries are given; in column 3 are listed the unpolarized differential cross-sections which were used to calculate the values of $P(d\sigma/d\Omega)$ (column 4). The unpolarized differential cross-sections for free n-p scattering at 95 MeV were obtained by interpolating between the results of STAHL and RAMSEY (6) at 91 MeV; RANDLE, SKYRME, SNOWDEN, TAYLOR, WOOD and URIDGE (7) at 133 MeV and THRESHER, VOSS and WILSON (8) at 105 MeV.

(6) R. H. STAHL and N. F. RAMSEY: *Phys. Rev.*, **96**, 1310 (1954).

(7) T. C. RANDLE, D. M. SKYRME, M. SNOWDEN, A. E. TAYLOR, E. WOOD and F. URIDGE: *Proc. Phys. Soc., A* **69**, 760 (1956).

TABLE I.

θ (c.m.)	e %	(mb/sr)	(mb/sr)
22.5	1.26 \pm 0.28	9.6	1.37 \pm 0.31
29.8	1.50 \pm 0.33	8.4	1.43 \pm 0.31
41.0	2.80 \pm 0.53	6.8	2.16 \pm 0.41
52.5	3.55 \pm 0.36	5.5	2.22 \pm 0.23
61.5	4.94 \pm 0.56	4.7	2.64 \pm 0.30
76.0	2.70 \pm 0.35	4.0	1.23 \pm 0.16
78.5	3.40 \pm 0.30	3.9	1.51 \pm 0.13
88.5	2.46 \pm 0.28	4.0	1.12 \pm 0.13
98.5	2.33 \pm 0.42	4.3	1.14 \pm 0.21
108.0	0.62 \pm 0.42	4.8	0.34 \pm 0.23
118.5	0.43 \pm 0.48	5.4	0.26 \pm 0.29
128.5	-0.48 \pm 0.31	6.3	-0.34 \pm 0.22
138.5	-0.14 \pm 0.25	7.4	-0.12 \pm 0.21
149.0	-0.64 \pm 0.22	8.9	-0.65 \pm 0.22
159.5	-0.33 \pm 0.21	10.7	-0.40 \pm 0.25

In column 4 the uncertainties quoted are purely statistical with the exception of the values for 22.5° , 29.8° and 41.0° where the uncertainties have been increased in view of the air correction applied to these measurements. There is, in addition, an estimated uncertainty of $\pm 3\%$ in the value of the unpolarized differential cross-section as well as $\pm 8\%$ in the value of P_2 due to the uncertainty in the beam polarization. The uncertainty associated with the value used for $d\sigma/d\Omega$ could introduce a small error in the shape of the polarization cross-section curve and hence in the value of the coefficients given below but the $\pm 8\%$ error in P_1 can only change the absolute and not the relative value of the coefficients.

The experimental results are shown in Fig. 2 together with the least squares fit which is given by:

$$P \frac{d\sigma}{d\Omega} \sin \theta ((1.17 \pm 0.11)P_0(\cos \theta) + (2.34 \pm 0.23)P_1(\cos \theta) + (0.21 \pm 0.26)P_2(\cos \theta)) .$$

A least squares fit with two terms gives

$$P \frac{d\sigma}{d\Omega} = \sin \theta ((1.12 \pm 0.09)P_0(\cos \theta) + (2.28 \pm 0.21)P_1(\cos \theta)) .$$

The « χ^2 -square » probability of the 3-term fit is 16% and 7% for the 2-term fit so that the need for the third term is not established.

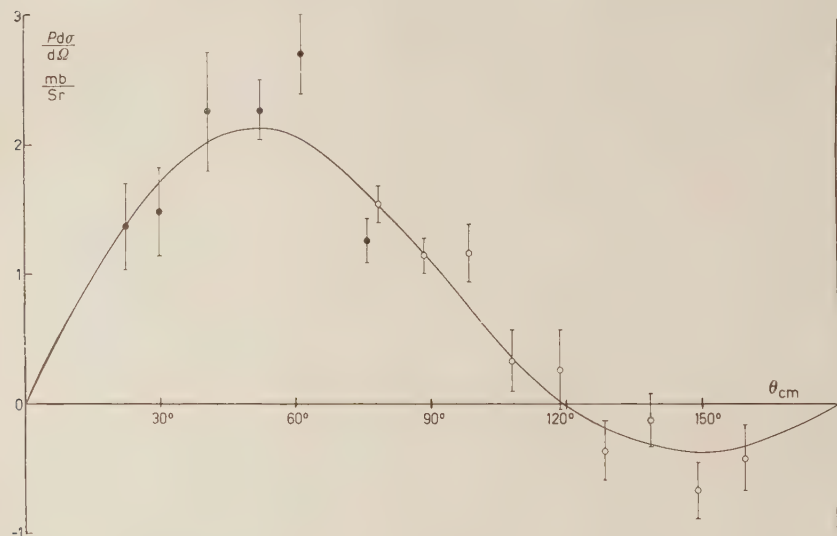


Fig. 2. — The variation of $P(d\sigma/d\Omega)$ with centre of mass scattering angle. The solid circles show the results obtained from the detection of scattered neutrons and the open circles are the results from the detection of recoil protons. The solid line is that obtained by a least squares fit of the form

$$P(d\sigma/d\Omega) = \sin \theta (aP_0(\cos \theta) + bP_1(\cos \theta) + cP_2(\cos \theta)) .$$

If the revised value for the beam polarization is used the original results of HILLMAN and STAFFORD are given by

$$P \frac{d\sigma}{d\Omega} = \sin \theta ((0.78 \pm 0.30)P_0(\cos \theta) + (1.96 \pm 0.69)P_1(\cos \theta) - (0.39 \pm 0.78)P_2(\cos \theta)) ,$$

which is in satisfactory agreement.

9. — Discussion.

These measurements were undertaken as part of a programme aimed at providing information for a complete phase shift analysis at this energy. This analysis can only be completed when measurements of the neutron-proton and proton-proton unpolarized differential cross-sections and the proton-proton

polarized differential cross-section are all available. However, there are certain observations that are worth while making at this stage.

Evidence for *D* wave interaction would be provided by the need for the $P_2(\cos \theta)$ term. This term is small and by itself would not be convincing but the preliminary results of a measurement of the proton-proton polarization at 95 MeV (TAYLOR and WOOD: private communication) indicate that the magnitude of the coefficient of the $P_1(\cos \theta)$ term in their experiment is 1.3 ± 0.1 . As there is no evidence in their experiment for any *F*-wave interaction this term arises from *P-P* interference effects whose contribution to the $P_1(\cos \theta)$ coefficient in the neutron-proton case will be one quarter of 1.3 ± 0.1 i.e. 0.33 ± 0.03 . The coefficient of $P_1(\cos \theta)$ required to fit the neutron proton results is 2.34 ± 0.23 and this disparity indicates the existence of appreciable *S-D* interference effects.

* * *

Our grateful thanks are extended to Dr. R. J. N. PHILLIPS for theoretical discussions; Dr. J. J. THRESHER, Dr. R. G. P. Voss and Dr. R. WILSON for the loan of equipment; Mr. E. W. SHARRATT for his help in always providing liquid hydrogen when required; Mr. F. URIDGE for help with the experiment and the cyclotron crew for their willing co-operation.

RIASSUNTO (*)

La polarizzazione libera neutrone-protone è stata misurata ad angoli nel sistema del centro di massa da 20 a 160°. Le asimmetrie furono ottenute usando rivelatori fissi e ruotando il piano di polarizzazione del fascio neutronico rispetto al piano di scattering per mezzo di un lungo solenoide. La sezione d'urto di polarizzazione fu trovata fortemente non antisimmetrica intorno a circa 90° nel sistema del centro di massa e furono ottenute prove di un'interazione di onde *D*.

(*) Traduzione a cura della Redazione.

Integral-Darstellung kausaler Kommutatoren.

R. JOST

Physikalisches Institut der E. T. H. - Zürich

H. LEHMANN

Institut für theoretische Physik der Universität - Hamburg

(ricevuto il 20 Marzo 1957)

Zusammenfassung. — Die Struktur des Kommutators von Feldoperatoren wird untersucht. Für das Matrixelement zwischen Eigenzuständen des Impulsoperators wird eine Integral-Darstellung angegeben. Dabei ist die mikroskopische Kausalität und das Spektrum des Impulsoperators berücksichtigt.

1. — Eigenschaften eines kausalen Kommutators.

Die Kausalität drückt sich in der Feldtheorie bekanntlich durch das Verschwinden des Kommutators (bzw. Antikommunitors) geeignet gewählter Feldgrößen für raumartige Distanzen aus. Wir wollen im folgenden einige mathematische Methoden behandeln, die vielleicht für Untersuchungen über die Auswirkung der Kausalitätsbedingung von Interesse sind.

Der Einfachheit halber diskutieren wir skalare Feldgrößen $A(x), B(x)$. Dann gilt:

$$(1.1) \quad [A(x), B(x')] = 0 \quad \text{falls} \quad (x - x')^2 = (\mathbf{x} - \mathbf{x}')^2 - (x_0 - x'_0)^2 > 0 .$$

Daher verschwindet auch das Matrixelement:

$$(1.2) \quad \langle P, \alpha | [A(x), B(x')] | Q, \beta \rangle = 0 , \quad \text{für } (x - x')^2 > 0 .$$

Die Zustände $|P, \alpha\rangle$ und $|Q, \beta\rangle$ seien dabei Eigenzustände des Energie-Impulsvektors zu den Eigenwerten P und Q . α und β sind zusätzliche Variable, die die Zustände eindeutig beschreiben.

Offenbar gilt $P_0 \geq 0$, $P^2 \leq 0$ und $Q_0 \geq 0$, $Q^2 \leq 0$; d.h. P und Q liegen im Vorkegel.

Unter Benutzung der Invarianz gegen Translationen folgt für das Matrixelement (1.2)

$$(1.3) \quad \langle P, \alpha | [A(x), B(x')] | Q, \beta \rangle =$$

$$= \exp \left[i(Q - P) \frac{x + x'}{2} \right] \langle P, \alpha | [A(\xi/2), B(-\xi/2)] | Q, \beta \rangle .$$

Dabei wurde $\xi = x - x'$ gesetzt.

Demnach genügt es, die Funktion

$$(1.4) \quad F(\xi) = i \langle P, \alpha | [A(\xi/2), B(-\xi/2)] | Q, \beta \rangle$$

zu diskutieren.

Neben der Kausalität liefert die Struktur des Eigenwertspektrums des Energie-Impulsevektors eine wichtige Bedingung für $F(\xi)$. Durch Summation über Zwischenzustände folgt nämlich

$$(1.5) \quad F(\xi) = \frac{1}{(2\pi)^4} \int d^4k \left\{ \exp \left[i\xi \left(k - \frac{P+Q}{2} \right) \right] \tilde{G}_1(k) - \exp \left[-i\xi \left(k - \frac{P+Q}{2} \right) \right] \tilde{G}_2(k) \right\} - \frac{1}{(2\pi)^4} \int d^4q \exp [iq\xi] \left\{ \tilde{G}_1 \left(q + \frac{P+Q}{2} \right) - \tilde{G}_2 \left(-q + \frac{P+Q}{2} \right) \right\} .$$

Dabei sind die Funktionen $\tilde{G}_1(k)$ und $\tilde{G}_2(k)$ nur dann von Null verschieden, wenn k zum Spektrum des Energie-Impulsvektors gehört; d.h. höchstens wenn k im Vorkegel liegt.

Die Funktion $F(\xi)$ hat also die folgenden bemerkenswerten Eigenschaften:

a) $F(\xi)$ verschwindet außerhalb des Lichtkegels.

b) Die Fouriertransformierte $\tilde{F}(q) = \int d^4\xi \exp [-iq\xi] F(\xi)$ verschwindet außerhalb der Vereinigungsmenge des Vorkegels mit Spitze in $-\frac{1}{2}(P+Q)$ und des Nachkegels mit Spitze in $\frac{1}{2}(P+Q)$ (1).

(1) Diese Bedingung (b) wird sich in vielen Fällen verschärfen lassen. Etwa wenn — in einem bestimmten Modell — vorausgesetzt wird, daß (abgesehen vom Vakuumzustand) der kleinste Eigenwert des Operators $-P^2$ und damit die Ruhmasse des leichtesten Teilchens von Null verschieden ist. Dieser Fall läßt sich mit unserer Methode ebenfalls leicht behandeln.

Der Versuch, eine möglichst allgemeine Klasse von Funktionen mit den Eigenschaften *a)* und *b)* mittels einer Darstellung zu erfassen, bildete den Anlaß zur vorliegenden Untersuchung. Wir werden aber die Problemstellung im folgenden verallgemeinern. Die entsprechenden Resultate scheinen brauchbar zu sein.

Wir bemerken noch, daß es offenbar keine wesentliche Einschränkung bedeutet, $(P+Q) = (1, 0, 0, 0)$ zu setzen. Der Fall $(P+Q)^2 = 0$, der damit ausgeschlossen ist, wird nicht von großer Bedeutung sein.

2. – Die mathematische Problemstellung.

Das folgende betrachten wir als zweckmäßige Verallgemeinerung und Präzisierung der Fragenstellung aus § 1:

Es sei $F(\xi) = F_R(\xi) - F_A(\xi)$, wobei $F_R(\xi)$ und $F_A(\xi)$ Distributionen⁽²⁾ sind, die außerhalb des Vor- resp. Nachkegels verschwinden. Es sei weiterhin bekannt, daß $\tilde{F}(q) = \int d^4\xi \exp[-iq\xi]F(\xi)$ im Doppelkegel $|q_0| + |\mathbf{q}| < 1$ verschwinde. Man suche eine Darstellung für $\tilde{F}(q)$.

Der Zusammenhang zwischen der neuen und der alten Problemstellung ist, daß das Komplement zur Vereinigungsmenge des von $(-1, 0, 0, 0)$ ausgehenden Vor- und des von $(1, 0, 0, 0)$ ausgehenden Nachkegels, d.h. das Gebiet in dem $\tilde{F}(q)$ aus § 1 verschwindet, sich als Vereinigung der Doppelkegel $|q_0| + |\mathbf{q} - \mathbf{a}| < |\mathbf{a}| - 1$ darstellen läßt.

Es soll hier freilich erwähnt werden, daß wir das eben formulierte mathematische Problem nicht in Strenge behandeln werden. Unsere Untersuchung macht bescheidene mathematische Ansprüche, sollte aber für die Physik hinreichend sein.

Aus der Tatsache, daß der Doppelkegel $|q_0| + |\mathbf{q}| < 1$ symmetrisch zur Ebene $q_0 = 0$ ist, folgt, daß wir $F(\xi_0, \xi)$ in einen symmetrischen Teil $\frac{1}{2}[F(\xi_0, \xi) + F(-\xi_0, \xi)]$ und einen antisymmetrischen Teil $\frac{1}{2}[F(\xi_0, \xi) -$

$F(-\xi_0, \xi)]$ zerlegen können, die beide die ursprünglichen Voraussetzungen erfüllen (einschließlich der Zerlegbarkeit in retardierte und avancierte Distributionen).

Weiter leuchtet es ein, daß der symmetrische Teil sich als Ableitung nach ξ_0 einer antisymmetrischen Distribution schreiben läßt, die selbst wieder alle Voraussetzungen erfüllt. (Siehe Anhang).

Es genügt also eine Darstellung für antisymmetrische $F(\xi)$ anzugeben. Diese kann man ohne Einschränkung wie folgt ansetzen.

$$(2.1) \quad F(\xi_0, \xi) = F_R(\xi_0, \xi) - F_R(-\xi_0, \xi).$$

(2) Wir sprechen immer von temperierten Distributionen L. SCHWARZ: *Théorie des Distributions* (Paris, 1951), Vol. II, p. 93.

Jetzt gehen wir von der Feststellung aus, daß eine in ξ bezüglich der orthochronen Lorentzgruppen invariante, in ξ_0 antisymmetrische Distribution außerhalb des Lichtkegels verschwindet. Dasselbe gilt auch von ihrer Fouriertransformierten. Es sei dann $L(\xi; \eta)$ in ξ eine derartige Distribution, in η sei $L(\xi; \eta)$ unendlich oft differenzierbar und jede Ableitung sei durch ein passendes Polynom in η beschränkt (³). Nun dürfte

$$(2.2) \quad F(\xi_0, \xi) = L(\xi_0, \xi; \xi)$$

eine völlig hinreichende Klasse von antisymmetrischen außerhalb des Lichtkegels verschwindenden Distributionen sein.

Durch Fouriertransformation entsteht aus (2)

$$(2.3) \quad \tilde{F}(q_0, \mathbf{q}) = \int d^3u \tilde{L}(q_0, \mathbf{q} - \mathbf{u}; \mathbf{u}),$$

wobei

$$(2.4) \quad \tilde{L}(q; \mathbf{u}) = (2\pi)^{-3} \int d^4\xi \int d^3\eta \exp[-iq\xi - iu\eta] L(\xi; \eta)$$

eine in q_0 ungerade, in q orthochron-lorentz-invariante Distribution, in \mathbf{u} eine stark abfallende Distribution (⁴) ist.

Die Gleichungen (2.2) und (2.3) sind vollständig äquivalent, so daß wir (2.3) als Bedingung für das Verschwinden von $F(\xi_0, \xi)$ außerhalb des Lichtkegels auffassen können. Es handelt sich jetzt darum, $\tilde{L}(q; \mathbf{u})$ so zu wählen, daß $\tilde{F}(q_0, \mathbf{q})$ im Doppelkegel $|q_0| + |\mathbf{q}| < 1$ verschwindet.

3. – Das Verschwinden vom $\tilde{F}(q_0, \mathbf{q})$ im Doppelkegel.

Wir setzen nun an

$$(3.1) \quad \tilde{L}(q; \mathbf{u}) = \varepsilon(q_0) \hat{\phi}(q_0^2 - \mathbf{q}^2, \mathbf{u})$$

wobei $\hat{\phi}$ für negatives erstes Argument verschwindet (⁵).

$$(3) \quad \int q(\xi) L(\xi; \eta) d^4\xi \in O_M$$

für jede Testfunktion $q(\xi) \in S_\xi$. L. SCHWARTZ: l. c., p. 99.

(⁴) L. SCHWARTZ: l. c., p. 100.

(⁵) Schreibt man analog

$$L(\xi; \eta) = \varepsilon(\xi_0) \Phi(\xi_0^2 - \xi^2, \eta),$$

$\hat{\Phi}(\kappa^2, \mathbf{u})$ soll in κ^2 eine Distribution sein. Wir beschränken uns also auf Distributionen L , die die Darstellung (3.1) gestatten.

Unser Ziel ist es, den folgenden Satz zu beweisen.

Satz 1: Notwendig und hinreichend dafür, daß $\tilde{F}(q_0, \mathbf{q})$ (2.3) in $|q_0| + |\mathbf{q}| < 1$ verschwindet ist, daß $\hat{\Phi}(\kappa^2, \mathbf{u})$ in $\kappa^2 + \mathbf{u}^2 < 1$ verschwindet.

Beweis:

a) Die Bedingung ist hinreichend: setzt man (3.1) in (2.3) ein, so erhält man

$$(3.2) \quad \tilde{F}(q_0, \mathbf{q}) = \varepsilon(q_0) \int d^3 u \hat{\Phi}(q_0^2 - (\mathbf{q} - \mathbf{u})^2, \mathbf{u}).$$

Es wird $\hat{\Phi}(\kappa^2, \mathbf{u})$ also über die Kugel $\kappa^2 + (\mathbf{u} - \mathbf{q})^2 = q_0^2$ integriert. Diese Kugel ist ganz in der Kugel $\kappa^2 + \mathbf{u}^2 \leq (|q_0| + |\mathbf{q}|)^2$ enthalten. Daraus folgt die Behauptung.

b) Die Bedingung ist notwendig: wir zeigen dies zunächst für stetige $\hat{\Phi}(\kappa^2, \mathbf{u})$. Es ist dann zu zeigen, daß aus dem Verschwinden von

$$(3.3) \quad \tilde{F}_1(q_0^2, \mathbf{q}) = \int d^3 u \int d\kappa^2 \delta(q_0^2 - \kappa^2 - (\mathbf{q} - \mathbf{u})^2) \hat{\Phi}(\kappa^2, \mathbf{u})$$

in $|q_0| + |\mathbf{q}| < 1$ folgt: $\hat{\Phi}(\kappa^2, \mathbf{u}) = 0$ für $\kappa^2 + \mathbf{u}^2 < 1$ und zwar für stetiges $\hat{\Phi}$. Es scheint bequemer, eine Variablentransformation vorzunehmen:

$$(3.4) \quad \left\{ \begin{array}{l} \eta_0 = \frac{1 - \kappa^2 - \mathbf{u}^2}{1 + \kappa^2 + \mathbf{u}^2}; \quad \kappa^2 = \frac{1 - \eta_0^2 - \eta^2}{(1 + \eta_0)^2}; \\ \eta = \frac{2\mathbf{u}}{1 + \kappa^2 + \mathbf{u}^2}; \quad \mathbf{u}^2 = \frac{\eta}{1 + \eta_0}. \end{array} \right.$$

Offensichtlich gilt

$$(3.5) \quad \eta_0^2 + \eta^2 = \frac{(1 - \kappa^2 - \mathbf{u}^2)^2 + 4\mathbf{u}^2}{(1 + \kappa^2 + \mathbf{u}^2)^2} \leq 1.$$

so gilt formal

$$\hat{\Phi}(\kappa^2, \mathbf{u}) = \frac{4i}{(2\pi)} \frac{\partial}{\partial \kappa^2} \theta(\kappa^2) \int d\kappa^2 \int d^3 \eta \exp[-i\mathbf{u}\eta] J_0(\alpha\kappa) \Phi(\kappa^2, \eta)$$

wobei J_0 die Besselfunktion der Ordnung Null ist.

$$\Delta(\kappa^2, x_0^2 - \mathbf{x}^2) = \frac{1}{4\pi} \frac{\partial}{\partial \kappa^2} \theta(\kappa^2) J_0(\kappa \sqrt{x_0^2 - \mathbf{x}^2})$$

ist die bekannte invariante Funktion.

Wir haben uns also im η -Raum nur mit dem Innern der Einheitskugel zu befassen.

Weiter ergibt sich aus dem Verschwinden von \tilde{F}_1 im Doppelkegel

$$(3.6) \quad \int d^4\eta \Psi(\eta) \delta(\gamma_0\eta_0 + \gamma\eta - \varrho) = 0,$$

wobei

$$(3.6') \quad \left\{ \begin{array}{l} \gamma_0 = \frac{q_0^2 - \mathbf{q}^2 + 1}{\sqrt{(q_0^2 - \mathbf{q}^2 + 1)^2 + 4\mathbf{q}^2}}, \quad \gamma = \frac{2\mathbf{q}}{\sqrt{(q_0^2 - \mathbf{q}^2 + 1)^2 + 4\mathbf{q}^2}}, \\ \varrho = \frac{1 + \mathbf{q}^2 - q_0^2}{\sqrt{(q_0^2 - \mathbf{q}^2 + 1)^2 + 4\mathbf{q}^2}} \end{array} \right.$$

und

$$(3.7) \quad \Psi(\eta) = (1 + \eta_0)^{-4} \hat{\Phi}(\boldsymbol{\alpha}^2, \mathbf{u}),$$

gesetzt ist. $\Psi(\eta)$ ist für $\eta_0^2 + \eta^2 > 1$ Null zu setzen. Natürlich gilt (3.6) nur in dem durch (3.6') vermittelten Bild des Doppelkegels, das ist für

$$(3.8) \quad \gamma_0^2 + \gamma^2 = 1, \quad \gamma_0 > 0, \quad \frac{\varrho}{\sqrt{1 - \gamma_0^2}} > 1.$$

Anschaulich bedeuten (3.6) und (3.8), daß das Integral von $\Psi(\eta)$ über jede Ebene, die den Zylinder $|1 + \eta_0| > 0$, $\eta^2 < 1$ nicht trifft, verschwindet. Zu zeigen bleibt dann, daß daraus das Verschwinden von $\Psi(\eta)$ für $\eta_0 > 0$ folgt. Das ist gemäß (3.7) und (3.4) mit der Aussage von Satz 1 gleichbedeutend.

Dieser Nachweis geschieht auf Grund des folgenden Hilfsatzes.

Hilfsatz: Die stetige Funktion $\chi(\eta)$ verschwinde außerhalb eines beschränkten Gebietes. Sie habe außerdem die Eigenschaft, daß ihr Integral über jede Ebene, die einen gegebenen endlichen (abgeschlossenen) konvexen Bereich \mathfrak{B} nicht trifft, verschwindet. Dann verschwindet $\chi(\eta)$ außerhalb \mathfrak{B} .

In unserem Fall ist der Bereich \mathfrak{B} der oben erwähnte Zylinder.

Wir verschieben den Beweis des Hilfsatzes. Den allgemeinen Fall des Satzes führt man auf den eben behandelten zurück, indem man die Distributionen $F_1(q_0^2, \mathbf{q})$ und $\Phi(\boldsymbol{\alpha}^2, \mathbf{u})$ durch geglättete Funktionen ersetzt. Es sei etwa $\alpha(\boldsymbol{\alpha}^2)$ eine unendlich oft stetig differentierbare Funktion, die stark abnimmt, ebenso $\beta(\mathbf{u})$. Dann definiere man

$$(3.9) \quad \tilde{F}_1(q_0^2, \mathbf{q}) = \int d^3u \int d\boldsymbol{\alpha}^2 F_1(q_0^2 - \boldsymbol{\alpha}^2, (\mathbf{q} - \mathbf{u})) \alpha(\boldsymbol{\alpha}^2) \beta(\mathbf{u}).$$

Offenbar ist

$$(3.10) \quad \tilde{\tilde{F}}_1(q_0^2, \mathbf{q}) = \int d^3u \tilde{\tilde{\Phi}}(q_0^2 - (\mathbf{q} - \mathbf{u})^2, \mathbf{u})$$

mit

$$(3.11) \quad \tilde{\tilde{\Phi}}(\varkappa^2, \mathbf{u}) = \int d^3v \int d\lambda^2 \hat{\hat{\Phi}}(\varkappa^2 - \lambda^2, \mathbf{u} - \mathbf{v}) \alpha(\lambda^2) \beta(\mathbf{v}).$$

Man kann nun leicht eine Folge α_k, β_k so finden, daß

a) $\tilde{\tilde{F}}_{1k} \rightarrow \tilde{\tilde{F}}_1, \hat{\hat{\Phi}}_k \rightarrow \hat{\hat{\Phi}}$ für $k \rightarrow \infty$.

b) $\tilde{\tilde{F}}_{1k}$ im «geschrumpften» Doppelkegel $|q_0| + |\mathbf{q}| < 1 - \varepsilon$ verschwindet.

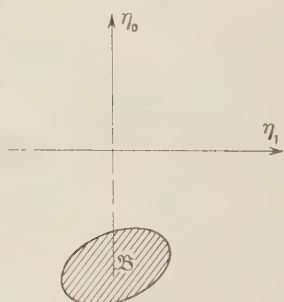
Auf Grund des schon bewiesenen verschwindet $\hat{\hat{\Phi}}_k$ in $\varkappa^2 + \mathbf{u}^2 - (1 - \varepsilon)^2$. Da $\varepsilon > 0$ dabei beliebig ist, verschwindet $\hat{\hat{\Phi}}$ also in $\varkappa^2 + \mathbf{u}^2 < 1$.

Es bleibt jetzt noch der

Beweis des Hilfsatzes (6). Der anschaulichkeit halber beziehen wir uns zunächst auf den 2-dimensionalen Fall und legen ein Koordinatensystem

zur Grunde, wie es in Fig. 1 angedeutet ist.

Das wesentliche dabei ist, daß die Halbebene $\eta_0 \geq 0$ von \mathfrak{B} einen nicht verschwindenden Abstand hat. Offenbar gilt



für jedes stetige $f(\eta_0)$. Wir wählen $f(\eta_0) = \eta_0$, schreiben also

$$(3.12) \quad \int_0^\infty d\eta_0 \int d\eta_1 f(\eta_0) \chi(\eta) = 0 .$$

Fig. 1. – Wahl des Koordinatensystems im Beweis des Hilfsatzes.

$$(3.13) \quad \int_0^\infty d\eta_0 \int d\eta_1 \eta_0 \chi(\eta) = 0 .$$

Jetzt drehen wir das Koordinatensystem um einen Winkel δ :

$$(3.14) \quad \begin{cases} \eta'_0 = \eta_0 \cos \delta + \eta_1 \sin \delta \\ \eta'_1 = -\eta_0 \sin \delta + \eta_1 \cos \delta , \end{cases}$$

(6) Wir verdanken diesen Beweis Herrn F. J. DYSON, dem wir auch hier unseren Dank aussprechen möchten. Er ersetzt den ursprünglichen, nicht elementaren Beweis der Autoren.

Falls δ klein genug ist, hat $\eta'_0 > 0$ immer noch einen nicht verschwindenden Abstand von \mathfrak{B} . Also gilt

$$(3.15) \quad \int_0^\infty d\eta'_0 \int d\eta'_1 \eta'_0 \chi'(\eta') = 0,$$

wobei $\chi'(\eta') = \chi(\eta)$ zu setzen ist. In den alten Variablen

$$(3.16) \quad \int d\eta_0 \int d\eta_1 (\eta_0 \cos \delta + \eta_1 \sin \delta) \chi(\eta) = 0, \quad \eta_0 \cos \delta + \eta_1 \sin \delta > 0.$$

Nun wird das Integrationsgebiet $\eta_0 \cos \delta + \eta_1 \sin \delta > 0$ aufgespalten in $\eta_0 > 0$, das Gebiet I: $\eta_1 < 0$ und $-\eta_1 \operatorname{tg} \delta > \eta_0 > 0$ und das Gebiet II: $\eta_1 > 0$ und $0 > \eta_0 > -\eta_1 \operatorname{tg} \delta$. Wegen (13) also

$$(3.17) \quad \begin{aligned} \sin \delta \int_0^\infty d\eta_0 \int d\eta_1 \eta_1 \chi(\eta) - \int_{(I)} d\eta_0 \int d\eta_1 (\eta_0 \cos \delta + \eta_1 \sin \delta) \chi(\eta) + \\ + \int_{(II)} d\eta_0 \int d\eta_1 (\eta_0 \cos \delta + \eta_1 \sin \delta) \chi(\eta) = 0. \end{aligned}$$

Sei $\chi(\eta) = 0$ für $\eta_0^2 + \eta_1^2 \geq R^2$ und $|\chi(\eta)| < A$ dann findet man leicht die Abschätzung

$$(3.18) \quad \left| \int_{(I)} d\eta_0 \int d\eta_1 (\eta_0 \cos \delta + \eta_1 \sin \delta) \chi(\eta) \right| < 2R^3 A \delta \sin \delta.$$

Entsprechendes gilt für das Integral über (II). Jetzt dividiert man (3.17) durch δ und geht mit $\delta \rightarrow 0$. Es folgt

$$(3.19) \quad \int_0^\infty d\eta_0 \int d\eta_1 \eta_1 \chi(\eta) = 0.$$

Da das Koordinatensystem (abgesehen von der erwähnten Einschränkung) willkürlich war, folgt, daß mit $\chi(\eta)$ auch $l(\eta)\chi(\eta)$, wobei $l(\eta)$ ein beliebiges lineares Polynom ist, die Eigenschaft hat, über jede Halbebene, die \mathfrak{B} nicht enthält, integriert Null zu ergeben. Wegen der Stetigkeit von $l(\eta)\chi(\eta)$ kann man auch über jede Gerade integrieren, die \mathfrak{B} nicht trifft und erhält Null. $l(\eta)\chi(\eta)$ erfüllt demnach dieselben Voraussetzungen wie $\chi(\eta)$. Anwendung von

Induktion führt deshalb zu

$$(3.20) \quad \int_0^\infty d\eta_0 \int d\eta_1 P(\eta_0, \eta_1) \chi(\eta) = 0,$$

wobei $P(\eta_0, \eta_1)$ ein beliebiges Polynom ist. (3.20) gilt in jeder Halbebene, die \mathfrak{B} nicht enthält. Wegen der Vollständigkeit der Polynome verschwindet $\chi(\eta)$ in jeder solchen Halbebene. Da \mathfrak{B} konvex ist, also $\chi(\eta) = 0$ für $\eta \notin \mathfrak{B}$.

Der Beweis für den n -dimensionalen Fall läßt sich offensichtlich genau so führen. An Stelle der einen Transformation (3.14) hat man deren $(n-1)$ zu betrachten:

$$(3.21) \quad \begin{cases} \eta'_0 = \eta_0 \cos \delta + \eta_k \sin \delta \\ \eta'_k = -\eta_0 \sin \delta + \eta_k \cos \delta \\ \eta'_l = \eta_l \end{cases} \quad \begin{cases} k = 1, 2, \dots, n-1 \\ l \neq k, l \neq 0 \end{cases}$$

(3.18) ändert sich in unwesentlicher Weise. An Stelle von (3.19) tritt

$$(3.22) \quad \int_0^\infty d\eta_0 \int d^{n-1}\eta \eta \chi(\eta) = 0$$

und an die Stelle von (3.20) ein n -faches Integral, das ein beliebiges Polynom $P(\eta_0, \eta_1, \dots, \eta_{n-1})$ enthält.

Als Anwendung des Satzes 1 bestimmen wir die Funktionen $\hat{\phi}(z^2, \mathbf{u})$, die zu der Problemstellung aus § 1 gehören. Wie in § 2 erwähnt wurde, verschwindet das entsprechende $F(q_0, \mathbf{q})$ für alle Doppelkegel $|q_0| + |\mathbf{q} - \mathbf{a}| < |\mathbf{a}| - 1$. Daher verschwindet $\hat{\phi}(z^2, \mathbf{u})$ in allen Kugeln $z^2 + |\mathbf{u} - \mathbf{a}|^2 < (|\mathbf{a}| - 1)^2$, $|\mathbf{a}| > 1$. $\hat{\phi}(z^2, \mathbf{u})$ ist also höchstens im Zylinder $|\mathbf{u}| \leq 1$ von Null verschieden. Als Folgerung daraus ergibt sich, daß $L(\xi; \eta)$ gemäß (3.1) und (2.4) in η eine regulär-analytische Funktion ist. Damit ist der Ansatz (2.2) wohl hinlänglich gerechtfertigt.

Weiterhin bemerken wir, daß es leicht möglich ist, Satz 1 auf allgemeinere Gebiete zu erweitern, da der zum Beweis benutzte Hilfssatz für beliebige endliche konvexe Bereiche formuliert ist.

Im Hinblick auf Anwendungen geben wir folgenden Satz an, den man durch elementare Betrachtungen erhält (⁷):

(⁷) Die Wahl des Gebietes in dem $\tilde{F}(q_0, \mathbf{q})$ verschwindet, entspricht der in Fußnote (¹) erwähnten verschärften Spektrumsbedingung.

Satz 2: Notwendig und hinreichend dafür, daß $\tilde{F}(q_0, \mathbf{k})$ außerhalb

$$(|q_0| + a)^2 \geq \mathbf{q}^2 + b^2 \quad (a, b \geq 0)$$

verschwindet, ist, daß $\hat{\Phi}(\varkappa^2, \mathbf{u})$ nur in

$$|\mathbf{u}| \leq a$$

und

$$\varkappa \geq \text{Max} \{0; b - \sqrt{a^2 - \mathbf{u}^2}\}$$

von Null verschieden ist ($\varkappa = +\sqrt{\varkappa^2}$).

4. – Die Funktion $\tilde{F}_R(k_0, \mathbf{k})$.

Falls $\hat{\Phi}(\varkappa^2, \mathbf{u})$ in (3.2) für $\varkappa^2 \rightarrow \infty$ genügend stark abfällt, dann existiert

$$(4.1) \quad \tilde{F}_R(k_0, \mathbf{k}) = \frac{1}{2\pi i} \int_{-\infty}^{\infty} \frac{F(q_0, \mathbf{k})}{q_0 - k_0} dq_0 .$$

für $\text{Im}[k_0] > 0$ und stellt für $\text{Im}[k_0] \rightarrow 0$ die Fouriertransformierte von $F_R(\xi_0, \xi)$ dar.

Einsetzen von (3.2) liefert

$$(4.2) \quad \tilde{F}_R(k_0, \mathbf{k}) = \int d^3 u \hat{\Phi}_R(k_0^2 - (\mathbf{k} - \mathbf{u})^2, \mathbf{u})$$

mit

$$(4.3) \quad \hat{\Phi}_R(\varkappa^2, \mathbf{u}) = \frac{1}{2\pi i} \int_0^\infty d\lambda^2 \frac{\Phi(\lambda^2, \mathbf{u})}{\lambda^2 - \varkappa^2} .$$

$\hat{\Phi}_R(\varkappa^2, \mathbf{u})$ ist in \varkappa^2 in der von 0 bis ∞ längs der positiven reellen Achse aufgeschnittenen komplexen Ebene regulär analytisch. Daraus folgt, daß $\tilde{F}_R(k_0, \mathbf{k})$ regulär analytisch ist, falls $\text{Im}[k]$ im Vorgegel liegt. Diese Eigenschaft ist charakteristisch für die Fouriertransformierte einer retardierten Distribution.

Nun folgt aber aus (4.3)

$$(4.4) \quad \hat{\Phi}_R(\varkappa^2, \mathbf{u}) = \frac{(\varkappa^2 + 1)^m}{2\pi i} \int_0^\infty d\lambda^2 \frac{\hat{\Phi}(\lambda^2, \mathbf{u})}{(\lambda^2 + 1)^m (\lambda^2 - \varkappa^2)} + \mathfrak{R}_{m-1}(\varkappa^2) ,$$

wobei $\mathfrak{R}_{m-1}(\varkappa^2)$ ein Polynom vom Grade $(m - 1)$ in \varkappa^2 mit Koeffizienten, die Funktionen von \mathbf{u} sind, darstellt. Nun läßt sich zu einer vorgegebenen Distribution Φ immer ein m so wählen, daß (4.4) sinnvoll ist. Falls $\tilde{F}_R(k_0, \mathbf{k})$ über-

haupt existiert, ist es notwendig von der Form

$$(4.5) \quad \tilde{F}_R(k_0, \mathbf{k}) = \frac{1}{2\pi i} \int d^3 u \int d\lambda^2 \frac{[k_0^2 - (\mathbf{k} - \mathbf{u})^2 + 1]^m \hat{\phi}(\lambda^2, \mathbf{u})}{(\lambda^2 + 1)^m [\lambda^2 - k_0^2 + (\mathbf{k} - \mathbf{u})^2]} + \mathfrak{R}_{2(m-1)}(k_0, \mathbf{k}),$$

wobei $\mathfrak{R}_{2(m-1)}(k_0, \mathbf{k})$ ein Polynom von Grade $2(m-1)$ in k_0, k_1, k_3, k_0 darstellt.

Für den Fall, daß $\tilde{F}(q_0, \mathbf{q})$ im Doppelkegel verschwindet, also $\hat{\phi}$ in $\lambda^2 + \mathbf{u}^2 < 1$ Null ist, liest man aus (4.5) leicht Regularitätsgebiete von $\tilde{F}_R(k_0, \mathbf{k})$ ab. Es gilt z.B. der folgende

Satz 3: Falls $\tilde{F}(q)$ in $|q_0 + \mathbf{q}| < 1$ verschwindet und falls $\tilde{F}_R(k)$ existiert, dann ist es für

$$(4.6) \quad \mu^2 < \text{Max}[0; (1 - |\mathbf{q}|^2 - q_0^2)]$$

regulär analytisch. Dabei ist $\mu = \text{Im}[k]$ und $q = \text{Re}[k]$.

Folgerung (8): $\tilde{F}_R(k)$ ist regulär in $|k_\nu| < \frac{1}{2}(\sqrt{3} - 1)$.

Beweis: Nach (4.5) ist $\tilde{F}_R(k_0, \mathbf{k})$ regulär solange $k_0^2 - \lambda^2 - (\mathbf{k} - \mathbf{u})^2$ für $\lambda^2 + \mathbf{u}^2 \geq 1$ nicht verschwindet. Trennt man in Real- und Imaginärteil, so muß

$$(4.7) \quad q_0^2 + \mu^2 < \lambda^2 + (\mathbf{q} - \mathbf{u})^2$$

sein, sobald $\lambda^2 + \mathbf{u}^2 \geq 1$ und $\mu q_0 - \mu(\mathbf{q} - \mathbf{u}) = 0$ ist.

Nun ist aber bei festen \mathbf{q} das Minimum von $\lambda^2 + (\mathbf{q} - \mathbf{u})^2$ gleich $(1 - |q_\nu|)^2$. Demnach ist $\tilde{F}_R(k)$ regulär für $\mu^2 < (1 - |\mathbf{q}|)^2 - q_0^2$. Andererseits ist $\tilde{F}_R(k)$ trivialerweise regulär für $\mu^2 < 0$. Der Satz gilt natürlich auch für gerades $\tilde{F}(q)$, wie aus § 2 folgt. (Anhang).

Zur Herleitung der Folgerung schreibe man $k_\nu = \varrho_\nu \exp[i\varphi_\nu]$; dann bedeutet (4.6)

$$(4.8) \quad \sum_{k=1}^3 \varrho_k^2 \sin^2 \varphi_k + \varrho_0^2 \cos^2 \varphi_0 < [1 - (\sum_1^3 \varrho_k^2 \cos^2 \varphi_k)^{\frac{1}{2}}]^2 + \varrho_0^2 \sin^2 \varphi_0,$$

oder

$$(4.9) \quad \sum_0^3 \varrho_\nu^2 < \frac{1}{2} + 2[\frac{1}{2} - (\sum_1^3 \varrho_k^2 \cos^2 \varphi_k)^{\frac{1}{2}}]^2 + 2\varrho_0^2 \sin^2 \varphi_0.$$

Will man eine Abschätzung vom Typus der Folgerung, so setze man $\varrho_\nu = \varrho$ und $\varphi_\nu = 0$. Die entstehende quadratische Ungleichung führt zur Folgerung.

(8) Diese Folgerung entspricht einem Satze, den N. N. BOGOLIUBOV am International Congress on Theoretical Physics in Seattle (September 1956) mitgeteilt hat. Wir möchten Herrn N. N. BOGOLIUBOV für anregende Diskussionen danken.

ANHANG

Es sei

$$(A.1) \quad F(\xi_0, \xi) = F_R(\xi_0, \xi) + F_R(-\xi_0, \xi).$$

Behauptet wird die Existenz von

$$(A.2) \quad G(\xi_0, \xi) = G_R(\xi_0, \xi) - G_R(-\xi_0, \xi)$$

derart, daß $F(\xi) = (\partial/\partial\xi_0)G(\xi)$ ist. Wir verlangen etwas mehr und setzen

$$(A.3) \quad F_R(\xi) = \frac{\partial G_R(\xi)}{\partial \xi_0}.$$

(A.3) bedeutet ⁽⁹⁾

$$(A.4) \quad F_R(\varphi) = -G_R\left(\frac{\partial \varphi}{\partial \xi_0}\right),$$

wodurch $G_R(\psi)$ für alle ψ definiert ist, für welche $\int_{-\infty}^{\infty} \psi d\xi_0 = 0$ ist. Nun sei $\alpha(\xi_0) \in S_{\xi_0}$, verschwinde in $\xi_0 > -1$ und erfülle $\int \alpha(\xi_0) d\xi_0 = 1$.

Ein beliebiges ψ wird jetzt aufgespalten in

$$(A.5) \quad \psi(\xi_0, \xi) = \chi(\xi_0, \xi) + \alpha(\xi_0) \int_{-\infty}^{\xi_0} \psi(\tau, \xi) d\tau.$$

Da

$$\int_{-\infty}^{\infty} \chi(\xi) d\xi_0 = 0,$$

ist

$$(A.6) \quad \varphi(\xi_0, \xi) = \int_{-\infty}^{\xi_0} \chi(\tau, \xi) d\tau \in S.$$

Jetzt definiert man

$$(A.7) \quad G_R(\psi) = -F_R(\varphi)$$

und $G(\xi_0, \xi)$ durch (A.2).

⁽⁹⁾ L. SCHWARTZ: l.c., Vol. I, Ch. II. Testfunktionen immer aus S (Vol. II, p. 89).

G_R verschwindet außerhalb des Vorkegels. In der Tat: falls ψ den Träger außerhalb des Vorkegels hat, dann gilt dasselbe auch von χ , da es von $\alpha(\xi_0)$ gilt. Aber die Aussage gilt auch von φ , da jede Gerade $\xi = \text{const.}$ mit dem Vorkegel nur eine Halbgerade gemeinsam hat.

Also ist $G_R(\psi) = 0$.

Schließlich haben $\tilde{F}(q)$ und $\tilde{G}(q)$ denselben Träger, denn es gilt

$$(A.8) \quad \tilde{F}(\varphi) = -i\tilde{G}(p_0\varphi),$$

wodurch $\tilde{G}(\psi)$ für ungerades ψ definiert ist. Für gerades ψ aber ist $\tilde{G}(\psi) = 0$.

RIASSUNTO (*)

Si esamina la struttura del commutatore degli operatori di campo. Si dà una rappresentazione integrale per l'elemento di matrice tra stati propri dell'operatore d'impulso, tenendo conto della causalità microscopica e dello spettro dell'operatore d'impulso stesso.

(*) Traduzione a cura della Redazione.

Low's General Equation.

W. KRÓLIKOWSKI (*)

Physikalisches Institut der E.T.H. - Zürich

(ricevuto il 25 Marzo 1957)

Summary. — This note contains a derivation of a formally exact relation in the field theory between the elements of the S matrix corresponding to a given number of particles. This relation is similar in form to Low's equation (¹), but all elements of the S matrix associated with different numbers of particles but one distinguished are here eliminated (²). The derivation of this relation is based on the equation for a distinguished component of the state vector corresponding to a given number of particles. Low's general equation obtained here contains the interaction operator of the given number of particles. So far, this operator can be evaluated practically only by expanding it in the coupling constant.

1. The equation for a distinguished component of the state vector.

We consider an arbitrary quantized system, e.g., a system of interacting fields, described in the Schrödinger picture by the state equation

$$(1) \quad \left(i \frac{\partial}{\partial t} - H \right) \Psi(t) = 0,$$

where H is the total energy of the system ($\hbar = 1$).

(*) Permanent address: Institute of Physics of the Polish Academy of Sciences, Warsaw.

(¹) F. E. Low: *Phys. Rev.*, **97**, 1392 (1955); G. F. CHEW and F. E. Low: *Phys. Rev.*, **101**, 1570, 1579 (1956); G. F. CHEW: *Theory of Pion Scattering and Photoproduction* (Berlin, 1957, to be published).

(²) FUKUDA and KOVACS published recently (*Phys. Rev.*, **104**, 1784 (1956)) a method of successive elimination of these different amplitudes in the fixed-source meson theory. This method of elimination is similar to the New Tamm-Dancoff procedure.

We take into account a situation, when we are interested in a distinguished component Ψ_{\parallel} of the state vector Ψ (2,3). E.g., this component may describe a given number of particles, when we are considering a system of interacting fields.

Denote by P_{\parallel} the projection operator which acting on the state vector Ψ produces its component Ψ_{\parallel} . The projection operator $P_{\perp} = 1 - P_{\parallel}$ acting on Ψ produces its component $\Psi_{\perp} = \Psi - \Psi_{\parallel}$. We have, of course,

$$(2) \quad P_{\parallel}^2 = P_{\parallel}, \quad P_{\perp}^2 = P_{\perp}, \quad P_{\parallel}P_{\perp} = 0 = P_{\perp}P_{\parallel}.$$

In the equation (1) we may write $H = P_{\parallel}HP_{\parallel} + P_{\perp}HP_{\perp} + P_{\parallel}HP_{\perp} + P_{\perp}HP_{\parallel}$. Now, we transform the equation (1) by means of the following unitary transformation:

$$(3) \quad \begin{cases} \Psi_F(t) = \exp [i(P_{\parallel}HP_{\parallel} + P_{\perp}HP_{\perp})t] \Psi(t), \\ O_F(t) = \exp [i(P_{\parallel}HP_{\parallel} + P_{\perp}HP_{\perp})t] O \exp [-i(P_{\parallel}HP_{\parallel} + P_{\perp}HP_{\perp})t]. \end{cases}$$

Since the operators P_{\parallel} and P_{\perp} commute with $P_{\parallel}HP_{\parallel} + P_{\perp}HP_{\perp}$, we obtain

$$(4) \quad i \frac{\partial}{\partial t} \Psi_F(t) = [P_{\parallel}H_F(t)P_{\perp} + P_{\perp}H_F(t)P_{\parallel}] \Psi_F(t).$$

Multiplying this equation by P_{\parallel} and P_{\perp} respectively, we get

$$(5) \quad \begin{cases} i \frac{\partial}{\partial t} \Psi_{F\parallel}(t) = P_{\parallel}H_F(t)P_{\perp}\Psi_{F\perp}(t), \\ i \frac{\partial}{\partial t} \Psi_{F\perp}(t) = P_{\perp}H_F(t)P_{\parallel}\Psi_{F\parallel}(t), \end{cases}$$

where $\Psi_F = P_{\parallel}\Psi_F = \Psi_{F\parallel}$ and $\Psi_{F\perp} = P_{\perp}\Psi_F = \Psi_{F\perp}$. Eliminating now from the first equation (5) the component $\Psi_{F\perp}$ by means of the second equation we have

$$(6) \quad i \frac{\partial}{\partial t} \Psi_{F\parallel}(t) = P_{\parallel}H_F(t)P_{\perp}\Psi_{F\perp}(t_0) - i \int_{t_0}^t dt' K_F(t, t') \Psi_{F\parallel}(t'),$$

where

$$(7) \quad K_F(t, t') = P_{\parallel}H_F(t)P_{\perp}H_F(t')P_{\parallel}.$$

(2) W. KRÓLIKOWSKI and J. RZEWUSKI: *Nuovo Cimento*, **3**, 260 (1956); *Bull. Acad. Pol. Sci. Cl. III*, **4**, 19 (1956).

(3) W. KRÓLIKOWSKI and J. RZEWUSKI: *Nuovo Cimento*, **4**, 1212 (1956).

Going back to the Schrödinger picture and making use of (2) we obtain the following equation of the component Ψ_{\parallel} of the state vector Ψ :

$$(8) \quad \left(i \frac{\partial}{\partial t} - P_{\parallel} H P_{\parallel} \right) \Psi_{\parallel}(t) = P_{\parallel} H P_{\perp} \exp[-iP_{\perp} H P_{\perp}(t-t_0)] \Psi_{\perp}(t) - \\ - i \int_{t_0}^t dt' K(t-t') \Psi_{\parallel}(t'),$$

where

$$(9) \quad K(t-t') = P_{\parallel} H P_{\perp} \exp[-iP_{\perp} H P_{\perp}(t-t')] P_{\perp} H P_{\parallel}.$$

In the case, when $\Psi_{\perp}(t_0) = 0$ and $t_0 \rightarrow -\infty$, we may go over from (8) to a time-independent equation by means of the substitution

$$\Psi_{\parallel}(t) = \chi_{\parallel} \exp[-iWt].$$

Then we get

$$(10) \quad [W - P_{\parallel} H P_{\parallel} - U(W)] \chi_{\parallel} = 0,$$

where (*)

$$(11) \quad U(W) = -i \int_0^{\infty} dt K(t) \exp[iWt] = P_{\parallel} H P_{\parallel} \frac{1}{W - P_{\perp} H P_{\perp}} + i\varepsilon P_{\perp} H P_{\perp}.$$

In the case $\Psi_{\perp}(t_0) = 0$ and $t_0 \rightarrow -\infty$ the integro-differential equation (with respect to time) (8) is equivalent to the following purely differential equation (with respect to time)

$$(12) \quad \left(i \frac{\partial}{\partial t} - P_{\parallel} H P_{\parallel} - V \right) \Psi_{\parallel}(t) = 0,$$

if the following equation defines the operator V uniquely:

$$(13) \quad V = -i \int_0^{\infty} dt K(t) \exp[i(P_{\parallel} H P_{\parallel} + V)t],$$

(cf. (*)).

(*) We understand the integral (11) so, that the oscillating part of its integrand vanishes for $t \rightarrow \infty$. For this purpose we may use the integrating factor $\exp[-\varepsilon t]$, where $\varepsilon > |\text{Im } W|$ and let $\varepsilon \rightarrow 0$ after all calculations are carried out.

By means of the substitution

$$\Psi_{\parallel}(t) = \chi_{\parallel} \exp[-iWt]$$

we obtain from (12) the time-independent equation

$$(14) \quad (W - P_{\parallel}HP_{\parallel} - V)\chi_{\parallel} = 0,$$

which is equivalent to (10), if (13) determines the operator V uniquely. Then we have

$$(15) \quad V\chi_{\parallel} = U(W)\chi_{\parallel},$$

what may be seen also directly from (13), (14) and (11).

The equations (12) and (14) have the form of Schrödinger equations but the « potential » V is here a complex (= non-Hermitian) operator (in general it is an integral operator) (cf. (2)). Its imaginary part is due to the instability of states described by the distinguished component Ψ_{\parallel} , e.g., states with a given number of particles, when we consider a system of interacting fields. We have in general $W = \bar{E} - i\Gamma$, where \bar{E} is the expectation value of the energy $P_{\parallel}HP_{\parallel} + \text{Re } V$ in the state χ_{\parallel} and $1/\Gamma$ is the life-time of this state. In order to evaluate the interaction operator V in the case of a field theory we must for the present expand it with respect to the coupling constant of the interacting fields.

Now we take into account a system of interacting fields and denote by Ψ the distinguished component of Ψ describing a given number N_0 of physical particles.

Let us denote by $|\lambda(N_0)\rangle$ vectors forming an orthogonal representation related to a given number N_0 of physical particles appearing in the system of interacting fields. Here $\lambda(N_0)$ is a set of eigenvalues of a complete system of commuting observable determining states of N_0 physical particles. N_0 is (speaking more strictly) a given set of total numbers of physical particles corresponding to the different fields under consideration. We assume here also that the whole Fock representation given by the vectors $|\lambda(N)\rangle$ for all N is orthogonal. We have thus (*)

$$(16) \quad P_{\parallel} = P_{N_0}, \quad P_{\perp} = \sum_{N \neq N_0} P_N,$$

(*) If the representation given by vectors $|\lambda(N)\rangle$ were non-orthogonal, the operators (16) might be defined by

$$\begin{aligned} P_N &= \sum_{\lambda(N)} |\lambda(N)\rangle \langle \lambda(N)| = \sum_{\lambda(N)} |\lambda(N)\rangle \langle \lambda(N)| = \sum_{\lambda(N)} \sum_{N'} \sum_{\lambda'(N')} |\lambda(N)\rangle \overset{\circ}{g}_{\lambda(N)\lambda'(N')}^{\lambda(N)\lambda'(N')} \langle \lambda'(N')| = \\ &= \sum_{\lambda(N)} \sum_{N'} \sum_{\lambda'(N')} |\lambda(N)\rangle \overset{\circ}{g}_{\lambda(N)\lambda'(N')}^{\lambda(N)\lambda'(N')} \langle \lambda'(N')|, \end{aligned}$$

where

$$P_N = \sum_{\lambda(N)} |\lambda(N)\rangle \langle \lambda(N)|.$$

We assume further that i) among other representations for N_0 particles given by $|\lambda(N_0)\rangle$ there is one, for which the vectors $|\lambda(N_0)\rangle$ represent asymptotic forms of scattering eigenstates of total energy of the system corresponding to eigenvalues $E_{\lambda(N_0)}$:

$$(17) \quad \begin{cases} (E_{\lambda(N_0)} - H)\Phi_{\lambda(N_0)}^{(\pm)} = 0, \\ \Phi_{\lambda(N_0)}^{(\pm)} = |\lambda(N_0)\rangle + \frac{1}{E_{\lambda(N_0)} - H \pm ie} (H - E_{\lambda(N_0)}) |\lambda(N_0)\rangle, \end{cases}$$

and ii) the operators

$$(18) \quad \begin{cases} U(\hat{H}, W) = P(H - \hat{H})P + U(W), \\ V(\hat{H}) = P(H - \hat{H})P + V, \end{cases}$$

are free from divergences (renormalization), where \hat{H} is given by

$$\hat{H} = \sum_N \sum_{\lambda(N)} |\lambda(N)\rangle E_{\lambda(N)} \langle \lambda(N)|.$$

We note that, if we construct as above the operator \hat{H} , for which $|\lambda(N)\rangle$ are the eigenstates with eigenvalues $E_{\lambda(N)}$:

$$(19) \quad (E_{\lambda(N)} - \hat{H}) |\lambda(N)\rangle = 0,$$

then

$$(20) \quad (H - E_{\lambda(N)}) |\lambda(N)\rangle = \hat{H} |\lambda(N)\rangle,$$

where \hat{H} is defined by

$$(21) \quad H = \hat{H} + \frac{1}{H},$$

where vectors $|\lambda(N)\rangle = |\lambda(N)\rangle$ and $|\lambda(N)\rangle$ would form two mutually contragradient representations:

$$\langle \lambda(N) | \underline{\lambda'(N')} \rangle = \delta_{\lambda(N)\lambda'(N')} = \begin{cases} 1 & \lambda(N) = \lambda'(N'), \\ 0 & \lambda(N) \neq \lambda'(N'), \end{cases}$$

and where

$$\hat{g}_{\lambda(N)\lambda'(N')}^{\lambda(N)\lambda'(N')} = \langle \lambda(N) | \lambda'(N') \rangle, \quad \hat{g}_{\lambda(N)\lambda'(N')}^{\lambda(N)\lambda'(N')} = \langle \lambda(N) | \lambda'(N') \rangle.$$

In the conventional renormalization method, \hat{H} is identical with the (renormalized) energy of the free fields and \hat{H} represents their (renormalized) interaction energy.

Note that the operators P_{\parallel} and P_{\perp} commute with \hat{H} and hence we have $P_{\parallel}\hat{H}P_{\parallel} = \hat{H}P_{\parallel}$, $P_{\perp}HP_{\parallel} = P_{\perp}\hat{H}P_{\parallel}$. Thus

$$(22) \quad P_{\parallel}\hat{H}P_{\parallel}|\lambda(N_0)\rangle = \hat{H}|\lambda(N_0)\rangle, \quad P_{\perp}HP_{\parallel}|\lambda(N_0)\rangle = P_{\perp}\hat{H}|\lambda(N_0)\rangle.$$

From (22) it follows that, if $|\lambda(N_0)\rangle$ are eigenstates of \hat{H} , we have also

$$(23) \quad (E_{\lambda(N_0)} - P_{\parallel}\hat{H}P_{\parallel})|\lambda(N_0)\rangle = 0.$$

Introducing into (8), (10) and (12), (14) the operator $P_{\parallel}\hat{H}P_{\parallel}$ describing the energy of N_0 free physical particles, we can see that the operators $U(\hat{H}, W)$ and $V(\hat{H})$ given by (18) are the interaction operators between these particles, and must vanish asymptotically for scattering states. Thus, for scattering states of N_0 particles we have

$$(24) \quad W = E_{\lambda(N_0)} = E \quad (\bar{E} = E_{\lambda(N_0)}, \Gamma = 0),$$

where E is an eigenvalue of the total energy of the system. Writing $\chi_{\parallel} = \chi_{\lambda(N_0)}$ we obtain from (15)

$$(25) \quad V\chi_{\lambda(N_0)} = U(E_{\lambda(N_0)})\chi_{\lambda(N_0)}.$$

It will be shown in the next Section that for scattering states of N_0 particles

$$(26) \quad \chi_{\lambda(N_0)} = \Phi_{\lambda(N_0)\parallel}^{(+)} \equiv P_{\parallel}\Phi_{\lambda(N_0)\parallel}^{(+)},$$

In general, however, we have $\Phi_{\lambda(N_0)\parallel}^{(+)} = P_{\parallel}\Phi_{\lambda(N_0)}^{(+)} \neq \Phi_{\lambda(N_0)}^{(+)}$ (i.e. $\Phi_{\lambda(N_0)\parallel}^{(+)}$ is not a stationary state, in spite of the fact that here $\Gamma = 0$).

From similar arguments, as above, we can see that for bound states of N_0 particles (or scattering on bound states) W is in general complex (since V is complex) and we have $W \neq E$, $\chi_{\parallel} \neq \Phi_{\parallel} = P\Phi$, where Φ is an eigenstate of the total energy of the system corresponding to the eigenvalue E :

$$(E - H)\Phi = 0.$$

If $(\text{Im } V)\chi_{\parallel} = 0$ (in this case $P_{\parallel} = 0$, but the reverse implication is not true, as it is seen for scattering states), then $W = E$, $\chi_{\parallel} = \Phi_{\parallel}$ and, moreover, $\Phi = P_{\parallel}\Phi_{\perp}$, Φ_{\perp} (i.e. Φ_{\perp} is a stationary state). The case $(\text{Im } V)\chi_{\parallel} \neq 0$ occurs, when χ_{\parallel} is a ground state of N_0 particles.

2. – The S matrix.

As is well known (cf. (1)), the elements of the S matrix for transitions $\lambda(N_0) \rightarrow \lambda'(N_0)$ may be represented in the form

$$(27) \quad \langle \lambda'(N_0) | S | \lambda(N_0) \rangle = \delta_{\lambda(N_0)\lambda(N_0)} - 2\pi i \delta(E_{\lambda(N_0)} - E_{\lambda'(N_0)}) T_{\lambda'(N_0)}(\lambda(N_0)) ,$$

where

$$(28) \quad T_{\lambda'(N_0)}(\lambda(N_0)) = \langle \lambda'(N_0) | (H - E_{\lambda(N_0)}) \Phi_{\lambda(N_0)}^{(+)} \rangle .$$

Here $\Phi_{\lambda(N_0)}^{(+)}$ is given by (17).

Multiplying the first equation (17) by P_{\parallel} and P_{\perp} respectively, we obtain

$$(29) \quad \begin{cases} (E_{\lambda(N_0)} - P_{\parallel} H P_{\parallel}) \Phi_{\lambda(N_0)\parallel}^{(+)} = P_{\parallel} H P_{\perp} \Phi_{\lambda(N_0)\perp}^{(+)} , \\ (E_{\lambda(N_0)} - P_{\perp} H P_{\perp}) \Phi_{\lambda(N_0)\perp}^{(+)} = P_{\perp} H P_{\parallel} \Phi_{\lambda(N_0)\parallel}^{(+)} . \end{cases}$$

From the second equation (29) we have

$$(30) \quad \Phi_{\lambda(N_0)\perp}^{(+)} = \frac{1}{E_{\lambda(N_0)} - P_{\perp} H P_{\perp} + i\varepsilon} P_{\perp} H P_{\parallel} \Phi_{\lambda(N_0)\parallel}^{(+)} ,$$

(there is no inhomogeneous term, because $\Psi_{\perp}(t_0) = 0$, $t_0 \rightarrow -\infty$). Inserting (30) in the first equation (29) we get the equation

$$(10') \quad [E_{\lambda(N_0)} - P_{\parallel} H P_{\parallel} - U(E_{\lambda(N_0)})] \Phi_{\lambda(N_0)\parallel}^{(+)} = 0 ,$$

where

$$(11') \quad U(E_{\lambda(N_0)}) = P_{\parallel} H P_{\perp} \frac{1}{E_{\lambda(N_0)} - P_{\perp} H P_{\perp} + i\varepsilon} P_{\perp} H P_{\parallel} ,$$

(of course $P_{\parallel} H P_{\perp} + U(E) = P_{\parallel} \overset{\circ}{H} P_{\perp} - U(\overset{\circ}{H}, E)$). Here $\Phi_{\lambda(N_0)\parallel}^{(+)} = P_{\parallel} \Phi_{\lambda(N_0)}^{(+)}$ and $\Phi_{\lambda(N_0)\perp}^{(+)} = P_{\perp} \Phi_{\lambda(N_0)}^{(+)}$. Comparing (10') and (10) and using (24) we obtain

⁽¹⁾ B. LIPPmann and J. SCHWINGER: *Phys. Rev.*, **79**, 469 (1950); M. GELL-MANN and M. L. GOLDBERGER: *Phys. Rev.*, **91**, 398 (1953); H. ECKSTEIN and K. TANAKA: *Phys. Rev.*, **104**, 259 (1956).

$\chi_{\parallel \lambda(N_0)} = \Phi_{\lambda(N_0)\parallel}^{(+)}$ i.e. (26). Instead of (10') we may write thanks to (26) and (25) the equation

$$(14') \quad (E_{\lambda(N_0)} - P_{\parallel} H P_{\parallel} - V) \Phi_{\lambda(N_0)\parallel}^{(+)} = 0$$

(of course $P_{\parallel} H P_{\parallel} + V = P_{\parallel} \overset{\circ}{H} P_{\parallel} + V(\overset{\circ}{H})$).

Now, the transition amplitudes (28) may be—by virtue of (30), (11'), (26) and (25)—rewritten in the form

$$\begin{aligned} (31) \quad T_{\lambda'(N_0)}(\lambda(N_0)) &= \langle \lambda'(N_0) | [P_{\parallel}(H - E_{\lambda'_0(N_0)}) P_{\parallel} + P_{\parallel} H P_{\parallel}] \Phi_{\lambda(N_0)\parallel}^{(+)} \rangle = \\ &= \langle \lambda'(N_0) | [P_{\parallel}(H - E_{\lambda'(N_0)}) P_{\parallel} + U(E_{\lambda(N_0)})] \Phi_{\lambda(N_0)\parallel}^{(+)} \rangle = \\ &= \langle \lambda'(N_0) | U(E_{\lambda'(N_0)}, E_{\lambda(N_0)}) \Phi_{\lambda(N_0)\parallel}^{(+)} \rangle = \\ &= \langle \lambda'(N_0) | V(E_{\lambda'(N_0)}) \Phi_{\lambda(N_0)\parallel}^{(+)} \rangle. \end{aligned}$$

From (14') we obtain

$$(32) \quad \Phi_{\lambda(N_0)\parallel}^{(+)} = |\lambda(N_0)\rangle + \frac{1}{E_{\lambda(N_0)} - P_{\parallel} H P_{\parallel} - V + i\varepsilon} V(E_{\lambda(N_0)}) |\lambda(N_0)\rangle.$$

Thus, (31) takes the form

$$\begin{aligned} (33) \quad T_{\lambda'(N_0)}(\lambda(N_0)) &= \langle \lambda'(N_0) | V(E_{\lambda'(N_0)}) |\lambda(N_0)\rangle + \\ &+ \langle \lambda'(N_0) | V(E_{\lambda'(N_0)}) \frac{1}{E_{\lambda(N_0)} - P_{\parallel} H P_{\parallel} - V + i\varepsilon} V(E_{\lambda(N_0)}) |\lambda(N_0)\rangle. \end{aligned}$$

Note that the vectors $\Phi_{\lambda(N_0)\parallel}^{(+)}$ are not orthogonal, because

$$\langle \Phi_{\lambda(N_0)\parallel}^{(+)} | \Phi_{\lambda'(N_0)\parallel}^{(+)} \rangle = \langle \Phi_{\lambda(N_0)\parallel}^{(+)} | P_{\parallel} \Phi_{\lambda'(N_0)\parallel}^{(+)} \rangle = \delta_{\lambda(N_0)\lambda'(N_0)} - \langle \Phi_{\lambda(N_0)\parallel}^{(+)} | P_{\perp} \Phi_{\lambda'(N_0)\parallel}^{(+)} \rangle.$$

It is consistent with the fact that the « potential » V is complex (= non-Hermitian). The same can be said of solutions of equation (41) other than scattering states $\Phi_{\lambda(N_0)\parallel}^{(+)}$, if such solutions, say χ_b , representing bound states (or scattering on bound states), exist for the given number N_0 of particles.

Note further that the two systems of vectors $\chi_{\parallel\alpha}$ and $\chi_{\parallel}^{\alpha}$ satisfying the equations

$$(15') \quad (W_{\alpha} - P_{\parallel} H P_{\parallel} - V) \chi_{\parallel\alpha} = 0$$

and

$$(34) \quad (W_{\alpha}^* - P_{\parallel} H P_{\parallel} - V^*) \chi_{\parallel}^{\alpha} = 0$$

(and the same boundary conditions) are mutually contragradient:

$$(35) \quad \langle \chi_{\parallel}^{\alpha} \chi_{\parallel \alpha'} \rangle = \delta_{\alpha \alpha'} = \begin{cases} 1 & \alpha = \alpha' , \\ 0 & \alpha \neq \alpha' . \end{cases}$$

Here V^* is the Hermitian conjugate of V . Ths, if the χ_{\parallel} 's form a complete system of vectors (a non-orthogonal basis) in the subspace of N_0 particles, we have

$$(36) \quad P_{\parallel} = \sum_{\alpha} \chi_{\parallel \alpha} \langle \chi_{\parallel}^{\alpha} \rangle = \sum_{\alpha} \chi_{\parallel}^{\alpha} \langle \chi_{\parallel \alpha} \rangle = \sum_{\alpha, \alpha'} \chi_{\parallel \alpha} \langle g^{\alpha \alpha'} \rangle \chi_{\parallel \alpha'} = \sum_{\alpha, \alpha'} \chi_{\parallel}^{\alpha} \langle g_{\alpha \alpha'} \rangle \chi_{\parallel}^{\alpha'},$$

where

$$(37) \quad g^{\alpha \alpha'} = \langle \chi_{\parallel}^{\alpha} \chi_{\parallel}^{\alpha'} \rangle, \quad g_{\alpha \alpha'} = \langle \chi_{\parallel \alpha} \chi_{\parallel \alpha'} \rangle.$$

Assuming that the vectors $\Phi_{\lambda(N_0)}^{(+)}(\chi_b)$, χ_b form a complete system in the subspace of N_0 particles, we obtain from (33), by means of (36) (putting there $(\chi_{\parallel \alpha}) = (\varphi_{\lambda(N_0)\parallel}, \chi_{\parallel b})$) and by virtue of the fact that $V(E_{\lambda(N_0)}) = P_{\parallel} V(E_{\lambda(N_0)}) P_{\parallel}$,

$$(38) \quad T_{\lambda(N_0)}(\lambda'(N_0)) = \langle \lambda'(N_0) | V(E_{\lambda'(N_0)}) \Phi_{\lambda(N_0)\parallel}^{(+)} \rangle = \langle \lambda'(N_0) | V(E_{\lambda(N_0)}) | \lambda(N_0) \rangle + \\ + \sum_{\lambda(N_0)} \frac{\langle \lambda'(N_0) | V(E_{\lambda(N_0)}) \Phi_{\lambda(N_0)\parallel}^{(+)} \rangle \langle \Phi_{\lambda(N_0)\parallel}^{(+)} | V(E_{\lambda(N_0)}) | \lambda(N_0) \rangle}{E_{\lambda(N_0)} - E_{\lambda'(N_0)} + i\varepsilon} + \\ + \sum_b \frac{\langle \lambda'(N_0) | V(E_{\lambda(N_0)}) \chi_b \rangle \langle \chi_b | V(E_{\lambda(N_0)}) | \lambda(N_0) \rangle}{E_{\lambda(N_0)} - E_b + i\Gamma_b + i\varepsilon},$$

($W_b = E_b - i\Gamma_b$). The term $\langle \lambda'(N_0) | V(E_{\lambda'(N_0)}) | \lambda(N_0) \rangle$ represents the Born approximation for the transition $\lambda(N_0) \rightarrow \lambda'(N_0)$, but with the exact interaction operator $V(E_{\lambda(N_0)}) = P_{\parallel}(H - E_{\lambda(N_0)})P_{\parallel} + V$ of N_0 particles.

The equation (38) connects the quantities

$$T_{\lambda(N_0)}(\lambda(N_0)) = \langle \lambda'(N_0) | V(E_{\lambda'(N_0)}) \Phi_{\lambda(N_0)\parallel}^{(+)} \rangle$$

and

$$X_{\lambda(N_0)}(\lambda(N_0)) = \langle \lambda'(N_0) | V^*(E_{\lambda'(N_0)}) \Phi_{\lambda(N_0)\parallel}^{(+)} \rangle^*$$

with the interaction operator $V(E_{\lambda(N_0)})$. Apart from (38) we obtain easily another equation, in which the rôles of T and X are interchanged and $V^*(E_{\lambda(N_0)})$ appears instead of $V(E_{\lambda(N_0)})$ (and $-i\Gamma_b$ instead of $+i\Gamma_b$). This equation together with (38) forms a simultaneous system of two equations for T and X . Shortening $\lambda \equiv \lambda(N_0)$, we have

$$(39) \quad \left\{ \begin{array}{l} T_{\lambda}(\lambda) = \langle \lambda' | V(E_{\lambda'}) | \lambda \rangle + \sum_{\lambda''} \frac{T_{\lambda}(\lambda'') X_{\lambda}^*(\lambda'')}{E_{\lambda} - E_{\lambda''} + i\varepsilon} + \sum_b \frac{\langle \lambda' | V(E_{\lambda'}) \chi_b \rangle \langle \chi_b | V(E_{\lambda}) | \lambda \rangle}{E_{\lambda} - E_b + i\Gamma_b + i\varepsilon} , \\ X_{\lambda}(\lambda) = \langle \lambda' | V^*(E_{\lambda}) | \lambda \rangle + \sum_{\lambda''} \frac{X_{\lambda}(\lambda'') T_{\lambda}^*(\lambda'')}{E_{\lambda} - E_{\lambda''} + i\varepsilon} + \sum_b \frac{\langle \lambda' | V^*(E_{\lambda}) \chi_b \rangle \langle \chi_b | V^*(E_{\lambda}) | \lambda \rangle}{E_{\lambda} - E_b - i\Gamma_b + i\varepsilon} . \end{array} \right.$$

If for N_0 particles under consideration no bound states exist, then in (39) $\sum_b = 0$.

If for the system under consideration the number N_0 of particles cannot change in real transitions, then the « potential » V is real (= Hermitian) and so the vectors $\Phi_{\lambda_i}^{(+)}, \chi_{\lambda b}$ form an orthogonal system. In this case (38) reduces to the form

$$(40) \quad T_{\lambda}(\lambda) = \langle \lambda' | V(E_{\lambda}) | \lambda \rangle + \sum_{\lambda} \frac{T_{\lambda}(\lambda') T_{\lambda}^*(\lambda'')} {E_{\lambda} - E_{\lambda} + i\varepsilon} + \sum_b \frac{\langle \lambda' | V(E_{\lambda'}) \chi_{\lambda b} \rangle \langle \lambda | V(E_{\lambda}) \chi_{\lambda b} \rangle^*}{E_{\lambda} - E_b + i\varepsilon}.$$

If the imaginary part of the « potential » V is small in comparison with its real part, then one may neglect in (38) the influence of the imaginary part in the numerators. So we obtain the following approximate equation

$$(41) \quad T_{\lambda}(\lambda) = \langle \lambda' | V(E_{\lambda}) | \lambda \rangle + \sum_{\lambda} \frac{T_{\lambda}(\lambda') T_{\lambda}^*(\lambda'')}{E_{\lambda} - E_{\lambda} + i\varepsilon} + \sum_b \frac{\langle \lambda' | V(E_{\lambda'}) \chi_{\lambda b} \rangle \langle \lambda | V(E_{\lambda}) \chi_{\lambda b} \rangle^*}{E_{\lambda} - E_b + i\Gamma_b + i\varepsilon}.$$

The above results give a relation between scattering amplitudes and the interaction operator of particles, in which they differ from dispersion relations, that allow for a discussion of the energy dependence of scattering amplitudes independently of the interaction operator.

Low's general equation obtained in this paper may be of some importance only when it is able to give more information about scattering amplitudes than the corresponding dispersion relations (when they exist in the given case). Instead, the equation for the distinguished component of the state vector corresponding to the definite number of particles gives, of course in principle, all possible information about these particles.

The method of this paper may be extended to the general case of scattering transitions with a change of the number of particles: $\lambda(N_1) \rightarrow \lambda'(N_2)$ (cf. (5)).

* * *

I am extremely indebted to Professor W. PAULI and Professor R. JOST for the hospitality in E.T.H. in Zürich and for helpful discussions.

(5) W. KRÓLIKOWSKI: *A General Equation for Scattering Amplitudes* (to be published in *Acta Phys. Polon.*).

RIASSUNTO (*)

La presente nota contiene una derivazione di una relazione formalmente esatta in teoria del campo fra gli elementi della matrice S corrispondente a un dato numero di particelle. Tale relazione è simile nella forma all'equazione di Low, salvo l'eliminazione di tutti gli elementi della matrice S associati con differenti numeri di particelle meno uno. La derivazione di questa relazione è basata sull'equazione per una componente distinta del vettore di stato corrispondente a un dato numero di particelle. L'equazione generale di Low qui ottenuta contiene l'operatore di interazione del dato numero di particelle. Per ora, tale operatore può essere praticamente calcolato solo sviluppandolo in potenze della costante d'accoppiamento.

(*) Traduzione a cura della Redazione.

On the Viscous Fluid Model in Multiple Production of Mesons.

M. HAMAGUCHI

Institute of Theoretical Physics, Kyoto University - Kyoto, Japan

(ricevuto il 27 Marzo 1957)

Summary. — The viscous effects in the hydrodynamical description of multiple production of particles in high energy collisions are discussed quantitatively. The multiplicity of the particles and the angular distribution (mean plateau) in the laboratory frame of reference are numerically calculated, and these results are compared with those obtained by RÖZENTAL *et al.* It is also shown that the viscous coefficients can be roughly estimated by the comparison with experimental data.

1. — Introduction.

In a recent paper (¹) the multiple production of mesons has been discussed using the viscous fluid model. The basic assumption of this model is that the entropy of the total system is not conserved by the influence of viscosity during the hydrodynamical expanding process of the meson cloud surrounding the nucleons. The entropy distribution has a conspicuous increase in the extreme point of the fluid motion of the system, where the viscous effects are remarkable (discussed in I, Sect. 2). From the view point of the second law of thermodynamics, however, the maximum point of the entropy is deemed as the equilibrium state of the system. So, we believe that the above assumption is necessary for a true description of such phenomena. Our model is somewhat similar to Heisenberg's theory (²) in regard to the standpoint of the increase of the entropy of the system.

The developments of the above idea were already given in I. In this case, we have followed only the hydrodynamical expression in the centre of mass

(¹) M. HAMAGUCHI: *Nuovo Cimento*, **4**, 1242 (1956), hereafter referred to as I.

(²) W. HEISENBERG: *Zeits. f. Phys.*, **133**, 65 (1952).

system, but we shall transform here this expression into that of the laboratory frame of reference which is given in Sect. 3 of this paper.

At first, the limits of the application of the perturbation method with respect to the viscosity are given in detail in Sect. 2.

In Sect. 4, we set the scattering angle $\bar{\theta}_1$ in such a way that the meson shower produced by a nucleon-nucleon collision contains half the energy of the incident nucleon in the laboratory system, and calculate the so called «mean plateau» (Table I). The multiplicity of the particle is also given in Table I. From the above results, we see that the viscous effect has no such a large contribution that the effect is verified by the experiments. But, the energy and the scattering angle in flight of the greater part of the produced particles, which is at the maximum point of the particle distribution, are very sensitive to the viscosity (see Sect. 3).

If we are permitted to estimate the viscosity according to the kinetic gas theory, the ordinary viscous coefficient has generally a large value. As pointed out in Sect. 2, the order of magnitude of the viscous coefficient determined by our perturbation calculation is incompatible with that obtained by the usual gas theory for the (incident) energy region $10^5 \sim 10^7$ GeV. But, we pay attention to the fact that both methods on the different standpoints are compatible for the energy region lower than $10^{4.5}$ GeV.

In conclusion, we have determined the viscosity by the comparison with the experimental data for the energy region $10^5 \sim 10^7$ GeV (for example, mean plateau). We can report here the fact that this determination does not contradict the perturbation method.

2. – Preliminary.

In this section, we shall explain in full detail the limits of application of the perturbation method with respect to the viscous coefficients. From eqs. (51), (52) in I, the condition to assure the utility of the perturbation method is given as follows:

$$(1) \quad \left| \gamma \eta \left(\frac{E}{2MA} \right)^{3.541} \right| (*) < 1 \quad (c = 1),$$

where E is the energy of the incident nucleon in the laboratory frame of reference. As was shown in I, we also use the relation between transversal and longitudinal viscosities $\zeta \sim -2\eta$ ($\eta < 0$), and chose $|\epsilon_1^*/\epsilon_0^*|$ as the value of γ in the above expression. From the relation (1), we have for the incident energy

(*) The formalism given in I holds also for the transformation $\eta \rightarrow \gamma\eta$ without any modification.

$E = 10^5 \sim 10^7$ GeV

$$(2) \quad \begin{cases} |\gamma\eta| \leq 10^{-17}; & \text{for } E = 10^5 \text{ GeV}, \\ |\gamma\eta| \leq 10^{-24}; & \text{for } E = 10^7 \text{ GeV}, \end{cases}$$

respectively, where the atomic weight $A=1$ is assumed for the nucleon-nucleon collision.

Now, we shall estimate the values $|\varepsilon_1^*/\varepsilon_0^*|$ and $|\varepsilon_2^*/\varepsilon_0^*|$, in which ε_1^* , ε_2^* are restricted with eqs. (24'), (30) of I.

$$\begin{cases} \varepsilon_1^* > 2.12 \cdot \frac{1}{A^{0.47}} \cdot \frac{\xi^{1.13}}{t^{1.66}}, \\ \varepsilon_2^* > 0.5 \cdot \frac{1}{A^{0.155}} \cdot \frac{\xi^{1.845}}{t^{2.69}}. \end{cases}$$

Considering the case that the equations of motion were reduced under the condition $t \gg \xi \gg A$, the values of γ satisfy

$$(3) \quad \gamma = |\varepsilon_1^*/\varepsilon_0^*| \geq 10^{-31} \sim 10^{-32},$$

for the energy $E = 10^5 \sim 10^7$ GeV, respectively. On this occasion, we have used $\xi \sim 10A$, $t \sim 10000A$, A being the width of the meson cloud in Lorentz contraction. Hereafter, we shall use the value γ given by the above relation, because $|\varepsilon_2^*/\varepsilon_0^*|$ has a small value compared with that of (3). Substituting the relation given by the footnote (*) into the relation (2), the following relations are obtained,

$$|\gamma\eta_0| \leq \frac{1}{2.7} \cdot 10^{-20} \sim \frac{1}{2.7} \cdot 10^{-21},$$

(*) The viscous term in relativistic hydrodynamics has the expression,

$$\eta \frac{\partial v}{\partial x},$$

where v is the four-velocity. In order to rewrite the above expression into the viscous term in C.G.S. unit, we use the relation

$$v^1 = \frac{u/c}{\sqrt{1 - (u/c)^2}}.$$

As a result, η in our expression is written over as follows:

$$\eta = \eta_0 c \cdot (1 - u^2/c^2)^{\frac{3}{2}},$$

where η_0 and c are the viscosity expressed in C.G.S. units, and the light velocity, respectively. It is of interest to notice that if the Lorentz contraction $(1 - u^2/c^2)^{\frac{1}{2}} \approx A/a = \exp[-L] = \sqrt{2Mc^2/E}$ is used, the above relation becomes as follows:

$$\eta = \eta_0 c \cdot (2Mc^2/E)^{\frac{3}{2}}.$$

for $E = 10^5 \sim 10^7$ GeV, respectively. Moreover, if we insert (3) into the above relation, we have

$$(4) \quad \begin{cases} |\eta_0| \leq 4 \cdot 10^{10}; & \text{for } E = 10^5 \text{ GeV}, \\ |\eta_0| \leq 4 \cdot 10^7; & \text{for } E = 10^7 \text{ GeV}. \end{cases}$$

On the other hand, if we allow the use of the usual gas theory, the viscosity η_0^* is given by

$$\eta_0^* \approx m_\pi \cdot n \cdot \bar{u} \bar{l} = m_\pi \bar{u} / \sigma \quad (3),$$

where $\bar{u} \approx c$ in the conical scattering of the fluid motion, and $\sigma = 1/(n\bar{l})$ is the scattering cross-section which has $\pi \cdot (h/m_\pi c)^2 \approx 3.4 \cdot 10^{-26}$ cm² in the case of the strong $\pi\pi$ interactions. If we consider the meson cloud as the assembly of a boson gas, finally, we obtain

$$\eta_0^* \approx 2.4 \cdot 10^{11} \text{ dyne} \cdot \text{s/cm}^2,$$

where the mass of the meson $m_\pi = 2.7 \cdot 10^{-25}$ g.

It can't be helped that the above results are inconsistent with condition (4) obtained by the perturbation calculation. But we lay emphasis on the fact that our perturbation method is compatible with the results of the usual kinetic gas theory for the energy region of $E \leq 10^{4.5}$ GeV.

For the energy region considered in our present problem, $E = 10^5 \sim 10^7$ GeV, we shall then determine $\gamma\eta_0$ by comparison with the experiments.

3. - Physical quantities in the laboratory system.

3.1. Angular distribution. - As is well known, the transformation from the scattering angle θ in the centre of mass system (c-m-system) into $\bar{\theta}$ in the laboratory frame of reference (L-system) is given by the following relation,

$$(5) \quad \operatorname{tg} \bar{\theta} \approx \bar{\theta} = \frac{u_k \sqrt{1 - V^2} \cdot \sin \theta}{u_k \cdot \cos \theta + V},$$

u_k and V are the velocity of the particle in c-m-system, and the relative velocity between c-m-system and L-system, respectively. Analogously to Landau's method (4), we can write the relation,

$$(6) \quad u_k \cdot \cos \theta + V = 1 + \cos \theta + \frac{1}{2v_k^2},$$

(3) S. Z. BELENKIJ and L. D. LANDAU: *U. F. N.*, **56**, 309 (1955).

(4) L. D. LANDAU: *Izv. An. SSSR.* **17**, 51 (1953).

where v_k is the four velocity in free scattering of the particle in e-m-system.

Since the last term on the right side of eq. (6) can't be neglected for $(1 + \cos \theta)$ when θ is nearly equal π , we estimate this as follows:

$$\frac{1}{2v_k^2} \approx -2\gamma\eta \cdot \exp[7.082L] \cdot (1 + \cos \theta),$$

for reasons we shall make clear in our following discussions.

We have now to prove that the right hand side of eq. (6) under the above consideration of our arguments, in case of $\theta \approx \pi$, satisfies the condition,

$$(1 - 2\gamma\eta \cdot \exp[7.082L]) \cdot (1 + \cos \theta) \gg \frac{1}{2v_k^2}.$$

This relation is written over again as

$$(7) \quad \theta \gg \frac{1}{(1 - \gamma\eta \cdot \exp[7.082L])} \cdot \frac{1}{v_k}.$$

θ and v_k , used in (7), were already given by eqs. (43), (49) of I,

$$(43.I) \quad \theta \sim \exp[-\lambda] \cdot (1 - 3\gamma\eta \cdot \exp[7.082\lambda]),$$

$$(49.I) \quad v_k \sim \exp\left[-\frac{L}{6} + \lambda + \frac{1}{3}\sqrt{L^2 - \lambda^2}\right] \cdot \left(1 + 2\gamma\eta \cdot \exp[7.082\lambda] + \frac{\gamma\eta}{2}\sqrt{\frac{L-\lambda}{L+\lambda}} \cdot \exp[7.082\lambda] - \frac{3}{4}\gamma\eta \cdot \exp\left[4.416\lambda + \frac{4}{3}(2L - \sqrt{L^2 - \lambda^2})\right] + \frac{3}{2}\gamma\eta - \frac{9}{4}\gamma\eta \cdot \exp[6.082\lambda] + \gamma\eta \cdot \exp[7.082L]\right).$$

Inserting the above relations into the condition (7), we have

$$\begin{aligned} & \frac{1}{(1 - \gamma\eta \cdot \exp[7.082L])} \cdot \exp\left[\frac{L}{6} - \frac{1}{3}\sqrt{L^2 - \lambda^2}\right] \cdot \\ & \cdot \left(1 + \gamma\eta \cdot \exp[7.082\lambda] - \frac{\gamma\eta}{2}\sqrt{\frac{L-\lambda}{L+\lambda}} \cdot \exp[7.082\lambda] + \frac{3}{4}\gamma\eta \cdot \exp\left[4.416\lambda + \frac{4}{3}(2L - \sqrt{L^2 - \lambda^2})\right] - \frac{3}{2}\gamma\eta + \frac{9}{4}\gamma\eta \cdot \exp[6.082\lambda] - \gamma\eta \cdot \exp[7.082L]\right) \ll 1. \end{aligned}$$

We see that the left hand side in the above relation has the values $\sim \exp[-L/6]$ and ~ 1 when $\lambda = 0$ and $\lambda = \lambda_{\max}$ respectively. Now that the above condition holds for all the region of λ satisfying $\lambda < \lambda_{\max}$, we may proceed to the estimation of the last term in eq. (6).

Then, the transformation formula from the centre of mass system into the laboratory frame of reference becomes as follows:

$$(8) \quad \bar{\theta} = \frac{\sqrt{1 - V^2}}{(1 - 2\gamma\eta \cdot \exp[7.082L])} \cdot \operatorname{tg} \frac{\theta}{2}.$$

Now, we shall define $\operatorname{tg}(\theta/2)$ by the following relation in order to take into consideration the angle θ of order ~ 1 ,

$$(9) \quad \operatorname{tg} \frac{\theta}{2} = \frac{\exp[-\lambda] \cdot (1 + 3A \cdot \exp[7.082\lambda])}{1 + 3A},$$

where $A = -\gamma\eta$. As is seen in eq. (9), the angle for $\lambda \approx 0$ has $\theta \approx \pi/2$ which is a permissible maximum angle in c-m system. For the particle flying to the opposite direction in c-m system, we may substitute $\operatorname{tg}((\pi - \theta)/2)$ for $\operatorname{tg}(\theta/2)$ in eq. (8).

$$(9') \quad \operatorname{tg} \frac{\pi - \theta}{2} = \frac{1}{\operatorname{tg}(\theta/2)} = \frac{\exp[\lambda] \cdot (1 - 3A \cdot \exp[7.082\lambda])}{1 - 3A}.$$

Using the relation, $\sqrt{1 - V^2} = \exp[-L]$, we finally obtain the transformation formula between c-m system and L-system,

$$(10) \quad \bar{\theta} = \exp[-L - \lambda] \cdot \frac{(1 + 3A \cdot \exp[7.082 \cdot |\lambda|])}{1 - 3A} \cdot (1 + 2\gamma\eta \cdot \exp[7.082L]),$$

where $|\lambda|$ means the absolute value of λ , and λ, A have positive sign for the particle flying to the right side in c-m system and negative sign for the left side, respectively.

In this connection, we shall mention the scattering angle of the greater part of the produced particles in the L-system. Since the variable λ satisfying the above consideration was given by eq. (44) in I,

$$(44.I) \quad \lambda \approx \frac{L}{\sqrt{2}} \cdot \left\{ 1 + \frac{3\gamma\eta}{4} \cdot \left(-0.829 \cdot \frac{\exp[5.008L]}{L} + 2.933 \cdot \exp[5.008L] - 8.624 \cdot \exp[4.847L] \right) \right\},$$

we applied the above condition to eq. (10), and obtained

$$\bar{\theta} \approx \exp \left[-\frac{\sqrt{2} + 1}{\sqrt{2}} L \right] \cdot (1 + 2\gamma\eta \cdot \exp [7.082L]).$$

In the above expression, we have considered only the term of maximum contribution of viscous effects.

If we estimate the viscosity as follows,

$$(11) \quad \begin{cases} \gamma\eta \approx -(0.1 \div 0.9) \cdot 10^{-17}; & (E = 10^5 \text{ GeV}), \\ \dots \\ \gamma\eta \approx -(0.1 \div 0.9) \cdot 10^{-24}; & (E = 10^7 \text{ GeV}), \end{cases}$$

which is given in Table I, we have

$$(1 + 2\gamma\eta \cdot \exp [7.082L]) = \left[1 + 2\gamma\eta \cdot \left(\frac{E}{2} \right)^{3.541} \right] \approx \begin{cases} (0.9 \div 0.2); & E = 10^5 \text{ GeV}, \\ (0.9 \div 0.1); & E = 10^7 \text{ GeV}. \end{cases}$$

Therefore, we see that the scattering angle for the greater part of the produced particles is very sensitive to the viscosity.

3.2. Energy and particle distributions. — In this section, we ask for the expression of the energy in the laboratory frame of reference analogously to Landau's method.

The energy distribution in L-system is connected with that of c-m system by the relation,

$$(12) \quad m\bar{v}_k = \frac{mv_k + P_x \cdot V}{\sqrt{1 - V^2}},$$

where $m\bar{v}_k$, mv_k are the energy in the laboratory and the c-m systems respectively, and P_x is the momentum projected in the x -direction parallel to the trajectory of the incident nucleon in c-m system. In the extreme relativistic case, eq. (12) can be written as

$$m\bar{v}_k = mv_k \cdot (1 + \cos \theta) / \sqrt{1 - V^2},$$

by using $P_x \approx mv_k \cdot \cos \theta$. If we consider eq. (9), the above relation becomes

$$m\bar{v}_k = mv_k \cdot \exp [L] \cdot \frac{2}{1 + \exp [-2\lambda] \cdot (1 + 3A \cdot \exp [7.082\lambda])^2} \approx m\bar{v}_k \cdot \exp [L].$$

In this expression, we may consider that the above approximate transformation formula is valid, even if λ varies from 0 to L , provided that the following relations are satisfied:

$$0 < \exp[-2\lambda] < 1,$$

and

$$3A \cdot \exp[7.082\lambda] < 1,$$

which signifies the applicability of the condition of our perturbation method.

Under the same arguments as above, we obtain

$$m\bar{v}_k \approx mv_k \cdot \exp[L - \lambda],$$

in the flight of the particles into the direction of the left side in e-m system. Inserting these relations into (49) in I, we have for the energy distribution (L-system)

$$(13) \quad mv_k \sim M \cdot \exp \left[\frac{5}{6}L + \lambda + \frac{1}{3}\sqrt{L^2 - \lambda^2} \right] \cdot \left(1 + \gamma\eta \cdot \exp[7.082L] - \frac{9}{4}\gamma\eta \cdot \exp[6.082L] + \frac{3}{2}\gamma\eta + 2\gamma\eta \cdot \exp[7.082 \cdot |\lambda|] + \frac{\gamma\eta}{2} \sqrt{\frac{L - |\lambda|}{L + |\lambda|}} \cdot \exp[7.082 \cdot |\lambda|] - \frac{3}{4}\gamma\eta \cdot \exp \left[4.416 \cdot |\lambda| + \frac{3}{4}(2L - \sqrt{L^2 - \lambda^2}) \right] \right),$$

where λ has positive sign for the particles flying to the right side in e-m system, and negative sign for those flying to the left side, respectively.

In the next place, we shall discuss the particle distribution which is given by eq. (42) in I. For the benefit of the following calculation, we are content with the normalization constant of the non viscous term as a substitute for that of the particle distribution. This means that for the present there is no alternative except this method. If we expand the exponential distribution in the vicinity of the maximum point under the condition, $\int dN = N$, and use $N = KA \cdot \exp[L/2]$ (see (2.I), (46.I)), we obtain

$$(14) \quad dN = \frac{KA}{\sqrt{2\pi L}} \cdot \exp \left[-\frac{L}{2} + \sqrt{L^2 - \lambda^2} \right] \cdot \left(1 + \frac{3\gamma\eta}{2} \sqrt{\frac{L - |\lambda|}{L + |\lambda|}} \cdot \exp[7.082 \cdot |\lambda|] - \frac{9\gamma\eta}{4} \cdot \exp \left[4.416 \cdot |\lambda| + \frac{4}{3}(2L - \sqrt{L^2 - \lambda^2}) \right] \right) d\lambda,$$

where $|\lambda|$ means the absolute value of λ .

Under the same considerations as the above mentioned, we can obtain the normalization constant of the energy distribution (12), which is the same as the result obtained by LANDAU. In this case, we have used, $\int m\bar{v}_k \cdot dN = E$, as the conditional equation. Then, we have the energy distribution (L-system).

$$(13') \quad m\bar{v}_k = \frac{5\sqrt{5}}{2\sqrt{3}} \cdot \frac{M}{K} \cdot \exp \left[\frac{5}{6} L + \lambda + \frac{1}{3} \sqrt{L^2 - \lambda^2} \right] \cdot \\ \cdot \left(1 + \gamma\eta \cdot \exp [7.082L] - \frac{9}{4} \gamma\eta \cdot \exp [6.082L] + \frac{3}{2} \gamma\eta + 2\gamma\eta \cdot \exp [7.082 \cdot |\lambda|] + \right. \\ \left. + \frac{1}{2} \gamma\eta \left| \frac{L - |\lambda|}{L + |\lambda|} \right| \cdot \exp [7.082 \cdot |\lambda|] - \frac{3\gamma\eta}{4} \cdot \exp \left[4.416 \cdot |\lambda| + \frac{4}{3} (2L - \sqrt{L^2 - \lambda^2}) \right] \right).$$

In this connection, we shall discuss the viscous effects on the energy of the greater part of the produced particles. If we insert the condition (44.I) which satisfies the above consideration into eq. (13'), we obtain

$$m\bar{v}_k \approx Mc^2 \cdot \exp \left[\frac{8 + 5\sqrt{2}}{6\sqrt{2}} \cdot L \right] \cdot (1 + \gamma\eta \cdot \exp [7.082L]),$$

where the second term in the brackets signifies the maximum effect of the viscosity. Analogously to the method followed in the discussion of the angular distribution, we also adopt the relation (11) for the viscous coefficient. So, we have

$$m\bar{v}_k \approx Mc^2 \cdot \left(\frac{E}{2Mc^2} \right)^{(8+5\sqrt{2})/12\sqrt{2}} \cdot \left(1 + \gamma\eta \cdot \left(\frac{E}{2Mc^2} \right)^{3.541} \right),$$

and

$$\left(1 + \gamma\eta \cdot \left(\frac{E}{2Mc^2} \right)^{3.541} \right) \approx \begin{cases} (0.96 \sim 0.61); & E = 10^5 \text{ GeV}, \\ (0.95 \sim 0.53); & E = 10^7 \text{ GeV}. \end{cases}$$

From the above results, we can conclude the possibility that the above energy decreases in half the energy in non-viscous treatments by using the maximum viscosity inserted in Table I.

4. – Comparison with experiments.

In this section, we discuss the relations between the viscosity, the mean plateau, and the multiplicity of the produced particles. For this purpose, we shall rewrite the particle and the energy distributions, and the scattering angle into the parametric expression by means of the variable transformation

$\lambda \rightarrow L \cdot \delta$. Using the relation $L = \ln \sqrt{E/2}$ for eq. (14), we have

$$(A) \quad dN = \frac{K \sqrt{\ln(E/2)^{\frac{1}{2}}}}{\sqrt{2\pi}} \left\{ \left(\frac{E}{2}\right)^{-\frac{1+12+|\delta|}{2}} + \frac{3\gamma\eta}{2} \sqrt{\frac{1-|\delta|}{1+|\delta|}} \cdot \right. \\ \left. \cdot \left(\frac{E}{2}\right)^{-\frac{1}{4}+\frac{1}{2}\sqrt{1-\delta^2}+3\cdot541\cdot|\delta|} - \frac{9\gamma\eta}{4} \cdot \left(\frac{E}{2}\right)^{13/12-\frac{1}{6}\sqrt{1-\delta^2}+2\cdot208\cdot|\delta|} \right\} d\delta,$$

where $|\delta| = |\lambda|/L$ means the absolute value of δ , and $M = C - 1$. By the same method as the above, we obtain from eq. (13')

$$(B) \quad m\bar{v}_k = \frac{5\sqrt{5}}{2\sqrt{3}} \cdot \frac{1}{K} \cdot \left(\frac{E}{2}\right)^{5/12+\delta/2+\frac{1}{6}\sqrt{1-\delta^2}} \cdot \\ \cdot \left[1 + \gamma\eta \cdot \left(\frac{E}{2}\right)^{3.541} - \frac{9\gamma\eta}{4} \cdot \left(\frac{E}{2}\right)^{3.041} + 2\gamma\eta \cdot \left(\frac{E}{2}\right)^{3.541\cdot|\delta|} + \right. \\ \left. + \frac{\gamma\eta}{2} \sqrt{\frac{1-|\delta|}{1+|\delta|}} \cdot \left(\frac{E}{2}\right)^{3.541\cdot|\delta|} - \frac{3\gamma\eta}{4} \cdot \left(\frac{E}{2}\right)^{2.208\cdot|\delta|+\frac{2}{3}(2-\sqrt{1-\delta^2})} \right].$$

The scattering angle, given by eq. (10), becomes as follows:

$$(C) \quad \bar{\theta} = \left(\frac{E}{2}\right)^{-(1+\delta)/2} \cdot \frac{(1 + 2\gamma\eta \cdot (E/2)^{3.541} - 3\gamma\eta \cdot (E/2)^{3.541\cdot|\delta|})}{1 - 3\gamma\eta}.$$

We shall now determine $\delta_{\frac{1}{2}}$ satisfying the relation

$$\int_{\delta_{\frac{1}{2}}}^1 m\bar{v}_k \cdot dN / \int_{-1}^1 m\bar{v}_k \cdot dN = \frac{1}{2},$$

in which $m\bar{v}_k$ and dN are given by the above eqs. (A), (B). $\delta_{\frac{1}{2}}$ means a parameter corresponding to such an angle that it contains half the energy E . The above relation is written over as follows:

$$(D) \quad \left(1 + \gamma\eta \cdot \left(\frac{E}{2}\right)^{3.541} - \frac{9}{4} \gamma\eta \cdot \left(\frac{E}{2}\right)^{3.041} \right) \cdot \int_{\delta_{\frac{1}{2}}}^1 \left(\frac{E}{2}\right)^{(\delta/2)+\frac{1}{6}\sqrt{1-\delta^2}} \cdot d\delta + \\ + 2\gamma\eta \cdot \int_{\delta_{\frac{1}{2}}}^1 \left(1 + \sqrt{\frac{1-|\delta|}{1+|\delta|}} \right) \cdot \left(\frac{E}{2}\right)^{(\delta/2)+\frac{1}{6}\sqrt{1-\delta^2}+3.541\cdot|\delta|} d\delta - \\ - 3\gamma\eta \cdot \int_{\delta_{\frac{1}{2}}}^1 \left(\frac{E}{2}\right)^{\frac{5}{3}+(\delta/2)+2.208\cdot|\delta|} d\delta = \left(\frac{E}{2}\right)^{\frac{5}{3}} \cdot \frac{2\sqrt{6}\pi}{5\sqrt{5} \cdot \sqrt{\ln(E/2)^{\frac{1}{2}}}}.$$

TABLE I.

E (GeV)	$\delta_{\frac{1}{2}}$	$\gamma\eta$ $(\gamma > 0, \eta < 0)$	Half Angle (L-system) $\theta_{\frac{1}{2}}$	Mean Plateau (Experimental Value ~ 1.2 m)	Multiplicity N/N_L
10^6	0.52	0	$2.684 \cdot 10^{-4}$	4.026 m	$1 (N \approx 28, \text{ for } K=2)$
$2 \cdot 10^6$			$1.585 \cdot 10^{-4}$	2.378 m	
$4 \cdot 10^6$			$9.359 \cdot 10^{-5}$	1.404 m	
10^5	0.5	$0.113 \cdot 10^{-17}$	$2.696 \cdot 10^{-4}$	4.045 m	$1 + 2.26 \cdot 10^{-5}$
	0.45	$0.362 \cdot 10^{-17}$	$2.683 \cdot 10^{-4}$	4.024 m	$1 + 7.25 \cdot 10^{-5}$
	0.4	$0.546 \cdot 10^{-17}$	$2.693 \cdot 10^{-4}$	4.04 m	$1 + 1.09 \cdot 10^{-4}$
	0.35	$0.683 \cdot 10^{-17}$	$2.726 \cdot 10^{-4}$	4.09 m	$1 + 1.37 \cdot 10^{-4}$
	0.3	$0.787 \cdot 10^{-17}$	$2.773 \cdot 10^{-4}$	4.16 m	$1 + 1.58 \cdot 10^{-4}$
	0.25	$0.865 \cdot 10^{-17}$	$2.843 \cdot 10^{-4}$	4.27 m	$1 + 1.73 \cdot 10^{-4}$
	0.2	$0.925 \cdot 10^{-17}$	$2.939 \cdot 10^{-4}$	4.41 m	$1 + 1.85 \cdot 10^{-4}$
	0.15	$0.971 \cdot 10^{-17}$	$3.059 \cdot 10^{-4}$	4.59 m	$1 + 1.95 \cdot 10^{-4}$
	0.54	0	$6.946 \cdot 10^{-6}$		$1 (N \approx 90, \text{ for } K=2)$
	0.5	$0.372 \cdot 10^{-24}$	$5.753 \cdot 10^{-6}$		$1 + 7.65 \cdot 10^{-6}$
10^7	0.45	$0.541 \cdot 10^{-24}$	$5.989 \cdot 10^{-6}$		$1 + 1.11 \cdot 10^{-5}$
	0.4	$0.582 \cdot 10^{-24}$	$7.924 \cdot 10^{-6}$		$1 + 1.2 \cdot 10^{-5}$
	0.35	$0.681 \cdot 10^{-24}$	$8.532 \cdot 10^{-6}$		$1 + 1.4 \cdot 10^{-5}$
	0.3	$0.751 \cdot 10^{-24}$	$9.252 \cdot 10^{-6}$		$1 + 1.54 \cdot 10^{-5}$
	0.25	$0.803 \cdot 10^{-24}$	$1.011 \cdot 10^{-5}$		$1 + 1.65 \cdot 10^{-5}$
	0.2	$0.839 \cdot 10^{-24}$	$1.120 \cdot 10^{-5}$		$1 + 1.72 \cdot 10^{-5}$

The applicable regions of the perturbation theory are given by

$$|\gamma\eta| \leq 10^{-17}; \quad \text{for } E = 10^6 \text{ GeV},$$

$$|\gamma\eta| \leq 10^{-24}; \quad \text{for } E = 10^7 \text{ GeV},$$

respectively.

By a suitable estimation of $\gamma\eta$ for the energy region $E = 10^5 \sim 10^7$ GeV, we can obtain $\delta_{\frac{1}{2}}$ satisfying the above condition (D).

For the special case, $\gamma\eta = 0$, we have

$$\delta_{\frac{1}{2}} = \begin{cases} 0.52; & \text{for } E = 10^5 \text{ GeV}, \\ 0.54; & \text{for } E = 10^7 \text{ GeV}, \end{cases}$$

which is somewhat different from that obtained by ROZENTAL *et al.* (5). This difference may depend on the accuracy of numerical calculation. By the way, the domain of δ in our calculation has been devided into fourty sections.

Table I shows the relations between $\delta_{\frac{1}{2}}$ and $\gamma\eta$ for the energy $E = 10^5 \sim 10^7$ GeV. No parts, which disagree with the limit of application of our theory, are inserted in this Table.

Substituting these values $\delta_{\frac{1}{2}}, \gamma\eta$ into the relation (C), we obtain the angle $\bar{\theta}_{\frac{1}{2}}$ and show this in the fourth column of the Table.

We shall now assume that the meson showers are produced in depth of the order ~ 100 g/cm². This altitude is 15 km distant from the position detected by HAZEN *et al.* (6). Then, we obtain the Table of mean plateau under the consideration of the above circumstance.

From the Table I, we see that the viscosity has such a little effect that the difference of the mean plateau can not be discriminated by the experiments.

Table I shows also the value of plateau for twice and fourfold the energy, in the case of $\delta_{\frac{1}{2}} = 0.52, \gamma\eta = 0$.

Considering that the mean plateaus have a little change in spite of the large fluctuation of the viscosity, it might be permitted to suppose $-\gamma\eta \approx (0.1 \sim 0.09) \cdot 10^{-17}$ for the energy $E = 10^5$ GeV.

Moreover, the multiplicity of the produced particles is given in the last column of the Table, in which N and N_L correspond to the produced particle number in our model and that in Landau's one $\gamma\eta = 0$, respectively.

5. - Discussions and conclusions.

We have seen in Table I that $\delta_{\frac{1}{2}}$ grows gradually downwards as the viscosity increases. Since the former and the latter bring on the increasing and the decreasing effects respectively for the angle $\bar{\theta}$ in relation (C), $\bar{\theta}$ has

(5) I. L. ROZENTAL and D. S. ČERNAVSKIJ: *U. F. N.*, **52**, 185 (1954). They had obtained, $\delta_{\frac{1}{2}} = 0.54 \sim 0.55$, for the same energy region.

(6) W. E. HAZEN: *Phys. Rev.*, **85**, 455 (1952); W. E. HAZEN, R. E. HEINEMAN and E. S. LENNOX: *Phys. Rev.*, **86**, 198 (1952).

a minimum value $2.683 \cdot 10^{-4}$ at $\delta_{\frac{1}{2}} = 0.45$ ($-\gamma\eta = 0.36 \cdot 10^{-17}$), and afterward increases in its value. Also, the mean plateau traces the same inclination as the above mentioned. But, it is worth while to notice that the mean plateau has roughly a value $\sim 4m$ for $E = 10^5$ GeV in spite of the fluctuation of the viscous coefficient. So to speak, this means that the viscosity has not a remarkable effect for the mean plateau.

The value of the plateau for twice the above energy is nearly equal to the experimental value.

From the last column of the Table, we see that the viscous effects are also very negligible for the multiplicity of the produced particles.

But, as pointed out in Sect. 3'1, 3'2, the scattering angle and the energy of the greater part of the produced particles are very sensitive to the viscosity. Therefore, we may think that the viscous coefficients obtained by us are determined more exactly provided that these above quantities are detected by the experiments.

In Sect. 2, we have expressed the relation between the kinetic gas theory and our perturbation calculation in respect to the viscosity, and emphasized that both results are consistent for the energy region $E \leq 10^{4.5}$ GeV, which may depend on the technique of our perturbation calculation. But, it will be a general tendency of the perturbation method that such bounds appear customary. In conclusion, this fact does not always mean that the statistical model of the elementary particles can not be used in a wholesale way for our present energy region.

We have treated here the case for Reynolds number $R > 1$, which signifies the ratio of the effect of inertia and the viscous effect in relativistic hydrodynamics, according to the perturbation method. The treatments under the circumstance satisfying $R \leq 1$ (?) still have not been given by reason of the unavoidable difficulty of treating the differential equation in relativistic hydrodynamics.

* * *

Finally, the author wishes to express his appreciation to Profs. H. YUKAWA and T. INOUE for their continuous interest in this work. He is also much indebted to Miss K. UEMURA for her numerical calculations. And this work was performed under the financial aid of the « Yukawa Yomiuri Fellowship ».

(?) M. HAMAGUCHI: *Progr. Theor. Phys.*, **15**, 588 (1956). A different attempt to attack this problem was given.

RIASSUNTO (*)

Si discutono quantitativamente gli effetti viscosi nella descrizione idrodinamica della produzione multipla delle particelle nelle collisioni di alta energia. Si calcolano numericamente la molteplicità delle particelle e la distribuzione angolare (plateau medio) nel sistema del laboratorio, e questi risultati si confrontano con quelli ottenuti da ROZENTAL *et al.* Si dimostra anche che i coefficienti di viscosità si possono grossolanamente valutare per confronto coi dati sperimentali.

(*) *Traduzione a cura della Redazione.*

**On the Relation between the Lee Model
and Ordinary Meson Theory.**

G. F. DELL'ANTONIO

*Istituto di Scienze Fisiche dell'Università - Milano
Istituto Nazionale di Fisica Nucleare - Sezione di Milano*

F. DUIMIO (*)

*C.E.R.N. Theoretical Study Division at the Institute for Theoretical Physics
University of Copenhagen*

(ricevuto il 28 Marzo 1957)

Summary. — Some features of a possible generalization of the Lee-model are examined. It is shown that it can be considered as an approximation of the neutral scalar meson theory with fixed sources, obtained by introducing a cut-off on the total energy of the mesons.

1. — Introduction.

The simple model of a renormalizable field theory proposed by T. D. LEE ⁽¹⁾ has raised much discussion. In particular, by analyzing its mathematical aspects PAULI and KÄLLÉN ⁽²⁾ have emphasized the existence of a critical value g_{cr} of the renormalized coupling constant g in connection with the shape of the cut-off function. If $g > g_{cr}$, one obtains typical consequences such as non-hermiticity of the Hamiltonian and the appearance of «ghosts», and not even the introduction of an indefinite metric makes it possible to construct a satisfactory theory (for example the S -matrix is not unitary in this case). When there is no cut-off, then $g_{cr} = 0$, i.e. for any value of $g \neq 0$ one gets

(*) On leave of absence from the Istituto di Scienze Fisiche dell'Università, Milano.

(¹) T. D. LEE: *Phys. Rev.*, **95**, 1329 (1954).

(²) G. KÄLLÉN and W. PAULI: *Dan. Mat. Fys. Medd.*, **30**, no. 7 (1955).

a theory with these unpleasant features. On the other hand, it is well known that a scalar neutral meson theory with fixed nucleons is renormalizable and exactly soluble, both with and without cut-off.

The aim of this paper is to examine whether the Lee model can be regarded as a kind of approximation of the neutral scalar theory, to look for the possibility of further approximations, and to study their limits of applicability.

First of all we notice that the one-nucleon problem in the Tamm-Dancoff approximation (0-meson and 1-meson states taken into account) is very similar to the one-V-particle problem of the Lee model. The difference consists in the fact that, in the TD case, the nucleon in a 1-meson state is regarded as identical with the nucleon in a 0-meson state, whereas in the Lee case they are looked upon as different particles (V and N); consequently the renormalization proceeds differently in the two cases. In both cases, however, one may regard these theories as derived from the neutral scalar theory, with a cut-off on the allowed numbers of mesons, independent of a possible «normal» cut-off on meson frequencies. Now, we can look for the next approximations, i.e. for extended Lee models related to the original one as the higher TD approximations are to the first.

We would like to remark in this connection that these «Lee approximations» of the one-nucleon problem may have a better chance than TD approximations of having a physical meaning (we use this word in a rather vague sense, principally due to the vague hope that a neutral scalar theory may somehow give useful suggestions on the behaviour of a «true» meson theory). Namely we suppose a nucleon which «cannot» emit mesons to be of a nature somewhat different from a nucleon which «can».

There are two essential possibilities for these approximations:

- a) an introduction of a cut-off on frequencies, and a cut-off on the meson number, independent of each other;
- b) introduction of a cut-off of a more general type which acts both on frequencies and on the meson number.

HABER-SCHAIM and THIRRING (3) have investigated an approach of the *a*) type which, already in the 2-meson approximation, gives very complicated formal equations. However, they worked with a symmetrical pseudo-scalar theory.

A simple theory of the *b*) type follows from the introduction of an energy cut-off. This theory is essentially an approximation of the neutral scalar theory with fixed sources, obtained cutting-off the states in which the total

(3) U. HABER-SCHAIM and W. THIRRING: *Nuovo Cimento*, **1**, 100 (1955).

energy of the mesons is greater than a fixed value. In such a way we impose an upper limit to the frequencies of each meson and at the same time, due to the finiteness of the rest-mass of the mesons, to their number.

The cut-off functions will therefore depend not only on the frequency of the meson which performs the transition (emission or absorption), but also on the total energy of the other mesons in the state.

2. - General formalism.

Let us consider the Hamiltonian

$$(1) \quad \begin{cases} H = H_0 + H_{\text{int}}, \\ H_0 = \sum_i M_i \sum_{p_i} a_i^*(\mathbf{p}_i) a_i(\mathbf{p}_i) + \sum_k b^*(\mathbf{k}) b(\mathbf{k}), \\ H_{\text{int}} = -\frac{1}{\sqrt{v}} \sum_i g_{0i} \sum_{p_i=p_{i+1}+k} [2\omega(k)]^{-\frac{1}{2}} \{f(\Omega) a_i(\mathbf{p}_i) a_{i+1}^*(\mathbf{p}_{i+1}) b^*(\mathbf{k}) + \text{e.c.}\}, \end{cases}$$

where $b(\mathbf{k})$ and $b^*(\mathbf{k})$ are absorption and emission operators of mesons (π) with momentum \mathbf{k} and mass μ . $\omega(\mathbf{k}) = (\mu^2 + \mathbf{k}^2)^{\frac{1}{2}}$. Everywhere we put $\hbar = c = 1$. $a_i(\mathbf{p})$ and $a_i^*(\mathbf{p})$ are absorption and emission operators of « i -nucleons » N_i , with mass M_i . They satisfy the commutation relations

$$(2) \quad \begin{cases} [b(\mathbf{k}), b^*(\mathbf{k}')] = \delta_{\mathbf{k}, \mathbf{k}'}, & \{a_i(\mathbf{p}), a_j^*(\mathbf{p}')\} = \delta_{ij} \delta_{\mathbf{p}, \mathbf{p}'}, \\ [b(\mathbf{k}), b(\mathbf{k}')] = [b(\mathbf{k}), a_i(\mathbf{p})] = \{a_i(\mathbf{p}), a_j(\mathbf{p}')\} = \dots = 0, & \end{cases}$$

g_{0i} are the unrenormalized coupling constants for the transitions $N_i \rightleftarrows N_{i+1} + \pi$.

For the sake of simplicity we hereafter make the assumption that all g_{0i} are equal to a given g_0 , and all M_i equal to a given M (*).

The energy cut-off operator $f(\Omega)$ is a given function of the operator $\Omega = \sum_k \omega(k) b^*(\mathbf{k}) b(\mathbf{k})$ total energy of the mesons, such that

$$f(\Omega) |\Omega'\rangle = f(\Omega') |\Omega'\rangle$$

for every state $|\Omega'\rangle$ satisfying $\Omega |\Omega'\rangle = \Omega' |\Omega'\rangle$.

(*) No essential change in the results would derive from the supposition that all M_i can be different, but fulfill the conditions $M_i < M_{i+1} + \mu$. Otherwise we should be faced with a problem of unstable particles. This case, in the context of the Lee model, has been examined by GLASER and KÄLLÉN ().

(⁴) O. GLASER and G. KÄLLÉN: *Nucl. Phys.*, **2**, 706 (1957).

As it can be easily verified, the operators

$$(3) \quad \left\{ \begin{array}{l} Q_1 = \sum_i i \sum_{p_i} a_i^*(\mathbf{p}_i) a_i(\mathbf{p}_i) - \sum_k b^*(\mathbf{k}) b(\mathbf{k}) \\ Q_2 = \sum_i \sum_{p_i} a_i^*(\mathbf{p}_i) a_i(\mathbf{p}_i), \end{array} \right.$$

commute with the total Hamiltonian. They are therefore constants of motion.

We shall consider as physical states the states with $Q_1 = 0$. For example, if we have a physical state with one nucleon and j mesons, the nucleon must be denoted by N_j . So the Hilbert space of our physical states, \mathcal{H}_0 , will be the subspace of the total Hilbert space \mathcal{H} , spanned by the eigenstates of H_0 , belonging to the eigenvalue 0 of the operator Q_1 . These eigenstates will be denoted in an occupation number representation by symbols such as ⁽⁵⁾

$$(4) \quad |\{n_p^{(0)}\}_\alpha, \{n_p^{(1)}\}_\beta \dots \{n_k\}_i\rangle,$$

which expresses that α N_0 -nucleons, β N_1 -nucleons ..., i mesons with given momenta are present in the state. They form a complete orthonormal system in \mathcal{H} .

Following the renormalization custom, we introduce:

- a) Mass renormalization terms of the form $= \delta M_i \sum_{p_i} a_i^*(\mathbf{p}_i) a_i(\mathbf{p}_i)$.
- b) Renormalized field operators

$$(5) \quad a'_i(\mathbf{p}_i) = a_i(\mathbf{p}_i)/C_i.$$

- c) Renormalized coupling constants g_i^r related to g_0 by

$$(6) \quad g_i^r = C_i C_{i+1} Z_i g_0.$$

The eigenstates of the total Hamiltonian \bar{H} (including mass renormalization terms) with $Q_1 = 0$ describe physical « clothed » states. They can be expressed as linear combinations of states (4). For example the physical « clothed » single nucleon state $|N_0\rangle$ can be developed in the following way ⁽⁵⁾:

$$(7) \quad |N_0\rangle = D_0 \left\{ |N_0\rangle + \sum_1^\infty \varphi_0^{(j)} [\{n_k\}_j] |N_j \{n_k\}_j\rangle \right\}.$$

⁽⁵⁾ We use notations similar to those used in the paper by Th. W. RUIJGROK and L. VAN HOVE: *Physica*, **22**, 880 (1956).

This particular state has to satisfy the equation

$$(8) \quad \bar{H}|\mathbf{N}_0\rangle = M|\mathbf{N}_0\rangle.$$

That is, the state $|\mathbf{N}_0\rangle$ has to be eigenstate of \bar{H} , with eigenvalue M , the « experimental » mass.

All the other eigenstates of \bar{H} , with $Q_1 = 0$, and eigenvalues ranging from $M - \mu$ to ∞ , with proper boundary conditions will describe scattering states.

In accord with our assumptions a state $|\mathbf{N}_i\rangle$, with $i \neq 0$, satisfying the equation

$$\bar{H}|\mathbf{N}_i\rangle = M_i|\mathbf{N}_i\rangle,$$

has no physical meaning because it belongs to a subspace \mathcal{H} , of the total Hilbert space \mathcal{H} , with eigenvalue of $Q_1 \neq 0$. But a state of the form $b^*(\mathbf{k}_1) \dots b^*(\mathbf{k}_i) |\mathbf{N}_i\rangle$, having $Q_1 = 0$ should have a physical meaning: it should represent a state compound of a clothed nucleon plus i free mesons (obviously it is not an eigenstate of \bar{H}), something which we might call an asymptotic physical state (*).

As it will appear from the following, where we shall use only special forms of the cut-off function, it is useful to redefine such asymptotic states as states $|\mathbf{N}_i\{\mathbf{n}'_{\mathbf{k}}\}_i\rangle_{as}$ obtained by applying i creation operators of mesons to a state which is solution of the equation (*)

$$(9) \quad \bar{H}[\{\mathbf{n}'_{\mathbf{k}}\}_i]|\mathbf{N}_i\rangle = M|\mathbf{N}_i\rangle,$$

where $\bar{H}[\{\mathbf{n}'_{\mathbf{k}}\}_i]$ is the total Hamiltonian with the cut-off operator $f(\Omega + \Omega'[\{\mathbf{n}'_{\mathbf{k}}\}_i])$ instead of $f(\Omega)$, $\Omega'[\{\mathbf{n}'_{\mathbf{k}}\}_i]$ being the total energy of the free mesons in the state $|\mathbf{N}_i\{\mathbf{n}'_{\mathbf{k}}\}_i\rangle_{as}$.

The equations (8) and (9) are sufficient to determine the quantities δM_i ; and the coefficients of the development of $|\mathbf{N}_0\rangle$ and of $|\mathbf{N}_i\rangle$

$$(10) \quad |\mathbf{N}_i\rangle = D_i[\{\mathbf{n}'_{\mathbf{k}}\}_i] \left\{ |\mathbf{N}_i\rangle + \sum_1^\infty \varphi_i^{(j)}[\{\mathbf{n}'_{\mathbf{k}}\}_i; \{\mathbf{n}_{\mathbf{k}}\}_j] |\mathbf{N}_{i+j}\{\mathbf{n}_{\mathbf{k}}\}_j\rangle \right\}.$$

We notice again that $|\mathbf{N}_i\rangle$ in itself has no physical meaning; only the state $|\mathbf{N}_i\{\mathbf{n}'_{\mathbf{k}}\}_i\rangle_{as}$ has the just described physical meaning of an asymptotic state.

(*) We use the word « asymptotic » in a sense similar to the one it has in the papers by L. VAN HOVE: *Physica*, 21, 901 (1955); 22, 343 (1956) or H. EKSTEIN: *Nuovo Cimento*, 4, 1017 (1956).

(**) More care should be taken in defining asymptotical states with more than one nucleon, but we don't need them for our purposes.

In order to determine the renormalization quantities C_i , D_i , and Z_i we impose the following conditions:

$$(11) \quad \langle 0 | a'_i | N_i \rangle = 1 \quad (\text{field operators renormalization})$$

$$(12) \quad \langle N_i | N_i \rangle = 1 \quad (\text{normalization})$$

$$(13) \quad g_i^r f[\mathcal{Q}'(\{n'_k\}_i) + \omega] = \\ = g_0 \langle N_{i+1} | b(\mathbf{k}) \sum_j \sum_{\mathbf{p}_j = \mathbf{p}_{i+1} + \mathbf{k}} f[\mathcal{Q}'(\{n'_k\}_i) + \mathcal{Q}] a_j(\mathbf{p}_j) a_{j+1}^*(\mathbf{p}_{j+1}) b^*(\mathbf{k}) | N_i \rangle \\ (\text{charge renormalization}).$$

Conditions (11) gives immediately $D_i = C_i$.

From the definition of $|N_i\rangle$ it is evident that the C_i and the $q_i^{(j)}$, for $i \neq 0$, are functions of the energy of the mesons present in the complete asymptotical state. As a consequence, if g_0 is a constant, the g_i^r , $i \neq 0$ will also be functions of the energy of the mesons.

The equations (8), (9) can be solved exactly. Omitting the lengthy but trivial calculations, we quote the results:

$$(14) \quad q_i^{(j)}[\{n'_k\}_i; \{n_k\}_i] = \prod_{k=1}^s \frac{g_0}{(2v)^k} (\omega_k!)^{-1} \{ \omega^{-1}(k) f[\mathcal{Q}'(\{n'_k\}_i) + \mathcal{Q}'(\{n_k\}_i)] \},$$

where the symbol \prod^s means symmetrized product. For example:

$$q_1^{(2)}[\omega_0; \omega_1 \omega_2] = \begin{cases} \frac{g_0^2}{2v} \frac{1}{2\omega_1^{\frac{3}{2}} \omega_2^{\frac{3}{2}}} f(\omega_0 + \omega_1 + \omega_2)[f(\omega_0 + \omega_1) + f(\omega_0 + \omega_2)], & \text{for } \omega_1 \neq \omega_2, \\ \frac{g_0}{2v} \frac{1}{2^{\frac{3}{2}} \omega_1^{\frac{3}{2}}} f(\omega_0 + 2\omega_1) f(\omega_0 + \omega_1), & \text{for } \omega_1 = \omega_2, \end{cases}$$

$$(15) \quad \delta M_i[\{n'_k\}_i] = -\frac{g_0^2}{2v} \sum_k f^2[\mathcal{Q}'(\{n'_k\}_i) + \omega]/\omega^2.$$

From (12)

$$(16) \quad C_i^{-2}[\{n'_k\}_i] = 1 + \frac{g_0^2}{2v} \sum_k f^2[\mathcal{Q}'(\{n'_k\}_i) + \omega]/\omega^3 + \frac{1}{2} \frac{g_0^4}{(2v)^2} \cdot$$

$$\cdot \sum_k \sum_{k'} \frac{1}{4} \frac{1}{\omega^3 \omega'^3} f^2[\mathcal{Q}'(\{n'_k\}_i) + \omega + \omega'] \{ [f[\mathcal{Q}'(\{n'_k\}_i) + \omega] + f[\mathcal{Q}'(\{n'_k\}_i) + \omega']]^2 + \dots \}.$$

and from (13)

$$(17) \quad Z_i[\{n'_k\}_i; \omega] = 1 + \frac{g_0^2}{2v} \sum_{k'} \frac{1}{\omega'^3} f^2[\mathcal{Q}'(\{n'_k\}_i) + \omega + \omega'] \cdot \\ \cdot [f[\mathcal{Q}'(\{n'_k\}_i) + \omega'] f^{-1}[\mathcal{Q}'(\{n'_k\}_i) + \omega] + \dots].$$

3. – One-meson case.

As a first simple example we consider the case in which the cut-off function has the form $f(x) = \theta(2\mu - x)$.

The function $\theta(y)$ is the step function equal to 1 for $y > 0$ and to 0 for $y < 0$ (*).

We are now in the case considered by LEE, but with our particular cut-off function. One obtains immediately (using $\theta^2 = \theta$)

$$(18) \quad \varphi_0^{(1)}(\omega) = \frac{g_0}{(2v)^{\frac{1}{2}}} \theta(2\mu - \omega)/\omega^{\frac{1}{2}},$$

$$(19) \quad \varphi_i^{(j)} = 0 \quad \text{for } i + j \geq 2$$

$$(20) \quad \delta M_0 = -\frac{g_0^2}{2v} \sum_k \theta(2\mu - \omega)/\omega^2,$$

$$(21) \quad C_0^{-2} = 1 + \frac{g_0^2}{2v} \sum_k \theta(2\mu - \omega)/\omega^3,$$

$$(22) \quad C_i = 1 \quad \text{for } i \geq 1,$$

$$(23) \quad Z_i = 1 \quad \text{for all } i$$

The expectation value of the operator $\sum_k b^*(\mathbf{k})b(\mathbf{k})$, number of mesons in the state $|N_0\rangle$, must obviously be less than 1. We can write the inequality

$$(24) \quad 0 \leq \langle N_0 | \sum_k b^*(\mathbf{k})b(\mathbf{k}) | N_0 \rangle = C_0^{-2} \frac{g_0^2}{2v} \sum_k \theta(2\mu - \omega)/\omega^3 \leq 1.$$

From (21) and (24) follow the well known results that the value of C_0 must lie between 0 and 1, and that there is an upper limit for $g_0' = C_0 C_0 Z_0 g_0 = C_0 g_0$,

(*) To avoid the troubles pointed out by PAULI and KÄLLÉN (2) (p. 11, footnote) we can use a function $\theta'(y)$ of the form

$$\theta'(y) = \begin{cases} 1, & \text{for } y > 0, \\ \delta g(y), & \text{for } y < 0, \end{cases}$$

with $0 < \delta \ll 1$ and $g(y)$ a continuous function tending to 0 faster than $1/y$ as $y \rightarrow \infty$. So all the relations involving the function $\theta(y)$ which appear in the following, are to be considered approximate relations obtained, dropping all terms involving $\delta g(y)$, or powers of it.

given by

$$(25) \quad g_{0\text{crit.}}^r = \left\{ \frac{1}{2v} \sum_k \theta(2\mu - \omega)/\omega^3 \right\}^{-\frac{1}{2}}.$$

for $g_0^r > g_{0\text{crit.}}^r$ one obtains the inconsistencies pointed out by PAULI and KÄLLÉN.

4. – Two-meson case.

We are now going to consider the case in which

$$f(x) = \theta(3\mu - x).$$

The general results (14)–(17) assume the form:

$$(26) \quad \begin{cases} \varphi_0^{(1)}(\omega) = \frac{g_0}{(2v)^{\frac{1}{2}}} \theta(3\mu - \omega)/\omega^{\frac{3}{2}}, \\ \varphi_1^{(1)}(\omega_0; \omega) = \frac{g_0}{(2v)^{\frac{1}{2}}} \theta(3\mu - \omega_0 - \omega)/\omega^{\frac{3}{2}}, \\ \varphi_0^{(2)}(\omega_1\omega_2) = \begin{cases} \frac{g_0^2}{2v} \frac{1}{2\omega_1^{\frac{3}{2}}\omega_2^{\frac{3}{2}}} \theta(3\mu - \omega_1 - \omega_2)[\theta(3\mu - \omega_1) + \theta(3\mu - \omega_2)], & \text{for } \omega_1 \neq \omega_2, \\ \frac{g_0^2}{2v} \frac{1}{2^{\frac{1}{2}}\omega_1^3} \theta(3\mu - 2\omega_1)\theta(3\mu - \omega_1), & \text{for } \omega_1 = \omega_2, \end{cases} \\ \varphi_i^{(0)} = 0, \quad \text{for } i + j \geq 3. \end{cases}$$

$$(27) \quad \begin{cases} \delta M_0 = -\frac{g_0^2}{2v} \sum_k \theta(3\mu - \omega)/\omega^2, \\ \delta M_1(\omega_0) = -\frac{g_0^2}{2v} \sum_k \theta(3\mu - \omega_0 - \omega)/\omega^2, \\ \delta M_i = 0, \quad \text{for } i \geq 2, \end{cases}$$

$$(28) \quad \begin{cases} C_0^{-2} = 1 + \frac{g_0^2}{2v} \sum_k \theta(3\mu - \omega)/\omega^3 + \\ \quad + \frac{1}{2} \frac{g_0^4}{(2v)^2} \sum_k \sum_{k'} \frac{1}{4} \frac{1}{\omega^3 \omega'^3} \theta(3\mu - \omega - \omega')[\theta(3\mu - \omega) + \theta(3\mu - \omega')]^2, \\ C_1^{-2}(\omega_0) = 1 + \frac{g_0^2}{2v} \sum_k \theta(3\mu - \omega_0 - \omega)/\omega^3, \\ \quad C_i = 1, \quad \text{for } i \geq 2, \end{cases}$$

$$(29) \quad \left\{ \begin{array}{l} Z_0(\omega) = 1 + \frac{g_0^2}{2v} \sum_k \frac{1}{\omega'^3} \theta^{-1}(3\mu - \omega) \theta(3\mu - \omega') \theta(3\mu - \omega - \omega') = \\ \qquad \qquad \qquad = 1 + \frac{g_0^2}{2v} \sum_k \theta(3\mu - \omega - \omega')/\omega'^3 = C_1^{-2}(\omega) \quad (*) , \\ Z_i = 1, \end{array} \right. \quad \text{for } i \geq 1.$$

The impositions on the expectation value of the number of mesons give for the state $|N_1\rangle$

$$(30) \quad 0 \leq \langle N_1 | \sum_k b^*(\mathbf{k}) b(\mathbf{k}) | N_1 \rangle = C_1^2(\omega_0) \frac{g_0^2}{2v} \sum_k \theta(3\mu - \omega_0 - \omega)/\omega^3 \leq 1 .$$

We have now

$$g_1^r(\omega_0) = C_1(\omega_0) g_0 ,$$

from (30) we obtain a limitation to the values of

$$(31) \quad g_1^r(\omega_0) \leq \left\{ \frac{1}{2v} \sum_k \theta(3\mu - \omega_0 - \omega)/\omega^3 \right\}^{-\frac{1}{2}} = g_{1\text{crit}}^r(\omega_0) ,$$

for the state $|N_0\rangle$ we have the condition

$$(32) \quad 0 \leq \langle N_0 | \sum_k b^*(\mathbf{k}) b(\mathbf{k}) | N_0 \rangle = C_0^2 \left\{ \frac{g_0^2}{2v} \sum_k \theta(3\mu - \omega)/\omega^3 + \right. \\ \left. - \frac{g_0^4}{(2v)^2} \sum_k \sum_k \frac{1}{4} \frac{1}{\omega^3 \omega'^3} \theta(3\mu - \omega - \omega') [\theta(3\mu - \omega) + \theta(3\mu - \omega')]^2 \right\} \leq \\ \leq 2 - C_0^2 \frac{g_0^2}{2v} \sum_k (3\mu - \omega)/\omega^3 .$$

It is identical to the condition $0 \leq C_0^2 \leq 1$. When it is satisfied, pathological states are excluded.

5. – Concluding remarks.

Further, it is possible to consider cases in which an increasing number of mesons are taken into account, assuming

$$f(x) = \theta(n\mu - x) ,$$

(*) This equality $Z_i = C_{i+1}^{-2}$ presents itself also in the model of Ruijgrok and Van Hove (5).

when $n \rightarrow \infty$, $f(x) \rightarrow 1$, i.e. the operator $f(\Omega)$ becomes the identity operator. The upper limit of the allowed energies of the mesons is shifted to infinity.

The results (14)–(17) assume the form

$$(33) \quad \left\{ \begin{array}{l} \varphi_1^{(j)}[\{n'_k\}_i; \{n_k\}_j] = \prod_i^r \frac{g_0}{(2v)^{\frac{1}{2}}} (n_k!)^{-\frac{1}{2}} \omega^{-\frac{1}{2}}(k), \\ \delta M_i[\{n'_k\}_i] = -\frac{g_0^2}{2v} \sum_k \frac{1}{\omega^2}, \\ C_i^{-2}[\{n'_k\}_i] = \exp \left[\frac{g_0^2}{2v} \sum_k \frac{1}{\omega^3} \right], \\ Z_i[\{n'_k\}_i; \omega] = \exp \frac{g_0^2}{2v} \sum_k \frac{1}{\omega^3}. \end{array} \right.$$

All these quantities become independent of $\{n_k\}$, and i and coincide with the quantities $\varphi^{(j)}[\{n_k\}]$, δM , C , and Z obtained from the neutral scalar meson theory with point sources.

This supports our initial assertion that our theory can be considered as an approximation of the neutral scalar theory obtained, taking into account only states in which the mesons have an energy less than a fixed value (this is due to the choice of the step function for the $f(x)$ and the definition (9)).

We hope that the method outlined in this note may be of some use when applied to more realistic cases of meson theories, because of its possibility to give a sharp definition, in terms of energy, of the «ignorance zone», that is of the energy region in which other phenomena not taken into account in the schematization of the meson theory as a closed one, become important.

* * *

We thank Professor P. CALDIROLA for his interest in this work, and our colleagues of the Theoretical Section of the Universities of Milan and Pavia for helpful comments.

One of us (D.F.) wants to express his gratitude to several members and guests at the Institute for Theoretical Physics in Copenhagen for comments and discussions. Particularly, thanks are due to Dr. G. KÄLLÉN for useful advices and criticism.

RIASSUNTO

Si esaminano alcuni aspetti di una possibile generalizzazione del modello di Lee. Si mostra come essa possa essere considerata come un'approssimazione della teoria mesonica scalare neutra con sorgenti fisse ottenute con l'introduzione di un taglio sull'energia totale dei mesoni.

Angular Correlations in High Energy Fission (*).

L. MARQUEZ

Centro Brasileiro de Pesquisas Físicas - Rio de Janeiro, Brasil

(ricevuto il 28 Marzo 1957)

Summary. — The existence of an angular correlation between the incident beam of nucleons and the fission fragments in high energy fission of heavy elements leads to the conclusion that the number of neutrons evaporated before fission is probably zero or very small.

1. — Introduction.

It seems to be now established that when a high energy nucleon collides with a heavy nucleus, and the collision leads to fission, the events take place in the following way:

The incoming nucleon develops a nucleonic cascade inside the heavy nucleus.

The nucleonic cascade can be absorbed in the nucleus or can come out of it. From the work of BELOVITSKII *et al.* (¹), it seems that the change from one case to the other takes place around incident nucleon energy of 150 MeV.

The nucleus is left with a large excitation energy forming a compound nucleus which decays by fission and by the emission of many neutrons.

We can assume, as BLATT and WEISSKOPF (²) do in a similar case, that all the reactions of the decay of the excited nucleus take place through elementary reactions in which only two products are formed. This will be true

(*) This work was done under the auspices of the Conselho Nacional de Pesquisas of Brazil.

(¹) G. E. BELOVITSKII, T. A. ROMANOVA, L. V. SOUKHOV and I. M. FRANK: *Zh. Exper. Teor. Fiz.*, **29**, 573 (1955).

(²) J. M. BLATT and V. F. WEISSKOPF: *Theoretical Nuclear Physics* (New York, 1952), p. 374.

if the time between reactions is longer than the transit time of nucleons over the nucleus.

The decay of the excited nucleus can now take place according to three different schemes.

In scheme I, the first event is the fission of the heavy nucleus, with the emission of the neutrons taking place from the excited fission fragments. The reactions will be as follows:

$$\begin{array}{ll} H_0 = F_0 + G_0 & \\ F_0 = F_1 + n & G_0 = G_1 + n \\ F_1 = F_2 + n & G_1 = G_2 + n \\ \text{etc.} & \text{etc.} \end{array}$$

Here H means heavy nucleus, F and G are fission fragments. This scheme has been suggested already (3).

In scheme II there are neutrons emitted before fission, and neutrons emitted from the fission fragments. The reactions will be as follows:

$$\begin{array}{ll} H_0 = H_1 + n & \\ H_1 = H_2 + n & \\ \text{etc.} & \\ \\ H_m = F_0 + G_0 & \\ F_0 = F_1 + n & G_0 = G_1 + n \\ F_1 = F_2 + n & G_1 = G_2 + n \\ \text{etc.} & \text{etc.} \end{array}$$

A third scheme proposed by GOECKERMANN and PERLMAN (4), in which all the neutrons were emitted before fission, seems to be ruled out by the experiment of HARDING and FARLEY (5). They irradiated U with 147 MeV protons and measured the ratio $N_0(f, n)/N_{90}(f, n)$ of the intensity of neutrons emitted at an angle of 0° with the fission fragments, and at an angle of 90° with the fission fragments, and found 1.27 ± 0.11. Although they interpreted their result as meaning that, of the 13 neutrons emitted in the process, 2.5

(3) L. MARQUEZ: *Nuovo Cimento*, **12**, 288 (1954).

(4) R. H. GOECKERMANN and I. PERLMAN: *Phys. Rev.*, **76**, 628 (1949).

(5) G. N. HARDING and F. J. M. FARLEY: *Proc. Phys. Soc., A* **69**, 853 (1956).

were emitted after fission, it has been shown (⁶) that their result is compatible with the emission of all the neutrons after fission, according to scheme I.

2. - Angular correlations.

WOLKE (⁷) has measured the angular correlation of one of the fission products of Bi when irradiated with 450 MeV protons, and he found the distribution $N_\theta(p, f) = 1 + 0.13 \cos^2 \theta$ between the proton beam and the fragments. LOZHIN *et al.* (⁸) have measured in plates the angular distribution of the fission of U with 660 MeV protons and found the correlation $N_\theta(p, f) = 1 + 0.29 \sin^4 \theta$ between the proton beam and the fragments.

From the data of STEINER and JUNGERMAN (⁹), we extrapolate that the fission cross-section for Bi with 450 MeV protons is about 0.23 barn and for U with 660 MeV protons about 1.3 barn. $\pi\lambda^2$ for protons of 450 MeV is 1.17 mb and for protons of 660 MeV it is 0.73 mb. This means that, to add up to the experimental cross-sections, we have to take the partial waves to $l = 13$ and $l = 41$ respectively. Even if there is some angular momentum leaving with the nucleonic cascade, the compound nucleus will have a large spin.

On scheme I, the existence of the angular correlation can be readily understood. This angular correlation means quantum mechanically that the fission fragments are emitted with orbital angular momentum of 0 and 1 in the case of Bi and 0, 1 and 2 in the case of U.

Since the average direction of the nucleonic cascade is the same as the direction of the incoming proton, it does not matter for defining a direction whether the cascade comes out or is absorbed in the nucleus. If the first event to happen to the excited nucleus is the fission, this will have a direct angular correlation with the direction of the incoming proton.

There are still several questions to be answered, such as why the coefficients have the values that they have, and why the angular correlation of U is peaked at 0° below proton energy of 60 MeV and at 90° above proton energy of 60 MeV.

On this scheme the angular distribution $N_\theta(p, n)$ of neutrons with respect to the incident proton beam can be calculated, and it turns out $1 + 0.004 \cos^2 \theta$ for Bi, and $1 - 0.008 \cos^2 \theta$ for U. As can be seen, they are practically symmetric. A forward cone due to the neutrons from the nucleonic cascade will be superimposed on this distribution.

(⁶) L. MARQUEZ: *Proc. Phys. Soc.* (to be published).

(⁷) R. L. WOLKE: *Bull. Am. Phys. Soc.*, **1**, 165 (1956).

(⁸) O. V. LOZHIN, N. A. PERFILOV and V. P. SHAMOV: *Zh. Exper. Teor. Fiz.*, **29**, 292 (1955).

(⁹) H. M. STEINER and J. A. JUNGERMAN: *Phys. Rev.*, **101**, 807 (1956).

It is also possible in scheme I that there is an angular correlation $N_\theta(f, n)$ between the fission fragment and the emitted neutrons due to the emission of the first neutron with angular momentum equal or greater than one. We guess that this correlation is small, strongly reduced by the remaining neutrons, and cannot be separated from the correlation due to the motion of the fission fragments. There might be also a small correlation $N_\theta(n, n)$ between any two neutrons, due to the emission of two consecutive neutrons from the same fission fragment with angular momentum equal or greater than one. We guess also that this correlation would be small and strongly reduced by the remaining neutrons.

In scheme II, the angular correlation between the incident proton or the nucleonic cascade and the fission fragments has to be preserved through the angular correlation of the intermediary neutrons. That means that all the neutrons evaporated before fission are emitted with angular momentum equal or greater than one.

The first neutron emitted would have to have a strong angular correlation $N_\theta(p, n)$ with the proton beam or the nucleonic cascade. Each emitted neutron would have to have a strong angular correlation $N_\theta(n_i, n_{i+1})$ with the following neutron, and the last neutron emitted before fission would have to have a strong angular correlation $N_\theta(n_m, f)$ with the fission fragments.

We have made calculations considering all the emissions until fission with $l = 1$. The three distributions mentioned in the previous paragraph would have the form $a_0 - a_2 \cos^2 \theta$. We found that, with values for the coefficients in the range of other measurements of nuclear angular distributions, the number of neutrons emitted before fission would be zero. We also found that, in the best of cases, the number of neutrons emitted before fission in Bi would be 4 and in U would be 2.

We then made calculations considering all the emissions before fission with $l = 2$. The three distributions would have the form $a_0 - a_2 \cos^2 \theta + a_4 \cos^4 \theta$. We found again that, with values of the coefficients in the range of other measurements, the number of neutrons emitted before fission would be zero, or perhaps one, and the largest number of neutrons emitted before fission would be 4 in U and 7 in Bi.

In the case of scheme II, there should be also an angular correlation $N_\theta(p, n)$ between the incoming proton and any neutron. We found that $N_{180}(p, n)/N_{90}(p, n) = 1 - 0.12m$, where m is the number of neutrons emitted before fission and the relation is true within 10%. There would be superimposed on this correlation the forward cone of neutrons from the nucleonic cascade.

In the case of scheme II, there should be also an angular correlation $N_\theta(n, n)$ between any two neutrons if there were two or more neutrons emitted before fission. If three or more neutrons were emitted before fission, this

angular correlation should be more asymmetric than the angular correlation between the proton beam and the fission fragments, in spite of the smearing from the neutrons emitted after fission.

In conclusion, there are 4 kinds of angular correlations in high energy fission. They are $N_\theta(p, f)$, $N_\theta(p, n)$, $N_\theta(f, n)$ and $N_\theta(n, n)$. There are measurements of the first and third, but there is not any measurement of the other two correlations. All the experimental data are compatible with scheme I and indicate contradictions with scheme II. A few more measurements could settle the problem of the qualitative mechanism of high energy fission, which is certainly a preliminary step to any attempt at a quantitative theory of high energy fission.

RIASSUNTO (*)

L'esistenza di una correlazione angolare tra il fascio di nucleoni incidente e i frammenti di fissione nella fissione ad alta energia di elementi pesanti porta alla conclusione che il numero di neutroni evaporati prima della fissione è probabilmente zero o molto piccolo.

(*) Traduzione a cura della Redazione

On the Measurements of the Pion-Proton Elastic Scattering in Nuclear Emulsions.

G. FERRARI, E. MANARESI and G. QUAREN

Istituto Nazionale di Fisica Nucleare - Sezioni di Bologna e Padova

(ricevuto il 29 Marzo 1957)

Summary. — The scanning methods for the photographic emulsions, used in the study of the pion-proton elastic scattering, are discussed. A particular method is described, which is useful in the research of the backwards scatterings ($135^\circ < \theta_{\text{c.m.}} < 180^\circ$). It has been employed in order to detect some eventual contribution of waves with $l > 1$, by analysing the behaviour of $d\sigma/d\Omega$ in this angular interval. The analysis of $d\sigma/d\Omega$ for the scattering process $\pi^+ + p$ at 120 MeV, based on 871 events, shows that no wave with $l > 1$ is present in a measurable quantity. The phase-shifts of the S and P waves result:

$$\alpha_3 = -10.3 \pm 2.9; \quad \alpha_{33} = 31.8 \pm 1.6; \quad \alpha_{31} = -2.6 \pm 1.6.$$

The study of the pion-proton interaction up to 300 MeV energy has been very much improved in the last years. The phenomenon seems to be rather clear in its general lines and the ensemble of the results obtained in numerous experiments already permits a theoretical treatment of the problem. So far, however, the available data are not sufficient to give a definite answer to the fundamental hypothesis, such as the rigorous validity of the charge independence principle, or, for instance, to determine the pion-nucleon coupling constant exactly ⁽¹⁾.

From the experimental point of view the situation is such that more precise and accurate measurements are needed, in order to solve the present uncertainties. In the elastic scattering experiments, the most convenient technique, for the rapidity and the statistical precision, seems to be at present

(1) G. PUPPI and A. STANGHELLINI: *Nuovo Cimento*, **5**, 1305 (1957).

the counter-technique. However, we think that the use of different techniques may be helpful for two reasons: the information they add and the better estimation of the systematic errors, proper to each technique, which arises from the comparison of the results obtained in different ways.

The photographic emulsions have been used by several authors, who measured the differential cross-sections of the pion-proton elastic scattering. Usually the pions are sent directly into the emulsions and the hydrogen, contained in the gelatine, constitutes the target.

The criteria for the identification of the pion-proton elastic scattering are based on the well defined kinematics of this two body process and have been described and discussed in previous papers (^{2,3}).

Our purpose here is to discuss the problems, which are tied to the usual methods of scanning in this kind of experiments, and also to present a different method, which provided us with good results in the determination of the differential cross-section of the scattering process $\pi^+ + p$ at 120 MeV for $135^\circ < \theta_{\text{c.m.}} < 180^\circ$.

The usual methods are: track-scanning and area-scanning. The track-scanning is certainly the method, which provides the most reliable results. Unfortunately it can be employed only when the cross-section is rather large, i.e. when the mean free path in the emulsion is sufficiently short, so that good statistics may be reached in a reasonable time. This becomes possible for the scattering process $\pi^+ + p$ at energies near resonance. In the other cases, if the work needed for track-scanning becomes prohibitive, one uses preferably the area-scanning, which is in fact more rapid than the precedent method. The success of the area-scanning more as for every other method depends on the observability conditions of the emulsion, i.e. the quality of the processing, the back-ground and the flux of the tracks.

Even with the best conditions the efficiency of the scanners is never complete. As was discussed in previous papers (^{3,4}), the inefficiency is not completely independent of the type of event and this fact may be seriously critical in the scattering experiments. One finds a sensible dependence of the inefficiency on the angle between the scattering plane and the emulsion surfaces; it is stronger for the planes near the vertical one. The inefficiency also depends on the scattering angle. For the smallest angles, the recoil-proton is very short and it is therefore hard to see it, until its range overcomes 10 microns; a cut-off at about 15° of the scattering angle is needed at energies around 100 MeV of the incident pions. The corresponding inefficiency rate was carefully examined

(²) G. GOLDHABER: *Phys. Rev.*, **89**, 1187 (1953).

(³) L. FERRETTI, E. MANARESI, G. PUPPI, G. QUAREN and A. RANZI: *Nuovo Cimento*, **1**, 1238 (1955).

(⁴) J. OREAR: *Phys. Rev.*, **96**, 1417 (1954).

by OREAR (⁴) and by FERRETTI *et al.* (⁵), by studying the Coulomb interference. Equally, the events, in which the scattering angle is very large, present difficulties for the scanning. Here the recoil proton is rather fast and its track has many gaps; besides its direction is near the incident pion. Especially in the case of a high density of tracks, it frequently happens that an accidental superposition of some tracks of the beam conceals the point origin of the recoil proton track, simulating its continuation, so that such an event may be lost also by a careful scanning. For this reasons, other authors, working with a high flux of tracks/cm², do not take into account the scattering angles larger than 160°. In the emulsions used by FERRETTI *et al.*, the flux is rather low ($5 \cdot 10^4$ tracks/cm²); thus a reasonable efficiency was also reached for the angles near 180°. From several checks, the inefficiency rate, within the experimental uncertainties, turned out to be the same in the whole angular interval from 15° up to 180°. However, a certain bias in the angular region near 180° could not be excluded.

The differential cross-section found in that experiment was better determined by a new way of scanning, whose method we describe here. The same emulsions of the earlier experiment, were used, i.e. a stack of 20 stripped emulsions (Ilford G-5, 600 µm thick, 7 cm \times 11 cm) exposed to the positive pions of (132 ± 5) MeV produced by the synchrocyclotron of Chicago.

The beam enters through one of the smallest faces of the stack parallel to the longest edges and it is concentrated in the central part (~ 3 cm) of the emulsions. The scanner observes the A_iB_i sections of the plates perpendicular to the mean direction of the beam; the sections are 44 mm long and at a distance of 5 mm from each other, as indicated in Fig. 1.

One observes in immersion with an eyepiece, of $8 \times$ magnification a $55 \times$ objective and with a field of ~ 300 µm of diameter. One searches for the gray and black tracks, i.e. those tracks having a density compatible with the one corresponding to a recoil proton. If they form an angle smaller than 30° with the mean direction of the beam, the tracks are followed in the opposite sense of movement of the beam until they go out of the emulsion or appear associated with an interaction which occurred in the emulsion itself. Many of the tracks we followed were due to recoil-protons of the elastic scattering $\pi^+ + p$. Because the angular limit, assumed for the choice of the tracks to be followed, the $\pi^+ + p$ events we found are all characterized by a large scattering angle of the pion.

We have taken into account only the events whose center is less than 5 mm

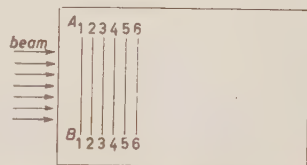


Fig. 1 - Position of an emulsion with respect to the beam. The sections A_iB_i have been observed

far from the observed section A_iB_i . The events having $\theta_{\text{c.m.}} < 135^\circ$ were not considered.

The scanning method described above is more rapid than the area-scanning; in fact the frequency rate for the events $\pi^+ + p$ with $\theta_{\text{c.m.}} > 135^\circ$ is 4 per scanner per day, whereas the corresponding rate for the area scanning is 0.4 events per scanner per day.

A further advantage over the area-scanning method, consists in avoiding the difficulties of observation, already mentioned when referring to the area-scanning. Many scatterings have been found having θ_{lab} near 180° and a scattering plane perpendicular to the emulsion surfaces; it is most unlikely that these events could have been found with the area-scanning method.

However, this type of scanning does not find all the $\pi^+ + p$ backscatterings which occur in the part of the gelatine of volume $A_iB_i \times d \times 500 \mu\text{m}$ before the observed section A_iB_i . A $\pi^+ + p$ scattering originating in the mentioned volume may be detected with this scanning method only if the recoil proton crosses the section A_iB_i . For the scatterings, we have considered ($\theta_{\text{c.m.}} > 135^\circ$, $E = 120 \text{ MeV}$), the proton has a range in the emulsion longer than 10 mm and the angle, which it forms with the incident pion, is smaller than 23° . An event is not observed, if the recoil-proton suffers a nuclear interaction or goes out of the emulsion before it crosses AB . Only this last possibility is very important in our case. In order to calculate the factors $f(\theta) = v(\theta)/v_0(\theta)$ which permit the true frequencies $v(\theta)$ to be obtained from the observed ones, $v_0(\theta)$, one must, at each scattering angle, account for all the parameters which are required to distinguish in the emulsion a $\pi^+ + p$ event with a certain θ , and the corresponding probabilities of their occurrence. These parameters are:

- d , distance from the section AB , varying between 0 and 5 mm; the ionization energy loss being small in this length, we have assumed that the cross-section does not change, i.e. all values of h have the same probability;
- z , depth of the event in the emulsion; all z 's have the same probability;
- Φ , angle between the scattering plane and the vertical plane, which contains the incident pion; Φ is isotropically distributed;
- α_1 , α_2 , projected and dip angles of the incident pion direction. The angular spread of the beam is 4° . The distributions of α_1 , and α_2 , have been carefully determined.

An analytical calculation of the factor $f(\theta)$ is rather easy if $\alpha_1 = \alpha_2 = 0$. Although the angular spread is small, it influences the factors $f(\theta)$ appreciably and therefore it is necessary to introduce it in the calculation. In this case the analytical calculation becomes very complicated, but the difficulty can

be overcome by applying the Montecarlo method. This was done using a mechanical device, with which the $\pi^- + p$ events were represented in the space by the different θ 's and the various parameters d , r , ϕ , z_1 , and z_2 . The function $f(\theta)$, we have obtained in this way, is drawn in Fig. 2.

The calculation was performed by assuming the section AB of infinite length. In the experiment, AB is somewhat longer than the width of the beam, which is concentrated in the central part of the plate; thus the experimental condition is equivalent to that assumed in the calculation. The error in the determination of the values $f(\theta)$ is smaller than 1% and therefore it is negligible if compared with the statistical errors.

Following the experimental procedure, we have described above, 348 $\pi^- - p$ events were found in the angular interval $135^\circ \div 180^\circ$.

They were divided in three groups, corresponding to angular intervals of 15° . The frequencies were obtained, taking into account for each event the

corresponding factor $f(\theta)$ deduced from the curve of Fig. 2. The angular distribution of these scatterings appears in Fig. 3 together with the similar distribution obtained with the 165 events found with the area-scanning. The two distributions, within the experimental errors, are in good agreement. So the reliability of the previous results obtained by area-scanning is confirmed also for this angular interval. We have averaged the two distributions and the average distribution has been normalized to the value of the cross-section for $135^\circ < \theta_{\text{cm}} \leq 180^\circ$, $\sigma_{135^\circ \div 180^\circ} = (27.4 \pm 2.2) \text{ mb}$ as obtained by the area-scanning.

In the Fig. 4, the differential cross-section $d\sigma/d\Omega$ is reported; it is based on 871 events, which were found partly with the previous area-scanning, partly with the new one. The total cross-section is $\sigma_t = (96.6 \pm 8.7) \text{ bm}$.

Fig. 3 – Angular distributions of the back-scatterings found with the new scanning (full lines) and with the previous area-scanning (dotted lines).

The experimental data are fitted by an analytical expression for $d\sigma/d\Omega$, where the pion-proton interaction is described in the S and P states taking into account also the Coulomb interference.

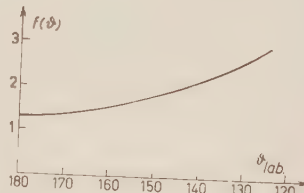


Fig. 2. Correction factors for each scattering angle in the laboratory system.

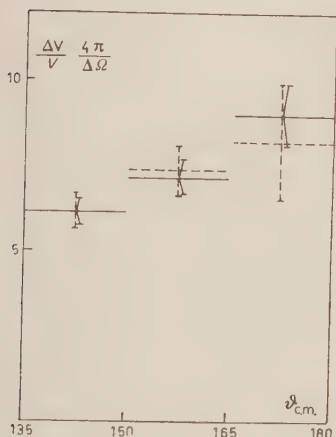


Fig. 3 – Angular distributions of the back-scatterings found with the new scanning (full lines) and with the previous area-scanning (dotted lines).

The experimental data are fitted by an analytical expression for $d\sigma/d\Omega$, where the pion-proton interaction is described in the S and P states taking into account also the Coulomb interference.

The best fit was made with the electronic computer, Avidae, of the Argonne National Laboratory by H. L. ANDERSON and W. C. DAVIDON (5). The resulting phase-shifts, according to the Fermi solution, are:

$$\chi_3 = -12.3 \pm 2.9, \quad \chi_{33} = 31.8 \pm 1.6, \quad \chi_{31} = -2.6 \pm 1.6.$$

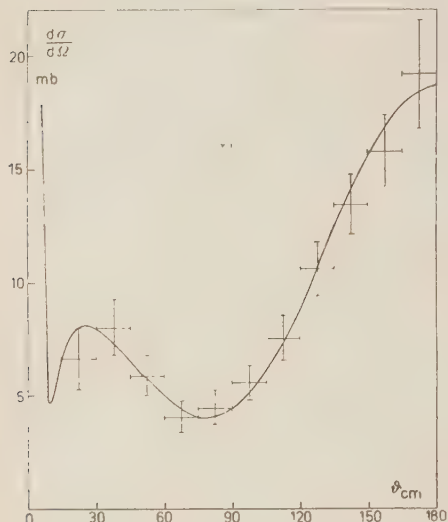


Fig. 4. — Differential cross-section for the process $\pi^+ + p = \pi^+ + p$ at 120 MeV.

The coefficients of the lower powers of the cosine are also affected, but we think that, in this case, the detection of the *D*-wave is mainly linked to the possibility of detecting terms of $\cos^3 \theta$ and $\cos^1 \theta$. Obviously these terms are most important for angles near 0° and 180°. However the forward cross-section is strongly distorted by the Coulomb interference with respect to the behaviour given by $\sum c_n \cos^n \theta$. This does not happen appreciably, for the backward scattering.

The method of scanning, we have used, could be very useful for the search for the *D*-wave in the scattering experiments with the nuclear emulsion technique. The result we have obtained shows that at 120 MeV the *D*-wave is not present in a measurable amount. Therefore it would be interesting to pursue the research at higher energies.

These values agree very well with those given by FERRETTI *et al.*

H. L. ANDERSON and W. C. DAVIDON have clearly demonstrated that the available data in this energy range are not sufficient to reveal any contribution of the *D*-wave, which consequently must be very small here. Some evidence on a contribution of the *D*-wave was recently given by Russian authors (6) working up to 300 MeV. However, the problem of the presence of the *D*-wave (or other waves of higher *l*) is still open: only new precise experiments shall lead to definite conclusions. As it is well known, the presence of a *D*-wave may lead to terms proportional to $\cos^3 \theta$ and $\cos^1 \theta$ in the expression for $d\sigma/d\Omega$.

(5) H. L. ANDERSON and W. C. DAVIDON: *Nuovo Cimento*, **5**, 1238 (1957).

(6) A. I. MUKHIN, E. B. OZEROV, B. M. PONTECORVO, E. L. GRIGORIEV and N. A. MITIN: *Proc. C.E.R.N. Symposium*, **2**, 204 (1956).

We should like to acknowledge with thanks the helpful assistance given us by Prof. G. PUPPI and we should like also to thank very gratefully Drs. H. L. ANDERSON and W. C. DAVIDON who provided us with the careful phase-shift analysis, and Dr. F. CAVINATO who helped us in the Montecarlo calculation.

RIASSUNTO

Si disentono i metodi di osservazione delle emulsioni fotografiche impiegate per lo studio dell'urto elastico pion-proton e viene descritto inoltre un metodo particolarmente utile per la ricerca degli eventi $\pi + p$ a grande angolo d'urto ($135^\circ < \theta_{\text{c.m.}} < 180^\circ$), con lo scopo di rilevare, dall'analisi dell'andamento della $d\sigma/d\Omega$ in questo intervallo angolare, eventuali contributi di onde con $l > 1$. L'analisi della $d\sigma/d\Omega$ per il processo $\pi^+ + p$ a 120 MeV, basata su 871 eventi, mostra che onde con $l > 1$ non sono presenti in quantità misurabile. Gli sfasamenti delle onde S e P risultano:

$$z_3 = -12.3 \pm 2.9; \quad z_{33} = 31.8 \pm 1.6; \quad z_{31} = -2.6 \pm 1.6.$$

π^+ - Proton Scattering at 100 MeV.

R. GESSAROLI and G. QUAREN

Istituto di Fisica dell'Università - Bologna

G. DASCOLA, S. MORA and G. TODESCO

Istituto di Fisica dell'Università - Parma

(ricevuto il 29 Marzo 1957)

Summary. — The differential cross-section $d\sigma/d\Omega$ for the elastic process $\pi^+ + p$ at 100 MeV has been measured. 621 events were found in photographic emulsion. The phase-shift analysis gives the following values for the S and P waves:

$$\alpha_3 = -10.6 \pm 1.9; \quad \alpha_{33} = 21.7 \pm 1.2; \quad \alpha_{31} = -2.5 \pm 1.3.$$

The differential cross-section of the $\pi^+ + p$ scattering at 100 MeV has been measured, using a stack of nuclear emulsions (20 stripped emulsions, 600 μm thick, 7 cm \times 11 cm) exposed to the pion beam of (132 ± 5) MeV of the Chicago Synchrocyclotron. The same stack was used earlier by FERRETTI *et al.* (1) and recently by G. FERRARI *et al.* (2), who studied the $\pi^+ + p$ scattering at 120 MeV. More details on the exposure, the methods of scanning and the analysis of the events are reported in their papers.

For this experiment, the scanning was made at a certain distance from the edge of the emulsion, through which the 132 MeV pions enter, so that their mean energy decreases down to ~ 100 MeV, because of the ionization energy-losses. The energy of the interacting pions was measured in many $\pi^+ + p$ events by means of the range of the recoil-proton and the scattering angle.

It resulted a mean energy of 100 MeV and an energy spread of about 12 MeV.

(1) L. FERRETTI, E. MANARESI, G. PUPPI, G. QUAREN and A. RANZI: *Nuovo Cimento*, **1**, 1238 (1955).

(2) G. FERRARI, E. MANARESI and G. QUAREN: *Nuovo Cimento*, **5**, 1651 (1957).

Firstly area-scanning was made and later the results were completed following the scanning method described by G. FERRARI *et al.* (2).

With the area-scanning 424 events were found in the angular interval $15^\circ < \theta_{\text{c.m.}} < 180^\circ$ and with the second method of scanning 197 having $135^\circ < \theta_{\text{c.m.}} < 180^\circ$. The total cross-section is $\sigma_x = (62.4 \pm 8.0)$ mb.

The differential cross-section, based on the results of both scannings, is drawn in Fig. 1. The phase-shift analysis has been made taking into account *S* and *P*-waves and Coulomb terms.

The maximum likelihood calculation has been carried out by means of the electronic computer, Avidac, of the Argonne Laboratory (3). Only the events found with the area-scanning were used for that calculation, but the results do not change adding the 197 events, we later found in the angular interval $135^\circ \div 180^\circ$. The phase-shift corresponding to the Fermi solution are:

$$\alpha_3 = -10.6 \pm 1.9, \quad \alpha_{33} = 21.7 \pm 1.2, \quad \alpha_{31} = -2.5 \pm 1.3.$$

These values are consistent with those obtained by other Authors at energies higher and lower than 100 MeV. From the behaviour of the differential cross-section, drawn in Fig. 1, it appears that the destructive Coulomb interference is well confirmed again by this new experiment.

* * *

We should like to thank gratefully Drs. H. L. ANDERSON and W. C. DAVIDON for the careful phase-shift analysis and the scanning groups of the Bologna and Parma laboratories for their valuable collaboration.

(3) F. ANDERSON and W. C. DAVIDON: *Nuovo Cimento*, **5**, 1238 (1957).

RIASSUNTO

È stata misurata la sezione d'urto differenziale $d\sigma/d\Omega$ del processo d'urto elastico $\pi^+ + p$ a 100 MeV. La tecnica usata è quella delle emulsioni fotografiche. L'analisi, basata su 621 eventi, ha dato i seguenti sfasamenti delle onde *S* e *P*:

$$\alpha_3 = -10.6 \pm 1.9; \quad \alpha_{33} = 21.7 \pm 1.2; \quad \alpha_{31} = -2.5 \pm 1.3.$$

π^+ -Proton Scattering at 83 MeV.

L. FERRETTI and G. QUAREN

Istituto di Fisica dell'Università - Bologna

M. DELLA CORTE and T. FAZZINI

Istituto di Fisica dell'Università - Firenze

(ricevuto il 29 Marzo 1957)

Summary. — In photographic emulsion 274 events $\pi^+ + p = \pi^- + p$ have been found. The energy of the pions extends between 70 and 90 MeV; the mean energy is 83 MeV. The phase-shift analysis gives, for the S and P waves, the following values:

$$\alpha_3 = -12.3 \pm 2.9; \quad \alpha_{33} = 12.0 \pm 2.2; \quad \alpha_{31} = -3.1 \pm 1.0.$$

The pion-proton scattering in the low energy region, below 100 MeV, has been so far not very much investigated. The experimental data are not sufficiently numerous and precise; the biggest difficulty comes from the smallness of the cross-section, which does not allow good statistics in the experiments. However, from the theoretical point of view, it would be very interesting to know the values of the phase shifts and their energy dependence up to few MeV. In fact, the extrapolation down to zero energy of the P -wave phase-shifts should provide, the value of the pion-proton coupling constant according to the fixed source theory given by CHEW and LOW⁽¹⁾. Obviously the result of such calculation will be the more reliable the more the extrapolation is drawn from the values corresponding to the smallest energies.

Using the emulsion stack mentioned in the previous paper⁽²⁾ and fol-

(¹) G. PUPPI and A. STANGHELLINI: *Nuovo Cimento*, **5**, 1305 (1957).

(²) L. FERRETTI, E. MANARESI, G. PUPPI, G. QUAREN and A. RANZI: *Nuovo Cimento*, **1**, 1238 (1955); G. DASCOLA, R. GESSAROLI, S. MORA, G. QUAREN and G. TODESCO: *Nuovo Cimento*, **5**, 1658 (1957).

lowing the same experimental procedure, we have measured the differential cross-section for the π^+ -proton scattering in the energy interval 70–90 MeV. By area-scanning 274 of such events were found, having $15^\circ < \theta_{cm} < 180^\circ$. The mean energy of the interacting pions is 83 MeV, as obtained from measurements of recoil-proton range and scattering angle. The total cross-section has been evaluated on the basis of the number of the events, the flux of the pions, crossing the scanned volume, and the number per cm^3 of hydrogen atoms; its value is $\sigma_t = (34 \pm 4) \text{ mb}$.

The differential cross-section appears in Fig. 1.

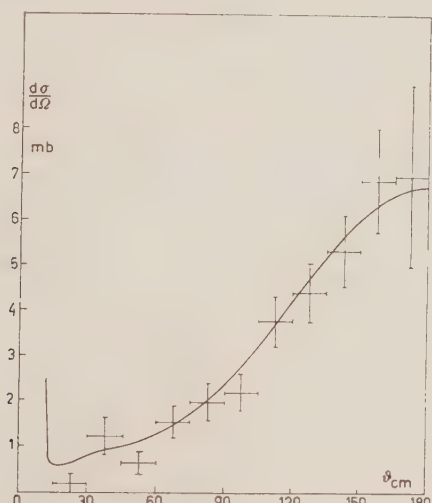


Fig. 1. – Differential cross-section for the process $\pi^+ + p \rightarrow \pi^+ + p$ at 83 MeV.

The best fit has been obtained by the assumption that only S and P -waves are present and the Coulomb interference is destructive.

The formula given by F. T. SOLMITZ⁽³⁾ was used: the resulting phase-shifts, according to the Fermi solution, are the following:

$$\alpha_3 = -12.3 \pm 2.9, \quad \alpha_{33} = 12.0 \pm 2.2, \quad \alpha_{31} = -3.1 \pm 1.0.$$

The S phase-shift seems to be rather bigger and the $P_{\frac{1}{2}}$ phase-shift rather smaller than that expected by considering the values obtained by other authors in the same energy interval. However the disagreement may be con-

⁽³⁾ F. T. SOLMITZ: *Phys. Rev.*, **94**, 1799 (1954).

tained within the errors. The $P_{\frac{1}{2}}$ phase-shift is consistent with the majority of the results available up to now. For these energies it is certainly small and negative.

* * *

We are most grateful to Dr. A. M. SONA for her collaboration and to the scanning teams of the Bologna and Florence laboratories.

RIASSUNTO

Sono stati trovati in emulsioni fotografiche 274 eventi $\pi^+ + p = \pi^+ + p$ nell'intervallo energetico $70 \div 90$ MeV. L'energia media è 83 MeV. L'analisi in fasi ha dato i seguenti valori degli sfasamenti delle onde S e P :

$$\alpha_3 = -12.3 \pm 2.9; \quad \alpha_{33} = 12.0 \pm 2.2; \quad \alpha_{31} = -3.1 \pm 1.0.$$

On the Angular Correlation in the β -Decay of μ -Mesons Observed in Photographic Emulsion.

B. BHOWMIK (*), D. EVANS and D. J. PROWSE

H. H. Wills Physical Laboratory, University of Bristol

(ricevuto il 6 Aprile 1957)

Summary. — The anisotropy of the distribution in the angle θ , between the direction of emission of the positron and that of the μ -meson, has been measured in stripped emulsion stacks exposed to the cosmic radiation. Assuming a distribution of the form $(1+a \cos \theta)$ a value of -0.081 ± 0.05 has been obtained for « a ». This result is compared with those obtained by other workers and the depolarizing effects of photographic emulsion are discussed.

1. — Introduction.

Since the suggestion by LEE and YANG (1) that non-conservation of parity might be observed by studying the angular correlations in the $\pi\mu e$ decay, and the report by C. CASTAGNOLI *et al.* (2) of preliminary results from events observed in photographic emulsion, which showed that the effect, if it existed, must be small, many groups (3-7) have independently investigated the aniso-

(*) On leave from the University of Delhi.

(1) T. D. LEE and C. N. YANG: *Phys. Rev.*, **104**, 254 (1956).

(2) C. CASTAGNOLI, C. FRANZINETTI and A. MANFREDINI: *The Arogadro Conference on Fundamental Physics*, Turin, 1956). (In press for *Suppl. Nuovo Cimento*).

(3) N. N. BISWAS, M. CECCARELLI and J. CRUSSARD: *Nuovo Cimento*, **3**, 756 (1957).

(4) C. CASTAGNOLI, C. FRANZINETTI and A. MANFREDINI: *Nuovo Cimento*, **3**, 684 (1957).

(5) Private communication from P. H. FOWLER, University of Minnesota.

(6) J. I. FRIEDMAN and V. L. TELELDI: Circulated preprints to appear in *Phys. Rev.*

(7) R. L. GARWIN, L. M. LEDERMAN and M. WEINRICH: Circulated preprint to appear in *Phys. Rev.*

tropy in emulsion of the distribution of the angle θ , between the direction of emission of the positron and that of the μ -meson. The conditions in these experiments have differed considerably, and it has been established that an anisotropy in the distribution of θ , can be detected.

The present communication gives the measurements carried out on the μ -e decays from π -mesons stopped in four stacks of photographic emulsions exposed during high altitude balloon flights to the cosmic radiation, discusses the internal consistency of the results and compares them with those obtained by other workers.

2. - Experimental technique.

The $\pi\text{-}\mu$ events were found by area-scanning the emulsions. Only those events in which the μ -mesons were stopped within a single emulsion strip have been utilized in this experiment. The π -meson decays were noted whether or not a positron secondary was observed from the μ -meson. Thus there is no bias in picking up events in which the decay positron is emitted preferentially in one favoured direction. The events for which no positron was seen at first were carefully scrutinized, and in every case the secondary was found when a 30 μm cut-off from the surface or glass interface was imposed on all events. Since all secondaries were found there is no bias against the inclusion of positrons emitted in any direction, which might otherwise have arisen.

The projected angle between the initial direction of the μ -meson and the decay positron was measured with an ocular protractor to within $\frac{1}{2}^\circ$. The dip of each track was measured over the initial rectilinear portion. In some instances for the μ -meson the track length used in this measurement was as short as 20 μm , because the particle is very rapidly scattered; for the positron it was always possible to use the first 100 μm . The dip measurements were made to the nearest μm and the dip angles calculated on the basis of a shrinkage factor of 2.0.

The mean shrinkage factor obtained by measuring the processed thickness of a number of the emulsions used was $2.0 \pm .1$, where .1 is the standard deviation. The effect on the final results of errors in this factor has been carefully considered. In general the forward/backward ratio is unchanged by use of a different shrinkage factor (e.g. 1.8 and 2.2). The maximum effect occurs for space angles near 90° when the dip angles are close to 45° , and the overall change in the distribution is to make angles in the forward hemisphere slightly smaller and angles in the backward hemisphere slightly larger or vice versa. The effect is symmetrical about 90° and if the distribution in $\cos\theta$ were isotropic it would have no effect on the sum of the $\cos\theta$ values; however, because the distribution is asymmetrical, there is a small systematic effect

which amounts to about 4% in the value of $\sum \cos \theta$ for a change of 5% in the shrinkage factor. An underestimate of the shrinkage factor leads to an under-estimate of the asymmetry and vice versa.

3. — Results.

The predicted form for the required angular distribution for a spin $\frac{1}{2}$ particle is $(1+a \cos \theta)$. The mean value of $\cos \theta$ is, therefore, $a/3$. The determination of this quantity provides the best method of obtaining the value

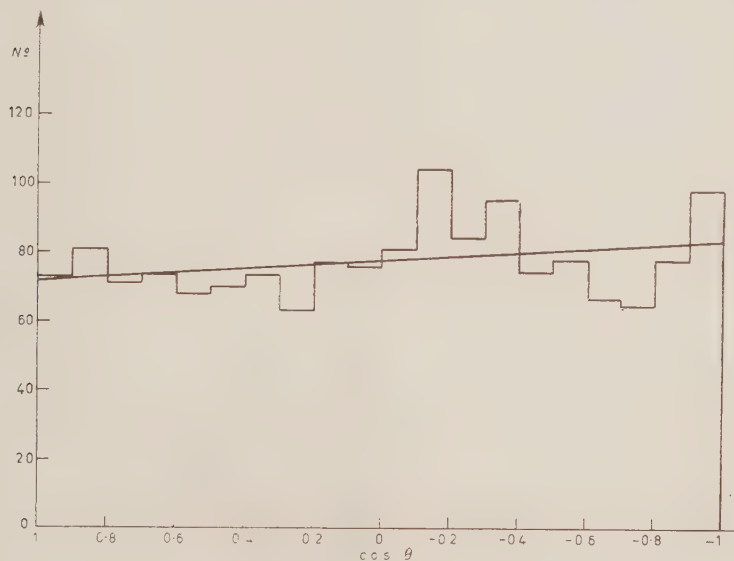


Fig. 1.

of « a », since all the information provided by the experimental data is used. The standard deviation of the distribution of $(\cos \theta)$, if it were rectilinear, is ± 0.6 , and since the distribution in this case is approximately rectilinear, the standard deviation on the mean value of $\cos \theta$ from n observations will be $0.6/n^{\frac{1}{2}}$.

The results from 1562 events are shown in Fig. 1. The backward excess is 6.5% and the value of $\sum \cos \theta$ for these events is — 42.24, giving a mean value for « a » of — .081 with a standard deviation of .045, which allowing for the possible shrinkage factor error becomes .050. The backward excess is slightly more than would be expected for this value of « a », because of a

larger number of events in the $\cos \theta$ interval 0 to -0.5 . The line corresponding to $a = .08$ is shown in Fig. 1. The results are again shown in Fig. 2 for four equal intervals of $\cos \theta$. The line $1 - .08 \cos \theta$ is again drawn. A χ^2 test on this line gives a Pearson probability of 0.8 compared with 0.7 for an isotropic distribution in $\cos \theta$. The difference between these two probabilities is hardly

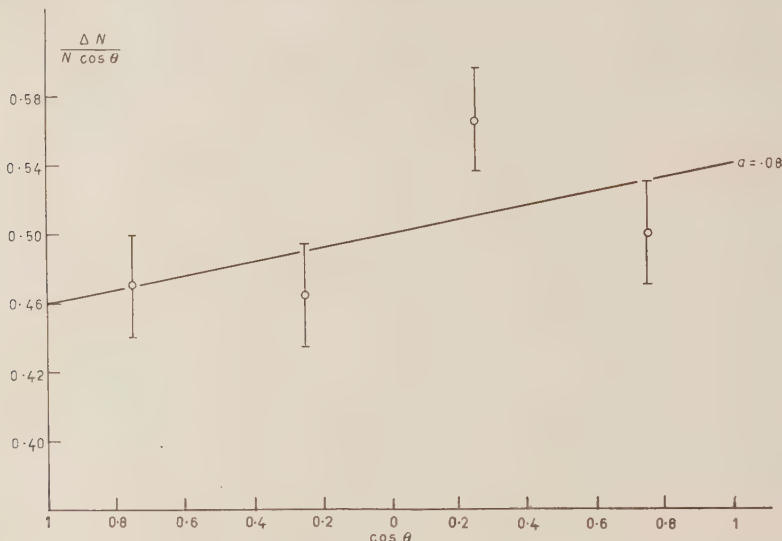


Fig. 2.

significant. All the information is not however used in this method of analysis and the difficulty of obtaining « a » by a best fit line is thus well illustrated. The value obtained from all the information available ($a = .08 \pm .05$) is 1.5 standard deviations from zero.

4. — Discussion.

The results of WU *et al.* (8) on the β -decay of aligned ^{60}Co nuclei and those of GERWIN *et al.* (7) which gave a value of « a » $= 0.33 \pm .03$ for the β -decay of μ -mesons arrested in carbon, are consistent with the two component neutrino theory of LEE and YANG (9) and of LANDAU (10). Using nuclear emulsion as

(8) C. S. WU, E. AMBLER, R. W. HAYWARD, D. D. HOPPER and R. P. HUDSON: Circulated preprint to appear in *Phys. Rev.*

(9) T. D. LEE and C. N. YANG: *Phys. Rev.* (in press).

(10) L. LANDAU, *Nuclear Physics*, **3**, 127 (1957).

the stopping medium for the μ -mesons, GERWIN *et al.* obtained a value of $0.18 \pm .03$ for « a » (this value has been obtained by taking into account the finite time width of their counter gate). This decrease in « a » might be explained by depolarising effects in emulsion which would occur due either to the presence of large transient fields, or to the stopping of the μ -mesons in portions of the emulsion influenced locally by stable fields of considerable strength (e.g. where electron capture to form mesonium were possible). In the former case it would be reasonable to assume the probability of a μ -meson being depolarized to be proportional to the time for which it is present in the emulsion before it decays. If this were so, one would expect a difference in the value of « a » obtained under the conditions of the present experiment to that obtained by the Columbia group, due to the difference in the time intervals for which the μ -mesons are observed after being stopped ($t = 0 \div \infty$ for this experiment and $t = 0.75 \div 2.0 \mu\text{s}$ for that of the Columbia group). It can be shown that under these conditions, the ratio

$$\frac{\text{effective } \langle a \rangle t = .75 \div 2.0 \mu\text{s}}{\text{effective } \langle a \rangle t = 0 \div \infty} = 0.65.$$

In addition, to enable a direct comparison to be made between the Columbia result and those obtained in emulsion using the procedure of the present experiment, account must be taken of the 25 MeV cut-off employed by the former group on the counter system for the detection of the β -particles. The energy dependence of the asymmetry deduced from the two-component neutrino theory is given by:

$$N(x, \theta) = x^2(3 - 2x + p(2x - 1)) dx d(\cos \theta),$$

where

$$x = \frac{\text{energy of electron}}{\text{max allowed electron energy}}.$$

Integrating this expression over the energy limits observed in the two types of experiments, one obtains:

$$\frac{\text{effective } \langle a \rangle x = \frac{1}{2} \div \frac{1}{1}}{\text{effective } \langle a \rangle x = 0 \div \frac{1}{1}} = 1.31.$$

The lower value for « a » obtained, while being in accordance with the energy dependence deduced from the two component neutrino theory, is clearly inconsistent with the form of depolarization assumed above and together with the lack of correlation between the size of the time gate and the value of « a » observed by the Columbia group, suggests that the process is very rapid and might be associated with a single component in the emulsion, which for example, provides a source of free electrons for the formation of mesonium.

Table I gives the details of the results for emulsion of other workers and Fig. 3a shows a scatter diagram of the values of «*a*» obtained together with the standard deviations quoted and the weighted mean «*a*» from all the observations. These results are just consistent with a common mean.

TABLE I.

Group	Exposure	Field	« <i>a</i> »
GARWIN <i>et al.</i>	Machine	—	$-0.13 \pm .03$ (*)
FRIEDMAN <i>et al.</i>	Machine	10^{-3} gauss	$-0.174 \pm .038$
BISWAS <i>et al.</i>	Machine	10^{-3} »	$-0.095 \pm .04$
CASTAGNOLI <i>et al.</i>	Cosmic ray	< 1 »	$-0.222 \pm .067$
FOWLER <i>et al.</i>	Cosmic ray	< 1 »	$-0.01 \pm .03$
Present experiment	Cosmic ray	< 1 »	$-0.08 \pm .05$

(*) This value takes into account the energy cut-off imposed (see text).

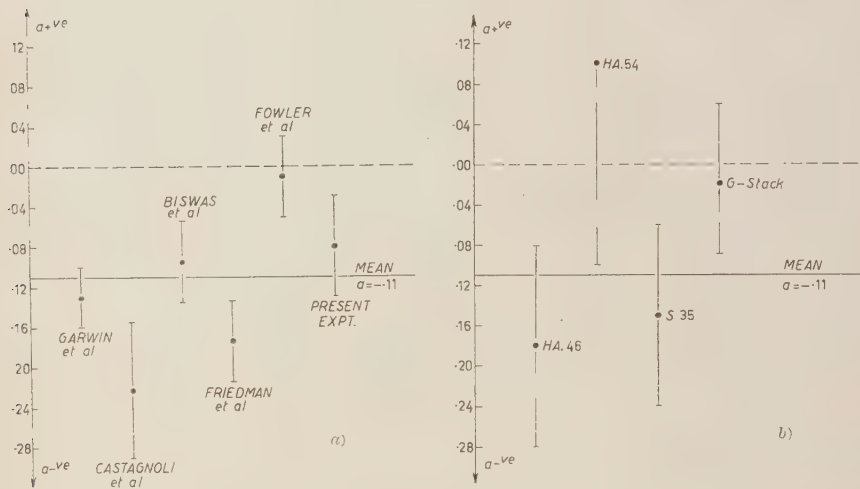


Fig. 3.

In Table II, the results of the present experiment have been analysed with respect to the stacks in which they were obtained and Fig. 3b shows the resulting scatter diagram for «*a*», the mean «*a*» from all observations being again shown. Although the errors are very large, due to the small number of events found in the individual stacks, when the results of Fig. 3a are taken into account, it seems just possible that in emulsion either a value of about -0.16 is obtained for «*a*», or a large degree of depolarization

TABLE II.

Stack	Locality of flight	Max. alt.	Time at alt.	Number of events	$\langle a \rangle$
HA 46	Oxford (England)	87 000	6 hours	331	$-.18 \pm .10$
HA 54	Cardington (England)	70 000	4 "	89	$+.10 \pm .20$
S 35	Sardinia (Italy)	85 000	7 "	425	$-.15 \pm .09$
G-stack	Novi Ligure (Italy)	83 000	7 "	717	$-.02 \pm .07$
				1 562	$-.08 \pm .045$

occurs reducing the asymmetry to a very small amount. In any case it appears possible that the results considered here are inconsistent with a unique magnitude of the asymmetry of the $\cos \theta$ distribution in emulsion. Variations between stacks are not inconceivable, as some of the substances added to stabilize the latent image are paramagnetic, and small variations in the quantities of these substances might make appreciable differences to the depolarizing properties of different stacks.

* * *

We should like to thank Dr. G. N. FOWLER, Dr. R. H. DALITZ, Professor C. F. POWELL and Professor M. H. L. PRYCE for many stimulating discussions. We are greatly indebted to Professor C. F. POWELL for his constant encouragement and advice. Our thanks are due to the other members of the laboratory for their co-operation and especially to Mrs. A. EVANS, Mrs. A. HOWSE and Miss M. PEARCE for much of the microscope work.

D. E. thanks the University of Bristol for a graduate scholarship and B. B. is indebted to the British Council and the Colombo plan authorities for financial assistance.

RIASSUNTO (*)

L'anisotropia della distribuzione dell'angolo θ tra la direzione di omissione del positrone e quella del mesone μ è stata misurata in pacchi di emulsioni pelate esposti alla radiazione cosmica. Assumendo per la distribuzione una forma del tipo $(1+a \cos \theta)$, si è ottenuto per a un valore di $-.081 \pm .05$. Si confronta questo risultato con quelli ottenuti da altri sperimentatori e si discutono gli effetti depolarizzanti dell'emulsione fotografica.

(*) Traduzione a cura della Redazione.

Effetti galvanomagnetici nel germanio.

G. C. DELLA PERGOLA

Istituto Superiore P. T., Fondazione « Ugo Bordoni » - Roma

D. SETTE

*Istituto Superiore P. T., Fondazione « Ugo Bordoni » - Roma
Istituto Nazionale di Ultracustica - Roma*

(ricevuto il 7 Aprile 1957)

Riassunto. — Vengono esposti i risultati di una serie di misure di resistività e di effetto Hall effettuate, a temperatura ambiente, su alcuni campioni monocristallini di germanio del tipo « p » e del tipo « n ». Sono riportati i valori della resistività e del coefficiente di Hall in funzione dell'intensità del campo di induzione magnetica (fra 0.15 e 1.0 Wb/m²) e dell'orientazione del campo e della corrente rispetto agli assi cristallografici dei campioni. I risultati vengono confrontati con quelli prevedibili teoricamente in base alle attuali conoscenze sulla struttura delle bande di valenza e di conduzione del germanio. Per quanto riguarda il germanio « n », il confronto è pienamente soddisfacente. Si constata che il valore del rapporto fra le masse efficaci longitudinale e trasversale degli elettroni di conduzione è compreso fra 8 e 12. Per quanto riguarda il germanio « p », non è possibile effettuare una interpretazione teorica completa dei dati sperimentali, non esistendo attualmente, a causa della notevole complessità delle superfici d'energia della banda di valenza del germanio, una trattazione matematica soddisfacente. Facendo uso di una teoria approssimata, si possono tuttavia giustificare in parte i risultati sperimentali. Non possono però essere spiegati i fenomeni di anisotropia.

1. — Introduzione.

I fenomeni della magnetoresistenza e dell'effetto Hall nei semiconduttori sono direttamente collegati alla struttura delle bande di valenza e di conduzione.

La teoria delle proprietà elettriche dei semiconduttori è stata sviluppata, in un primo tempo, essenzialmente facendo uso della ipotesi semplificatrice che le superfici di energia costante nella zona ridotta di Brillouin siano di forma sferica. Ciò conduce spesso a risultati che sono in notevole disaccordo con l'esperienza, particolarmente per quanto riguarda gli effetti galvanomagnetici.

Alcune recenti esperienze di risonanza ciclotronica (¹-⁶), unitamente a misure di altro tipo ed a considerazioni teoriche, hanno permesso di determinare, con un discreto grado di approssimazione, la struttura delle bande di energia del germanio e del silicio. Sulla base delle attuali conoscenze su questa struttura sono stati fatti vari tentativi per interpretare teoricamente gli effetti galvanometrici nei cristalli di questi elementi.

In tale situazione, hanno particolare interesse le misure degli effetti galvanometrici in campioni di germanio aventi diverse orientazioni: esse consentono infatti di controllare e completare le indicazioni fornite dalle esperienze di risonanza ciclotronica. Misure di questo tipo erano già state effettuate da PEARSON e SUHL (1951) (⁷), con una precisione che si è però dimostrata insufficiente per un proficuo confronto con la teoria. Appare quindi evidente l'utilità di dati più precisi.

Nel presente lavoro si è cercato di determinare sperimentalmente l'andamento del coefficiente di Hall e della resistività nel germanio, sia di tipo « p » che di tipo « n », in funzione dell'intensità del campo di induzione magnetica e delle orientazioni di esso e della corrente rispetto agli assi cristallografici dei campioni. I risultati sono stati confrontati con le indicazioni ottenibili mediante le teorie attualmente esistenti. In particolare, nel caso del germanio « n », tali risultati concordano con quelli ottenuti da GOLDBERG e DAVIS (⁸) mentre la presente ricerca era in corso.

2. – Metodo di misura e risultati sperimentali.

Le misure sono state effettuate a temperatura ambiente, fra 0,15 e 1,03 Wb/m², con il metodo e l'apparecchiatura altrove descritti (⁹).

(¹) G. DRESSELHAUS, A. F. KIP e C. KITTEL: *Phys. Rev.*, **92**, 827 (1953).

(²) G. DRESSELHAUS, A. F. KIP e C. KITTEL: *Phys. Rev.*, **98**, 368 (1955).

(³) B. LAX, H. J. ZEIGER, R. N. DEXTER e E. S. ROSENBLUM: *Phys. Rev.*, **93**, 1418 (1954).

(⁴) C. KITTEL: *Physica*, **20**, 829 (1954).

(⁵) R. N. DEXTER, H. J. ZEIGER e B. LAX: *Phys. Rev.*, **95**, 567 (1954).

(⁶) R. N. DEXTER, H. J. ZEIGER e B. LAX: *Phys. Rev.*, **104**, 637 (1956).

(⁷) G. L. PEARSON e H. SUHL: *Phys. Rev.*, **83**, 768 (1951).

(⁸) C. GOLDBERG e R. E. DAVIS: *Phys. Rev.*, **102**, 1254 (1956).

(⁹) G. C. DELLA PERGOLA e D. SETTE: *Alta Frequenza*, **25**, 140 (1956).

Sono stati usati campioni aventi la forma di parallelepipedi allungati (circa 1,5 mm \times 3 mm \times 20 mm). Detti campioni sono stati ricavati da grossi monocristalli, dai quali sono stati tagliati in modo che il lato maggiore fosse parallelo alla direzione cristallografica (100) o alla direzione (110). I campioni di tipo «p» avevano una resistività di circa $14 \Omega \text{ cm}$ ($\sim 2 \cdot 10^{14}$ atomi accettatori per cm^3); quelli di tipo «n» avevano una resistività compresa fra 14 e $16 \Omega \text{ cm}$ ($\sim 10^{14}$ atomi donatori per cm^3).

Sono stati determinati l'andamento della resistività ϱ , e quello del coefficiente di Hall, R , in funzione della intensità del campo di induzione magnetica, B , per le tre seguenti orientazioni della corrente e del campo rispetto agli assi cristallografici:

	I	B
1	(100)	(001)
2	(110)	(001)
3	(110)	(1 $\bar{1}$ 0)

L'intensità della corrente nei campioni è stata tenuta all'incirca pari a 2 mA, avendo cura che essa non variasse durante ogni singola esperienza, nei limiti di precisione del dispositivo potenziometrico di misura (1/10 000). I valori della resistività e del coefficiente di Hall sono stati determinati a meno di un fattore di proporzionalità, dipendente dalle dimensioni dei campioni e dai parametri del circuito di misura, che si è avuto cura di mantenere rigorosamente costanti. Poichè per gli scopi del presente lavoro hanno interesse soltanto le variazioni percentuali della resistività e del coefficiente di Hall, non ha molta importanza conoscere con grande precisione i valori numerici di questi fattori di proporzionalità per ϱ e R .

Una particolare cura è stata invece dedicata alla misura dell'intensità del campo B , che è stata effettuata mediante un flussometro a risonanza nucleare (¹⁰), con un errore inferiore a una parte su mille.

I risultati sperimentali sono illustrati dai grafici 1, 2, 3, 4 e 5, nei quali sono riportati i valori di ϱ/ϱ_0 e R/R_0 (ϱ_0 e R_0 essendo definiti, rispettivamente, dalle relazioni: $\varrho_0 = \lim_{B \rightarrow 0} \varrho$, $R_0 = \lim_{B \rightarrow 0} R$), in funzione dell'intensità del campo d'induzione magnetica B e dell'orientazione di esso e della corrente rispetto agli assi cristallografici.

Poichè non è possibile una determinazione sperimentale diretta di R_0 , esso è stato determinato, caso per caso, mediante estrapolazione dei dati relativi ai più bassi valori dell'intensità del campo per i quali la misura è stata effettuata.

(¹⁰) V. ANDRESCIANI E D. SETTE: *Ric. Sci.*, **26**, 1101 (1956).

Le misure sono state effettuate, per ogni orientazione, su vari campioni, tagliati dai medesimi monocrystalli, di tipo «n» o «p». I risultati ottenuti con campioni dello stesso tipo orientati allo stesso modo sono perfettamente concordanti; perciò si è ritenuto sufficiente riportare i dati relativi ad un solo campione per ciascuno dei vari casi presi in esame.

3. - Germanio di tipo «p».

Le Fig. 1, 2 e 3 illustrano i risultati delle misure effettuate sui campioni di tipo «p». A questi risultati, purtroppo, non è possibile dare una interpretazione teorica soddisfacente. Infatti il calcolo dei coefficienti galvanomagnetici per il germanio «p» è, dal punto di vista matematico, estremamente difficoltoso, essendo

molto complessa la struttura della banda di valenza, che è stata resa nota dai risultati delle esperienze di risonanza ciclotronica.

Ci siamo perciò limitati ad effettuare un confronto fra i risultati sperimentali da noi ottenuti e quelli deducibili mediante la teoria semplificata di Willardson, Harman e Beer (WHB) (11) fondata sull'ipotesi di superfici d'energia sferiche, che ha permesso di spiegare alcuni dati sperimentali ottenuti dagli autori di essa su campioni di tipo «p» con corrente perpen-

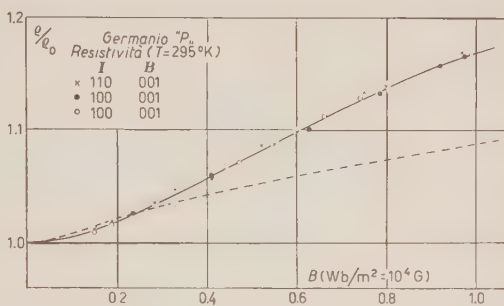


Fig. 1. - Dipendenza della resistività dall'intensità del campo di induzione magnetica \mathbf{B} in campioni orientati di germanio «p».

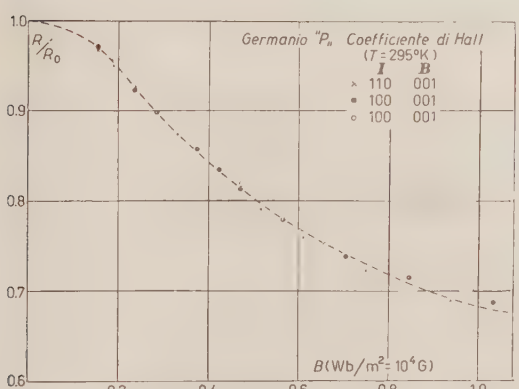


Fig. 2. - Dipendenza del coefficiente di Hall dall'intensità del campo di induzione magnetica \mathbf{B} in campioni orientati di germanio «p».

dicolare alla direzione cristallografica (111). Questa teoria ha il pregio di spiegare le forti variazioni di g e R con l'intensità del campo di induzione magne-

(11) T. C. HARMAN, R. K. WILLARDSON e A. C. BEER: *Phys. Rev.*, **96**, 1512 (1954).

tica, attribuendole essenzialmente alla presenza delle cosiddette « lacune veloci », dotate di una piccola massa efficace e di una elevata mobilità. La presenza di queste lacune è stata confermata dalle esperienze di risonanza ciclotronica.

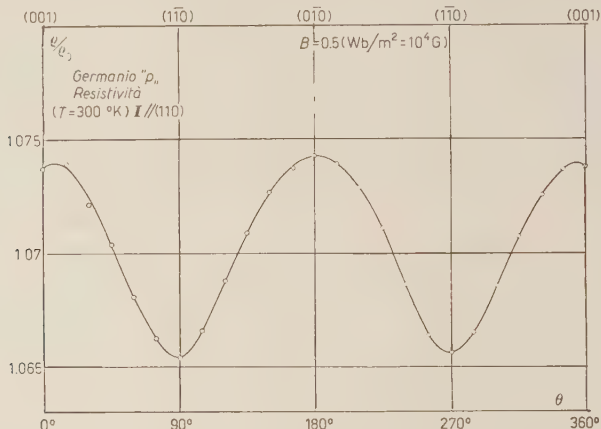


Fig. 3. — Dipendenza dell'effetto di magnetoresistenza dalla direzione del campo di induzione magnetica \mathbf{B} nel germanio « p ». Nella figura è rappresentato l'andamento della resistività in funzione dell'angolo compreso fra la direzione di \mathbf{B} e la direzione cristalografica (001).

Nella teoria di WHB è tenuto conto anche della presenza di elettroni nella banda di conduzione, anch'essa supposta con superfici d'energia sferiche. Nella espressione del coefficiente di Hall e della resistività intervengono pertanto sei parametri: le concentrazioni n_1 , n_2 e n_3 e le mobilità μ_1 , μ_2 e μ_3 , rispettivamente degli elettroni, delle lacune normali e di quelle veloci. Fra questi parametri intercorrono tre relazioni:

$$\left\{ \begin{array}{l} \sigma = \frac{1}{\rho} = e(n_1\mu_1 + n_2\mu_2 + n_3\mu_3), \\ R_0 = -\frac{3\pi}{8e} (n_1\mu_1^2 - n_2\mu_2^2 - n_3\mu_3^2)/(n_1\mu_1 + n_2\mu_2 + n_3\mu_3)^2, \\ n_1(n_2 + n_3) \simeq 3 \cdot 10^{32} T^3 \exp[-0.785/kT]. \end{array} \right.$$

Restano pertanto da determinare tre parametri. Utilizzando i dati illustrati nella Tabella I, dedotti in parte dai risultati ottenuti da WHB, si ottiene per $\rho = 14 \Omega \text{ cm}$ e $T = 300^\circ \text{K}$:

$$n_1 = 1.5 \cdot 10^{12} \text{ cm}^{-3}; \quad n_2 = 2 \cdot 10^{14} \text{ cm}^{-3}; \quad n_3 = 4 \cdot 10^{12} \text{ cm}^{-3}.$$

TABELLA I.

μ_1	μ_2	μ_3/μ_2	μ_3	n_3/n_2
3 900 (cm ² /V s)	1 900 (cm ² /V s)	8	15 200 (cm ² /V s)	0.02

Se ne deduce per R_0 il valore $R_0 = 6 \cdot 10^4$ cm³/coulomb, che è in buon accordo con il valore ottenuto da noi sperimentalmente ($5.7 \cdot 10^4$ cm³/coulomb).

L'andamento teorico delle curve che esprimono R/R_0 e ϱ/ϱ_0 in funzione dell'intensità del campo di induzione magnetica (tratteggiato nelle Fig. 1 e 2) può essere allora calcolato mediante la teoria di WHB e precisamente usando le formule (10) e (11) del loro lavoro (11).

Per quanto riguarda il coefficiente di Hall si ha un buon accordo con i dati sperimentali. Per quanto riguarda invece l'effetto di magnetoresistenza si nota un sensibile scarto fra la curva teorica e quella sperimentale. Ciò è probabilmente da attribuire al fatto che i valori da noi supposti validi per i rapporti μ_3/μ_2 e n_3/n_2 sono stati ottenuti da WHB con misure relative a campioni orientati differentemente da quelli usati nel corso della presente ricerca. Poichè la teoria di WHB è fondata sulla ipotesi di superfici d'energia sferiche, essa non può, evidentemente, spiegare in modo soddisfacente gli effetti di anisotropia, effetti che sono abbastanza sensibili, come risulta anche dai risultati sperimentali illustrati nella Fig. 3.

In linea di principio, con una conveniente scelta dei valori da attribuire ai vari parametri che intervengono nel calcolo, dovrebbe essere possibile ottenere un migliore accordo fra questa teoria ed i risultati sperimentali. Purtroppo, però, non esiste un criterio che permetta di effettuare tale scelta in base a qualche ipotesi plausibile.

Si potrebbero, ad esempio, mantenere inalterati i valori delle concentrazioni n_1 , n_2 e n_3 (che sono evidentemente indipendenti dall'orientazione) e quelli delle mobilità μ_1 e μ_2 (le cui variazioni non producono sensibili spostamenti delle curve teoriche), e far variare invece il valore della mobilità delle lacune veloci, μ_3 , giacchè questo è il parametro da cui dipendono principalmente le variazioni di ϱ e R . Si osserva, però, che, mentre l'accordo fra la curva teorica della resistività e quella sperimentale non migliora sensibilmente, si ha un notevole disaccordo con l'esperienza per quanto riguarda il valore di R_0 e l'andamento del rapporto R/R_0 in funzione dell'intensità del campo. Ad esempio, supponendo $\mu_3/\mu_2 = 10$ ($\mu_3 = 19\,000$ cm²/Vs), si ottiene $R_0 = 7.76 \cdot 10^4$ cm³/coulomb e, per $B = 0.75$ Wb/m², si ha $\varrho/\varrho_0 = 1.092$ e $R/R_0 = 0.61$.

Inoltre va osservato che, se si utilizzano le informazioni fornite dalle misure

di risonanza ciclotronica sui valori delle componenti del tensore di massa efficace per calcolare le componenti del tensore della mobilità, mediante la relazione

$$\mu_{ij} \propto m_{ij}^{-\frac{5}{2}}$$

(che è generalmente valida quando la mobilità è determinata essenzialmente dalle interazioni fra i portatori di carica e le vibrazioni reticolari), si ottengono valori che non sono in accordo con quelli illustrati nella Tabella I.

Si può pertanto concludere che la teoria di WHB, pur essendo sufficiente

per una interpretazione approssimata dei dati sperimentali, va opportunamente corretta per tener conto degli effetti di anisotropia.

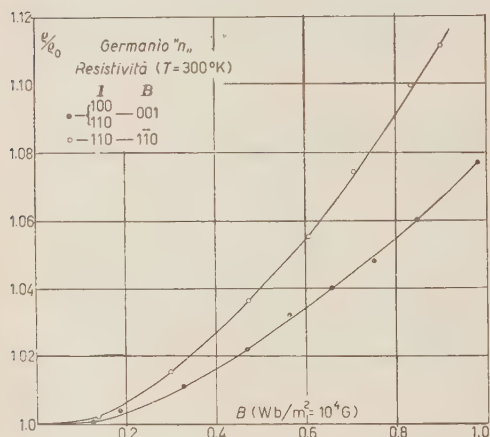


Fig. 4. — Dipendenza della resistività dall'intensità del campo di induzione magnetica B in campioni orientati di germanio « n ».

soldi di rotazione. Pertanto il tensore della resistività ha due sole componenti distinte, una longitudinale m_l e una trasversale, m_t .

Vari autori (12,13) hanno effettuato il calcolo dei coefficienti galvanomagnetici nell'ipotesi di superfici d'energia sferoidali. Per l'interpretazione dei nostri risultati ci siamo serviti dei calcoli eseguiti da ABELES e MEIBOOM (13). Questi ottengono le espressioni del coefficiente di Hall e dei coefficienti di magnetroresistenza, per varie orientazioni del campo e della corrente rispetto agli assi cristallografici, in funzione del parametro $K = m_l/m_t$.

I risultati sperimentali sono in ottimo accordo con le previsioni teoriche. Mediante un confronto quantitativo è possibile determinare, entro certi limiti,

4. — Germanio di tipo « n ».

Le Fig. 4 e 5 illustrano i risultati delle misure effettuate su campioni di tipo « n ». In questo caso è possibile dare una corretta interpretazione teorica ai risultati sperimentali. Infatti la struttura della banda di conduzione del germanio è relativamente semplice, le superfici d'energia essendo ellissoidi di rotazione.

Pertanto il tensore della resistività ha due sole componenti distinte, una longitudinale m_l e una trasversale, m_t .

(12) M. SHIBUYA: *Phys. Rev.*, **95**, 1385 (1954).

(13) S. MEIBOOM e B. ABELES: *Phys. Rev.*, **95**, 31 (1954).

il valore del parametro K . Dai dati sperimentali relativi all'effetto di magneto-resistenza si deduce che K deve essere compreso fra 8 e 12. Una determinazione più accurata non è possibile, perché i valori teorici dei coefficienti galvanomagnetici sono assai poco sensibili alle variazioni di K . Inoltre le variazioni percentuali del coefficiente di Hall con l'intensità del campo (v. Fig. 5) sono, nel germanio di tipo «n», molto piccole, e spesso dello stesso ordine di grandezza dell'errore sperimentale. Per le curve della Fig. 5 questo non supera il 3%.

L'esperienza conferma tuttavia le previsioni teoriche secondo le quali le variazioni della resistività e del coefficiente di Hall con corrente in direzione (110) e campo in direzione (110) sono maggiori di quelle che si hanno con corrente in direzione (100) e (110) e campo in direzione (001).

Le indicazioni ottenute nella presente ricerca inducono a ritenere che il valore di K alla temperatura ambiente, sia sensibilmente inferiore a quello fornito dalle esperienze di risonanza ciclotronica ($K = 20$). Questo risultato è in accordo con altri ottenuti in precedenza nel corso di analoghe ricerche, le quali avevano fra l'altro permesso di stabilire un limite superiore pari a 15.6 per il valore di K (8,14).

Va notato, comunque, che il divario fra i nostri risultati e quelli delle esperienze di risonanza ciclotronica è probabilmente soltanto apparente. Infatti una teoria corretta degli effetti galvanomagnetici nel germanio di tipo «n» dovrebbe tener conto, come è stato recentemente osservato (15), oltre che della anisotropia delle superfici d'energia, anche di quella relativa ai processi di collisione che determinano la mobilità dei portatori di carica. In tal caso è necessario introdurre un tensore del tempo di rilassamento. Con superfici d'energia sferoidali questo tensore avrà due sole componenti distinte, τ_i e τ_t , relative alle direzioni degli assi principali degli ellissoidi dell'energia. Il para-

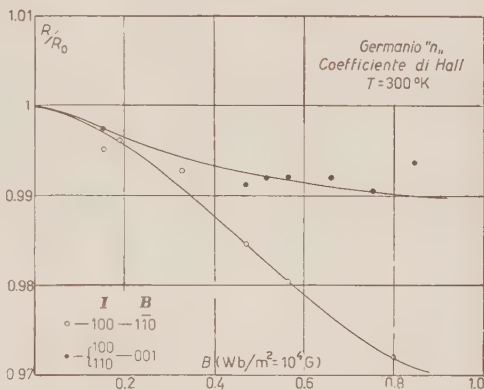


Fig. 5. - Dipendenza del coefficiente di Hall dall'intensità del campo di induzione magnetica B in campioni orientati di germanio «n».

(14) G. C. DELLA PERGOLA e D. SETTE: *Phys. Rev.*, **104**, 598 (1956).

(15) C. HERRING e E. VOGT: *Phys. Rev.*, **101**, 944 (1956).

metro K risulterebbe allora definito dalla relazione

$$K = \frac{m_l}{m_t} \frac{\tau_t}{\tau_l},$$

mentre le espressioni teoriche dei coefficienti galvanomagnetici restano inalterate.

Va inoltre ricordato che le esperienze di risonanza ciclotronica sono state eseguite alla temperatura di 4 °K e, d'altra parte, la struttura delle bande d'energia, e quindi il valore del rapporto m_l/m_t , sono probabilmente variabili con la temperatura, con una legge che, però, non è ancora conosciuta.

S U M M A R Y

Resistivity and Hall effect's measurements were performed at room temperature on n-type and p-type oriented germanium single crystals, as a function of intensity of magnetic induction, between 0.15 and 1.0 Wb/m². The results of the measurements were compared with theoretical expectations based on the present knowledge of germanium band structure. The comparison is satisfactory for n-type germanium; the ratio of longitudinal to transverse electron effective masses has been found to be between 8 and 12. The valence band structure of germanium is so complicate that no mathematical treatment has been developed to compare the results of measurements of galvanomagnetic effects in p-type germanium with theory. An approximate theory has been however used to partially explain the experiment; the observed anisotropy however can not be explained in this way.

The Flux of Primary Cosmic Ray α -Particles over Sardinia.

H. H. ALY (*) and C. J. WADDINGTON

H. H. Wills Physical Laboratory - Bristol, England

(ricevuto l'8 Aprile 1957)

Summary. — The flux of α -particles in the primary cosmic radiation has been determined over Sardinia, geomagnetic latitude, λ , 41° N. A nuclear emulsion technique was employed. The result obtained of 72 ± 9 α -particles/m²·sr·s, was considerably higher than the only other directly comparable experimental result, but was in good agreement with the predicted value. The implications of this result are discussed.

1. — Introduction.

It has been shown (^{1,2}), that α -particle and heavy primary fluxes obtained over Europe are lower than those obtained at similar geomagnetic latitudes over America. These differences have been interpreted as being due to the inadequacy of using geomagnetic theory to calculate the true cut-off energies at different geographical localities (¹). The correctness of this interpretation has been confirmed by the measurements of positions of the «cosmic ray equator» (³), and by the direct measurement of the cut-off energies of multiply charged particles (^{1,4}).

A recent determination of the α -particle flux over Sardinia by DE MARCO *et al.* (⁵) gave a value of (39 ± 8.6) α -particles/m²·sr·s; appreciably lower than the value predicted from other observations on the geomagnetic anomaly.

(*) On leave of absence from the College of Arts and Science, Baghdad.

(¹) C. J. WADDINGTON: *Nuovo Cimento*, **3**, 930 (1956).

(²) H. FAY: *Zeits. f. Naturf.*, **10a**, 572 (1955).

(³) J. A. SIMPSON, K. B. FENTON, J. KATZMAN and D. C. ROSE: *Phys. Rev.*, **102**, 1648 (1956).

(⁴) P. H. FOWLER and C. J. WADDINGTON: *Phil. Mag.*, **1**, 637 (1956).

(⁵) A. DE MARCO, A. MILONE and M. REINHARZ: *Nuovo Cimento*, **3**, 1150 (1956).

This determination was, however, of low statistical weight, and the experimental procedure appeared to be open to criticism. For these reasons the $\bar{\alpha}$ -particle flux over Sardinia has been re-determined using a nuclear emulsion method similar to those previously employed in this laboratory.

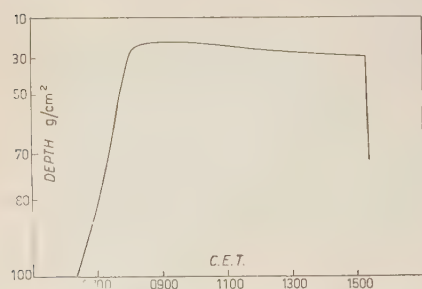


Fig. 1. — Flight curve as determined by radar, visual observation and radiosonde.

The flight curve, Fig. 1, was determined by radar, visual observation and radiosonde equipment.

2.2. Track selection. — Emulsions near the centre of the stack were scanned along lines parallel to the top edge. These lines were separated by a distance of one centimeter and were at least one centimeter from the outside edges. Tracks crossing these scanning lines were recorded if they satisfied the following selection criteria. Each track:

- (i) had to have a length of more than 6 mm per emulsion;
- (ii) had to have a grain density of at least three times the minimum value;
- (iii) had to make an angle with the vertical of less than 60° .

All particles whose tracks were found in this manner were traced through the stack until they either left, interacted, or were brought to rest. Altogether, in a total scanning length of 48 cm the tracks of 242 particles were found. Of these, 65 were identified as α -particles, 78 came to rest, 83 left the stack, and 16 produced low energy disintegrations.

2.3. Track measurement. — Six hundred grains were counted on every track before it was traced through the emulsions. In addition, as a check on the detection efficiency (see Appendix), a measurement was made on every track of the depth in the emulsion at which it had been detected.

For those particles which were brought to rest in the stack, the range and

grain density were sufficient to identify the particle. The distribution of these parameters is shown in Fig. 2. It can be seen that these particles were all singly charged.

Before measuring the scattering parameters of the remaining particles their charges were provisionally estimated by a visual inspection. Scattering measurements were then made on twenty 500 μm cells on the tracks of particles thus identified as being singly charged, and on fifty such cells on those identified as α -particles. In both cases a $4D$ replacement cut-off was applied, and noise was eliminated by a procedure similar to that used by FOWLER and WADDINGTON (4).

The variation of scattering parameter with grain density is shown in Fig. 3. This figure shows that the α -particles are clearly resolved from those of single charge.

It should be noted that, due to the high level of distortion in this stack, the scattering parameters obtained for the α -particles can only be regarded as upper limits to the true values. It will be seen later (Sect. 4) that the true scattering parameters must all have been of less than $0.008^\circ/100 \mu\text{m}$. That these identifications of charge are essentially correct is supported by the observed characteristics of the disintegrations, and by the measured value for the α -particle mean

This value is in excellent agreement

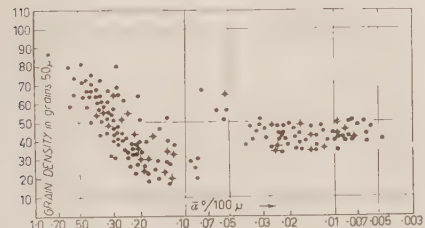


Fig. 3. - The variation of grain density and scattering parameter for all particles not brought to rest in the stack. Those particles which interacted are indicated by +.

free path of (17.6 ± 5) cm of emulsion. This value is in excellent agreement with those found previously (6,7).

(6) C. J. WADDINGTON: *Phil. Mag.*, **1**, 105 (1956).

(7) M. V. K. APPA RAO, R. R. DANIEL and K. A. NEELAKANTAN: *Proc. Ind. Acad.*, **43**, 181 (1956).

3. - Results.

In order to calculate the flux of α -particles observed in the emulsions it was necessary to allow for the shielding of some of the scanned area, since the scanning lines were not independent of each other. For this reason the total scanned length has to be reduced to a true effective length of 30 cm. Thus the flux of α -particles in the emulsions was (38 ± 5) α -particles/m²·sr·s. To extrapolate this value to that at the top of the atmosphere corrections were made for the absorption of α -particles in the matter above the point of detection, and for the production of secondary α -particles by heavier particles above the stack. The latter correction was applied by solving diffusion equations for the various components of the primary radiation (⁴), using the heavy primary flux values found by FAY (²) at the same geographic locality, and the fragmentation probabilities of FOWLER *et al.* (⁹). Applying these corrections the flux of primary α -particles at the top of the atmosphere was found to be:

$$(72 \pm 9) \text{ } \alpha\text{-particles/m}^2 \cdot \text{sr} \cdot \text{s}.$$

4. - Discussion.

From the α -particle energy spectrum published by FOWLER and WADDINGTON (¹) this flux value gives a cut-off energy of $2.0^{+0.30}_{-0.25}$ GeV per nucleon for multiply charged particles over Sardinia, where the quoted errors are solely those due to the statistical error in the flux determination. This value of the cut-off energy may be compared with that of 1.8 GeV per nucleon predicted by geomagnetic theory (¹⁰), and that of 2.25 GeV per nucleon predicted on the assumption that over Europe there is a 4° shift southward of the «cosmic ray» latitudes with respect to the geomagnetic latitudes (¹). It can be seen that the result obtained in this experiment is consistent with either picture, but is quite inconsistent with that obtained by DE MARCO *et al.* (⁵), since the flux value quoted by them corresponds to a cut-off energy of $3.6^{+0.6}_{-1.1}$ GeV per nucleon.

* * *

We are grateful to Professor C. F. POWELL for the hospitality of his laboratory. One of us, C. J. W., wishes to thank the Royal Society for the award of a Mackinnon Research Studentship.

(⁸) M. F. KAPLON, J. H. NOON and G. W. RACETTE: *Phys. Rev.*, **95**, 1408 (1954).

(⁹) P. H. FOWLER, R. R. HILLIER and C. J. WADDINGTON: *Phil. Mag.*, **2**, 293 (1957).

(¹⁰) F. S. JORY: *Phys. Rev.*, **102**, 1167 (1956).

APPENDIX

The efficiency of detection of α -particles.

The procedure of checking the detection of efficiency achieved in this experiment closely followed that adopted previously (1), and the reader is referred

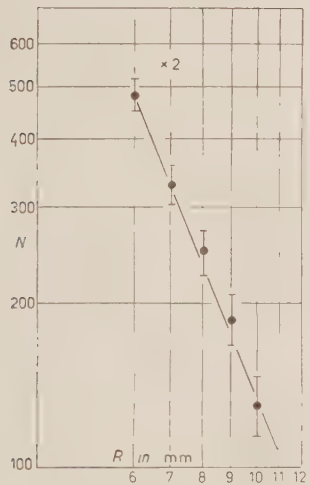


Fig. 4. — The integral length distribution of all the tracks found by scanning. For convenience of representation all values have been increased by a factor two.

to that paper for details. Essentially there are various possible ways in which a track might not have been detected by the scanner, who in this case was one of us (H.H.A.), and these are checked as follows.

(i) The integral length distribution of all the tracks is shown in Fig. 4. It can be seen that there is no apparent evidence for the missing of short tracks.

(ii) Fig. 5 shows the grain density distribution of the singly charged particles compared to that of the α -particles, and shows that the possibility of missing α -particles due to an underestimate of their grain density was small.

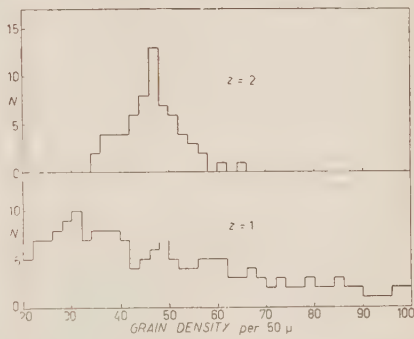


Fig. 5. — The distribution of grain density for singly and doubly charged particles.

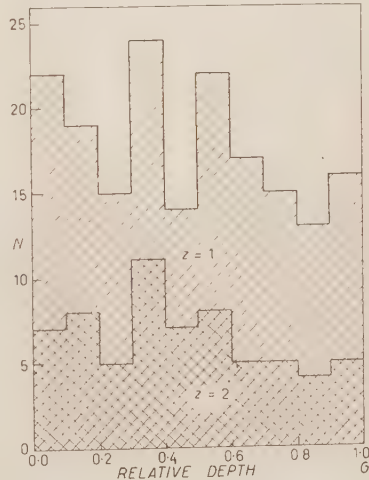


Fig. 6. — The distribution of depth in the emulsion at which each track was detected.

(iii) In all 48 tracks found in one scan should have been, and were, observed in a second scan, thus showing that there can have been little indiscriminate missing of tracks.

(iv) The measurements of the depth in the emulsions at which each track was found are shown in Fig. 6. This figure shows that the scanning efficiency has been sensibly constant throughout the depth of emulsion.

It must, therefore, be concluded that few, if any, of the α -particles present in the scanned area have not been detected.

RIASSUNTO (*)

Si è determinato sulla Sardegna (latitudine geomagnetica, λ , 41° N) il flusso delle particelle α nella radiazione cosmica primaria, servendosi di una tecnica a base di emulsioni nucleari. Il risultato ottenuto ((72 ± 9) particelle $\alpha/m^2 \cdot sr \cdot s$) è stato considerevolmente più elevato del solo altro risultato sperimentale confrontabile col nostro, ma si trova in buon accordo col valore previsto. Si discutono le conseguenze implicite in tale risultato.

(*) Traduzione a cura della Redazione.

Parity Violation and the Spin of the Λ^0 Particle.

F. CERULUS

CERN - Geneva

(ricevuto il 13 Aprile 1957)

Summary. — The ratio of non-mesonic to mesonic decay is calculated using a phenomenological hamiltonian for the Λ -decay interaction and for the pion-nucleon interaction. In the calculation the absorption by the nucleons of charged and neutral virtual pions from the Λ is taken into account, and parity conservation in the Λ -decay is not assumed. If parity were strongly violated, a comparison of the results of the calculation with experiment would indicate that the Λ has spin $\frac{1}{2}$. If the parity violation is slight, spin $\frac{3}{2}$ is still possible. The value of the ratio of non-mesonic to mesonic decay is calculated numerically for ${}^4\text{He}_\Lambda$, ${}^4\text{H}_\Lambda$ and ${}^9\text{Be}_\Lambda$ under different assumptions about spin and parity.

1. — Introduction.

In a recent article RUDERMAN and KARPLUS⁽¹⁾ derived a relation between the ratio of mesonic to non-mesonic decays of hypernuclei and the spin of the Λ^0 .

Since the publication of this analysis, the belief in the conservation of parity in weak interactions has been heavily shaken, and it seems useful to enquire into the effects of a possible parity violation on the Λ -decay.

If parity is not conserved, the (real or virtual) pion may be emitted on two different l -waves and these transitions will be governed by two different coupling constants λ_+ and λ_- . Interference terms will arise, giving an asymmetric angular distribution of the decay of an oriented Λ^0 -particle, but in the calculation of the decay rates no terms with λ_+ , λ_- will show up.

⁽¹⁾ M. RUDERMAN and R. KARPLUS: *Phys. Rev.*, **102**, 247 (1956) (henceforth cited as R.K.; we follow closely the notation of these authors).

It will appear from the analysis that the ratio of mesonic to non-mesonic decay will, for a given spin j of the Λ^0 , lie between the two possible values obtained in the case of parity conservation, the exact value being determined by the ratio λ_+/λ_- .

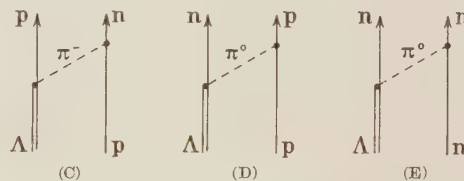
In comparing the results of the experiment with the calculation one should keep in mind that not all decay modes are observable, or could be distinguished one from the other. The following mesonic decays occur:

$$(A) \quad \Lambda^0 \rightarrow p + \pi^- ,$$

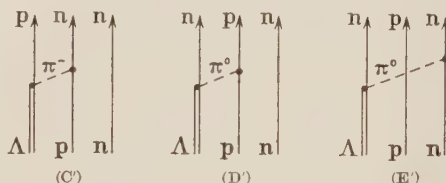
$$(B) \quad \Lambda^0 \rightarrow n + \pi^0 .$$

The last one should be half as frequent as the first for theoretical reasons (2-4) which seem not to be contradicted by experiment.

The non-mesonic decays can occur by exchange of a virtual π^- or π^0 -meson; the graphs for this phenomenon are



Experimentally there is no way to distinguish strictly which of the three graphs (C), (D) or (E) is responsible for a non-mesonic decay of a hyper-nucleus containing neutrons and protons. Let us take e.g. the case of the ${}^3H_{\Lambda}$. Its non-mesonic decay is described by three graphs



The deuteron-like binding of the n and p has the effect that the $\pi^{0,-}$ will be absorbed by a nucleon having already a certain momentum, say p , in the center of mass system of the hypernucleus.

(2) B. D'ESPAGNAT et J. PRENTKI: *Nuovo Cimento*, **3**, 1045 (1956).

(3) R. GATTO: *Nuovo Cimento*, **2**, 318 (1956).

(4) G. TAKEDA: *Phys. Rev.*, **101**, 1547 (1956).

If $-k$ is the momentum of the pion

in (C')	the p	has a momentum	k
	one n	» » »	$p - k$
	one n	» » »	$-p$
in (D')	the p	» » »	$p - k$
	one n	» » »	k
	one n	» » »	$-p$
in (E')	the p	» » »	$-p$
	one n	» » »	k
	one n	» » »	$p - k$

It is easy to see when one takes the Fourier transform of the deuteron wave function ⁽⁵⁾ describing approximately the $n+p$

$$\varphi_b(x) = \frac{1}{x} \exp[-\sqrt{ME_b}x](1 - \exp[-x]),$$

i.e.

$$\varphi_b(p) \sim \frac{1}{ME_b + p^2} - \frac{1}{(\sqrt{ME_b} + 1)^2 + p^2},$$

(where $E_b = 2.2$ MeV and $\sqrt{ME_b} = 45$ MeV $= 0.32 m_\pi c^2$) that for $p = k = 3$ (in units $\hbar = c = m_\pi = 1$) a graph gives 1/500 of its contribution with $p = 0$. In this approximation one may therefore neglect the interference effects between (D') and (E'), and only retain those between (C') and (D'); in the latter we neglect the p -dependence. An analogous reasoning could be made for other nuclei; the confinement of a nucleon wave function in the region of the nucleus will produce a momentum spectrum of a width $1/2R$ which will always be small compared with the momentum $k = 3.0$ resulting from the π -capture.

As far as the observability of the non-mesonie decay is concerned, all three graphs will give rise to a visible process at the end of a hypernucleus track, because even in case (E) it is reasonable to assume that one or more charged particles of a few MeV will be ejected along with the two fast neutrons. (Compare e.g. the absorption of a π^- by a nucleus, giving a σ -star, 70% of which are visible in emulsion). Anyhow, it would be quite easy to allow in the calculation for some loss of these events.

(5) L. HULTHÉN: *Arkiv Mat. Astron. Fysik*, **28A**, No. 5 (1941).

The mesonic decay into neutral particles (Type (B)) will probably not be observed, the decay neutrons having only 5.5 MeV. If one wanted to include it, it should be counted among the «non-mesonic» decays, as no charged π will be seen in the desintegration.

One should therefore calculate the ratio of the decay rates

$$Q = \frac{\text{rate of } [(C) + (D)] + \text{rate of } (E)}{\text{rate of } (A)}.$$

2. - Calculation.

We take the interaction operator given by R.K. for process (Λ)

$$(1) \quad H_i = \int d\mathbf{r} \psi_{\nu}^{(p)}(\mathbf{r}) \int d\mathbf{r}' T_{\nu\mu}(\mathbf{r} - \mathbf{r}') \varphi(\mathbf{r}') \psi_{\mu}^{(\Lambda)}(\mathbf{r}).$$

The operator $T_{\nu\mu}$ consists of two terms which project the system $\pi + p$ on two states of the same total angular momentum as the Λ^0 but with different parity.

The Fourier transform of $T_{\nu\mu}$ is

$$(2) \quad T_{\nu\mu}(\mathbf{k}) = \lambda_+ k^{j-\frac{1}{2}} \left[\sqrt{\frac{j-\mu+1}{2j+2}} Y_{j+\frac{\mu+r}{2}} \left(\frac{\mathbf{k}}{k} \right) \delta_{\nu, \frac{1}{2}} - \sqrt{\frac{j+\mu+1}{2j+2}} Y_{j+\frac{\mu+r}{2}} \left(\frac{\mathbf{k}}{k} \right) \delta_{\nu, -\frac{1}{2}} \right] + \\ + \lambda_- k^{j-\frac{1}{2}} \left[\sqrt{\frac{j+\mu}{2j}} Y_{j-\frac{\mu+r}{2}} \left(\frac{\mathbf{k}}{k} \right) \delta_{\nu, \frac{1}{2}} + \sqrt{\frac{j-\mu}{2j}} Y_{j-\frac{\mu+r}{2}} \left(\frac{\mathbf{k}}{k} \right) \delta_{\nu, -\frac{1}{2}} \right].$$

The coupling constants λ_+ and λ_- have different dimensions:

$$[\lambda_+] = [L][\lambda_-].$$

The decay rate of a free Λ^0 into free p and π^- is then given by

$$(3) \quad R_{\text{charged mesonic}} = \frac{1}{2\pi} [\lambda_+^2 q^{2j+2} + \lambda_-^2 q^{2j}],$$

where $q = 0.73$ is the momentum of the π^- .

If parity is conserved, one of the two terms in (3) has to be zero.

For calculating the non-mesonic decay one proceeds along the same lines as in R.K. The matrix element $M_{(-)}(k)$ from graph (C) is given in R.K. The matrix element $M_{(0)}(k)$ from (D) is related to $M_{(-)}(k)$ in the following manner: because of the rule $|\Delta I| = \frac{1}{2}$ the vertex $(\bar{n}\pi^0\Lambda)$ introduces a factor $-1/\sqrt{2}$ compared to the vertex $(\bar{p}\pi^- \Lambda)$ and $(\bar{p}\pi^0 p)$ because of charge independence of nuclear forces gives a factor $1/\sqrt{2}$ as compared to $(\bar{n}\pi^- p)$.

The sign of the momentum of the pion is changed so as to have the same final state in both $(M_{(-)})$ and $(M_{(+)})$:

$$\langle p, \mathbf{k}; n, -\mathbf{k} | .$$

Consequently

$$M_{(-)}(\mathbf{k}) + M_{(+)}(\mathbf{k}) = g\sqrt{2}\sqrt{\varrho_p} \frac{(\bar{u}^{(N)}\sigma \cdot \mathbf{k} u^{(N)})\{\bar{u}_\nu^{(N)}[T_{\nu\mu}(\mathbf{k}) + \frac{1}{2}T_{\nu\mu}(-\mathbf{k})]u_\mu^{(N)}\}}{k^2 + 1 - [\sqrt{k^2 + M^2} - M']^2},$$

$u^{(N)}$ are the normalized spinors of the nucleons.

The desintegration rate, after summing over the different spin states of the end-particles, is then

$$(4) \quad R_{\text{charged non-mesonic}} = \frac{1}{\pi} g^2 \varrho_p \frac{M}{[M(M' - M) + 1]^2} k^{2j+2} \cdot \left\{ \lambda_+^2 k^2 \left[\frac{5}{4} + (-1)^{j+\frac{1}{2}} \right] + \lambda_-^2 \left[\frac{5}{4} + (-1)^{j-\frac{1}{2}} \right] \right\}.$$

The matrix element from graph (E) is obtained from the one from (C) by introducing again the factor $1/\sqrt{2}$ because of the vertex $(\bar{n}\pi^0\Lambda)$ and $-1/\sqrt{2}$ because of $(\bar{n}\pi^0n)$, i.e. by multiplying $M_{(-)}(k)$ with $\frac{1}{2}$.

The rate calculated from it is then

$$(5) \quad R_{\text{neutral non-mesonic}} = \frac{1}{4\pi} g^2 \varrho_n \frac{M}{[M(M' - M) + 1]^2} k^{2j+2} (\lambda_+^2 k^2 + \lambda_-^2) .$$

The ratio of non-mesonic to mesonic decay is consequently

$$(6) \quad Q = 2g^2 \frac{M}{[M(M' - M) + 1]^2} k^2 \left(\frac{k}{q} \right)^{2j} [\varrho_p P_+(j) + \frac{1}{2} \varrho_n P_0],$$

with

$$P_+(j) = \frac{\eta^2 k^2 [1.25 + (-1)^{j+\frac{1}{2}}] + 1.25 + (-1)^{j-\frac{1}{2}}}{\eta^2 q^2 + 1},$$

$$P_0 = \frac{\eta^2 k^2 + 1}{\eta^2 q^2 + 1},$$

$$\eta = \frac{\lambda_+}{\lambda_-} \text{ (in units } \lambda_\pi).$$

The variation of $P_+(j)$ and P_0 with η and j is shown in Table I.

TABLE I.

$\eta =$	0	0.5	1	2	∞
P_+ $j = \frac{1}{2}, \frac{5}{2}, \dots$	2.25	2.49	2.94	3.60	4.24
P_\perp $j = \frac{3}{2}, \frac{7}{2}, \dots$	0.25	4.70	13.40	26.0	38.2
P_0	1	2.84	6.46	11.7	16.7

Putting in the numerical values in (6) we obtain

$$(7) \quad Q = (1.32 \varrho_p P_+(j) + 0.33 \varrho_n P_0) \cdot (4.1)^{2j} .$$

3. – Applications.

For the lightest hyperfragments where the particles may be assumed to be approximately free and the exclusion principle does not forbid certain states for the decay nucleus, we can use (7). For ϱ_p we have to take

$$Z \cdot \int \varrho_p(\mathbf{r}) \varrho_\Lambda(\mathbf{r}) d\mathbf{r} ,$$

to account for the extension of the Λ outside the nucleus. A similar expression is used for ϱ_n .

For ${}^4\text{He}_\Lambda$ we took

$$\varrho_\Lambda(r) = \frac{\sqrt{2M'E_b}}{2\pi r^2} \exp[-2\sqrt{2M'E_b}r] ,$$

where M' is the reduced mass of the Λ^0 and the ${}^3\text{He}$ nucleus, and $E_b = 1.7$ MeV is the Λ binding energy.

For $\varrho_p(r)$ and $\varrho_n(r)$ we took the density of an s -state in the shell-model, taking as the radius of ${}^3\text{He}$ $1.7 \cdot 10^{-13}$ cm⁽⁶⁾. Because the structures of ${}^4\text{He}_\Lambda$ and

(6) For ${}^1\text{He}$ the radius as found from electron scattering experiments is $1.5 \cdot 10^{-13}$ cm (R. W. McALLISTER and R. HOFSTADTER: *Phys. Rev.*, **102**, 851 (1956)). The wave function of the ${}^3\text{He}$ has probably a somewhat larger extension than that of ${}^4\text{He}$, because the ${}^3\text{He}$ is less tightly bound.

${}^4\text{H}_\Lambda$ are probably very alike and the binding energy of the Λ is about the same in both hypernuclei, we may use the above estimate for ${}^4\text{H}_\Lambda$ as well.

With the foregoing data we get Table II.

TABLE II.

	$j = \frac{1}{2}$			$j = \frac{3}{2}$		
	$\eta = 0$	$\eta = 1$	$\eta = \infty$	$\eta = 0$	$\eta = 1$	$\eta = \infty$
$Q_{{}^4\text{He}\Lambda}$	2.3	3.6	6.1	6.1	230	640
$Q_{{}^4\text{H}\Lambda}$	1.3	3.0	6.1	6.1	130	370

For heavier nuclei the exclusion principle forbids certain states to the decay nucleon because these are already occupied by other nucleons.

In a rough way, this can be accounted for as shown in R.K. Making the same approximation, $I^2 \approx \frac{1}{4}$, one gets for a nucleus with $Z = N = 4$, $\varrho_p = \varrho_n = 3/8\pi$ as in R.K., the results of Table III.

TABLE III.

$j = \frac{1}{2}$			$j = \frac{3}{2}$		
$\eta = 0$	$\eta = 1$	$\eta = \infty$	$\eta = 0$	$\eta = 1$	$\eta = \infty$
$Q_{Z=4}^{N=4}$	6.4	11.5	21	21	690
					1800

These new values confirm the conclusion that the spin of the Λ^0 could not be larger than $\frac{3}{2}$. To make more precise statements from a comparison with experiment, it would be necessary to have statistics allowing to get rather precise experimental values of Q for the various hypernuclei.

If from another type of experiment it would become apparent that parity is strongly violated in the Λ -decay, one could conclude that the spin has to be $\frac{1}{2}$, because $j = \frac{3}{2}$, $\eta \approx 1$ gives in all cases a much too large Q , compared with the known facts.

We gratefully acknowledge an important remark by Dr. B. d'ESPAGNAT and a stimulating discussion with Prof. B. FERRETTI.

RIASSUNTO (*)

Si calcola il rapporto del decadimento non mesonico al mesonico per mezzo di un'hamiltoniana fenomenologica per l'interazione del decadimento Λ e per l'interazione pione-nucleone. Nel calcolo si tien conto dell'assorbimento nei nucleoni di pioni carichi e neutri virtuali del Λ e non si postula conservazione di parità nel decadimento Λ . Se la parità fosse fortemente violata, il confronto dei risultati del calcolo coll'esperienza indicherebbe che il Λ ha spin $\frac{1}{2}$. Se la violazione della parità è di modesta entità è ancora possibile lo spin $\frac{3}{2}$. Si calcola numericamente il valore del rapporto del decadimento non mesonico al mesonico per ${}^4\text{He}_\Lambda$, ${}^3\text{H}_\Lambda$ e ${}^9\text{Be}_\Lambda$ con differenti ipotesi sullo spin e la parità.

(*) Traduzione a cura della Redazione.

On the Equivalence Theorem for the Massless Neutrino.

L. A. RADICATI

Istituto di Fisica dell'Università - Pisa

B. TOUSCHEK

Scuola di Perfezionamento in Fisica Nucleare dell'Università - Roma

Istituto Nazionale di Fisica Nucleare - Sezione di Roma

(ricevuto il 15 Aprile 1957)

Summary. — A new proof is presented of the Serpe-Fierz equivalence theorem for the free neutrino case. The interaction of neutrinos with their sources is seen to restrict the freedom in the neutrino description. It is proved that the only two state theory for the neutrino which does not give rise to double β -decay is the Weyl-Lee-Yang theory.

Recently LEE and YANG ⁽¹⁾ have proposed to apply WEYL's ⁽²⁾ two component theory of the neutrino to the β -decay process. The result is a theory in excellent agreement with the new information on weak interactions recently published by WU, LEDERMAN *et al.* ⁽³⁾,

It has been pointed out by SERPE ⁽⁴⁾, FIERZ ⁽⁵⁾ and by MC LENNAN ⁽⁶⁾ that Weyl's theory is completely equivalent to the theory of Majorana ⁽⁷⁾ with zero neutrino mass. In the present note we want to illustrate this equivalence.

⁽¹⁾ T. D. LEE and C. N. YANG: *Phys. Rev.*, **105**, 1671 (1957).

⁽²⁾ H. WEYL: *Zeits. f. Phys.*, **56**, 330 (1929); see also W. PAULI: *Hand. d. Phys.*, vol. **24/1**, p. 225 (Berlin 1933).

⁽³⁾ C. S. WU, E. AMBLER, R. HUDSON, R. HAYWORD, D. D. HOPPES and R. P. HUDSON: *Phys. Rev.*, **105**, 1413 (1957); R. L. GARWIN, L. M. LEDERMAN and M. WEINRICH: *Phys. Rev.*, **105**, 1415 (1957).

⁽⁴⁾ J. SERPE: *Physica*, **18**, 295 (1952).

⁽⁵⁾ FIERZ: Private communication to one of us.

⁽⁶⁾ Private communication from Prof. FIERZ to one of us.

⁽⁷⁾ E. MAJORANA: *Nuovo Cimento*, **14**, 171 (1937).

We begin by giving a different proof of the equivalence theorem which does not make explicit use of spinor calculus.

Let us first consider the case of a free neutrino. We assume that this particle has spin $\frac{1}{2}$ and mass zero. The Majorana neutrino is then represented by a q -number field μ_ϱ (ϱ = spinor index) with the property (in Majorana gauge which is used throughout)

$$(1) \quad \mu_\varrho^+ = \mu_\varrho .$$

The plane wave representation of μ_ϱ is:

$$(2) \quad \mu_\varrho(\mathbf{x}) = \frac{1}{\sqrt{2}} \sum_{\mathbf{p}, s=\pm 1} a(\mathbf{p}, s) u_\varrho(\mathbf{p}, s) \exp[i\mathbf{p} \cdot \mathbf{x}] + \text{H.C.} ,$$

(H.C. stand for hermitian conjugate), where $u(\mathbf{p}, s)$ satisfies the equations

$$(3) \quad (\alpha \cdot \mathbf{p} - |\mathbf{p}|) u(\mathbf{p}, s) = 0 ; \quad (\sigma \cdot \mathbf{p} - s|\mathbf{p}|) u(\mathbf{p}, s) = 0$$

Here α and β are the usual Dirac matrices and $a(\mathbf{p}, s)$ is a destruction operator defined by the anticommutation relations

$$(4) \quad \{a \cdot (\mathbf{p}, s), a(\mathbf{p}', s')\} = 0 ; \quad \{a(\mathbf{p}, s), a^+(\mathbf{p}', s')\} = \delta_{\mathbf{p}, \mathbf{p}'} \delta_{ss'} .$$

For every given value of the momentum vector \mathbf{p} the Majorana neutrino can therefore be formed in any one of the two states corresponding to $s = \pm 1$.

We shall call a theory of this type a two state theory of the neutrino, to be distinguished from the four state theory of an ordinary fermion.

The Lagrangian

$$(5) \quad \mathcal{L} = -\mu \gamma_4 \gamma_\mu \frac{\partial}{\partial x_\mu} \mu ,$$

is invariant under the substitution

$$(6) \quad P \mu(\mathbf{x}) P^{-1} = i \gamma_4 \mu(-\mathbf{x}) ,$$

which will be interpreted as representing space reflection, since it acts in this way on the equations of motion.

We now consider a set of spinors:

$$(7) \quad \sqrt{2} \lambda = (1 - \gamma_5) \mu , \quad \sqrt{2} \lambda^+ = (1 + \gamma_5) \mu ,$$

where the second equation follows from the first because of (1) and $\gamma_5^* = -\gamma_5$.

Using $\gamma_5 = -(\boldsymbol{\alpha} \cdot \mathbf{e})(\boldsymbol{\sigma} \cdot \mathbf{e})$ valid for an arbitrary unit vector \mathbf{e} and (3), we find from (2) that the Fourier representation of λ is:

$$(8) \quad \lambda_e = \sum_{\mathbf{p}} (a(\mathbf{p}+) u_e(\mathbf{p}+) \exp[i\mathbf{p} \cdot \mathbf{x}] + a^*(\mathbf{p}-) u_e^*(\mathbf{p}-) \exp[-i\mathbf{p} \cdot \mathbf{x}]).$$

The operator λ therefore destroys neutrinos with spin parallel to their momentum and creates neutrinos with spin antiparallel. The operator λ^+ does the opposite. The expressions $\frac{1}{2}(1 \mp \gamma_5)$ are « Nullteiler ». Their eigenvalues are 1 and 0, and it is therefore clear that there must exist a gauge of the γ 's in which λ are two component spinors.

The number of components however depends on the gauge and is in no way significant for the physical content of the theory. To see that the operators λ , λ^+ defined by equations (7) are identical to those of Weyl's theory we consider the Lagrangian

$$(9) \quad \mathcal{L}' = -\lambda^+ \gamma_4 \gamma_\mu \frac{\partial}{\partial x_\mu} \lambda,$$

which has also been used by YANG and LEE. We show that $\mathcal{L}' = \mathcal{L} + \frac{1}{2}(\partial J_\nu / \partial x_\nu)$ where

$$(10) \quad J_\nu = \mu \gamma_4 \gamma_\mu \gamma_5 \mu.$$

For by using (7) we have

$$\mathcal{L}' = -\mu \gamma_4 \gamma_\mu \frac{\partial}{\partial x_\mu} \mu + \mu \gamma_4 \gamma_\mu \gamma_5 \frac{\partial}{\partial x_\mu} \mu.$$

Now, because of the anticommutation of the operators μ and because of $\gamma_1 \gamma_\mu \gamma_5 = -(\gamma_4 \gamma_\mu \gamma_5)^T$ one has $\mathcal{L}' = \mathcal{L} + \frac{1}{2}(\partial / \partial x_\mu)(\mu \gamma_4 \gamma_\mu \gamma_5 \mu)$. The two Lagrangians (9) and (5) therefore differ by a divergence. The transformation (7) is therefore a canonical transformation.

Since the LEE and YANG neutrino is completely defined in terms of the Lagrangian (9) and the condition

$$(11) \quad \lambda = -\gamma_5 \lambda$$

and since the latter is obviously satisfied by (7) this proves the complete equivalence of the two theories

Under the reflection (6) λ and λ^+ undergo the transformations

$$(12) \quad \begin{cases} P\lambda(\mathbf{x})P^{-1} = i\gamma_4 \lambda^+(-\mathbf{x}), \\ P\lambda^+(\mathbf{x})P^{-1} = i\gamma_4 \lambda(-\mathbf{x}). \end{cases}$$

We observe that, if one insists on calling λ the operator which destroys neutrinos and λ^+ the operator which destroys antineutrinos the reflection transformation (12) requires the replacement of neutrinos by antineutrinos (*). It is clear that if for certain interactions the replacement of neutrinos by antineutrinos if forbidden parity will not in general be conserved.

It must be considered an advantage of the Weyl-Lee-Yang (WLY) theory that it insures that the mass of the neutrino is zero. For one has identically (because of $(1 - \gamma_5)\gamma_4(1_1 - \gamma_5) = 0$) $\lambda^+\gamma_4\lambda = 0$. If one wanted to describe massive neutrinos by means of λ and λ^+ , the mass term would be of the form

$$\lambda\gamma_4\lambda + \lambda^+\gamma_4\lambda^+.$$

In the Majorana theory, on the other hand, $m = 0$ has to be imposed as a separate condition. This condition can also be formulated by an invariance requirement (*). For if $m = 0$ the Lagrangian (5) is invariant under the transformation:

$$(13) \quad \mu' = \exp [i\gamma_5\alpha]\mu,$$

with arbitrary real α . Also (13) insures that the mass is zero. Under (13) λ and λ^+ undergo the transformation

$$(14) \quad \lambda' = \exp [-i\alpha]\lambda, \quad \lambda^{+'} = \exp [+i\alpha]\lambda^+.$$

This invariance property, which is automatically satisfied in the WLY theory and in Majorana's theory provided that $m = 0$ allows one to determine a constant of the motion. A local conservation law of a scalar quantity requires the definition of a vector density. Now, it is well known that the Majorana neutrino does not allow the formation of a vector and an antisymmetrical tensor. This is due to the anticommutation of the neutrino operators and the fact that $(\gamma_4\gamma_\mu)^T = \gamma_5\gamma_\mu$ and $(\gamma_4\gamma_{[\mu\nu]})^T = \gamma_4\gamma_{[\mu\nu]}$. It follows that the Majorana neutrino can have neither charge nor magnetic moment. The Majorana neutrino however allows the formation of a pseudo-vector, namely $\mu\gamma_4\gamma_\mu\gamma_5\mu$ and therefore the definition of a pseudo-charge

$$(15) \quad q = - \int d^3x \mu\gamma_5\mu,$$

(*) This would still be the case with the most general representation of (6), namely $P_\mu(x)P^{-1} = \exp [i\delta\gamma_5]\gamma_4\mu(-x)$ with arbitrary real δ .

(**) B. Touschek: *Nuovo Cimento*, **5**, 754, 1281 (1957); **5**, 1281 (1957).

in terms of the WLY operators one has for q'

$$(15') \quad q' = - \int d^3x \lambda^+ \lambda ,$$

and it is easily seen that because of (2), or (8), it follows that

$$(16) \quad q = n_p - n_a ,$$

where n_p is the number of neutrinos with their spin parallel and n_a the number of neutrinos with their spin anti-parallel to the direction of \mathbf{p} . (We shall refer to them as « parallel » and « antiparallel » neutrinos). It is also seen immediately that q must be a « pseudocharge » for a space reflexion replaces n_p by n_a and viceversa.

We now want to consider the sources of the neutrino field. Restricting ourselves to non derivative couplings the most general form of the source Lagrangian will be

$$(17) \quad -H' = \lambda^+ \gamma_4 S + S^+ \gamma_4 \lambda ,$$

where S is a spinor made up in general of an odd number of spinor operators and an arbitrary number of boson operators. It will be assumed that S transforms like μ under proper Lorentz transformations but that (17) is not in general reflection invariant. It can further be assumed that the operators S and S^+ anticommute with λ and λ^+ so that instead of (17) one may also write

$$(17') \quad -H' = \lambda^+ \gamma_4 S + \lambda \gamma_4 S^+ .$$

It is immediately seen that this Hamiltonian is still much more general than the specific theory proposed by LEE and YANG. For suppose that one has $S = S^+$, then because of (7) one has

$$(18) \quad -H' = \sqrt{2} \mu \gamma_4 S \quad (\text{for } S = S^+)$$

and this is exactly the form of the source Lagrangian which one would have expected for the Majorana neutrino and which—as it is well known—leads to the possibility of double β -decay without the emission of neutrinos. For β -decay one would in general have $S = O_i e^+(n^+ \gamma_4 O_i p)$, where O_i are a set of γ operators and e^+ , p , n are the spinor operators which destroy respectively a positron, a proton and a neutron. For $S = S^+$ it is necessary that S be of the form $O_i e^+_i (n^+ \gamma_4 O_i p) + (p^+ O_i \gamma_4 n) e^+_i O_i$.

As a result the type of neutrino emitted does not depend on the isotopic

spin component of the emitting nucleon: the same neutrino can be emitted or absorbed with the emission of an electron or a positron.

It is therefore quite clear that to get the theory of Lee and Yang it is not sufficient to use Weyl's two component theory, but an additional requirement is needed, which defines the selection of the proper source functions of the neutrino. It is therefore this requirement which «makes» the theory of Lee and Yang and not the introduction of Weyl spinors which—as it has been shown—are completely equivalent to those of the Majorana theory.

LEE and YANG therefore make a specific choice of the interaction Lagrangian which in the case of β -decay can be thus described:

The «parallel» neutrino is labelled as «neutrino», the «antiparallel» particle as antineutrino. The interaction is chosen in such a way that it conserves the number of Fermi particles minus the number of antifermions.

It has been shown by one of us (?) that it is possible to define this choice of interaction by means of an invariance requirement. The conservation of the number of fermions minus antifermions is one of the possible interpretations of the constant of the motion defined by this invariance.

The invariance principle is based on a gauge group containing (13) and (14) and the supplementary transformation

$$(19) \quad \psi'_i = \exp [il_i\alpha] \psi_i,$$

for the i -th (not necessarily spinor) field. It is clear that because of (19) S will transform as $\exp[i\Delta l\alpha]$, where Δl is the difference of the numbers l of the particles destroyed and those created in conjunction with the creation of a parallel neutrino.

Because of (14) we must have $\Delta l = -1$. It is also immediately obvious that (13), (19) exclude the possibility of a Majorana type coupling (18), for with $S^+ = S$ we must have $\Delta l = 0$; the emission of a neutrino on the other hand requires $\Delta l = \pm 1$. It is also seen that double β -decay is impossible without the emission of neutrinos. For it follows from charge conservation and the conservation law implied by the invariance (13), (19) that

$$(20) \quad \Delta((l_p - l_+ \pm \frac{1}{2})N \mp T_3 + q) = 0.$$

Here l_p and l_+ are respectively the l -numbers of proton and positron, N is the nucleon number, equal to the number of nucleons minus antinucleons and T_3 is the third component of the isotopic spin. The \mp signs depend on whether in neutron decay a «parallel» or «antiparallel» neutrino is emitted.

Now, for double β -decay we have $|\Delta T_3| = 2$ and we must therefore have $\Delta q = 2$ so that at least two neutrinos must be emitted.

It therefore appears that the WLY theory is the only formulation of the β -decay involving a two state neutrino which does not give rise to double β -decay without emission of free neutrinos.

* * *

One of us wishes to thank Prof. FIERZ for communication of a proof of this theorem.

RIASSUNTO

Si dà una nuova dimostrazione del teorema di equivalenza di Serpe e Fierz. Si dimostra che l'interazione fra i neutrini e le loro sorgenti limita l'arbitrarietà della descrizione del campo neutrinico e che l'unica teoria a due stati del neutrino che non dia luogo al doppio decadimento β è la teoria di Weyl-Lee-Yang.

Systematics of Λ^0 and θ^0 Decay (†).

F. EISLER, R. PLANO and N. SAMIOS

Nevis Cyclotron Laboratory, Columbia University - Irvington, New York

M. SCHWARTZ and J. STEINBERGER (*)

Brookhaven National Laboratory - Upton, New York

(ricevuto il 17 Aprile 1957)

Summary. — Systematic observations on 528 Λ^0 - θ^0 production events in propane have yielded the following information: 1) There exists a neutral Λ^0 decay; $\Lambda^0 \rightarrow \pi^0 + n$ and the fraction of Λ^0 's decaying in this mode is $.32 \pm .05$. 2) The θ_1^0 component has a neutral decay mode, very probably $\theta_1^0 \rightarrow \pi^0 + \pi^0$. The θ^0 therefore very probably has even spin. The fraction $P(\theta_1^0 \rightarrow \pi^0 + \pi^0)$ is $.14 \pm .06$. The branching ratio $\frac{P(\Lambda^0 \rightarrow \pi^0 + n)}{P(\Lambda^0 \rightarrow \pi^- + n)}$ is in good agreement with the $I = \frac{1}{2}$ selection rule; the branching ratio $\frac{P(\theta^0 \rightarrow 2\pi^0)}{P(\theta^0 \rightarrow \pi^+ + \pi^-)}$ seems to be in disagreement. 3) $(51 \pm 7.5)\%$, or just one half of the θ^0 mesons escape the chamber and are to be identified with the θ_2^0 -meson proposed by GELL-MANN and PAIS (4). The question of the existence of additional (parity doublet) decay modes is discussed. 4) The decays $\Lambda^0 \rightarrow \frac{u^- + p + \nu}{e^- + p + \nu}$ are not observed and the fraction of such decays is less than 2%. 5) The 3 particle decay modes of the θ_1^0 have not been observed and are therefore very unlikely to exceed 2% of all θ_1^0 decays. 6) Preliminary measurements yield lifetimes $\tau_{\theta_1^0} = (.95 \pm .08) \cdot 10^{-10}$ s and $\tau_{\Lambda^0} = (2.8 \pm .2) \cdot 10^{-10}$ s. 7) For the θ_2^0 we obtain a lower limit of the lifetime, which together with the results of LANDE *et al.* (5) brackets the θ_2^0 lifetime ($3 < \theta_2^0 < 10 \cdot 10^{-8}$ s).

1. — Introduction.

The observation, in considerable number, of strange particle production events in the bubble chamber, with clearly visible origin, enables us to study the decay processes of the Λ^0 and θ^0 particles. In particular, the observations

(†) Supported by a joint program of the Office of Naval Research and the Atomic Energy Commission.

(*) Permanent address, Columbia University.

on electron-positron pairs produced by γ -rays resulting from such decays permit the analysis of neutral decay modes of the Λ^0 and 0^0 . γ -rays, almost certainly due to strange particle decays, have previously been observed with electronic techniques (^{1,2}), but under conditions in which the origin, whether Λ^0 , 0^0 , or Σ^+ , was not clear and where the nature of the particular decay mode could not be studied.

2. - Outline of experiment.

The experimental technique is briefly the following. We look at events in the bubble chamber in which at least one Λ^0 or one 0^0 is produced by the incoming π^- and is observed to decay in the chamber, and in which definitely no charged strange particles are produced. The latter is established by the requirement that all charge particles in the production event stop in the chamber and show no decay secondaries. We assume the associated production hypothesis to be established, and hence that in all of these events, two neutral strange particles were actually produced, even though only one of them was observed. If, say, a Λ^0 is seen, then it is assumed that a 0^0 also traverses the chamber *whether or not its decay is visible*. In this sense the Λ^0 observation serves as the detector of the 0^0 and will henceforth be referred to as a « 0^0 signature ». As we have previously pointed out (³), it is usually possible to determine whether the reaction was with a free proton, e.g., $\pi^- + p \rightarrow \Lambda^0 - 0^0$, by noting whether the Λ^0 energy corresponds to that expected from its production angle (measured) and the beam energy (known). In those cases ($\sim 40\%$) which do fit a production in hydrogen, the direction and momentum of the 0^0 is known *with or without the observation of its decay*.

The converse situation exists for the Λ^0 . The observation of a 0^0 without production of an associated charged strange particle demonstrates the production of a Λ^0 either directly or through an intermediary Σ^0 , and in a good fraction of the cases ($\sim 40\%$) the direction of propagation and momentum of the Λ^0 are known as well. Observations of 0^0 production without associated charged strange particles will be termed « Λ^0 signatures ». These « signatures » make it possible to identify nuclear interactions, or unusual decay modes of the particle, even though its normal decay is unobserved. This then is the basic technique of the experiment.

There is a reasonable probability ($\sim 7\%$) that a γ -ray produced in the decay of one of these particles will produce an electron-positron pair some-

(¹) S. L. RIDGEWAY, D. BERLEY and G. B. COLLINS: *Phys. Rev.*, **104**, 513 (1956).

(²) B. MOYER and J. OSHER: *Proc. of the Sixth Annual Rochester Conference*.

(³) R. BUDDE, M. CHRETIEN, J. LEITNER, N. SAMIOS, M. SCHWARTZ and J. STEINBERGER: *Phys. Rev.*, **103**, 1827 (1956).

where in the chamber. At these energies (in the neighborhood of 100 MeV or more) both members of the pair are emitted very close to the direction of the γ -ray. The energy of the γ -ray is determined by the curvature of electron and positron in the magnetic field. Events in which materialized γ -rays are associated with « 0^0 or Λ^0 signatures » can serve therefore to establish the neutral decays of these particles and give information on the nature of these decays and their relative probabilities.

3. - Experimental details.

3·1. Apparatus. - The chamber is 12 in. in diameter and 8 in. deep, and in a magnet which produced 13.7 kG in the center, and 13.2 kG at the periphery. The average field is 13.4 kG. The expanded propane has a density of .425 g/cm³. The partial density of hydrogen is .088 g/cm³. The size of the chamber is such that of the order of 80-90% of the Λ^0 and 0^0 particles produced in the chamber also decay in it.

3·2. Beam and exposure. - The beam is collimated in the manner previously described (³) but an additional lead collimator directly in front of the chamber limits the beam aperture to a width of 4 in. in the dimension of the depth of the chamber and $5\frac{3}{4}$ in. in the dimension of the height of the chamber. This insures that all events are produced in a central region as far as these two dimensions are concerned. The only unfavorable events, unfavorable because of short potential path of the Λ 's and 0 's, are collisions close to that chamber wall at which the particles leave. Three beam momenta are employed: 980 MeV/c, 1.30 GeV/c, and 1.43 GeV/c. The beams are defined to a momentum interval of $\pm 1\%$. The pictures have between 10 and 20 beam tracks each and on the average an event of the type analyzed here appears in one out of ~ 50 -100 frames.

3·3. Selection of events. - The pictures are examined as reprojected images which are either life size or somewhat larger. We have searched systematically for events in which the incoming π^- meson suffers a collision and one or more V particles appear. All such events are tabulated provided all the prongs of the star, if any, come to the end of their range in the chamber and clearly show no decay. All chosen events are therefore examples of the productions of an associated 0^0 and Λ^0 (which may be the daughter of a Σ^0) pair (*), whether both, or only one of them is actually found.

(*) This is of course on the assumption that the selection rules for associated production are strictly valid, and events produced by the small ($\sim .1 \div .01\%$) K^- contamination can be neglected.

The V particles are identified as Λ^0 's or Θ^0 's in the manner previously reported (3), except that in addition we now know the momenta of the two prongs, and the energy of the V is obtainable both in this way or using the angular correlations as before. It must be remarked that the background of V's which are not of strange particle origin is negligibly small, and it is possible to select the events by means of inspection and rough measurement and calculation.

4. — Results.

4.1. *Numbers and types of observed neutral production events.* — The number of events which have been found in approximately 20 000 pictures are tabulated in Table I.

TABLE I.

168	π^- interactions with both Λ^0 and Θ^0 observed.
251	π^- interactions with only Λ^0 observed.
109	π^- interactions with only Θ^0 observed.
528	total number of events.

The 419 events in which the Λ^0 is seen will be called « Θ^0 signatures ». Similarly, the 277 events in which the Θ^0 is seen will be called « Λ^0 signatures ».

4.2. *Neutral decay of the Θ^0 .* — Consider the following possibilities for neutral decay modes of the Θ_1^0 :

- | | |
|-----|------------------------------------------------|
| (1) | $\Theta_1^0 \rightarrow \pi^0 + \pi^0$ |
| (2) | $\Theta_1^0 \rightarrow \pi^0 + \pi^0 + \pi^0$ |
| (3) | $\Theta_1^0 \rightarrow \gamma + \gamma$ |
| (4) | $\Theta_1^0 \rightarrow \gamma + \pi^0$. |

These decays are observed through the materialization of the γ -rays in the chamber. The γ -rays we expect here have between fifty and several hundred MeV. The main materialization process is pair production, either internal or in the liquid. The probability of internal conversion is $\sim .6\%$. The composition of the chamber liquid is C_3H_8 and the density is 425 g/cm^3 . The mean free path for γ -rays of this energy range in this material is 200 cm. The average track length of a particle produced in the chamber is ~ 15 cm, and if 3 cm are required for detection, the conversion probability in the propane is $12/200 = 6\%$. The total conversion probability is then 6.6% . The reactions

(1)-(4) are observed with efficiencies which depend on the number of γ -rays which are emitted. Reaction (1) 24%, reaction (2) 34%, reaction (3) 13%, and reaction (4) 19%.

It is clear that in this experiment we will rarely see more than one of the γ -rays at a time. Nevertheless, it is possible in principle to establish the decay mode by studying the spectrum of the photons in the θ^0 rest system. The transformation to the rest system is unambiguously possible in the case of hydrogen events, and can be attempted in the other cases more or less accurately by assuming a θ^0 energy and momentum most consistent with energy and momentum balance of the observed Λ^0 and charged particles. If one of the decay modes is dominant, even a crude analysis may then make it possible to select this mode. Even a poor knowledge of the average γ -ray energy may suffice, since this varies from 246 MeV in the case of 2γ emission (reaction (3)) to 82 MeV for the case of $3\pi^0$ emission (reaction (2)).

It should be remembered that the angles of the members of the pair with respect to the γ -ray are very small, $\sim mc^2/E$, so that the members of the pair usually determine the γ -ray direction to a few tenths of a degree.

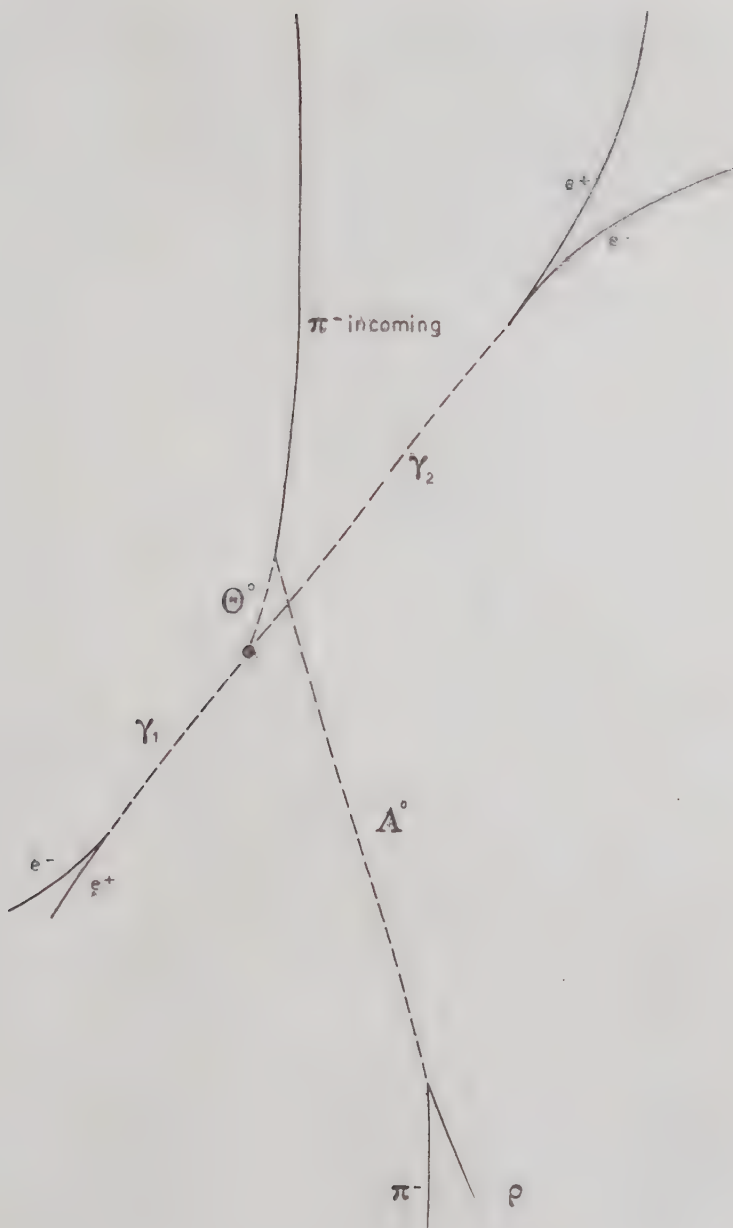
The neutral θ^0 decays are then studied in this experiment by investigating those « θ^0 signatures » in which a positron electron pair also appears in the picture. The line of flight of the pair must intersect the line of flight of the θ^0 , which is well defined for the hydrogen events and more poorly defined for the others.

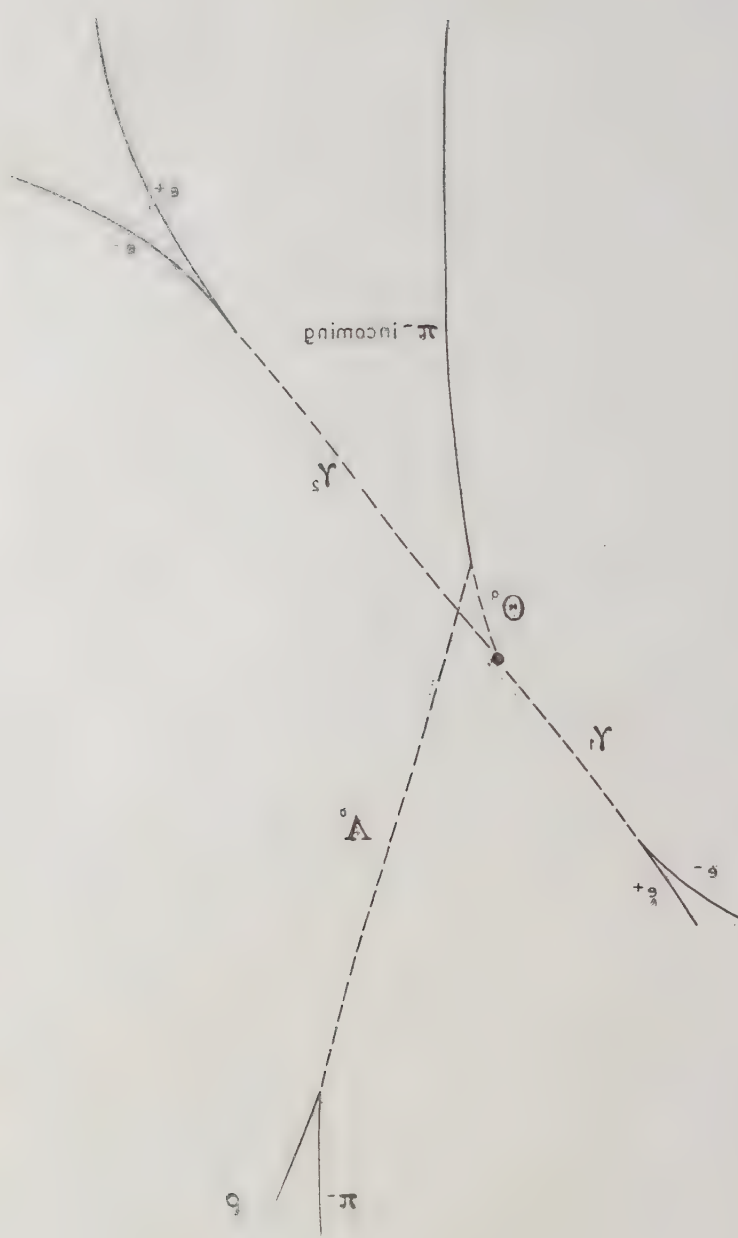
It is necessary to study the possibility of chance coincidence between a « θ^0 signature » and a γ -ray. We have analyzed some rolls of film to find the frequency of occurrence of electron-positron pairs. These pairs fall into 3 categories.

a) Pairs clearly originating in some other event in the chamber, i.e., pointing to a star or to a stopping incoming beam track. These we ignore, because we do not accept them in those cases where a θ^0 signature is also in the same picture.

b) Pairs pointing in the direction opposite to the incident beam. There are a rather large number of these; approximately one in 25 pictures show such a pair. They are produced chiefly by the radiation of the electron contamination in the beam in the aluminium walls of the chamber. We have decided not to include any such γ -rays among our events, since by excluding them we exclude a large fraction (approximately $\frac{1}{2}$) of the background, while missing only a very small fraction (perhaps $\sim 5\%$) of the real events.

c) All other electron-positron pairs. There is one in about 20 pictures, and we estimate the probability that the direction of propagation and the energy of such a γ -ray are accidentally consistent with θ^0 decay to be approximately 1/50 in hydrogen events and 1/10 in non-hydrogen events.





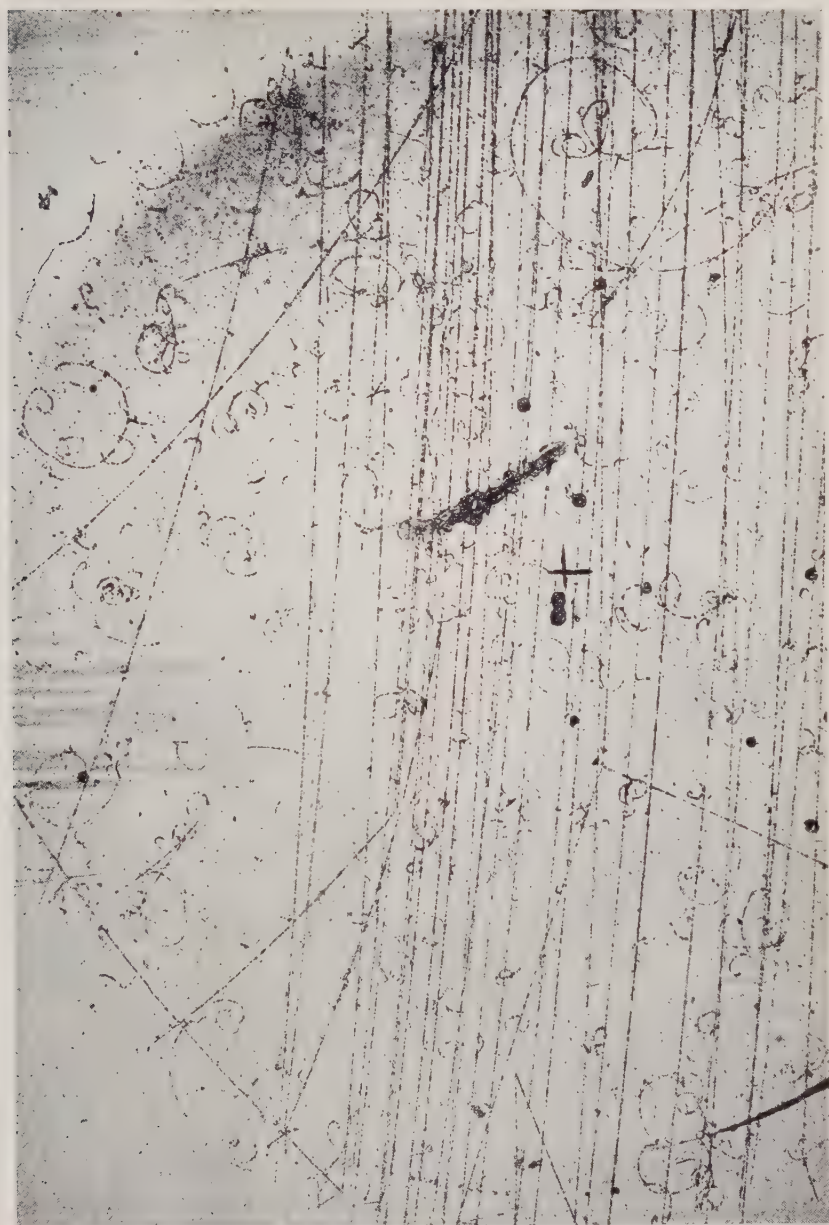


Fig. 1. - An event in which a 0° signature, that is an interaction which produces a visible Λ^0 , is associated with two electron positron pairs. The γ -rays producing the pairs come from a common origin in the chamber and are probably due to the decay of the 0° .

Event No. 1621/60.

So far we have observed 251 θ^0 signatures in which the θ^0 is not observed to decay into charged particles and of these perhaps 40% are in hydrogen. The chance events in hydrogen collisions are therefore $\sim 251 \times .4 \times 1/20 \times 1/50 = .1$ which is negligible. All hydrogen events can therefore be assumed to be real. The number of expected non-hydrogen chance coincidences is $\sim 251 \times .6 \times 1/20 \times 1/10 \simeq .75$. There is then a good possibility that one of the events in Table II is a chance event, but the probability that chance events seriously affect the results can be ignored.

We have observed seven θ^0 signatures with associated γ -rays which meet our criteria. In one of these, two γ -rays materialize, so that there are altogether eight γ -rays. One of these events is reproduced in Fig. 1. The details of the events are tabulated in Table II.

TABLE II.

Case No.	H ₂ prod. Yes/No	No. of γ -rays	Angle between θ^0 and γ	θ^0 mo- mentum MeV/c	γ -ray energy (MeV)	γ -ray energy in θ^0 cm MeV	Path length of θ^0 before decaying (cm)	Lifetime of θ^0 in rest sys- tem in 10^{-10} s
8380/69	No	1	25°	600	114 ± 15	54 ± 8	1.8	.52
3336/34	No	1	55°	1020	85 ± 20	94 ± 22	.8	.14
3903/35	Yes	1	30°	620	230 ± 20	120 ± 10	3.3	.89
7722/40	Yes	1	40°	470	165 ± 20	118 ± 15	1.9	.65
1621/60	No	2	108°	620	102 ± 10	205 ± 25	2.5	.62
			24°		250 ± 100	113 ± 40		
1269/46	No	1	5°	760	237 ± 20	73 ± 25	4.4	.95
4769/9	Yes	1	67°	1080	95 ± 10	148 ± 15	5.3	.88

A histogram of the energy distribution of the seven γ -rays in the center of mass system of the decaying θ^0 is shown in Fig. 2.

We wish to make the following points:

1) It is clear that the θ_1^0 has at least one neutral decay mode and that γ -rays are produced, either directly or through π^0 decay.

2) The average number of γ -rays produced in θ_1^0 decay, referred to the number of θ_1^0 's decaying in the normal, charged decay $\theta_1^0 \rightarrow \pi^+ + \pi^-$, is

$$\frac{\text{number of } \gamma\text{'s observed with } \theta^0 \text{ signatures}}{\text{number of } \theta^0 \rightarrow \pi^+ + \pi^- \text{ observed with } \theta^0 \text{ signatures} \times .066} = \frac{8 - .75}{.066 \times 168} = .65 \pm .25.$$

3) The γ -rays do not have a unique energy.

4) The average γ -ray energy is 155 ± 25 . The error here indicates the

statistical uncertainty that can be expected from 8 events, if the distribution is as broad as indicated in Fig. 2.

5) The 2 γ -rays in event 1621/60 cannot have the same π^0 as parent, on the basis of their energies and the angle between them.

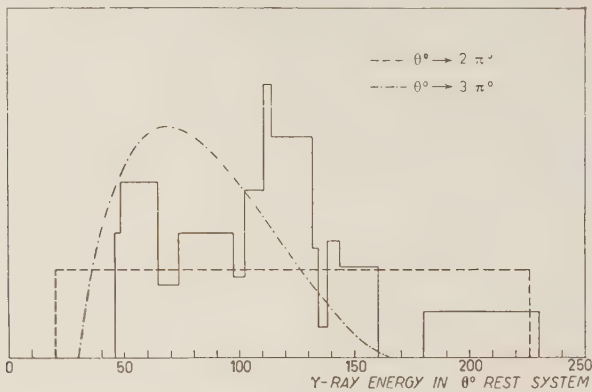


Fig. 2. -- A plot of the energy spectrum of observed γ -rays from alternate 0° decay, in the rest system of the 0° . Drawn in for comparison is the spectrum for $2\pi^0$ decay as well as the spectrum for $3\pi^0$ decay.

We now discuss the neutral decay modes (1)-(4) in terms of the data.

1) $0_1^0 \rightarrow 2\pi^0$. Here we expect a uniform γ -ray spectrum between 20 and 226 MeV, with a mean energy of 123 MeV. This is in good agreement with the data, as can be seen in Fig. 2.

2) $0_1^0 \rightarrow 3\pi^0$. Using a non-relativistic phase space distribution for the π^0 we expect a spectrum of the form

$$N(E_\gamma) = \left\{ 1 - \frac{1}{4E_\gamma E_{\pi^0}^{\max}} (m_{\pi^0} - 2E_\gamma)^2 \right\}^{\frac{1}{3}},$$

where $E_{\pi^0}^{\max}$ is the maximum π^0 kinetic energy. This spectrum has been plotted in Fig. 2. It gives an average γ -ray energy of 82 MeV and is also consistent with the observed data.

On the other hand, if this mode exists, there is a very strong presumption that the charged mode, $0_1^0 \rightarrow \pi^\pm + \pi^\mp + \pi^0$ exists with at least equal probability. We would then expect to find of the order of $(8 - .75)/(6 \cdot .066) = 18$ or more charged decays, but none have been found. It is therefore very dif-

ficult to believe that the $3\pi^0$ decay mode can exist with anything like the observed probability.

3) $\theta_1^0 \rightarrow 2\gamma$. Here we expect a unique γ -ray energy of 246 MeV, clearly inconsistent with the observations.

4) $\theta_1^0 \rightarrow \pi^0 + \gamma$. Here we expect one-third of the γ -rays to have the unique energy 229 MeV and the rest to be distributed uniformly between 17 and 246 MeV. The average energy would be 164 MeV, and this seems outside the experimental error.

On the basis of this evidence there is then a very strong presumption that the θ_1^0 can decay into two neutral pions. So far we have not seen an event in which 2 γ -rays from the same π^0 convert in the chamber, but a single such even could remove any ambiguity, since the combined energy of the two γ 's in the rest system of the θ^0 would have to be 246 MeV, for the $2\pi^0$ decay mode.

Assuming then that the observed γ -rays are due to this decay mode, we can calculate its relative probability,

$$\frac{P(\theta_1^0 \rightarrow 2\pi^0)}{P(\theta_1^0 \rightarrow 2\pi)} = \frac{\frac{8}{4} - .75}{\frac{.066}{1.066} + \frac{.75}{168}} = .14 \pm .06.$$

4.3. θ_2^0 decay of the θ^0 and lifetime of θ_2^0 . From the data of Table I it is also possible to obtain the fraction of the θ^0 decays which are unseen because of either a long lifetime or an unobservable neutral decay mode. It is first necessary, however, to correct the observations for those θ_1^0 's which decay in the usual fashion but leave the chamber before decaying. The average path length in the chamber is ~ 15 cm and the average observed θ^0 momentum is 500 MeV/c. The lifetime is $0.95 \cdot 10^{-10}$ s. The chief contribution to θ_1^0 's decaying outside the chamber comes from production events which occur close to the far wall. The beam traverses only the central 10 cm of the 20 cm chamber depth, and so the loss through the glass surfaces is negligible. We estimate a total loss of $(10 \pm 5)\%$. The corrected number is then $168/9 = 187$ events with both Λ^0 and θ^0 appearing. The events *without* the θ^0 must also be corrected for the relatively greater efficiency of finding events if the θ^0 is also there. On the basis of double scanning of about 10% of the film we estimate an efficiency of $\sim 93\%$ for double events and 85% for single events. The 251 single Λ^0 events must therefore be corrected to $(251 \cdot 93)/85 = 275$. The corrected number of θ^0 signatures is $168 + 275 = 443$, and the fraction of $\theta_1^0 \rightarrow \pi^+ + \pi^-$ to all θ^0 's is $P(\theta_1^0 \rightarrow \pi^+ + \pi^-)/P(\theta^0) = 187/443 = .42 \pm .05$. The

error includes the statistical error as well as the estimated systematic detection error. To get the total θ_1^0 fraction it is necessary to add the neutral decay fraction. So $P(\theta_1^0 \rightarrow 2\pi)/P(\theta^0) = (.42 \pm .05)/(.86 \pm .055) = .49 \pm .075$. The important result is that *one half of the θ^0 mesons decay with the short θ_1^0 half life, and the other half escape detection* in the chamber. It is immediate to connect these missing θ^0 mesons with the θ_2^0 which is predicted by GELL-MANN and PAIS (4), and which is expected to account for 50% of the θ^0 's. This experimental result is another striking confirmation of the theory, which is already strongly supported by the discovery by LANDE *et al.* (5) of neutral particles with mass probably close to that of the θ^0 and with 3 particle decay modes, viz:

$$\theta_2^0 \left\{ \begin{array}{l} \rightarrow \pi^\pm + \pi^\mp + \pi^0 \\ \rightarrow \pi^\pm + \mu^\mp + \nu \\ \rightarrow \pi^\pm + e^\mp + \nu. \end{array} \right.$$

In the latter experiments the lifetime was bracketed between 10^{-7} and $5 \cdot 10^{-9}$ s. We have not observed any decays of this sort. We would detect these particles as a long lived V component, non-coplanar in its decay, appearing in θ^0 signatures.

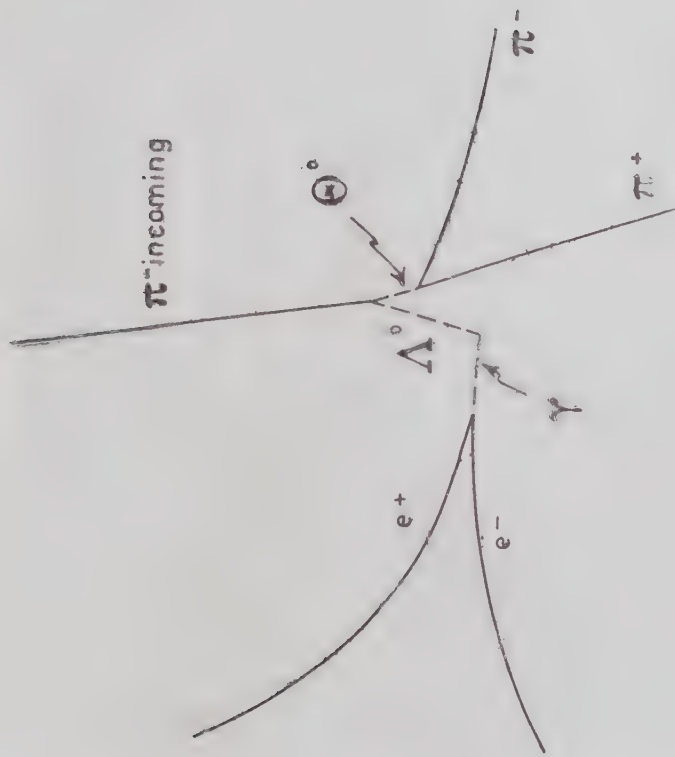
The total number of θ_2^0 's in these signatures is just $\frac{1}{2} \cdot 419 = 210$. The average time in the chamber of such a θ_2^0 , based on observed θ_1^0 properties, is $3.6 \cdot 10^{-10}$ s, in the θ^0 rest system. The total θ_2^0 time in the chamber is therefore $7.5 \cdot 10^{-8}$ s. Since no such decays were observed, it is reasonably safe to put a lower limit for the θ_2^0 lifetime at $\sim 3 \cdot 10^{-8}$ s. The θ_2^0 lifetime, using also the result of LANDE *et al.* (5) for the upper limit, must then be between 3 and $10 \cdot 10^{-8}$ s.

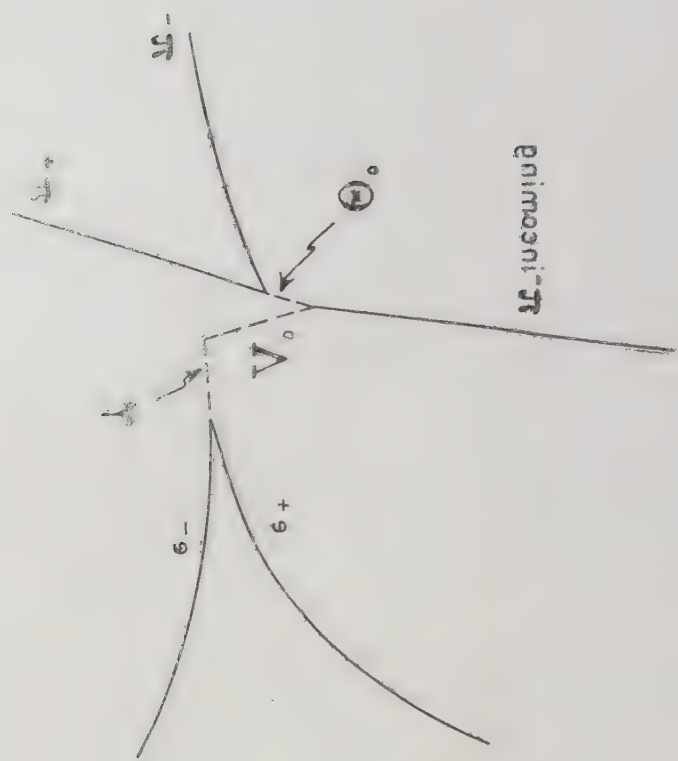
4·4. Three particle charged decays of the θ_1^0 . — As already pointed out, no θ^0 charged decays, inconsistent with the two π decay modes, were observed. 168 $\theta_1^0 \rightarrow \pi^+ + \pi^-$ decays were seen in association with Λ^0 's. We can conclude that the probability for charged decay of the θ_1^0 in other modes is most probably less than $\sim 2\%$.

4·5. Neutral Λ^0 decay. — We have observed 5 events in which γ -rays are associated with Λ^0 signatures. One of these events is shown in Fig. 3. The details are presented in Table III. The observed γ -ray spectrum in the Λ^0

(4) M. GELL-MANN and A. PAIS: *Phys. Rev.* **97**, 1387 (1955).

(5) K. LANDE, E. BOOTH, J. IMPEDUGLIA, L. LEDERMAN and W. CHINOWSKY: *Phys. Rev.*, **103**, 1901 (1956).





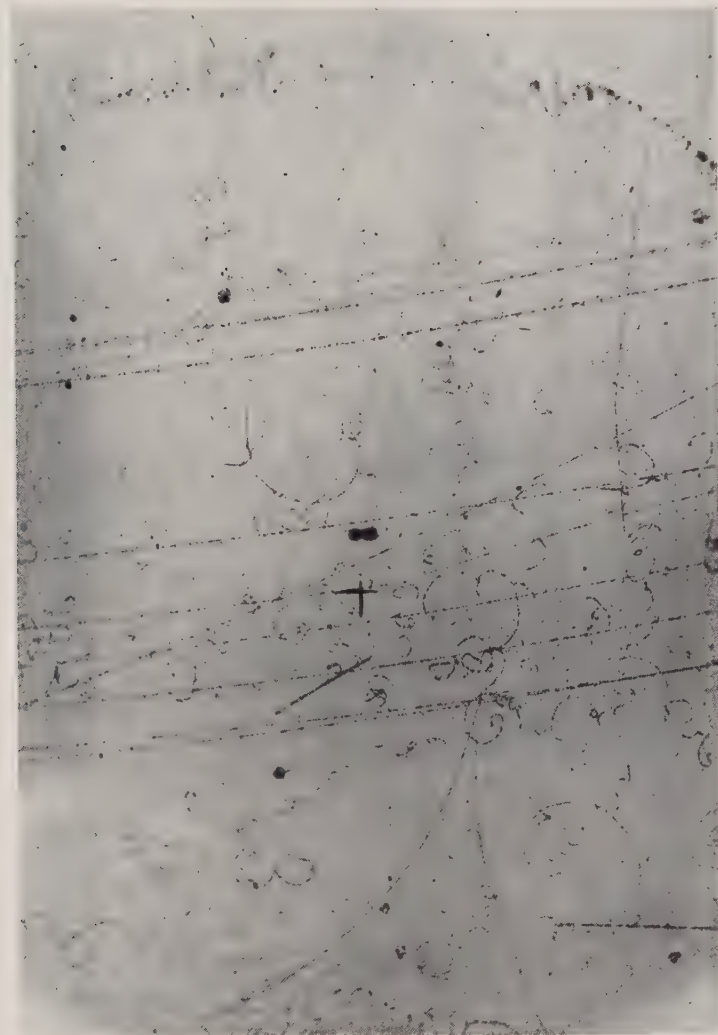
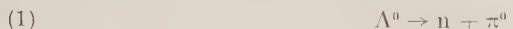


Fig. 3. An event in which a θ^0 , produced in a free proton collision of the incident $\pi^- : \pi^- + p \rightarrow \theta^0 + \Lambda^0$, is accompanied by an electron positron pair. The line of flight of the γ -ray producing the pair intersects the line of flight of the Λ^0 as calculated from the kinematics. Event No. 9922, 85.

TABLE III. — *Neutral Λ^0 Decay Events.*

Case No.	H_2 prod. Yes/No	No. of γ -rays	Angle between Λ^0 and γ	Λ^0 Mo- mentum MeV/c	γ -ray energy	γ -ray energy in Λ^0 cm	Path length of Λ^0	Lifetime of Λ^0 in rest system (10^{-10} s)
9922/85	Yes	1	95°	560	97 ± 10	113 ± 11	2.25	1.5
8502/83	Yes	1	16°	650	145 ± 10	82 ± 6	4.6	2.6
7446/4	Yes	1	24°	1140	277 ± 22	137 ± 11	3.3	.88
1086/56	Yes	1	85°	890	76 ± 10	87 ± 12	2.2	.92
4760/65	No	1	100°	750	80 ± 10	102 ± 12	3.6	.18

rest system has been plotted in Fig. 4. We may compare the properties of these γ -rays with those expected in the reactions



and



In (1) we expect a continuous γ -ray spectrum flat from 32 to 134 MeV, with an average energy of 84 MeV. We actually observe an average energy of 104 ± 30 , with a distribution in reasonable agreement. In (2), we expect a mono-energetic γ -ray of 165 MeV, clearly inconsistent with the data. We therefore conclude that the dominant neutral decay mode of the Λ^0 is into a π^0 and neutron.

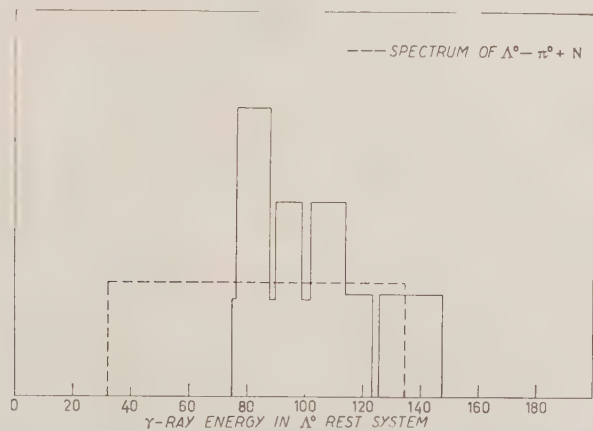


Fig. 4. — A plot of the energy spectrum of observed γ -rays from alternate Λ^0 decay, in the rest system of the Λ^0 . Drawn in is the spectrum for decay into neutron and π^0 .

To determine the relative frequency of this decay we first correct the number of observed events by the expected accidental coincidences. This is done, just as in the θ^0 decay, for the 109 Λ^0 signatures without the Λ^0 . The number of accidental events is then $109 \cdot .6 \cdot 1/20 \cdot 1/10 = .33$. We then obtain for the fraction of Λ^0 's undergoing neutral decay

$$\frac{P(\Lambda^0 \rightarrow \pi^0 + n)}{P(\Lambda^0)} = \frac{\frac{5 - .33}{2 \cdot .066}}{\frac{5 - .33}{2 \cdot .066} + 168} = .175 \pm .09 \text{ (*)}.$$

The neutral decay rate can also be determined by comparing the number of Λ^0 signatures to the number of these in which the Λ^0 is also detected. As in the discussion of θ^0 decay, we have to make a correction of 10% for the Λ^0 decaying outside the chamber. The number of Λ^0 - θ^0 events is therefore again $168/.9 = 187$. The number of single θ^0 's must be corrected for a differential inefficiency for detecting single events: $106 \cdot (93/85) = 119$. The total number of Λ signatures is then $119 + 168 = 287$, and the fraction of charged decays is $187/287 = .65 \pm .05$ where the error is chiefly due to uncertainty in the efficiency corrections. The fraction of Λ^0 's, which are missed, presumably because of neutral decay, is $35 \pm 6\%$. This is in reasonable agreement with the observations on the observed γ -rays; certainly, the disagreement does not justify the introduction of other neutral decay modes. Combining the two results we get, for the fraction of Λ^0 's undergoing neutral decay

$$\frac{P(\Lambda^0 \rightarrow \pi^0 + n)}{P(\Lambda^0)} = .32 \pm .05$$

4·6. Alternate charged Λ^0 decay. — It must be expected that the Λ^0 can decay into other charged modes,



The phase space for these modes, however, is some hundreds of times smaller than the phase space for the dominant mode. We have not observed any examples of these modes compared to 168 charged decays accompanying

(*) *Note added in proof.* - In rescanning the film 2 more γ -rays attributed to Λ^0 decay have been found in the same film. This changes the fraction undergoing neutral decay to $P(\Lambda^0 \rightarrow \pi^0 + n)/P(\Lambda^0) = 0.23 \pm 0.09$.

Λ^0 signatures. We can therefore place a reasonably safe upper limit of 2% for the relative frequency of the combination of these two modes.

4.7. Λ^0 and 0^0 lifetimes. τ In the case of 182 0^0 events and 304 Λ^0 events we have measured the actual path length, the potential path length, as well as the momentum. It is noted here that the measurements are preliminary and are being repeated with better accuracy. The lifetimes reported here must therefore be considered preliminary. The average potential time of the Λ^0 's in the chamber was $9 \cdot 10^{-10}$ s, that of the 0^0 's, $3.5 \cdot 10^{-10}$ s, in either case large ($\sim 3\sigma$) compared to the observed lifetime. It is therefore possible to treat the data by tabulating the potential times, and the observed times, and dividing the number observed to decay at a given time t by the fraction of

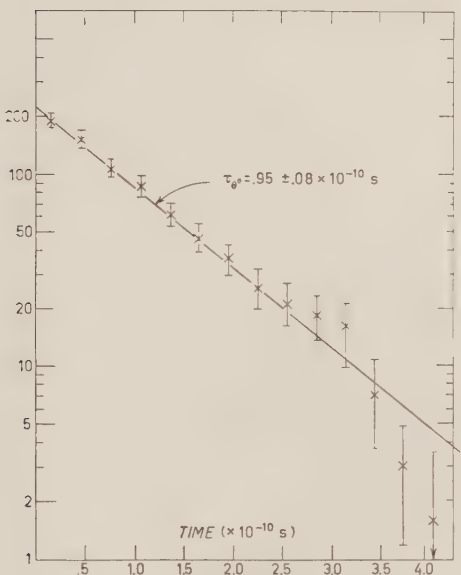


Fig. 5. — Integral decay time distribution of 182 0^0 decays.

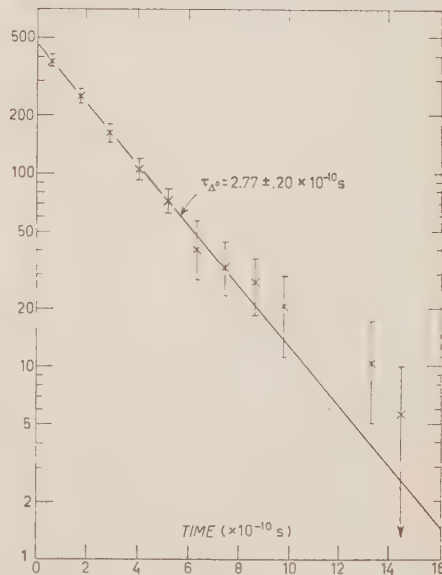


Fig. 6. — Integral decay time distribution of 304 Λ^0 decays.

all potential times exceeding t . The observed decays are plotted in Fig. 5 and 6 and for 0^0 's and Λ^0 's respectively. The lifetimes we get are $\tau_{0^0} = .95 \pm .08$ and $\tau_{\Lambda^0} = 2.77 \pm .2$. These values agree best with the most recent data (14) but are considerably better statistically.

5. - Some comments.

5.1. The $\Delta I = \frac{1}{2}$ selection rule for the decay of strange particles. — It has often been pointed out (6) that strange particle decay reactions may be restricted by the selection rule $\Delta I = \frac{1}{2}$. This is made plausible by several experimental observations:

- 1) The Ξ^- hyperons are observed to decay into Λ^0 and π^- . The decay into a nucleon and pion would be forbidden by this selection rule since the Ξ^- has $I = \frac{1}{2}$ and a pion-nucleon system of charge $-e$ has $I_z = -\frac{3}{2}$ and therefore $I = \frac{3}{2}$.
- 2) The ratio of decays $(\tau^{+1} \rightarrow \pi^+ + 2\pi^0)/(\tau^+ \rightarrow 2\pi^+ + \pi^-)$ is experimentally $\sim .33 \pm .07$ (6) in good agreement with the value (6) .325 expected for pseudo-scalar τ mesons for $\Delta I = \frac{1}{2}$ (6).
- 3) The rate $K^+ \rightarrow \pi^+ + \pi^0$ is about 500 times less probable than the rate $0_1^0 \rightarrow 2\pi$. This can be understood if it is supposed that these particles have zero spin, $I = \frac{1}{2}$. The K^+ decay is then forbidden by this selection rule, since the only possible state for a π^+ and π^0 with angular momentum zero has isotopic spin two.

This selection rule also has as consequences definite ratios for charged to neutral decay for Λ^0 and 0^0 . Consider first the Λ^0 decay. The Λ^0 has isotopic spin zero, and the final pion-nucleon state with $I = \frac{1}{2}$, as required by the rule, is with probability $\frac{2}{3}$ charged and $\frac{1}{3}$ neutral. The expected fraction of neutral decays is therefore $\frac{1}{3}$, in excellent agreement with the experimental result obtained here.

In the case of the 0^0 decay the situation is slightly more complicated, since it is known from $K_{\pi 2}$ decay that the selection rule is at least weakly violated. If this violation is disregarded, as a first approximation, then in the decay of 0^0 particles of even spin the final two pion state has either $T = 0$ or $T = 2$ and the $T = 2$ state is forbidden by $\Delta I = \frac{1}{2}$. The $T = 0$ state has a probability $\frac{1}{3}$ of being neutral and $\frac{2}{3}$ of being charged, so that we would expect again just one-third of the 0_1^0 decays to be into two π^0 's. If the violation of the selection rule in K^+ decay is recognized, and if it assumed that the additional matrix element has $\Delta I = \frac{3}{2}$ (rather than $\Delta I = \frac{5}{2}$), it is possible to get the magnitude of this amplitude from the rate of the decay $K^+ \rightarrow \pi^+ + \pi^0$. It has been

(6) See for example R. H. DALITZ: *Proc. Phys. Soc.*, **69**, 527 (1956); G. TAKEDA: *Phys. Rev.*, **101**, 1547 (1956)

shown by DALITZ⁽⁶⁾ that

$$\frac{|a_3|^2}{|a_1|^2 + |a_3|^2} = \frac{4}{3} \frac{P(K^+ \rightarrow \pi^+ + \pi^0)}{P(\Theta_1^0 \rightarrow 2\pi)},$$

and

$$\frac{P(\Theta^0 \rightarrow 2\pi^0)}{P(\Theta_1^0 \rightarrow 2\pi)} = \frac{|a_1 + \sqrt{2}a_3|^2}{3(|a_1|^2 + |a_3|^2)},$$

were a_1 is the amplitude of the $\Delta I = \frac{1}{2}$ decay and a_3 is the amplitude of the $\Delta I = \frac{3}{2}$ decay.

$|a_3/a_1|$ can then be evaluated from the K^+ lifetime $((1.2 \pm .05) \cdot 10^{-8} \text{ s})$ ^(7,8), the fraction of K^+ decay into two pions $(28.9 \pm 2.7)\%$ ⁽⁹⁾ and from the Θ^0 lifetime $(.95 \pm .08) \cdot 10^{-10} \text{ s}$ from this experiment. $|a_3/a_1| = .055$. The fraction of neutral Θ^0 decay is then still undetermined because of the unknown relative phase of a_3 and a_1 , but must be within the limits

$$.29 \geq \frac{P(\Theta_1^0 \rightarrow 2\pi^0)}{P(\Theta_1^0 \rightarrow 2\pi)} \leq .38.$$

Our experimental value of $.14 \pm .06$ is outside of the range of theoretical values, so at least in this decay the inadequacy of the $\Delta I = \frac{1}{2}$ rule seems to be indicated (*).

5.2. Parity conjugation and doubling. — It has been proposed on theoretical grounds by LEE and YANG⁽¹⁰⁾ that the particles of strangeness ± 1 , that is, the Λ^0 , Σ^0, \pm , K^\pm and Θ^0 exist each in two states of opposite parity. The theory recently elaborated by SCHWINGER⁽¹¹⁾ has such a structure. The theoretical motivation has changed recently, with the discovery of parity non-conservation in β and μ decay. It may nevertheless be useful to discuss

(7) V. FITCH and R. MOTLEY: *Phys. Rev.*, **101**, 496 (1956).

(8) L. W. ALVAREZ, F. S. CRAWFORD, M. L. GOOD and M. L. STEVENSON: *Phys. Rev.*, **101**, 503 (1956).

(9) R. W. BIRGE, D. H. PERKINS, J. R. PETERSON, D. H. STORK and M. N. WHITHEAD: *Nuovo Cimento*, **4**, 834 (1956).

(*) *Note added in proof.* — Prof. R. H. DALITZ has kindly informed us that all present experimental results including the one on Θ^0 decay reported here can be reconciled with a dominant $\Delta I = \frac{1}{2}$ selection rule, if it is supposed that the violation occurs not only in the $\Delta I = \frac{3}{2}$ mode, but in about equal measure in $\Delta I = \frac{5}{2}$. Specifically he points out that $a_3/a_1 = -0.12$; $a_5/a_1 = -0.08$ can reconcile the observations.

(10) T. D. LEE and C. N. YANG: *Phys. Rev.*, **102**, 290 (1956).

(11) J. SCHWINGER: *Phys. Rev.*, **104**, 1164 (1956).

the experimental situation on this point. Our most important result in this connection is the fact that *just one-half of the θ^0 particles* which are produced in association with Λ^0 's in our chamber *decay in the 2π mode*. The other half are long lived and must be presumed to be the complementary θ_2^0 particles. If parity conjugate particles also exist, we would have 4 θ^0 particles, θ_{1+}^0 , θ_{2+}^0 , θ_{1-}^0 , θ_{2-}^0 and in general four sets of lifetimes and decay modes. Of these, only one is expected to have the short observed mean life of the θ_1^0 and dominantly the 2π decay mode. The others are expected to have a long life. We should then expect to see only one quarter of the θ^0 particles materializing in the chamber contrary to the experimental result. The fact that no trace of the parity conjugate modes is observed is a clear indication that the theory is not tenable in this form. In order, nevertheless, to maintain the theory it would be necessary to assume:

- 1) That the θ_{1-}^0 and θ_{2-}^0 are produced only in association with Λ_-^0 . This is permissible but completely *ad hoc*, and
- 2) The Λ_-^0 is long lived, and therefore not observed in the chamber. According to the data of Fig. 6 the Λ_-^0 lifetime would have to be at least 10^{-8} s. In this connection it must be remembered that the absorption experiments of K^- in hydrogen (¹²) show that there are no long lived Σ^+ or Σ^- particles with appreciable abundance, and
- 3) The θ_{1-}^0 and θ_{2-}^0 lifetimes are greater than $3 \cdot 10^{-8}$ s.

The last assumption is no difficulty. On the other hand, the first two, especially the second, must be considered most unlikely. The really striking experimental fact is that there is no trace whatever of the parity doublets.

The original motivation for the introduction of the parity conjugates was of course the fact that the τ^+ and θ^+ decay into states of opposite parity. The violation of parity conservation in decay processes involving the neutrino changes the problem markedly, although the question of parity conservation in processes not involving the neutrino is not yet clear.

In this connection it has been pointed out to us in conversations with T. D. LEE that it is possible to construct now quite different structures of parity doublets, for which the decay interaction is invariant under parity conjugation and therefore, of course, violates parity conservation. In such a theory the θ_{1+}^0 and θ_{1-}^0 have identical decay modes and lifetime, and the same is true of Λ_+^0 and Λ_-^0 as well as θ_{2+}^0 and θ_{2-}^0 . Such a theory is in agree-

(¹²) L. W. ALVAREZ, H. BRADNER, P. FALK-VAIRANT, J. D. GOW, A. H. ROSENFIELD, F. T. SOLMITZ and R. D. TRIPP: *University of California Radiation Laboratory Report* (UCRL 3583) (1956).

ment with our experimental results since the 0_{1+}^0 and 0_{1-}^0 have identical properties and cannot be distinguished in this experiment. The predictions of this theory are then identical with the predictions of the theory without doubling. For this reason, the only motivations for the introduction of this type of doubling theory at the present time would have to be of a theoretical nature. The only experiments which seem capable of demonstrating the existence of such doublets are experiments in which both production and decay angles of the Λ^0 and 0^0 are observed. There are then certain asymmetries possible, as pointed out by LEE and YANG (13), which must, if they exist, be referred to parity doublets. On this point the evidence available to date must be considered inadequate.

* * *

We gratefully acknowledge the help of Dr. R. BUDDY in the design of the chambers, the very kind help of Mr. E. HOYLE in the difficult reconstruction of the magnet, and valuable discussions with Drs. LEE and LEDERMAN. One of us (J.S.) wishes to acknowledge the generous support of the Guggenheim Memorial Foundation and the hospitality of the Brookhaven National Lab. as well as that of the Istituto di Fisica, Università, Roma.

(13) T. D. LEE and C. N. YANG: *Phys. Rev.*, **104**, 822 (1956).

(14) H. BLUMENFELD, E. T. BOOTH, L. M. LEDERMAN and W. CHINOWSKY: *Phys. Rev.*, **102**, 1184 (1956).

RIASSUNTO (*)

L'osservazione sistematica di 528 eventi Λ^0 - 0^0 in propano ha dato i seguenti risultati: 1) Esiste un decadimento Λ^0 neutro; $\Lambda^0 \rightarrow \pi^0 + n$ e la frazione di Λ^0 che decadono in questo modo è $.32 \pm .05$. 2) La componente 0_1^0 ha un modo di decadimento neutro, molto probabilmente $0_1^0 \rightarrow \pi^0 + \pi^0$. Il 0^0 ha pertanto molto probabilmente spin pari.

La frazione $\frac{P(0_1^0 \rightarrow \pi^0 + \pi^0)}{P(0_1^0 \rightarrow 2\pi)}$ è $.14 \pm .06$. Il rapporto $\frac{P(\Lambda^0 \rightarrow \pi^0 + n)}{P(\Lambda^0 \rightarrow \pi^- + n)}$ è in buon accordo con

la regola di selezione $I = \frac{1}{2}$; il rapporto $\frac{P(0^0 \rightarrow 2\pi^0)}{P(0^0 \rightarrow \pi^+ + \pi^-)}$ sembra invece in disaccordo.

3) $(51 \pm 7.5)\%$, cioè, metà dei mesoni 0^0 sfuggono dalla camera e si debbono identificare con i mesoni 0_2^0 proposti da GELL-MANN e PAIS (4). Si discute l'esistenza di altri modi di decadimento (doppietto di parità). 4) I decadimenti $\Lambda^0 \rightarrow \frac{\mu^- + p + \nu}{e^- + p + \nu}$ non si osservano e la frazione di tali decadimenti è inferiore al 2%. 5) I modi di decadimento del 0_1^0 in 3 particelle non sono stati osservati ed è pertanto assai poco probabile che eccedano il 2% del totale dei decadimenti di 0_1^0 . 6) Misure preliminari danno vite media $\tau_{0_1^0} = (.95 \pm .08) \cdot 10^{-10}$ s e $\tau_{\Lambda^0} = (2.8 \pm .2) \cdot 10^{-10}$ s. 7) Per il 0_2^0 otteniamo per la vita media un limite inferiore che assieme ai risultati di LANDE *et al.* (5) inquadra la vita media di tale particella fra $(3 < \theta_2^0 < 10) \cdot 10^{-8}$ s.

(*) Traduzione a cura della Redazione.

Gravitational Forces and Quantum Field Theory.

P. GULMANELLI and E. MONTALDI

*Istituto di Scienze Fisiche dell'Università - Milano
Istituto Nazionale di Fisica Nucleare - Sezione di Milano*

(ricevuto il 17 Aprile 1957)

Summary. — The Gamow-Teller hypothesis, according to which an exchange of neutrino pairs could give rise to a gravitational type potential between nucleons, is re-examined. By introducing a new boson field it is shown that this guess cannot be valid at least in the frame of the usual linear field theories.

1. – Introduction.

It is the purpose of this paper to develop some ideas that have already been discussed in a previous letter ⁽¹⁾, and to give results that allow us to draw a definite conclusion on the matter.

As is well known, several attempts have been made to explain gravitational forces in terms of elementary processes typical of quantum field theory.

GAMOW and TELLER ⁽²⁾ were the first to put forward the hypothesis that exchange of a pair of virtual neutrinos between two nucleons could give rise to an interaction of a gravitational type between the two particles. Later CORBEN ⁽³⁾ suggested a scheme by which the Gamow-Teller hypothesis is re-interpreted in the frame of the usual β -theories. Namely the interaction between two nucleons appears as the result of a fourth order process, in which the exchange of two virtual neutrinos is accompanied by the emission and

⁽¹⁾ P. BOCCIERI and P. GULMANELLI: *Nuovo Cimento*, **5**, 1016 (1957).

⁽²⁾ G. GAMOW and E. TELLER: *Phys. Rev.*, **51**, 289 (1937); G. GAMOW: *Phys. Rev.*, **71**, 550 (1947).

⁽³⁾ H. C. CORBEN: *Nuovo Cimento*, **10**, 1485 (1953).

reabsorption of two electrons. This last circumstance implies the appearance of two closed loops, that make impossible the actual calculation of the corresponding matrix element.

Owing to the un-renormalizability of β -theory, one would in any case obtain ambiguous results. In order to circumvent these difficulties of calculation, it has also been proposed to introduce a form factor (⁴). But, apart from the current criticism applying to non-local type theories, the results will obviously depend in an essential way on the choice of the form factor.

This being the situation, another scheme (¹) has recently been suggested in which the fundamental idea of an exchange of virtual neutrinos is kept fixed, whereas the interaction is modified by the introduction of a new field in such a way as to reach finite and unique results.

In the following section we perform the detailed calculation of the interaction potential acting between two nucleons, which one obtains with this model in the static approximation. As it will be seen, the momentum space representation of the potential does not show the $(\Delta p)^2$ -dependence corresponding to a $1/r$ type potential in co-ordinate space.

2. - The static approximation potential.

The suggested scheme is based on the introduction of a boson field, associated with a hypothetical X particle, having a mass greater than the nucleon mass, and coupled with the nucleon and lepton fields. Without any loss of generality, we shall restrict ourselves to a neutral scalar field and therefore the elementary processes involved will be only the following two:

$$(1) \quad N \rightleftharpoons X + \nu, \quad X \rightleftharpoons P + e.$$

The condition we impose on the μ , mass of the X particle, that it must be greater than M , suffices to prevent the decay of the free neutron into an X particle. One of the two coupling constants, g_1 and g_2 , corresponding to the elementary interactions (1), can be fixed by means of the resulting relationship between the product $g_1 g_2$ and the mean lifetime for β -decay.

In this scheme also the lowest order interaction between two nucleons takes place through the exchange of two virtual neutrinos. The process is still a fourth order one, but it does not involve electrons and therefore does not show the unpleasant features connected with the presence of closed loops.

For the sake of simplicity, we have performed the detailed calculations for the case of the neutron-neutron interaction, assuming a direct coupling

(⁴) P. BUDINI: *Nuovo Cimento*, **10**, 1486 (1953).

between the φ_x field and the ψ_n and ψ_v fields:

$$(2) \quad H_{\text{int.}} = g_1 \bar{\psi}_n \psi_v \varphi_x + \text{h.c.}$$

Denoting by p , q and p' , q' the momentum-energy four-vectors of the ingoing, respectively outgoing neutrons, and putting $\Delta p = p' - p = q - q'$ and $\mathbf{p} = p_\mu \gamma^\mu$, the S -matrix element, to the order here considered, is given by the sum of the following term

$$(3) \quad S^I = -\frac{g_1^4}{4!} \delta(p + q - p' - q') \cdot \int d^4k \frac{(\bar{\psi}_{\nu'}(\mathbf{p}' - \mathbf{k})\psi_{\nu})(\bar{\psi}_q(\mathbf{q} - \mathbf{k})\psi_v)}{[(k - p')^2 - i\varepsilon][(k - \Delta p)^2 + \mu^2 - i\varepsilon][(k - q')^2 - i\varepsilon](k^2 + \mu^2 - i\varepsilon)},$$

and of the similar expression S^{II} one obtains by interchanging p' and q' .

By means of Feynman's formula

$$(4) \quad \frac{1}{abcd} = 6 \int_0^1 dx \int_0^x dy \int_0^y dz [(a - b)z + (b - c)y + (c - d)x + d]^{-4},$$

eq. (3) becomes

$$(5) \quad S^I = -\frac{g_1^4}{4} \delta(p + q - p' - q') \int_0^1 dx \int_0^x dy \int_0^y dz \int d^4k \cdot \frac{(\bar{\psi}_{\nu'}(\mathbf{p}' - \mathbf{k} - \mathbf{q}x + \mathbf{q}'y - \mathbf{p}z)\psi_{\nu})(\bar{\psi}_q(\mathbf{q} - \mathbf{k} - \mathbf{q}x + \mathbf{q}'y - \mathbf{p}z)\psi_v)}{(k^2 + A)^4},$$

where one has put

$$(6) \quad A = M^2 \{ (x - y + z)^2 + \theta(1 - x)(y - z) + (\theta' - \theta)z(x - y) + \div (1 + \varrho)(1 - x + y - z) - 1 \}$$

and

$$(7) \quad \theta = \frac{(\Delta p)^2}{M^2}, \quad \theta' = \frac{(p - q)^2}{M^2}, \quad \varrho = \left(\frac{\mu}{M} \right)^2.$$

It can be easily seen that A is always greater than zero, so that one can straightway put $\varepsilon = 0$. The integration over k can be easily done and gives

the following result:

$$(8) \quad S^r = -\frac{g_1^4}{24} \pi^2 i \delta(p + q - p' - q') \int_0^1 dx \int_0^x dy \int_0^y dz \cdot$$

$$\begin{aligned} & (\psi_{\nu}(iM - \mathbf{q}^r - \mathbf{q}'y - iMz)\psi_{\rho})(\bar{\psi}_{\nu}(iM - iMx + iMy - \mathbf{p}z)\psi_{\sigma}) \\ & - \frac{g_1^4}{48} \pi^2 i \delta(p + q - p' - q') (\bar{\psi}_{\nu} \gamma_{\lambda} \psi_{\rho})(\bar{\psi}_{\sigma} \gamma_{\lambda} \psi_{\sigma}) \int_0^1 dx \int_0^x dy \int_0^y dz \cdot \frac{1}{A^2}, \end{aligned}$$

which can be suitably rewritten as follows:

$$(9) \quad S^r = -\frac{g_1^4}{24} \pi^2 i \delta(p + q - p' - q') \cdot$$

$$\begin{aligned} & \left\{ iM(\bar{\psi}_{\nu} \psi_{\rho})(\bar{\psi}_{\sigma} \mathbf{p} \psi_{\sigma}) \int_0^1 dx \int_0^x dy \int_0^y dz \frac{(x - y + z)(x - y + z - 1)}{A^2} \right. \\ & - M^2(\bar{\psi}_{\nu} \psi_{\rho})(\bar{\psi}_{\sigma} \psi_{\sigma}) \int_0^1 dx \int_0^x dy \int_0^y dz \frac{1 - x + y - z}{A^2} - \\ & - (\bar{\psi}_{\nu} (\mathbf{p} - \mathbf{q}) \psi_{\rho})(\bar{\psi}_{\sigma} (\mathbf{p} - \mathbf{q}) \psi_{\sigma}) \int_0^1 dx \int_0^x dy \int_0^y dz \frac{z(x - y)}{A^2} + \\ & \left. + \frac{1}{2} (\bar{\psi}_{\nu} \gamma_{\lambda} \psi_{\rho})(\bar{\psi}_{\sigma} \gamma_{\lambda} \psi_{\sigma}) \int_0^1 dx \int_0^x dy \int_0^y dz \frac{1}{A} \right\}. \end{aligned}$$

For the present purpose, it will suffice to consider the non-relativistic approximation of eq. (9). In this approximation the $(\mathbf{p} - \mathbf{q})$ term is negligible and \mathbf{p} reduces simply to iM , so that eq. (9) becomes:

$$(10) \quad S^r = -\frac{g_1^4}{24} \pi^2 i \delta(p + q - p' - q') (\bar{\psi}_{\nu} \psi_{\rho})(\bar{\psi}_{\sigma} \psi_{\sigma}) \cdot$$

$$\left\{ \frac{1}{2} \int_0^1 dx \int_0^x dy \int_0^y dz \frac{1}{A} - M^2 \int_0^1 dx \int_0^x dy \int_0^y dz \frac{(x - y + z - 1)^2}{A^2} \right\}.$$

Similarly one has, for the matrix element S^{II} :

$$(11) \quad S^{\text{II}} = -\frac{g_1^4}{24} \pi^2 i \delta(p + q - p' - q') (\bar{\psi}_p \psi_p) (\bar{\psi}_q \psi_q) \cdot \\ \cdot \left\{ \frac{1}{2} \int_0^1 dx \int_0^x dy \int_0^y dz \frac{1}{B} - M^2 \int_0^1 dx \int_0^x dy \int_0^y dz \frac{(x - y + z - 1)^2}{B^2} \right\},$$

where

$$(12) \quad B = M^2 \left\{ (-y + z)^2 + (\theta' - \theta)(1 - x)(y - z) + \right. \\ \left. + \theta z(x - y) + (1 + \varrho)(1 - x + y - z) - 1 \right\}.$$

We now notice that in this approximation one can still put $\theta' = 0$.

The integration over the auxiliary variables becomes then possible and gives for S^{I} the following result

$$(13) \quad S^{\text{I}} = -\frac{g_1^4}{24} \pi^2 i \delta(p + q - p' - q') \left(\frac{1}{2} H - M^2 K \right),$$

where

$$(14) \quad H = \frac{1 + \varrho + \theta}{2\theta} [(\varrho + \theta) \ln(\varrho + \theta) - \varrho \ln \varrho + (\varrho - 1) \ln(\varrho - 1) - \\ - (\varrho + \theta - 1) \ln(\varrho + \theta - 1)] - \frac{1}{2} - \frac{1}{2\theta} [(\varrho + \theta) \ln(\varrho + \theta) - \varrho \ln \varrho] + \\ + \frac{1}{2} \varrho \ln \varrho - \frac{1}{2} (\varrho - 1) \ln(\varrho - 1),$$

$$(15) \quad K = \frac{1 + \varrho + \theta}{2\theta} [(2\varrho + 2\theta - 1) \ln(\varrho + \theta) - (2\varrho - 1) \ln \varrho + \\ + 2(\varrho - 1) \ln(\varrho - 1) - 2(\varrho + \theta - 1) \ln(\varrho + \theta - 1)] - \\ - \frac{1}{2\theta} [(3\varrho + 3\theta - 1) \ln(\varrho + \theta) - (3\varrho - 1) \ln \varrho + 2(\varrho - 1) \ln(\varrho - 1) - \\ - 2(\varrho + \theta - 1) \ln(\varrho + \theta - 1)] - 1 + \left(\varrho - \frac{1}{2} \right) \ln \varrho - (\varrho - 1) \ln(\varrho - 1).$$

The corresponding expression for S^{II} follows from (13) by changing θ into $-\theta$ (cf. (6) and (12)).

It is now evident that the asymptotic behaviour of the sum $S^{\text{I}} + S^{\text{II}}$, in the limit for $\theta \rightarrow 0$, is not of the form $1/\theta$, and this means that in co-ordinate space the static interaction potential between the two neutrons does not

behave, at great distances, as $1/r$. *The Fourier transform of the leading term turns out to be of the form $\sim (1/r) \ln r$.*

All these results obviously do not depend on the particular choice we have made for the φ_x field.

A different tensor direct coupling (iso-spin also included) would imply changes in the spinor coefficients only, and would leave unmodified the structure of those integrals, which determine the θ -dependence of the interaction potential.

It is clear, therefore, that although capable of reproducing the results of the ordinary β -theories, the proposed model cannot give an interaction potential of a gravitational type.

This necessarily leads us to conclude that, at least *in the frame of the usual linear field theories, it is not possible to explain gravitational forces in terms of an exchange of neutrino pairs.*

* * *

We wish to express our gratitude to Professor P. CALDIROLA for his kind interest in this work.

We like to thank also our friends P. BOCCIERI and A. LOINGER for useful discussions.

RIASSUNTO

Viene ripresa in esame l'ipotesi di Gamow e Teller secondo cui uno scambio di coppie di neutrini potrebbe condurre a un potenziale di tipo gravitazionale tra nucleoni. Mediante l'introduzione di un nuovo campo bosonico si dimostra che questa supposizione non può essere valida almeno nell'ambito delle ordinarie teorie lineari di campo.

NOTE TECNICA

Diborane-gas filled Counting Tubes for Measuring Thermic Neutrons.

O. J. ORIENT and E. I. VIZSOLYI

Central Research Institute for Physics - Budapest

(ricevuto il 5 Febbraio 1957)

Summary. — A method for producing adequately pure diborane gas free from electron-negative impurities is described; further the results of comparative research work on diborane-filled and boron-fluoride filled counting tubes are given. According to the results of measurements, the operating characteristics of the diborane-filled tubes coincide with those of the boron-fluoride filled tubes, the only difference being that the efficiency of the diborane-filled tubes is double of that of the boron-fluoride filled tubes.

1. — Introduction.

For the detection of thermic neutrons the boron-isotope of mass-number 10 can be utilized. Slow electrons cause the following nuclear reaction:



In consequence of the nuclear reaction, either 2.3 MeV or 2.78 MeV energy is liberated as the kinetic energy of the ${}^3_3\text{Li}$ nucleus and particle α coming into being. In the first case, the nucleus ${}^3_3\text{Li}$ remains in an excited state and will emit the surplus of energy in form of γ -rays. Along their whole range, the two nuclei produce about 70 : 80 000 ion pairs. The cross-section of the effect of the reaction follows the $1/r$ law through a very large range. Its value is at a 1 eV about $100 \cdot 10^{-24} \text{ cm}^2$, at 0.025 eV about $708 \cdot 10^{-24} \text{ cm}^2$.

Neutron-counting tubes are filled mostly with different gaseous compounds of boron. Let us have a look on the compounds of boron that may be considered as filling-gases for neutron-counting tubes.

TABLE I.

Boron-Halogens			Boron-Alkyls			Borans		
BX_3	tension		BR_3	tension		B_nH_{n+4}	tension	
	400 mm Hg	760 mm Hg		400 mm Hg	760 mm Hg		400 mm Hg	760 mm Hg
BF_3	-108.3 °C	101.7 °C	$\text{B}(\text{CH}_3)_3$	34.7 eC	20.2 °C	B_2H_6	99.6 °C	86.5 °C
BCl_3	3.6 °C	+12.7 °C	$\text{B}(\text{C}_2\text{H}_5)_3$		+95.0 °C	B_4H_{10}	+0.8 °C	+16.3 eC
BBr_3	+70.0 °C	+91.7 °C	$\text{B}(\text{C}_3\text{H}_7)_3$		+156.0 °C	B_5H_9	+40.8 °C	+58.1 eC
BJ_3		+210.0 °C				B_5H_{11}	+51.2 °C	+67.0 °C

There are a very large number of borie compounds, but only a few of them are gaseous at room temperature.

In the following table some of the characteristics of the more important boric compounds are listed, i.e. boron-halogens, boron-alkyls and borans (Table I). The tabulated values show that the first members of each group are gases, the following ones are liquids and the further ones solids. As the efficiency of the counters goes increasing with the increase of the pressure of the gas, our interest is principally focussed on the boron-fluorid, the boron-methyl and the diborane compounds, characterized by considerable tension values.

Counting-tubes filled with boron halides and boron alkyls are described in the literature and are in current use. Each molecule of these compounds contains one atom of boron.

Each molecule of the different boranes, however contains several atoms of boron. It is evident that the effectiveness of the detection of the particles can be increased even without the separation of the isotopes, merely by increasing the number of the atoms of boron present in the molecules. On the other hand, the gas B_2H_6 can presumably be enriched with a better effectiveness, in spite of its lesser stability, than the gas BF_3 , since the ratio of the masses of the atoms of boron and hydrogen in the molecules of the diborane is more favourable than the ratio of the masses of the atoms of boron and fluorine in the molecules of the boron-fluoride. Therefore, we took an interest in the properties of the different borane varieties. The state of affairs up to now is, that no adequate borane-filled counting-tubes have been constructed so far (1).

Thus the problem set was, on the one hand, to produce a correspondingly pure diborane-gas, free from all electron-negative impurity (as oxygen, carbon dioxide, aqueous vapour and silanes), on the other hand, the comparison of the operating characteristics of our diborane-filled counting tubes with the characteristics of the boron-fluoride tubes in use up to the present.

(1) S. A. KORFF: *Electron and Nuclear Counters* (1955), p. 97.

2. — The synthesis of the diborane.

The synthesis of the diborane is a two-step process. In the first step, a complex of boron-fluoride-ether was synthetized, then, in the second one, the complex of boron-fluoride-ether was treated with lithium-aluminium-hydride.

The method for producing a boron-fluoride-ether was a further development of a synthesis elaborated by one of the authors (2) on basis of the following formulas:

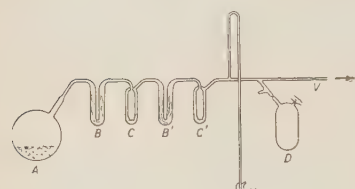


Fig. 1.

In order to remove impurities, the whole system is exposed to a high vacuum and heated thoroughly, then removed from the pumping system. Upon heating the content of the retorte A to 518 °C, the production of the gas begins according to formula (1). The generated gas passes through the U-shaped tubes B and B' respectively, filled with glass-silk, then through the traps C and C', cooled with ice, resp. with carbonic acid snow. By this procedure the gas is purified from the sublimated boron-fluoride and from accidental hydrogen-fluoride traces. The purified gas concentrates in recipient D, filled with ether and cooled by liquid air. When the vigorous generation of the gas ceases, the recipient D is disconnected from the system by sealing off. Now recipient D contains the ether and the boron-fluoride condensed within it. The recipient is kept for 48 hours in liquid air, during which time the complex formation from the boron-fluoride, solid at this temperature, and the ether will be completed.

Now recipient D is sealed to the apparatus shown on Fig. 2, in which the production of the gas diborane will take place.

In the retorte of the apparatus shown on Fig. 1 dry, completely pulverized potassie tetrafluorborate and boron-oxide is fed in and the recipient B is filled with ether p.a. The quantities of the ingredients are calculated in such manner that from 140 g of KBF_4 and 105 g of B_2O_3 , there should be won about 15-16 l gas BF_3 , and that this should be absorbed by the surplus of 270 ml of ether.

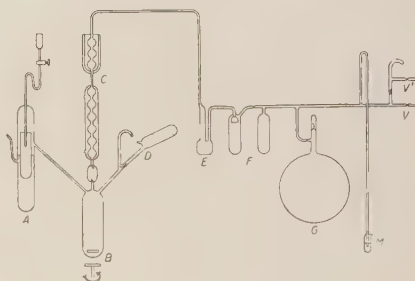
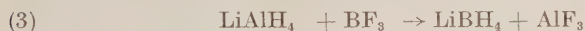


Fig. 2.

(2) E. VIZSOLYI: *KFKI Kôzl.* 3. évf. 3. sz. 293 (1955).

The diborane gas is produced according to the following formulas:



Formula (5) characterizes the whole process, on base of which FINHOLT, Bond and SCHLESINGER (³) produced diborane gas; the fact that in etheric medium the reaction proceeds in two steps was proved by SHAPIRO and others (⁴) (since the generation of the diborane is not continuous, and the reaction starts only upon adding a surplus of BF_3). The higly violent reaction is slowed down by the etheric medium, whose application is necessary on this ground too.

For the production of the diborane we utilized the apparatus shown on Fig. 2. In the feeder *A* an etheric solution of lithium-aluminium-hydride was put. The reactive vessel was provided with a stirrer. The vessel *D*, provided with a break-off-seal contained the complex of boron-fluoride, prepared as described above. The cooling-system *C* is cooled by air, by circulating water, resp. with dry ice; the freezing-vessels *E* also are cooled by dry ice.

A high vacuum is established throughout the whole system and the whole system is baked out. Then the etheric solution of the lithium-aluminium-hydride is poured into the vessel. In order to purify the product from impurities (traces of air and water), the mixture is to be thawed up and freezed again several times. Then the vessel is disconnected from the pump. Now the break-off-seal of vessel *D* is removed and the boron-fluoride-ether complex flows into the reacting-vessel *B*. At the same time the etheric solution of lithium-aluminium-hydride is thawed up. We put in movement the magnetic stirring apparatus of vessel *B*, and lightly open the tap conducting to the feeder. Upon this, while the mercury is slowly dripping, the etheric solution of lithium-aluminium-hydride is fed over into the vessel *B*, which already contains a complex of boron-fluoride-ether. Now the gas diborane is generated readily, even with effervescence. Most part of the ether remains in the freezing-vessel, and the manometer shows the pressure of the produced gas. We discontinue the production of the gas when new doses of lithium-aluminium-hydride do not cause effervescence any more, and the reading of the manometer does not change any more. The recipient vessel will be disconnected from the gas-generating apparatus ahead of the freezing-tank *F*.

Further, the produced gaseous diborane has to be purified from the traces of ether and the impurities of polyborane-hydrogene coming into being in the course of the reaction. For that purpose the freezing tank *F* is cooled by liquid air for as long as 48-72 hours, in which time the diborane and part of the impurities (the polyboranes and traces of ether) will also be frozen out quantitatively, while the soiling hydrogene does not freeze. The break-off-seal between the recipient system and the pump is opened and the diborane is purified from the hydrogene by means of a high vacuum. Then by sealing

(³) A. E. FINHOLT, A. C. BOND and H. I. SCHLESINGER: *Journ. Am. Chem. Soc.*, **69**, 1199 (1947).

(⁴) I. SHAPIRO, H. G. WEISS, M. SCHMICH, SOL SKOLNIK and G. B. L. SMITH: *Journ. Am. Chem. Soc.*, **74**, 901 (1952).

off, the system is disconnected definitively from the pump and the cooling by liquid air instantly replaced by cooling with carbonic-acid snow. Then the diborane thaws and vessel *G*, after having been sealed off in its turn will be filled with purified diborane-gas, whose pressure is shown by the manometer; the traces of ether and the polyborane remain in the trap cooled by carbonic-acid snow.

3. Construction and vacuum technique of the counting tubes.

The construction of the counting tubes is shown on Fig. 3 in axial section. The cathodes are made of nickel foil of 0.1 mm thickness. The diameter of the tubes is 15 mm. The anodes, made of 0.1 mm diameter tungsten wire, are provided with a tungsten spring. The working length of the anode wire is 80 mm. The outer tubes are made of Jena-glass (16/III), as this kind of glass does not contain any boron.



Fig. 3.

The tubes are sealed to a manifold, and a vacuum of 10^{-6} mm is produced. After that they are baked at 350°C for 3 hours, in order to remove the absorbed water and other impurities. After the baking the tubes are cooled to room-temperature and filled with diborane to 20 cm of mercury.

For comparison, with the same vacuum-technique, some tubes were filled with boron-fluoride, equally to the pressure of 20 cm mercury. The shape and the size of these tubes were similar to those of the diborane containing tubes.

4. - Measuring apparatus.

In the course of the measurement and research work, neutrons are most often accompanied by intensive γ -radiation, which give rise to electrons coming from the walls of the counter. The neutron-counters are therefore operated in the proportionality range. The α -particles, originating from the neutrons, cause a primary ionization about 2-3 times the size of that originated by the electrons resulting from the γ -rays. The two kinds of impulses can be separated by means of an adequate electronic impulse-amplitude discriminator. That is why we compared the tubes filled with the two different kinds of gas in the proportionality range only.

The block-diagramm of the measuring apparatus is shown on Fig. 4.

A preliminary amplifier amplifies the signal produced on the load resistance ($1.5 \text{ M}\Omega$) of the counting tube. The preliminary amplifier is followed by a discriminator. The signal is fed from the discriminator on to a scale of 1000.

The shape of the signal may be checked on the screen of the oscilloscope plugged to the output of the amplifier. The high voltage is smoothly adjustable between 1000 and 3000 V and can be continually controlled by means of a meter instrument. The amplification of the amplifier is adjustable in 10 steps between 50 and 500.

The transmission of the amplifier is smooth up to a frequency of 500 kHz.

The main data of the discriminator are as follows: threshold adjustable between 5 V and 55 V, the uncertainty of the discrimination being less than 150 mV; the discriminating capacity is of $3 \cdot 10^5$ periodic signals pro secund; the length of the output-signal is of 3 μ s and its amplitude is smoothly adjustable from 0 to 20 V.

For the actioning of the neutron-counters we utilized a natural radioactive neutron-source. This neutron-source was a Ra-Be preparation with an amount of 100 mg radium. This source emits fast neutrons mainly with an energy of 4-5 MeV. For their slowing down a cylindrical block of paraffine was utilized. For the neutron-counter to be measured a circular hole was made in the block. The distance of the axis of the cylinder of paraffine was about 15 cm. The tubes to be measured were fitting exactly in the holes; by this fact it was assured that the tubes of the same size and dimensions will receive slow neutron radiation of the same intensity even if they are interchanged.

5. - Results of the measurements.

The operating characteristic of the boron-fluoride filled neutron-counting tubes displays a relatively broad (proportional) plateau. This means that the number of the impulses registered is between certain limits almost independent of the most important three auxiliary parameters: the working tension of the tube, the amplification factor, and the setting of the discriminator threshold. This is due to the fact that the maximal background impulses originated from the γ -rays are considerably smaller than the overwhelming majority of the impulses due to the neutron-counting (5).

Measurements have been executed for the establishment of the operating characteristics of the tubes filled with boron-fluoride and those filled with diborane. In the first line, the proportional plateau has been examined. The operating data of the diborane-filled and those of the boron-fluoride filled tubes are listed on Table II. During the measurements the amplification of the preliminary amplifier was permanently set on an amplifying factor of 150, the discriminator threshold to 5 V.

It is apparent that the data of the diborane-filled tubes are similar to those of the boron-trifluoride filled ones. The slope of the characteristics of tubes

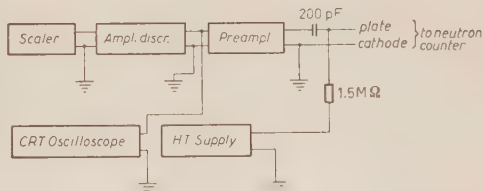


Fig. 4.

(5) B. ROSSI and H. STAUB: *Ionization Chambers and Counters* (1949), p. 193.

TABLE II.

	Plateau threshold V	Plateau length V	Plateau slope %/V	Counting rate
BF_3	2000	220	0.122 ± 0.02	3080 ± 59
B_2H_6	2020	220	0.114 ± 0.012	6100 ± 85

Relative increase in efficiency = 1.981 ± 0.065 .

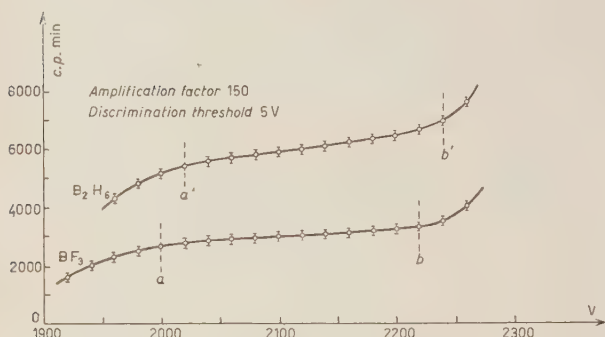


Fig. 5.

forming part of the figure indicates the average of the impulses counted on the plateau of the tube with diborane and of that with boron-trifluoride, as well as the quotient of the two figures; the quotient indicates the relative increase of efficiency of the diborane-filled tubes as compared with the boron-trifluoride filled ones. This value was found to be 1.981 ± 0.065 , i.e. the efficiency of the tubes with diborane, within the errors of the measurement, is the double of those with boron-trifluoride.

In conclusion it may be stated that the operating characteristics of the diborane filled tubes and those of the boron-trifluoride filled tubes are the same, except that the efficiency of the tubes filled with diborane is double.

RIASSUNTO (*)

Si descrive un metodo per produrre agevolmente diborano gassoso puro esente da impurità elettronegative; si danno inoltre i risultati di lavori di ricerca sul confronto di tubi di contatori riempiti con diborano o con fluoruro di boro. Dalle misure eseguite risulta che le caratteristiche di funzionamento dei tubi riempiti di diborano coincidono con quelle dei tubi riempiti con fluoruro di boro, l'unica differenza essendo che il rendimento dei tubi riempiti di diborano è doppio di quello dei tubi riempiti di fluoruro di boro.

(*) Traduzione a cura della Redazione.

of both kinds is the same on a 220 V long plateau (portion $a-b$, resp. $a'-b'$ on the figure), within the error of the measurements.

The voltage corresponding to the beginning of the plateau of the diborane-filled tubes, (a') is higher than that of the boron-fluoride filled tubes, (a). Beside these data the table

Stereoscopy in Bubble Chambers.

P. BASSI, A. LORIA, J. A. MEYER (*), P. MITTNER and I. SCOTONI

Istituto di Fisica dell'Università - Padova

Istituto Nazionale di Fisica Nucleare - Sezione di Padova

(ricevuto il 17 Aprile 1957)

Summary. — Exact and approximate methods are given for the reconstruction of the position of a point in a bubble chamber, photographed with two cameras having parallel optic axes. In the appendix procedures are suggested for the direct reconstruction of a straight line and for the determination of the radius of curvature of a cylindrical helix with axis parallel to the optic axes.

The spatial reconstruction of events in bubble chambers may be carried out by means of two photographs taken through objectives of the same type, situated at equal distances from the front plate, and having their optic axes perpendicular to it. It is this type of optical system, often used in practice owing to its simplicity and suitability, which will be considered here.

The treatment is limited to quite elementary considerations of geometric optics, since our aim was only to outline a general simple method for the stereoscopic analysis of the events taking place in a bubble chamber: we think that the physics of the various problems, including the evaluation and discussion of errors, could more profitably be studied case by case.

Let us suppose that the two objectives are free from aberrations, that they have the same focal length and that each has its principal points coincident: the importance of the aberrations will, in fact, be estimated case by case while, as will become evident from what follows, the considering of different focal lengths or non-coincident principal points only introduces inessential complications.

The data necessary for the reconstruction may be taken either directly from measurements on the photographs, or from reprojected images.

(*) Now at CEN, Saclay, France.

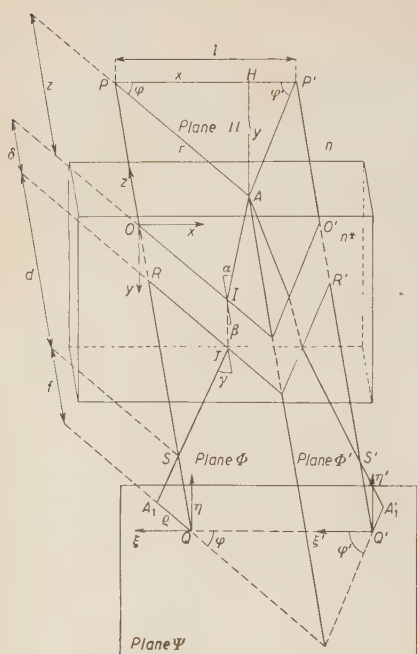


Fig. 1. - Assonometric projection.

n and n^* are the refractive indices of the liquid, supposed to be homogeneous, and of the front glass respectively.

Further:

A : is a point object;

A_1 : its image on the film;

P : its projection on the optic axis;

r : its distance from the optic axis;

ϱ : the distance of the image from the optic axis;

the line $AIJS A_1$ represents a light ray passing through S , which helps to form A_1 : note that this lies in a plane Φ which passes through the optic axis. φ is the angle formed by this plane with that which contains the optic axes, which may be taken as being horizontal.

Π is the plane which passes through A and is normal to the optic axes: it contains P and P' ; α , β and γ are the angles which the three segments of the ray form with the normal to the front plate.

The cartesian coordinate systems used are: in the object space the system $Oxyz$, and in the photograph the system $Q\xi\eta$. In addition, the polar coordinate systems $P\varphi\rho$ on plane Π , and $Q\varphi\varrho$ on the photograph will be used.

1. - Geometrical representation.

In the assonometric projection of Fig. 1 the front plate of the bubble chamber and the plane Ψ of the film, which is supposed to be parallel to the plate, are clearly recognizable.

Dashed letters concern elements specifically related to the right-hand objective; other letters refer to general geometric elements, or common to both objectives, or specifically related to the left-hand objective.

The symbols are as follows:

S : principal point of the objective;

f : focal length;

d : distance between the principal point and the outward face of the front glass;

δ : thickness of the front glass;

l : distance between the optic axes.

Points Q on the film and R on the outward face of the front glass individualize the optic axis.

Further:

A : is a point object;

A_1 : its image on the film;

P : its projection on the optic axis;

r : its distance from the optic axis;

ϱ : the distance of the image from the optic axis;

the line $AIJS A_1$ represents a light ray passing through S , which helps to form A_1 : note that this lies in a plane Φ which passes through the optic axis. φ is the angle formed by this plane with that which contains the optic axes, which may be taken as being horizontal.

Π is the plane which passes through A and is normal to the optic axes: it contains P and P' ; α , β and γ are the angles which the three segments of the ray form with the normal to the front plate.

The cartesian coordinate systems used are: in the object space the system $Oxyz$, and in the photograph the system $Q\xi\eta$. In addition, the polar coordinate systems $P\varphi\rho$ on plane Π , and $Q\varphi\varrho$ on the photograph will be used.

2. - The reconstruction of a point object from measurements on the photographs: exact procedure.

From the photographs one may directly measure angles φ and φ' . From Fig. 1 one has

$$(1) \quad r = \frac{l \sin \varphi'}{\sin(\varphi + \varphi')}.$$

On the other hand one has from Fig. 2:

$$(2) \quad r = d \operatorname{tg} \gamma + \delta \operatorname{tg} \beta + z \operatorname{tg} \alpha,$$

but

$$\operatorname{tg} \gamma = \frac{\varrho}{f},$$

$$\sin \alpha = \frac{\varrho}{n} (\varrho^2 + f^2)^{-\frac{1}{2}},$$

$$\sin \beta = \frac{\varrho}{n^*} (\varrho^2 + f^2)^{-\frac{1}{2}}.$$

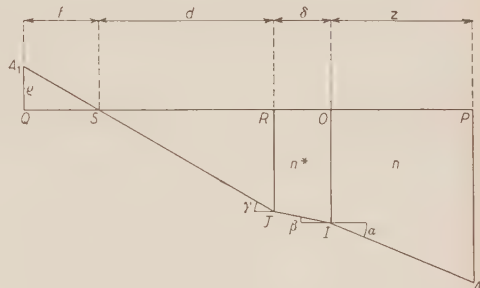


Fig. 2. - Plane Φ . Path of light ray $AIJS A_1$.

Substituting in (2) one obtains

$$(3) \quad r = \varrho \left\{ \frac{d}{f} + \delta [n^{*2} f^2 + (n^{*2} - 1) \varrho^2]^{-\frac{1}{2}} + z [n^2 f^2 + (n^2 - 1) \varrho^2]^{-\frac{1}{2}} \right\},$$

from which

$$(4) \quad z = \left\{ \frac{l \sin \varphi'}{\varrho \sin(\varphi + \varphi')} - \frac{d}{f} - \delta [n^{*2} f^2 + (n^{*2} - 1) \varrho^2]^{-\frac{1}{2}} \right\} \{n^2 f^2 + (n^2 - 1) \varrho^2\}^{\frac{1}{2}}.$$

Thus having determined the distance z of the plane from the outward face of the front plate, and the polar co-ordinates ϱ and r within this plane, the problem is solved.

With the method described above one makes, in effect, a transformation of plane polar coordinates: one starts in fact from a knowledge of ϱ , q and q' (q' is unnecessary information), one obtains r as a function of q and q' , and then z as a function of ϱ , q and q : one then makes use of q , together with r , on the plane Π determined by z .

It is possible to obtain direct transformation formulae for cartesian co-ordinates, so avoiding the measurement or calculation of angles. One notes, in fact, that calling i the magnification in the photograph, one has $i = \xi/x = -\eta/y = \varrho/r$: bearing in mind that $\varrho^2 = \xi^2 + \eta^2$ then from (3) one obtains $x = x(\xi, \eta, z)$ and $y = y(\xi, \eta, z)$, and similarly for the right-hand objective $x' = x'(\xi', \eta', z)$ and $y' = y'(\xi', \eta', z)$. But $x(\xi, \eta, z) = x'(\xi', \eta', z) = l$.

One thus obtains $z(\xi, \eta, \xi', \eta')$ and then x, y, x', y' as functions of ξ, η, ξ', η' .

One may further note that $y = y'$, which allows us to find the relationship

between η and η' and to express x , y and z as functions of ξ , η and ξ' only (η' is unnecessary information). The relationships are, however, complex and this favours the use of plane-polar coordinates. If the cartesian coordinates x and y are required, these are obviously given by the following expressions:

$$(5) \quad \begin{cases} x = \frac{l \sin \varphi' \cos \varphi}{\sin(\varphi + \varphi')} \\ y = \frac{l \sin \varphi' \sin \varphi}{\sin(\varphi + \varphi')} \end{cases}$$

3. Reconstruction of a point object from measurements on the photographs: approximate procedure.

When α , β and γ are sufficiently small one may put

$$\operatorname{tg} \alpha \cong \frac{\operatorname{tg} \gamma}{n} \quad \text{and} \quad \operatorname{tg} \beta \cong \frac{\operatorname{tg} \gamma}{n^*}.$$

Expression (4) then reduces to

$$(6) \quad z \cong n \left(\frac{f l \sin \varphi'}{\varrho \sin(\varphi + \varphi')} - d - \frac{\delta}{n^*} \right).$$

One may also arrive at equality (6) by expanding in series expression (3) and taking only the first terms.

With this approximation the transformation in cartesian coordinates is very simple.

Using now the procedure which was only outlined for the exact solution, one has

$$(7) \quad \frac{x}{\xi} = \frac{y}{\eta} \cong \frac{1}{f} \left(d + \frac{\delta}{n^*} + \frac{z}{n} \right),$$

and similar equalities for the right-hand objective. But

$$x - x' = l \cong \frac{\xi - \xi'}{f} \left(d + \frac{\delta}{n^*} + \frac{z}{n} \right),$$

from which

$$(8) \quad \begin{cases} x = \frac{l \xi}{\xi - \xi'}, \\ y = \frac{l \eta}{\xi - \xi'}, \\ z \cong n \left(\frac{l f}{\xi - \xi'} - d - \frac{\delta}{n^*} \right). \end{cases}$$

Since $y = y'$ one sees that in this approximation the relationship between η and η' is simply $\eta = \eta'$. Note that this property is very useful for identifying in both photographs the same point on a given track. As it would

otherwise be very long and difficult, if not impossible, to identify a certain number of corresponding images of bubbles, it is advisable to design the photographic system in such a way that this approximation is sufficient.

Further it is well known that in the situation represented by Fig. 1 the image of a straight line produced by an objective is not another straight line; in fact in that situation an objective gives rectilinear images only for those straight lines which intersect its own optic axis. BLACKETT⁽¹⁾ has discussed this type of distortion for the case of the Wilson Cloud Chamber ($n = 1$).

In the approximation considered, this effect is ignored and a straight line transforms as a straight line. The simplified equations for a straight line in space are of the type $x = pz - q$, $y = tz + r$; combining these expressions with (8) one may eliminate ξ' and z and so obtain a relation between ξ and η , which is linear.

It is to be noted that the exact formulae (4) and (5) and the approximate formula (6) conserve their validity even if points S and S' are not equidistant from the front plate and even if the focal lengths of the objectives are different. The only data relative to the right hand objective which is used is in fact the angle φ' which is independent of S' and f' .

4. — Reconstruction of a point object from a reprojection of the photographs: approximate procedure.

Suppose that both pictures are reprojected simultaneously onto a plane Σ , parallel to the plane of the film, with a reference system as shown in Fig. 3. U and U' are the projections of Q and Q' : the length $l = kl$ of the segment UU' is also the separation of the optic axes in the re-projection: A_2 and A'_2 are the projections of A_1 and A'_1 , and X and Y the coordinates of A_2 . In the known approximation the segment $A_2A'_2$, whose length will be indicated by ξ , is parallel to the abscissa.

Let j be the magnification in the re-projection: A'_2 will be to the left of, coincident with, or to the right of A_2 according to whether k is less than, equal to, or greater than $(i \cdot j)$; Fig. 3 represents the case of $k > (i \cdot j)$.

Calling \bar{A} the intersection of UA_2 and $U'A'_2$, with coordinates X and Y , one has at once:

$$(9) \quad \begin{cases} x = \frac{X}{k} - \frac{Xl}{kl - \xi}, \\ y = \frac{Y}{k} - \frac{Yl}{kl - \xi}. \end{cases}$$

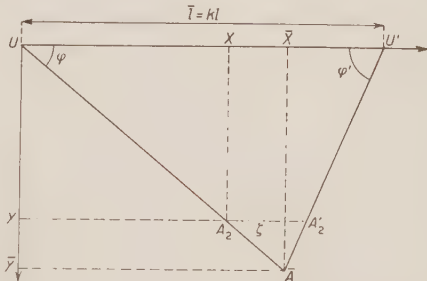


Fig. 3. — Plane Σ . Reprojection of a point A .

⁽¹⁾ P. M. S. BLACKETT: *Proc. Roy. Soc., 154*, 573 (1936).

Note that to obtain the exact values of x and y it is not necessary to know i and j : it is sufficient to know k .

It is further to be noted that $r = \bar{U}\bar{A}/k$, $\varrho = UA_2/j$ so that $r/\varrho = j/k$, $U\bar{A}/UA_2 = jl/(kl - \zeta)$ and finally, by substituting in (6)

$$(10) \quad z \cong n \left(f \frac{jl}{kl - \zeta} - d - \frac{\delta}{n^*} \right).$$

For $k = (i \times j)$, as $A_2 = A'_2 = \bar{A}$, then $x = X/k$, $y = Y/k$ and formula (10) reduces to $z \cong n((fj/k) - d - (\delta/n^*))$.

For $k < (i \times j)$ formula (9) and (10) are still valid if one changes the sign of ζ .

A second approximation for z may also be used. The first approximation (10) may be written

$$z = K \frac{1}{1 - (\zeta/k)} - K',$$

where $K = nj/k$ and $K' = n(d + \delta/n^*)$, which may be expanded as

$$z = K \left(1 + \frac{\zeta}{kl} + \frac{\zeta^2}{k^2 l^2} + \frac{\zeta^3}{k^3 l^3} + \dots \right) - K',$$

where

$$h = \frac{nij}{k^2 l} = \frac{n}{kl} \left(d + \frac{\delta}{n^*} \right) \quad \text{and} \quad h' = K - K' = n \left(\frac{fj}{k} - d - \frac{\delta}{n^*} \right).$$

In the appendix, for simplicity's sake, we have used, neglecting in the expansion the terms of order higher than the first,

$$(11) \quad z \cong h\zeta + h'$$

* * *

One of us (J.A.M.) wishes to acknowledge a grant from the Conselho Nacional de Pesquisas (Brazil).

APPENDIX

Normal procedures allow one to arrive at a measurement of any geometrical element from the coordinates of the points which define it: occasionally calculating machines could be employed to elaborate the various items of information such as cartesian coordinates and angles: to speed up even more the work automatic systems (converters) could be used to feed the information directly into the machine. It will be seen, case by case, if it is more convenient to examine the photographs directly or to reproject them.

Sometimes it will be more convenient to renounce the method of reconstruction by points in favour of some other procedure of a synthetic character: three examples follow, based on the reprojection of the photographs.

1. – Direction of a straight line in space and the use Wulff's Disc.

Let A and B be two points of a straight line b in the object space: let A' be the distance between them. Projecting from U and U' the images of these points, one obtains (Fig. 4) A and B , whose coordinates with respect to the $X'Y$ system are, as has been shown, proportional to the real values x and y .

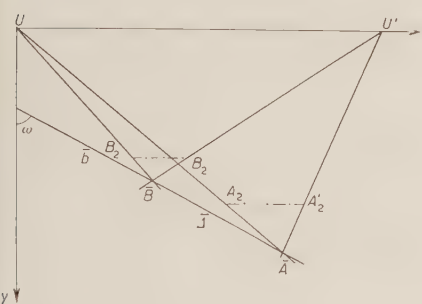


Fig. 4. – Plane Σ . Azimuth of a straight line b . Direct construction from the images of two points.

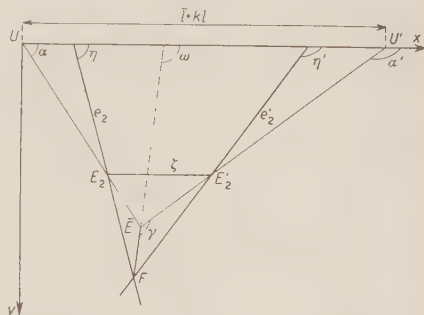


Fig. 5. – Plane Σ . Dip and azimuth of a straight line from the azimuth of its reprojected images.

The angle ω which the straight line \bar{b} makes with the X axis is then the azimuth of b with respect to the x axis when one takes z as the polar axis. The dip with respect to the xy plane, which we will indicate with ε , is the complement of the zenith angle in the same reference system. The coordinate z of any point is a function of ζ given, according to the required approximation, by formula (10) or (11). Making use of (11) one has

$$\varepsilon = \operatorname{tg}^{-1} \frac{hk(\zeta_B - \zeta_A)}{\bar{l}}.$$

It is also possible to calculate ω and ε from the azimuth of the reprojected images of the straight line and from the angular coordinates of the projected images of any of its points: these angles are represented respectively with η , η' and α , α' in Fig. 5.

One has

$$(E'_2 \bar{E}) = \frac{\zeta(U' \bar{E})}{kl} = \frac{\zeta \sin \alpha}{\sin(\alpha' - \alpha)},$$

and

$$(E'_2 F) = \frac{\zeta \sin \eta}{\sin(\eta' - \eta)},$$

from which

$$(EF) = \zeta g^{\frac{1}{2}},$$

where

$$g(\eta, \eta', \alpha, \alpha') = \frac{\sin^2 \alpha}{\sin^2 (\alpha' - \alpha)} + \frac{\sin^2 \eta}{\sin^2 (\eta' - \eta)} - 2 \frac{\sin \alpha \sin \eta \cos (\alpha' - \eta')}{\sin (\alpha' - \alpha) \sin (\eta' - \eta)}.$$

Using formula (11) one obtains

$$\varepsilon = \operatorname{tg}^{-1} h k g^{-\frac{1}{2}}.$$

One has further

$$\omega = \alpha' + \gamma - 180^\circ,$$

but

$$\sin \gamma = \frac{(E'_2 F) \sin (\alpha' - \eta')}{E F},$$

and finally

$$\omega = \alpha' + \sin^{-1} \frac{\sin \eta \sin (\alpha' - \eta') g^{-\frac{1}{2}}}{\sin (\eta' - \eta)} - 180^\circ.$$

A knowledge of the angles ω and ε for the lines concerned, is sufficient for resolving rapidly various problems of spherical geometry with the aid of a stereographic projection which maintains the angles (Wulff's disc).

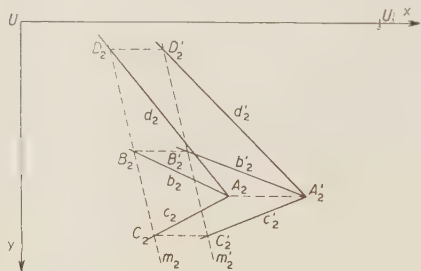


Fig. 6. — Plane Σ . Coplanarity test.

fixes the plane. It then follows that if B_2 and B'_2 are the images of a point B on b , while C_2 and C'_2 are the two images having the same separation of the point C on c , then the intersection D_2 of d_2 with m_2 must be equally separated from the intersection D'_2 of d'_2 with m'_2 : m_2 and m'_2 are obviously the images of m , the intersection of the plane bcd with that selected for the test.

2. — Coplanarity test.

Let A be a point in the object space which is common to the three straight lines b, c, d . In the reprojection (Fig. 6) there will be two distinct images, one from each objective. If the lines b, c, d are coplanar, their intersections with a plane will be in line: in the particular case of a plane normal to the z axis these intersections must give pairs of images with constant separation z , depending only on the value of z which

3. — Momentum of a particle crossing a magnetic field.

Referring to the preceding considerations concerning the geometrical layout, let us now suppose the presence of a uniform magnetic field H , parallel to the z axis.

A particle of momentum p will describe an arc of a helix wound on a cylinder parallel to z of radius

$$R_c = \frac{p \cos \varepsilon}{300H},$$

where ε is the dip of the tangent to the arc with respect to the xy plane; R_c is in cm if P is measured in eV/c and H in gauss.

An arc of a helix, which is small in comparison with R_c , practically lies on the osculating plane passing through its mid-point M and can be considered as a circular arc with radius

$$R = \frac{p}{300H \cos \varepsilon}.$$

Let us suppose that this arc ends at points A and B and let us call σ the sagitta. It is well known that if $\sigma \ll R$ then one may put

$$R = \frac{l^2}{8\sigma}.$$

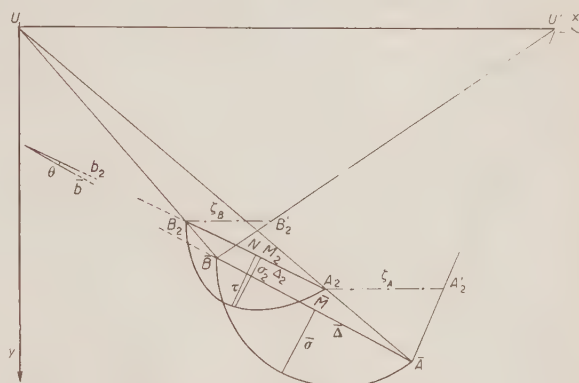


Fig. 7. — Plane Σ . Reprojection of a cylindrical helix.

In Fig. 7 the significance of the arc of circle which joins A and B is obvious; the curve A_2B_2 is the image obtained by reprojection through the left hand objective. Since the sagitta lies in a plane normal to the z axis, σ_2 is parallel to σ and one has simply,

$$\sigma = \frac{l}{kl - \zeta_M} \sigma_2.$$

In this paragraph let us use approximation (11): then

$$\zeta_M = \frac{\zeta_A + \zeta_B}{2}.$$

The chord A_2 , instead, undergoes an apparent rotation θ about the z axis, which we can measure directly in the reprojection as the angle between b_2 and \bar{b} .

We now approximate the curve A_2B_2 to an arc of a circle and indicate with τ its sagitta, i.e. the length of the segment of the perpendicular to A_2 from its mid-point N onto the curve.

For the apparent radius \mathcal{R} , which may be measured by direct comparison of the curve A_2B_2 with standard calibrated circular arcs we have

$$\mathcal{R} = \frac{A_2^2}{8\tau}.$$

The separation between N and the image M_2 of M is small, so that with good approximation $\tau = \sigma_2 \cos \theta$.

One then has

$$R = \mathcal{R} \frac{kl - \zeta_M}{l} \frac{\Delta^2}{\Delta_2^2} \cos \theta .$$

Since

$$\Delta^2 = \frac{\Delta^2}{k^2} + h^2(\zeta_B - \zeta_A)^2 ,$$

and

$$\cos \varepsilon = \bar{A}[\bar{A}^2 + h^2 k^2 (\zeta_B - \zeta_A)^2]^{-\frac{1}{2}} ,$$

one finally obtains for the momentum the expression

$$p = 300H\mathcal{R} \left(k - \frac{\zeta_A + \zeta_B}{2l} \right) \frac{\bar{A}[\bar{A}^2 + h^2 k^2 (\zeta_B - \zeta_A)^2]^{\frac{1}{2}}}{k^2 \Delta_2^2} \cos \theta .$$

The same procedure may be applied to the right hand image in order to decrease the error by taking into account both results.

RIASSUNTO

Si espongono un metodo esatto ed altri approssimati per ricostruire da due fotografie, prese ad assi ottici paralleli, la posizione di un punto interno ad una camera a bolle. In appendice si esamina come risalire direttamente alla direzione di una retta nello spazio ed alla curvatura di un arco di elica cilindrica con asse parallelo agli assi ottici.

Accuracy Limits in the Measurement of Time Intervals Defined by Scintillation Counter Pulses.

S. COLOMBO (*), E. GATTI and M. PIGNANELLI (+)

Laboratori CISE e Politecnico - Milano

(ricevuto il 17 Aprile 1957)

Summary. — Accuracy limits of the time of occurrence of an event detected by a scintillation counter are investigated. Two methods «non linear» and «linear» for extracting time information from the output current pulse of the photomultiplier are compared taking into account statistics of photoelectron emission, transit time and multiplication spread in the phototube and finite width of the response of the phototube to one photoelectron. Resolution obtained by the «non linear» method is better, but linear method dispenses from an amplitude selection of pulses.

1. — Introduction.

A method was introduced ⁽¹⁾ and an instrument described ⁽²⁾ for the measurement of time intervals defined by means of the output pulses of two scintillation counters.

The theoretical analysis of the maximum resolutive powers obtainable on the basis of scintillator and phototube properties induced us to analyse the problem in its general aspect and permitted us to determine the resolution limit and the factors for the choice of the two proposed methods (non linear and linear) in utilizing the pulses at the output of the phototube.

We have to estimate the accuracy with which we can evaluate the time position of the interaction between a charged particle and the sensitive element of a scintillation counter. For this purpose, the chain of processes that lead to the detection of the particle is given ⁽³⁾:

(*) Politecnico di Milano, now Agip Nucleare.

(+) Istituto Nazionale di Fisica Nucleare, Sezione di Milano.

(1) C. COTTINI, E. GATTI and G. GIANNELLI: *Nuovo Cimento*, **4**, 156 (1956).

(2) C. COTTINI and E. GATTI: *Nuovo Cimento*, **4**, 1550 (1956).

(3) E. BALDINGER and W. FRANZEN: *Advances in Electronics and electron physics*, vol. VIII (New York, 1956).

- 1) Slowdown in the scintillator and excitation of optically active states or direct emission of photons by Čerenkov effect.
- 2) Decay of the excited states and consequent emission of light.
- 3) Collection of light.
- 4) Emission of photoelectrons by the photocathode of the phototube.
- 5) Formation of the electronic cascade (avalanche).
- 6) Processing the output current pulse of the phototube, by mean of a suitable electronic instrument.

We shall overlook the details of the processes 1), 2), 3) and take into account only their influence through the photocathode illumination function $I(t)$ which may be considered as continuous function of time (a justified approximation as far a photoelectron emission is concerned) considering the low photoelectronic yield of 5-10%.

It is assumed therefore that the photoelectron emission, following a given illumination, obey the Poisson distribution. The illumination can be normalized so that:

$$\int_0^{\infty} I(t) dt = R ,$$

where R is the average number of electrons emitted as a consequence of a scintillation.

As far as concerns point 5) the essential properties of the electronic photomultiplier are taken into account by indicating the response to a photoelectron emitted by the photocathode as follows:

$$(1) \quad U(t) = Af(t + h) ,$$

where A is the gain of the phototube characterized by the average value A and by a relative root-mean square error ε_A .

The variance ε_A^2 is due to a fluctuation in the amplification of individual photoelectrons (mainly due to multiplication on the first dynode) which is supposed (4,5) equal to

$$(2) \quad \varepsilon_A^2 = \frac{1}{g - 1} ,$$

where g is the secondary emission factor, considered to be equal for all dynodes.

The function $f(t)$ characterizes the pulse form which is so normalized as:

$$\int_0^{\infty} f(t) dt = 1 .$$

(4) J. SHARPE: *Nuclear Radiation Detectors* (London, 1955), p. 104.

(5) G. A. MORTON: *Proceedings Geneva Conference*, vol. XIV, p. 255.

To this shape is assigned the width λ^2 , defined as a second moment

$$\lambda^2 = \int_0^\infty (t - a)^2 \cdot f(t) dt ,$$

where a is the center of gravity of $f(t)$. It can be assumed that this width is given by

$$(3) \quad \lambda^2 = (n - 1)\varepsilon_{dd}^2 ,$$

where n is the number of dynodes, and ε_{dd} the root mean square error in the transit time between two successive dynodes.

h is a statistical variable having the time dimension with an average value 0 and r.m.s. error ε_{ph} . This variable accounts for a fluctuation in the time interval between the instant of emission of the photoelectron and the instant in which the center of gravity of the current pulse, due to a photo-electron, arrives at the output.

It may be supposed that these fluctuations are due mainly to the transit between the cathode and the first dynode. They will be taken into account by attributing to h the variance:

$$(4) \quad \varepsilon_{ph}^2 = \varepsilon_{dd}^2 + \frac{\varepsilon_{dd}^2}{g - 1} ,$$

where ε_{dd} is the r.m.s. error in the transit time of a photoelectron between cathode and first dynode.

No statistic fluctuation has been considered for the shape of the pulse following a photoelectron. Moreover no non-linearity due to space charge saturation has been considered.

Now (point 6) let us introduce a scheme of the electronic instrument, that will help to determine precisely, as far as «seen» by the instrument itself, the occurrence time of a current pulse $i(t)$ from the photomultiplier. In connection with the quoted instrument (1), we suppose that the output current of the phototube $i(t)$ is integrated on the output capacity of the phototube itself, paralleled to the input capacity of an electronic sharp cut-off tube and that the relationship between the input voltage and the anodic current I_a of the tube is linear until the cut-off is reached.

The anode current is applied to an high Q resonant circuit having a period larger than t_i , which is the time spent to bring the tube to cut-off.

For $t < t_i$, the anode current I_a will be

$$I_a(t) = K \int_0^t i(t') dt' ,$$

t , being the time necessary to bring the tube to cut-off through the accumulation of charge $C(t_i)$, while for $t > t_i$, the anodic current is a constant $KC(t_i)$.

If I_a is this function and $I_a(p)$ his Laplace transform, the voltage at the

terminals of the resonant circuit is:

$$(5) \quad V(p) = Z(p)I_a(p) = Z(p) \frac{1}{p} \bar{i}(p),$$

where $\bar{i}(p)$ is the transform of $i(t)$, i.e. of $i(t)$ considered = 0 for $t > t_i$ and $Z(p)$ is the impedance of the resonant circuit.

From equation (5) it can be concluded that, except for a constant, the phase of the oscillation $V(t)$, which is equal to $\arg V(j\omega)$, is equal to $\arg \bar{i}(j\omega)$.

If we suppose that the instrument is sensitive to the oscillation phase considered at an instant t^* given by an external time reference, we see that it registers the arrival of pulse $i(t)$ at a time μ equal to:

$$(6) \quad \mu = \frac{1}{\omega} \arg \bar{i}(j\omega).$$

If, for the time being, $\bar{i}(p)$ is so normalized as

$$\int_0^\infty \bar{i}(t) dt = 1,$$

$\bar{i}(p)$ can be written as follows:

$$(7) \quad \bar{i}(p) = 1 - p \int_0^\infty t \bar{i}(t) dt + \frac{p^2}{2} \int_0^\infty t^2 \bar{i}(t) dt - \dots.$$

Moreover, if the period corresponding to the angular frequency ω of the resonant circuit is long with respect to the duration of pulse $i(t)$, it can be concluded from (7) that:

$$(8) \quad \arg \bar{i}(j\omega) = \omega \int_0^\infty t \bar{i}(t) dt.$$

Therefore the « machine time » is the center of gravity of current pulse $\bar{i}(t)$. For such scheme the problem is therefore reduced to that of determining the variance in position of the center of gravity of current pulse $i(t)$ following a scintillation (*). This method of working will be called briefly « non linear ».

Further on we shall deal with the case where cut-off charge $C(t_i)$ is never

(*) It has been tacitly assumed that the phase is measurable with a negligible error: this was experimentally proved (2).

reached. This method of working will be called «linear» and, in that case, instead of $i(t)$, the whole pulse $i(t)$ will be used for the purpose of measurement.

The introduction of a fixed variable (center of gravity of $i(t)$ or $\bar{i}(t)$) to which the instrument is sensitive, permits the straightforward deduction from the statistic properties of photoelectron emission and electronic multiplication in the phototube⁽⁶⁻⁸⁾ of the variance of the machine time, taking also into account the finite width of the pulse following each photoelectron.

The shape of the average pulse resulting from a scintillation due to a finite pulse width of the phototube response has been considered by LEWIS and WELLS⁽¹⁰⁾ but the statistic implications have not been dealt with.

2. - Resolution in an ideal case of non-linear working.

An ideal photomultiplier is considered giving the following output pulse

$$V(t) = A \cdot \delta(t),$$

for a photoelectron emitted at its cathode, where A is a constant and $\delta(t)$ is the Dirac function.

Under such hypothesis it will be enough to determine the variance in the center of gravity of the first Q photoelectrons in order to have the measurement of the statistical dispersion introduced by one of the two measurement channels. Q is the charge necessary to cut off the electronic tube. It should be further supposed that the law of illumination is constant in time (in other words, the electronic tube is cut off in a time short in comparison with the duration of the scintillation).

If f is the average emission frequency of the photoelectrons and hence $\exp[-ft]$ is the probability of finding at time t the first photoelectron, the position of the center of gravity of the first Q photoelectrons (see calculation in Appendix I) is:

$$\frac{1}{f} \frac{Q+1}{2},$$

and its variance

$$(9) \quad \frac{1}{f^2} \left(\frac{1}{3} Q + \frac{1}{2} + \frac{1}{6Q} \right).$$

If we suppose the average frequency f being equal to the initial one due to a scintillation corresponding to an illumination $I(t) = (R/\tau) \exp[-t/\tau]$ in

⁽⁶⁾ R. F. POST and L. I. SHIFF: *Phys. Rev.*, **80**, 1113 (1950).

⁽⁷⁾ G. A. MORTON: *Nucleonics*, **10**, no. 3, 39 (1952).

⁽⁸⁾ G. H. MINTON: *Journ. of Research of the National Bureau of Standards*, **57**, no. 3, Sept. 1956.

⁽⁹⁾ Z. BAY, V. P. HENRY and H. KANNER: *Phys. Rev.*, **100**, 1197 (1955).

⁽¹⁰⁾ I. A. D. LEWIS and F. H. WELLS: *Millimicrosecond Pulse Techniques* (London, 1954).

which R electrons are totally emitted with a decay constant τ , we obtain for the variance:

$$(10) \quad \varepsilon_{c, em}^2 = \frac{1}{3} \frac{\tau^2 Q}{R^2} \left[1 + \frac{3}{2} \frac{1}{Q} + \frac{1}{2} \frac{1}{Q^2} \right].$$

Formula (10) corresponds to the expression

$$\frac{1}{2} \frac{\tau^2 Q}{R^2} \left(1 + \frac{1}{Q} \right),$$

which is, according to our notation and the uniform illumination hypothesis, the one given by MINTON (*) at the beginning of p. 124 of the quoted paper.

This expression is obtained by Minton by taking the arithmetic average of the variances of emission time of the first, second ... Q -th photoelectron.

It is now supposed that the photomultiplier introduces a fluctuation of variance ε_{ph}^2 in the delay between the output pulse and a photoelectron causing it.

If $t_1, t_2 \dots t_Q$ are the emission times for 1st, 2nd ... Q th photoelectron, each of these times will be affected, by reason of the phototube, by a variance ε_{ph}^2 . Consequently the center of gravity, which is the average of $t_1, t_2 \dots t_Q$, will have a variance, due to this cause, equal to

$$(11) \quad \varepsilon_{c, ph}^2 = \frac{\varepsilon_{ph}^2}{Q}.$$

Leaving this simple case, we will now face the problem from such point of view that permits hypotheses more in accord with actual physical behaviour at the expense of some approximations of mathematical character.

3. - Resolution in the case of non-linear working.

A general law of illumination $I(t)$ of the photocathode is considered, while for the photomultiplier a response $V(t) = Af(t + h)$ is considered according to the observations at the introduction.

In the absence of statistical fluctuations, $i(t)$ would be given by

$$\underline{i}(t) = I(t) * f(t).$$

A statistical fluctuation corresponding either to ΔK electrons emitted in addition to the average in the time between σ and $\sigma + \Delta\sigma$ or to an amplification $A(1 + \Delta K)$ relatively greater by ΔK than the average one for a certain electron emitted at time σ , brings the current to

$$i(t) = I(t) * f(t) + \Delta K f(t - \sigma).$$

The disturbance considered (to the purpose of reasoning ΔK positive) has a double effect on the « machine variable » (for a more exact deduction,

reference is to be made to Appendix II): a direct effect due to the displacement of the center of gravity resulting from the presence of the disturbance current which, between σ and t_i , is different from zero, and an indirect effect due to the displacement of the cut-off time t_i ; t_i is actually shorter because the charge $C(t_i)$ necessary to the cut-off is also reached by the contribution of the charge due to the disturbance current in the time interval between σ and t_i .

In fact, for the variance of the center of gravity, due to the statistic of the emission and of the gain A , we obtain by means of the procedure reported in Appendix II:

$$(12) \quad \varepsilon_{c, \text{em}, A}^2 = (1 + \varepsilon_A^2) \frac{\left[\int_0^{t_i} dt \int_0^t f(t) dt \right]^2 * I(t_i)}{\left[\int_0^{t_i} i(t) dt \right]^2} .$$

By a similar calculation (Appendix III) the variance of the center of gravity due to the fluctuations in the mean transit times characterized by the variance $\varepsilon_{\text{ph}}^2$ is:

$$(13) \quad \varepsilon_{c, \text{ph}}^2 = \varepsilon_{\text{ph}}^2 \frac{\left[\int_0^{t_i} f(t) dt \right]^2 * I(t_i)}{\left[\int_0^{t_i} i(t) dt \right]^2} ,$$

and finally, by summing up the variances due to the various effects studied, we obtain:

$$(14) \quad \varepsilon_c^2 = \frac{(1 + \varepsilon_A^2) \left[\int_0^{t_i} dt \int_0^t f(t) dt \right]^2 * I(t_i) + \varepsilon_{\text{ph}}^2 \left[\int_0^{t_i} f(t) dt \right]^2 * I(t_i)}{\left[\int_0^{t_i} i(t) dt \right]^2} .$$

By means of (14) ε_c^2 is expressed as a function of t_i but for the purpose of experimental comparison ε_c^2 must be expressed in terms of $C(t_i)$, that is the charge necessary for the cut-off.

C is a function of t_i and its average value is:

$$(15) \quad C(t_i) = \int_0^{t_i} [I(t) * f(t)] dt .$$

Between (14) and (15), t_i can be eliminated and ε_c^2 can be expressed as a function of $C(t_i)$.

For the sake of simplicity, we have assumed in the numerical calculations an illumination

$$I(t) = \frac{R}{\tau} \exp \left[-\frac{t}{\tau} \right] ,$$

and a phototube « response »

$$f(t) = \frac{\sqrt{5}}{\lambda} \left\{ \exp \left[- \frac{\sqrt{5}}{2\lambda} t \right] - \exp \left[- \frac{\sqrt{5}}{\lambda} t \right] \right\},$$

though a function of type

$$\frac{\sqrt{m}}{\lambda m!} \left(\sqrt{m} \frac{t}{\lambda} \right)^m \exp \left[- \sqrt{m} \frac{t}{\lambda} \right],$$

would have been more in line with the real response of the phototube.

In Figs. 1 and 2, $\varepsilon_{e, em, A}^2$ and $\varepsilon_{e, ph}^2$ are shown as functions of C/R and in Figs. 3 and 4 as functions of Q/R where Q is the number of photoelectrons emitted at the cathode up to the time t_i .

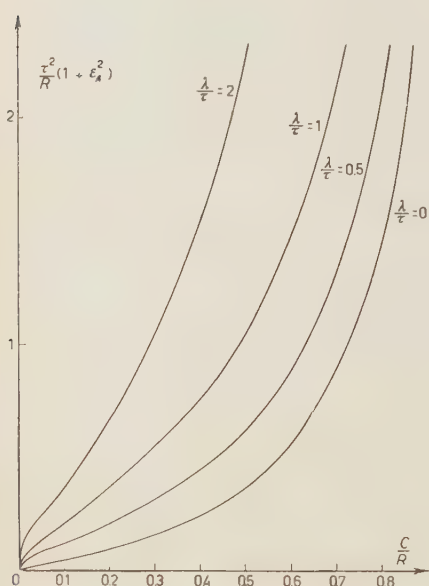


Fig. 1. « Machine time » variance due to emission and amplification statistics versus the ratio of cut off charge C to total charge R .

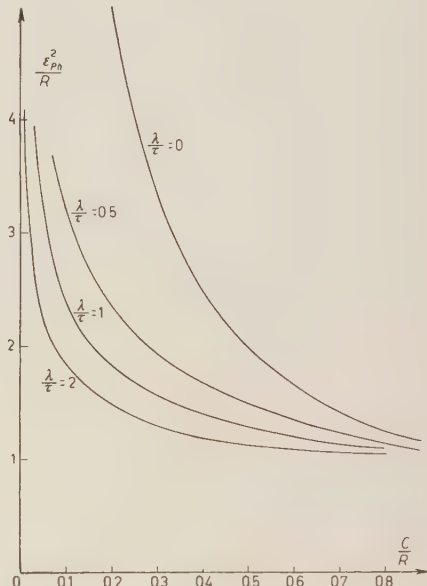


Fig. 2. — « Machine time » variance due to average transit time variance ε_{ph}^2 versus the ratio of cut off charge C to total charge R .

In Fig. 5 the relation between C/R and t/τ is shown, while Fig. 6 shows the relation between C/R and Q/R .

From equation (15) we note that when $t_i = 0$, also $C = 0$, but when $C = 0$ the instrument is affected at least by the variance due to the statistical emission of the first photoelectron and therefore ε_e^2 instead of 0, is equal to τ^2/R^2 .

By this consideration (12) can be corrected to be

$$(16) \quad \varepsilon_{c, em, A}^2 = \frac{\tau^2}{R^2} + (1 + \varepsilon_A^2) \frac{\left[\int_0^{t_i} dt \int_0^t f(t) dt \right]^2 * I(t_i)}{\left[\int_0^{t_i} f(t) dt \right]^2} .$$

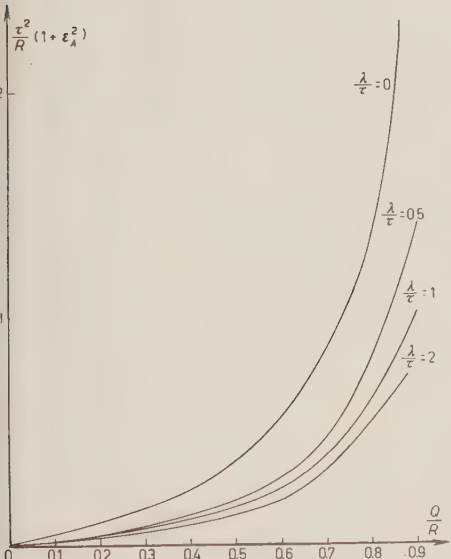


Fig. 3. — « Machine time » variance due to emission and amplification statistics versus the ratio of the Q photoelectrons emitted until t_i , to the R photoelectrons totally emitted.

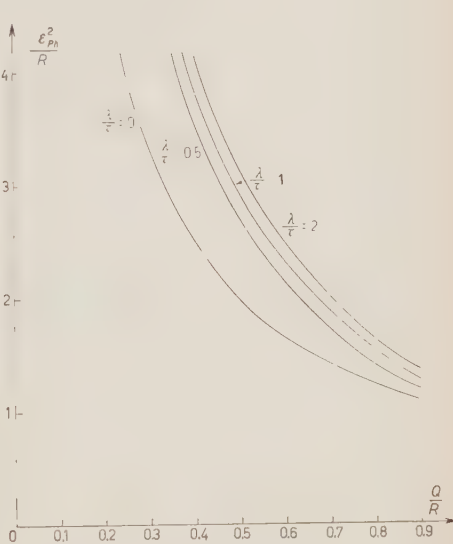


Fig. 4. — « Machine time » variance due to average transit time variance ε_{ph}^2 versus the ratio of the Q photoelectrons emitted until t_i , to the R photoelectrons totally emitted.

In Appendix IV the formula (16) is evaluated in the hypothesis that led to (10): by comparison it is clear that the approximation made in deducing (16) have not led to significant errors.

Apart from the statistical fluctuations, the position of the center of gravity varies with the variations of C/R and hence, once C is fixed at a certain working condition, depends from R or, actually, from the amplitude of the pulses accepted: working with the non-linear method, this dependence imposes a selection, by means of slow measurement channels, of a limited amplitude band for the accepted pulses. This necessity is what has conducted to the development of the so called fast-slow coincidences.

This dependence of « machine time » on C/R can be evaluated easily by

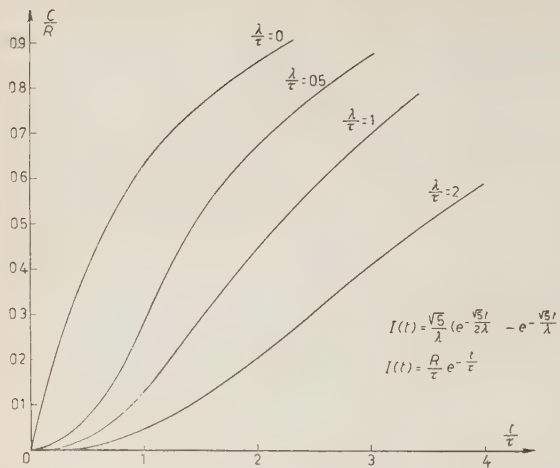
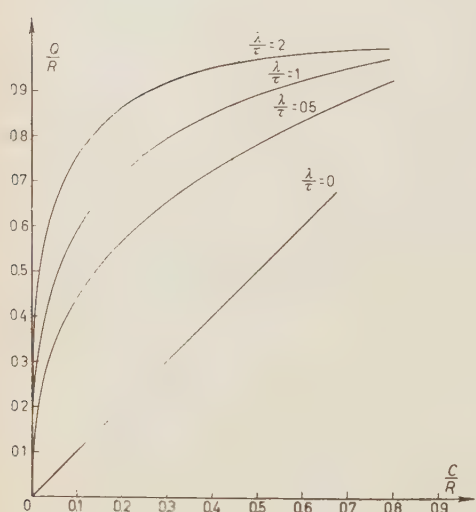


Fig. 5. - Charge collected versus time.

by possible irregularity in the illumination function due for instance to possible differences in the decay time between different points of the scintillator.

Fig. 6. - Charge collected versus number of photoelectrons emitted with phototube response « width » λ as parameter.

eliminating t_i from:

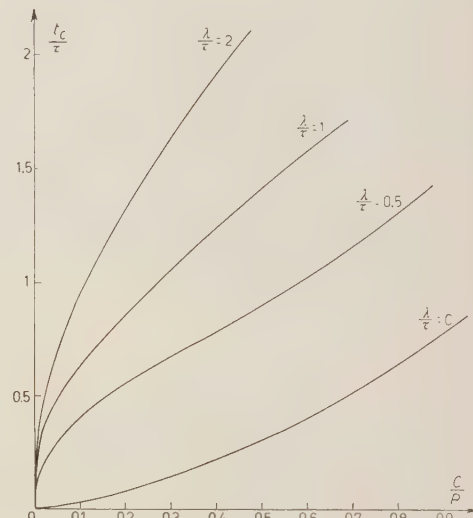
$$t_c = \frac{\int_0^{t_i} i(t) dt}{\int_0^{t_i} i(t) dt},$$

and

$$C(t_i) = \int_0^{t_i} i(t) dt.$$

The results of this calculation are reported graphically in Fig. 7.

No evaluation has been made of the errors caused

Fig. 7. - « Machine time » dependence from pulse height R .

4. – Resolution in the case of ballistic linear working.

In the case of «ballistic linear working», in which the total pulse of the current from the phototube is impressed on the oscillating circuit, possibly by means of a linear amplifier though not necessarily very fast, the calculations are particularly simple because there is no more need to introduce the «response» $f(t)$ of the phototube with finite width but it is enough to consider a response $A\delta(t+h)$ with h affected by a variance ε_{ph}^2 and A by a variance ε_A^2 .

Moreover a disturbance for example in the form of an additional electron emitted between σ and $\sigma + \Delta\sigma$ does no more than displace the center of gravity by its very presence. For details of calculation we refer to Appendix V. For the variance ε_c^2 we obtain:

$$\varepsilon_c^2 = \frac{1}{R} \left[(1 + \varepsilon_A^2) \frac{1}{R} \int_0^\infty (\sigma - t)^2 I(\sigma) d\sigma + \varepsilon_{ph}^2 \right],$$

and in accordance with the hypothesis of an illumination law given by

$$I(t) = \frac{R}{\tau} \exp \left| -\frac{|t|}{\tau} \right|,$$

we obtain

$$(17) \quad \varepsilon_c^2 = \frac{\varepsilon_{ph}^2 + \tau^2(1 - \varepsilon_A^2)}{R}.$$

5. Resolution in the case of non-ballistic linear working.

It will be interesting to see now how (17) is modified when the period T of the resonant circuit can no longer be considered long enough with respect to the duration of the phototube pulse. In this case the «machine variable» is defined with reference to (6) by:

$$\mu = \frac{1}{\omega} \arg i(j\omega),$$

and therefore it would be necessary to consider again the phototube response $f(t)$ of «finite width». However, only the case where $i(t)$ can be confused with the illumination law $I(t)$ was studied, since in the linear case the total pulse is considered and not only its first part; this does not seem to lead to substantial differences in the evaluation of the «machine variable» variances.

We obtain (referring to Appendix VI):

$$(18) \quad \varepsilon_c^2 = \frac{\tau^2}{R} (1 + \varepsilon_A^2) \frac{1 + 2\omega^2\tau^2}{1 + 4\omega^2\tau^2} + \frac{\varepsilon_{ph}^2}{R} \left(1 + \frac{2\omega^4\tau^4}{1 + 4\omega^2\tau^2} \right).$$

It is physically reasonable that, with the increase in ω , a decrease takes place in the variance due to the emission statistics and to the variance in amplification, as an appreciable number of contributions to the output current, that have greater variance, take place at a time when they excite the resonant current with an almost opposite phase to that determined by the first photoelectrons and therefore have little weight in altering the resulting oscillation phase. Conversely, the little effect that a few photoelectrons have in determining the final phase is such that the error due to transit times is increased.

Finally it is noteworthy that the linear working does not introduce any systematic change in the position of « machine time » with the change in the scintillation amplitude.

6. – Conclusions.

From Fig. 1 it can be pointed out that the variance $\varepsilon_{c,em,A}^2$, which increases linearly with C/R , for small C/R , in the case of narrow width of the phototube response ($\lambda \rightarrow 0$) increases more rapidly when the response width λ increases. This is noticed by observing Fig. 6 which shows that large response widths are corresponded by high Q/R even with relatively small C/R .

Opposite behaviour is seen in Fig. 2 for $\varepsilon_{c,ph}^2$: this variance diminishes, C/R being constant, with the increase of λ , because the number of photoelectrons, of which transit times are averaged, though with different weights, is increased.

The total value of « the machine time » variance ε_c^2 which is related to the value observable as a width of line $W_{\frac{1}{2}}$ in a coincidence experiment ($W_{\frac{1}{2}} = \sqrt{2} \cdot 2.56 \cdot \varepsilon_c$, where $\sqrt{2}$ is introduced in order to take into account the presence of the two measurement channels) is obtained by adding the ordinates of the graphs in Figs. 1 and 2, taking into consideration the scale values determined by τ , ε_A , ε_{ph} .

The value $1/3$ was assumed for ε_A^2 , substituting $g = (4)$ in equation (2).

In Figs. 8 and 9 the graphs of ε_c^2 , having taken the respective values of 6 and 2 for τ/ε_{ph} , are shown. These values have been chosen by assigning, in accordance with (4), the value $\varepsilon_{ph} = 5 \cdot 10^{-1}$ s for the phototube RCA 6342, and $3 \cdot 10^{-9}$ s, which is the characteristic decay time of the faster organic scintillators, for τ .

From the examination of Fig. 8 and 9 it may be concluded that by considering all the parameters except λ to be fixed, the minimum value of $\varepsilon_c^2(\tau\varepsilon_{ph} R)$ does not change appreciably; only the value C/R , corresponding to the very wide minima observed, changes. Physically, this means that, with phototubes having equal geometry and working conditions between cathode and first dynode but having different λ (due for example to different geometry and working conditions of the successive multiplying dynodes) the maximum resolution obtainable does not change appreciably. The value of the minima calculated can be approximated by the formula

$$(19) \quad \varepsilon_c^2 = \sqrt{\frac{4}{3}(1 + \varepsilon_A^2)} \frac{\tau\varepsilon_{ph}}{R},$$

which is calculated from (14) with the hypothesis of constant illumination R/τ

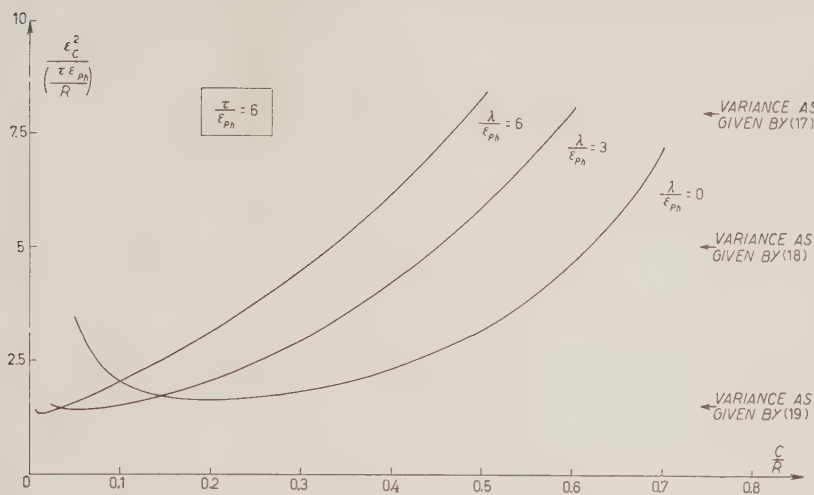


Fig. 8. - « Machine time » variance for definite $\tau/\epsilon_{ph} = 6$ versus C/R . The arrows at the right give, respectively from top to bottom, the variance calculated for the ballistic linear working, for the linear working with $\omega\tau = 1$ and the variance as given by the rough formula (19).

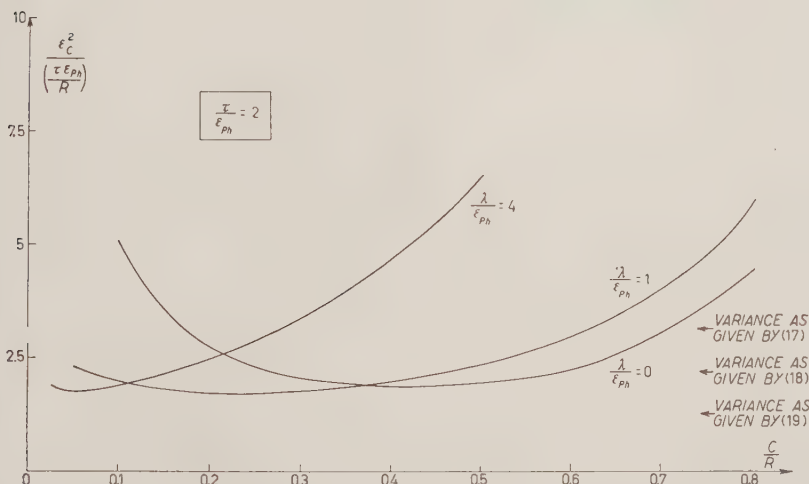


Fig. 9. - « Machine time » variance for definite $\tau/\epsilon_{ph} = 2$ versus C/R . The arrows at the right give, respectively from top to bottom, the variances calculated for the ballistic linear working, for the linear working with $\omega\tau = 1$, and the variance as given by the rough formula (19).

and zero width of $f(t)$ ($\lambda = 0$). The (14) gives:

$$\varepsilon_{c,\text{em},A,\text{ph}}^2 = \frac{1}{3} \frac{\tau^2 Q}{R^2} (1 + \varepsilon_A^2) + \frac{\varepsilon_{\text{ph}}^2}{Q},$$

and its minimum (19) is obtained for

$$R = \sqrt{\frac{3}{1 + \varepsilon_A^2}} \frac{\varepsilon_{\text{ph}}}{\tau}.$$

The value $\lambda \varepsilon_{\text{ph}}$ of the parameter appearing in Figs. 8 and 9, is given, recalling (3) and (4), by:

$$\left| \frac{(n-1)(g-1)}{1 + (g-1)\alpha^2} \right|^{\frac{1}{2}},$$

where: $\alpha = \varepsilon_{\text{at}}/\varepsilon_{\text{ld}}$,

Assuming that $n = 10$ and $g = 4$, and assigning to α a value range of 0.5 to 2 we see that parameter $\lambda \varepsilon_{\text{ph}}$ varies in the range between 4 to 1.5.

A larger width λ of $f(t)$ should be compensated by a greater amplification, since the minimum of the curve of Figs. 8 and 9 is obtained from lower values of $C R$. These broad minima however show that the working conditions for $C R$ are not critical for obtaining the « machine time » minimum variance.

It is interesting to observe that the introduction of an amplifier between phototube and cut-off tube can be considered as equivalent to an increase of the width λ characteristic of the phototube, and therefore it seems possible to affirm that the introduction of a fast amplifier does not reduce the resolving power.

The curves of Fig. 7 permit us to find, at certain non-linear working conditions, the width admissible in the amplitude of the band of the accepted pulses, so as not to exceed assigned limits of the systematic error caused by the dependence of the « machine time » on R .

In Figs. 8 and 9 are shown the values for ballistic working and for linear working with $\omega \tau = 1$.

On the whole, the linear method introduces greater variance with respect to that encountered with the non-linear method (greater to a negligible extent for rather small $\tau \varepsilon_{\text{ph}}$) but it also offers the advantage of not presenting any systematic error dependent on the amplitude of the pulses in question. For this reason the linear method is advisable where very fast scintillators or Čerenkov light are used, or when it is not convenient to diminish the counting intensity which in the non-linear method is reduced on account of the necessary amplitude selection.

* * *

We wish to thank heartily Dr. S. ALBERTONI for helpful discussions on the mathematical developments.

List of symbols.

A	gain of the phototube;
\bar{A}	average gain of the phototube;
$C(t)$	change collected at the output of the photomultiplier from 0 to t ;
$\underline{C}(t)$	idem without statistical fluctuation;

f	mean frequency of photoelectron emission in the case of steady illumination
$f(t)$	average shape of current pulse at the output of the photomultiplier as due to one photoelectron emitted at $t = 0$;
g	secondary emission multiplication factor;
h	statistical variable accounting for a fluctuation in average transit time in the phototube. His variance is equal to ε_{dh}^2 ;
$I(t)$	law of illumination of the photocathode as a consequence of a scintillation;
$i(t)$	current output pulse of the photomultiplier;
$\bar{i}(t)$	current output pulse of the photomultiplier considered $= 0$ for $t > t_i$;
$i(t)$	current output pulse of the photomultiplier as the theoretical average if no statistical fluctuations were present;
$Q(t)$	number of photoelectrons emitted in the time interval $0 - t$;
R	mean number of photoelectrons emitted as consequence of one scintillation;
t_c	center of gravity of $\bar{i}(t)$ or of $i(t)$;
t_i	time in which the cut off of the electronic tube has been reached;
ε_A^2	relative variance of A ;
ε_c^2	variance of the center of gravity of $\bar{i}(t)$ or $i(t)$;
$\varepsilon_{c, \text{em}, A, ph}^2$	idem as due respectively to statistics of photoelectron emission, fluctuations in gain, fluctuations in average transit time;
ε_{cd}^2	variance in transit time of one photoelectron between photocathode and first dynode;
ε_{dd}^2	variance in transit time of one electron between two successive dynodes (assumed equal for all couples);
ε_{ph}^2	variance of the time interval between the emission of one photoelectron and the center of gravity of the consequent current output pulse;
ε_μ^2	variance of μ ;
n	number of secondary emission dynodes;
λ	$\langle \text{width} \rangle$ of $f(t)$; λ^2 is the second moment of $f(t)$ referred to its center of gravity;
μ	time as measured by the instrument working in the linear non ballistic way (it is equal to t_c in the ballistic case);
τ	decay time of an illumination having a law $(R/\tau) \exp [-t/\tau]$.

APPENDIX I

If f is the mean frequency of photoelectron emission and t_i is the emission time of i -th photoelectron, the probability density of a $(i+1)$ -th event, occurring at time t is:

$$(1.1) \quad P(t) = f \exp [-f(t - t_i)].$$

The position of center of gravity of the first Q photoelectrons is:

$$(1.2) \quad t_{c,Q} = \frac{t_1 + t_2 + \dots + t_Q}{Q},$$

where the times $t_1, t_2 \dots t_Q$ refer respectively to emission of 1st, 2nd ... and Q -th photo-electron. We have to calculate the density of probability $P_{c,Q}(t_c)$ of observing the center of the first Q events at time t_c . Obviously $P_{c,1}$ is:

$$P_{c,1}(t_c) = f \exp [-ft_c].$$

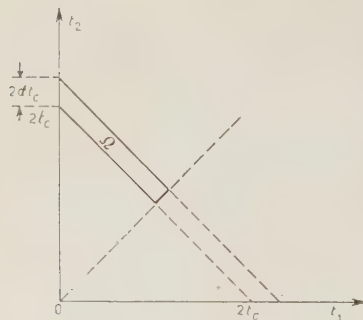


Fig. 10. - Surface of integration for $Q = 2$.

In order to calculate the value of $P_{c,2}$ we observe that:

$$(1.3) \quad P(t_1) dt_1 \cdot P(t_2 - t_1) dt_2,$$

is the probability that first and second photoelectron are emitted respectively in the time intervals $t_1, (t_1+dt_1)$ and $t_2, (t_2+dt_2)$.

By integration of Eq. (1.3) over t_1 and t_2 in an allowed region Ω defined by the bounds: $t_1 \leq t_2$ and $t_c \leq (t_1+t_2)/2 \leq t_c + dt_c$, (this region can be represented as in Fig. 10) we obtain:

$$P_{c,2}(t_c) dt_c = \iint_{\Omega} P(t_1) \cdot P(t_2 - t_1) dt_1 dt_2,$$

$P_{c,2}$ can be rewritten as:

$$(1.4) \quad P_{c,2}(t_c) = 2 \int_0^{t_c} P(t_1) \cdot P(2t_c - 2t_1) dt_1.$$

Substituting into Eq. (1.4) the expression of $P(t)$ as given by (1.1) we find:

$$P_{c,2}(t_c) = 2f^2 \exp [-2ft_c] \int_0^{t_c} \exp [ft_1] dt_1.$$

Similarly, in order to obtain $P_{c,3}$ we can calculate the integral: (in the region Σ as in Fig. 11)

$$P_{c,3}(t_c) dt_c = \iint_{\Sigma} P(t_1) \cdot P(t_2 - t_1) \cdot P(t_3 - t_2) dt_1 dt_2 dt_3,$$

equal to this integral:

$$P_{c,3}(t_c) = 3f^3 \exp [-3ft_c] \int_0^{t_c} dt_1 \int_{t_1}^{t_c} \exp [ft_1] \cdot \exp [ft_2] dt_2.$$

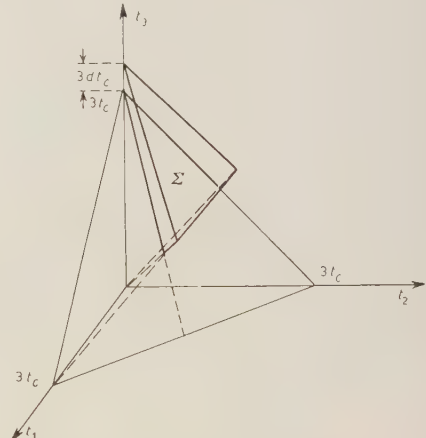


Fig. 11. - Volume of integration for $Q = 3$.

And finally, for Q photoelectrons we may write:

$$(1.5) \quad P_{c,q}(t_c) = Q! f^Q \exp [-Qf t_c] \int_1^{\infty} \int_2^{\infty} \cdots \int_{q-1}^{\infty} \exp [ft_1] \exp [ft_2] \cdots \exp [ft_{q-1}] dt_1 dt_2 \cdots dt_{q-1},$$

where the limits of integration are:

$$\text{integral} \quad 1^{\circ} \quad 2^{\circ} \quad \dots \quad (Q-2)^{\circ} \quad (Q-1)$$

$$\text{sup. limit } t_1 = t_c \quad t_2 = \frac{Q}{Q-1} \left(t_c - \frac{t_1}{Q} \right) \cdots \quad t_{q-2} = \frac{Q}{3} \left(t_c - \sum_{i=1}^{q-3} t_i \right) \quad t_{q-1} = \frac{Q}{2} \left(t_c - \sum_{i=1}^{q-2} t_i \right)$$

$$\text{inf. limit } t_1 = 0 \quad t_2 = t_1 \quad \dots \quad t_{q-2} = t_{q-3} \quad t_{q-1} = t_{q-2}.$$

The integrals (1.5) for $Q = 1, 2, 3, 4$ and corresponding characteristic functions $G_{c,q}(p)$ have been calculated; from which follows directly that the mean value and the variance of t_c are given by:

	mean value	variance
$Q = 1$	$\frac{1}{f}$	$\frac{1}{f^2}$
$Q = 2$	$\frac{3}{2} \frac{1}{f}$	$\frac{5}{4} \frac{1}{f^2}$
$Q = 3$	$2 \frac{1}{f}$	$\frac{14}{9} \frac{1}{f^2}$
$Q = 4$	$\frac{5}{2} \frac{1}{f}$	$\frac{30}{16} \frac{1}{f^2}$

from which, by induction:

$$\text{mean value of } t_{c,a} = \frac{Q+1}{2} \frac{1}{f},$$

$$\text{variance of } t_{c,a} = \frac{1}{f^2} \frac{1^2 + 2^2 + \cdots + Q^2}{Q^2} = \frac{1}{f^2} \left(\frac{1}{3} Q + \frac{1}{2} + \frac{1}{6Q} \right).$$

APPENDIX II

The mean current $\underline{i}(t)$ and the perturbed current $i(t)$, at time t , are expressed by:

$$(2.1) \quad \underline{i}(t) = f(t) * I(t),$$

$$(2.2) \quad i(t) = \underline{i}(t) + \Delta K f(t - \sigma),$$

Likewise $\underline{C}(\underline{t}_i)$ and $C(t_i)$ are respectively the mean charge collected until t_i , mean time of cut off, and the charge collected until the time t_i :

$$(2.3) \quad \underline{C}(\underline{t}_i) = \int_0^{\underline{t}_i} [f(t) * I(t)] dt ,$$

$$(2.4) \quad C(t_i) = \int_0^{t_i} [f(t) * I(t)] dt + \Delta K \int_{\sigma}^{t_i} f(t - \sigma) dt .$$

The Eq. (2.4) can be rewritten as:

$$(2.5) \quad C(t_i) = \int_0^{\underline{t}_i} [f(t) * I(t)] dt + \Delta t [f(t) * I(t)] + \Delta K \int_{\sigma}^{t_i} f(t - \sigma) dt ,$$

where $t_i = \underline{t}_i + \Delta t$.

Recalling that must be $\underline{C}(\underline{t}) = C(t_i)$, from Eq. (2.3) and Eq. (2.5), it follows that:

$$0 = \Delta t [f(t) * I(t)] + \Delta K \int_{\sigma}^{t_i} f(t - \sigma) dt ,$$

from which

$$(2.6) \quad \Delta t = - \Delta K \frac{\int_{\sigma}^{t_i} f(t - \sigma) dt}{\underline{i}(t)} .$$

This will be employed afterwards. From (2.2), t_c is defined by:

$$(2.7) \quad t_c = \frac{\int_0^{\underline{t}_i} \underline{i}(t) dt + \Delta K \int_{\sigma}^{\underline{t}_i} f(t - \sigma) dt}{\int_0^{\underline{t}_i} \underline{i}(t) dt + \Delta K \int_{\sigma}^{\underline{t}_i} f(t - \sigma) dt} =$$

$$(2.8) \quad = \frac{\frac{\int_0^{\underline{t}_i} \underline{i}(t) dt}{\int_0^{\underline{t}_i} \underline{i}(t) dt} + \Delta K \frac{\int_{\sigma}^{\underline{t}_i} f(t - \sigma) dt}{\int_0^{\underline{t}_i} \underline{i}(t) dt}}{1 + \Delta K \frac{\int_{\sigma}^{\underline{t}_i} f(t - \sigma) dt}{\int_0^{\underline{t}_i} \underline{i}(t) dt}} .$$

And this, since the terms proportional to ΔK are $\ll 1$, for no very small values of t_i ,

can be written as:

$$(2.9) \quad t_c = \frac{\int_0^{t_i} \underline{i}(t) dt}{\int_0^{t_i} \underline{i}(t) dt} + \Delta K \left[\frac{\int_{\sigma}^{t_i} \underline{f}(t-\sigma) dt}{\int_0^{t_i} \underline{i}(t) dt} - \frac{\int_{\sigma}^{t_i} \underline{f}(t-\sigma) dt \cdot \int_0^{t_i} \underline{i}(t) dt}{\left(\int_0^{t_i} \underline{i}(t) dt \right)^2} \right].$$

Subtracting from this expression the corresponding one which gives t_c , we obtain:

$$(2.10) \quad \Delta t_c = \frac{\int_0^{t_i} \underline{i}(t) \int_0^t \underline{i}(t) dt - \underline{i}(t) \int_0^{t_i} \underline{i}(t) dt}{\left[\int_0^{t_i} \underline{i}(t) dt \right]^2} \Delta t + \Delta K \left[\frac{\int_{\sigma}^{t_i} \underline{f}(t-\sigma) dt}{\int_0^{t_i} \underline{i}(t) dt} - \frac{\int_{\sigma}^{t_i} \underline{f}(t-\sigma) dt \cdot \int_0^{t_i} \underline{i}(t) dt}{\left(\int_0^{t_i} \underline{i}(t) dt \right)^2} \right],$$

and recalling that Δt is given by Eq. (2.6)

$$(2.11) \quad \Delta t_c = \frac{\frac{\int_{\sigma}^{t_i} \underline{f}(t-\sigma) dt}{\int_0^{t_i} \underline{i}(t) dt} - \frac{\int_{\sigma}^{t_i} \underline{f}(t-\sigma) dt}{\int_0^{t_i} \underline{i}(t) dt}}{\frac{\int_0^{t_i} \underline{i}(t) dt}{\int_0^{t_i} \underline{i}(t) dt}} \Delta K.$$

From which calculating the first of the two integrals of numerator:

$$(2.12) \quad \Delta t_c = \frac{\frac{\int_0^{t_i} dt \int_{\sigma}^t \underline{f}(t-\sigma) dt}{\int_0^{t_i} [\underline{f}(t) * I(t)] dt}}{\frac{\int_0^{t_i} [\underline{f}(t) * I(t)] dt}{\int_0^{t_i} [\underline{f}(t) * I(t)] dt}} \Delta K.$$

In agreement with the preceding analyses, ΔK can be interpreted in two ways.

First we suppose that ΔK photoelectrons are emitted over the mean between the time σ and $(\sigma+d\sigma)$. The variance of ΔK , according to Poisson statistics, is equal to the mean number of events between σ and $(\sigma+d\sigma)$, namely $I(\sigma) d\sigma$.

By adding the variances over every interval $\Delta\sigma$ from $t=0$ to $t=t_i$ we find:

$$(2.13) \quad \varepsilon_{c, em}^2 = \int_0^{t_i} \left[\frac{\int_{\sigma}^{t_i} dt \int_{\sigma}^t \underline{f}(t-\sigma) dt}{\int_0^{t_i} [\underline{f}(t) * I(t)] dt} \right]^2 I(\sigma) d\sigma = \frac{\left[\int_0^{t_i} dt_i \int_0^{t_i} \underline{f}(t_i) dt_i \right]^2 * I(t_i)}{\left[\int_0^{t_i} [\underline{f}(t) * I(t)] dt \right]^2}.$$

Second we define ΔK as a perturbation arising from variations in the gain. If ε_A^2 is the variance of the average gain for a singular photoelectron emitted at time σ , the contribution to variance of the center of gravity is:

$$\varepsilon_A^2 \left[\frac{\int_{\sigma}^{t_i} dt \int_{\sigma}^t \underline{f}(t-\sigma) dt}{\int_0^{t_i} [\underline{f}(t) * I(t)] dt} \right]^2,$$

and by adding the variances, for every photoelectron emitted between $t = 0$ and $t = t_i$

$$(2.14) \quad \varepsilon_{c,A}^2 = \varepsilon_A^2 \int_0^{t_i} \left[\frac{\frac{1}{\sigma} \int_0^t f(t-\sigma) dt}{\int_0^{t_i} [f(t) * I(t)] dt} \right]^2 I(\sigma) d\sigma = \varepsilon_A^2 \frac{\left[\int_0^{t_i} dt_i \int_0^{t_i} f(t_i) dt_i \right]^2 * I(t_i)}{\left[\int_0^{t_i} [f(t) * I(t)] dt \right]^2} .$$

From Eq. (2.13) and (2.14) the variance in center position, arising from emission statistics and fluctuations in gain is given by:

$$(2.15) \quad \varepsilon_{c,\text{em},A}^2 = (1 + \varepsilon_A^2) \frac{\left[\int_0^{t_i} dt_i \int_0^{t_i} f(t_i) dt_i \right]^2 * I(t_i)}{\left[\int_0^{t_i} [f(t) * I(t)] dt \right]^2} .$$

APPENDIX III

The average value of the current output pulse of the phototube is:

$$\underline{i}(t) = f(t) * I(t) .$$

Now we suppose that the shape of current due to one photoelectron emitted, at time σ , in consequence of a light quantity $I(\sigma)\Delta\sigma$ [where $\Delta\sigma$ is chosen in order to obtain $I(\sigma)\cdot\Delta\sigma = 1$] is $f(t-\sigma+h)$ rather than the average shape $f(t-\sigma)$.

In consequence the current is:

$$(3.1) \quad i(t) = \underline{i}(t) - f(t-\sigma) + f(t-\sigma+h) \simeq \underline{i}(t) + h \frac{df(t-\sigma)}{dt} .$$

Similarly the charge $C(t)$ becomes:

$$(3.2) \quad C(t) = \underline{C}(t) + hf(t-\sigma) .$$

By this equation, we can calculate, as well as in Appendix II, the variation Δt of t_i in regard to t_i arising from the considered transit time variation:

$$(3.3) \quad \Delta t = -h \frac{f(t-\sigma)}{\underline{i}(t)} .$$

By the definition of t_c and by Eq. (3.3), as above for Eq. (2.11) of Appendix II,

we find:

$$(3.4) \quad \Delta t_c = -h \frac{\frac{1}{\sigma} \int_{t_i}^t f(t-\sigma) dt}{\int_0^{t_i} [f(t) * I(t)] dt}.$$

h is a statistical variable accounting for a fluctuation in average transit time whose variance is ε_{ph}^2 , hence by adding the contributions due to any photoelectron, we have

$$(3.5) \quad \varepsilon_{c, ph}^2 = \varepsilon_{ph}^2 \left[\frac{\left| \int_0^{t_i} f(t) dt \right|^2 * I(t_i)}{\int_0^{t_i} [f(t) * I(t)] dt} \right]^2.$$

APPENDIX IV

By means of hypotheses used for Eq. (10) and (16) we can determine that:

$$(4.1) \quad \varepsilon_c^2 = \frac{\tau^3}{3} \frac{1}{R} \frac{C}{R} + \frac{\tau^2}{R^2}.$$

For to make a comparison with the Eq. (6) we put $C = Q - 1$ (from which, for very small value of C , follows that is taken in consideration the first photoelectron alone) and by (4.1) we have:

$$(4.2) \quad \varepsilon_c^2 = \frac{\tau^2}{3} \frac{Q}{R^2} \left(1 + \frac{2}{Q} \right).$$

APPENDIX V

Working in linear ballistic way, we can calculate, as in Appendix II, $\varepsilon_{c, em, A}^2$. Now we put in the integrals of Eq. (2.7) $t_i = \infty$; hence t_c is function of ΔK only and not of Δt . Then Eq. (2.10) can be written:

$$(5.1) \quad \Delta t_c = \frac{\Delta K}{\left[\int_0^\infty \underline{i}(t) dt \right]^2} \left[\int_0^\infty \underline{i}(t) dt \cdot \int_\sigma^\infty t f(t-\sigma) dt - \int_0^\infty t \underline{i}(t) dt \cdot \int_\sigma^\infty f(t-\sigma) dt \right].$$

In this case the shape assumed, for the output current of the multiplier tube, is

thing of no moment, and for semplicity we may choose: $f(t - \sigma) = \delta(t - \sigma)$. We find:

$$\int_0^\infty \underline{i}(t) dt = \int_0^\infty [\delta(t) * I(t)] dt = R,$$

where R is the total number of photoelectrons emitted. Then Eq. (5.1) becomes:

$$\Delta t_c = \frac{\Delta K}{R^2} \left[R\sigma - \int_0^\infty t \underline{i}(t) dt \right].$$

Remembering that

$$t_c = \frac{\int_0^\infty t \underline{i}(t) dt}{R},$$

we have:

$$\Delta t_c = \frac{\Delta K}{R} [\sigma - t_c],$$

and consequently (Appendix II)

$$(5.2) \quad \varepsilon_{c,\text{em}\,A}^2 = (1 + \varepsilon_A^2) \frac{1}{R^2} \int_0^\infty (\sigma - t_c)^2 I(\sigma) d\sigma.$$

On the other hand, for the variance arising from the fluctuations in the transit time, we have:

$$(5.3) \quad \varepsilon_{c,\text{ph}}^2 = \frac{\varepsilon_{\text{ph}}^2}{R}.$$

APPENDIX VI

First we shall calculate the « machine time » variance due to emission statistics and to gain fluctuations, then the variance due to transit time fluctuations.

Since the contribution given to total current by each photoelectron is $\delta(t - \sigma)$ and, as we suppose that the scintillation is $I(t) = (R/\tau) \exp[-t/\tau]$ the mean current and the perturbed current respectively are:

$$(6.1) \quad \underline{i}(t) = \frac{R}{\tau} \exp \left[-\frac{t}{\tau} \right],$$

$$(6.2) \quad i(t) = \frac{R}{\tau} \exp \left[-\frac{t}{\tau} \right] + \Delta K \delta(t - \sigma),$$

where ΔK , defined as in Appendix II, is a perturbation at time σ .

The Laplace transform of Eq. (6.1) and (6.2) are:

$$(6.3) \quad \underline{i}(p) = \frac{R}{1 + p\tau},$$

$$(6.4) \quad i(p) = \frac{R}{1 + p\tau} + \Delta K \exp [-\sigma p].$$

If μ here is the « machine time » from (6) we obtain:

$$\omega\mu = \arg i(j\omega).$$

Substituting $j\omega$ for p in (6.3) and (6.4), we find:

$$(6.5) \quad \operatorname{tg} \omega\underline{\mu} = -\omega\tau,$$

$$(6.6) \quad \operatorname{tg} \omega\mu = -\frac{(1 + \omega^2\tau^2)\Delta K \sin \omega\sigma + R\omega\tau}{(1 + \omega^2\tau^2)\Delta K \cos \omega\sigma + R},$$

where $\underline{\mu}$ is the mean value of μ .

In order to obtain the variance of μ , expressed in terms of ΔK ; we must calculate: $\Delta\mu = \mu - \underline{\mu}$.

By subtracting Eqs. (6.5) from (6.6) and being $\Delta\mu$ small with respect to μ , it follows that

$$\frac{d}{d\mu} (\operatorname{tg} \omega\mu) \Delta\mu = -\frac{(1 + \omega^2\tau^2)\Delta K \sin \omega\sigma + R\omega\tau}{(1 + \omega^2\tau^2)\Delta K \cos \omega\sigma + R} + \omega\tau,$$

and finally:

$$(6.7) \quad \Delta\mu = \frac{\omega\tau \cos \omega\sigma - \sin \omega\sigma}{\omega R} \Delta K.$$

In the calculation of the variance of μ the two meanings of ΔK must be taken into account. By the same considerations made in Appendix II in order to obtain (2.13) and (2.14) we find

$$(6.8) \quad \varepsilon_{\mu, em, A}^2 = (1 + \varepsilon_A^2) \int_0^\infty \left| \frac{\omega\tau \cos \omega\sigma - \sin \omega\sigma}{\omega R} \right|^2 \frac{R}{\tau} \exp \left[-\frac{\sigma}{\tau} \right] d\sigma = (1 + \varepsilon_A^2) \frac{\tau^2}{R} \frac{1 + 2\omega^2\tau^2}{1 + 4\omega^2\tau^2}.$$

For small ω in comparison with τ , (6.8) becomes (5.2) where one uses $I(\sigma) = R/\tau \exp [-\sigma/\tau]$.

Let us calculate now the variance in the machine time due to the transit time fluctuations in the phototube.

As in Appendix III, we suppose that for the electron delivered at about the time σ , the response of the phototube is $\delta(t - \sigma + h)$ instead of $\delta(t - \sigma)$.

This perturbation carries the current, whose mean value is given by (6.1) to the value

$$(6.9) \quad i(t) = \frac{R}{\tau} \exp \left| -\frac{t}{\tau} \right| + \delta(t - \sigma + h) - \delta(t - \sigma),$$

and its transform is

$$(6.10) \quad i(p) = \frac{R}{1 + p\tau} + \exp [-(\sigma - h)p] - \exp [-\sigma p].$$

For sufficiently small h

$$(6.11) \quad i(p) = \frac{R}{1 + p\tau} + p \exp [-\sigma p] \cdot h.$$

By substituting $j\omega$ to p in (6.11), recalling (6), we obtain:

$$(6.12) \quad \operatorname{tg} \omega\mu = \frac{(1 + \omega^2\tau^2)\omega h \sin \omega\sigma - R\omega\tau}{(1 + \omega^2\tau^2)\omega h \cos \omega\sigma + R}.$$

As it has been done before in order to obtain (6.7), we calculate $\Delta\mu = \mu - \underline{\mu}$ [where $\underline{\mu}$ is given by (6.5)], thus obtaining:

$$(6.13) \quad \Delta\mu = \frac{\omega\tau \sin \omega\sigma + \cos \omega\sigma}{R} h.$$

By the same considerations made in Appendix III in order to obtain (3.5) we obtain

$$(6.14) \quad \varepsilon_{\mu, \text{ph}}^2 = \varepsilon_{\text{ph}}^2 \int_0^\infty \left| \frac{\omega\tau \sin \omega\sigma + \cos \omega\sigma}{R} \right|^2 \frac{R}{\tau} \exp \left[-\frac{\sigma}{\tau} \right] d\sigma = \frac{\varepsilon_{\text{ph}}^2}{R} \left[1 + \frac{2\omega^4\tau^4}{1 + 4\omega^2\tau^2} \right].$$

For small ω in comparison with τ , (6.14) become (5.3). By adding (6.8) to (6.14) we obtain:

$$(6.15) \quad \varepsilon_{\mu, \text{em}, A, \text{ph}}^2 = \frac{\tau^2}{R} (1 + \varepsilon_A^2) \frac{1 + 2\omega^2\tau^2}{1 + 4\omega^2\tau^2} + \frac{\varepsilon_{\text{ph}}^2}{R} \left(1 + \frac{2\omega^4\tau^4}{1 + 4\omega^2\tau^2} \right).$$

RIASSUNTO

Si esaminano i limiti della precisione nel valutare la posizione temporale di un evento rivelato con un contatore a scintillazione. Si confrontano due metodi «non lineare» e «lineare» impiegati per ottenere informazioni su tale tempo dall'impulso di corrente del fotomoltiplicatore, tenendo conto della statistica di emissione dei fotoelettroni, del tempo di transito e della variazione del fattore di moltiplicazione nel fototubo, e della larghezza finita della risposta del fototubo ad un photoelettrone. La risoluzione ottenuta col metodo «non lineare» è migliore, ma il metodo «lineare» non richiede selezione in ampiezza degli impulsi.

LETTERE ALLA REDAZIONE

(La responsabilità scientifica degli scritti inseriti in questa rubrica è completamente lasciata dalla Direzione del periodico ai singoli autori)

A Note on the Energy Gap Model of Superconductivity (*).

M. J. BUCKINGHAM

Department of Physics, Duke University - Durham, N. C.

(ricevuto il 9 Ottobre 1956)

The fact that the measured specific heat and thermal conductivity of superconductors becomes so small at low temperatures — even falling exponentially — has led to the suggestion of a gap in the energy level spectrum above the lowest energy value.

BARDEEN (¹) has shown that if one assumes, as well as a gap, that the matrix elements for optical type transitions are the same as for the system without a gap, one obtains magnetic properties similar to those described by London's equation, and in particular, the Meissner effect.

It is the purpose of this note to point out that no system could obey these assumptions which in fact contradict a general theorem, and that Bardeen's conclusion is invalid. The theorem results from the dependence between the energy levels of a system and the matrix elements mentioned, and is a necessary and sufficient condition for the gauge invariance of the current density.

The proof is given here only for a homogeneous system of electrons at absolute zero temperature; generalization will be discussed in a later publication, together with other aspects of the results.

Consider a system of electrons at absolute zero temperature, in a state, described by $|0\rangle$, with energy E_0 . Let $|k\rangle$ represent a complete set of states with energy eigenvalues E_k .

In the presence of a small magnetic field described by the vector potential function $\mathbf{A}(\mathbf{r})$, the current density component $j_\mu(\mathbf{q})$, ($\mu = 1, 2, 3$) arising from the \mathbf{q} Fourier component of $\mathbf{A}(\mathbf{r})$ is given to first order in \mathbf{A} by

$$j_\mu(\mathbf{q}) = -\frac{e^2 n}{mc} \left[A_\mu(\mathbf{q}) + \frac{1}{2} \sum_{k \neq 0} \sum_{\nu=1}^3 \left\{ \frac{\langle 0 | e^{i\mathbf{q} \cdot \mathbf{r}} \nabla_\mu + \nabla_\mu e^{i\mathbf{q} \cdot \mathbf{r}} | k \rangle \langle k | e^{-i\mathbf{q} \cdot \mathbf{r}} \nabla_\nu + \nabla_\nu e^{-i\mathbf{q} \cdot \mathbf{r}} | 0 \rangle}{(2m/\hbar^2)(E_0 - E_k)} A_\nu(\mathbf{q}) + \text{compl. conj.} \right\} \right].$$

(*) Supported in part by the National Science Foundation.

(¹) J. BARDEEN: *Phys. Rev.*, **97**, 1724 (1955).

where \mathbf{r} stands for the co-ordinate of one electron and the gradient is with respect to the same electron co-ordinate (the matrix elements are independent of which electron because of the antisymmetry of the wave functions); n is the number of electrons per unit volume. We can write this perturbation expression for the current as:

$$(1) \quad j_\mu(\mathbf{q}) = -\frac{e^2 n}{mc} \sum_{\nu=1}^3 [\delta_{\mu\nu} - S_{\mu\nu}(\mathbf{q})] A_\nu(\mathbf{q});$$

putting q for the magnitude of \mathbf{q} , we assert that

$$(2) \quad \sum_{\mu,\nu=1}^3 \frac{q_\mu q_\nu}{q^2} S_{\mu\nu}(\mathbf{q}) = 1.$$

If H represents the Hamiltonian operator for the system of electrons in the absence of the field, the commutator of H and $\exp[i\mathbf{q} \cdot \mathbf{r}]$, where \mathbf{r} is the co-ordinate of one electron can be used to prove the following identity:

$$(3) \quad \sum_{\mu=1}^3 i q_\mu \{ \langle k | \exp[i\mathbf{q} \cdot \mathbf{r}] \nabla_\mu + \nabla_\mu \exp[i\mathbf{q} \cdot \mathbf{r}] | k' \rangle \} = \\ = (2m/\hbar^2)(E_{k'} - E_k) \langle k | \exp[i\mathbf{q} \cdot \mathbf{r}] | k' \rangle.$$

Using also the completeness of the set $|k\rangle$, the proof of the theorem (2) follows immediately.

Now the fact that $S_{\mu\nu}(\mathbf{q})$ is a function only of \mathbf{q} means that it must be of the form

$$S_{\mu\nu}(\mathbf{q}) = a(q) \frac{q_\mu q_\nu}{q^2} + b(q) \delta_{\mu\nu};$$

the theorem (2) now reduces to $a + b = 1$ and contracting the tensor,

$$\text{Trace } S_{\mu\nu}(\mathbf{q}) = a + 3b.$$

Using these relations we can now write the current component (1) in the alternative forms:

$$(a) \quad j_\mu(\mathbf{q}) = \frac{e^2 n}{mc} \sum_{\nu=1}^3 (S_{\mu\nu}(\mathbf{q}) - \delta_{\mu\nu}) A_\nu(\mathbf{q}),$$

$$(b) \quad = \frac{e^2 n}{mc} \frac{1}{2} \sum_{\nu=1}^3 (\text{Tr } S_{\mu\nu}(\mathbf{q}) - 3) \left(\delta_{\mu\nu} - \frac{q_\mu q_\nu}{q^2} \right) A_\nu(\mathbf{q}).$$

$$(c) \quad = \frac{e^2 n}{mc} \frac{1}{2} \sum_{\alpha,\beta,\nu=1}^3 S_{\alpha\beta}(\mathbf{q}) \left(\delta_{\alpha\beta} - 3 \frac{q_\alpha q_\beta}{q^2} \right) \left(\delta_{\mu\nu} - \frac{q_\mu q_\nu}{q^2} \right) A_\nu(\mathbf{q}),$$

The last two forms exhibit gauge invariance explicitly through the factor $(\delta_{\mu\nu} - (q_\mu q_\nu/q^2))$. The theorem (2) is thus a sufficient condition to ensure gauge invariance of the current. It is easy to see that it is also necessary. Thus although our

proof is for a special system, the theorem must nevertheless be true for any system in which the current is expressible in the form (1).

Returning now to Bardeen's discussion of the gap model of superconductors we see that the assumption of unchanged matrix elements and altered energy differences is inconsistent with the identity (3), and that the theorem (2) is not satisfied; indeed, if ϵ is the size of the energy gap, $S_{\mu\nu}(\mathbf{q}) \rightarrow 0$, for $q/\epsilon \rightarrow 0$.

The form for the current (*a*), used by Bardeen, then reduces to London's equation as found by Bardeen. The form (*b*) would give $\frac{2}{3}$ times this value and the form (*c*) would give zero, the result for an insulator rather than a superconductor.

* * *

The author is indebted to Dr. M. R. SCHAFROTH for a number of helpful discussions of this work, which was carried out during a stay at the School of Physics, University of Sydney and he wishes also to express his thanks to Professor H. MESSEL for his generous hospitality.

Note added in proof.

In the following letter of this issue, Dr. J. BARDEEN points out that, in a one particle picture, there is an effective velocity dependent interaction. This is, of course, true but as stated above, our theorem can be generalized; both to a finite temperature and to a system with many *different* types of particles interacting with *x*-space forces only. Any system can be represented in this way, if necessary by going right back to the electrons and nuclei. The theorem remains true in the form (2) for any system in which the current can be expressed in the form (1).

We cannot agree, however, that the matrix elements or the quantity $S_{\mu\nu}(\mathbf{q})$ depend on the choice of gauge: they are intrinsic properties of the *field-free* system. An assumption concerning the matrix elements and energy levels relates to the system itself and cannot refer only to a particular choice of gauge or field. Bardeen's assumptions mean that $S_{\mu\nu}(\mathbf{q}) \rightarrow 0$ as $q \rightarrow 0$, i.e. not only that $b(q) \rightarrow 0$ but also that $a(q) \rightarrow 0$. It is claimed that no system could have this property.

The author wishes to thank Dr. BARDEEN for a copy of his note and for some comments.

Gauge Invariance and the Energy Gap Model of Superconductivity.

J. BARDEEN

University of Illinois - Urbana, Illinois

(ricevuto il 12 Ottobre 1956)

It is true, as pointed out by BUCKINGHAM⁽¹⁾, that one can not assume that the matrix elements of the energy gap model are the same as those of a system without a gap if one uses an arbitrary gauge. In the writer's opinion, this does not invalidate the arguments made concerning the connection between the energy gap model and magnetic properties nor the usefulness of this approach to a phenomenological theory of superconductivity.

The difficulties arise from the fact that in the one-particle picture an energy gap corresponds to a velocity dependent operator. One might write for the energy of an electron with momentum p :

$$E(p) = \frac{p^2}{2m} + g(p),$$

where $g(p)$ is presumed to vary rapidly from 0 to ϵ as p crosses the Fermi surface. In a gauge invariant theory, one would have to include terms in the expressions for the current and magnetic interaction which come from $g(p)$ ⁽²⁾.

In the earlier note⁽³⁾, one assumed that when the gauge is chosen so that $\text{div } \mathbf{A} = 0$, the matrix elements of the current operator and of the magnetic interaction to excited states of the actual many-body particle system in a superconductor are similar to those of a one-particle model without gap. A Meissner effect is obtained since the matrix elements go to zero with the wave vector q of the magnetic field while the energy denominator remains finite. It is the function $b(q)$, in Buckingham's notation, which is determined by this procedure. As far as the writer is aware, there are no general theorems which preclude the possibility that $b(q) \rightarrow 0$ or remains less than unity as $q \rightarrow 0$ ⁽⁴⁾. In either case, a Meissner effect would result.

BUCKINGHAM, in effect, argues that when similar assumptions concerning the matrix elements are made with a general gauge, one gets inconsistent results. This

⁽¹⁾ J. BARDEEN: *Phys. Rev.*, **97**, 1724 (1955). A more complete account is to appear in a forthcoming article on *Theory of Superconductivity*, in *Encyclopedia of Physics*, vol. XV (Heidelberg).

⁽²⁾ M. R. SCHAFROTH: *Phys. Rev.*, **100**, 502 (1955), has argued that one can not have a Meissner effect in a system with finite correlation length, but has not shown that the actual correlation length in superconductors is not effectively infinite.

⁽³⁾ M. J. BUCKINGHAM: *Nuovo Cimento*, **5**, (1956).

⁽⁴⁾ The writer is indebted to a discussion with Dr. F. E. Low in early 1955 on the question of gauge invariance from this point of view.

is true, for one then determines a combination of $a(q)$ and $b(q)$, and the sum of these can not go to zero with q . There is, however, nothing inconsistent about making this assumption for the special gauge, $\text{div } \mathbf{A} = 0$, and to use the criterion of gauge invariance to get general expressions which apply in any gauge.

There are good reasons for the choice $\text{div } \mathbf{A} = 0$ aside from simplicity⁽⁵⁾. If a different choice, $\mathbf{A}' = \mathbf{A} + \text{grad } \varphi$, is made, the magnetic perturbation can be minimized by expanding in terms of a set of functions

$$\Psi'_i = \exp [-(ie/\hbar c) \sum \varphi(r_\alpha)] \Psi_i,$$

instead of the functions Ψ_i appropriate to zero field. This corresponds to making a gauge transformation to one for which $\text{div } \mathbf{A} = 0$. If it is assumed that \mathbf{A}' is small and an expansion is made in terms of Ψ_i one is in effect expanding Ψ'_i in terms of Ψ_i . Further, the matrix elements of \mathbf{A} (with $\text{div } \mathbf{A} = 0$) important for penetration phenomena are similar to those which determine absorption of electromagnetic radiation.

The last point is important. Perhaps the greatest value of this approach to superconductivity is to see what sort of phenomenological theories it leads to. If for a given excitation energy the matrix elements (and thus absorption) are nearly the same as those of a normal metal, the diamagnetism is small and $b(q) \sim 1$ for the corresponding q . If there is a Meissner effect, $b(q)$ will become appreciably less than unity for small q , say $q < q_s$. The nature of the phenomenological theory depends on whether or not the product of q_s and the penetration depth λ is greater than or smaller than unity. If $q_s \lambda \ll 1$, one finds a non-local theory of the type suggested by Pippard. If matrix elements depart from normal values for excitation energies $< \Delta E$, one

expects $hq_s \sim (dp/dE)_F \Delta E$. The qualitative nature of the theory is not very sensitive as to whether the departure is in the matrix elements or energies of the excited states.

One can not, of course, be sure that any model which gives an energy spectrum corresponding to an energy gap will yield a Meissner effect. In particular, if the energy gap is of the sort which arises in band theory from a periodic perturbation, and the lower bands are completely filled and the upper bands completely empty, one can show by sum rules that terms corresponding to Landau diamagnetism vanish. Although the energy gap model has considerable empirical backing, the ultimate test will be to derive the properties from a sound microscopic theory.

* * *

The author is indebted to Dr. BUCKINGHAM for raising these questions which were not treated adequately in the original communication and for sending a copy of his note prior to publication.

Note added in proof.

In a many-particle formulation, it is necessary to consider excited states of the collective modes (lattice vibrations and plasma oscillations) as well as those of the individual particles. [See J. BARDEEN and D. PINES: *Phys. Rev.*, **99**, 1140 (1955)]. In a general gauge, \mathbf{A}' , the matrix elements which come from $\varphi(r_\alpha)$ in the expansion of Ψ'_i in terms of Ψ_i are similar to those encountered in the perturbation expansion of a small electrostatic potential, $\varphi(r)$. For a slowly varying $\varphi(r)$ (corresponding to small q), the important excited states are those which have a varying charge density and which are described in terms of collective co-ordinates. On the other hand, the true magnetic interactions which come from A ($\text{div } A = 0$) connect mainly with individual particle excit-

(5) J. BARDEEN: *Phys. Rev.*, **81**, 469 (1951).

ations in which there is no long range variation in charge density.

One may divide $S_{\mu\nu}$ into two parts, one $S_{\mu\nu}^c$ which comes from collective excitations and another $S_{\mu\nu}^i$ which comes from individual particle excitations. If for q small, the former comes mainly from φ and the latter from A , one would expect to find

$$S_{\mu\nu}^c = \frac{q_\mu q_\nu}{q^2}.$$

$$S_{\mu\nu}^i = b(q) \left(\delta_{\mu\nu} - \frac{q_\mu q_\nu}{q^2} \right).$$

There is no reason why $b(q)$ may not go to zero as $q \rightarrow 0$ as a result of a finite energy denominator and vanishing matrix elements for individual particle excitations.

Because of the way in which subsidiary conditions limit individual particle excitations in the Bohm-Pines formulation to those which involve no long range charge fluctuations, a direct calculation of $S_{\mu\nu}^i$ would be difficult. On physical grounds, however, one would not expect a magnetic field to excite collective modes.

Ambipolar Diffusion in a Magnetic Field in the Case of Glow Discharge.

S. N. GOSWAMI

Hooghly Mohsin College - Chinsura, India

(ricevuto il 13 Novembre 1956)

The positive column of a glow discharge has a linear fall of potential along it. Consequently, along the axis of the discharge tube, $N_+ = N_- = N$. In such type of discharge, ambipolar diffusion also occurs, for which the guiding equations are ⁽¹⁾

$$(1) \quad n_+ \bar{v}_{x+} = -D_+ \frac{dn_+}{dx} + K^+ X n_+$$

and

$$(2) \quad n_- \bar{v}_{x-} = -D_- \frac{dn_-}{dx} - K^- X n_-$$

From these equations the coefficient of ambipolar Diffusion D_a turns out to be

$$(3) \quad D_a = \frac{D_+ K_- + D_- K_+}{K_+ + K_-}$$

ALBERT SIMSON ⁽²⁾ has however shown that no ambipolar diffusion occurs when the plasma is subjected to a magnetic

field perpendicular to the direction of the applied electric field. This fact can also be realised if, following LOEB, one writes,

$$(4) \quad n_+ \bar{v}_{x+} = -D_+ \frac{dn_+}{dx} + K^+ X n_+ - K'_+ H \bar{v}_{y+} n_+$$

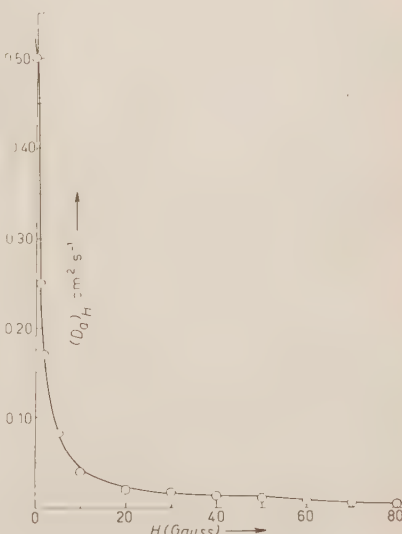


Fig. 1.

⁽¹⁾ L. B. LOEB: *Fundamental Processes of Electrical Discharge in Gases* (New York, 1939), p. 587.

⁽²⁾ A. SIMON: *Phys. Rev.*, **98**, 317 (1955).

and

$$(5) \quad n_- \bar{v}_{x-} = -D_- \frac{dn_-}{dx} - K_- X n_- - K'_- H \bar{v}_y n_-,$$

To simplify matters, one may assume that there exists a correlation between \bar{v}_x and \bar{v}_y and further, taking that correlation to be linear one obtains the following ambipolar diffusion coefficient in the usual way,

$$(6) \quad (D_a)_H = \frac{D_+ K_- + D_- K_+}{K_+ + K_-} \left(\frac{1}{1 + \beta H} \right)$$

where $\beta \approx 1$ at a pressure of 1 mm Hg

Eq. (6) shows that $(D_a - H)$ curve is a rectangular hyperbola (Fig. 1). At a field of the order of 100 G, it is seen that the value of the coefficient of ambipolar diffusion is very small (.005) in comparison to that in the absence of the magnetic field (.50), in conformity with the observations of SIMON.

* * *

Thanks are due to Dr. T. ROY for very helpful discussions in the course of the work.

A Method for Measuring the Relaxation Time T_1 .

T. GHOSE, S. K. GHOSH and D. K. ROY

Institute of Nuclear Physics - Calcutta, India

(ricevuto il 5 Febbraio 1957)

CARR and PURCELL⁽¹⁾ introduced a method for measuring the relaxation time T_1 from the growth or vanishing of the second free induction signal, avoiding totally the diffusion effect, which was subsequently used by HOLCOMB and NORBERG⁽²⁾ and others⁽³⁾. They also pointed out the possibility of using the growth of the primary echo due to the second and third pulses P_{23} . It will be shown that besides the growth, the exact null point determination of this echo P_{23} gives a very neat method of measuring T_1 .

The amplitude of this particular echo is given by,

$$M_0 \left[1 - (1 - \cos \varepsilon_1) \exp \left(-\frac{\tau_1}{T_1} \right) \right] \sin \varepsilon_2 \sin^2 \frac{\varepsilon_3}{2} \exp \left[-\frac{2(\tau_2 - \tau_1)}{T_2} \right] \exp \left[-\frac{5}{3} k (\tau_2 - \tau_1)^3 \right],$$

where ε_1 , ε_2 , ε_3 are the angles through which the moment vector is nutated by the first, second and third rf-pulses respectively. τ_1 and τ_2 are respectively the intervals of the second and third rf-pulses from the first pulse. Evidently the best choice of angles in the case of studying the growth of the echo - the characteristic time of which gives T_1 — will be $\varepsilon_1 = 90^\circ$, $\varepsilon_2 = 90^\circ$ and $\varepsilon_3 = 180^\circ$. But choosing the angles as $\varepsilon_1 = 180^\circ$; $\varepsilon_2 = 90^\circ$ and $\varepsilon_3 = 180^\circ$, the echo signal can be made to vanish for a particular separation between the first and the second pulse, (while the interval between the second and third pulse is held fixed), as given by,

$$\tau_{\text{null}} = T_1 \log_e 2.$$

The null point is quite sharp and can be determined quickly. The accuracy of measurement depends on how slowly the interval τ_1 can be varied, on its exact determination and on ascertaining the exact point of vanishing of the echo below the noise level. Thus T_1 can be easily obtained eliminating the damping effect due to diffusion. The superiority of this method over those using the second induction

(¹) H. Y. CARR and E. M. PURCELL: *Phys. Rev.*, **94**, 630 (1954).

(²) D. F. HOLCOMB and R. E. NORBERG: *Phys. Rev.*, **98**, 1074 (1955).

(³) R. J. BLUME: *Bull. Am. Phys. Soc.*, **1**, II, 397 (1956).

decay signal lies in the fact that no arrangement for preventing the receiver from saturation is needed here as required in the latter case. For glycerine, T_1 is obtained as 34 ms using this method.

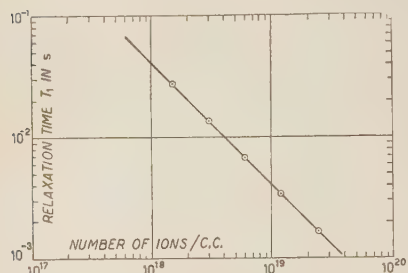


Fig. 1. — Curve showing the variation of relaxation time T_1 with different concentrations of FeCl_3 solution at 14 MHz.

A systematic measurement of T_1 has been carried out at 14 MHz for protons in water containing different concentrations of FeCl_3 . The results are plotted graphically in Fig. 1 which gives a smooth straight line as expected theoretically. The absolute magnitude of T_1 at any concentration, however, differs appreciably from that given by BLOEMBERGEN⁽⁴⁾ who carried out measurements at 29 MHz. Recently NOLLE and MORGAN⁽⁵⁾ and also BLOOM⁽⁶⁾ have observed field-dependence of T_1 for protons in aqueous solutions of $\text{Cr}(\text{H}_2\text{O})_6^{+++}$, $\text{Mn}(\text{H}_2\text{O})_x^{++}$, $\text{Co}(\text{H}_2\text{O})_x^{+}$.

We also think that the deviation of our results from those of Bloembergen may be due to such a cause and intend to explain quantitatively the exact field dependence of T_1 , both from theoretical and experimental points of view.

* * *

The authors thank Prof. A. K. SAHA and Mr. B. M. BANERJEE for their encouragement.

⁽⁴⁾ N. BLOEMBERGEN: *Thesis* (Utrecht, 1948).

⁽⁵⁾ A. W. NOLLE and L. O. MORGAN: *Bull. Am. Phys. Soc.*, **1**, II, 92 (1956).

⁽⁶⁾ A. L. BLOOM: *Journ. Chem. Phys.*, **25**, 793 (1956).

Interactions of μ -Mesons Underground (19.0 MeV).

S. NARANAN, P. V. RAMANAMURTY, A. B. SAHIAR and B. V. SREEKANTAN

Tata Institute of Fundamental Research - Bombay

(ricevuto il 6 Febbraio 1957)

Several workers (^{1,12}) working underground with cloud chambers, photographic emulsions, and Geiger counters have obtained for μ -mesons underground, cross-section for their nuclear interactions of the order of 10^{-3} cm²/nucleon. Following BRADDICK and HENSBY (¹³), other workers (^{4,14}) working underground

(¹) E. P. GEORGE and J. EVANS: *Proc. Phys. Soc.*, A **63**, 1248 (1950).

(²) E. P. GEORGE and J. EVANS: *Proc. Phys. Soc.*, A **68**, 829 (1955).

(³) A. LOVATI, A. MURA, C. SUCCI and G. TAGLIAFERRI: *Nuovo Cimento*, **10**, 1201 (1953).

(⁴) H. J. J. BRADDICK, W. NASH and A. W. WOLFENDALE: *Phil. Mag.*, **42**, 1277 (1951).

(⁵) H. J. J. BRADDICK and B. LEONTIC: *Phil. Mag.*, **45**, 1287 (1954).

(⁶) S. KANEKO, T. KUBOZOE, M. OKAZAKI and K. TAKAHATA: *Journ. Phys. Soc. Japan*, **10**, 600 (1955).

(⁷) M. L. T. KANNAGARA and M. ZIVKOVIC: *Phil. Mag.*, **44**, 797 (1953).

(⁸) P. H. BARRETT, L. M. BOLLINGER, G. COCCONI, Y. EISENBERG and K. I. GREISEN: *Rev. Mod. Phys.*, **24**, 133 (1952).

(⁹) E. AMALDI, C. CASTAGNOLI, A. GIGLI and S. SCIUTI: *Nuovo Cimento*, **9**, 969 (1952).

(¹⁰) P. E. ARGAN, A. GIGLI and S. SCIUTI: *Nuovo Cimento*, **11**, 530 (1954).

(¹¹) D. KESSLER and R. MAZE: *Physica*, **12**, 69 (1956).

(¹²) C. CASTAGNOLI, A. GIGLI and S. SCIUTI: *Nuovo Cimento*, **10**, 893 (1953).

(¹³) H. J. J. BRADDICK and G. HENSBY: *Nature*, **144**, 1912 (1939).

(¹⁴) E. P. GEORGE, J. L. REDDING and P. T. TRENT: *Proc. Phys. Soc.*, A **66**, 533 (1953).

with cloud chambers had reported comparatively very large cross-sections ($4 \div 5 \cdot 10^{-2}$) cm²/nucleon for the production of single penetrating secondaries by penetrating particles underground, the so called « associated pairs of penetrating particles » (A.P.P's).

With a view to study these interactions, the present experiment was performed with a multiplate cloud chamber inside an abandoned railway tunnel at Khandala (1790 ft. a.s.l.), 80 miles from Bombay, during February-June 1954. The cloud chamber was run inside the tunnel, in a temperature-controlled trailer caravan. The rock (*) over the apparatus was equivalent to 180 m of water (180 m w.e.). The cloud chamber was 45 cm in diameter, and had an illuminated depth of 12.5 cm. It had seven, half-inch thick lead plates inside, and a 10.5 cm lead block above, and was triggered by a triple coincidence system of Geiger counters consisting of one counter tray above, and two counter trays below the chamber.

In a total of 6884 photographs obtained in 1300 h of cloud chamber operation, we have 33 events where a penetrating particle is accompanied by, or has produced inside the chamber, a

(*) The density of the rock was 2.9 g/cm³.

single secondary particle which apparently penetrates one or two lead plates. These events if interpreted as examples of the associated pair production (A.P.P.) would give, for this type of phenomenon a cross-section of the same order of magnitude as that given by previous workers^(4,14) namely $(4 \pm 5 \cdot 10^{-21}) \text{ cm}^2/\text{nucleon}$. However we will see below that almost all the above secondaries are consistent with being knock-on electrons.

In all the above cases where the secondary particle stops in a plate in the chamber, its track appears to be minimum ionizing in the compartment above the plate. Protons stopping in a lead plate 1.25 cm thick would appear to ionize heavily in the compartment above the plate. π - or μ -mesons would also appear to ionize heavily, except for those which stop in the bottom 3 mm of the plate, which would appear to ionize minimum. Thus, since the particles are minimum ionizing in all our cases, one is led to believe that a large majority of these secondaries could not be protons or π or μ -mesons stopping in the plate.

There are 25 photographs of knock-on electron showers, where at least one of the shower particles appears to penetrate one plate, and stops in the next, showing thereby that it is not rare for an electron to appear to penetrate one half-inch lead plate (2.2 radiation lengths). Thus, most of the secondaries which appear to penetrate one plate in the above mentioned 33 cases could be knock-on electrons, which may have produced a shower in the lead plate, with only one shower particle emerging from this plate.

We now, therefore, try to interpret these 33 events as knock-on electrons and so consider them together with all the other knock-on electrons and knock-on electron cascades observed by us. Taking D'ANDLAU's⁽¹⁵⁾ experimental re-

sults on the fluctuations in the number of electrons below a lead layer two radiation lengths thick, and using the energy spectrum of electrons in equilibrium with μ -mesons in lead at a total depth of 190 m.w.e., calculated from Bhabha's⁽¹⁶⁾ theory, we can show that the calculated⁽¹⁷⁾ and observed ratios of $N(1)/N (> 1)$ namely 0.79 ± 0.3 and 0.55 ± 0.1 respectively, are in agreement within the statistical errors. $N(1)$ is the number of cases where only one electron emerges below the lead plate 2 radiation lengths thick, and $N (> 1)$ is the number of cases where more than one electron emerge from the lead plate.

The above results and discussion show that all these apparently penetrating secondaries could be explained as knock-on electrons and that it is not necessary to invoke a special phenomenon like the production of A.P.P.'s with a comparatively large cross-section. These results are in agreement with those of APPAPILLAI *et al.*⁽¹⁸⁾ and BRADDICK and LEONTIC⁽¹⁹⁾ who have since drawn similar conclusions.

Working below such a large thickness of rock (180 m.w.e.), we have observed in our cloud chamber, 6 cases of nuclear interactions of the penetrating particles underground. Five of these photographs are typical penetrating showers, while one photograph has a heavily ionizing particle coming out of the lead plate, together with some soft component. The photograph of one of the penetrating showers is reproduced in Fig. 1. Three of these interactions have their origin inside the chamber, two have a possible origin in the 10.5 cm lead block above the chamber, and one of them was possibly produced in the rock of the tunnel.

(16) H. J. BHABHA: *Proc. Roy. Soc., A* **168**, 829 (1938).

(17) S. NARANAN: *Banaras, Thesis* (1956) (unpublished).

(18) V. APPAPILLAI, A. W. MAILVAGANAM and A. W. WOLFENDALE: *Phil. Mag.*, **45**, 1059 (1954).

(15) C. D'ANDLAU: *Journ. Phys. Rad.*, **16**, 176 (1955).



Fig. 1. -- Photograph of a nuclear interaction produced by a penetrating particle underground (190 m w.e.). The heavily ionizing particle coming out of the third plate and going to the left edge of the photograph may be a heavy unstable particle which has stopped and decayed in the fourth plate. The secondary particle probably stops in the last plate after penetrating two plates. Local gas turbulence has distorted the other heavily ionizing track in the third compartment.

Ignoring the interaction in the rock and the very weak interaction in the lead plate, and so taking the other four interactions, and noting a traversal of 984 m of lead by the μ -mesons, we evaluate an upper limit of the cross-section for the production of penetrating showers by μ -mesons of mean energy 47 GeV (total depth 190 m w.e.) as

$$\sigma_{\text{p.sh.}}(\varepsilon \geq 1 \text{ GeV}) = \\ = (5.7 \pm 2.8) \cdot 10^{-30} \text{ cm}^2/\text{nucleon},$$

ε being the estimated energy of the interactions. This value is of the same order of magnitude ($1.2 \div 4.0 \cdot 10^{-30} (\text{cm}^2/\text{nucleon})$) as that obtained by other underground cloud chamber workers (³⁻⁵) working at much lower mean energies ($6 \div 14$ GeV) of μ -mesons. Very recently HIGASHI *et al.* (¹⁹) working under 200 m w.e., have reported a cross-section of $(2.9 \pm 1.1) \cdot 10^{-31} \text{ cm}^2/\text{nucleon}$, for production of showers of energies > 7 GeV.

We would like to point out here that the particles producing the interactions observed by us could not be identified as μ -mesons, but are assumed to be μ -mesons. The penetrating particles observed below a total depth of 190 m w.e., cannot be a part of the nuclear interacting component produced in the atmosphere, since the latter is rapidly absorbed in the rock with an absorption length of half a metre of rock. The observed events could therefore be either produced by μ -mesons which could penetrate this thickness of the rock by virtue of their weak interactions with matter, or they are produced by locally generated nuclear interacting secondaries of the μ -meson interactions in the rock. Very recently KITAMURA and ODA (²⁰) have calculated that below 200 m w.e.,

(¹⁹) S. HIGASHI, M. ODA, T. OSHIO, H. SHIBATA, K. WATANABE and Y. WATASE: *Progr. Theor. Phys.*, **16**, 250 (1956).

(²⁰) T. KITAMURA and M. ODA: *Progr. Theor. Phys.*, **16**, 252 (1956).

the ratio of the frequency of occurrence of the nuclear interactions produced by π -mesons to the frequency of those produced by μ -mesons is 1.75, for interactions of threshold energies ≥ 1 GeV. This uncertainty about the nature of the penetrating particles producing the interactions, leads us to regard the above cross-section as an upper limit for the nuclear interactions of μ -mesons underground.

The above mentioned observed upper limit of the cross-section is not in disagreement with the theoretical value of $\sigma_{\text{p.sh.}}(\varepsilon > 1 \text{ GeV}) = 3.1 \cdot 10^{-30} \text{ cm}^2/\text{nucleon}$ calculated, as first indicated by GEORGE and EVANS (¹), by interpreting the interactions as the photonuclear interactions of the virtual photons associated with μ -mesons in flight. The poor statistics available for cloud chamber results do not permit any definite conclusions regarding the variation of this cross-section with increasing energy of μ -mesons.

Two cases of large angle scatterings of penetrating particles have been observed, where the two particles having mean (+) scattering angles of $2.6^{+0.4}_{-0.3}$ degrees and $1.7^{+0.4}_{-0.2}$ degrees have scattered through $(13.5 \pm 0.5)^\circ$ and $(22.5 \pm 0.5)^\circ$ respectively, in one of the lead plates inside the chamber. If these scatterings are due to nuclear scattering of μ -mesons, then they give a cross-section of σ (scattering) $= (6.3 \pm 4.5) \cdot 10^{-31} \text{ cm}^2/\text{nucleon}$, for μ -mesons in lead. The experimental limitations in the measurement of small scattering angles, do not permit us to state anything about the anomalous cross-section (²¹) (*) for large angle scattering of high energy μ -mesons.

The following main results were ob-

(²¹) B. LEONTIC and A. W. WOLFENDALE: *Phil. Mag.*, **44**, 1101 (1953).

(*) These authors have summarized the results of sea level experiments on large angle scatterings of μ -mesons.

(+) The large angles were excluded while taking the mean of the scattering angles in the other plates.

tained for the electronic component in equilibrium with μ -mesons underground. (a) the average number of electrons in equilibrium with a μ -meson in lead is $0.172^{+0.012}_{-0.002}$ in good agreement with the value 0.164 calculated from Bhabha's (16) theory. (b) The numbers of knock-on cascade showers of energies (*) greater than 600 MeV and 1.5 GeV, are $(7.0 \pm 1.4) \cdot 10^{-5}$ and $(2.0 \pm 0.75) \cdot 10^{-5}$ per meson per g/cm^2 of lead respectively, again in good agreement with the values of $9.5 \cdot 10^{-5}$ and $2.26 \cdot 10^{-5}$ per meson per g/cm^2 of lead calculated from Bhabha's theory.

In conclusion, we would like to state that in conformity with other later experiments (5,18) there is no evidence for the existence of a large cross-section for a special phenomenon called the associated production of penetrating particles (A.P.P.). The results on the equilibrium electronic component, are in

agreement with the theoretical expectations. The upper limit of $(5.7 \pm 2.8) \cdot 10^{-31} \text{ cm}^2/\text{nucleon}$, for nuclear interactions of the underground μ -mesons of mean energy 47 GeV is, within statistics, of the same order of magnitude as the cross-section obtained by other cloud chamber workers at lower mean energies of μ -mesons (3–15 GeV). The cross-section for large angle scattering of μ -mesons is of the same order of magnitude as the cross-section for nuclear interactions.

* * *

We have great pleasure in thanking Professor H. J. BHABHA, F.R.S., for his keen interest in the work and for helpful discussions. We have pleasure in thanking Dr. A. W. WOLFENDALE for his comments, and Mr. B. GUZDER for the prompt construction of the caravan trailer and the invaluable help rendered in transporting it to the tunnel. Thanks are also due to Mr. K. F. DINSHAW for his help in running the chamber, and to Messrs. D. COWASJEE & Co. for permission to work in the tunnel.

(*) The energies of the showers were estimated using Hazen's (22) experimental results.

(22) W. E. HAZEN: *Phys. Rev.*, **99**, 911 (1955).

Nucleon-Surface Interaction and the (p, n) Reactions.

J. SAWICKI and Z. SZYMANSKI

Institute of Physics, Polish Academy of Sciences - Warsaw

(ricevuto il 14 Febbraio 1957)

Recently ⁽¹⁾ (*) the angular distribution and the neutron polarization of the neutron from (p, n) reactions were calculated under the assumption that a direct mechanism of the type as proposed by AUSTERN *et al.* ⁽²⁾ is the primary mechanism operative in a (p, n) reaction. This mechanism dominates over the compound nucleus formation in a number of particular cases, when we are dealing with a reaction far away the pronounced resonances of the excitation curve and for nuclei containing one outer nucleon (or a few nucleons) the most loosely bound with a double magic (or with closed subshells) core. It applies, before all, to sufficiently small energies (***) of the incident protons, when the only neutron that can be knocked out from the nucleus is the outer one.

Following AUSTERN *et al.* ⁽²⁾ and similarly as in I we assume that the neutron which is initially the most loosely bound (with a spin-zero core) and which is in state of total angular momentum j_i , orbital angular momentum l_i and z -component m_i , is knocked out from the surface of the nucleus by the incoming proton which is then captured into a state of total angular momentum j_f , orbital angular momentum l_f and z -component m_f .

It was assumed in I that the knock-out mechanism is due to the interaction of the incident proton with the target neutron i.e. the potential V_{np} . It seems, therefore, interesting to investigate the contributions to the reaction from the interactions of both the nucleons with the surface of the core in the sense of the Bohr-Mottelson model.

In the case of target nuclei considered here (one or a few nucleons outside the core) the equilibrium deformations of the core are expected to be rather small (almost spherical nucleus). Only vibrational excitations of the surface should, therefore, contribute. That means that the rotational excitations of the target nucleus are to be neglected. In this situation the weak coupling approximation for the nucleon-

(¹) J. SAWICKI: *Phys. Rev.*, **104**, 1441 (1956) and *Act. Phys. Pol.*, in the press.

(*) Further referred to as I.

(²) N. AUSTERN, S. T. BUTLER and H. MC MANUS: *Phys. Rev.*, **92**, 350 (1953).

(***) One must remember, however, that the energy has to be sufficiently high ($\sim 5 \div 15$ MeV) to neglect the compound formation important at small energies.

surface interaction is applicable. The contributions to the (p, n) transition operator due to these interactions consists then of an additional proton-neutron interaction via virtual phonon excitations of the surface plus similar proton (neutron) selection terms. These interactions are of the type of particle-core-particle couplings i.e. interactions of the 2-nd order in the coupling constant.

The neutron and the proton are assumed to interact with the surface via the usual interactions (in the notations of BOHR and BOHR and MOTTELSON⁽³⁾):

$$(1a) \quad H_{\text{int}}^{(p)}(\mathbf{r}_p, \alpha_\mu) = -V_0^{(p)}R_0\delta(r_p - R_0) \sum_{\mu=-2}^{+2} \alpha_\mu Y_{2\mu}(\Omega_p),$$

$$(1b) \quad H_{\text{int}}^{(n)}(\mathbf{r}_n, \alpha_\mu) = -V_0^{(n)}R_0\delta(r_n - R_0) \sum_{\mu} \alpha_\mu Y_{2\mu}(\Omega_n),$$

$$(2) \quad H_{\text{int}} = H_{\text{int}}^{(p)} + H_{\text{int}}^{(n)},$$

where $V_0^{(p)}$, $V_0^{(n)}$ are the square well depths approximate to the bound proton and neutron (*).

All the particle-core couplings are to be written in the form of the (second order perturbation) operator:

$$(3) \quad \Delta V = \sum_{H'_0 \alpha'} \frac{H_{\text{int}} | H'_0 \alpha' \rangle \langle H'_0 \alpha' | H_{\text{int}} }{E_0 - H'_0},$$

where E_0 is the total energy of the system in the initial and final states and $|H'_0 \alpha'\rangle$ denotes an eigenket of the unperturbed hamiltonian:

$$(4) \quad H_0 = H_s + T_n + T_p + V_n + V_p,$$

where H_s is the hamiltonian of the surface; $T_p(T_p)$ and $V_n(V_n)$ denote the kinetic and potential energies of the proton (neutron), respectively.

The energy H'_0 of an intermediate state is the sum of the proton energy $H_0'^{(p)}$, the neutron energy $H_0'^{(n)}$ and the phonon energy $= \hbar\omega$ (there is only one phonon transition involved).

The (p, n) reaction amplitude is calculated according to I in the spirit of Tobocman's⁽⁴⁾ with the only difference that the transition operator V_{np} is replaced by $V_{np} + \Delta V$.

For the sake of numerical computations we shall confine ourselves to the bound states S (i.e. $l_i = l_f = 0$), where the spin-orbit coupling does not operate. To simplify the computations the spin-orbit coupling will be neglected in the V_p and V_n potentials.

The initial state of the system corresponding to our scattering problem is:

$$(5) \quad |E_0; i\rangle = |000\rangle \cdot \Psi_i[\mu_i] \cdot \Psi[\mu_p],$$

(3) A. BOHR: *Kgl. Dan. Mat. Fys. Medd.*, **26**, no. 14 (1952); A. BOHR and B. MOTTELSON: *Kgl. Dan. Mat. Fys. Medd.*, **27**, no. 16 (1953).

(*) This point is discussed below.

(4) W. TOBOCMAN: *Phys. Rev.*, **94**, 1655 (1954).

where $|000\rangle = |N = 0, R = 0, m_R = 0\rangle$ denotes the unperturbed state of the surface and the wave function of the bound state of the neutron is assumed according to I in the form:

$$(6) \quad \Psi_i[\mu_i] = \mathcal{R}_0^{-\varepsilon_i}(r_n) \cdot Y_{00}(\Omega_n) \cdot \chi_{\mu_i}(\sigma_n),$$

and the incident proton wave is:

$$(7) \quad \Psi_p[\mu_p] = \sum_{L_p M_p} b^*(L_p M_p) \mathcal{R}_{L_p}^{E_p + \varepsilon_f}(r_p) Y_{L_p M_p}(\Omega_p) \chi_{\mu_p}(\sigma_p).$$

The final state « equivalent » in the sense of Toboeman's theory may be written as:

$$(8) \quad \langle E_0; f | = \langle 000 | \cdot \Psi_f^*[\mu_f] \cdot \Psi_n[\mu_n],$$

where:

$$(9) \quad \Psi_f^*[\mu_f] = \mathcal{R}_0^{*-e_f}(r_p) \cdot Y_{00}^*(\Omega_p) \cdot \chi_{\mu_f}(\sigma_p),$$

denotes the bound state of the proton and

$$(10) \quad \Psi_n[\mu_n] = \begin{cases} 0, & \text{for } r_n < R_0, \\ \sum_{L M_L} a(L M_L) \mathcal{R}_L^{*E_0 + \varepsilon_f} \cdot Y_{L M_L}^*(\Omega_n) \cdot \chi_{\mu_n}^*(\sigma_n), & \text{for } r_n \geq R_0, \end{cases}$$

is the outgoing neutron wave. The « Toboeman radius » is assumed to be the nuclear radius R_0 ($R_0 = 1.45 \cdot A \cdot 10^{-13}$ cm).

The intermediate states are:

$$(11) \quad |H'_0 \alpha' \rangle = |NRm_R\rangle \cdot \Psi[\mu'_p] \cdot \Psi[\mu'_n],$$

where

$$(12) \quad \Psi[\mu'_p] = \mathcal{R}_0'^{H(p)}(r_p) \cdot Y_{l'_p m'_p}(\Omega_p) \cdot \chi_{\mu'_p}(\sigma_p),$$

$$(13) \quad \Psi[\mu'_n] = \mathcal{R}_0'^{H(n)}(r_n) \cdot Y_{l'_n m'_n}(\Omega_n) \cdot \chi_{\mu'_n}(\sigma_n).$$

The summation over all the intermediate states $\sum_{\alpha' H'_0}$ is to be understood as the operator:

$$(14) \quad \int dH'_0^{(p)} \int dH'_0^{(n)} \int dH'_0 \sum_{NRm_R} \sum_{l'_p m'_p} \sum_{l'_n m'_n} \sum_{\mu_p} \sum_{\mu_n} \delta(H'_0 - H_0^{(p)} - H_0^{(n)} - N\hbar\omega).$$

After performing all the angular spin and other integrations and summations, making use of the properties of the operators α_μ , the well known formula for the products of two spherical harmonics, the properties of the vector addition coefficients and various orthogonality relations we finally obtain the correction to the reaction

amplitude due to the operator ΔV in the form:

$$(15) \quad \langle E_0; f | \Delta V | E_0; i \rangle = \Delta M(\mu_p, \mu_i \rightarrow \mu_f \mu_n) = \delta_{\mu_p \mu_f} \cdot \delta_{\mu_i \mu_n} (\text{const}_1 \cdot \cos 2\theta - \text{const}_2).$$

The $^{29}\text{Si}(p, n)^{29}\text{P}$ reaction ($l_i = l_f = 0$) is considered similarly as in I. The binding energies are $\varepsilon_i = 8.194$ MeV, $\varepsilon_f = 2.691$ MeV, $E_0 = -2.194$ MeV which corresponds to the energy of the incident protons $E_p = 6$ MeV. $\hbar\omega$ calculated according to BOHR (3) = 4.955 MeV.

The numerical computations using various approximations were performed in two cases: 1) disregarding the Coulomb effects of the incident proton wave; 2) including Coulomb effect.

In both the cases the selfaction terms appear more important than the mutual n-p interaction terms. The correction to the reaction amplitude coming from ΔV was found to be nearly isotropic. To estimate the relative contribution of the correction considered herein to the total (p, n) process according to I the main part of the reaction amplitude was taken to be

$$(16) \quad \langle E_0; f | V_{np} | E_0; i \rangle = M(\mu_p, \mu_i \rightarrow \mu_f \mu_n),$$

V_{np} being of the form: $V_{np} = (V_1 + V_2 \boldsymbol{\sigma}_n \cdot \boldsymbol{\sigma}_p) \delta(\mathbf{r}_n - \mathbf{r}_p)$.

For the numerical estimation V_{np} was taken to be:

$$(17) \quad V_{np} = \frac{4\pi\hbar^2}{M} \delta(\mathbf{r}_n - \mathbf{r}_p) \left\{ \frac{a_1 + a_0}{2} + \frac{a_1 - a_0}{2} P_\sigma \right\},$$

where $a_1 = 4.31 \cdot 10^{-13}$ cm and $a_0 = -24.34 \cdot 10^{-13}$ cm are the triplet and the singlet n-p scattering lengths, respectively, and $P_\sigma = \frac{1}{2}(1 + \boldsymbol{\sigma}_n \cdot \boldsymbol{\sigma}_p)$. Hence:

$$(18) \quad M(\mu_p \mu_i \rightarrow \mu_f \mu_n) = M_{00} \left\{ \frac{a_1 + a_0}{2} \delta_{\mu_p \mu_f} \cdot \delta_{\mu_i \mu_n} + \frac{a_1 - a_0}{2} \delta_{\mu_i \mu_f} \cdot \delta_{\mu_p \mu_n} \right\},$$

where M_{00} is given in I.

The angular distribution is given by:

$$(19) \quad \alpha(\theta) = \sum_{\mu_n \mu_i} \sum_{\mu_p \mu_f} |M(\mu_p \mu_i \rightarrow \mu_n \mu_f) + \Delta M(\mu_p \mu_i \rightarrow \mu_n \mu_f)|^2.$$

The numerical values of the relative contributions of the operator ΔV are given by:

$$(20) \quad x = \frac{\alpha(\theta) - \alpha_0(\theta)}{\alpha_0(\theta)},$$

where

$$(21) \quad \alpha_0(\theta) = \sum_{\mu_n \mu_i} \sum_{\mu_p \mu_f} |M(\mu_p \mu_i \rightarrow \mu_n \mu_f)|^2.$$

The numerical values of x ($\theta = 0$) for the cases 1) and 2) are +4.25% and 12.04%, respectively. With the increase of θ , x increases to $\sim 20\%$ in the minimum of $\alpha_0(\theta)$. The form of the resulting angular distribution remains unchanged.

The correction due to ΔV increases the differential cross-section by a small amount. The numerical results are to be trusted only rather qualitatively because of great uncertainty in the numerical values of the constant coefficients in V_{np} and the values $V_0^{(p)}$, $V_0^{(n)}$. The latter were assumed to be the square well depths corresponding to the bound states of the outer nucleons, while BRINK⁽⁵⁾ assumes an optical model square well for the neutron inelastically scattered from a heavy nucleus. On the other hand, HAYAKAWA and YOSHIDA⁽⁶⁾ use square wells approximate to bound states for the scattering of protons from ^{24}Mg .

It seems possible that the most reasonable choice would be to use bound state square wells for those terms of Eq. (16) where respective $H_{int}^{(-)}$ operate on bound states and to use optical model square wells when operating on free scattering states. This should increase the effect of ΔV .

* * *

The authors are indebted to Dr. M. GUNTHER for a helpful discussion.
A more extensive paper on this subject will appear in *Acta Physica Polonica*.

⁽⁵⁾ D. M. BRINK: *Proc. Phys. Soc.*, A **68**, 994 (1955).

⁽⁶⁾ S. HAYAKAWA and S. YOSHIDA: *Proc. Phys. Soc.*, A **68**, 656 (1955).

A Non-Linear Theory of Phase Oscillations Induced by Radiation Fluctuations in Synchrotrons.

A. N. MATVEEV

State University - Moscow

(ricevuto l'11 Marzo 1957)

It was shown in (1) that radiation fluctuations induce phase oscillations of electrons in synchrotrons. Similar results for betatron oscillations were reported in papers (2,3). A generalization of the results, reported in (1), for AG-synchrotrons was given in (1,4).

In papers (1,4,5) a linear theory was used. This linear theory is valid only when amplitudes of oscillations are small. The main chance of the theory is that about losses of electrons due to oscillations. These losses are significant only when amplitudes of oscillations are large enough. Therefore one has to abolish the above mentioned restriction about the smallness of oscillations. In other words it is necessary to consider a non-linear theory of phase oscillations, induced by radiation fluctuations.

A non-linear stochastic equation for phase oscillations induced by radiation fluctuations has the form:

$$(1) \quad \ddot{\Psi} + \gamma \dot{\Psi} + f^2 [\cos \varphi_s - \cos (\varphi_s + \Psi)] = \frac{k\omega\alpha}{\lambda E_s} [W_s - \sum_i \varepsilon_i \delta(t - t_i)],$$

where

$$\Psi = \varphi - \varphi_s, \quad \lambda = 1 + L/2\pi R_0, \quad \omega = \frac{e}{R_0 \lambda}, \quad f^2 = \frac{k\omega^2 \alpha}{2\pi \lambda} \frac{eV_0}{E_s},$$

$$\gamma = (4 - \alpha) \frac{2\omega r_0}{3R_0} \left(\frac{E_s}{mc^2} \right)^3, \quad r_0 = \frac{e^2}{mc^2}, \quad \frac{\delta \langle R \rangle}{\langle R \rangle} = \alpha \frac{\delta E}{E_s}, \quad W_s = \frac{2}{3} \frac{ce^2}{R_0^2} \left(\frac{E_s}{mc^2} \right)^4,$$

(1) M. SANDS: *Phys. Rev.*, **97**, 470 (1955).

(2) A. A. SOKOLOV and J. M. TERNOV: *Dokl. Akad. Nauk SSSR*, **92**, 537 (1953); *Zu. Éksper. Teor. Fiz.*, **25**, 698 (1953).

(3) A. A. SOKOLOV and J. M. TERNOV: *Dokl. Akad. Nauk SSSR*, **97**, 823 (1954); *Zu. Éksper. Teor. Fiz.*, **28**, 432 (1955).

(4) A. A. KOLOMENSKIY: *Zu. Éksper. Teor. Fiz.*, **30**, 207 (1956).

(5) A. N. MATVEEV: *Dokl. Akad. Nauk SSSR*, **108**, 432 (1956).

L is the total length of straight sections of a synchrotron;
 R_0 is the radius of curvature of the synchrotron;
 ϵ is the energy of the photon;
 φ is the phase of the rf-field (radio-frequency field);
 k is the order of the harmonics of a rf-field, eV_0 is the amplitude of the rf-field.

When Ψ is small the Eq. (1) may be transformed into the linear stochastic Eq. (2) of paper ⁽⁶⁾.

Putting

$$\zeta = \int_0^t f dt, \quad \Psi = uz, \quad u = \exp\left(-\frac{1}{2} \int_0^\zeta q d\zeta\right), \quad q = \frac{f'}{f} + \frac{\gamma}{f}, \quad z' = \frac{dz}{d\zeta}, \quad \text{etc.,}$$

we obtain instead of Eq. (1) the following equation:

$$(2) \quad z'' + \frac{1}{u} [\cos \varphi_s - \cos (\varphi_s + uz)] = \frac{k\omega\alpha}{\lambda E_s u f} [W_{1s} - \sum_i \epsilon_i \delta(\zeta - \zeta_i)],$$

where we have omitted the term $-(q^2/4) + (q'/2)z$ which is small. We can also neglect terms proportional to u' . Therefore for the free motion of the system in consideration we have

$$(3) \quad \frac{z'^2}{2} + \frac{1}{u^2} [uz \cos \varphi_s - \sin (\varphi_s + uz)] = Q = \text{const},$$

and bound states correspond to the following values of Q :

$$(4) \quad -\frac{1}{u^2} \sin \varphi_s = Q_{\min} < Q < Q_{\max} = \frac{1}{u^2} (-2\varphi_s \cos \varphi_s + \sin \varphi_s).$$

An influence of quantum fluctuations of a radiation may be taken into account in the following manner. It follows from Eq. (2) and (3), that

$$(5) \quad \Delta z' = -\frac{k\omega\alpha}{\lambda E_s u f} \epsilon, \quad \langle \Delta Q \rangle = \frac{1}{2} \langle (\Delta z')^2 \rangle.$$

Using the condition (4) for the existence of bound states we can write the condition that electron losses be small in the following form

$$(6) \quad \frac{55\pi}{32\sqrt{3}} \frac{k\alpha}{\lambda(4-\alpha)} \frac{r_0}{R_0} \frac{hc}{e^2} \frac{mc^2}{eV_0} \left(\frac{E_s}{mc^2}\right)^3 \ll (\sin \varphi_s - \varphi_s \cos \varphi_s).$$

It is easily seen that this condition (6) of the non-linear theory is stronger than the corresponding condition of the linear theory. This condition confirms the assertion ^(5,7), that the utilization of an alternating gradient principle is inevitable for energies of electrons of few GeV.

⁽⁶⁾ A. N. MATVEEV: *Dokl. Akad. Nauk SSSR*, **109**, 495 (1956).

⁽⁷⁾ A. N. MATVEEV: *Dokl. Akad. Nauk SSSR*, **107**, 671 (1956).

Emission of an Electron Pair in a K^+ -Decay (*).

R. LEVI-SETTI (+) and W. SLATER

*The Enrico Fermi Institute for Nuclear Studies
The University of Chicago, Chicago, Illinois*

(ricevuto il 20 Marzo 1957)

In an emulsion stack (1) exposed to 4.5 GeV π^- from the Berkeley Bevatron, a K^+ particle has been observed which decays at rest into a low energy π^+ and two lightly ionizing particles. Fig. 1 contains a photograph of the event. The measured data are given in Table I.

The K^+ is ejected from a $(14+1\pi)$ star and travels 5.4 cm through 50 pellicles. Its mass, from multiple scattering vs. range (constant sagitta) is $(1070 \pm 350) m_e$. We assume in the following that this particle has the known K^+ mass, $M_K = 966 m_e$. No associated strange particles were detected among the other prongs of the primary star. The π^+ secondary, identified by its decay, $\pi-\mu-e$, has a range of 2.01 mm in three pellicles, corresponding in this stack to an energy at ejection of 9.6 MeV.

Because of the large dip angles of the light secondaries e_1 and e_2 , 74° and 78° , respectively, and because of their very low ionization (~ 10 blob/100 μm), a special procedure was necessary to measure their scattering. A profile of each track in two pellicles was obtained by plotting the y and z co-ordinates of the individual blobs. Scattering was then measured on these plots, the cells being defined by constant displacements in z instead of in x , as done for flatter tracks. The distortion vector has been measured in both pellicles; its magnitude both times being 25 μm , corresponding to 20 covans. The sagittae have been accordingly corrected, before applying noise elimination. The values of $p\beta$ for e_1 and e_2 are (47 ± 10) and (50 ± 11) MeV/c respectively. The relative blob densities of e_1 and e_2 compared with that of steep electrons from μ^+ -decays are 0.91 ± 0.14 and 1.07 ± 0.14 . Scattering and ionization results are consistent with e_1 and e_2 being electrons. To conserve charge, these particles must be an electron-positron pair.

(*) Work supported by the Greenewalt Nuclear Physics Fund, the Office of Naval Research, and the Atomic Energy Commission.

(+) On leave of absence from the University of Milan.

(¹) R. LEVI SETTI and W. SLATER: *Nuovo Cimento*, in press.



Fig. 1. — Photomicrograph of event EFINS-K15. Event observed by P. J. Kliauga.

TABLE I.

Particle	Dip angle (degrees)	Polar angle (degrees)	Observed length or range (mm)	$p\beta$ (from scattering (MeV/c)
π^+	-63 ± 2	-8 ± 1	$2.01 \pm .10$	—
e_1	-76 ± 3	0 ± 5	1.7	47 ± 10
e_2	-74 ± 3	58 ± 5	1.7	50 ± 11

K^+ decays involving the emission of electron pairs, identified as K_{π^0} ⁽²⁾ and K_{μ^0} modes⁽³⁾ have provided evidence for the identity of the neutral particles emitted in these decays. Analogous evidence for the $K_{\pi^0}(\tau')$ is provided by the present event.

We can, following an analysis similar to that of HOANG *et al.*⁽³⁾, treat the pair as a single fictitious particle whose 4-momentum $P_0 = P_{e_1} + P_{e_2}$. From the data in Table I we can evaluate:

$$M_K c^2 = |P_0| = (12.9 \pm 3.6) \text{ MeV}$$

$$E_0 = eP_4/i = (97 \pm 15) \text{ MeV}$$

$$|\mathbf{p}_0| = (96 \pm 15) \text{ MeV/c}$$

$$\beta_0 = 0.991 \pm 0.002.$$

If we first assume that this event represents $K^+ \rightarrow \pi^+ + e^+ + e^- + x$,

$$M_x c^2 = (M_K c^2 - E_{\pi^+} - E_0)^2 - (\mathbf{p}_0 + \mathbf{p}_{\pi^+})^2 c^2 = (238 \pm 28) \text{ MeV}.$$

Since this mass corresponds to no known particle, we assume that at least two neutral particles are included in the decay. This rules out, for example, a possible direct decay $K_{\pi^0}^+ \rightarrow \pi^+ + (e^+ + e^- + \gamma)$. We further assume that the electron pair arises from Dalitz' alternate π^0 decay, by internal conversion $\pi^0 \rightarrow e^+ + e^- + \gamma$ ⁽⁴⁾. This is supported by the proximity of the apex of the pair to the point of K^+ decay (the points are, in fact, indistinguishable) and by the measured values of the electron energies. Writing the decay scheme $K^+ \rightarrow \pi^+ + \pi^0 \rightarrow [e^+ + e^- + \gamma] + y$, we can estimate limits for M_y . The scalar product $(P_{\pi^0} - P_0)^2$ gives the following relation between the energy of the π^0 and the angle θ between \mathbf{p}_0 and \mathbf{p}_{π^0} :

$$(1) \quad \gamma(1 - \beta\beta_0 \cos \theta) = (M_0^2 + M_{\pi^0}^2)c^2/2M_{\pi^0}E_0 = 0.71 \pm 0.11,$$

where $E_{\pi^0} = (1 - \beta^2)^{-\frac{1}{2}}M_{\pi^0}c^2$.

A plot of $|\mathbf{p}_{\pi^0}| = \beta\gamma M_{\pi^0}c$ vs. $\cos \theta$ is shown in Fig. 2. We calculate the limiting

⁽²⁾ F. ANDERSON, G. LAWLOR and T. E. NEVIN: *Proc. of the Pisa Conference* (June 1955), *Suppl. Nuovo Cimento*, **4**, 225 (1956) and *Nuovo Cimento*, **2**, 608 (1955).

⁽³⁾ G. YEKUTIELI, M. E. KAPLON and T. F. HOANG: *Phys. Rev.*, **101**, 506 (1956).

⁽⁴⁾ R. H. DALITZ: *Proc. Phys. Soc.*, **A 64**, 667 (1951).

values of M_y from:

$$(2) \quad \left\{ \begin{array}{l} M_y c^2 = [(M_K c^2 - E_{\pi^+} - E_{\pi^0})^2 - (\mathbf{p}_{\pi^+} + \mathbf{p}_{\pi^0})^2 c^2]^{\frac{1}{2}}, \\ = [(M_K c^2 - E_{\pi^+} - E_{\pi^0})^2 - (p_{\pi^+} + p_{\pi^0} \cos \varphi)^2 c^2 - (p_{\pi^0} \sin \varphi)^2 c^2]^{\frac{1}{2}}, \end{array} \right.$$

where $\cos \varphi = \mathbf{p}_{\pi^+} \cdot \mathbf{p}_{\pi^0} / \mathbf{p}_{\pi^+} + \mathbf{p}_{\pi^0}$.

In this event, the angle between \mathbf{p}_{π^+} and \mathbf{p}_{π^0} is very small (8°), so that $\varphi \approx \theta$. With this approximation, using (1), and inserting numerical values from Table I, we can rewrite (2)

$$(2') \quad M_y^2 = (7.91 - 5.88\gamma) M_{\pi^0}^2.$$

Fig. 2 implies $\gamma_{\min} = 1.06 \pm 0.05$ so $M_y(\max)$ is $(1.30 \pm 0.11) M_{\pi^0}$. γ_{\max} from formula (1) is 176, obviously exceeding the available energy. It is determined therefore by the condition $M_y = 0$.

Within the framework of our initial assumption that the observed electron is a « Dalitz Pair », we conclude that y , if it represents a single particle, may be a photon or neutral pion, a neutrino being excluded by the assumption that all K-mesons are bosons.

K^+ decays into a single π^+ (\circ) with a continuous energy spectrum in the region $0 \div 50$ MeV (K_{π^+}) have been attributed to the alternate τ -decay mode ($^*(\circ)$): $\tau^+ \rightarrow \pi^+ + 2\pi^0$. In fact, no stopping π^+ from K^+ 's have been found to exceed the maximum allowed energy of 54 MeV for this decay, except of course the monoenergetic π^+ 's (108 MeV) from K_{π^2} . The event here analyzed strongly suggests the presence of at least one π^0 among the secondaries of K_{π^3} , and furthermore shows that the assumption of another π^0 being emitted is compatible with the kinematics of the decay.

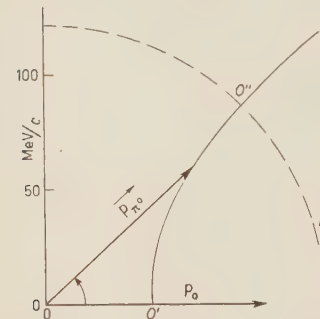


Fig. 2. — a) Locus of the points satisfying the equation $\gamma(1 - \beta_0 \cos \theta) = 0.71$; b) Circle of radius $0.0'' = p_{\pi^0 \max}$; corresponding to $M_y = 0$.

of another π^0 being emitted is compatible with the kinematics of the decay.

* * *

It is a pleasant duty to thank Dr. E. J. LOFGREN and his co-workers of the University of California Radiation Laboratory for their kind assistance in obtaining and carrying out the exposures used in the present investigation. We are also indebted to Professor V. L. TELELDI for helpful discussions and criticism.

Note. — After completion of the present manuscript, we received a preprint by G. HARRIS, J. OREAR, and S. TAYLOR (Nevis Report No. 31, Lifetime of the Neutral Pion) in which two events similar to the one described here are mentioned.

(*) J. CRUSSARD, M. F. KAPLON, J. KLARMANN and J. H. NOON: *Phys. Rev.*, **93**, 253 (1954).

(0) R. H. DALITZ: *Proc. Phys. Soc.*, A **77**, 710 (1953); A. PAIS: *Phys. Rev.*, **86**, 663 (1953).

**A Discussion of the Possibility of Detecting Asymmetries
in the Λ^0 Decay.**

G. MORPURGO

*Istituto di Fisica e Scuola di Perfezionamento in Fisica Nucleare dell'Università - Roma
Istituto Nazionale di Fisica Nucleare - Sezione di Roma*

(ricevuto il 20 Marzo 1957)

This note is a continuation of a previous one⁽¹⁾ in which the angular distributions in the decay of an hyperon were discussed under the hypothesis of parity non conservation in the weak interactions. Spin $\frac{1}{2}$ will be assumed for the hyperon.

Call φ the angle between the plane of production and the plane of decay of the hyperon, and θ the angle between the line of flight of the produced hyperon (in the center of mass system of the colliding pion and nucleon) and the line of flight of the decay products of the hyperon (in its rest system); then the general expected form of the distribution in θ and φ , if parity is not conserved in the decay of the hyperon is $I(\theta, \varphi) = 1 + C \sin \theta \sin \varphi$. Integrating over θ the distribution in φ results

$$(1) \quad I(\varphi) = 1 + B \sin \varphi.$$

The constant B was given in⁽¹⁾; it is:

$$(2) \quad B = (-i) \frac{\pi}{4} \frac{ab^* + a^*b}{|a|^2 + |b|^2} \frac{\lambda_{\frac{1}{2}} \lambda_{-\frac{1}{2}}^* - \lambda_{-\frac{1}{2}} \lambda_{\frac{1}{2}}^*}{|\lambda_{\frac{1}{2}}|^2 + |\lambda_{-\frac{1}{2}}|^2},$$

where the same notation as in⁽¹⁾ has been used; the constants a and b characterize here the parity mixture in the decay; and the constants λ characterize the polarization of the produced hyperon; more precisely it is:

$$\langle \sigma_y \rangle = (-i) \frac{\lambda_{\frac{1}{2}} \lambda_{-\frac{1}{2}}^* - \lambda_{-\frac{1}{2}} \lambda_{\frac{1}{2}}^*}{|\lambda_{\frac{1}{2}}|^2 + |\lambda_{-\frac{1}{2}}|^2},$$

the y axis being normal to the plane of production.

⁽¹⁾ G. MORPURGO: *Nuovo Cimento*, **4**, 1222 (1956); also **3**, 1069 (1956).

The purpose of this note is to examine the dependence of $\langle \sigma_y \rangle$ on the angle of production of the hyperon and, in particular 1) to determine the production angle at which the polarization may be expected to be maximum 2) to determine the maximum amount of the asymmetry in $I(\varphi)$ which may be found, in the most favourable conditions if one integrates over all the possible production angles. We shall confine to low energies of the produced Λ^0 , K^0 pair (2), so that the outgoing Λ^0 K^0 wave may be characterized by three complex parameters a_0 , a_1 and a_2 describing the amplitudes of an s and two p waves. In the following θ' will be the production angle of the K^0 meson in the center of mass system.

In terms of the three complex parameters introduced above, one may easily write the polarization appearing in (2) as:

$$(3) \quad \langle \sigma_y \rangle = (-i) \sqrt{\frac{3}{2}} \sin \theta' \left\{ \frac{(a_2^* a_0 - a_2 a_0^*) + \sqrt{3} \cos \theta' (a_2^* a_1 - a_1^* a_2)}{|a_0|^2 + \frac{3}{2}|a_2|^2 - 3 \cos^2 \theta' (|a_1|^2 - \frac{1}{2}|a_2|^2) + \sqrt{3} \cos \theta' (a_0 a_1^* + a_1 a_0^*)} \right\}$$

Assume now, as it seems to be the case experimentally (2), that the angular distribution in the center of mass system shows a pronounced minimum at 180° . Then it follows that

$$(4) \quad a_0 \simeq a_1 \sqrt{3},$$

which is the condition for the vanishing of the scattered intensity at 180° . Expression (3) may then be rewritten as

$$\langle \sigma_y \rangle = \frac{x \sqrt{2} \sin \delta \sin \theta'}{1 + \cos \theta' + \frac{1}{2} x^2 (1 - \cos \theta')},$$

where δ is the relative phase between a_1 and a_2 and x is defined as $|a_2|/|a_1|$; x may be determined experimentally from the angular distribution (3).

It is apparent that the polarization is proportional to $\sin \delta$ on which we know nothing; assuming that it does not vanish we may ask, for a given x , which is the angle for which the polarization has a maximum. We find:

$$(5) \quad \cos \theta' = \frac{x^2 - 2}{x^2 + 2},$$

the polarization being then just equal to $\sin \delta$.

In order to detect an asymmetry one should therefore collect mainly the events produced at an angle satisfying (5).

We may next ask what may be the maximum asymmetry in $I(\varphi)$, found if we collect all the events, independently of their production angle, and when the most favourable assumption is made:

$$(6) \quad \frac{ab^* + ba^*}{|a|^2 + |b|^2} = 1.$$

(*) Such as in the PUPPI and cow. experiment now in progress at Bologna.

(**) The angular distribution is in fact, under the assumption (4):

$$I(\theta') = (1 + \cos \theta')^2 + \frac{1}{2} x^2 \sin^2 \theta'.$$

The ratio between the number N_+ of events with φ from 0 to π , and the number N_- with φ from π to 2π is then:

$$(7) \quad \frac{N_+}{N_-} = \frac{\int_0^\pi [(1+\cos\theta')^2 + \frac{1}{2}x^2 \sin^2\theta' - \frac{x}{\sqrt{2}} \sin\delta \sin\theta'(1+\cos\theta')] \sin\theta' d\theta'}{\int_0^\pi [(1+\cos\theta')^2 + \frac{1}{2}x^2 \sin^2\theta' + \frac{x}{\sqrt{2}} \sin\delta \sin\theta'(1+\cos\theta')] \sin\theta' d\theta'} = \\ = \frac{\frac{8}{3} + \frac{2}{3}x^2 - \frac{\pi}{2\sqrt{2}}x \sin\delta}{\frac{8}{3} + \frac{2}{3}x^2 + \frac{\pi}{2\sqrt{2}}x \sin\delta}$$

It appears from this expression that even if (6) is satisfied and $\sin\delta=1$, an experimentally detectable asymmetry may be found only for x having a value in a rather restricted interval ⁽⁴⁾.

An accurate determination of the angular distribution so as to have some indication on the value of x may be therefore interesting. If x does not have a value such as to make N_+/N_- (7) sufficiently different from unity, one should try, in spite of the smaller statistics to collect only events having angles of production near to (5).

Notice that a discussion like the one made here is possible also without the condition (4) and should be repeated when a determination of the parameters of the angular distribution will be available.

* *

My interest in this question arose in conversations with Prof. J. STEINBERGER whom I would like to thank.

⁽⁴⁾ The most favourable of x is 2; for such a value and if $(ab^* + a^*b)/(|a|^2 + |b|^2) = 1$, $\sin\delta = 1$, one would get $N_+/N_- = 0.41$.

The Nuclear Potential for the K^+ -Mesons.

C. MARCHI, G. QUARENÌ and A. VIGNUDELLI

Istituto di Fisica dell'Università - Bologna

G. DASCOLA and S. MORA

Istituto di Fisica dell'Università - Parma

(ricevuto il 4 Aprile 1957)

In recent papers on the K^+ nuclear interaction, it has been discussed whether the K^+ -nuclei forces are attractive or repulsive.

OSBORNE⁽¹⁾ first suggested an attractive nuclear potential, whereas the next works⁽²⁾ have shown that the opposite solution is more reliable, i.e. a repulsive potential of the order of 10 MeV. This conclusion was suggested by considerations based on the collected data for the $K^+ + p$ process, the inelastic and elastic scattering by nuclei. We have attempted to give a stronger evidence to the repulsive potential from the elastic interaction of the K^+ -mesons with the nuclei, which seems to be the more

favorable process for an analysis of this kind.

Like the previous works, the data have been obtained by an experiment performed with photographic emulsions exposed to the K^+ -beam of the bevatron of Berkeley.

The analysis was restricted only to the small scattering angles, between 3° and 26° , because of the following reasons: *a)* In this angular interval, the shape of the cross-section is strongly affected by the Coulomb interference and therefore most sensible to the sign of the real part of the nuclear potential; *b)* From the experimental point of view, the smaller the scattering angle, the easier the distinction between elastic and inelastic scattering; *c)* The cross-section is relatively large for the smallest scattering angles.

The energy interval we have considered goes from 50 to ~ 120 MeV. The mean energy, to which refers the scattering angle distribution is 80 MeV. This value corresponds to the mean value of $(1/p\beta)^2$, weighted on the track

(¹) L. S. OSBORNE: *Phys. Rev.* **102**, 296 (1956).

(²) N. N. BISWAS, L. CECCARELLI-FABBRECHESI, M. CECCARELLI, K. GOTTSSTEIN, N. C. VARSHNEYA and P. WALOSCHEK: *Nuovo Cimento*, **5**, 123 (1957); G. COCCONI, G. PUPPI, G. QUARENÌ and A. STANGHELLINI: *Nuovo Cimento*, **5**, 172, (1957); M. BALDO-CEOLIN, M. CRESTI, N. DALLAPORTA, M. GRILLI, L. GUERRIERO, M. MERLIN, G. A. SALANDIN and G. ZAGO: *Nuovo Cimento*, **5**, 402 (1957).

observed at different energies, which is the dynamic factor contained in the Rutherford formula. As for the small

section is drawn, shows that the experimental points are in good agreement with the cross-section calculated for

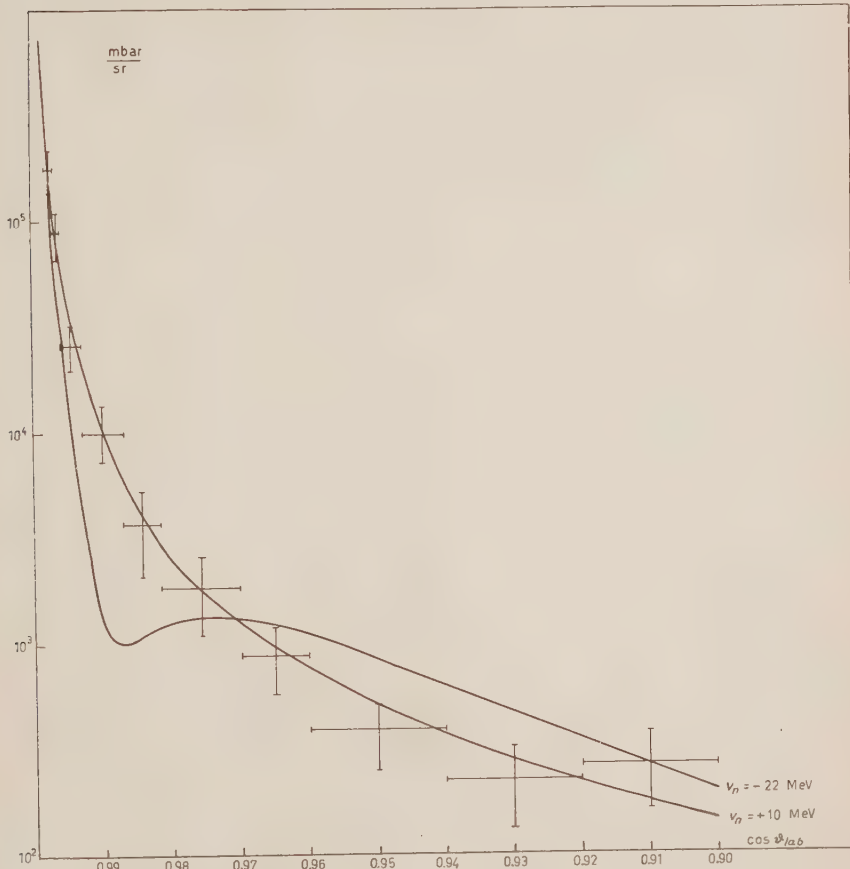


Fig. 1. — Differential cross-section for the K^+ nuclei elastic scattering at 80 MeV in nuclear emulsions. The two curves, fitting the experimental points, correspond to the real potentials $V_n = +10$ MeV and $V_n = -22$ MeV.

angles the coulombian term is in fact the most important. The mean value of 80 MeV corresponds also to the average energy of the events, which were found.

Fig. 1, where the differential cross-

$V_n = +10$ MeV. The calculation has been made by means of the optical model. The imaginary part of the potential was neglected, the mean free path of the K^+ -mesons in nuclear matter being very long, according to the small cross-section

for the incoherent scattering at this energy. The W.K.B. approximation was used as suggested by COSTA and PATERGNANI⁽³⁾.

* * *

We should like to thank Dr. GOLDHABER, who kindly provided us with

the emulsions, Dr. PATERGNANI for useful discussions, Dr. GESSAROLI for her help in the calculations and the scanning groups of the Bologna and Parma laboratories. We are also most grateful to the Town Council of Bologna for supporting us with financial help.

(3) G. COSTA and G. PATERGNANI: *Nuovo Cimento*, **5**, 448 (1957).

On Parity Non-Conservation in the Decay of Strange Particles.

N. DALLAPORTA and F. FERRARI

Istituto di Fisica dell'Università - Padova

Istituto Nazionale di Fisica Nucleare - Sezione di Padova

(ricevuto il 5 Aprile 1957)

Following the suggestion of LEE and YANG (¹), experiments have been performed in order to test the conservation of parity in weak interactions. So far most of these experiments (²) have been concerned with β -decay and in such process it appears that parity is in fact not conserved. However, in all these cases this may be connected with the peculiar nature of the neutrino: for a particle of vanishing mass, scalar and pseudoscalar interactions should always give rise to the same effects for all observable phenomena (³). Thus in some respects the non-conservation of parity in β -decay should mean transitions from an initial state of definite parity to a final state whose parity has no definite eigenvalue.

In this note some consequences of the non-conservation of parity in K-meson and hyperon decays will be considered.

At first sight, in order to solve in the easiest way the τ -0 puzzle, one could consider that the decay of K-mesons and hyperons is similar to β -decay and, therefore, assume a transition from an initial state, with definite parity, to a final state with either parity (*). However, the situation may be more complicated because

(¹) T. D. LEE and C. N. YANG: *Phys. Rev.*, **102**, 290 (1956); **104**, 254 (1956); **104**, 822 (1956).

(²) C. S. WU, E. AMBLER, R. W. HAYWARD, D. D. HOPPES and R. P. HUDSON: *An experimental test of parity conservation in beta decay* (preprint); R. L. GARWIN, L. LEDERMAN and M. WEINRICH: *Observations of the failure of conservation of parity and charge conjugation in meson decays: the magnetic moment of the muon* (preprint); B. BHOWMIK, D. EVANS and D. J. PROWSE: *On the angular correlation in the beta decay of ν -mesons observed in photographic emulsions* (preprint); N. N. BISWAS, M. CECCARELLI and J. CRUSSARD: *Nuovo Cimento*, **5**, 756 (1957).

(³) J. TIOMNO and C. N. YANG: *Phys. Rev.*, **79**, 495 (1950); A. SALAM: *Nuovo Cimento*, **5**, 299 (1957); B. F. TOUSCHEK: *Nuovo Cimento*, **5**, 754 (1957); T. D. LEE and C. N. YANG: *Parity non-conservation and a two component theory of the neutrino* (preprint); S. ONEDA: *A two component theory of the neutrino and the K-meson decays comprising two neutrinos* (preprint); J. WERLE and S. ONEDA: *Parity conservation and neutrino mass* (preprint).

(*) An objection to this assumption could be the following: if the non-conservation of parity should be linked to interacting states in which parity is not a diagonal observable, as appears to be the case for the neutrino, it is not certain that it would be applicable to decays which contain only pions and nucleons in final states. However neutrino states could be considered as intermediate states in the decay processes and would justify the lack of conservation of parity even in this case.

there is the additional fact that it cannot be excluded *a priori* that even the initial state could be without a well defined parity. This has first been considered by LEE and YANG (¹) and developed independently by SCHWINGER (²) and by BUDINI and FONDA (³) in order to introduce a possible $\text{KK}\pi$ interaction. Since the experimental indications cannot actually be considered as either proving or disproving the existence of the $\text{KK}\pi$ interaction, it may be useful not to overlook the possibility that the K-mesons and hyperons should be quantum mechanical mixtures of both parities.

Let us then consider as the most general case that even strong interactions should contain all four terms Y+K+N , Y+K-N , Y-K+N , Y-K-N and therefore be a mixture of scalar and pseudoscalar interactions.

The hyperon-boson wave produced in the pion-proton collision (*) can be written as

$$(1) \quad \left\{ \begin{array}{l} \frac{1}{2} A^{-1} \sum_M \left\{ (\lambda_M^{++} \chi_S^M + \lambda_M^{-+} \chi_S^{-M}) \theta + (\lambda_M^{-+} \chi_S^M + \lambda_M^{++} \chi_S^{-M}) \bar{\theta} + \right. \\ \left. + (-1)^{|M| - \frac{1}{2}} [(\lambda_M^{++} \chi_S^{-M} + \lambda_M^{-+} \chi_S^{-M}) \theta - (\lambda_M^{-+} \chi_S^{-M} - \lambda_M^{++} \chi_S^{-M}) \bar{\theta}] \right\} . \\ A = 2 \sum_M (\lambda_M^{*++} \lambda_M^{++} + \lambda_M^{*-+} \lambda_M^{-+}) . \end{array} \right.$$

In this formula the symbols of Morpurgo (⁵) have been used: χ and θ are the wave functions of the hyperon and of the K-meson; equal indices (+ +) means that the coefficient refers to states in which the hyperon and the K-meson are produced with the same parity, while different indices (+ -) means that the parities are different.

In what follows we will only consider hyperon decays. In fact the decay of the K-meson is complicated by the variety of its decay modes; on the other hand there is only one form of the final state for hyperons. Furthermore, as the hyperons have spin $> \frac{1}{2}$, there is the possibility of characteristic angular correlations due to the non-conservation of parity in their decay processes.

Let us now see what expression (1) implies, assuming that parity is not conserved in weak interactions: each wave function χ_{+} , χ_{-} gives rise to an outgoing wave function which will be a superposition of two waves ψ_{+} , ψ_{-} with opposite parities, that is

$$(2) \quad \left\{ \begin{array}{l} \chi_S^M \rightarrow a \psi_S^M + b \psi_S^{-M}, \\ \chi_S^{-M} \rightarrow c \psi_S^M + d \psi_S^{-M}. \end{array} \right.$$

As we do not know the effect of parity non-conservation on the probability rates a , b , c and d , we will start by assuming that these are completely arbitrary. Then, for the simplest case, in which the hyperon has spin $\frac{1}{2}$, the expressions for

(*) J. SCHWINGER: *Phys. Rev.*, **104**, 1164 (1956).

(¹) P. BUDINI and L. FONDA: *Nuovo Cimento*, **5**, 306, 666 (1957).

(²) G. MORPURGO: *Nuovo Cimento*, **3**, 1069 (1956); **4**, 1222 (1956).

(*) The target proton is unpolarized and therefore one must average over the spin direction of the proton itself.

the θ and φ distributions are given by:

$$(3) \quad \begin{cases} I_{\frac{1}{2}}(\theta) = \frac{1}{2} [1 + A_1 P_1(\cos \theta)], \\ I_{\frac{1}{2}}(\varphi) = \frac{1}{2\pi} [1 + A_1 \cos \varphi + B_1 \sin \varphi], \end{cases}$$

where θ is the angle between the line of flight (in the rest system of the decaying hyperon) of the π^- produced in the decay and the line of flight of the hyperon, φ is the angle between the plane of production and the plane of decay and

$$\begin{aligned} A_1 &= \frac{a^*d + ad^* + b^*c + bc^*}{a^2 + b^2 + c^2 + d^2} A^{-1} (\lambda_{\frac{1}{2}}^{*++} \lambda_{\frac{1}{2}}^{-+} - \lambda_{-\frac{1}{2}}^{*++} \lambda_{-\frac{1}{2}}^{-+} + \lambda_{\frac{1}{2}}^{*-+} \lambda_{\frac{1}{2}}^{++} - \lambda_{-\frac{1}{2}}^{*-+} \lambda_{-\frac{1}{2}}^{++}), \\ A_1 &= \frac{\pi}{4} \frac{a^*d + ad^* + b^*c + bc}{a^2 + b^2 + c^2 + d^2} A^{-1} (\lambda_{\frac{1}{2}}^{*++} \lambda_{\frac{1}{2}}^{-+} + \lambda_{\frac{1}{2}}^{*-+} \lambda_{\frac{1}{2}}^{++} + \lambda_{\frac{1}{2}}^{*-+} \lambda_{-\frac{1}{2}}^{-+} + \lambda_{-\frac{1}{2}}^{*-+} \lambda_{-\frac{1}{2}}^{++}), \\ B_1 &= i \frac{\pi}{4} \frac{a^*b + ab^* + c^*d + cd^*}{a^2 + b^2 + c^2 + d^2} A^{-1} (\lambda_{\frac{1}{2}}^{*++} \lambda_{-\frac{1}{2}}^{++} - \lambda_{-\frac{1}{2}}^{*++} \lambda_{\frac{1}{2}}^{++} + \lambda_{\frac{1}{2}}^{*-+} \lambda_{-\frac{1}{2}}^{-+} - \lambda_{-\frac{1}{2}}^{*-+} \lambda_{\frac{1}{2}}^{-+}). \end{aligned}$$

From formula (3) we see that in the most general case, we should obtain a $\cos \theta$ asymmetry term in the θ distribution and $\cos \varphi$ and $\sin \varphi$ terms in the φ distribution.

The cases considered by Morpurgo are obtained:

1) For the non-conservation of parity only in the final state, by putting c and $d = 0$.

2) For the parity doublet hypothesis alone by putting $a=d=1$, $c=b=0$. In the second of these cases the $\sin \varphi$ term is now lacking, in the first one, the θ distribution is isotropic, and there is only the $\sin \varphi$ term.

We may now consider other possibilities.

3) The parity is not determined in the initial hyperon state, but there is only one final state (let us say only the s state, if the transition probabilities to the p state are very small compared with those to the s state), in which case we put $a=c=1$, $b=d=0$ and we find isotropy both in the θ and in the φ distributions. As a result, this case cannot be experimentally distinguished from a transition from an initial to a final state both of definite parity.

4) Let us assume that parity non-conservation has no effect on the value of the transition rate, so that $a=c$ and $b=d$. This case does not differ qualitatively from the general one in which a , b , c and d have purely arbitrary values.

5) Finally, if the strong YKN interactions imply a well defined parity, and therefore a definite type of coupling, we must put either λ^{++} or λ^{-+} equal to zero. We then get a distribution which is quite similar to that of case 1), with an asymmetry only in the φ distribution.

From these results one concludes that the angular correlation phenomena in hyperon decays are not very sensitive to the fact that the initial state of the hyperon

may or may not be in a state of definite parity. Generally, the existence or non existence of the asymmetries in the angular distributions should give us an indication as to whether parity is conserved or not in the transition to final states of different parity, rather than information about the parity of the hyperon itself.

Only the general case and case 4), with the term in $\cos \theta$, should be an indication that the hyperon is in a state of no definite parity; but the lack of this term does not necessarily mean that the parity of the hyperon has a definite value.

Other phenomena connected with different interaction processes of strange particles will perhaps turn out to be a more sensitive test for the existence of the $KK\pi$ interaction, and thus indirectly for the state of parity of K-mesons and hyperons.

Further Results on Antiproton Annihilations.

E. AMALDI, C. CASTAGNOLI, M. FERRO-LUZZI, C. FRANZINETTI and A. MANFREDINI

*Istituto di Fisica dell'Università - Roma
Istituto Nazionale di Fisica Nucleare - Sezione di Roma*

(ricevuto il 6 Aprile 1957)

As part of a collaboration between the laboratories of Berkeley and Rome — started about a year ago (¹) — a stack of 140 pellicles (each 600 μm thick and $10 \times 15 \text{ cm}^2$ of area) was exposed to the flux of antiprotons produced by the Bevatron of the Radiation Laboratory and examined in our department in Rome. In this stack 14 events have been found which may be interpreted as due to antiprotons: of them

- 4 annihilate at rest;
- 5 annihilate in flight, releasing a visible energy larger than their kinetic energy;
- 5 produce a star having a visible energy smaller than their kinetic energy. Direct measurements indicate that they have a protonic mass but their interpretation is ambiguous.

The emulsions were exposed to the 700 MeV/c antiproton beam — the geometry of the experiment being essen-

tially the same as described in a previous paper (²). In the present case the $(700 \pm 4\%) \text{ MeV}/c$ reference orbit went through our stack at 1 in. from the left hand side corner. The pion flux at the high momentum side (left side) was $2 \cdot 10^5 \pi^-/\text{cm}^2 \pm 7\%$ and at the low momentum side was $1 \cdot 10^5 \pi^-/\text{cm}^2 \pm 10\%$. The momentum dispersion was $\Delta p/p = 0.7\%$ per inch.

The examination of the stack started at the beginning of June and it was finished at the end of December. The method of «scanning along the track» was used, each track being followed starting at 5 mm from the leading edge of the stack.

All tracks forming an angle of less than 3° with respect to the pion beam and having a specific ionization $g/g_0 = 2.0 \pm 0.4$ were selected and examined. None of those which could be interpreted as antiprotons had an angle larger than 1° .

Care was taken to estimate the residual range of the four antiprotons which

(¹) O. CHAMBERLAIN, W. W. CHUPP, G. GOLDHABER, E. SEGRÉ, C. WIEGAND, E. AMALDI, G. BARONI, C. CASTAGNOLI, C. FRANZINETTI, A. MANFREDINI: *Phys. Rev.*, **101**, 909 (1956); *Nuovo Cimento*, **3**, 447 (1956).

(²) O. CHAMBERLAIN, W. W. CHUPP, A. G. EKSPONG, G. GOLDHABER, S. GOLDHABER, E. J. LOFGREN, E. SEGRÉ, C. WIEGAND, E. AMALDI, G. BARONI, C. CASTAGNOLI, C. FRANZINETTI and A. MANFREDINI: *Phys. Rev.*, **102**, 94 (1956).

ANTIPROTON MASS MEASUREMENTS (*)

TABLE I. - Annihilation at rest.

Event no.	Total observ. range (cm)	Method					Average on values of column 4, 5, 6, 7
		$R - H\varrho$ ()	$R - \bar{w}$ ()	$R - \langle \theta \rangle$ ()	constant sagitta	$R - w/w_0$ (†)	
(1)	(2)	(3)	(4)	(5)	(6)	(7)	
4	12.60	1.00 ± 0.03	1.10 ± 0.08	—	0.93 ± 0.07	1.12 ± 0.10	1.03 ± 0.04
5	10.63	1.05 ± 0.06	0.95 ± 0.10	0.91 ± 0.14	1.32 ± 0.22	0.95 ± 0.09	0.98 ± 0.07
6	11.99	0.99 ± 0.06	1.08 ± 0.08	1.03 ± 0.16	1.00 ± 0.15	1.09 ± 0.20	1.02 ± 0.06
7	12.01	0.99 ± 0.05	1.08 ± 0.08	1.05 ± 0.16	—	1.18 ± 0.10	1.11 ± 0.06

Average values 1.00 ± 0.02 1.06 ± 0.04 0.98 ± 0.09 0.98 ± 0.06 1.07 ± 0.05 1.04 ± 0.03

(‡) Range versus momentum method. The momentum is deduced from the magnetic rigidity at the point of entry in the stack.

(§) Range versus average gap length (at the point of entry).

(×) Range versus scattering (at the point of entry).

(†) Range versus relative ionization density [see (‡)], measured on the terminal part of the track.

TABLE II. - Annihilation in flight.

Event no.	Total observ. range (cm)	Method			Average value
		$H\varrho - \bar{w}$ ()	$\langle \theta \rangle - \bar{w}$ (×)	$w - R$ (†)	
8	5.90	1.07 ± 0.05	1.23 ± 0.12	1.10 ± 0.08	1.09 ± 0.04
9	11.03	0.89 ± 0.05	0.86 ± 0.07	1.07 ± 0.15	1.89 ± 0.04
10	8.05	1.06 ± 0.05	0.98 ± 0.09	1.16 ± 0.09	1.07 ± 0.04
11	4.29	1.14 ± 0.05	1.22 ± 0.13	0.90 ± 0.07	1.07 ± 0.04
12	5.29	1.12 ± 0.05	—	—	1.12 ± 0.05
13	5.96	1.09 ± 0.05	0.92 ± 0.08	1.07 ± 0.05	1.05 ± 0.03
14	4.90	1.00 ± 0.04	1.12 ± 0.11	1.58 ± 0.40	1.02 ± 0.04
15	4.15	1.12 ± 0.05	0.89 ± 0.09	1.39 ± 0.15	1.09 ± 0.04
16	5.92	1.01 ± 0.06	0.89 ± 0.14	0.93 ± 0.23	0.99 ± 0.05
17	0.95	1.01 ± 0.04	—	—	1.01 ± 0.04
	56.44	1.05 ± 0.01	0.97 ± 0.03	1.07 ± 0.03	1.04 ± 0.01

(‡) Magnetic rigidity versus average gap length (at the point of entry).

(×) Scattering versus average gap length (at the point of entry).

(†) Specific variation of gap length (at the point of entry).

(*) All masses are given in proton mass units. The angle between any of the listed anti-proton tracks and the pions (at the entry in the stack) was in all cases less than 1° .

TABLE III. - Data on antiproton annihilation stars.

Star No.	N_{π}	N_n	$\sum E_{\pi}$	$\sum E_{n\pi}$	$E_{\pi n}$	T_p	π-meson kinetic energies					$\sum E_{\pi/W}$	$E_{\pi,W}$	M/M_p	
							2	3	4	5	6				
5.4	0	2	0	135+16	151	0	-	-	-	-	-	0.081	0.081	1.03 ± 0.04	
5.5	2	0	> 280+280	0	> 560	0	> 140	> 140	-	-	-	0.300	-	0.300	0.98 ± 0.07
5.6	5	0	> 562+700	0	1262	0	51.8	90.5	> 140	> 140	0.674	-	0.674	1.02 ± 0.06	
5.7	0	3	0	51+24	75	0	-	-	-	-	-	0.040	0.040	1.11 ± 0.06	
5.8	1	4	> 140+140	57+32>	369	156	-	-	-	-	0.138	0.044	0.182	1.09 ± 0.04	
5.9	0	2	0	55+1671±12	50	-	-	-	-	-	-	0.038	0.038	0.90 ± 0.04	
5.10	1	10	28+140231+80	479	120	28.2	-	-	-	-	0.084	0.156	0.240	1.07 ± 0.04	
5.11 (*)	-	1	0	2.5+8	10.5	155	-	-	-	-	-	0.005	0.005	1.07 ± 0.04	
5.12 (*)	-	1	0	2.0+8	10.0	153	-	-	-	-	-	0.005	0.005	1.12 ± 0.05	
5.13 (*)	0	2	0	50+16	66	100	-	-	-	-	-	0.033	0.033	1.05 ± 0.03	
5.14 (*)	0	3	0	95+24	119	170	-	-	-	-	-	0.058	0.058	1.02 ± 0.04	
5.15 (*)	0	2	0	98+16	114	175	-	-	-	-	-	0.055	0.055	1.09 ± 0.04	
5.16	3	9	> 322+420324+72>	1138	146	90 ± 10.92 ± 10	140	-	-	0.370	0.197	0.567	0.99 ± 0.05		
7.17	3	4	> 300+420103+24	847	209	> 140	140	19 ± 2	-	0.347	0.061	0.408	1.01 ± 0.04		

(*) All energies in MeV.

(**) Dubious events (see text).

Code: N_{π} number of pions ejected from the annihilation star.
 N_n number of secondaries of nucleonic nature.
 $\sum E_{\pi,n}$ total kinetic energy + total rest mass of the ejected pions.
 $\sum E_{n\pi}$ total kinetic energy + assumed binding energy attributed to the secondaries of nucleonic nature.
 $E_{\pi n}$ total visible energy.
 T_p kinetic energy of the antiproton at the point of the interaction.
 M_p proton mass.

appeared to annihilate at rest (Table I): in all these cases the residual ranges R_r ⁽³⁾ — at the point of interaction — were found to be equal to (0 ± 50) μm .

These four events have been used for a better determination of the reference momentum which turned out to be (690 ± 7) MeV/c. Therefore the data of column 3 of Table I do not represent a mass determination but rather a check of the correct value of the reference momentum. The averages given in column 8 of the same table refer to the results collected in columns 4, 5 and 6.

Table III contains the data regarding the annihilation stars. Noteworthy is event 5-6 which annihilates at rest with emission of 5 minimum tracks and no other prongs. This and event 5-16 have a visible energy larger than $M_p c^2$. On the other hand, in five cases (marked with a cross in table III) the visible energy is smaller than the kinetic energy of the incident particle and therefore one cannot exclude that they are due to a background of positive protons.

When the visible energy is as small as in the events 5-11 and 5-12, a third interpretation is possible in terms of a charge exchange process, as already suggested in a previous paper in connection with event 5-1⁽⁴⁾. Small angle scatterings

($\theta < 15^\circ$) have been sought for a length of 118.26 cm track due to antiprotons in the energy interval between 50 and 200 MeV. Using the same procedure as outlined in⁽⁴⁾, we checked our efficiency in detecting small angle deflections: it proved to be close to 100% for angles having a horizontal projection of 2° or more. In a systematic search carried out independently by two observers, the four cases listed in table IV were found. These are the only p- scattering observed in this laboratory, apart from an inelastic scattering of 8° associated with Bl-Ro⁽¹⁾ at an energy of 80 MeV. In conclusion, summing all data we have observed only 5 small angle scatterings over a total length of 126.65 cm, at energies 50 to 200 MeV.

TABLE IV. — *Independent measurements on five deflections observed on antiproton tracks.*

Event	Observer 1	Observer 2	Average
5-5	$2^\circ 14'$	$2^\circ 20'$	$2^\circ 17'$
5-7	$2^\circ 48'$	$3^\circ 35'$	$3^\circ 12'$
5-9	$2^\circ 18'$	$2^\circ 10'$	$2^\circ 14'$
5-15	$2^\circ 45'$	$2^\circ 15'$	$2^\circ 30'$

* * *

⁽³⁾ G. BARONI, G. CORTINI and A. MANFREDINI: *Nuovo Cimento*, **1**, 473 (1955).

⁽⁴⁾ W. H. BARKAS, R. W. BIRGE, W. W. CHUFF, A. G. EKSPONG, G. GOLDHABER, S. GOLDHABER, H. H. HECKMAN, D. H. PERKINS, J. SANDWEISS, E. SEGRE, F. M. SMITH, D. H. STORK and L. VAN ROSSUM. Radiation Laboratory, University of California, Berkeley, Cal. and E. AMALDI, G. BARONI, C. CASTAGNOLI, C. FRANZINETTI and A. MANFREDINI. Istituto di Fisica dell'Università, Roma; Istituto Nazionale di Fisica Nucleare, Sezione di Roma, Italy. *Phys. Rev.*, **105**, 1037 (1957).

We have pleasure in thanking the Bevatron group and its leader Dr. E. J. LOFGREN, Prof. E. SEGRÈ, Prof. G. GOLDHABER for their help in planning and carrying out the exposure. Thanks are due to Prof. HOUTERMANS for allowing the processing of the stack to be made in the new plant of the Bern laboratory. We also acknowledge the assistance of Drs. TEUCHER and WINZELER in the processing operations.

Nuclear Interactions of Long-Lived Neutral Strange Particles (*).

R. AMMAR, J. I. FRIEDMAN, R. LEVI SETTI (+) and V. L. TELEGGI

*The Enrico Fermi Institute for Nuclear Studies
The University of Chicago - Chicago, Illinois*

(ricevuto il 16 Aprile 1957)

Preliminary scanning of an emulsion stack irradiated with a beam of neutral particles from the Berkeley bevatron has provided evidence for charge-exchange reactions of neutral, long-lived K-mesons yielding charged K-mesons of both strangenesses +1 and -1, and for the production of hyperons of strangeness -1. This evidence strongly supports the Gell-Mann-Pais model (¹) for a long-lived, neutral K-meson.

This stack, $(10 \times 15 \times 3.5)$ cm³ in size, was exposed so as to intercept only neutral particles emitted from a beryllium target at 45° with respect to the direction of the 6.3 GeV proton beam. The target received a total of $3 \cdot 10^{12}$ protons during the exposure. The setup, proceeding from the Be target to the stack, comprised a channel in the wall of a curved section of the bevatron, a lead collimator, a lead converter of about 5 radiation lengths thickness, and a sweeping magnet capable of deflecting a

particle of 7 GeV/c momentum by 0.12 rad. The stack was placed 1 m behind this magnet, at a total distance of 6 m from the target, in a position chosen to minimize the number of stray charged particles.

To date, about 10 cm³ of emulsion have been area scanned, partly under 12 (air) \times 10 magnification, and partly under 22 (oil) \times 10. The search was for decays and captures of heavy mesons and hyperons, as well as for hyperfragments. The following strange particle events were found:

(a) 3 heavy mesons each decaying at rest into three charged pions;

(b) 2 heavy mesons, decaying at rest with the emission of single relativistic secondaries;

(c) 1 heavy meson, captured at rest;

(d) 1 $\Sigma^- \rightarrow p + \pi^0$ decay at rest;

(e) 4 double-stars, connected by heavily ionizing tracks (events classed as « GOKS »).

A common feature of the events in categories (a) through (d) is that they originate from parent stars in the stack. These parent stars show no charged pri-

(*) Research supported by the Greengewalt Nuclear Physics Fund, the Office of Naval Research, and the Atomic Energy Commission.

(+) On leave of absence from the University of Milan.

(¹) M. GELL-MANN and A. PAIS: *Phys. Rev.*, **97**, 1387 (1955).

TABLE I. - Nuclear interaction

Event	Parent star	Suggested production process			Strange particle		
		Type (¹)	Visible Excitation Energy (MeV) (²)		θ_{lab}	Mass m_e (³)	Range mm
a) τ -mesons							
EFINS 1	2+0n		2.2	$K^0 + p \rightarrow \tau^+ + n$	29°	695 ± 250	67.7
EFINS 2	2+0n		4.4	$K^0 + p \rightarrow \tau^+ + n$	86°	1015 ± 350	13.8
EFINS 3	3+0n		38.4	$K^0 + p \rightarrow \tau^+ + n$	42°	890 ± 250	50.65
b) K^+ -mesons							
EFINS 1	3+0n		37.7	$K^0 + p \rightarrow K^+ + n$	89°	1110 ± 300	14.0
EFINS 2	1+0n		0	$K^0 + p \rightarrow K^+ + n$	45°	1290 ± 350	57.5
c) K^- -mesons							
EFINS 1	2+0n		8.4	$K^0 + n \rightarrow K^- + p$	36°	1065 ± 300	41.0
d) Σ^+							
EFINS 1	1+1n	(¹)		$K^0 + \bar{n} \rightarrow \Sigma^+ + (\pi)$	72°	2250 ± 850	1.28
e) GOKS	Type (¹)				Length of connecting track (μm)	Decay mode or capture	Co me
EFINS 1	12+0n	—		$K^0 + n \rightarrow \Sigma^+ + (\pi^+)$ $K^0 + (A, Z) \rightarrow \Lambda^0 + (A - 1, Z)$	80	Non- mesonic	May Σ
EFINS 2	4+0n	—		$K^0 + (A, Z) \rightarrow \Lambda^0 + (A - 1, Z)$	3.0	Non- mesonic	Poss hyp frag
EFINS 3	12+0n	—		$\bar{K}^0 + (A, Z) \rightarrow \Lambda^0 + (A - 1, Z)$	3.3	Non- mesonic	Poss hyp frag
EFINS 4	7+0n	—		$K^0 + (A, Z) \rightarrow \Lambda^0 + (A - 1, Z)$	4.7	Non- mesonic	Poss hyp frag

(1) Prongs less than 5 μm have been excluded.

(2) Lower limit, based on assumption of proton mass for evaporation particles.

(3) Determined from constant sagitta scattering using 3rd differences.

long-lived strange particles.

Particle	Secondary particles					
	Number of plates traversed	Range μm	Energy (MeV)	α_ℓ	Momentum unbalance (MeV/e)	Q (MeV)
π_2^+	1	92.4 \pm 5	1.59 \pm 0.05	170° 03'		
	3	18 860 \pm 650	33.84 \pm 0.7	62° 52'	2.0	75.2 \pm 1.0
	5	24 650 \pm 800	39.75 \pm 0.85	127° 05'		
π_3^-	1	35 \pm 2	0.9 \pm 0.024	171° 39'		
	8 (4)	(4)	36.1 (4)	97° 27'	(4)	73.7 \pm 1.6
	9	21 580 \pm 700	36.68 \pm 0.78	90° 54'		
π_2^+	1	148 \pm 6	2.08 \pm 0.05	176° 55'		
	6	14 680 \pm 510	29.15 \pm 0.61	166° 25'	2.8	74.8 \pm 1.0
	7	28 620 \pm 930	43.53 \pm 0.83	16° 40'		

Particle at about plateau ionization. Dip = 68°.

Particle at about plateau ionization. Dip = 42°.

Short recoil.

Interacts after 6.8 mm yielding a 4+0p star with a visible energy release of 16 MeV.

P	2	1 670 \pm 20	18.8 \pm 0.06	—	—	—	116.4 \pm 1.5
(μm)	R_2 (μm)	R_3 (μm)	R_4 (μm)	—	—	—	Visible energy release (MeV) (2)
307	8 044	—	—	—	—	—	63.0
4040	4 327	—	—	—	—	—	96.0
1 650	18 900	short recoil	short recoil	—	—	—	94.5
2 771	316	107.0	—	—	—	—	36.0

Pion leaves stack. It is assumed to be positive and its energy calculated from momentum balance.
Light track lost in tracing

maries, and involve (besides the strange particles) only a very low energy release in the form of a few evaporation tracks. Table I is a compilation of the results of measurements performed on these events.

A careful check of momentum balance and coplanarity of the secondaries from events (*a*) identified the latter as 3-body decays. Q -values of (75.2 ± 1) MeV, (73.7 ± 1.6) MeV, and (74.8 ± 1) MeV were determined, and are all consistent with the identification of events (*a*) as π -mesons. Fig. 1 shows mosaics of these events.

Identification of events (*b*) as K-mesons comes from direct mass determination (constant sagitta), and from the observation of their decays at rest. The modes of decay cannot be specified beyond the statement that the secondaries give about plateau ionization, owing to the steepness of their tracks. The assumption that these events represent decays rather than captures, which is equivalent to assigning a positive charge to these K-mesons, relies on the empirical fact that K^- captures lead rarely to a single relativistic particle.

Event (*c*) is identified as a K^- from mass measurement of the primary, and from its capture star; the latter consists of a single grey track and a recoil blob. The particle causing the grey track interacts in flight giving a 4-prong star.

Event (*d*) is identified as Σ^+ by the range of its decay proton $(1.670 \pm 20) \mu\text{m}$ and by mass measurement of the primary.

Of the four events in category (*e*), event EFINS 1 probably represents the capture of a heavy particle (K^- or Σ^-), as the connecting track has the appearance characteristic of a singly charged particle. The visible energy release in the capture is about 65 MeV on the assumption that the two secondary prongs are protons. Classification of this event as a hyperfragment cannot however be ruled out.

The other three «GOKS», giving

visible energy releases ≥ 36 , 95, and 96 MeV respectively, could be attributed either to non-mesic decays of hyperfragments or to captures.

Summarizing the results, we have observed 5 particles of positive strangeness, and at least 2, and possibly 6, of negative strangeness. The characteristics of the parent stars of the K^+ and K^- events strongly suggest that these particles originated from charge-exchange scatterings of neutral K-mesons. Fig. 2a shows the prong distribution of the individual parent stars, together with the range, R , and the angle θ_{lab} , of emission with respect to the incident beam direction of the associated K-mesons. On the assumption of the reaction $K(K) + \mathcal{N} \rightarrow K^+(K^-) + \mathcal{N}$ on a free nucleon \mathcal{N} , and for a given K^+ energy, the energy of the charged K-meson can be predicted as a function of the scattering angle θ_{lab} . Tentatively describing our charged K events by this reaction, such a calculation was made for these events, using the energy of the incident particle as a parameter. Satisfactory correlation between the predicted and observed quantities is found (Fig. 2b) for a unique incident energy of about 140 MeV, and this correlation remains meaningful when the Fermi energy of the target nucleon is taken into account. From this computation, now interpreted to describe quasi-nucleon collisions, the average energy transfer to the target nucleus can be estimated as about 55 MeV. Such a transfer is quite consistent with the visible energy release from the parent stars, viz. about 30 MeV.

The preceding analysis provides self-consistent evidence that the observed charged K-mesons are indeed produced by charge-exchange scattering. In addition, the primary neutral particles leading to the observed events all appear to have rather similar energies. This does not necessarily mean that the K^0 beam is monoenergetic. The effect could arise from the limited size of the stack and

R. AMMAR, J. I. FRIEDMAN, R. LEVI SETTI and V. L. TELELDI

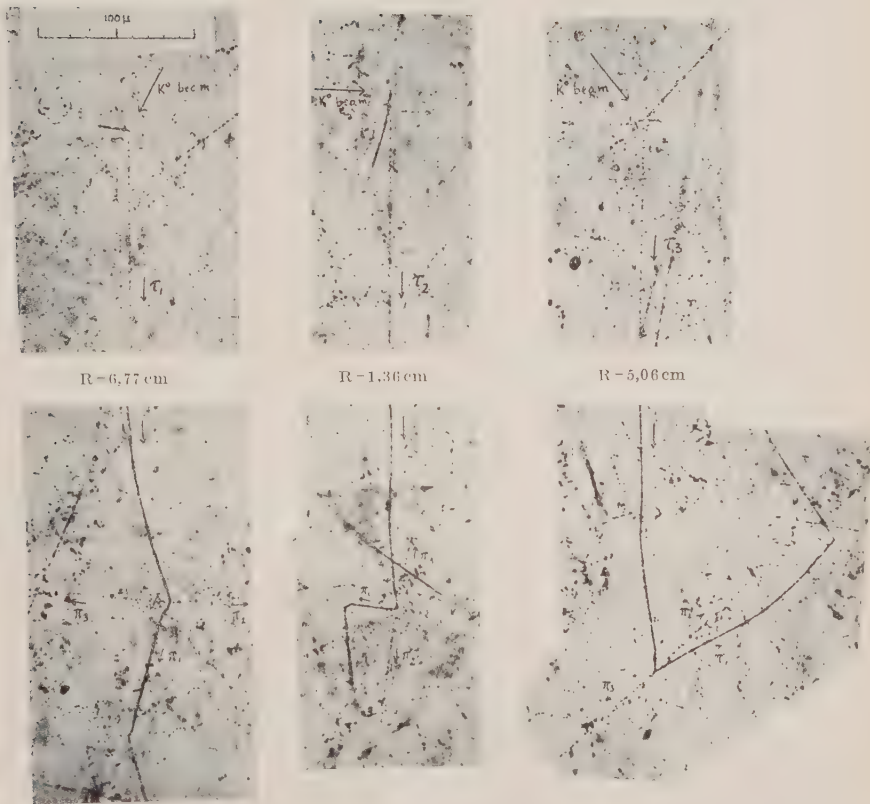


Fig. 1. — Photomicrographs of τ -mesons produced by long-lived neutral strange particles.

from a possible energy dependence in the charge-exchange cross section.

To strengthen our assumption that the neutral primaries giving rise to the analyzed events are indeed strange

shall assume that they also apply to neutron-induced stars, except for minor corrections. The threshold for the reaction $n + \pi \rightarrow K + Y + \pi$ is about 1.2 GeV assuming a Fermi energy of 20 MeV

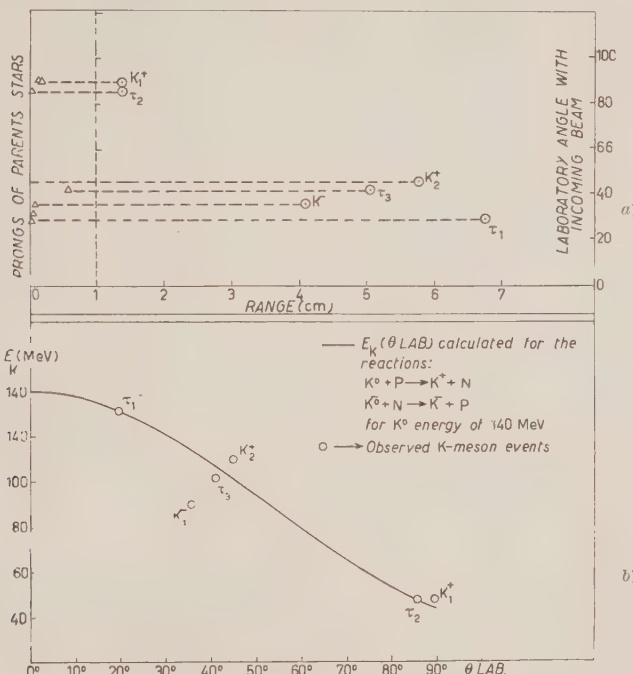


Fig. 2. — (a) Range vs. angle of emission from incident neutral beam direction of K -mesons, and prong distribution of their parent stars. (b) — Energy vs. laboratory scattering angle of charged K -mesons produced in the reaction $K^0(K^0) + \pi \rightarrow K^+(K^-) + \pi$ by neutral K -particles of 140 MeV on free nucleons; π ; \circ : Experimental points.

particles rather than neutrons, we have determined the flux of high energy neutrons incident upon the stack. The principle underlying this determination is that the total prong number distribution of stars has, even for primaries in the GeV range, an upper cut-off that is a sensitive function of the primary energy. Fig. 3, compiled from the data of several authors (²), shows this cut-off as a function of energy; though the experimental data were obtained with protons, we

for π . According to Fig. 3, this threshold energy corresponds to a cut-off at $n_{c.o.} = 16$; we shall take $n_{c.o.} = 15$ for incoming neutrons. Let $f(E)$ be the fraction of stars with $n \geq 14$ (*) [known approximately from experiment (²)], i.e.

(*) We include 14-prong stars to take into account stars produced by neutrons at threshold.

(²) J. I. FRIEDMAN: unpublished results; A. D. SPRAGUE, D. M. HASKIN, R. G. GLASSER and M. SCHEIN: *Phys. Rev.*, **94**, 994 (1954);

$f(E) = n_{14}(E)/N(E)$, where $N(E)$ is the total number of stars produced by neutrons of energy E . Our purpose is to determine the sum of all $N(E)$ for all $E \geq 1.2$ GeV. This sum, N_0 , is given by n_{14}/\bar{f} , where \bar{f} is a suitable average

It has to be borne in mind that not all 1.2 GeV neutrons are effectively above threshold for K^0 production, because: (1) H present in the emulsion has no Fermi energy; (2) the Fermi momentum lowers the threshold in only about half

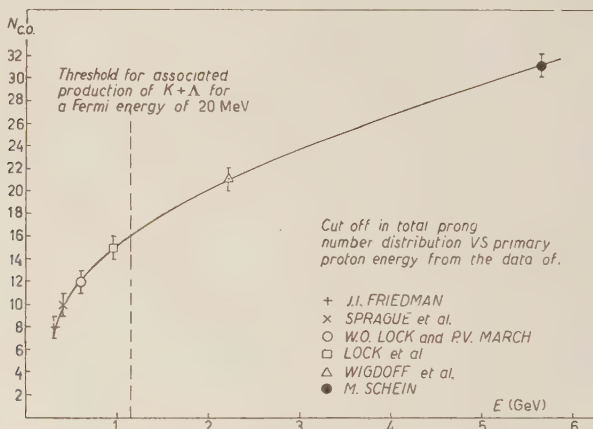


Fig. 3. - Cut-off in the prong number distribution of proton-induced stars in nuclear emulsion, as a function of proton energy.

of $f(E)$ over the neutron energy spectrum, and n_{14} is the number of stars having 14 or more prongs. Assuming a neutron spectrum as would result at 45° from proton-neutron scattering in a target nucleus with 20 MeV Fermi energy, one obtains $\bar{f} = 0.05$. Scanning a volume of 0.45 cm^3 in our stack, 2000 neutron stars were found, 6 of which had 14 or more prongs. With the preceding assumptions and a geometric interaction cross section, this would correspond to a flux of $8 \cdot 10^3/\text{cm}^2$ neutrons of energy greater than 1.2 GeV.

W. O. LOCK and P. V. MARCH: *Proc. Roy. Soc.*, A **230**, 222 (1955); W. O. LOCK, P. V. MARCH, H. MUIRHEAD and W. G. V. ROSSER: *Proc. Roy. Soc.*, A **230**, 215 (1955); M. WIGDOFF, C. P. LEAVITT, A. M. SHAPIRO, L. W. SMITH and C. E. SWARTZ: *Phys. Rev.*, **92**, 851 (1953); private communication from Professor Marcel SCHEIN, to whom we express our gratitude.

the collisions. Taking these facts into account, we estimate that the number of charged strange particles directly produced in the scanned volume by incoming neutrons is of the order of 1 particle/(mb production cross section at threshold). This represents an upper limit for events of the type described here, since a considerable fraction of neutron-produced charged K 's would escape from the stack. We conclude that the observed events were not produced by high energy neutrons. The validity of this conclusion might appear to rest on the assumed neutron spectrum. To see that this is not so, we consider as an alternative an extreme case, viz., a uniform neutron spectrum extending from 1.2 to 6 GeV. The f for such a distribution would be 0.25, leading to 0.2 charged strange particle event/(mb production cross section). Obviously, the probability of

escape would be even greater for this case.

There remains to consider the possibility that all or some of our events were produced by interactions of neutral K's locally produced in the stack. Such an origin of the events is even more unlikely than the one just discarded, because of its secondary character.

We are led to interpret our events as caused by interactions of long-lived neutral strange particles. From the dynamic arguments given above (Fig. 2) we conclude that they are most probably neutral K-mesons. From conservation of strangeness, they must comprise both K^0 and \bar{K}^0 ; it is most attractive to identify them with the coherent mixture proposed by GELLMANN and PAIS⁽¹⁾ to represent the long-lived 0_2 ⁽³⁾.

Our findings concerning the production of particles of negative strangeness by long-lived neutral K's are corroboration of the results of earlier experiments⁽⁴⁻⁶⁾ conducted along similar lines.

(2) K. LANDÉ, E. T. BOOTH, J. IMPEDUCIA, L. M. LEDERMAN and W. CHINOWSKY: *Phys. Rev.*, **103**, 1901 (1956); K. LANDÉ, L. M. LEDERMAN and W. CHINOWSKY: *Nevis*, **38** (February, 1957).

(4) W. F. FRY, J. SCHNEPS and M. S. SWAMI: *Phys. Rev.*, **103**, 1904 (1956).

(5) R. G. GLASSER and N. SEEMAN: *Bull. Am. Phys. Soc.*, Series II, **1**, no. 7, 320 (1956).

(6) Milan and Padua Groups: private communication. We are indebted to the authors for communicating their results prior to publication.

In conformity with the ideas underlying the concept of multiplets of strange particles, one might like to verify that the branching ratios of the various K^+ decay modes of particles produced under the conditions of the present experiment agree with those observed for K^+ produced in the collision of non-strange particles. Various experimental biases must, however, be overcome before our experiment can yield such information.

Although we are aware of the limitations of our statistics, we would like to point out that each of the three τ -decays observed involves a positive pion of less than 2 MeV. From experimental decay spectra⁽⁷⁾, it is known that positive pions in this energy range occur with a relative frequency of about $1 \cdot 10^{-2}$, and hence the probability of observing the present sample from a population of τ -mesons is rather small.

* * *

It is a pleasure to thank Professor G. WATAGHIN for helping with the arrangements for this exposure. The latter was made possible through the co-operative assistance of Dr. E. J. LOFGREN and his staff, to whom we wish to express our deepest appreciation. We thank Professor R. H. DALITZ for helpful discussions concerning the subject of this investigation.

(7) M. BALDO-CEOLIN, A. BONETTI, W. D. B. GREENING, S. LIMENTANI, M. MERLIN and G. VANDERHAEGE: to be published.

**On the Angular Correlation in μ -e Decays
Observed in Nuclear Emulsions Exposed in Magnetic Field.**

J. HEUGHEBAERT, M. RENÉ, J. SACTON (*) and G. VANDERHAEGHE (*)

*Institut de Physique de l'Université Libre de Bruxelles
Service de Physique Nucléaire*

(ricevuto il 27 Aprile 1957)

According to LEE and YANG (1), parity non-conservation in weak interactions can be tested by studying the successive decay processes:

$$(1) \qquad \pi \rightarrow \mu + \nu,$$

$$(2) \qquad \mu \rightarrow e + \nu + \nu.$$

If parity is not conserved in process (1), the μ -meson must be polarized along its initial direction of motion in the center of mass system of the π -meson; if moreover parity is not conserved in process (2), the distribution of the angle θ between the spin of the μ and the initial direction of motion of the electron must be asymmetric with respect to $\theta = \pi/2$. For μ -mesons decaying at rest, the probability distribution of θ is expected to be (1-4)

$$(3) \qquad W(\theta) d\theta \sim (1 + a \cos \theta) \sin \theta d\theta,$$

where « a » is the *asymmetry coefficient*. The existence of such an asymmetry in the angular distribution of the μ -decay electrons has already been shown by various experiments with counter technique (5) and with nuclear emulsions exposed to cosmic rays (6-8)

(*) Chercheur agréé de l'Institut Interuniversitaire des Sciences Nucléaires (Belgique).

(1) T. D. LEE and C. N. YANG: *Phys. Rev.*, **104**, 254 (1956).

(2) T. D. LEE and C. N. YANG: *Phys. Rev.*, **105**, 1671 (1957).

(3) C. BOUCHIAT and L. MICHEL: *Phys. Rev.*, **106**, 170 (1957).

(4) L. LANDAU: *Nuclear Physics*, **3**, 127 (1957).

(5) R. L. GARWIN, B. M. LEDERMAN and M. WEINRICH: *Phys. Rev.*, **105**, 1415 (1957).

(6) C. CASTAGNOLI, C. FRANZINETTI and A. MANFREDINI: *Nuovo Cimento*, **5**, 684 (1957).

(7) B. BHOWMIK, D. EVANS and D. J. PROWSE: *On the Angular Correlation in the β -Decay of μ -Mesons observed in Photographic Emulsion*. Preprint.

(8) P. H. FOWLER, P. S. FREIER, C. M. G. LATTES, E. P. NEY and S. J. ST. LORANT: *Angular Correlation in the π - μ -e Decay of Cosmic Ray Mesons*. Preprint.

or to artificial π^+ beams without external magnetic field (9-11). The value of the asymmetry coefficient might be reduced by various depolarizing factors, one of which is the presence of a magnetic field leading to the Larmor precession of the spin of the μ (8).

In the present letter, we propose a method by which the asymmetry coefficient can be reached by studying π - μ -e decays in nuclear emulsions exposed in a uniform and constant magnetic field, without needing the determination of the precession angle. The principle of the method is the following: let α be the angle between the initial momentum \mathbf{P}_μ of the μ and its projection \mathbf{P}'_μ along the magnetic field direction and let φ be the angle between the initial momentum \mathbf{P}_e of the electron and \mathbf{P}'_μ (Fig. 1). Assuming that the spin σ of the μ is initially orientated along \mathbf{P}_μ , the magnetic field will make σ rotate around a cone of aperture α whose axis is parallel to the field itself. The resulting angular displacement will depend on the magnitude of the spin, on the lifetime of the μ and on the intensity of the magnetic field but the angle θ between σ and \mathbf{p}_e will be necessarily comprised between the following limits:

$$|\alpha - \varphi| < \theta < \alpha + \varphi.$$

In such conditions, three cases can occur:

- I. $\varphi < \pi/2 - \alpha$, which implies $\theta < \pi/2$, i.e. the electron is certainly emitted forward;
- II. $\varphi > \pi/2 + \alpha$, which implies $\theta > \pi/2$, i.e. the electron is certainly emitted backward;
- III. $\pi/2 - \alpha \leq \varphi \leq \pi/2 + \alpha$, i.e. the electron may be emitted either forward or backward.

Let us now consider π^+ mesons decaying at rest in nuclear emulsion. The angular distribution of the μ -mesons will be isotropic. Let us then suppose that all π - μ -e events are completely observable whatever direction of emission of the μ and let us distribute the events in the three classes I, II, III defined above. Assuming the distribution law (3) for the decay electrons, the ratio $R = B/F$ of the numbers of events belonging to classes II and I is related to the asymmetry coefficient by the

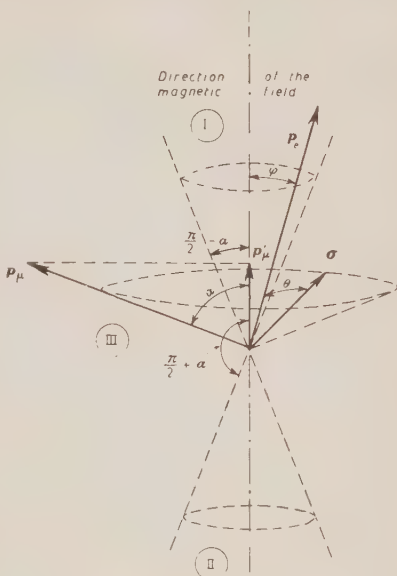


Fig. 1.

(9) J. L. FRIEDMAN and V. L. TELELDI: *Phys. Rev.*, **105**, 1681 (1957) and preprint.

(10) N. BISWAS, M. CECCARELLI and J. CRUSSARD: *Nuovo Cimento*, **5**, 756 (1957).

(11) M. F. KAPLON: private communication.

expression

$$(4) \quad R = \frac{k - a}{k + a},$$

from which follows

$$(5) \quad a = k \frac{1 - R}{1 + R},$$

where the constant k results from an integration as indicated in Appendix.

We are giving here, in a preliminary form, the first results obtained by this method in a stack of 5 emulsion sheets (Ilford G-5) of 2 in. \times 2 in. \times 600 μm exposed to the 37 MeV π^+ beam of the Rochester Synchro-cyclotron, in a magnetic field between 50 and 100 gauss perpendicular to the emulsion surface.

Up to now, we have observed 831 events: not only those entirely contained in the same sheet but also those contained in successive sheets, which avoids geometrical corrections. This was done by superposing the plates, two by two and working with an objective 30 \times Koristka.

The isotropy of the angular distribution of the μ -mesons was checked. The electron was not observed in nine cases ($\sim 1\%$) (*); 12 other events were eliminated because the end of the μ was near either surface of the emulsion.

We first applied the method described above to 500 events, assuming successively a magnetic field in the direction of one of three orthogonal axes x , y and z : z being perpendicular to the plane of the emulsion, x being in the direction of the π^+ beam and y being perpendicular to the plane (x , z). The results obtained are given in the three first lines of Table I.

TABLE I.

Direction	Number of events	B	F	$R = B/F$	Probability (%)
x	108	52	56	0.92	65 %
y	117	56	61	0.91	60 %
z	117	66	51	1.29	17 %
z	179	101	78	1.29	9 %

(*) The number indicated is the probability to observe an asymmetry greater than R , assuming an isotropic distribution.

It appears that the asymmetry is the most important in the z direction, which was the effective direction of the magnetic field.

Further, we applied the same method to 331 more events, considering only

(*) In four of these cases we observed a fast electron track beginning at respective distances of 15, 23, 38 and 40 μm from the end of the μ -track; in the 3 last cases the end of the μ -track does not lay in the prolongation of the electron track. Such cases are now submitted to a careful examination; a possible explanation might be the formation of mesonium (4, 9).

the z direction. The result obtained for the total of 831 events is given in the last line of Table I. The calculation of the asymmetry coefficient by formula (5) gives

$$a = -0.22 \pm 0.12.$$

The error quoted is the r.m.s. deviation, taking $R=1.29$ as *a priori* value.

Looking at the different causes of errors (errors in measurements, distortion, shrinkage factor), we come to the conclusion that, in the present experimental conditions, they cannot introduce any bias in the classification of events between classes I and II. However, some errors may systematically displace events from classes I and II to class III or vice-versa, so that convenient corrections will allow a better determination of the asymmetry coefficient.

On the basis of the present analysis, we have obtained a determination of the asymmetry coefficient which is in agreement with previous determinations (Table II) and we may conclude that the observed asymmetry is effectively corre-

TABLE II.

Group	Method	Number of events	a
Columbia (5)	Counters	—	-0.18 ± 0.03
Romé (6)	Nuclear Emulsions - Cosmic rays	1028	-0.222 ± 0.067
Bristol (7)	» » »	1562	-0.08 ± 0.05
Minneapolis (8)	» » »	2117	-0.03 ± 0.04
Chicago (9)	Nuclear emulsions - Machines - <i>without</i> magnetic field	2000	-0.174 ± 0.038
Göttingen (10)	» » »	2003	-0.095 ± 0.040
Rochester (11)	» » »	?	-0.19 ± 0.6
Our results	Nuclear emulsions - Machines - <i>with</i> magnetic field	831	-0.22 ± 0.12

lated with the orientation of the spin of the μ along its initial direction; indeed, as in Lederman's experiment (2), only this hypothesis allows a simple explanation of the role of the magnetic field.

We suggest that the comparison of more accurate values of the asymmetry coefficient obtained in nuclear emulsions exposed respectively *with* and *without* magnetic field could give some indication about depolarization by various factors (*).

* * *

We wish to thank Professors J. GÉHÉNIAU and G. P. S. OCCHIALINI for stimulating discussions and Professor L. MICHEL for pointing out to us the problem and helpful advice.

(*) Note added in proof: This view is supported by a recent experiment by OREAR and HARRIS (*Influence of strong magnetic field on depolarization of muons*. Preprint). Using a magnetic field of about 10 kilogauss, they find $a = -0.249 \pm 0.036$.

We are indebted to Professor J. VAN ISACKER for solving the mathematical part of the problem.

We wish to express our gratitude to Professor M. F. KAPLON who made possible the exposure of our plates to the Rochester Synchro-cyclotron.

We thank also the microscopists of the laboratory for their helpful contribution.

APPENDIX

Let γ be the angle between plane (σ, p_e) and plane (σ, H) , H being the magnetic field vector. The probability to include in our statistics an event with an electron emitted between θ and $\theta + d\theta$ may be expressed by

$$p(\theta) d\theta = (1 + a \cos \theta) \sin \theta d\theta \int_0^{2\pi} d\gamma \int_0^{\pi/2} \frac{\sin \alpha}{4\pi} d\alpha \Delta(\alpha, \gamma, \theta),$$

where $\Delta=1$ for events in class I and II and $\Delta=0$ for events in class III.

This expression may be written:

$$p(\theta) d\theta = [p_0(\theta) + ap_a(\theta)] d\theta,$$

where $p_0(\theta)$ is the symmetric term and $p_a(\theta)$ the asymmetric term. The ratio $R=B/F$ is then given by

$$R = \frac{\int_0^{\pi/2} p(\theta) d\theta}{\int_0^{\pi/2} p(\theta) d\theta} = \frac{\int_0^{\pi/2} [p_0(\theta) - ap_a(\theta)] d\theta}{\int_0^{\pi/2} [p_0(\theta) + ap_a(\theta)] d\theta} = \frac{k-a}{k+a},$$

where

$$k = \frac{\int_0^{\pi/2} p_0(\theta) d\theta}{\int_0^{\pi/2} p_a(\theta) d\theta},$$

The numerical value of the numerator is $\frac{1}{2}(1 - \pi/4) = 0.1073$. Making a change of variable $\gamma(\alpha, \theta, \varphi)$ the integral of $p_a(\theta)$ can be expressed by

$$\begin{aligned} \int_0^{\pi/2} p_a(\theta) d\theta &= \frac{1}{2} \int_0^{\pi/2} \sin \theta \cos \theta d\theta \int_0^{\pi/4-\theta/2} \sin \alpha d\alpha + \\ &+ \frac{1}{2\pi} \int_0^{\pi/2} \sin \theta \cos \theta d\theta \int_{\pi/4-\theta/2}^{\pi/4+\theta/2} \sin \alpha \arccos (\cosec \theta - \cotg \alpha \cotg \theta) d\alpha. \end{aligned}$$

The first term can be easily calculated and is equal to

$$\frac{1}{60} (7 - 4\sqrt{2}) = 0.0224 .$$

The second term has been calculated numerically and is equal to 0.0401.

Finally, we obtain

$$k = \frac{0.1073}{0.0224 + 0.0401} = 1.72 .$$

The Electronic Absorption Spectrum of Naphtotriazines.

M. SIMONETTA, G. FAVINI and V. PIERPAOLI

*Istituto di Chimica Industriale dell'Università di Milano
Laboratorio di Chimica Fisica*

(ricevuto il 3 Maggio 1957)

Recently⁽¹⁾ the ultraviolet spectra of benzotriazine and its derivatives were presented and a theoretical interpretation of the involved electronic transitions was given.

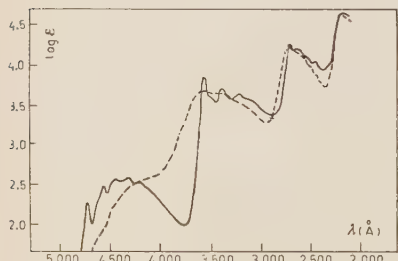


Fig. 1. — (2,1-e)-as-naphtotriazine:
in cyclohexane —; in methanol

Now (1,2-e)-as-naphtotriazine and (2,1-e)-as-naphtotriazine were prepared⁽²⁾ and the related ultraviolet spectra were taken both in cyclohexane and in methanol, using a Beckmann Quartz Spectrophotometer model D.U.

The observed bands are summarized

in Tables I and II, and shown in Figs. 1 and 2.

The assignment of bands was straightforward, also owing to the similarity of these spectra and the spectrum of benzo-

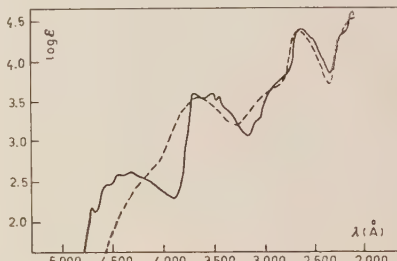


Fig. 2. — (1,2-e)-as-naphtotriazine:
in cyclohexane —; in methanol

triazine. For the (1,2-e)-as-naphtotriazine Pariser and Parr's semi-empirical molecular orbital treatment was performed to calculate the excited energy levels and the oscillator strengths for the $\pi \rightarrow \pi^*$ transitions. All the necessary empirical parameters were taken from previous calculations⁽¹⁾.

The results are collected in Table III, and compared with experiment; the agreement is quite satisfactory. The calculations will be published in full elsewhere.

⁽¹⁾ M. SIMONETTA, G. FAVINI, S. CARRÀ and V. PIERPAOLI: *Nuovo Cimento*, **4**, 1364 (1956).

⁽²⁾ R. FUSCO: *Gazz. Chim. It.*, in the press.

TABLE I. — *Observed bands of (2,1-e)-as-naphtotriazine.*

Band origin	Solvent	Wave number (cm ⁻¹)	ϵ
$n \rightarrow \pi^*$	cyclohexane	20 960	220
		21 740	325
		22 220	390
		23 000	405
		23 500	355
	methanol	(23 810)	400
1st $\pi \rightarrow \pi^*$	cyclohexane	27 590	7 500
		28 170	3 900
		29 200	5 150
		30 500	4 450
		27 400	5 000
		(29 000)	4 500
2nd $\pi \rightarrow \pi^*$	cyclohexane	35 970	18 800
		37 030	16 200
		38 100	12 600
		39 600	11 000
		35 800	16 800
	methanol		
3rd $\pi \rightarrow \pi^*$	cyclohexane	43 900	43 300
	methanol	43 900	44 500

TABLE II. — *Observed bands of (1,2-e)-as-naphtotriazine.*

Band origin	Solvent	Wave number (cm ⁻¹)	ϵ
$n \rightarrow \pi^*$	cyclohexane	21 050	170
		21 740	302
		22 350	420
		23 000	445
1st $\pi \rightarrow \pi^*$	cyclohexane	26 850	4 200
		28 170	4 050
		28 570	3 750
	methanol	27 030	3 750
2nd $\pi \rightarrow \pi^*$	cyclohexane	37 320	26 000
	methanol	36 630	24 000
3rd $\pi \rightarrow \pi^*$	cyclohexane	45 450	44 800
	methanol	45 500	34 400

TABLE III. - *Theoretical and experimental results for (1,2-e)-as-naphthotriazine.*

Transitions	teor. energy (eV)	teor. f	exp. energy (eV)	exp. f
first $\pi \rightarrow \pi^*$	3.73	0.043	3.35	0.058
second $\pi \rightarrow \pi^*$	4.65	0.13	4.54	0.36
third $\pi \rightarrow \pi^*$	5.54	0.20	5.58	(0.73)

EMENDATION

E. L. LOMON - A Soluble Model of Meson-Nucleon S -State Scattering, *Il Nuovo Cimento*, **4**, 106 (1956).

It is necessary to remove an ambiguity in the notation. At the beginning of Sect. 2 (page 116) we define operators which create a meson-nucleon system. This is only one of four type of «double operators» formed by combining creative (\bar{p} , \bar{q} , \bar{P} and \bar{Q}) or destructive (\tilde{p} , \tilde{q} , P and Q) nucleon operators into creative $\left(\frac{i}{\sqrt{2}\omega} P + \sqrt{\frac{\omega}{2}} Q, \text{etc.} \right)$ or destructive $\left(\frac{i}{\sqrt{2}\omega} P + \sqrt{\frac{\omega}{2}} Q, \text{etc.} \right)$ meson operators. The notation must distinguish between all four types. We thus stipulate that the presence or absence of a bar above an a or an α denotes respectively the creative or destructive properties of the operator with respect to the nucleon field. A bar or its absence below an a an α has a similar connotation with regard to the meson field.

In view of these definitions, the following alteration in Sect. 2 will remove the ambiguities:

on page 116 $\bar{\alpha}_\beta(k)$ should read $\underline{\alpha}_\beta(k)$
 $\bar{\alpha}_\beta(k')$ » » $\underline{\alpha}_\beta(k')$,

on page 117
in eq. (22) $\bar{\alpha}_\beta(k'')$ » » $\underline{\alpha}_\beta(k'')$,
in eq. (23) $\bar{\alpha}_\beta(k')$ » » $\underline{\alpha}_\beta(k')$
 $\bar{\alpha}_\beta(k'')$ » » $\underline{\alpha}_\beta(k'')$.

In addition, in the definition of $a_\beta(k')$ (page 116), $\bar{p}_\beta(k)$ should be replaced by $\bar{P}_\beta(k)$.

LIBRI RICEVUTI E RECENSIONI

C. KITTEL — *Introduction to Solid State Physics*. Wiley & Sons Inc., New York, 1956; pagg. xvii + 617, 69 tavole, prezzo 12 \$.

La parte della fisica che con termine moderno viene chiamata fisica dei solidi include argomenti di tipo assai diverso quali la conducibilità nei metalli, i cambiamenti di stato, l'assorbimento nei cristalli, i semiconduttori. Un criterio di unificazione può essere il fatto che le proprietà trattate dipendono in qua che modo dalla disposizione periodica degli atomi nel reticolo. Tuttavia è assai comune che chi lavora in fisica dei solidi abbia una competenza specifica in alcuni tipi di problemi e una conoscenza spesso soltanto superficiale dell'intero campo. Di qui l'utilità di un testo semplice ed esteso che possa servire a completamento della cultura professionale del ricercatore.

Il libro di KITTEL: *Introduction to solid state physics*, che appare ora in una seconda edizione arricchita di 200 pagine rispetto all'edizione originale del 1953, soddisfa pienamente questa esigenza.

Esso è pure raccomandabile per lo studente e per il giovane laureato che desideri orientarsi in fisica dei solidi.

Il testo consiste di 19 capitoli non necessariamente collegati l'uno all'altro, ma ordinati secondo il criterio di anticipare gli argomenti di carattere più generale e tradizionale.

Nei primi nove capitoli l'Autore presenta una descrizione delle strutture cristalline, una classificazione dei solidi, tratta le proprietà elastiche, termiche,

dielettriche, diamagnetiche e paramagnetiche.

In seguito l'Autore descrive il comportamento degli elettroni in un reticolo periodico sviluppando la teoria delle bande per passare poi alle applicazioni a metalli, leghe e cristalli semiconduttori.

Il modello degli elettroni liberi nei metalli, il ferromagnetismo, la superconduttività, sono pure egregiamente esposti in altrettanti capitoli.

Gli ultimi tre capitoli riguardano i fenomeni dovuti alla presenza di irregolarità nel reticolo cristallino. Assorbimento dovuto a centri di colore, luminescenza e crescita dei cristalli da dislocazioni sono qui trattati. La teoria dell'eccitone è pure presentata alla luce di recenti esperienze.

Pregio maggiore del libro è quello di presentare i fenomeni in modo semplice e chiaro, illustrandoli con le esperienze che li mettono in evidenza. I concetti teorici vengono direttamente collegati ai dati sperimentali, spesso con l'aiuto di modelli, mentre le trattazioni matematiche di carattere più astratto sono svolte nelle appendici.

Oltre ad essere chiaro ed informativo, il libro è meditato e molto curato nei dettagli.

Lungi dall'essere incoraggiato in semplificazioni apparenti e in imprecisioni, il lettore è stimolato a pensare da sè e ad approfondire maggiormente i vari argomenti.

Sono in questo di valido aiuto i problemi proposti alla fine di ogni capitolo

ed i richiami bibliografici alla letteratura più recente.

L'unico serio appunto che si possa fare è già stato anticipato dall'Autore nella prefazione alla seconda edizione ed è il non aver trattato alcuni rami della fisica dei solidi in fase di intenso sviluppo quali la fisica delle superficie e i fenomeni di anelasticità.

F. BASSANI

Particelle pesanti instabili, fascicolo della « Series of Selected Papers in Physics » pubblicata a cura della Società Giapponese di Fisica (Physical Society of Japan, pagine 286).

In questo fascicolo sono raccolti 31 articoli apparsi tra il 1947 ed il 1955 su riviste americane (11 articoli pubblicati sulla *Physical Review*), europee (8 articoli pubblicati sul *Nuovo Cimento*; 5 su *Nature London*; 4 sul *Philosophical Magazine*) e giapponesi; la scelta è stata limitata a quegli articoli originali nei quali sono descritti o nuove particelle instabili, o aspetti nuovi della loro fenomenologia, o interpretazioni generali del complesso insieme di fenomeni che comprende la produzione, l'interazione ed il decadimento dei mesoni pesanti e degli iperoni.

Il fascicolo è diviso in tre parti: nella prima, di carattere sperimentale, l'insieme dei lavori raccolti permette di seguire la genesi ed il successivo rapido accrescimento di questo nuovo campo di ricerca della fisica moderna. I primi lavori contengono i risultati della analisi della radiazione cosmica mediante le lastre nucleari e la camera di Wilson; le osservazioni del gruppo di Bristol (1947) sul decadimento $\pi\mu$; la scoperta del τ (Bristol 1949), del K_l (Bristol 1951), degli iperoni carichi (Milano 1953), dei frammenti pesanti eccitati (DANYSZ e PNIEWSKI 1953), del decadimento $\frac{1}{2}$ del K (Bristol 1954); il lavoro conclu-

sivo del G-stack (1955) sulla natura delle particelle pesanti instabili che fanno parte della radiazione cosmica. I risultati ottenuti mediante la tecnica della camera di Wilson sono ben rappresentati dai lavori del gruppo di Manchester (1947) sulle V neutre e cariche; dalle successive osservazioni del gruppo di Pasadena (1950) e di quello di Manchester (1951); dalla prima osservazione del θ^0 (Bloomington 1953), del Ξ (Pasadena 1954) e del $K_{\mu 2}$ (Parigi 1954). Seguono alcuni importanti articoli sulla produzione di mesoni pesanti mediante particelle accelerate artificialmente: le prime osservazioni su la produzione associata (Brookhaven 1954) e le prime abbondanti statistiche sui mesoni pesanti (Berkeley 1955). Chiude la prima parte il lavoro del gruppo di Berkeley (1955) sull'antiproton.

La seconda parte contiene tre articoli teorici: quello di PAIS sulle particelle V (1952); le osservazioni di GELL-MANN sullo spin isotopico delle particelle instabili (1953) e l'articolo di NISHIJIMA su una teoria indipendente dalla carica per i mesoni pesanti e gli iperoni (1955). La scelta compiuta per i lavori teorici mi sembra eccessivamente limitata e non troppo rappresentativa; sarebbe stato interessante trovare, in un fascicolo in cui la documentazione sperimentale è così accurata e completa, anche articoli teorici come quelli di GELL-MANN e PAIS (*Conferenza di Glasgow* 1954), di D'ESPAGNAT e PRENTKI (*Nuclear Physics* 1955), di DALITZ sulla indipendenza dalla carica nei frammenti leggeri (1956), ecc.

La terza parte è in giapponese e mi è impossibile, quindi, recensirla; contiene due lavori, pubblicati su riviste giapponesi nel 1953 e nel 1954 che, a quanto si può desumere dalla bibliografia, sono articoli riassuntivi sulla situazione sperimentale e sulle interpretazioni teoriche nel campo delle particelle pesanti instabili.

Come è facile notare, la scelta fatta esclude tutti gli articoli in cui sono state

scoperte particelle nuove e strane che in seguito non sono sopravvissute per più di qualche mese; malgrado ciò, tutta la nomenclatura dei mesoni pesanti e degli iperoni è, durante gli ultimi anni, radicalmente mutata, e risulta talvolta difficile seguire, negli articoli originali, il progressivo trasformarsi del nome e del simbolo di una stessa particella.

B. VITALE

H. PREUSS - *Integraltafeln zur Quantenchemie*. Springer-Verlag, Göttingen, 1956; pagg. IV+162; tavole 92. Prezzo L. 6450.

Il libro di PREUSS, *Integraltafeln zur Quantenchemie*, affiancandosi ad altro analogo di recente pubblicazione della scuola giapponese, contribuisce a colmare la lacuna costituita dalla mancanza di una sintesi unitaria del lavoro di numerosissimi autori che da vari anni cercano di alleggerire il faticoso calcolo numerico insito nei problemi di struttistica molecolare.

Lo studio della struttura elettronica della molecola rappresenta un tipico esempio di problema quantomeccanico di molte particelle. I metodi di lavoro che sono stati sviluppati per affrontare questo studio sono necessariamente dei metodi di risoluzione approssimati, nei quali la caratteristica comune è rappresentata dalla scelta della funzione d'onda polielettronica nella forma di un prodotto di funzioni d'onda monoelettroniche antisimmetrizzato. La scelta, poi, della forma di queste ultime caratterizza i due metodi di approssimazione più largamente usati. Come è noto, nel primo di questi metodi, le funzioni monoelettroniche adottate sono direttamente funzioni atomiche degli atomi che compongono la molecola (metodo degli orbitali atomici); mentre, nel secondo, le funzioni monoelettroniche prescelte sono funzioni d'onda estese a tutta la molecola (orbitali molecolari).

Di solito gli orbitali molecolari adottati nel secondo metodo vengono, a loro volta, approssimati da combinazioni lineari di orbitali atomici e pertanto le funzioni monoelettroniche base scelte in ambedue i metodi per la costruzione delle funzioni d'onda complessive sono, in definitiva, sempre gli orbitali atomici degli atomi costituenti la molecola.

Da lungo tempo i diversi Autori che si sono occupati di questi problemi hanno trovato conveniente adoperare, per le funzioni d'onda monoelettroniche atomiche, le funzioni idrogenoidi senza nodi di Slater.

In effetti, i risultati migliori raggiunti fino ad oggi nella trattazione dei problemi atomici vengono forniti dalle funzioni numeriche ottenute da Hartree-Fock con il metodo del campo «self consistente», ma si può dimostrare che esse sono descritte con sufficiente esattezza mediante una opportuna combinazione lineare delle funzioni di Slater le quali, pertanto, sono da considerarsi come buone funzioni base monoelettroniche atomiche, utilizzabili per lo studio di qualsiasi problema molecolare.

Ciò premesso, ogni calcolo numerico nei problemi di struttura molecolare si può affrontare con l'ausilio di un certo numero di integrali che coinvolgono le funzioni di Slater e i vari addendi dell'operatore Hamiltoniano: tipici, per esempio, l'integrale di sovrapposizione, quelli di attrazione nucleare e gli integrali di Coulomb, di scambio e ibridi di repulsione elettronica.

Nel manuale di PREUSS il lettore potrà trovare formule risolutive e tabelle numeriche per i principali tipi di questi integrali monocentrici e bicentrici e per un certo numero di integrali ausiliari.

I risultati trascritti sono, però, limitati a funzioni di Slater caratterizzate dai soli valori 1 e 2 del parametro n che rappresenta il numero quantico principale, e inoltre tutte le funzioni che compaiono in uno stesso integrale bicentrico sono relative al medesimo valore del

secondo parametro z che rappresenta la carica efficace del nucleo cui appartiene la funzione monoelettronica corrispondente. Il lettore, poi, avrebbe forse visto con piacere una maggiore estensione del campo di tabulazione. Queste limitazioni consentono di utilizzare il manuale di PREUSS soltanto per i problemi relativi a molecole omonucleari.

In realtà, sulla intestazione del volume è scritto «Erster Band», e c'è da sperare che l'Autore possa presto pubblicare dei volumi integrativi che estendano il campo di utilizzazione delle tabelle, sia raccogliendo l'abbondante materiale sparso nella letteratura (per gli integrali di sovrapposizione, per esempio, vi sono ottime tabelle molto estese della scuola di Mulliken), sia eseguendo il lavoro di calcolo numerico sulle basi delle formule risolutive pubblicate in questi ultimi anni dai numerosi Autori citati dal Preuss stesso.

E. SCROCCO

P. M. S. BLACKETT — *Lectures on Rock Magnetism*. The Weizmann Science Press of Israel, Jerusalem, 1956; pagg. II+129; tabelle 6; prezzo \$ 5.00.

Le ricerche sul magnetismo delle rocce hanno avuto recentemente sviluppi molto interessanti e promettenti; esse hanno aperto prospettive nuove in seno alla questione tanto dibattuta della origine e della storia, attraverso i tempi geologici, del campo magnetico terrestre, e hanno altresì portato nuovi elementi per la soluzione del problema riguardante il movimento di masse continentali, le une rispetto alle altre, o rispetto ai poli geografici.

Nel presente volumetto, *Lectures on Rock Magnetism*, di mole piuttosto limitata (pagg. 131), P. M. S. BLACKETT riesce a dare un'esposizione, per quanto molto sintetica, chiara ed acuta dei diversi problemi connessi con la interpre-

tazione di numerosi risultati sperimentali su alcune rocce ignee e sedimentarie, la cui direzione di magnetizzazione è risultata invertita rispetto a quella dell'attuale campo magnetico terrestre.

Nel primo capitolo viene discusso dall'autore questo punto fondamentale della trattazione: in esso, che è poi il più interessante dal punto di vista fisico, vengono esposte sotto forma critica alcune ipotesi avanzate; in particolare quelle di Néel, sulla esistenza di speciali processi fisici e chimici nei quali può essere invertito il senso nella direzione di magnetizzazione delle rocce rispetto al campo ambientale; in seguito viene discussa la possibilità che il dipolo magnetico della terra, al quale si pensa legato il suo campo magnetico, sia stato attraverso la storia geologica pressocchè sempre della stessa grandezza, ma che abbia invertito il suo verso repentinamente una o più volte.

L'Autore descrive piuttosto dettagliatamente, nel cap. II, alcuni lavori sperimentali condotti allo scopo di studiare l'origine dell'inversione della magnetizzazione di alcune rocce: egli conclude che, per quanto ci siano forti ragioni per ammettere una magnetizzazione in un campo terrestre invertito, (questo sarebbe suffragato dal fatto di non aver trovato differenza di natura fisica o chimica tra rocce normali e rocce invertite), pure si è ancora lontani da una soluzione definitiva del problema.

Nel cap. III sono raccolti e discussi recenti risultati sul movimento di masse terrestri interessanti parte dell'Europa, l'America, il Sud Africa, l'India e l'Australia; nella seconda parte dello stesso capitolo sono riportati altri risultati di misure su numerosi campioni (rocce sedimentarie e ignee).

Completono il volume tre appendici nelle quali sono trattati: un nuovo strumento di misura impiegato da P. M. S. BLACKETT e D. J. SUTTON, con alcuni risultati sperimentali ottenuti con lo stesso; la separazione di piccole quan-

tità di materiali magnetici ed infine l'inversione termica di materiali trattati magneticamente. È possibile infatti portare qualche sostanza magnetica ad uno stato tale che la sua magnetizzazione si possa invertire con una variazione di temperatura. Questa inversione termica della magnetizzazione di alcuni materiali può derivare dalla esistenza in essi di componenti magnetici diretti in verso opposto: il meccanismo attraverso il quale si realizza questo fenomeno varia da caso a caso.

Il libro è aggiornato fino ai più recenti lavori; alla fine di ogni capitolo una larga bibliografia mette lo studioso che ne avesse interesse nella possibilità di approfondire l'argomento.

L'Autore dichiara nella prefazione di avere voluto esercitare, nel redigere questo volumetto, uno stimolo per ulteriori ricerche in questo nuovo campo di studi che interessano tanto la fisica che la geologia e la geofisica. Penso che tale scopo sia stato raggiunto: è certo che solo attraverso nuovi metodi di indagine ed una estensione delle ricerche a zone sempre più vaste della terra, sarà possibile trarre dai risultati attuali e da quelli che verranno, conclusioni che potranno modificare profondamente le nostre idee sulla origine e la storia del campo magnetico terrestre e sui problemi geologici fondamentali.

Aggiungasi a questo interesse quello che riguarda la conoscenza più intima del vasto e complesso fenomeno della magnetizzazione della materia.

M. SANTANGELO

H. RICHTER — *Wahrscheinlichkeits-theorie*. Springer-Verlag, Berlin, 1956; pagg. XII+435; figg. 14; prezzo non indicato.

Il calcolo delle probabilità ha subito negli ultimi vent'anni una profonda revisione critica, che ha permesso anche di vedere i risultati classici da un punto

di vista unitario e di formulare i problemi nella maggiore generalità possibile. Tale nuova epoca del Calcolo delle probabilità può farsi datare nel 1933 quando apparve nella collezione « Ergebnisse der Mathematik und ihre Grenzgebiete » il volumetto di A. KOLMOGOROFF, *Grundbegriffe der Wahrscheinlichkeitsrechnung*.

Mentre un tempo la nozione di probabilità era lasciata piuttosto nel vago e frequenti richiami a fatti sperimentali e lunghi discorsi — spesso mascherati circoli viziosi — pretendevano di definire cosa si intendeva per probabilità, si preferisce oggi seguire una via assiomatica. Il calcolo delle probabilità diviene così un capitolo della teoria della misura e della integrazione secondo una data misura: la probabilità si introduce come una misura normalizzata.

Di qui la necessità per una moderna trattazione di calcolo delle probabilità di usare mezzi matematici elevati, che soltanto lettori molto specializzati possiedono. Bene ha fatto quindi l'A. a dedicare nella sua pregevole opera l'intero capitolo I ai fondamenti della teoria della misura e il cap. IV alla teoria dell'integrazione di una funzione misurabile (integrazione di Lebesgue-Stieltjes) in una o più variabili. L'esposizione di questi due capitoli è piana e la lettura riesce agevole per chi abbia le nozioni matematiche del nostro primo biennio delle Facoltà scientifiche universitarie. Tale scopo può essere raggiunto perché saggiamente l'A. limita la trattazione solo a quei risultati che gli occorrono nel seguito dell'opera.

Stabilite così nel cap. I le basi matematiche per poter proseguire, l'A. espone nel cap. II il concetto di probabilità dal punto di vista intuitivo e sperimentale, giustificando la necessità di una precisione matematica.

Nel cap. III è svolta la teoria elementare del Calcolo delle probabilità, da un punto di vista assiomatico, ed è messa in luce l'insufficienza degli schemi usati e la necessità di poter disporre di una

più larga nozione di probabilità. Perciò, stabiliti (come si è già detto) nel Cap. IV i fondamenti della teoria dell'integrazione, l'A. può finalmente passare nel Cap. V alla teoria generale dei campi di probabilità.

Egli definisce la densità di probabilità e le funzioni di ripartizione, sviluppando la teoria generale astratta delle probabilità.

Nel Cap. VI egli ritrova, come caso particolare della teoria generale, le ripartizioni classiche, in particolare quella gaussiana. L'ultimo capitolo è dedicato alle leggi limite del Calcolo delle probabilità.

L'opera è resa più attrente da una accurata scelta di esercizi proposti al lettore e di cui alla fine viene data la soluzione.

Il rigore e la modernità dell'esposizione, lo sviluppo graduale della trattazione, il fatto che l'A. ha esplicitamente rinunciato a soffermarsi troppo a lungo sull'analisi critica degli assiomi — analisi che sarebbe stata di alto interesse filosofico, ma che avrebbe condotto il lettore fuori della via maestra — rendono la lettura di questo trattato praticamente agevole a chi voglia con relativa rapidità rendersi conto delle moderne concezioni del calcolo delle probabilità.

S. FAEDO

Korpuskularoptik - Optics of Corpuscles, volume XXXIII dell'*Handbuch der Physik*, editore S. Flügge. Springer-Verlag, Berlino, 1956.

È uno dei primi volumi apparsi della nuova edizione dell'*Handbuch der Physik*. La grande mole delle conoscenze odierne in fisica sarà raccolta completamente entro pochi anni in questa poderosa opera, comprendente 54 volumi, e verrà suddivisa, cosa caratteristica della nuova edizione, in un numero di capitoli molto elevato (oltre 300), ciascuno dei quali è

affidato ad uno specialista dell'argomento. Secondo lo schema annunciato i compilatori sono per il 35% fisici degli Stati Uniti, per il 20% tedeschi e per il 10% inglesi. Il testo è riportato in una delle tre lingue, inglese, tedesco e francese, a scelta dell'autore. L'autorità del direttore della enciclopedia, la fama della casa editrice, la notorietà dei collaboratori assicurano all'impresa un successo pari a quello della vecchia edizione. Nessuna biblioteca importante potrà rinunciare a possedere la collezione che farà il punto sulla fisica generale, sulla fisica atomica e nucleare, sulla geofisica e sulla fisica stellare alla metà del secolo XX. L'organizzazione della materia è tale da invogliare molti fisici ad acquistare i volumi che trattano gli argomenti a cui sono interessati.

Il volume XXXIII contiene 5 capitoli di *Ottica elettronica*, i primi quattro scritti in tedesco e l'ultimo in inglese.

Il 1° capitolo, scritto dal dottor D. KAMKE dell'Università di Marburg, riguarda le *sorgenti di elettroni e di ioni*. Dopo un rapido richiamo ai processi di emissione, l'autore descrive numerosi tipi di sorgenti, corredando la trattazione con molti disegni e grafici. Soprattutto utile risulta la rassegna delle sorgenti di ioni, perchè la presente trattazione è la prima sull'argomento. Nella stesura dell'articolo l'autore si è proposto di illustrare essenzialmente le sorgenti per gli spettrometri di massa. Nessun cenno è fatto così alle sorgenti particolari impiegate per gli acceleratori ciclici e neppure a quelle di ioni a più cariche, che pure presentano oggi particolare interesse.

Il 2° capitolo è dedicato alla *Teorica dell'ottica elettronica*. Il prof. W. GLASER dell'Università di Vienna sviluppa anzitutto l'analogia fra l'ottica e lo studio della traiettoria degli elettroni, soffermandosi poi sulle proprietà dei campi elettrici e magnetici con simmetria di rotazione attorno ad un asse, usati per la deflessione dei fasci. Molto ampiamente

è trattata la teoria delle aberrazioni geometriche. Successivamente viene analizzato il comportamento dei fasci di elettroni in campi deflectenti, considerando anche i casi di sistemi dotati di asse principale curvo. Particolare attenzione è pure rivolta al problema degli effetti della carica spaziale nella formazione delle immagini. La parte finale del capitolo svolto da GLASER si stacca dalle trattazioni tradizionali: con i metodi della meccanica ondulatoria sono affrontati in modo brillante alcune questioni, fra cui la critica dei limiti dell'ottica elettronica geometrica, la soluzione di alcuni problemi relativi alla microscopia elettronica ed all'ottica fuori dell'approssimazione dei raggi parassiali. La trattazione dell'autore, ricca di contributi originali, è veramente felice e risulterà certamente fra i più bei capitoli dell'Encyclopedia.

Sul *microscopio elettronico* il dottor S. LEISEGANG di Berlino offre nel 3º capitolo del volume un quadro completo: accanto al microscopio convenzionale, usato in trasmissione, trovano largo spazio quelli per uso speciale, quali i microscopi ad ombra, a riflessione, ad emissione, ... Per ciascuno dei tipi l'autore descrive il principio di funzionamento, presenta i dati costruttivi e delinea i problemi pratici che si presentano nell'uso dei diversi strumenti. La lettura del testo è facilitata dalle numerose illustrazioni nitide e precise che permettono di sorprendere ogni particolare in schemi di apparecchi talvolta molto complessi. Scelti con estrema cura gli esemplari di fotografie ottenute con il microscopio elettronico.

Il 4º e 5º capitolo trattano rispettivamente degli *spettrometri di massa* e degli *spettrometri per raggi beta* e sono svolti, il primo dal dott. H. EWALD del Politecnico di Monaco, il secondo dal dott. T. R. GERHOLM dell'Università di Uppsala. Le trattazioni, riferendosi ad argomenti recentemente riassunti in altre brillanti rassegne (K. T. BAINBRIDGE,

nel 1º volume dell'*Experimental Nuclear Physics* edito da SEGRÈ, e K. SIEGBAHL e J. M. W. DUMOND nel volume *Beta and Gamma Spectroscopy* edito da SIEGBAHL) non presentano particolari novità. L'esposizione di entrambe le trattazioni è chiara e completa, i disegni e le fotografie riportate sono nettamente migliori di quelli presentate in altre precedenti rassegne.

A. LOVATI

W. H. SULLIVAN - *Trilinear Chart of Nuclides*. January 1957. Atomic Energy Commission, U.S.A.

Tra le numerose « Carte di Nuclidi » questa di W. H. SULLIVAN, uscita recentissimamente nella seconda edizione, ricca di dati e informazioni raccolti nella più recente letteratura (fino al luglio 1956) nel campo della fisica e della chimica nucleare, ci pare veramente utile in un laboratorio di ricerche nucleari.

Non occorre ricordare come sia facile la consultazione di tale carta in cui sono allineati gli isotopi, gli isobari, gli isotonni e gli isodiaferi e come per ogni nuclide siano riportati i valori della sezione efficace, l'abbondanza relativa, la massa atomica, il momento angolare, i modi di disintegrazione, i momenti di dipolo, ecc.

Conviene piuttosto segnalare come sia possibile, e con molta facilità, conoscere attraverso quali reazioni nucleari può ottersi un nuclide dai nuclidi « confinanti ».

Poiché le tabelle nucleari invecchiano rapidamente, perché sempre nuovi dati si aggiungono a quelli già noti e sempre più perfezionate informazioni vengono fornite da nuove ricerche sperimentali, un pregio materiale, ma notevole della Trilinear Chart è il seguente: francobolli relativi ai nuclidi nuovi o ai nuclidi che i nuovi risultati sperimentali hanno modificato vengono via via inviati dall'Autore in modo che la Carta sia sempre « up to date ». Dicasi questo un vantaggio

spicciolo, ma ci pare possa risolvere uno dei problemi più gravi inerenti alla durata delle attuali raccolte di dati nucleari.

F. DEMICHELIS

A. DAUVILLIER — *L'origine des Planètes*. Presses Universitaires de France, Paris, 1956. Nouvelle Collection Scientifique, 224 pagg. 10 tavole. Frs. 800.

I Pianeti hanno avuto origine in seguito a collisioni stellari, questa è la tesi dell'A. che impiega una ottantina di pagine per illustrare la sua nuova teoria dei Pianeti gemelli, e le rimanenti pagine del libro a criticare e demolire le teorie fino ad ora proposte.

La tesi dell'A. sarebbe insostenibile nell'universo quale noi lo osserviamo attualmente, poiché, data la piccola densità stellare, la probabilità di collisioni è praticamente nulla anche in periodi di tempo lunghissimi. Ecco che allora l'A. ha bisogno di creare l'ambiente perché la collisione si verifichi, e così egli postula che la nascita delle Stelle avvenga unicamente nel centro della galassia o nel nucleo degli ammassi stellari. A dire il vero, secondo le idee dell'A. gli ammassi servono unicamente a raccogliere le Stelle sfuggite al nucleo galattico ed a riportarle verso il centro per una specie di rigenerazione o di rinnovamento.

Da questo punto di vista la galassia diviene un sistema autonomo funzionante a ciclo chiuso e nel quale le stelle assumono ruolo analogo alle molecole nella teoria cinetica dei gas. Si hanno così tre specie di collisioni: chiamate dall'autore

pseudo-collisioni, collisioni centrali e collisioni radenti. Mentre le prime servono a mantenere un'equipartizione dell'energia tra le Stelle, quelle centrali darebbero origine a delle nuove Stelle giganti rosse mentre le ultime provocando la cattura di una Stella da parte di un'altra, porterebbero di conseguenza alla fusione dei due corpi celesti con l'espulsione di frammenti dai quali avrebbero origine i pianeti. L'eventuale interazione tra i frammenti produrrebbe a sua volta i Satelliti. Questa in poche parole la teoria dell'A. che se è notevole per la sua semplicità lascia d'altronde piuttosto perplessi per la necessità di ammettere la formazione delle Stelle in condizioni del tutto particolari.

Sappiamo oggi come per esempio la nebulosa di Orione sia una fucina di nuove Stelle senza che pertanto vi siano quei valori estremi di densità postulati dall'A. per sostenere la sua teoria. Appaiono anche strane le idee che l'A. sembra avere sul ruolo della materia interstellare dell'universo e sul ciclo evolutivo delle Stelle che non è certamente conforme ai risultati acquisiti dalla cosmologia osservativa.

Il libro si legge facilmente ma per le ragioni anzidette non è certamente raccomandabile per la formazione culturale dei giovani. Può essere molto utile invece come messa a punto critica sullo stato del problema qualora si tenga presente che lo smantellamento delle teorie precedenti viene fatto in funzione della nuova teoria presentata.

La veste tipografica è decorosa e conforme alle tradizioni dell'Editore.

G. RIGHINI

IL NUOVO CIMENTO

INDICI

DEL VOLUME V - SERIE X

1957

PRINTED IN ITALY

INDICE SISTEMATICO
PER NUMERI SUCCESSIVI DEL PERIODICO

N. 1° - 1 GENNAIO 1957

B. JOUVENT - Fermi Coupling and Mass and Charge Spectra of Bosons	pag. I
A. AGODI - On γ -Polarization Effects in Photonuclear Reactions	» 21
R. L. MILLS - Integral Equations for Meson Field Theory	» 30
W. CZYŻ and J. SAWICKI - Polarization of Nucleons from Photodisintegration of Deuterium	» 45
H. JOOS, J. LEAI FERREIRA and A. H. ZIMERMAN - A Special Representation for the Treatment of a System of two Dirac Particles	» 57
J. K. PERCUS and G. J. YEVICK - «Dynamical» Lagrangian for the Many Body Problem	» 65
C. C. GROSJEAN - Further Development of a New Approximate One-Velocity Theory of Multiple Scattering	» 83
A. BORGARDT - Possible Forms of Nonlinear Mesodynamics	» 102
N. DALLAPORTA and F. FERRARI - On the Λ -Nucleon Force and the Binding Energy of the Light Hyperfragments	» 111
N. N. BISWAS, L. CECCARELLI-FABBRICHESI, M. CECCARELLI, K. GOTTSSTEIN, N. C. VARSHNEYA and P. WALOSCHEK - Nuclear Scattering of K^+ -Mesons in the Energy Region of 80 MeV	» 123
P. BROVETTO and S. FERRONI - On the Paramagnetic Resonance Spectrum of Triphenylmethyl	» 142
F. GÜRSEY - General Relativistic Interpretation of Some Spinor Wave Equations	» 154
G. COCCONI, G. PUPPI, G. QUARENÌ and A. STANGHELLINI - K^+ -Meson Interaction with Nucleons and Nuclei	» 172
S. FRANCHETTI - On the Problem of the Static Helium Film - II. Effects due to the Smallness of One Dimension	» 183
R. HAAG - On the Physical Significance of the Redundant Solutions of the Low Equation	» 203
R. PLANO, N. SAMIOS, M. SCHWARTZ and J. STEINBERGER - Demonstration of the Existence of the Σ^0 Hyperon and a Measurement of its Mass . .	» 216
L. TENAGLIA - Proprietà elettromagnetiche del protone e rinormalizzazione della costante d'accoppiamento	» 220
L. TENAGLIA - Struttura del protone e scattering elettrone-protone	» 229
F. FERRERO, L. GONEILA, R. MALVANO, C. TRIBUNO and A. O. HANSON - Fast Neutron Component in Photonuclear Reactions	» 242

Note Tecniche:

J. E. LABY, Y. K. LIM and V. D. HOPPER - Level Flights with Expansible Balloons	pag. 249
M. DEBEAUVAIS, E. PICCIOTTO et S. WILGAIN - Arrêt de la diffusion des radio-éléments dans les émulsions nucléaires par exposition à basse température	» 260
M. SILVESTRI e N. ADORNI - Apparato per misure standard di scambio isotopico del deutero fra idrogeno e vapor d'acqua a pressione atmosferica e a 100 °C	» 266
S. FOCARDI, C. RUBBIA, G. TORELLI e F. BELLA - Metodi di comando rapido di rivelatori di tracce	» 275

Lettere alla Redazione:

M. W. FRIEDLANDER - The Lifetime of ${}^3\text{H}_\Lambda$ Hyperfragments	» 283
S. FURUCHI, Y. SUGAHARA, A. WAKASA and M. YONEZAWA - An Analysis of Rochester $K_{\mu 3}$ and K_{e3} Data	» 285
G. B. ZORZOLI - On the Decay of ${}^{141}\text{Ce}$	» 289
A. MARQUES, N. MARGEM and G. A. B. GARNIER - Mean Free Path of 4.3 GeV π^- -Mesons in Nuclear Emulsions	» 291
H. FAY - Electron-Photon Cascades of High Energy in Photographic Emulsions	» 293
A. SALAM - On Parity Conservation and Neutrino Mass	» 299
W. HEITLER Renormalization in Non-Relativistic Field Theories. (Remarks about the paper by Enz)	» 302
P. BUDINI and L. FONDA - Pion-Nucleon Interaction and Strange Particles	» 306
L. COLLI and U. FACCHINI - Further Measurements on n, p Reactions at 14 MeV - II. Sulphur, Aluminium, Iron, Copper, Nickel	» 309
U. L. BUSINARO and S. GALLONE - Asymmetric Equilibrium Shapes in the Liquid Drop Model	» 315
A. KIND - On the Sign of the Real Central Part of the Neutron-Nucleus Complex Potential	» 318

<i>Libri ricevuti e Recensioni</i>	» 321
----------------------------------------------	-------

N. 2 - 1° FEBBRAIO 1957

T. REGGE - On the Properties of Spin 2 Particles	pag. 325
A. J. APOSTOLAKIS, J. O. CLARKE and J. V. MAJOR - Spurious Scattering in Nuclear Emulsions	» 337
H. FUKUTOME and Y. NOGAMI - Remarks on the Fixed Extended Source Pion Theory	» 347
G. BERTOLINI, E. LAZZARINI and M. MANDELLI BETTONI - Directional Correlation of the 0.845 and 1.24 MeV γ -Rays of ${}^{56}\text{Fe}$	» 356
G. ALEXANDER and R. H. W. JOHNSTON - On the Relation between Blob-Density and Velocity of a Singly Charged Particle in G-5 Emulsion . .	» 363

S. JANNELLI e F. MEZZANARES - Caratteristiche delle disintegrazioni nucleari prodotte da protoni di 140 ± 6 MeV - II. Nuclei pesanti	pag. 380
W. E. FRAHN - Nucleon-Nucleus Interaction from the Statistical Model	» 393
M. BALDO-CEO LIN, M. CRESTI, N. DALLAPORTA, M. GRILLI, L. GUERRIERO, M. MERLIN, G. A. SALANDIN and G. ZAGO - Interactions of K^+ Mesons with Emulsion Nuclei between 40 and 160 MeV	» 402
C. CEO LIN and L. TAFFARA - On the Scattering of K^+ -Mesons by Nucleons in Perturbation Theory	» 435
G. COSTA and G. PATERGNANI - K^+ Nuclei Interactions According to the Optical Model	» 448
M. W. FRIEDLANDER, D. KEEFE and M. G. K. MENON - The Range in G-5 Nuclear Emulsion of Protons with Energies, 87, 118 and 146 MeV	» 461
U. FASOLI, C. MARONI, I. MODENA, E. POHL and J. POHL-RÜLING - On the Correlation of the Intensity of μ^- and μ^+ -Mesons with the Pressure at Sea-level, and with the Height of the 100 mb Layer	» 473
E. ARNOUS - Étude du nombre de mésons virtuels sur un modèle simple	» 483
L. v. LINDERN - Multiple Meson Production and Angular Distribution of Shower Particles Produced in Cosmic Ray «Jets»	» 491
L. COLLI, U. FACCHINI and S. MICHELETTI - Comparison between (n, p) and (p, p') Experiments on Intermediate Energy	» 502

Note Tecniche:

F. FERRERO, R. MALVANO and C. TRIBUNO - Camera di ionizzazione per raggi X fino a 31 MeV	» 510
----------------------------------------------------------------------------------------------------	-------

Lettere alla Redazione:

M. MIĘSOWICZ, O. STANISZ and W. WOLTER - Investigation of an Electromagnetic Cascade of Very High Energy in the First Stage of its Development	» 513
S. TOKUNAGA, K. NISHIKAWA and T. ISHII - Nuclear Disintegration Cascades by Heavy Primaries	» 517
N. NAKANISHI - On Lehmann's Method of Renormalization	» 520
W. E. FRAHN and R. H. LEMMER - Effective Nuclear Potentials	» 523
N. A. PORTER - The Effect of Ultra-Violet Converters on the Efficiency of Liquid Čerenkov Counters	» 526
C. MILONE, R. RICAMO and A. RUBBINO - C and Al Photoprotton Angular and Energy Distribution	» 528
C. MILONE, R. RICAMO and R. RINZIVILLO - Photoprottons from Oxygen up to 30 MeV	» 532

<i>Libri ricevuti e Recensioni</i>	» 535
----------------------------------------------	-------

N. 3 - 1° MARZO 1957

K. M. CROWE - The Masses of Light Mesons, K-Mesons and Hyperons in 1956	pag. 541
M. MILONE e E. BORELLO - Sulla struttura della glossofima allo stato solido	» 562
M. PIERUCCI - Sull'età dell'Universo	» 572

G. RIGAULT - Relazioni tra la struttura della blenda e il contenuto in gallio e indio	pag. 579
M. SIMONETTA e A. VACIAGO - Calcolo quantomeccanico della barriera di potenziale per l'inversione della molecola di fosfina	» 587
S. HIGASHI, T. OSHIO, H. SHIBATA, K. WATANABE and Y. WATASE - On the Cosmic Ray Penetrating Showers Underground	» 592
S. HIGASHI, T. OSHIO, H. SHIBATA, K. WATANABE and Y. WATASE - On the Multiple Penetrating Particles Underground	» 597
S. HAYAKAWA - A Possible Interpretation of the Multiple Penetrating Particles	» 608
M. ODA - A Calculation on the Structure of the Nucleonic Cascade in the Atmosphere	» 615
N. MIKOSHIBA - Quantum Fluid as a Common Model for Superfluidity and Supereconductivity	» 628
J. A. MCLENNAN jr. - Conformally Invariant Wave Equations for Non-Linear and Interacting Fields	» 640
L. VERDINI - Velocità delle onde elastiche e dissipazione interna nel metacrilato di polimetile	» 648
K. SYMANZIK - On Scattering at Very High Energies	» 659
P. BUDINI and L. FONDA - Non-Local Models of Pion-Nucleon, Pion-Hyperon Interactions	» 666
C. CASTAGNOLI, C. FRANZINETTI and A. MANFREDINI - Further Results on Parity Conservation in $\pi\mu\text{-e}$ Decays	» 684
G. WATAGHIN - On a Non-Local Relativistic Quantum Theory of Fields - I.	» 689

Note Tecniche:

M. R. E. BICHARA - Risultati di un oscillatore con transistore	» 702
P. J. GROUSE and H. D. RATHGEBER - A Geiger Counter Design Giving a Definite Counting Length	» 707
A. BARONE - Interferometro per misure di precisione della velocità degli ultrasuoni nei liquidi	» 717

Lettere alla Redazione:

L. A. RADICATI and S. ROSATI - On the Spin of the $K_{\mu 3}$ Meson	» 729
B. VITALE - Electromagnetic Properties of Nucleons and Barion-Heavy Meson Interactions	» 732
C. J. WADDINGTON - Observation on the Energy Spectra of Multiply Charged Nuclei in the Cosmic Radiation	» 737
E. R. CAIANIELLO - Propagation Kernels as Functions of the Masses	» 739
N. DALLAPORTA and F. FERRARI - On the Σ Hyperon-Nucleon Interaction Cross-Section	» 742
R. C. KUMAR, W. B. LASICH and F. R. STANNARD - The Mass Difference between the Σ^+ and Σ^- Hyperons	» 746
S. COLOMBO, C. COTTINI and E. GATTI - Improvements on a Multichannel Pulse Analyzer	» 748
T. GHOSE, S. K. GHOSH and D. K. ROY - Spin-Echoes with any Number of Pulses	» 751

B. F. TOUSCHEK - Parity Conservation and the Mass of the Neutrino	pag.	754
N. N. BISWAS, M. CECCARELLI and J. CRUSSARD - Angular Distribution of the μ -Decay as Test of Parity Conservation	"	756
M. GELL-MANN - Change of Isotopic Spin in the K_{π^2} Decay	"	758
B. FERRETTI - On the Conservation of Nucleons	"	761
<i>Libri ricevuti e Recensioni</i>	"	762

N. 4 - 1° APRILE 1957

M. FENOGLIO - Relazioni cristallografico-strutturali tra il difenile ed una serie di suoi nuovi derivati	pag.	765
A. CARRELLI and F. S. GAETA - A New Method for the Determination of the Acoustic Absorption Coefficient in Liquids	"	773
F. GÜRSEY - Relativistic Kinematics of a Classical Point Particle in Spinor Form	"	784
H. EZAWA, Y. TOMOZAWA and H. UMEZAWA - Quantum Statistics of Fields and Multiple Producton of Mesons	"	810
A. FERRO e G. MONTALENTI - Sulle variazioni delle proprietà magnetiche e meccaniche causate dall'idrogeno disciolto nel ferro	"	842
J. H. NOON, A. J. HERZ and B. J. O'BRIEN - An Observed Cosmic-Ray Flux of Light Elements at 41° N. Geomagnetic Latitude	"	854
H. S. GREEN - Separability of a Covariant Wave Equation	"	866
J. RAYSKI - Bilocal Field Theories and their Experimental Tests - II . .	"	872
B. JUDEK - Mass Measurements of Particles Stopping in the Emulsion by the Constant Sagitta Method	"	886
K. HIIDA and M. SAWAMURA - Some Relations Among Green's Functions	"	896
E. CLEMENTEL, C. VILLI and L. JESS - Phase Shift Analysis of Proton- Proton Scattering Experiments - II. Analysis of the Scattering Data from 18 to 260 MeV	"	907
A. SOKOLOV and B. KERIMOV - On the Scattering of Particles by a Force Centre According to the Radiation Damping Theory	"	921
L. BERTANZA, G. MARTELLI and B. TALLINI - Bubble Density along the Path of Ionizing Particles Crossing a Bubble Chamber	"	940
B. DE TOLLIS and R. S. LIOTTA - Interference in the Double Compton Effect	"	947
M. CARRASSI - The Spin Kinematics for a Charged Particle in a Uniform Magnetic Field	"	955
E. MONTALDI and M. PUSTERLA - Electron Scattering in Nuclear Field with Pair-Creation	"	961
A. HOSSAIN and D. J. PROWSE - On the 7.7 MeV Level of Carbon 12 . .	"	973
D. J. PROWSE - An Analysis of the Pairs Produced by ^{8}Be γ -Rays in Photographic Emulsions	"	977
R. OMNES - A System of General Relativistic Equations of Low Type . .	"	983
B. BHOWMIK, D. EVANS, S. NILSSON, D. J. PROWSE, F. ANDERSON, D. KEEFE, Á. KERNAN, N. N. BISWAS, M. CECCARELLI, P. WALOSCHEK, J. E. HOOPER, M. GRILLI and L. GUERRIERO - The Lifetime of Positive Heavy Mesons	"	994

Lettere alla Redazione:

K. M. CASE, C. N. YANG and R. KARPLUS - A Reply to Criticism by Mr. A. Gamba	pag. 1004
E. J. BURGE, J. H. DAVIES, I. J. VAN HEERDEN and D. J. PROWSE - On Some Aspects of Processing Thick Nuclear Emulsions	» 1005
G. STEPHENSON - A Classical Calculation of the Nucleon-Meson Coupling Constant.	» 1009
J. CSIKAI - Photographic Evidence for the Existence of the Neutrino	» 1011
S. v. FRIESEN and K. KRISTIANSSON - Further Evidence for a Longlived Neutral K-Particle	» 1013
P. BOCCIERI and P. GULMANELLI - Gravitational Forces and Quantum Theory	» 1016
R. PIONTELLI, G. POLI and L. PAGANINI - Electrochemistry of Metallic Single Crystals - I. Exchange Overvoltages on Silver and Copper	» 1018

Emendation:

A. KIND and L. JESS - On the Real Part of the Complex Potential Well of the Nucleus	» 1020
--------------------------------------------------------------------------------------------------	--------

N. 5 - 1° MAGGIO 1957

R. GATTO - Interference Effects between Members of Parity Doublets in the Lee-Yang Theory	pag. 1021
R. GATTO - The Annihilation of a Nucleon-Antinucleon System into a K-anti K Pair	» 1024
L. W. ALVAREZ, H. BRADNER, P. FALK-VAIRANT, J. D. GOW, A. H. RO- SENFELD, F. T. SOLMITZ and R. D. TRIPP - K- Interactions in Hydrogen .	» 1026
S. JANNELLI e F. MEZZANARES - Caratteristiche delle disintegrazioni nu- cleari prodotte da protoni di 140 ± 6 Mev - III. Nuclei leggeri	» 1047
J. K. PERCUS and G. J. YEVICK - Statistical Approach to the Domain of Action of Collective Co-ordinates in the Many Body Problem	» 1057
E. LOHRMANN - Multiple Meson Production in the Cosmic Radiation	» 1074
H. A. BUCHDAHL - Reciprocal Static Solutions of Field Equations Involving an Asymmetrical Fundamental Tensor	» 1083
K. HIIDA - A Kinematical Test for the Relation between the Coupling Constants in Meson Theory	» 1094
T. E. CRANSHAW and J. F. DE BEER - A Triggered Spark Counter	» 1107
S. MASCARENHAS - Thermodynamical Theory of Thermal Conduction of Dielectrics under Electric Fields	» 1118
J. B. KELLER - Bound of Phase Shifts	» 1122
TSAI-CHÜ - Determination of Distortion Vectors in Nuclear Emulsions . .	» 1128
C. B. A. MCCUSKER and F. C. ROESLER - New Experimental Evidence for the Tunnel Theory of Cosmic Ray « Jets »	» 1136
A. ASCOLI, M. ASDENTE and E. GERMAGNOLI - On the Atomic Displace- ments Produced by α -Particles in Germanium.	» 1145

M. S. SINHA and S. N. SENGUPTA - Evidence for a Heavy Neutral K-Particle and its Cascade Decay	pag. 1153
G. MORPURGO - Possible Explanations of the Decay Processes of the Pion in the Frame of the « Universal » Fermi Interaction	1159
E. CLEMENTEL and C. VILLI - On Neutron-Proton Scattering	1166
B. P. EDWARDS, A. ENGLER, M. W. FRIEDLANDER and A. A. KAMAL - The Production of Heavy Mesons and Hyperons by π^- -Mesons of 4.5 GeV/c	1188
V. GLASER and B. JAKŠIĆ - Electromagnetic Properties of Particles with Spin	1197
D. F. FALLA, M. W. FRIEDLANDER, F. ANDERSON, W. D. B. GREENING, S. LIMENTANI, B. SECHI-ZORN, C. CERNIGOI, G. IERNETTI and G. POIANI - Parent Stars of K^+ -Mesons	1203
L. I. SCHIFF - Effects of Proton Correlations on the Scattering of High-Energy Electrons from Nuclei	1223
H. L. ANDERSON and W. C. DAVIDON - Machine Analysis of Pion Scattering by the Maximum Likelihood Method	1238
A. AGODI and M. CINI - Charge Dependent Corrections to Dispersion Relations - I	1256
S. FRANCHETTI - On the Problem of the Static Helium Film - III. The Profile of the Film and its Dependence on Temperature	1266
B. F. TOUSCHEK - The Mass of the Neutrino and the Non-Conservation of Parity	1281
M. BERNARDINI, P. BROVETTO and S. FERRONI - Scattering of Fast Electrons by Polarized Nuclei	1292
G. PUPPI and A. STANGHELLINI - Determination of the Pion-Nucleon Interaction Coupling Constant from Scattering Experiments Using Dispersion Relations	1305
P. CALDIROLA e G. ROSSI - Effetti isotopici nell'adsorbimento di gas su solidi	1316

Lettere alla Redazione:

G. ALVIAL and S. STANTIC - Application of the Klausen Micrometer to the Measurements of Multiple Scattering of Elementary Particles in Nuclear Emulsions	1333
R. J. N. PHILLIPS - On the Phase-Shift Analysis of High-Energy p-p Scattering	1335
C. MILONE and R. RICAMO - Angular Distribution of Photoprottons from Oxygen	1338
J. J. SAKURAI - Associated Production of Strange Particles	1340
E. CLEMENTEL and C. VILLI - D Wave Effects in Positive Pion-Proton Scattering	1343
K. NISHIIMA - On the Theory of Leptons	1349
W. BEUSCH, H. KNOEPFEL, E. LOEFFE, D. MAEDER and P. STOLL - Thallium-Activated CsI for Scintillation Spectroscopy	1355
U. FANO - Angular Correlation of Radiations with Parallel Angular Momenta	1358
B. BOSCO - On the Nucleons Magnetic Moments Contribution to the Radiative Pion-Nucleon Scattering	1361
S. TANAKA - The Parity Non-Conservation and the Strength of the Interaction of Elementary Particles	1364
J. W. GARDNER - On the Solutions of the Fluctuation Problem in Cascade Showers	1368

M. P. MADAN - Law of Molecular Interaction for Kripton	pag. 1369
M. CINI and S. FUBINI - Some Remarks about a Paper by Fukutome and Nogami	» 1371
P. CALDIROLA e G. ROSSI - Influenza dell'adsorbimento e della migrazione superficiale sulla separazione isotopica nella diffusione di un gas attraverso una parete porosa	» 1374
<i>Libri ricevuti e Recensioni</i>	» 1377

N. 6 - 1° GIUGNO 1957

G. YEKUTIELI - Ionization at the Origin of High Energy Electron Positron Pairs	pag. 1381
W. A. COOPER, H. FILTHUTH, J. A. NEWTH, G. PETRUCCI, R. A. SALMERON and A. ZICHICHI - Examples of the Production of (K^0, K^0) and (K^0, K^+) Pairs of Heavy Mesons	» 1388
G. R. SCREATON - Meson Production by a Meson Nucleon Collision in the Heisenberg Representation	» 1398
P. S. FARAGÓ and L. JÁNOSSY - Review of the Experimental Evidence for the Law of Variation of the Electron Mass with Velocity	» 1411
P. GOSAR - A New Method for Solving Multiple Scattering Problems in Inhomogeneous Media	» 1437
M. S. HUQ - Radiation from ^{192}Pt and Proposed Decay Scheme	» 1456
B. J. O'BRIEN and J. H. NOON - Measurement of the Alpha Particle Flux at 41° N Geomagnetic Latitude Using Nuclear Emulsions	» 1463
V. S. BARAŠENKOV - On the Impossibility of the Hamiltonian Formulation of Theory with the Form-Factor	» 1469
P. MITTELSTAEDT - Zur Energieverteilung der inelastischen Streuung von K^+ -Mesonen an Kernen	» 1480
L. J. TASSIE - Inelastic Scattering of Electrons by Nuclei	» 1497
W. K. BURTON and A. H. DE BORDE - Derivation of the Functional Integral Formalism for Fermi Systems from the Canonical Formalism	» 1510
R. L. BRAHMACHARY - A Generalization of Reissner-Nordström Solution. II	» 1520
R. K. GUPTA and S. IHA - On the Neutron Deficient Isotopes of Thallium, ^{200}Tl and ^{202}Tl	» 1524
S. KAHANA and J. C. POLKINGHORNE - A Method for Calculating the Anomalous Magnetic Moment of the Electron	» 1528
D. AMATI and B. VITALE - Low Energy K-Nucleon Interaction	» 1533
D. KESSLER and R. MAZE - Expérience sur les gerbes pénétrantes produites par les mesons μ dans une grande chambre de Wilson sous terre	» 1540
W. E. FRAHN and R. H. LEMMER - Velocity-Dependent Nuclear Interaction	» 1564
S. GOTŌ - A Model for the Weak Interactions	» 1573
G. H. STAFFORD, C. WHITEHEAD and P. HILLMAN - Polarization in Neutron Proton Scattering at 95 MeV	» 1589
R. JOST and H. LEHMANN - Integral-Darstellung kausaler Kommutatoren	» 1598
W. KRÓLIKOWSKI - Low's General Equation	» 1611
M. HAMAGUCHI - On the Viscous Fluid Model in Multiple Production of Mesons	» 1622

G. F. DELL'ANTONIO and F. DUIMIO - On the Relation between the Lee Model and Ordinary Meson Theory	pag. 1636
L. MARQUEZ - Angular Correlations in High Energy Fission	» 1646
G. FERRARI, E. MANARESI and G. QUAREN - On the Measurements of the Pion-Proton Elastic Scattering in Nuclear Emulsions	» 1651
R. GESSAROLI, G. QUAREN, G. DASCOLA, S. MORA and G. TODESCO - π^+ -Proton Scattering at 100 MeV	» 1658
L. FERRETTI, G. QUAREN, M. DELLA CORTE and T. FAZZINI - π^+ -Proton Scattering at 83 MeV	» 1660
B. BHOWMIK, D. EVANS and D. J. PROWSE - On the Angular Correlation in the β -Decay of μ -Mesons Observed in Photographic Emulsion	» 1663
G. C. DELLA PERGOLA e D. SETTE - Effetti galvanometrici nel germanio	» 1670
H. H. ALY and C. J. WADDINGTON - The Flux of Primary Cosmic Ray α -Particles over Sardinia	» 1679
F. CERULUS - Parity Violation and the Spin of the Λ^0 Particle	» 1685
L. A. RADICATI and B. TOUSCHEK - On the Equivalence Theorem for the Massless Neutrino	» 1693
F. EISLER, R. PLANO, N. SAMIOS, M. SCHWARTZ and J. STEINBERGER - Systematics of Λ^0 and θ^0 Decay	» 1700
P. GULMANELLI and E. MONTALDI - Gravitational Forces and Quantum Field Theory	» 1716

Note Tecniche:

O. J. ORIENT and E. I. VIZSOLYI - Diborane-gas Filled Counting Tubes for Measuring Thermic Neutrons	» 1722
P. BASSI, A. LORIA, J. A. MEYER, P. MITTNER and I. SCOTONI - Stereoscopy in Bubble Chambers	» 1729
S. COLOMBO, E. GATTI and M. PIGNANELLI - Accuracy Limits in the Measurement of time Intervals Defined by Scintillation Counter Pulses	» 1739

Lettere alla Redazione:

M. J. BUCKINGHAM - A Note on the Energy Gap Model of Superconductivity	» 1763
J. BARDEEN - Gauge Invariance and the Energy Gap Model of Superconductivity	» 1766
S. N. GOSWAMI - Ambipolar Diffusion in a Magnetic Field in the Case of Glow Discharge	» 1769
T. GHOSE, S. K. GHOSH and D. K. ROY - A Method for Measuring the Relaxation Time T_1	» 1771
S. NARANAN, P. V. RAMANAMURTY, A. B. SAHAR and B. V. SREEKANTAN - Interactions of μ -Mesons Underground	» 1773
J. SAWICKI and Z. SZYMANSKI - Nucleon-Surface Interaction and the (p, n) Reactions	» 1777
A. N. MATVEEV - A Non-Linear Theory of Phase Oscillations Induced by Radiation Fluctuations in Synchrotrons	» 1782
R. LEVI-SETTI and W. SLATER - Emission of an Electron in Pair a K^- -Decay	» 1784
G. MORPURGO - A Discussion of the Possibility of Detecting Asymmetries in the Λ^0 Decay	» 1787

C. MARCHI, G. QUAREN, A. VIGNUDELLI, G. DASCOLA and S. MORA - The Nuclear Potential for the K^+ -Mesons	pag. 1790
N. DALLAPORTA and F. FERRARI - On Parity Non-Conservation in the Decay of Strange Particles	» 1793
E. AMALDI, C. CASTAGNOLI, M. FERRO-LUZZI, C. FRANZINETTI and A. MANDREDINI - Further Results on Antiproton Annihilations	» 1797
R. AMMAR, J. I. FRIEDMAN, R. LEVI SETTI and V. L. TELELDI - Nuclear Interactions of Long-Lived Neutral Strange Particles	» 1801
J. HEUGHEBAERT, M. RENÉ J. SACTON and G. VANDERHAEGHE - On the Angular Correlation in μ -e Decays Observed in Nuclear Emulsions Exposed in Magnetic Field	» 1808
M. SIMONETTA, G. FAVINI and V. PIERPAOLI - The Electronic Absorption Spectrum of Naphthotriazines	» 1814
<i>Emendation:</i>	
E. L. LOMON - A Soluble Model of Meson-Nucleon S-State Scattering	» 1816
<i>Libri ricevuti e Recensioni</i>	» 1817
<i>Indici del Volume V, Serie X, 1957</i>	» 1825

INDICE PER AUTORI

Le sigle L. e N.T., si riferiscono rispettivamente alle *Lettere alla Redazione* e alle *Note Tecniche*.

ADORNI N. (vedi SILVESTRI M.) (N. T.)	pag. 266
AGODI A. - On γ -Polarization Effects in Photonuclear Reactions	» 21
AGODI A. and M. CINI - Charge Dependent Corrections to Dispersion Relations - I	» 1256
ALEXANDER G. and R. H. W. JOHNSTON - On the Relation between Blob-Density and Velocity of a Singly Charged Particle in G-5 Emulsion	» 363
ALVAREZ L. W., H. BRADNER, P. FALK VAIRANT, J. D. GOW, A. H. ROSENFIELD, F. T. SOLMITZ and R. D. TRIPP - K Interactions in Hydrogen	» 1026
ALVIAL G. and S. STANTIC - Application of the Klausen Micrometer to the Measurements of Multiple Scattering of Elementary Particles in Nuclear Emulsions (L.)	» 1333
ALY H. H. and C. J. WADDINGTON - The Flux of Primary Cosmic Ray Alpha Particles over Sardinia	» 1679
AMALDI E., C. CASTAGNOLI, M. FERRO-LUZZI, C. FRANZINETTI and A. MANDREDINI - Further Results of Antiproton Annihilations (L.)	» 1797
AMATI D. and B. VITALE - Low Energy K-Nucleon Interaction	» 1533
AMMAR R., J. I. FRIEDMAN, R. LEVI SETTI and V. L. TELELDI - Nuclear Interactions of Long-lived Neutral Strange Particles (L.)	» 1801
ANDERSON F. (vedi BHOWMIK B.).	» 994
ANDERSON F. (vedi FALLA D. F.).	» 1203
ANDERSON H. L. and W. C. DAVIDON - Machine Analysis of Pion Scattering by the Maximum Likelihood Method.	» 1238

APOSTOLAKIS A. J., J. O. CLARKE and J. V. MAJOR	Spurious Scattering in Nuclear Emulsions	pag. 337
ARNOUS E.	Étude du nombre de mésons virtuels sur un modèle simple	» 483
ASCOLI A., M. ASDENTE and E. GERMAGNOII	- On the Atomic Displacements Produced by α -Particles in Germanium.	» 1145
ASDENTE M. (vedi ASCOLI A.)	» 1145
BALDO-CEO LIN M., M. CRESTI, N. DALLAPORTA, M. GRILLI, L. GUERRIERO, M. MERLIN, G. A. SALANDIN and G. ZAGO	- Interactions of K ⁺ -Mesons with Emulsion Nuclei between 40 and 160 MeV	» 402
BARAŠENKOV V. S.	- On the Impossibility of the Hamiltonian Formulation of Theory with the Formfactor	» 1469
BARDEEN J.	Gauge Invariance and the Energy Gap Model of Superconductivity (L.)	» 1766
BARONE A.	- Interferometro per misure di precisione della velocità degli ultrasuoni nei liquidi (N. T.)	» 717
BASSI P., A. LORIA, J. A. MEYER, P. MITTNER and I. SCOTONI	- Stereoscopy in Bubble Chamber (N. T.)	» 1729
BELLA F. (vedi FOCARDI S.) (N. T.)	» 275
BERNARDINI M., P. BROVETTO and S. FERRONI	- Scattering of Fast Electrons by Polarized Nuclei	» 1292
BERTANZA L., G. MARTELLI and B. TALLINI	- Bubble Density Along the Path of Ionizing Particles Crossing a Bubble Chamber.	» 940
BERTOLINI G., E. LAZZARINI and M. MANDELLI BETTONI	- Directional Correlation of the 0.845 and 1.24 MeV γ -Rays of ⁵⁶ Fe	» 356
BEUSCH W., H. KNOEPFEL, E. LOEPFE, D. MAEDER and P. STOLL	- Thallium-Activated CsI for Scintillation Spectroscopy (L.)	» 1355
BHOWMIK B., D. EVANS, S. NILSSON, D. J. PROWSE, F. ANDERSON, D. KEEFE, A. KERNAN, N. N. BISWAS, M. CECCARELLI, P. WALOSCHEK, J. E. HOOPER, M. GRILLI and L. GUERRIERO	- The Lifetime of Positive Heavy Mesons	» 994
BHOWMIK B., D. EVANS and D. J. PROWSE	- On the Angular Correlation in the β -Decay of μ -Mesons Observed in Photographic Emulsion	» 1663
BICHARA M. R. E.	- Risultati di un oscillatore con transistore (N. T.)	» 702
BISWAS N. N., L. CECCARELLI-FABBRICHESI, M. CECCARELLI, K. GOTTSSTEIN, N. C. VARSHNEYA and P. WALOSCHEK	- Nuclear Scattering of K ⁺ -Mesons in the Energy Region of 80 MeV	» 123
BISWAS N. N., M. CECCARELLI and J. CRUSSARD	- Angular Distribution of the μ -Decay as Test of Parity Conservation (L.)	» 756
BISWAS N. N. (vedi BHOWMIK B.)	» 994
BOCCHIERI P. and P. GULMANELLI	- Gravitational Forces and Quantum Theory (L.)	» 1016
BORELLO E. (vedi MILONE M.)	» 562
BORGARDT A.	- Possible Forms of Nonlinear Mesodynamics	» 102
BOSCO B.	- On the Nucleons Magnetic Moments Contribution to the Radiative Pion-Nucleon Scattering (L.)	» 1361
BRADNER H. (vedi ALVAREZ L. W.)	» 1026
BRAHMACHARY R. L.	- A Generalization of Reissner-Nordström Solution - II	» 1520
BROVETTO P. (vedi BERNARDINI M.)	» 1292
BROVETTO P. and S. FERRONI	- On the Paramagnetic Resonance Spectrum of Triphenylmethyl	» 142
BUCHDAHL H. A.	- Reciprocal Static Solutions of Field Equations Involving an Asymmetrical Fundamental Tensor	» 1083

BUCKINGHAM M. J. - A Note on the Energy Gap Model of Superconductivity (L.)	pag. 1763
BUDINI P. and L. FONDA - Pion-Nucleon Interaction and Strange Particles (L.)	» 306
BUDINI P. and L. FONDA - Non-local Models of Pion-Nucleon, Pion-Hyperon Interactions	» 666
BURGE E. J., J. H. DAVIES, I. J. VAN HEERDEN and D. J. PROWSE - On Some Aspects of Processing Thick Nuclear Emulsions (L.)	» 1005
BURTON W. K. and A. H. DE BORDE - Derivation of the Functional Integral Formalism for Fermi Systems from the Canonical Formalism.	» 1510
BUSINARO U. L. and S. GALLONE - Asymmetric Equilibrium Shapes in the Liquid Drop Model (L.)	» 315
CAIANIELLO E. R. - Propagation Kernels as Functions of the Masses (L.)	» 739
CALDIROLA P. e G. ROSSI - Effetti isotopici nell'adsorbimento di gas su solidi	» 1316
CALDIROLA P. e G. ROSSI - Influenza dell'adsorbimento e della migrazione superficiale sulla separazione isotopica nella diffusione di un gas attraverso una parete porosa (L.)	» 1374
CARRASSI M. - The Spin Kinematics for a Charged Particle in a Uniform Magnetic Field	» 955
CARRELLI A. and F. S. GAETA - A New Method for the Determination of the Acoustic Absorption Coefficient in Liquids	» 773
CASE K. M., N. C. YANG and R. KARPLUS - A Reply to Criticism by Mr. A. Gamba (L.)	» 1004
CASTAGNOLI C., C. FRANZINETTI and A. MANFREDINI - Further Results on Parity Conservation in π - μ -e Decays	» 684
CASTAGNOLI C. (vedi AMALDI E.) (L.)	» 1797
CECCARELLI M. (vedi BISWAS N. N.)	» 123
CECCARELLI M. (vedi BISWAS N. N.) (L.)	» 756
CECCARELLI M. (vedi BHOWMIK B.)	» 994
CECCARELLI-FABBRICHESI L. (vedi BISWAS N. N.)	» 123
CEOGLIN C. and L. TAFFARA - On the Scattering of K^+ -Mesons by Nucleons in Perturbation Theory	» 435
CERNIGOI C. (vedi FALLA D. F.)	» 1203
CERULUS F. - Parity Violation and the Spin of the Λ^0 Particle	» 1685
CINI M. (vedi AGODI A.)	» 1256
CINI M. and S. FUBINI - Some Remarks about a Paper by Fukutome and Nagami (L.)	» 1371
CLARKE J. O. (vedi APOSTOLAKIS A. J.)	» 337
CLEMENTEL E., C. VILLI and L. JESS - Phase Shift Analysis of Proton-Proton Scattering Experiments - II. Analysis of the Scattering Data from 18 to 260 MeV	» 907
CLEMENTEL E. and C. VILLI - On Neutron-Proton Scattering	» 1166
CLEMENTEL E. and C. VILLI - D Wave Effects in Positive Pion-Proton Scattering (L.)	» 1343
COCCONI G., G. PUPPI, G. QUARENÌ and A. STANGHELLINI - K^+ -Meson Interaction with Nucleons and Nuclei	» 172
COLLI L. and U. FACCHINI - Further Measurements on n, p Reactions at 14 MeV - II. Sulphur, Aluminium, Iron, Copper, Nickel (L.)	» 309
COLLI L., U. FACCHINI and S. MICHELETTI - Comparison between (n, p) and (p, p') Experiments on Intermediate Energy	» 502

COLOMBO S., C. COTTINI and E. GATTI - Improvements on a Multichannel Pulse Analyzer (L.)	pag. 748
COLOMBO S., E. GATTI and M. PIGNANELLI - Accuracy Limits in the Measurements of Time Intervals Defined by Scintillation Counter Pulses (N.T.)	» 1739
COOPER W. A., H. FILTHUTH, J. A. NEWTH, G. PETRUCCI, R. A. SALMERON and A. ZICHICHI - Examples of the Production of (K^0, K^0) and (K^+, K^0) Pairs of Heavy Mesons	» 1388
COSTA G. and G. PATERGNANI - K^+ Nuclei Interactions According to the Optical Model	» 448
COTTINI C. (vedi COLOMBO S.) (L.)	» 748
CRANSHAW T. E. and J. F. DE BEER - A Triggered Spark Counter	» 1107
CRESTI M. (vedi BALDO-CEOLIN M.)	» 402
CROWE K. M. - The Masses of Light Mesons, K-Mesons and Hyperons in 1956	» 541
CRUSSARD J. (vedi BISWAS N. N.) (L.)	» 756
CSIKAI J. - Photographic Evidence for the Existence of the Neutrino (L.)	» 1011
CZYŻ W. and J. SAWICKI - Polarization of Nucleons from Photodisintegration of Deuterium	» 45
DALLAPORTA N. (vedi BALDO-CEOLIN M.)	» 402
DALLAPORTA N. and F. FERRARI - On the Λ -Nucleon Force and the Binding Energy of the Light Hyperfragments	» 111
DALLAPORTA N. and F. FERRARI - On the Σ -Hyperon-Nucleon Interaction Cross-Section (L.)	» 742
DALLAPORTA N. and F. FERRARI - On Parity Non-Conservation in the Decay of Strange Particles (L.)	» 1793
DASCOLA G. (vedi GESSAROLI R.)	» 1658
DASCOLA G. (vedi MARCHI C.) (L.)	» 179
DAVIDON W. C. (vedi ANDERSON H. L.)	» 1238
DAVIES J. H. (vedi BURGE E. J.) (L.)	» 1005
DEBEAUVAIS M., E. PICCIOTTO et S. WILGAIN - Arrêt de la diffusion des radio-éléments dans les émulsions nucléaires par exposition à basse température (N. T.)	» 260
DE BEER J. F. (vedi CRANSHAW T. E.)	» 1107
DE BORDE A. H. (vedi BURTON W. K.)	» 1510
DELLA CORTE M. (vedi FERRETTI L.)	» 1660
DELL'ANTONIO G. F. and F. DUIMIO - On the Relation between the Lee Model and Ordinary Meson Theory	» 1636
DELLA PERGOLA G. C. e D. SETTE - Effetti galvanometrici nel Germanio	» 1670
DE TOLLIS B. and R. S. LIOTTA - Interference in the Double Compton Effect	» 947
DUIMIO F. (vedi DELL'ANTONIO G. F.)	» 1636
EDWARDS B. P., A. ENGLER, M. W. FRIEDLANDER and A. A. KAMAL - The Production of Heavy Mesons and Hyperons by π^- -Mesons of 4.5 GeV/c	» 1188
EISLER F., R. PLANO, N. SAMIOS, M. SCHWARTZ and J. STEINBERGER - Systematics of Λ^0 and θ^0 Decay	» 1700
ENGLER A. (vedi EDWARDS B. P.)	» 1188
EVANS D. (vedi BHOWMIK B.)	» 994
EVANS D. (vedi BHOWMIK B.)	» 1663
EZAWA H., Y. TOMOZAWA and H. UMEZAWA - Quantum Statistics of Fields and Multiple Production of Mesons	» 810
FACCHINI U. (vedi COLLI L. (L.)	» 309
FACCHINI U. (vedi COLLI L.)	» 502

FALK VAIRANT P. (vedi ALVAREZ L. W.)	pag. 1026
FALLA D. F., M. W. FRIEDLANDER, F. ANDERSON, W. D. B. GREENING, S. LIMENTANI, B. SECHI-ZORN, C. CERNIGOI, G. IERNETTI and G. POIANI - Parent Stars of K^+ -Mesons	» 1203
FANO U. - Angular Correlation of Radiations with Parallel Angular Mo- menta (L.)	» 1358
FARAGÒ P. S. and L. JÁNOSSY - Review of the Experimental Evidence for the Law of Variation of the Electron Mass with Velocity	» 1411
FASOLI U., C. MARONI, I. MODENA, E. POHL and J. POHL-RÜLING - On the Correlation of the Intensity of μ^- and μ^+ -Mesons with the Pressure at Sea-level, and with the Height of the 100 mb Layer	» 473
FAVINI G. (vedi SIMONETTA M.) (L.)	» 1814
FAY H. - Electron-Photon Cascades of High Energy in Photographic Emulsions (L.)	» 293
FAZZINI T. (vedi FERRETTI L.)	» 1660
FENOGLIO M. - Relazioni cristallografico-strutturali tra il difenile ed una serie di suoi nuovi derivati	» 765
FERRARI F. (vedi DALLAPORTA N.)	» 111
FERRARI F. (vedi DALLAPORTA N.) (L.)	» 742
FERRARI F. (vedi DALLAPORTA N.) (L.)	» 1793
FERREIRA J. (vedi JOOS H.)	» 57
FERRARI G., E. MANARESI, and G. QUARENİ - On the Measurements of the Pion-Proton Elastic Scattering in Nuclear Emulsions	» 1651
FERRERO F., L. GONELLA, R. MALVANO, C. TRIBUNO and A. O. HANSON - Fast Neutron Component in Photonuclear Reactions	» 242
FERRERO F., R. MALVANO and C. TRIBUNO - Camera di ionizzazione per raggi X fino a 31 MeV (N. T.)	» 510
FERRETTI B. - On the Conservation of Nucleons (L.)	» 761
FERRETTI L., G. QUARENİ, M. DELLA CORTE and T. FAZZINI - π^+ -Pro- ton Scattering at 83 MeV	» 1660
FERRO A. e G. MONTALENTI - Sulle variazioni delle proprietà magnetiche e meccaniche causate dall'idrogeno disciolto nel ferro	» 842
FERRO-LUZZI M. (vedi AMALDI E.) (L.)	» 1797
FERRONI S. (vedi BROVETTO P.)	» 142
FERRONI S. (vedi BERNARDINI M.)	» 1292
FILTHUTH H. (vedi COOPER W. A.)	» 1388
FOCARDI S., C. RUBBIA, G. TORELLI e F. BELLA - Metodi di comando rapido di rivelatori di tracce (N. T.)	» 275
FONDA L. (vedi BUDINI P.) (L.)	» 306
FONDA L. (vedi BUDINI P.)	» 666
FRAHN W. E. - Nucleon-Nucleus Interaction from the Statistical Model .	» 393
FRAHN W. E. and R. H. LEMMER - Effective Nuclear Potentials (L.) .	» 523
FRAHN W. E. and R. H. LEMMER - Velocity-Dependent Nuclear Interaction	» 1564
FRANCHETTI S. - On the Problem of the Static Helium Film - II. Effects due to the Smallness of One Dimension	» 183
FRANCHETTI S. - On the Problem of the State Helium Film - III. The Profile of the Film and its Dependence on Temperature	» 1266
FRANZINETTI C. (vedi CASTAGNOLI C.)	» 684
FRANZINETTI C. (vedi AMALDI E.) (L.)	» 1797
FRIEDLANDER M. W. - The Lifetime of 3H_A Hyperfragments (L.)	» 283

FRIEDLANDER M. W., D. KEEFE and M. G. K. MENON - The Range in G5 Nuclear Emulsion of Protons with Energies 87, 118 and 146 MeV	pag. 461
FRIEDLANDER M. W. (vedi EDWARDS B. P.)	» 1188
FRIEDLANDER M. W. (vedi FALLA D. F.)	» 1203
FRIEDMAN J. I. (vedi AMMAR R.) (L.)	» 1801
v. FRIESEN S. and K. KRISTIANSSON Further Evidence for a Longlived Neutral K-Particle (L.)	» 1013
FUBINI S. (vedi CINI M.) (L.)	» 1371
FUKUTOME H. and Y. NOGAMI Remarks on the Fixed Extended Source Pion Theory	» 347
FURUICHI S., Y. SUGAHARA, A. WAKASA and M. YONEZAWA - An Analysis of Rochester $K_{\mu 3}$ and $K_{e 3}$ Data (L.)	» 285
GAETA F. S. (vedi CARRELLI A.)	» 773
GALLONE S. (vedi BUSINARO U. L.) (L.)	» 315
GARDNER J. W. - On the Solutions of the Fluctuation Problem in Cascade Showers (L.)	» 1368
GARNIER G. A. B. (vedi MARQUES A.) (L.)	» 291
GATTI E. (vedi COLOMBO S.) (L.)	» 748
GATTI E. (vedi COLOMBO S.) (N. T.)	» 1739
GATTO R. Interference Effects between Members of Parity Doublets in the Lee-Yang Theory	» 1021
GATTO R. - The Annihilation of a Nucleon-Antinucleon System into a K-anti K Pair	» 1024
GELL-MANN M. - Change of Isotopic Spin in the $K_{\pi 2}$ Decay (L.)	» 758
GERMAGNOLI E. (vedi ASCOLI A.)	» 1145
GESSAROLI R., G. QUAREN, G. DASCOLA, S. MORA and G. TODESCO - π^+ -Proton Scattering at 100 MeV	» 1658
GHOSE T., S. K. GHOSH and D. K. ROY Spin-Echoes with Any Number of Pulses (L.)	» 751
GHOSE T., S. K. GHOSH and D. K. ROY - A Method for Measuring Relaxation Time T_1 (L.)	» 1771
GHOSH S. K. (vedi GHOSE T.) (L.)	» 751
GHOSH S. K. (vedi GHOSE T.) (L.)	» 1771
GLASER V. and B. JAKŠIĆ Electromagnetic Properties with Spin	» 1197
GONELLA L. (vedi FERRERO F.)	» 242
GOSAR P. A New Method for Solving Multiple Scattering Problems in Inhomogeneous Media	» 1437
GOTO S. - A Model for the Weak Interactions	» 1573
GOTTSTEIN K. (vedi BISWAS N. N.)	» 123
GOW J. D. (vedi ALVAREZ L. W.)	» 1026
GREEN H. S. - Separability of a Covariant Wave Equation	» 866
GREENING W. D. B. (vedi FALLA D. F.)	» 1203
GRILLI M. (vedi BALDO-CEO LIN M.)	» 402
GRILLI M. (vedi BHOWMIK B.)	» 994
GROSJEAN C. C. Further Development of a New Approximate One-Velocity Theory of Multiple Scattering	» 83
GROUSE P. J. and H. D. RATHGEBER A Geiger Counter Design Giving a Definite Counting Length (N. T.)	» 707
GUERRIERO L. (vedi BALDO-CEO LIN M.)	» 402
GUERRIERO L. (vedi BHOWMIK B.)	» 994
GULMANELLI P. (vedi BOCCIERI P.) (L.)	» 1016

GULMANELLI P. and E. MONTALDI - Gravitational Forces and Quantum Field Theory	pag. 1716
GUPTA R. K. and S. IHA - On the Neutron Isotopes of Thallium, ^{200}Tl and ^{202}Tl	» 1524
GÜRSEY F. - General Relativistic Interpretation of Some Spinor Wave Equations	» 154
GÜRSEY F. - Relativistic Kinematics of a Classical Point Particle in Spinor Form	» 784
HAAG R. - On the Physical Significance of the Redundant Solutions of the Low Equations	» 203
HAMAGUCHI M. - On the Viscous Fluid Model in Multiple Production	» 1622
HANSON A. O. (vedi FERRERO F.)	» 242
HAYAKAWA S. - A Possible Interpretation of the Multiple Penetrating Particles	» 608
HEITLER W. Renormalization in Non-Relativistic Field Theories (Remarks about the Paper by Enz) (L.)	» 302
HERZ A. J. (vedi NOON J. H.)	» 854
HEUGHEBAERT J., M. RENÉ, J. SACTON and G. VANDERHAEGHE - On the Angular Correlation in μ -e Decays Observed in Nuclear Emulsions Exposed in Magnetic Field (L.)	» 1808
HIGASHI S., T. OSHIO, H. SHIBATA, K. WATANABE and Y. WATASE - On the Cosmic Ray Penetrating Showers Underground	» 592
HIGASHI S., T. OSHIO, H. SHIBATA, K. WATANABE and Y. WATASE - On the Multiple Penetrating Particles Underground	» 597
HIIDA K. - A Kinematical Test for the Relation between the Coupling Constants in Meson Theory	» 1094
HIIDA K. and M. SAWAMURA - Some Relations Among Green's Functions	» 896
HILLMAN P. (vedi STAFFORD G. H.)	» 1589
HOOPER J. E. (vedi BHOWMIK B.)	» 994
HOPPER V. D. (vedi LABY J. E.) (N. T.)	» 249
HOSSAIN A. and D. J. PROWSE - On the 7.7 MeV Level of Carbon 12	» 973
HUQ M. S. - Radiation from ^{192}Pt and Proposed Decay Scheme	» 1456
IERNETTI G. (vedi FALLA D. F.)	» 1203
IHA S. (vedi GUPTA R. K.)	» 1524
ISHI T. (vedi TOKUNAGA S.) (L.)	» 517
JAKŠIĆ B. (vedi GLASER V.)	» 1197
JANNELLI S. e F. MEZZANARES - Caratteristiche delle disintegrazioni nucleari prodotte da protoni di 140 ± 6 MeV - II. Nuclei pesanti	» 380
JANNELLI S. e F. MEZZANARES - Caratteristiche delle disintegrazioni nucleari prodotte da protoni di 140 ± 6 MeV - III. Nuclei leggeri	» 1047
JÁNOSSY L. (vedi FARAGÒ P. S.)	» 1411
JESS L. (vedi CLEMENTEL E.)	» 907
JESS L. (vedi KIND A.)	» 1020
JOHNSTON R. H. W. (vedi ALEXANDER G.)	» 363
JOOS H., J. FERREIRA and A. H. ZIMERMAN - A Special Representation for the Treatment of a System of two Dirac Particles	» 57
JOST R. und H. LEHMANN - Integral-Darstellung kausaler Kommutatoren	» 1598
JOUVET B. - Fermi Coupling and Mass and Charge Spectra of Bosons	» 1
JUDEK B. - Mass Measurements of Particles Stopping in the Emulsion by the Constant Sagitta Method	» 886

KAHANA S. and J. C. POLKINGHORNE - A Method for Calculating the Anomalous Magnetic Moment of the Electron	pag. 1528
KAMAL A. A. (vedi EDWARDS B. P.)	» 1188
KARPLUS R. (vedi CASE K. M.) (L.)	» 1004
KEEFE D. (vedi FRIEDLANDER M. W.)	» 461
KEEFE D. (vedi BHOWMIK B.)	» 994
KELLER J. B. - Bound of Phase Shifts	» 1122
KERIMOV B. - (vedi SOKOLOV A.)	» 921
KERNAN A. (vedi BHOWMIK B.)	» 994
KESSLER D. et R. MAZE - Expérience sur les Gerbes Pénétrantes produites par les Mésons μ dans une grande Chambre de Wilson sous Terre	» 1540
KIND A. - On the Sign of the Real Central Part of the Neutron-Nucleus Complex Potential (L.)	» 318
KIND A. and L. JESS - On the Real Part of the Complex Potential Well of the Nucleus	» 1020
KNOEPFEL H. (vedi BEUSCH W.) (L.)	» 1355
KRISTIANSSON K. (vedi v. FRIESEN S.) (L.)	» 1013
KRÓLIKOWSKI W. - Low's General Equation	» 1611
KUMAR R. C., W. B. LASICH and F. R. STANNARD - The Mass Difference between the Σ^+ and Σ Hyperons (L.)	» 746
LAMY J. E., Y. K. LIM and V. D. HOPPER - Level Flights with Expandible Balloons (N. T.)	» 249
LASICH W. B. (vedi KUMAR R. C.) (L.)	» 746
LAZZARINI E. (vedi BERTOLINI G.)	» 356
LEHMANN H. (vedi JOST R.)	» 1598
LEMMER R. H. (vedi FRAHN W. E.) (L.)	» 523
LEMMER R. H. (vedi FRAHN W. E.)	» 1564
LEVI SETTI R. (vedi AMMAR R.) (L.)	» 1801
LEVI SETTI R. and W. SLATER - Emission of an Electron Pair in a K^+ Decay (L.)	» 1784
LIM Y. K. (vedi LABY J. E.) (N. T.)	» 249
LIMENTANI S. (vedi FALLA D. F.)	» 1203
von LINDERN L. - Multiple Meson Production and Angular Distribution of Shower Particles Produced in Cosmic Ray « Jets »	» 491
LIOTTA R. S. (vedi DE TOLLIS B.)	» 947
LOEPFE E. (vedi BEUSCH W.) (L.)	» 1355
LOHRMANN E. - Multiple Meson Production in the Cosmic Radiation	» 1074
LOMON E. L. - A Soluble Model of Meson-Nucleon S -State Scattering	» 1816
LORIA A. (vedi BASSI P.) (N. T.)	» 1729
MADAN P. - Law of Molecular Interaction for Kripton (L.)	» 1369
MAEDER D. (vedi BEUSCH W.) (L.)	» 1355
MAJOR J. V. (vedi APOSTOLAKIS A. J.)	» 337
MALVANO R. (vedi FERRERO F.)	» 242
MALVANO R. (vedi FERRERO F.) (N. T.)	» 510
MANARESI E. (vedi FERRARI G.)	» 1651
MANDELLI BETTONI M. (vedi BERTOLINI G.)	» 356
MANFREDINI A. (vedi CASTAGNOI C.)	» 684
MANFREDINI A. (vedi AMALDI E.) (L.)	» 1797
MARCHI C., G. QUARENIA, A. VIGNUDELLI, G. DASCOLA and S. MORA - The Nuclear Potential for the K^+ -Mesons (L.)	» 1790
MARGEM N. (vedi MARQUES A.) (L.)	» 291

MARONI C. (FASOLI U.)	pag. 473
MARQUES A., N. MARGEM and G. A. B. GARNIER - Mean Free Path of 4.3 GeV π^- -Mesons in Nuclear Emulsions (L.)	» 291
MARQUEZ L. - Angular Correlation in High Energy Fission	» 1646
MARTELII G. (vedi BERTANZA L.)	» 940
MASCARENHAS S. - Thermodynamical Theory of Thermal Conduction of Dielectrics under Electric Fields	» 1118
MATVEEV A. N. - A Non-Linear Theory of Phase Oscillations Induced by Radiation Fluctuations in Synchrotrons (L.)	» 1782
MAZE R. (vedi KESSLER D.)	» 1540
MCCUSKER C. B. A. and F. C. ROESLER - New Experimental Evidence for the Tunnel Theory of Cosmic Ray « Jets »	» 1136
MCLENNAN J. A. jr. - Conformally Invariant Wave Equations for Non- Linear and Interacting Fields	» 640
MENON M. G. K. (vedi FRIEDLANDER M. W.)	» 461
MERLIN M. (vedi BALDO-CEOLIN M.)	» 402
MEYER J. A. (vedi BASSI P.) (N. T.)	» 1729
MEZZANARES F. (vedi JANNELLI S.)	» 380
MEZZANARES F. (vedi JANNELLI S.)	» 1047
MICHELETTI S. (vedi COLLI L.)	» 502
MIEŚOWICZ M., O. STANISZ and W. WOLTER - Investigation of an Electro- magnetic Cascade of Very High Energy in the First Stage of its Deve- lopment (L.)	» 513
MIKOSHIBA N. - Quantum Fluid as a Common Model for Superfluidity and Superconductivity	» 628
MILLS R. L. - Integral Equations for Meson Field Theory	» 30
MILONE C., R. RICAMO and R. RINZIVILLO - Photoprottons from Oxygen up to 30 MeV (L.)	» 535
MILONE C. and R. RICAMO - Angular Distribution of Photoprottons from Oxygen (L.)	» 1338
MILONE C., R. RICAMO and A. RUBBINO - C and Al Photoproton Angular and Energy Distribution (L.)	» 528
MILONE M. e E. BORELLO - Sulla struttura della gliossima allo stato solido	» 562
MITTELSTAEDT P. - Zur Energieverteilung der inelastischen Streuung von K^+ -Mesonen an Kernen	» 1480
MITTNER P. (vedi BASSI P.) (N. T.)	» 1729
MODENA I. (vedi FASOLI U.)	» 473
MONTALDI E. and M. PUSTERLA - Electron Scattering in Nuclear Field with Pair-Creation	» 961
MONTALDI E. (vedi GULMANELLI P.)	» 1716
MONTALENTI G. (vedi FERRO A.)	» 842
MORA S. (vedi GESSAROLI R.)	» 1658
MORA S. (vedi MARCHI C.) (L.)	» 1790
MORPURGO G. - Possible Explanations of the Decay Processes of the Pion in the Frame of the « Universal » Fermi Interaction	» 1159
MORPURGO G. - A Discussion of the Possibility of Detecting Asymmetries in the Λ^0 Decay (L.)	» 1787
NAKANISHI N. - On Lehmann's Method of Renormalization (L.)	» 520
NARANAN S., P. V. RAMANAMURTY, A. B. SAHIAR and B. V. SREEKANTAN - Interactions of μ -Mesons Underground (190 MeV) (L.)	» 1773
NEWTH J. A. (vedi COOPER W. A.)	» 1388

NILSSON S. (vedi BHOWMIK B.)	pag.	994
NISHIJIMA K. - On the Theory of Leptons (L.)	»	1349
NISHIKAWA K. (vedi TOKUNAGA S.) (L.)	»	517
NOGAMI Y. (vedi FUKUTOME H.)	»	347
NOON J. H., A. J. HERZ and B. J. O'BRIEN - An Observed Cosmic-Ray Flux of Light Elements at 41° N Geomagnetic Latitude	»	854
NOON J. H. (vedi O'BRIEN B. J.)	»	1463
O'BRIEN B. J. (vedi NOON J. H.)	»	854
O'BRIEN B. J. and J. H. NOON - Measurement of the Alpha Particle Flux at 41° N. Geomagnetic Latitude using Nuclear Emulsions	»	1463
ODA M. - A Calculation of the Structure of the Nucleonic Cascade in the Atmosphere	»	615
OMNES R. - A System of General Relativistic Equations of Low Type	»	983
ORIENT O. J. and E. I. VIZSOLYI - Diborane-gas Filled Counting Tubes for Measuring Thermic Neutrons (N. T.)	»	1722
OSHIO T. (vedi HIGASHI S.)	»	592
OSHIO T. (vedi HIGASHI S.)	»	597
PAGANINI L. (vedi PIONTELLI R.) (L.)	»	1018
PATERGNANI G. (vedi COSTA G.)	»	448
PERCUS J. K. and G. J. YEVICK - «Dynamical» Lagrangian from the Many Body Problem	»	65
PERCUS J. K. and G. J. YEVICK - Statistical Approach to the Domain of Action of Collective Co-ordinates in the Many Body Problem	»	1057
PETRUCCI G. (vedi COOPER W. A.)	»	1388
PHILLIPS R. J. N. - On the Phase-Shift Analysis of High-Energy p-p Scattering (L.)	»	1335
PICCIOTTO E. (vedi DEBEAUV AIS M.) (N. T.)	»	260
PIERPAOLI V. (vedi SIMONETTA M.) (L.)	»	1814
PIERUCCI M. - Sull'età dell'Universo	»	572
PIGNANELLI P. (vedi COLOMBO S.) (N. T.)	»	1739
PIONTELLI R., G. POLI and L. PAGANINI - Electrochemistry of Metallic Single Crystals - I. Exchange Overvoltages on Silver and Copper (L.)	»	1018
PLANO R., N. SAMIOS, M. SCHWARTZ and J. STEINBERGER - Demonstration of the Existence of the Σ^0 Hyperon and a Measurement of its Mass	»	216
PLANO R., (vedi EISLER F.)	»	1700
POHL E. (vedi FASOLI U.)	»	473
POHL-RÜLING J. (vedi FASOLI U.)	»	473
POIANI G. (vedi FALLA D. F.)	»	1203
POLKINGHORNE J. C. (vedi KAHANA S.)	»	1528
POLI G. (vedi PIONTELLI R.) (L.)	»	1018
PORTER N. A. - The Effect of Ultra-Violet Converters on the Efficiency of Liquid Čerenkov Counters (L.)	»	526
PROWSE D. J. (vedi BHOWMIK B.)	»	1663
PROWSE D. J. (vedi HOSSAIN A.)	»	973
PROWSE D. J. - An Analysis of the Pairs Produced by ${}^8\text{Be}$ γ -Rays in Photographic Emulsions	»	977
PROWSE D. J. (vedi BHOWMIK B.)	»	994
PUPPI G. (vedi COCCONI G.)	»	172
PUPPI G. and A. STANGHELLINI - Determination of the Pion-Nucleon Interaction Coupling Constant from Scattering Experiments Using Dispersion Relations	»	1305

PUSTERLA M. (vedi MONTALDI E.)	pag. 961
QUARENIG. (vedi COCCONI G.)	» 172
QUARENIG. (vedi FERRARI G.)	» 1651
QUARENIG. (vedi FERRETTI L.)	» 1660
QUARENIG. (vedi GESSAROLI R.)	» 1658
QUARENIG. (vedi MARCHI C.) (L.)	» 1790
RADICATI L. A. and S. ROSATI - On the Spin of the $K_{\mu 3}$ Meson (L.)	» 729
RADICATI L. A. and B. F. TOUSCHEK - On Fierz' Equivalent Theorem for the Massless Neutrino	» 1693
RAMANAMURTY P. V. (vedi NARANAN S.) (L.)	» 1773
RATHGEBER H. D. (vedi GROUSE P. J.) (N.T.)	» 707
RAYSKI J. - Bilocal Field Theories and Their Experimental Tests - II	» 872
REGGE T. - On the Properties of Spin 2 Particles	» 325
RENÉ M. (vedi HEUGHEBAERT J.) (L.)	» 1808
RICAMO R. (vedi MILONE C.) (L.)	» 528
RICAMO R. (vedi MILONE C.) (L.)	» 535
RICAMO R. (vedi MILONE C.) (L.)	» 1338
RIGAULT G. - Relazioni tra la struttura della blenda e il contenuto in gallio e indio	» 579
RINZIVILLO R. (vedi MILONE M.) (L.)	» 535
ROESLER F. C. (vedi McCUSKER C. B. A.)	» 1136
ROSATI S. (vedi RADICATI L. A.) (L.)	» 729
ROSENFIELD A. H. (vedi ALVAREZ L. W.)	» 1026
ROSSI G. (vedi CALDIROLA P.)	» 1316
ROSSI G. (vedi CALDIROLA P.) (L.)	» 1374
ROY D. K. (vedi GHOSE T.) (L.)	» 751
ROY D. K. (vedi GHOSE T.) (L.)	» 1771
RUBBIA C. (vedi FOCARDI S.) (N.T.)	» 275
RUBBINO A. (vedi MILONE C.) (L.)	» 528
SACTON J. (vedi HEUGHEBAERT J.) (L.)	» 1808
SAHIAR A. B. (vedi NARANAN S.) (L.)	» 1773
SAKURAI J. J. - Associated Production of Strange Particles (L.)	» 1340
SALAM A. - On Parity Conservation and Neutrino Mass (L.)	» 299
SALANDIN G. A. (vedi BALDO-CEOGLIN M.)	» 402
SALMERON R. A. (vedi COOPER W. A.)	» 1388
SAMIOS N. (vedi PLANO R.)	» 216
SAMIOS N. (vedi EISLER F.)	» 1700
SAWAMURA M. (vedi HIIDA K.)	» 896
SAWICKI J. (vedi CZYZ W.)	» 45
SAWICKI J. and Z. SZYMANSKI - Nucleon-Surface Interaction and the (p, n) Reactions (L.)	» 1777
SCHIFF L. I. - Effects of Proton Correlations on the Scattering of High-Energy Electrons from Nuclei	» 1223
SCHWARTZ M. (vedi PLANO R.)	» 216
SCHWARTZ M. (vedi EISLER F.)	» 1700
SCREATOR G. R. - Meson Production by a Meson Nucleon Collision in the Heisenberg Representation	» 1398
SCOTONI I. (vedi BASSI P.) (N.T.)	» 1729
SECHI-ZORN B. (vedi FALLA D. F.)	» 1203
SENGUPTA S. N. (vedi SINHA M. S.)	» 1153
SETTE D. (vedi DELIA PERGOLA G. C.)	» 1670

SHIBATA H. (vedi HIGASHI S.)	pag.	592
SHIBATA H. (vedi HIGASHI S.)	»	597
SILVESTRI M. e N. ADORNI - Apparato per misure standard di scambio isotopico del deuterio fra idrogeno e vapor d'acqua a pressione atmosferica e a 100 °C (N. T.)	»	266
SIMONETTA M. e A. VACIAGO - Calcolo quantomeccanico della barriera di potenziale per la inversione della molecola di fosfina	»	587
SIMONETTA M., G. FAVINI and V. PIERPAOLI - The Electronic Absorption Spectrum of Naphthotriazines (L.)	»	1814
SINHA M. S. and S. N. SENGUPTA - Evidence for a Heavy Neutral K-Particle and its Cascade Decay	»	1153
SLATER W. (vedi LEVI SETTI R.) (L.)	»	1784
SOKOLOV A. and B. KERIMOV - On the Scattering of Particles by a Force Centre According to the Radiation Damping Theory	»	921
SOLMITZ F. T. (vedi ALVAREZ L. W.)	»	1026
SREEKANTAN B. V. (vedi NARANAN S.) (L.)	»	1773
STAFFORD G. H., C. WHITEHEAD and P. HILLMAN - Polarization in Neutron Proton Scattering at 95 MeV	»	1589
STANGHELLINI A. (vedi COCCONI G.)	»	172
STANGHELLINI A. (vedi PUPPI G.)	»	1305
STANISZ O. (vedi MI SOWICZ M.) (L.)	»	13
STANNARD F. R. (vedi KUMAR R. C.) (L.)	»	746
STANTIC S. (vedi ALVIAL G.) (L.)	»	1333
STEINBERGER J. (vedi PLANO R.)	»	216
STEINBERGER J. (vedi EISLER F.)	»	1700
STEPHENSON G. - A Classical Calculation of the Nucleon-Meson Coupling Constant (L.)	»	1009
STOLI P. (vedi BEUSCH W.) (L.)	»	1355
SUGAHARA Y. (vedi FURUCHI S.) (L.)	»	285
SYMANZIK K. - On Scattering at Very High Energies	»	659
SZYMANSKI Z. (vedi SAWICKI J.) (L.)	»	1777
TAFFARA L. (vedi CEOLIN C.)	»	435
TALLINI B. (vedi BERTANZA L.)	»	940
TANAKA S. - The Parity Non-Conservation and the Strength of the Interaction of Elementary Particles (L.)	»	1364
TASSIE L. J. - Inelastic Scattering of Electrons by Nuclei	»	1497
TELEGDI V. L. (vedi AMMAR R.) (L.)	»	1801
TENAGLIA L. - Proprietà elettromagnetiche del protone e rinormalizzazione della costante d'accoppiamento	»	220
TENAGLIA L. - Struttura del protone e scattering elettron-protone	»	229
TODESCO G. (vedi GESSAROI R.)	»	1658
TOKUNAGA S., K. NISHIKAWA and T. ISHII - Nuclear Disintegration Cascades by Heavy Primaries (L.)	»	517
TOMOZAWA Y. (vedi EZAWA H.)	»	810
TORELLI G. (vedi FOCARDI S.) (N. T.)	»	275
TOUSCHEK B. F. - Parity Conservation and the Mass of the Neutrino (L.)	»	754
TOUSCHEK B. F. - The Mass of the Neutrino and the Non-Conservation of Parity	»	1281
TOUSCHEK B. F. (vedi RADICATI L. A.)	»	1693
TRIBUNO C. (vedi FERRERO F.)	»	242

TRIBUNO C. (vedi FERRERO F.) (N. T.)	pag. 510
TRIPP R. D. (vedi ALVAREZ L. W.)	» 1026
TSAI-CHÜ - Determination of Distortion Vectors in Nuclear Emulsions	» 1128
UMEZAWA H. (vedi EZAWA H.)	» 810
VACIAGO A. (vedi SIMONETTA M.)	» 587
VANDERHAEGHE G. (vedi HEUGHEBAERT J.) (L.)	» 1808
VAN HEERDEN I. J. (vedi BURGE E. J.) (L.)	» 1005
VARSHNEYA N. C. (vedi BISWAS N. N.)	» 123
VERDINI L. - Velocità delle onde elastiche e dissipazione interna nel metacrilato di polimetile.	» 648
VIGNUDELLI A. (vedi MARCHI C.) (L.)	» 1790
VILLI C. (vedi CLEMENTEL E.)	» 907
VILLI C. (vedi CLEMENTEL E.) (L.)	» 1343
VILLI C. (vedi CLEMENTEL E.)	» 1166
VITALE B. - Electromagnetic Properties of Nucleons and Barion-Heavy Meson Interactions (L.)	» 732
VITALE B. (vedi AMATI D.)	» 1533
VIZSOLYI E. I. (vedi ORIENT O. J.) (N. T.)	» 1722
WADDINGTON C. J. - Observation on the Energy Spectra of Multiply Charged Nuclei in the Cosmic Radiation (L.)	» 737
WADDINGTON C. J. (vedi ALY H. H.)	» 1679
WAKASA A. (vedi FURUICHI S.) (L.)	» 285
WALOSCHEK P. (vedi BISWAS N. N.)	» 123
WALOSCHEK P. (vedi BHOWMIK B.)	» 994
WATAGHIN G. - On a Non-Local Relativistic Quantum Theory of Fields - I	» 689
WATANABE K. (vedi HIGASHI S.)	» 592
WATANABE K. (vedi HIGASHI S.)	» 597
WATASE Y. (vedi HIGASHI S.)	» 592
WATASE Y. (vedi HIGASHI S.)	» 597
WHITEHEAD C. (vedi STAFFORD G. H.)	» 1589
WILGAIN S. (vedi DEBEAUV AIS M.) (N. T.)	» 260
WOLTER W. (vedi MIĘSOWICZ M.) (L.)	» 513
YANG N. C. (vedi CASE K. M.) (L.)	» 1004
YEKUTIELI G. - Ionization at the Origin of High Energy Electron Positron Pairs	» 1381
YEVICK G. J. (vedi PERCUS J. K.)	» 65
YEVICK G. J. (vedi PERCUS J. K.)	» 1057
YONEZAWA M. (vedi FURUICHI S.) (L.)	» 285
ZAGO G. (vedi BALDO-CÉOLIN M.)	» 402
ZICHICHI A. (vedi COOPER W. A.)	» 1388
ZIMERMAN A. H. (vedi JOOS H.)	» 57
ZORZOLI G. B. - On the Decay of ^{141}Ce (L.)	» 289

INDICE ANALITICO PER MATERIE

APPARATI E STRUMENTI E TECNICA Sperimentale

Acoustic Absorption Coefficient in Liquids. A New Method for the Determination, <i>A. Carrelli and F. S. Gaeta</i>	pag. 773
Arrêt de la diffusion des radio-éléments dans les émulsions nucléaires par exposition à basse température (N.T.), <i>M. Debeauvais, E. Picciotto et S. Wilgain</i>	» 260
Bubble Density along the Path of Ionizing Particles Crossing a Bubble Chamber, <i>L. Bertanza, G. Martelli and B. Tallini</i>	» 940
Camera di ionizzazione per raggi X fino a 31 MeV (N.T.), <i>F. Ferrero, R. Malvano and C. Tribuno</i>	» 510
Diborane-Gas Filled Counting Tubes for Measuring Thermic Neutrons (N.T.), <i>O. J. Orient and E. I. Vizsolyi</i>	» 1722
Distortion Vectors in Nuclear Emulsions. Determination of	» 1128
Effect of Ultra-Violet Converters on the Efficiency of Liquid Čerenkov Counters (L.), <i>N. A. Porter</i>	» 526
Geiger Counter Design giving a Definite Counting Length (N.T.), <i>P. J. Grouse and H. D. Rathgeber</i>	» 707
Interferometro per misure di precisione della velocità degli ultrasuoni nei liquidi (N.T.), <i>A. Barone</i>	» 717
Klausen Micrometer, Application to the Measurements of Multiple Scattering of Elementary Particles in Nuclear Emulsions (L.), <i>G. Alvial and S. Stantic</i>	» 1333
Level Flights with Expansible Balloons (N.T.), <i>J. E. Laby, Y. K. Lim and V. D. Hopper</i>	» 249
Machine Analysis of Pion Scattering by the Maximum Likelihood Method, <i>H. L. Anderson and W. C. Davidon</i>	» 1238
Multichannel Pulse Analyzer, Improvements on (L.), <i>S. Colombo, C. Cottini and E. Gatti</i>	» 748
Non-Linear Theory of Phase Oscillations Induced by Radiation Fluctuations in Synchrotrons (L.), <i>A. N. Matveev</i>	» 1782
Oscillatore con transistore (N.T.), <i>M. R. E. Bichara</i>	» 702
Range in G5 Nuclear Emulsion of Protons with Energies 87, 118 and 146 MeV, <i>M. W. Friedlander, D. Keefe and M. G. K. Menon</i>	» 461
Relation between Blob-Density and Velocity of a Singly Charged Particle in G5 Emulsion, <i>G. Alexander and R. H. W. Johnston</i>	» 363
Relaxation Time T_1 , Method for Measuring (L.), <i>T. Ghose, S. K. Ghosh and D. K. Roy</i>	» 1771
Rivelatori di tracce, comando rapido (N.T.), <i>S. Focardi, C. Rubbia, G. Torelli e F. Bella</i>	» 275
Scambio isotopico del deuterio fra idrogeno e vapor d'acqua a pressione atmosferica e a 100° C, apparato per misure standard (N.T.), <i>N. Silvestri e N. Adorni</i>	» 266

Some Aspects of Processing Thick Nuclear Emulsions (L.), <i>E. J. Burge,</i> <i>J. H. Davies, I. J. Van Heerden and D. J. Prowse</i>	pag. 1005
Spin Echoes with Any Number of Pulses (L.), <i>T. Ghose, S. K. Ghosh</i> <i>and D. K. Roy</i>	» 751
Stereoscopy in Bubble Chamber (N.T.), <i>P. Bassi, A. Loria, J. A. Meyer,</i> <i>P. Mittner and I. Scoton</i>	» 1729
Thallium-Activated CsI for Scintillation Spectroscopy (L.), <i>W. Beusch,</i> <i>H. Knoepfel, E. Loepfe, D. Maeder and P. Stoll</i>	» 1355
Time Intervals Defined by Scintillation Counter Pulses. Accuracy Limits in the Measurements (N.T.), <i>S. Colombo, E. Gatti and M. Pignanelli</i>	» 1739
Triggered Spark Counter, <i>T. E. Cranshaw and J. F. De Beer</i>	» 1107

COSMICA (RADIAZIONE)

Alpha Particle Flux at 41° N Geomagnetic Latitude Using Nuclear Emulsions, <i>B. J. O'Brien and J. H. Noon</i>	» 1463
Correlation of the Intensity of μ and μ' Mesons with the Pressure at Sea-Level and with the Height of the 100 mb Layer, <i>U. Fasoli,</i> <i>C. Maroni, I. Modena, E. Pohl and J. Pohl-Rüling</i>	» 473
Cosmic-Ray Flux of Light Elements at 41° N Geomagnetic Latitude, <i>J. H. Noon, A. J. Herz and B. J. O'Brien</i>	» 854
Cosmic Ray Penetrating Showers Underground, <i>S. Higashi, T. Oshio,</i> <i>H. Shibata, K. Watanabe and Y. Watase</i>	» 592
Electromagnetic Cascade of Very High Energy in the First Stage of Its Development (L.), <i>M. Misowicz, O. Stanisz and W. Wolter</i>	» 513
Electron-Photon Cascades of High Energy in Photographic Emulsions (L.), <i>H. Fay</i>	» 293
Energy Spectra of Multiply Charged Nuclei in the Cosmic Radiation (L.), <i>C. J. Waddington</i>	» 737
Fluctuation Problem in Cascade Showers, Solutions of — (L.), <i>J. W. Gardner</i>	» 1368
Flux of Primary Cosmic Ray Alpha Particles over Sardinia, <i>H. H. Aly</i> <i>and C. J. Waddington</i>	» 1679
Gerbes pénétrantes produites par les mésons μ dans une grande chambre de Wilson sous terre, <i>D. Kessler et R. Maze</i>	» 1540
Interactions of μ -Mesons Underground (190 MeV) (L.), <i>S. Narayan,</i> <i>P. V. Ramanamurty, A. B. Sahiar and B. V. Sreekantan</i>	» 1773
Multiple Meson Production and Angular Distribution of Shower Particles Produced in Cosmic Ray « Jets », <i>L. von Lindern</i>	» 491
Multiple Meson Production in the Cosmic Radiation, <i>E. Lohrmann</i> . .	» 1074
Multiple Penetrating Particles, Possible Interpretation, <i>S. Hayakawa</i> .	» 608
Multiple Penetrating Particles Underground, <i>S. Higashi, T. Oshio,</i> <i>H. Shibata, K. Watanabe and Y. Watase</i>	» 597
Nuclear Disintegration Cascades by Heavy Primaries (L.), <i>S. Tokunaga,</i> <i>K. Nishikawa and T. Ishi</i>	» 517
Structure of the Nucleonic Cascade in the Atmosphere, a Calculation of —, <i>M. Oda</i>	» 615
Tunnel Theory of Cosmic Ray « Jets », New Experimental Evidence, <i>C. B. A. McCusker and F. C. Roesler</i>	» 1136

ELETTRODINAMICA E TEORIE DEI CAMPI.

a) CAMPI ELETTROMAGNETICI.

Anomalous Magnetic Moment of the Electron, a Method for Calculating,	
<i>S. Kahana and J. C. Polkinghorne</i>	pag. 1528
Bilocal Field Theories and Their Experimental Tests - II, <i>J. Rayski</i>	» 872
Conformally Invariant Wave Equations for Non-Linear and Interacting Fields, <i>J. A. McLennan jr.</i>	» 640
Dispersion Relations - I. Charge Dependent Corrections, <i>A. Agodi</i> and <i>M. Cini</i>	» 1256
«Dynamical» Lagrangian for the Many Body Problem, <i>J. K. Percus</i> and <i>G. J. Yevick</i>	» 65
Electromagnetic Properties of Particles with Spin, <i>V. Glaser</i> and <i>B. Jakšić</i>	» 1197
Fermi Coupling and Mass and Charge Spectra of Bosons, <i>B. Jouvet</i>	» 1
Fierz' Equivalent Theorem for the Massless Neutrino, <i>L. A. Radicati</i> and <i>B. F. Touschek</i>	» 1693
Functional Integral Formalism for Fermi Systems from the Canonical Formalism, <i>W. K. Burton</i> and <i>A. H. De Borte</i>	» 1510
Gravitational Forces and Quantum Field Theory, <i>P. Gulmanelli</i> and <i>E. Montaldi</i>	» 1716
Gravitational Forces and quantum Theory (L.), <i>P. Bocchieri</i> and <i>P. Gulmanelli</i>	» 1016
Green's Functions, Some Relations Among, <i>K. Hiida</i> and <i>M. Sawamura</i>	» 896
Hamiltonian Formulation of Theory with the Formfactor, Impossibility of —, <i>V. S. Barašenkov</i>	» 1469
Integral-Darstellung kausaler Kommutatoren, <i>R. Jost</i> und <i>H. Lehmann</i>	» 1598
Lehmann's Method of Renormalization (L.), <i>N. Nakanishi</i>	» 520
Leptons, Theory of — (L.), <i>K. Nishijima</i>	» 1349
Low Equations, Physical Significance of the Redundant Solutions of —, <i>R. Haag</i>	» 203
Low's General Equation, <i>W. Królikowski</i>	» 1611
Mass of the Neutrino and the Non-Conservation of Parity, <i>B. F. Touschek</i>	» 1281
Non-Local Relativistic Quantum Theory of Fields - I, <i>G. Wataghin</i>	» 689
Parity Conservation and Neutrino Mass (L.), <i>A. Salam</i>	» 299
Parity Conservation and the Mass of the Neutrino, <i>B. F. Touschek</i>	» 754
Parity Doublets in the Leé-Yang Theory, Interference Effects, <i>R. Gatto</i>	» 1021
Parity Non Conservation and the Strength of the Interaction of Elementary Particles (L.), <i>S. Tanaka</i>	» 1364
Pion Theory, Remarks on the Fixed Extended Source, <i>H. Fukutome</i> and <i>Y. Nogami</i>	» 347
Propagation Kernels as Functions of the Masses (L.), <i>E. Caianiello</i>	» 739
Remarks About a Paper by Fukutome and Nogami (L.), <i>M. Cini</i> and <i>S. Fubini</i>	» 1371
Renormalization in non Relativistic Field Theories (Remarks about the Paper by Enz) (L.), <i>W. Heitler</i>	» 302
Spin 2 Particles, Properties of —, <i>T. Regge</i>	» 325
System of General Relativistic Equations of Low Type, <i>R. Omnes</i>	» 983
Weak Interactions, a Model for —, <i>S. Gotō</i>	» 1573

b) CAMPI MESONICI E STRUTTURA DEL NUCLEONE.

Conservation of Nucleons (L.), <i>B. Ferretti</i>	pag. 761
Integral Equations for Meson Field Theory, <i>R. L. Mills</i>	» 30
Kinematical Test for the Relation between the Coupling Constants in Meson Theory, <i>K. Hiida</i>	» 1094
Lee Model and Ordinary Meson Theory, <i>G. F. Dell'Antonio</i> and <i>F. Duimio</i>	» 1636
Meson Production by a Meson Nucleon Collision in the Heisenberg Representation, <i>G. R. Sereaton</i>	» 1398
Nombre de mésons virtuels sur un modèle simple, <i>E. Arnous</i>	» 483
Nonlinear Mesodynamics, a Possible Form of —, <i>A. Borgardt</i>	» 102
Nucleon-Meson Coupling Constant, Classical Calculation of — (L.), <i>G. Stephenson</i>	» 1009
Nucleons Magnetic Moments Contribution to the Radiative Pion-Nucleon Scattering (L.), <i>B. Bosco</i>	» 1361
Pion-Nucleon Interaction and Strange Particles (L.), <i>P. Budini</i> and <i>L. Fonda</i>	» 306
Pion-Nucleon, Pion-Hyperon Interactions, Non-Local Models of —, <i>P. Budini</i> and <i>L. Fonda</i>	» 666
Proprietà elettromagnetiche del protone e rinormalizzazione della costante di accoppiamento, <i>L. Tenaglia</i>	» 220
Quantum Statistics of Fields and Multiple Production of Mesons, <i>H. Ezawa</i> , <i>Y. Tomozawa</i> and <i>H. Umezawa</i>	» 810
Struttura del protone e scattering elettrone-protone, <i>L. Tenaglia</i>	» 229
Viscous Fluid Model in Multiple Production, <i>M. Hamaguchi</i>	» 1622

MESONI π E μ .

Angular Correlation in μ -e Decays Observed in Nuclear Emulsions Exposed in Magnetic Field (L.), <i>J. Heughebaert</i> , <i>M. René</i> , <i>J. Sacton</i> and <i>G. Vanderhaeghe</i>	» 1808
Angular Correlation in the β -Decay of μ -Mesons Observed in Photographic Emulsions, <i>B. Bhownick</i> , <i>D. Evans</i> and <i>D. J. Prowse</i>	» 1663
Angular Distribution of the μ -Decay as Test of Parity Conservation (L.), <i>N. N. Biswas</i> , <i>M. Ceccarelli</i> and <i>J. Crussard</i>	» 756
Decay Processes of the Pion in the Frame of the Universal Fermi Interaction, Possible Explanations of —, <i>G. Morpurgo</i>	» 1159
Mean Free Path of 4.3 GeV π^- -Mesons in Nuclear Emulsions (L.), <i>A. Marques</i> , <i>N. Margem</i> and <i>G. A. B. Garnier</i>	» 291
Parity Conservation in π - μ -e Decays, Further Results, <i>C. Castagnoli</i> , <i>C. Franzinetti</i> and <i>A. Manfredini</i>	» 684

MESONI PESANTI, IPERONI E PARTICELLE STRANE

Analysis of Rochester $K_{\mu 3}$ and $K_{e 3}$ Data (L.), <i>S. Furuichi</i> , <i>Y. Sugahara</i> , <i>A. Wakasa</i> and <i>M. Yonezawa</i>	» 285
Annihilation of a Nucleon-Antinucleon System into a K-anti K Pair, <i>R. Gatto</i>	» 1024

Asymmetries in the Λ^0 Decay, Discussion of the Possibility of Detecting (L.), G. Morpurgo	pag. 1787
Change of Isotopic Spin in the K_{π^2} Decay (L.), M. Gell-Mann	» 758
Electromagnetic Properties of Nucleons and Barion-Heavy Meson Interactions (L.), B. Vitale	» 732
Emission of an Electron Pair in a K Decay (L.), R. Levi Setti and W. Slater	» 1784
Heavy Neutral K-Particle and Its Cascade Decay, Evidence for —, M. S. Sinha and S. N. Sengupta	» 1153
Hyperon-Nucleon Interaction Cross Section (L.), N. Dallaporta and F. Ferrari	» 742
Interactions of K-Mesons with Emulsions Nuclei between 40 and 160 MeV, M. Baldo-Ceolin, M. Cresti, N. Dallaporta, M. Grilli, L. Guerriero, M. Merlin, G. A. Salandin and G. Zago	» 402
K-Interactions in Hydrogen, L. W. Alvarez, H. Bradner, P. Fall, Vairant, J. D. Gow, A. H. Rosenfeld, F. T. Solmitz and R. D. Tripp	» 1026
K ⁺ -Meson Interaction with Nucleons and Nuclei, G. Cocconi, G. Puppi, G. Quarenii and A. Stanghellini	» 172
K ⁺ Nuclei Interactions According to the Optical Model, G. Costa and G. Paterniani	» 448
Δ Nucleon Force and the Binding Energy of the Light Hyperfragments, N. Dallaporta and F. Ferrari	» 111
Lifetime of ${}^3H_\Lambda$ Hyperfragments (L.), M. W. Friedlander	» 283
Lifetime of Positive Heavy Mesons, B. Bhowmik, D. Evans, S. Nilsson, D. J. Prouse, F. Anderson, D. Keele, A. Kernan, N. N. Biswas, M. Ceccarelli, P. Waloscheck, J. E. Hooper, M. Grilli and L. Guerriero	» 994
Longlived Neutral K-Particle (L.), S. Friesen and K. Kristiansson	» 1013
Low Energy K-Nucleon Interaction, D. Amati and B. Vitale	» 1533
Mass Difference between the Σ and Ξ Hyperons (L.), R. G. Kumar, W. B. Lasich and F. R. Stannard	» 746
Masses of Light Mesons, K-Mesons and Hyperons in 1956, K. M. Crowe	» 541
Mass Measurements of Particles Stopping in the Emulsion by the Constant Sagitta Method, B. Judek	» 886
Nuclear potential for the K ⁺ -Mesons (L.), C. Marchi, G. Quarenii, A. Vignudelli, G. Dascola and S. Mora	» 1790
Nuclear Scattering of K-Mesons in the Energy Region of 80 MeV, N. N. Biswas, L. Ceccarelli-Fabbrichesi, M. Ceccarelli, K. Gottstein, N. C. Varshneya and P. Waloscheck	» 123
Parent Stars of K ⁺ -Mesons, D. F. Falla, M. W. Friedlander, F. Anderson, W. D. B. Greening, S. Limentani, B. Sechi-Zorn, C. Cernigoi, G. Ier netti and G. Poiani	» 1203
Parity Non-Conservation in the Decay of Strange Particles (L.), N. Dallaporta and F. Ferrari	» 1793
Parity Violation and the Spin of the Λ^0 Particle, F. Cerulus	» 1685
Production of Heavy Mesons and Hyperons by π^- -Mesons of 4.5 GeV/c, B. O. Edwards, A. Engler, M. W. Friedlander and A. A. Kamal	» 1188
Production of (K^0 , K^0) and (K^+ , K^0) Pairs of Heavy Mesons, W. A. Cooper, H. Filthuth, J. A. Newth, G. Petrucci, R. A. Salmeron and A. Zichichi	» 1388
Reply to Criticism by Mr. A. Gamba (L.), K. M. Case, N. C. Yang and R. Karplus	» 1004

Scattering of K ⁺ -Mesons by Nucleons in Perturbation Theory, <i>C. Ceolin</i> and <i>L. Taffara</i>	pag. 435
Σ Hyperon-Nucleon Interaction Cross-Section (L.), <i>N. Dallaporta</i> and <i>F. Ferrari</i>	» 742
Σ ⁰ Hyperon and a Measurement of Its Mass, Demonstration of the Existence of —, <i>R. Plano</i> , <i>N. Samios</i> , <i>M. Schwartz</i> and <i>J. Steinberger</i>	» 216
Spin of the K _{μ3} Meson (L.), <i>L. A. Radicati</i> and <i>S. Rosati</i>	» 729
Strange Particle, Associated Production of —, (L.), <i>J. J. Sakurai</i>	» 1340
Systematics of Λ ⁰ and Θ ⁰ Decay, <i>F. Eisler</i> , <i>R. Plano</i> , <i>N. Samios</i> , <i>M.</i> <i>Schwartz</i> and <i>J. Steinberger</i>	» 1700
 MOLECOLE	
Barriera di potenziale per l'inversione della molecola di fosfina, calcolo quantomeccanico, <i>M. Simonetta</i> e <i>A. Vaciago</i>	» 587
Electronic Absorption-Spectrum of Naphtotriazines (L.), <i>M. Simonetta</i> , <i>G. Favini</i> and <i>V. Pierpaoli</i>	» 1814
Law of Molecular Interaction for Kripton (L.), <i>M. P. Madan</i>	» 1369
 NEUTRINO	
Photographic Evidence for the Existence of the Neutrino (L.), <i>J. Csilai</i>	» 1011
 NUCLEI (FISICA NUCLEARE)	
a) FORZE E MODELLI NUCLEARI	
Effective Nuclear Potentials (L.), <i>W. E. Frahn</i> and <i>R. H. Lemmer</i>	» 523
Liquid Drop Model, Asymmetry Equilibrium Shapes (L.), <i>U. L. Busi-</i> <i>naro</i> and <i>S. Gallone</i>	» 315
Nucleon-Nucleus Interaction from the Statistical Model, <i>W. E. Frahn</i>	» 393
Real Part of the Complex Potential Well of the Nucleus, <i>A. Kind</i> and <i>L. Jess</i>	» 1020
Sign of the Real Central Part of the Neutron-Nucleus Complex Po- tential (L.), <i>A. Kind</i>	» 318
Velocity-Dependent Nuclear Interaction, <i>W. E. Frahn</i> and <i>A. H. Lemmer</i>	» 1564
 b) REAZIONI NUCLEARI	
Angular Correlation in High Energy Fission, <i>L. Marquez</i>	» 1646
Angular Distribution of Photoprottons from Oxygen (L.), <i>C. Milone</i> and <i>R. Ricamo</i>	» 1338
Antiproton Annihilations. Further Results (L.), <i>E. Amaldi</i> , <i>C. Castagnoli</i> , <i>M. Ferro-Luzzi</i> , <i>C. Franzinetti</i> and <i>A. Manfredini</i>	» 1797
C and Al Photoprotton Angular and Energy Distribution (L.), <i>C. Milone</i> , <i>R. Ricamo</i> and <i>A. Rubbino</i>	» 528

Disintegrazioni nucleari prodotte da protoni di 140 ± 6 MeV - II. Nuclei pesanti, <i>S. Jannelli e F. Mezzanares</i>	pag. 380
Disintegrazioni nucleari prodotte da protoni di 140 ± 6 MeV - III. Nuclei leggeri, <i>S. Jannelli e F. Mezzanares</i>	» 1047
Fast Neutron Component in Photonuclear Reactions, <i>F. Ferrero, L. Gonella, R. Malvano, C. Tribuno and A. O. Hanson</i>	» 242
γ Polarization Effects in Photonuclear Reactions, <i>A. Agodi</i>	» 21
(n, p) and (p, p') Experiments on Intermediate Energy, <i>L. Colli, U. Facchini and S. Micheletti</i>	» 502
n, p Reactions at 14 MeV, further Measurements - II. Sulphur, Aluminium, Iron, Copper, Nickel (L.), <i>L. Colli and U. Facchini</i>	» 309
Nuclear Interactions of Long-Lived Neutral Strange Particles (L.), <i>R. Ammar, J. I. Friedman, R. Levi Setti and V. L. Telegdi</i>	» 1801
Nucleon-Surface Interaction and the (p, n) Reactions (L.), <i>J. Sawicki and Z. Szymanski</i>	» 1777
Pairs Produced by ^8Be γ -Rays in Photographic Emulsions, <i>D. J. Prowse</i>	» 977
Photoprottons from Oxygen up to 30 MeV (L.), <i>C. Milone, R. Ricamo and R. Rinzivillo</i>	» 535
Polarization of Nucleons from Photodisintegration of Deuterium, <i>W. Czyz and J. Sawicki</i>	» 45
Spurious Scattering in Nuclear Emulsions, <i>A. J. Apostolakis, J. O. Clarke and J. V. Major</i>	» 337

c) STRUTTURA DEI NUCLEI

Neutron Isotopes of Thallium, ^{200}Tl and ^{202}Tl , <i>R. K. Gupta and S. Iha</i>	» 1524
7.7 MeV Level of Carbon 12, <i>A. Hossain and D. J. Prowse</i>	» 973

QUANTISTICA (MECCANICA)

Bound of Phase Shifts, <i>J. B. Keller</i>	» 1122
Covariant Wave Equation, Separability of —, <i>H. S. Green</i>	» 866
Special Representation for the Treatment of a System of two Dirac Particles, <i>H. Joos, J. Ferreira and A. H. Zimerman</i>	» 57
Spin Kinematics for a Charged Particle in a Uniform Magnetic Field, <i>M. Carrassi</i>	» 955
Statistical Approach to the Domain of Action of Collective Co-ordinates in the Many Body Problem, <i>J. K. Percus and G. J. Yevick</i>	» 1057

RADIOATTIVITÀ

Angular Correlation of Radiations with Parallel Angular Momenta (L.), <i>U. Fano</i>	» 1358
Decay of ^{111}Ce (L.), <i>G. B. Zorzoli</i>	» 289
Directional Correlation of the 0.845 and 1.24 MeV γ -Rays of Fe, <i>G. Bertolini, E. Lazzarini and M. Mandelli Bettoni</i>	» 356
Radiation from ^{192}Pt and Proposed Decay Scheme, <i>M. S. Huq</i>	» 1456

RELATIVITÀ

Età dell'Universo, <i>M. Pierucci</i>	pag. 572
Field Equations Involving an Asymmetrical Fundamental Tensor, Reciprocal Static Solutions, <i>H. A. Buchdahl</i>	» 1083
Generalization of Reissner-Nordström Solution - II, <i>R. L. Brahmachary</i>	» 1520
Relativistic Kinematics of a Classical Point Particle in Spinor Form, <i>F. Gürsey</i>	» 784
Review of the Experimental Evidence for the Law of Variation of the Electron Mass with Velocity, <i>P. S. Farago</i> and <i>L. Jánossy</i>	» 1411
Spinor Wave Equations, General Relativistic Interpretation, <i>F. Gürsey</i>	» 154

SCATTERING E IONIZZAZIONE

<i>D</i> Wave Effects in Positive Pion-Proton Scattering (L.), <i>E. Clementel</i> and <i>C. Villi</i>	» 1343
Double Compton Effect, Interference in —, <i>B. De Tolla</i> and <i>R. S. Liotta</i>	» 947
Effects of Proton Correlations on the Scattering of High Energy Electrons from Nuclei, <i>L. I. Schiff</i>	» 1223
Electron Scattering in Nuclear Field with Pair-Creation, <i>E. Montaldi</i> and <i>M. Pusterla</i>	» 961
Energieverteilung der inelastischen Streuung von K^+ -Mesonen an Kernen, <i>P. Mittelstaedt</i>	» 1480
Inelastic Scattering of Electrons by Nuclei, <i>L. S. Tassie</i>	» 1497
Ionization at the Origin of High Energy Electron Positron Pairs, <i>G. Yekutieli</i>	» 1381
Multiple Scattering, further Development of a New Approximate One-Velocity Theory, <i>C. C. Grosjean</i>	» 83
Multiple Scattering Problems in Inhomogeneous Media. New Method for Solving —, <i>P. Gosar</i>	» 1437
Neutron-Proton Scattering, <i>E. Clementel</i> and <i>C. Villi</i>	» 1166
Phase-Shift Analysis of High-Energy p-p Scattering (L.), <i>A. J. N. Phillips</i>	» 1335
Phase-Shift Analysis of Proton-Proton Scattering Experiments - II. Analysis of the Scattering Data from 18 to 260 MeV, <i>E. Clementel</i> , <i>C. Villi</i> and <i>L. Jess</i>	» 907
Pion-Nucleon Interaction Coupling Constant from Scattering Experiments Using Dispersion Relations, <i>G. Puppi</i> and <i>A. Stanghellini</i>	» 1305
Pion-Proton Elastic Scattering in Nuclear Emulsions, Measurements of, <i>G. Ferrari</i> , <i>E. Manaresi</i> and <i>G. Quarenì</i>	» 1651
Polarization in Neutron Proton Scattering at 95 MeV, <i>G. H. Stafford</i> , <i>C. Whitehead</i> and <i>P. Hillman</i>	» 1589
π^+ -Proton Scattering at 100 MeV, <i>R. Gessaroli</i> , <i>G. Quarenì</i> , <i>G. Dascola S. Mora</i> and <i>G. Tedesco</i>	» 1658
π^+ -Proton Scattering at 83 MeV, <i>L. Ferretti</i> , <i>G. Quarenì</i> , <i>M. Della Corte</i> and <i>T. Fazzini</i>	» 1660
Scattering of Fast Electrons by Polarized Nuclei, <i>M. Bernardini</i> , <i>P. Brovetto</i> and <i>S. Ferroni</i>	» 1292

Scattering at Very High Energies, <i>K. Symanzik</i>	pag.	659
Scattering of Particles by a Force Centre According to the Radiation		
Damping Theory, <i>A. Sokolov</i> and <i>B. Kerimov</i>	»	921
Soluble Model of Meson-Nucleon <i>S</i> -State Scattering, <i>E. L. Lomon</i>	»	1816

STRUTTURA DELLA MATERIA

Atomic Displacements Produced by α -Particles in Germanium, <i>A. Ascoli</i> , <i>M. Asdente</i> and <i>E. Germagnoli</i>	»	1145
Effetti galvanometrici nel germanio, <i>G. C. Della Pergola</i> e <i>D. Sette</i>	»	1670
Effetti isotopici nell'adsorbimento di gas su solidi, <i>P. Caldirola</i> e <i>G. Rossi</i>	»	1316
Electrochemistry of Metallic Single Crystals - I. Exchange Overvoltages on Silver and Copper (L.), <i>R. Piontelli</i> , <i>G. Poli</i> and <i>L. Paganini</i>	»	1018
Gliossima allo stato solido, struttura della —, <i>M. Milone</i> e <i>E. Borello</i>	»	562
Helium Film Static - II. Effects due to the Smallness of One Dimension, <i>S. Franchetti</i>	»	183
Helium Film Static - III. The Profile of the Film and Its Dependence on Temperature, <i>S. Franchetti</i>	»	1266
Paramagnetic Resonance Spectrum of Triphenylmethyl, <i>P. Brovetto</i> and <i>S. Ferroni</i>	»	142
Relazioni cristallografico-strutturali tra il difenile ed una serie di suoi nuovi derivati, <i>M. Fenoglio</i>	»	765
Relazioni tra la struttura della blenda e il contenuto in gallio e indio, <i>G. Rigault</i>	»	579
Separazione isotopica nella diffusione di un gas attraverso una parete porosa, influenza dell'adsorbimento e della migrazione superficiale (L.), <i>P. Caldirola</i> e <i>G. Rossi</i>	»	1374
Superconductivity, Gauge Invariance and the Energy Gap Model (L.), <i>J. Bardeen</i>	»	1766
Superconductivity, a Note on the Energy Gap Model (L.), <i>M. J. Buckingham</i>	»	1763
Superfluidity and Superconductivity, Quantum Fluid as a Common Model, <i>N. Mikoshiba</i>	»	628
Thermodynamical Theory of Thermal Conduction of Dielectrics under Electric Fields, <i>S. Mascarenhas</i>	»	1118
Variazioni delle proprietà magnetiche e meccaniche causate dall'idro- geno disciolto nel ferro, <i>A. Ferro</i> e <i>G. Montalenti</i>	»	842
Velocità delle onde elastiche e dissipazione interna nel metacrilato di polimetile, <i>L. Verdini</i>	»	648

INDICE DELLE RECENSIONI

J. R. MENTZER - <i>Scattering and Diffraction of Radio Waves</i>	pag. 321
ALBERT EINSTEIN - <i>The Meaning of Relativity</i>	» 321
<i>Process Chemistry</i> , Vol. I; Editors F. R. BRUCE, J. M. FLETCHER, H. H.	
HYMAN and J. J. KATZ	» 322
A. MÜNSTER - <i>Statistische Thermodynamik</i>	» 322
R. HAASE - <i>Thermodynamik der Mischphasen</i>	» 323
E. BODEWIG - <i>Matrix Calculus</i>	» 323
<i>Handbuch der Physik</i> - Herausgegeben von S. FLÜGGE, Band I	» 535
K. HAUFFE - <i>Oxydation von Metallen und Metallegierungen</i>	» 536
F. CONFORTO - <i>Abelsche Funktionen und algebraische Geometrie</i>	» 537
F. BITTER - <i>Currents, Fields, and Particles</i>	» 538
E. J. DIJKSTERHUIS - <i>Die Mechanisierung des Weltbildes</i>	» 539
W. HEITLER - <i>Elementary Wave Mechanics with Applications to Quantum Chemistry</i>	» 539
A. S. THOMPSON and O. E. RODGERS - <i>Thermal Power from Nuclear Reactors</i>	» 762
<i>Proceedings of the International Conference on the Peaceful Uses of Atomic Energy</i> , Geneva, 8-20 August 1955, Vol. 7. <i>Nuclear Chemistry and Effects of Irradiation</i>	» 763
<i>Progress in Nuclear Energy</i> , serie II. <i>Reactors</i> , Vol. I - Editors: R. A. CHARPIE, D. J. LITTLER, D. J. HUGHES, M. TROCHERIS	» 1377
Z. KOPAL - <i>Astronomical Optics and Related Subjects</i>	» 1377
<i>Quantum Theory of Fields</i> , fascicolo della « Series of Selected Papers in Physics » pubblicata a cura della Società Giapponese di Fisica	» 1379
A. DUSCHEK - <i>Vorlesungen über höhere Mathematik</i> , I Bd., II Auflage . .	» 1379
C. KITTEL - <i>Introduction to Solid State Physics</i>	» 1817
<i>Particelle pesanti instabili</i> , fascicolo della « Series of Selected Papers in Physics », pubblicata a cura della Società Giapponese di Fisica	» 1818
H. PREUSS - <i>Integraltafeln zur Quantenchemie</i>	» 1819
P. M. S. BLACKETT - <i>Lectures on Rock Magnetism</i>	» 1820
H. RICHTER - <i>Wahrscheinlichkeitstheorie</i>	» 1821
<i>Korpuskularoptik - Optics of Corpuscles</i> , vol. XXXIII dell' <i>Handbuch der Physik</i>	» 1822
W. H. SULLIVAN - <i>Trilinear Chart of Nuclides</i>	» 1823
A. DAUVILLIER - <i>L'origine des Planètes</i>	» 1824

Fine del Volume V, Serie X, 1957

PROPRIETÀ LETTERARIA RISERVATA

Direttore responsabile: G. POLVANI

Tipografia Compositori - Bologna

Questo fascicolo è stato licenziato dai torchi il 27-V-1957

